Catalytic Asymmetric Reduction of Alkenes

Inaugural-Dissertation

zur

Erlangung des Doktorgrades

der Mathematisch-Naturwissenschaftlichen Fakultät

der Universität zu Köln

vorgelegt von

Wencke Leinung Genannt Policardo

aus Stendal

angenommen im Jahr 2025

CONTENTS

ABSTRACT

Over the past two decades, organocatalytic asymmetric transfer hydrogenation of alkenes has seen significant advances. Inspired by enzymes, chemists have developed catalytic strategies that employ small organic chiral molecules as catalysts and biomimetic dihydrogen donors as reducing agents, to achieve high levels of enantioselectivity. Beyond classical steric and electronic effects, it is now well recognized that noncovalent interactions, such as hydrogen bonding, ion pairing and London dispersion, play a decisive role in determining reactivity and selectivity. This understanding has opened new avenues for rational catalyst design in asymmetric transfer hydrogenation reactions.

The first part of this dissertation investigates the first report of asymmetric counteranion-directed catalysis (ACDC) describing the transfer hydrogenation of α,β-unsaturated aldehydes. Particular emphasis is placed on the role of noncovalent interactions, especially London dispersion, in governing stereocontrol. Computational studies revealed that an isopropyl group in the reducing agent engages in key dispersion interactions, contributing significantly to enantioselectivity. Building on this insight, a second-generation catalyst was designed, incorporating analogous *dispersion energy donors* into the catalyst scaffold. This modified system overcame limitations of the original, and mechanistic analysis confirmed that the enhanced enantioselectivity resulted directly from intended dispersion interactions.

The second part of this work focuses on the development of an enantioselective reduction of α-alkyl styrenes. While activated alkenes such as enals, enones, nitroolefins, and α-(2-hydroxyphenyl) styrenes can be reduced enantioselectively using established organocatalytic methods, analogous asymmetric transformations of less functionalized substrates remain underdeveloped. Here, a Brønsted acid-catalyzed, chemo- and enantioselective ionic hydrogenation of α-alkyl styrenes was established using silanes in combination with benzoic acid. Mechanistic investigations support a pathway proceeding via a stabilized carbocation intermediate and a transient silylated catalyst species, with catalyst turnover dependent on the presence of a protic additive. Density functional theory highlights key noncovalent interactions, including cation–π interactions, that govern enantioselectivity.

KURZZUSAMMENFASSUNG

In den letzten zwei Jahrzehnten wurden bedeutende Fortschritte bei der organokatalytischen asymmetrischen Transferhydrierung von Alkenen erzielt. Inspiriert von Enzymen haben Chemiker katalytische Strategien entwickelt, bei denen kleine organische chirale Moleküle als Katalysatoren und biomimetische Wasserstoffdonatoren als Reduktionsmittel eingesetzt werden, um eine hohe Enantioselektivität zu erreichen. Über klassische sterische und elektronische Effekte hinaus ist heute allgemein anerkannt, dass nichtkovalente Wechselwirkungen wie Wasserstoffbrückenbindungen, Ionenpaarbildung und London-Dispersion eine entscheidende Rolle bei der Bestimmung der Reaktivität und Selektivität spielen. Dieses Verständnis hat neue Wege für das rationale Katalysatordesign in asymmetrischen Transferhydrierungsreaktionen eröffnet.

Der erste Teil dieser Dissertation befasst sich mit dem ersten Bericht über asymmetrische Gegenanion-vermittelte Katalyse (asymmetric counteranion-directed catalysis, ACDC), in dem die Transferhydrierung von α,β-ungesättigten Aldehyden beschrieben wird. Besonderes Augenmerk wird dabei auf die Rolle nichtkovalenter Wechselwirkungen, insbesondere der London-Dispersion, bei der Steuerung der Stereokontrolle gelegt. Computergestützte Studien zeigten, dass eine Isopropylgruppe im Reduktionsmittel an wichtigen Dispersionswechselwirkungen beteiligt ist und erheblich zur Enantioselektivität beiträgt. Auf dieser Erkenntnis aufbauend wurde ein Katalysator der zweiten Generation entwickelt, der analoge Dispersionsenergiedonatoren in das Katalysatorgerüst integriert. Dieses modifizierte System überwand die Einschränkungen des Originals, und eine mechanistische Analyse bestätigte, dass die verbesserte Enantioselektivität direkt auf die beabsichtigten Dispersionswechselwirkungen zurückzuführen war.

Der zweite Teil dieser Arbeit konzentriert sich auf die Entwicklung einer enantioselektiven Reduktion von α-Alkylstyrolen. Während aktivierte Alkene wie Enale, Enone, Nitroolefine und α-(2-Hydroxyphenyl)styrole mit etablierten organokatalytischen Methoden enantioselektiv reduziert werden können, sind analoge asymmetrische Umwandlungen von weniger funktionalisierten Substraten noch unterentwickelt. Hier wurde eine Brønsted-Säure-katalysierte, chemo- und enantioselektive ionische Hydrierung von α-Alkylstyrolen unter Verwendung von Silanen in Kombination mit Benzoesäure etabliert. Mechanistische Untersuchungen stützen einen Reaktionsweg über ein stabilisiertes Carbokation-Intermediat und eine vorübergehende silylierte Katalysatorspezies, wobei der Katalysatorumsatz von der Anwesenheit eines protischen Additivs abhängt. Dichtefunktionaltheorie-Berechnungen heben wichtige nichtkovalente Wechselwirkungen hervor, darunter Kation-π-Wechselwirkungen, die die Enantioselektivität bestimmen.

LIST OF ABBREVIATIONS

Ac	acetyl
Alkyl	Alkyl
Aryl	Aryl
aq.	aqueous
atm	atmosphere
BALT	binaphthyl-allyl-tetrasulfone
BINOL	1,1'-bi-2-naphthol
BINSA	binaphthyl-2,2'-disulfonic acid
Bn	benzyl
Boc	*tert*-butyloxycarbonyl
BPTM	BINOL-derived phosphoryl bis((trifluoromethyl)-sulfonyl) methane
Bu	butyl
CBS	Corey–Bakshi–Shibata (reduction)
conc.	concentration
conv.	conversion
CPA	chiral phosphoric acid
Cy	cyclohexyl
d	doublet or day(s)
DCM	dichloromethane
DED	dispersion energy donor
DFT	density functional theory
DIA	distortion interaction analysis
DIBAL-H	diisobutylaluminium hydride
DMAP	4-dimethylaminopyridine
DMF	*N,N*-dimethylformamide
DSI	disulfonamide
E	educt
EDG	electron-donating group
ee	enantiomeric excess
EI	electron impact
ent	enantiomer
eq.	equivalent(s)

er	enantiomeric ratio
ESI	electrospray ionization
Et	ethyl
EWG	electron-withdrawing group
GC	gas chromatorgaphy
GP	general procedure
h	hour(s)
HE	Hantzsch ester
Hex	hexyl
HMBC	heteronuclear multiple bond correlation
HMDS	hexamethyldisilazane
HOMO	highest occupied molecular orbital
HPE	hexaphenylethane
HPLC	high performance liquid chromatography
HRMS	high resolution mass spectrometry
i	*iso*
IDP	imidodiphosphate
IDPi	imidodiphosphorimidate
iIDP	iminoimidodiphosphate
IGMH	Independent Gradient Model based on Hirshfeld partition
Int	intermediate
Int.	interactions
JINGLE	binaphthyl-2-2'-bis(sulfuryl)imide
LC	liquid chromatography
LDA	lithium diisopropylamide
LED	local energy decomposition
LUMO	lowest unoccupied molecular orbital
m	multiplet
m	*meta*
M	molar
Me	methyl
Mes	mesityl
min	minute(s)
MTBE	methyl *tert*-butyl ether

NADH/NAD$^+$	nicotinamide adenine dinucleotide
NADPH/NADP$^+$	nicotinamide adenine dinucleotide phosphate
Nap	naphthyl
NCI	noncovalent interactions
NLE	nonlinear effect
NMR	nuclear magnetic resonance (spectroscopy)
NOE	nuclear Overhauser effect
Ns	nitrobenzenesulfonyl
NTPA	*N*-triflyl phosphoramide
Nu	nucleophile
o	*ortho*
o2s	over two steps
p	pentet
P	product
p	*para*
PADi	phosphoramidimidate
Pent	pentyl
Ph	phenyl
Pr	propyl
q	quartet
quant.	quantitative
rac	racemic
rt	room temperature
SPINOL	1,1'-spirobiin-dane-7,7'-diol
t	*tert*
t	triplet or time
TBS	*tert*-butyldimethylsilyl
temp.	temperature
TADDOL	α,α,α',α'-tetraaryl-2,2-disubstituted 1,3-dioxolane-4,5-dimethanol
temp.	temperature
Tf	trifluoromethanesulfonyl (triflyl)
TFA	trifluoroacetic acid
THF	tetrahydrofuran
TIPS	triisopropylsilyl

TLC	thin-layer chromatography
TRIP	3,3'-bis(2,4,6-triisopropylphenyl)-1,1'-binaphthyl-2,2'-diyl hydrogenphosphate
TS	transition state
Ts	toluenesulfonyl (tosyl)
TTP	tetratriflylpropene
VANOL	3,3'-diphenyl-2,2'-bi-1-naphthol
VAPOL	2,2'-diphenyl-(4-biphenanthrol)
VTNA	variable-time normalization approach

1   INTRODUCTION

Owing to the development of hydrogenation, margarine became spreadable, fossil and biofuels available, and life-saving medicines a reality. From the breakfast table to the pharmacy shelf, hydrogenation reactions subtly shape our everyday lives.

What became a cornerstone in chemical synthesis, started in the late 19th century, when Paul Sabatier discovered the addition of hydrogen gas to unsaturated molecules in the presence of freshly reduced nickel.[1] Only shortly thereafter, the first transfer hydrogenation (the addition of hydrogen from a non-H_2 source), involving a disproportionation of 1,4-dihydroterephthalate, was reported by Emil Knoevenagel.[2] Both general strategies offer practical access to hydrogenated compounds, each with its own strengths and limitations. While hydrogenations provide clean and atom-economic transformations, transfer hydrogenations usually do not require high-pressure experimental set-ups and use readily available and easy-to-handle hydrogen sources. The first half of the 20th century was characterized by important developments in both fields. The Haber-Bosch process[3] (ammonia synthesis, 1905), the Bergius process[4] (coal liquefaction, 1913), and the Fischer-Tropsch process[5–7] (conversion of CO/H_2 syngas into liquid hydrocarbons, 1922) represent selected milestones that significantly influenced human life. The key to unlocking all of these powerful transformations lies in a well-known concept: catalysis.

The term *catalysis* was first introduced by Jöns Jakob Berzelius in 1835 and later established as a fundamental principle by Wilhelm Ostwald.[8,9] Substoichiometric amounts of a catalyst can accelerate a chemical reaction by providing an alternative reaction pathway with a lower activation energy barrier. While the catalyst interacts with the substrates and forms intermediates, it is ultimately regenerated and remains unchanged after the reaction. These inherent characteristics make catalysis a powerful and highly sought-after technology in industry, as reflected by the fact that approximately 90% of chemical processes and 60% of industrial products rely on the use of a catalyst today.[10]

In the mid-19th century, while catalysis was still in its infancy, a previously unrecognized three-dimensional complexity of chemical structures became apparent. Chemists made the puzzling observation that compounds with identical molecular formulae and constitution show different optical activity.[11] As Jacobus Henricus van't Hoff would later write: "*The theory is brought into accord with the facts if we consider the affinities of the carbon atom directed toward the corners of a tetrahedron of which the carbon atom itself occupies the center. […] When the four affinities of the carbon atom are satisfied by four univalent groups differing among themselves, two and not more than two different tetrahedrons are obtained, one of which is the reflected image of the other, they cannot be superposed; that is, we have here to deal with two structural formulas isomeric in space.*"[12] This structural insight, independently proposed in 1874 by van't Hoff and Joseph-Achille Le Bel, offered a theoretical basis for the existence of *enantiomers*

(from the Greek *enantios*, meaning "opposite", and *meros*, meaning "part") and their differing optical behavior.[13] The geometric property of being non-superposable on a mirror image was later termed *chirality*. It explains how enantiomers, despite sharing scalar physical properties, may exhibit distinct interactions in chiral environments, such as biological systems, or, most crucially, chiral catalysts.

Despite early attempts at asymmetric heterogeneous hydrogenation of alkenes, no groundbreaking discovery in enantioselective catalysis was made until the 1960s.[14] Pioneering work on homogeneous Rh- and Ru-catalyzed hydrogenations, along with the development of chiral phosphine ligands by chemists such as Wilkinson, Horner, and Mislow, among others, paved the way for a major breakthrough.[15] In 1968, William S. Knowles reported the Rh-catalyzed asymmetric hydrogenation of unsaturated carboxylic acids using chiral phosphines.[16] Although low enantioselectivities were initially obtained, continued efforts culminated in the development of the Monsanto (L)-DOPA process, in which the key step is the enantioselective hydrogenation of an enamide precursor to the protected α-amino acid.[17] The foundational work by Knowles—and later by Ryoji Noyori on Ru-catalyzed asymmetric hydrogenation of ketones[18]— was recognized with the Nobel Prize in Chemistry in 2001 (together with Sharpless) for their contributions to catalytic asymmetric hydrogenation reactions.[1]

These developments firmly established *asymmetric metal catalysis* as a powerful tool for enantioselective synthesis, providing an alternative to earlier stoichiometric approaches such as the chiral pool and auxiliary-based methods. Around the same time, *biocatalysis* emerged as a complementary paradigm, with enzymes offering exceptional stereoselectivity through well-defined active sites and simple functional group activation.[19] Drawing inspiration from nature, researchers began to explore whether similar control could be achieved using small organic molecules[20]. This ultimately led to the rise of *organocatalysis*—the third pillar of asymmetric catalysis—based on the ability of simple functional groups to mediate both reactivity and stereoselectivity.[21,22] Following the seminal reports by Benjamin List[23] and David W. C. MacMillan[24] in the early 2000s, various bioinspired asymmetric reductions of unsaturated molecules have been explored.[25–29] Utilizing small molecule catalysts as enzyme mimics, together with dihydrogen surrogates resembling NAD(P)H co-factors, organocatalytic transfer hydrogenations provide a mild and practical platform for reductive transformations without the need for metals.

---

[1] The 2001 Nobel Prize in Chemistry was shared with K. Barry Sharpless, who was awarded for his work on catalytic asymmetric oxidation reactions.

1.1 Fundamentals and Transition State Differentiation in Asymmetric Organocatalysis

Catalysis plays a central role in accelerating chemical reactions and enabling otherwise inaccessible transformations. The changes a catalyst induces in a chemical reaction can be visualized using a simplified model reaction coordinate diagram, where the Gibbs free energy is plotted against the progress of the reaction (Figure 1.1).
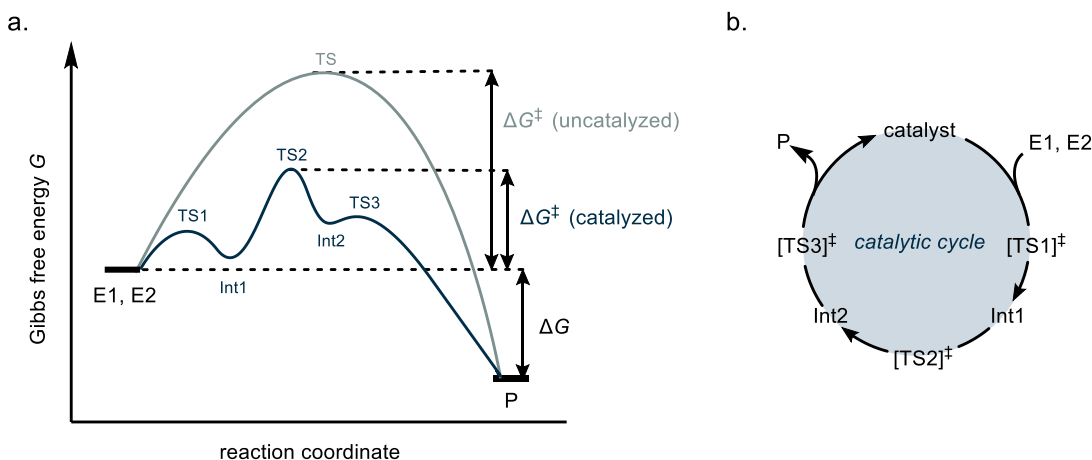
Figure 1.1 Catalysis: a. Energy diagram of a(n) (un)catalyzed reaction. b. Schematic representation of a catalytic cycle.

In the absence of a catalyst, the reactants (E1, E2) must overcome a single high-energy transition state (TS) to form the product (P). Under thermodynamic control, the reaction outcome is governed by the Gibbs free energy difference between the reactants and the products (ΔG), whereas under kinetic control, the determining factor is the activation free energy ($\Delta G^{\ddagger}$). Catalysis is inherently a kinetic phenomenon: while the overall Gibbs free energy difference remains unchanged, the catalyst lowers the activation energy by providing an alternative reaction pathway. This typically involves the formation of a substrate–catalyst complex, followed by a sequence of lower-energy transition states (TS1–TS3) and intermediates (Int1, Int2), which ultimately lead to product formation and catalyst regeneration.

In asymmetric catalysis, the origin of enantioselectivity lies in energetically different diastereomeric transition states that arise from a common substrate–chiral catalyst complex and evolve to opposite isoenergetic enantiomers (Figure 1.2). The difference in Gibbs free energy between competing transition states leading to major (*S*)-P and minor (*R*)-P is defined as $\Delta\Delta G^{\ddagger}$, and it directly correlates with the relative rate constants *k* of the reaction pathways according to equation (*1.1*), and thus with the product distribution. The ratio of the molar fractions $F_{(S)}$ and $F_{(R)}$ is defined as the *enantiomeric ratio* (er), while their difference corresponds to the *enantiomeric excess* (ee).[30]
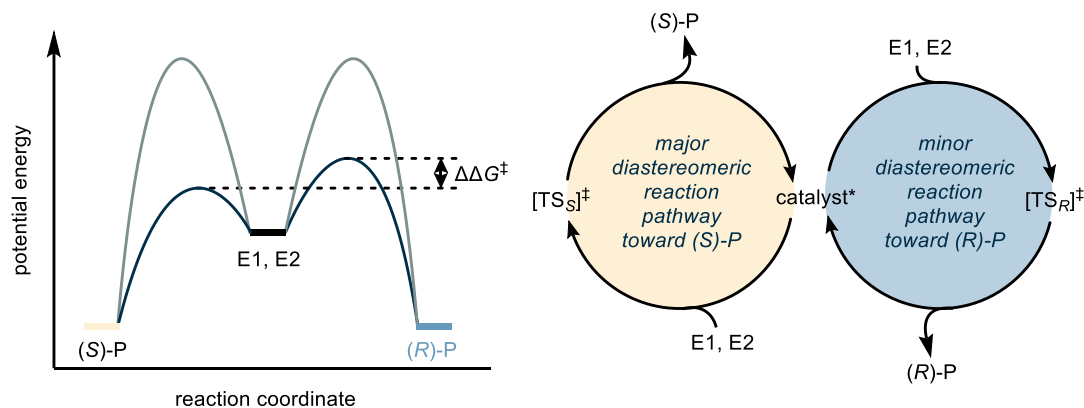
Figure 1.2 Asymmetric catalysis: a. Energy diagram of an asymmetric catalyzed (blue) and an uncatalyzed (gray) reaction. b. Schematic representation of diastereomeric pathways of an enantioselective catalytic reaction.

$$\frac{k_{(S)}}{k_{(R)}} = \frac{F_{(S)}}{F_{(R)}} = e^{-\frac{\Delta\Delta G^{\ddagger}}{RT}} \tag{1.1}$$

$$er = \frac{F_{(S)}}{F_{(R)}} \tag{1.2}$$

$$ee = \left| F_{(S)} - F_{(R)} \right| \tag{1.3}$$

The relative stability of competing transition states can be influenced by a variety of interactions. Destabilizing effects may arise from steric or electronic repulsion, leading to an increase in the activation energy barrier, while stabilizing contributions may include attractive noncovalent interactions that lower the transition state energy (Figure 1.3). In well-defined, covalently bound substrate–organocatalyst complexes, conformational freedom is restricted, making steric repulsion a particularly effective guiding element for stereocontrol. This behavior is consistent with the Lennard-Jones potential, which models steric interactions as highly distance-dependent.[31] In contrast, noncovalently bound substrate–organocatalyst complexes retain greater conformational flexibility and can undergo minor reorganizations to alleviate destabilizing effects. While noncovalent interactions are individually weaker, they are also less sensitive to distance and can act cooperatively. A transition state that benefits from multiple attractive interactions may achieve significant stabilization, and even small cumulative energy differences can result in high enantioselectivities.[32]

The balance between repulsion and flexible noncovalent stabilization is reminiscent of enzymatic catalysis. A network of weak, precisely oriented noncovalent interactions guides the geometry of transition states and enables high levels of enantiocontrol through cooperative binding modes.
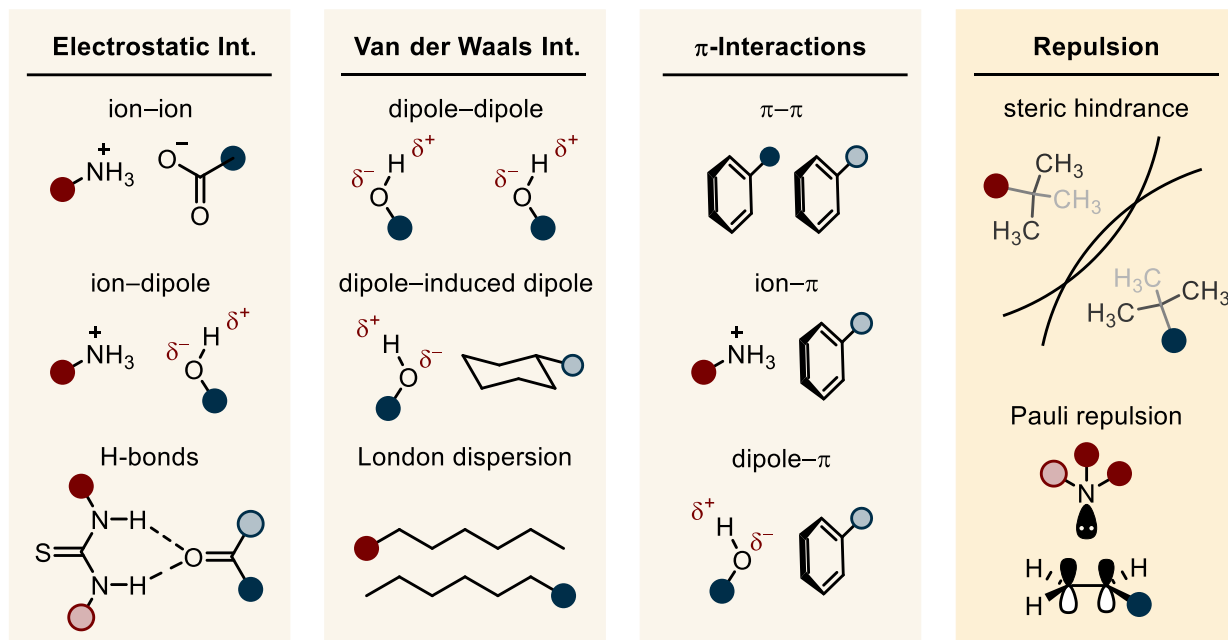
Figure 1.3 Representative noncovalent interactions that can stabilize transition states in organocatalyzed reactions vs. repulsion.

1.2 Historic Milestones in Asymmetric Organocatalysis

Asymmetric organocatalysis—the use of small chiral organic molecules as catalysts for enantioselective transformations—emerged as a fundamental strategy to access chiral molecules, alongside metal and enzymatic catalysis. In 2021, two decades after their seminal contributions, Benjamin List and David W. C. MacMillan were awarded the Nobel Prize in Chemistry for their development of the field.[33] Although earlier examples of (asymmetric) organocatalyzed reactions had been reported in the literature prior to their publications in 2000 (Figure 1.4), it was these two chemists who established organocatalysis as a distinct concept, recognized its broad potential, and introduced the term itself.[34]

In 1860, Justus von Liebig reported the dicyan hydrolysis to oxamide in the presence of acetaldehyde—the earliest documented example of achiral organocatalysis known to date.[35] The role of acetaldehyde, which remained unclear at the time, was recognized nearly 70 years later by Wolfgang Langenbeck. He referred to "organische Katalysatoren" (engl. *organic catalysts*) and compared their effect to that of enzymes.[36] The first example of iminium ion activation dates back to 1896, when Emil Knoevenagel employed secondary amines to catalyze the condensation of benzaldehyde with acetoacetate.[37] Although not fully recognized at the time, this transformation reflects a mechanistic principle central to modern iminium catalysis.
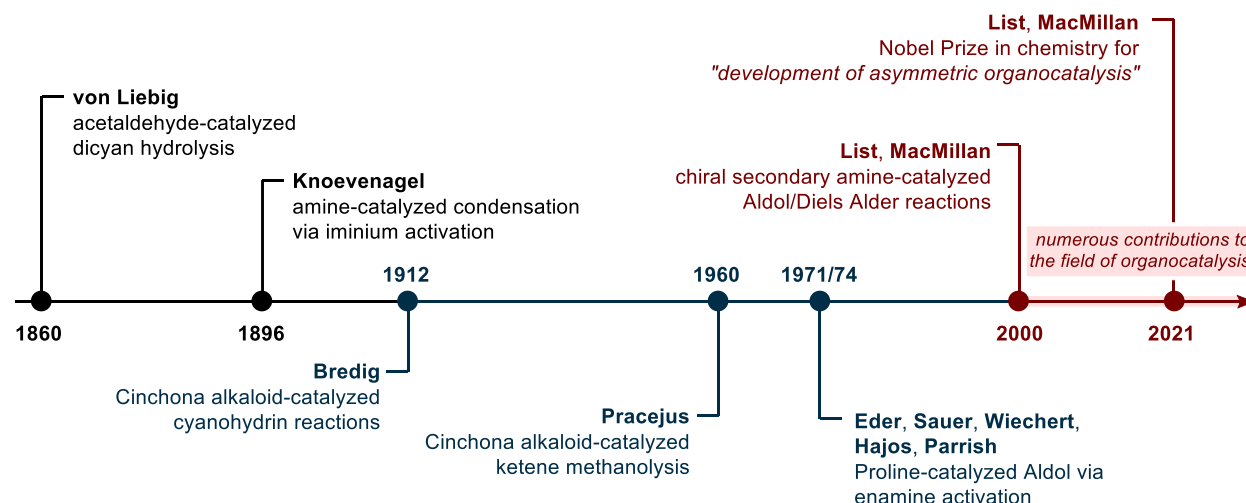
Figure 1.4 Selected historic milestones in organocatalysis: Achiral precedents (black), early asymmetric examples (blue), renaissance of asymmetric organocatalysis (red).

The first asymmetric organocatalytic reaction is attributed to Georg Bredig and Paul S. Fiske, who in 1912 explored the use of Cinchona alkaloids as catalysts for the addition of hydrogen cyanide to benzaldehyde.[38] Although enantiomeric excesses were not directly reported, later estimates based on optical rotation suggest low levels of enantioinduction (<10% ee). Nearly four decades later, Horst Pracejus reported one of the first highly enantioselective organocatalytic reactions, also using a Cinchona alkaloid to catalyze the addition of methanol to phenyl(methyl)ketene (87:13 er).[39] These pioneering studies exemplify how the inherent structural complexity of natural products like alkaloids can serve as a platform for asymmetric catalysis. Cinchona alkaloid derivatives, in particular, have since emerged as privileged chiral scaffolds across multiple catalytic modes, serving as Brønsted bases, nucleophilic catalysts, and chiral phase-transfer agents in a wide range of asymmetric transformations.[40,41] In the early 1970s, the proline-catalyzed intramolecular aldol cyclization was independently reported by Eder, Sauer, and Wiechert at Schering, and by Hajos and Parrish at Hoffmann–La Roche.[42,43] These studies mark foundational milestones in asymmetric organocatalysis, representing the first synthetically useful enantioselective syntheses of bicyclic ketones—key intermediates in steroid hormone production. Notably, Hajos and Parrish observed that (L)-proline functioned analogously to an enzyme, yet this biomimetic strategy was not pursued further at the time.

It was not until 2000 that List, Lerner, and Barbas rediscovered proline (**3**) as a highly effective catalyst for the asymmetric intermolecular aldol reaction of acetone (**1**) and isobutyraldehyde (**2**) via enamine activation[23] (Figure 1.5). In parallel, MacMillan introduced a complementary mode of organocatalysis (iminium ion activation), reporting the highly selective Diels–Alder reaction of α,β–unsaturated aldehydes and dienes catalyzed by a phenylalanine-derived imidazolidinone catalyst **7**.[24] Following the foundational

breakthroughs in 2000, numerous asymmetric organocatalytic reactions were developed over the next two decades by the chemical community. These advancements ultimately culminated in the Nobel Prize in 2021.
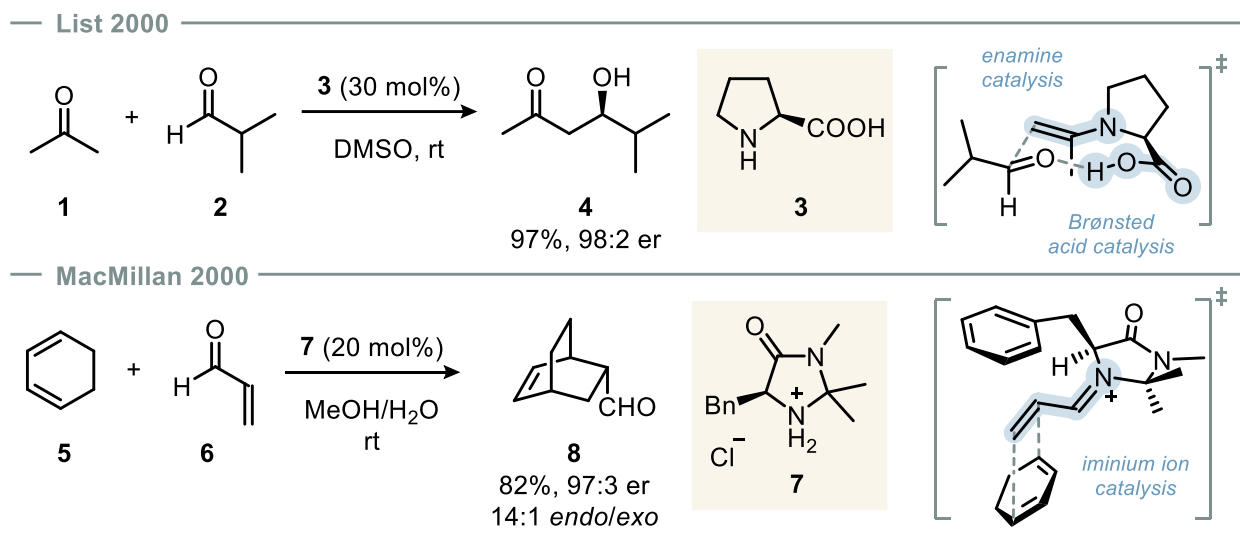
Figure 1.5 Seminal reports by List and MacMillan.

The two complementary activation modes described above fall under the category of covalent organocatalysis. Upon enamine formation between ketone **1** and (L)-proline, the highest occupied molecular orbital (HOMO) of the resulting intermediate is elevated relative to the HOMO of ketone **1**, facilitating nucleophilic attack. Simultaneously, the electrophilic reaction partner **2** is activated via Brønsted acid catalysis by the carboxyl group of proline, representing one of the earliest examples of bifunctional catalysis.[44] In contrast, iminium ion formation with catalyst **7** lowers the lowest unoccupied molecular orbital (LUMO) of enal **6**, enhancing its electrophilicity.[45] Beyond these two classic mechanisms, numerous other organocatalytic strategies have been developed. To systematically describe this growing field, various classification schemes have been introduced, focusing on catalyst functionality, activation mode, and reaction type. Notable frameworks include distinctions such as covalent versus noncovalent catalysis, and Brønsted acid/base versus Lewis acid/base mechanisms.[34,46]

1.3 Evolution of Chiral Brønsted Acids

1.3.1 Early Developments: From Hydrogen Bond Donors to Chiral Phosphoric Acids

Chiral Brønsted acid catalysis represents one of the most versatile strategies for enabling stereoselective transformations across a wide range of substrates. This approach typically involves activating electron-rich functional groups through hydrogen bonding or proton transfer. The mode of acid activation is influenced by the pK_a difference between catalyst and substrate: when hydrogen bonding occurs within the rate-

determining transition state, the mechanism aligns with general acid catalysis; full substrate protonation prior to the key transformation is characteristic of specific acid catalysis.[47,48] In the early development of asymmetric organocatalysis, diverse chiral hydrogen bond donors were introduced,[49] including thioureas[50], squaramides[51,52], and diols such as TADDOL **11**[53] and 1,1'-bi-2-naphthol (BINOL)-derived scaffolds[54] (Figure 1.6).
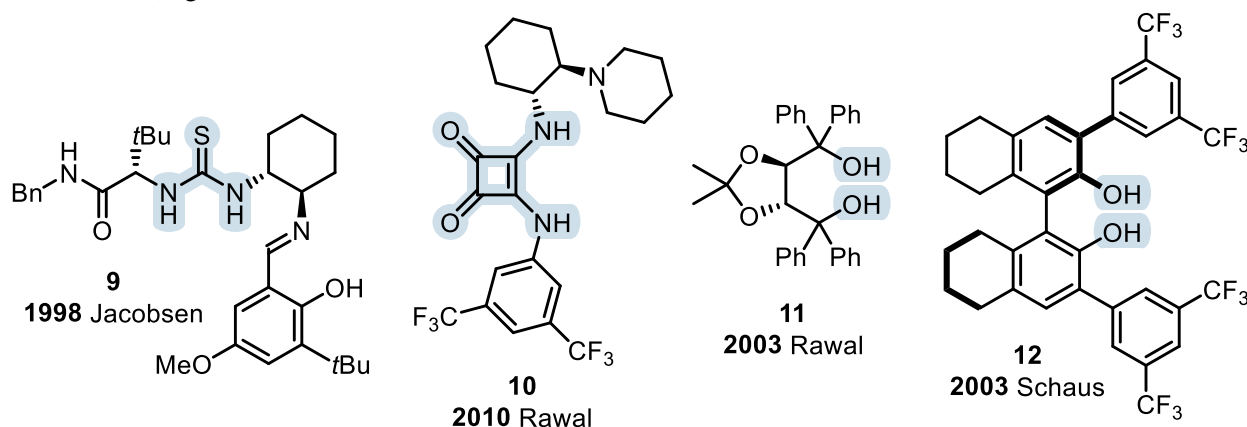
Figure 1.6 Early examples of weakly acidic chiral hydrogen bond donor catalysts.

Since the independent development of BINOL-derived chiral phosphoric acids (CPAs) by Akiyama[55] and Terada[56] in 2004, powerful chiral Brønsted acid catalysts featuring rigid and well-defined stereochemical environments have become central to asymmetric organocatalysis. As later revealed by further studies, however, the initial reports were in fact catalyzed by residual metal phosphate salts (predominantly Ca^{2+}). Acidification of the metal phosphate precatalysts was shown to be necessary to generate the free Brønsted acid form of the catalyst.[57–60] In addition to donating a proton, the phosphoryl oxygen can coordinate to substrates, imparting bifunctionality. Moreover, the 3,3'-substituents on the BINOL scaffold provide high modularity, allowing for customized catalyst design across a broad range of enantioselective transformations (Figure 1.7). TRIP (**15**), a privileged BINOL-derived chiral phosphoric acid bearing 2,4,6-triisopropylphenyl groups at the 3,3'-positions, has been successfully applied to a wide range of asymmetric transformations, including Mannich reactions, Friedel–Crafts alkylations, and transfer hydrogenations.[61] Introduced by List in 2005,[62] it is widely regarded as a benchmark CPA for the development and comparison of new chiral Brønsted acid catalysts.
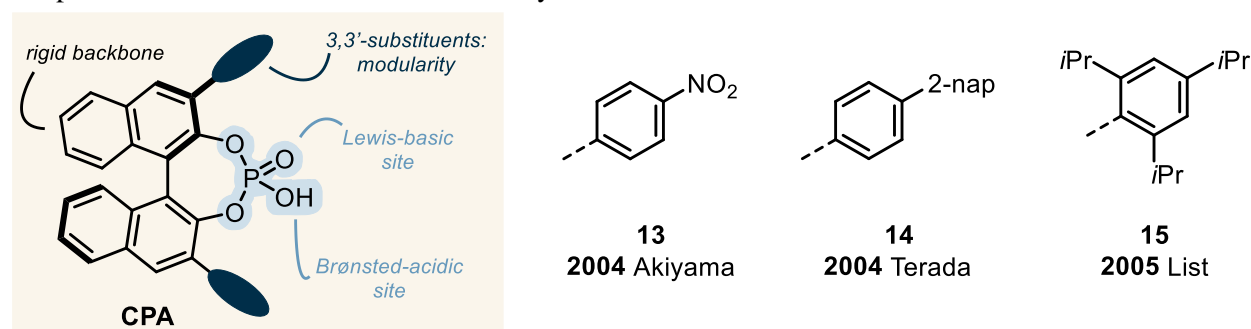
Figure 1.7 Early examples of moderately acidic BINOL-derived chiral phosphoric acids.

1.3.2 Toward Superacidity and Confinement
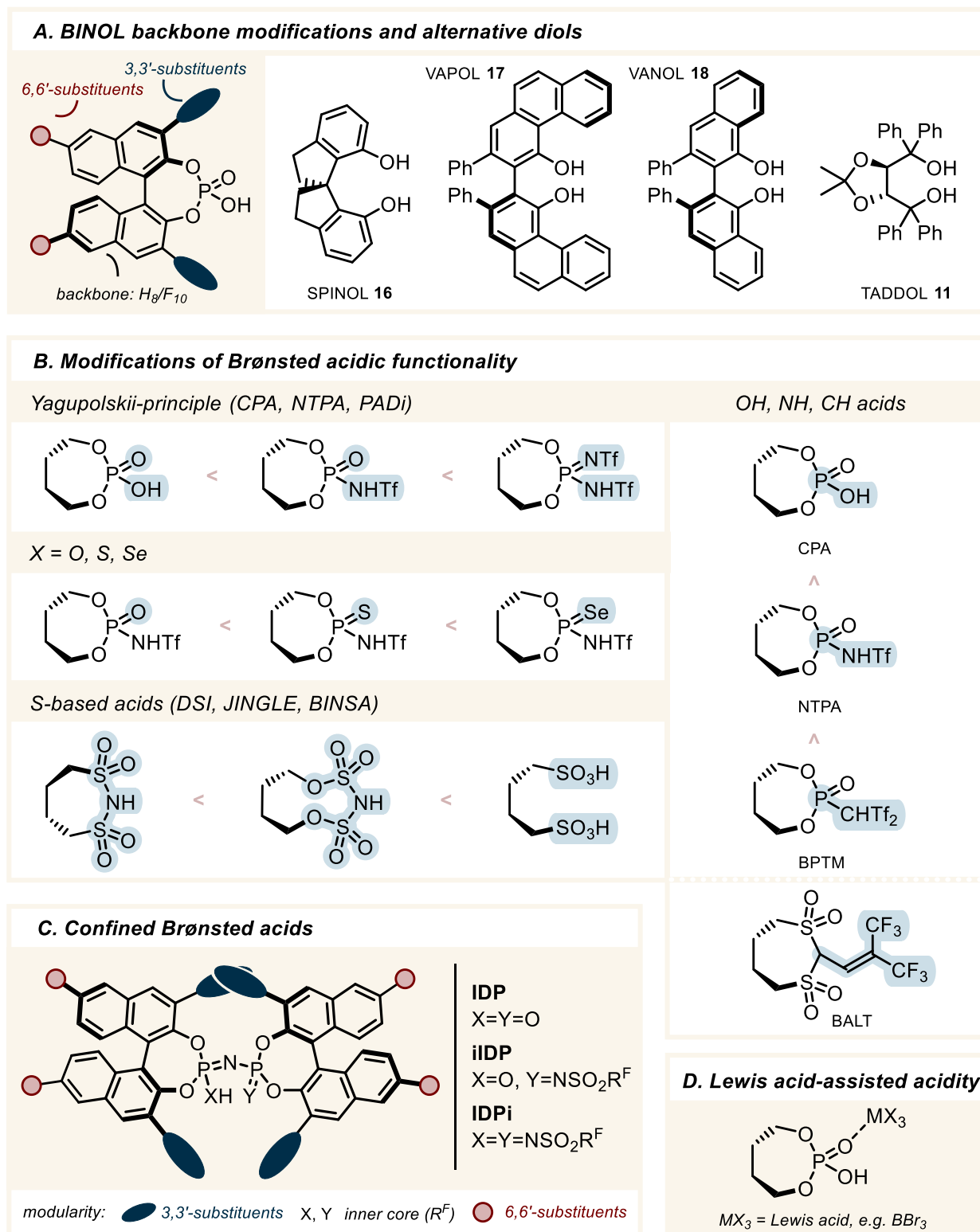
Figure 1.8 Representative strategies to modulate acidity and stereocontrol in chiral Brønsted acids.

The further development of Brønsted acid catalysts was guided by two interrelated principles: enhancing acidity and improving stereocontrol. Various structural strategies have been pursued to modulate the catalyst function (Figure 1.8).

The BINOL scaffold offers multiple handles for modification (Figure 1.8A): substitution of the 3,3'-aryl groups with electron-donating (EDG), electron-withdrawing (EWG) or neutral substituents can significantly influence both acidity and stereoselectivity.[63] Additional modifications to the BINOL backbone have also been reported, including partial saturation,[64] fluorination,[65–67] and substitution at the 6,6'-positions.[68] Although BINOL derived phosphoric acids remain the most widely used, catalysts featuring alternative diol backbones (such as SPINOL **16**) have in some cases outperformed BINOL analogs in terms of enantiocontrol.[69–71] Other examples include structurally more distinct diols, such as vaulted biaryls **17**[72–74] and **18**[75,76], and, less commonly, TADDOL **11**[77].

Beyond tuning the 3,3′-substituents and the diol scaffold, a complementary approach has focused on modifying the acidic functional group itself (Figure 1.8B). A prominent example is the formal substitution of one oxygen atom in BINOL-derived CPAs with a strongly electron-withdrawing *N*-triflyl group, yielding *N*-triflyl phosphoramides (NTPAs), as first reported by Yamamoto in 2006.[78] Replacement of both oxygen atoms was later achieved by List in 2016, resulting in highly acidic phosphoramidimidates (PADis).[79] These acid-strengthening modifications follow the Yagupolskii principle which provides a theoretical basis for the substantial acidification enhancement achieved through replacement of oxygen atoms with *N*-triflyl groups.[80,81]

Another strategy explored by Yamamoto involved exchanging the oxygen atom with sulfur or selenium.[82] In the context of enantioselective protonation of enol ethers, the observed reactivity trend correlates with the pK_a values in DMSO of achiral analogs: PhOH (pK_a = 18.0), PhSH (pK_a = 10.3), and PhSeH (pK_a = 7.1)[83].

A similar trend is observed among triflate-type acids in MeCN: TfOH (pK_a = 0.7), Tf$_2$NH (pK_a = 0.3), and Tf$_3$CH (pK_a = –3.7)[84]. Peng *et al.* synthesized BINOL-derived variants of the OH (CPA), NH (NTPA) and CH acid (BINOL-derived phosphoryl bis((trifluoromethyl)sulfonyl) methane, BPTM) and compared their performance. Supported by computational studies, the CH acidic 3,3'-diphenyl-substituted BPTM was shown to be the most acidic of the three catalyst classes (pK_a(MeCN) = 1.3).[85] Another chiral CH acid motif was introduced by List, who developed binaphthyl-allyl-tetrasulfones (BALT) as highly active chiral acids.[86]

In addition to these modifications, the phosphate group itself has been exchanged by other acidic, predominantly sulfur-based moieties. Disulfonimides (DSIs), reported by List[87] and later by Giernoth[88],
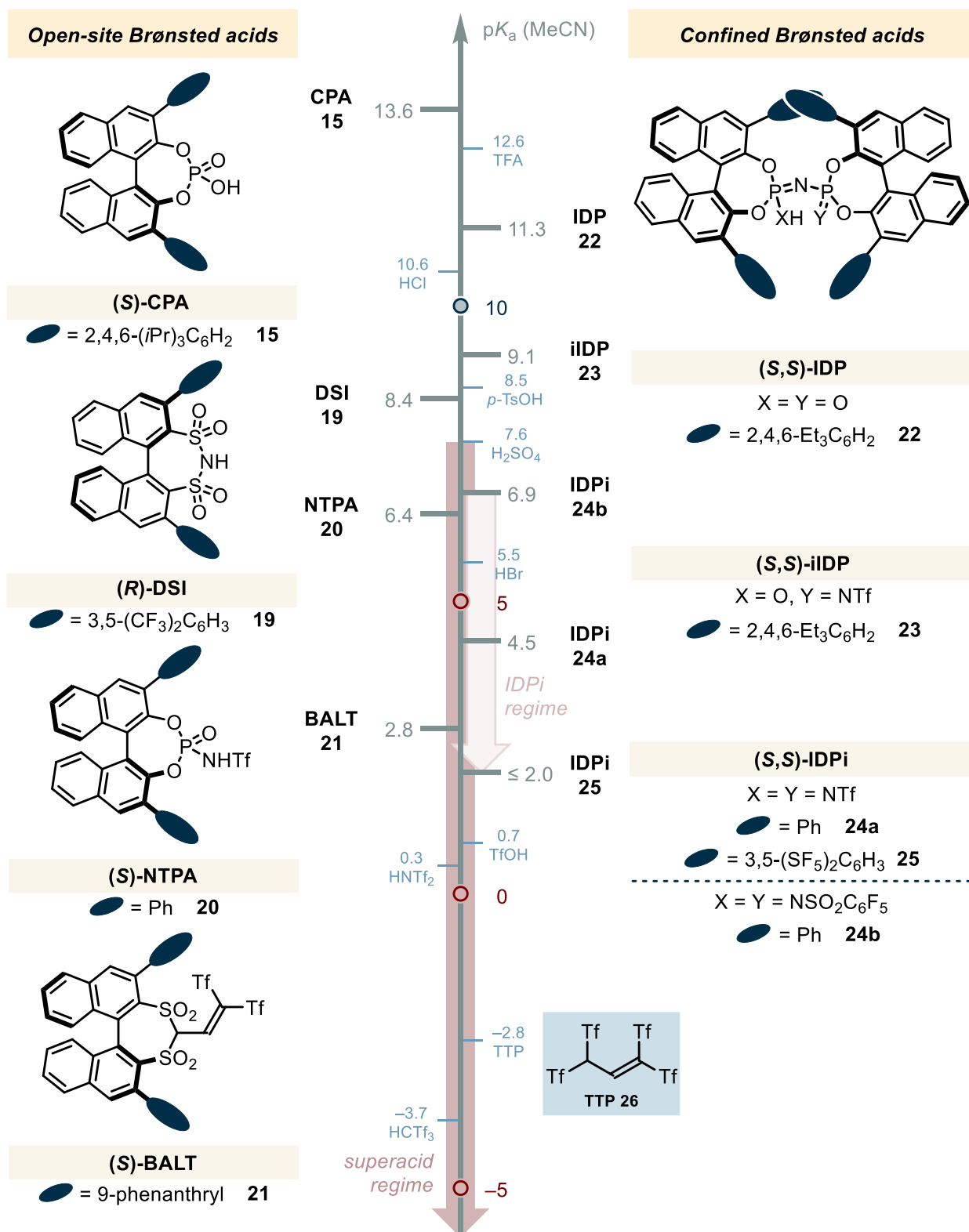
Figure 1.9 Brønsted acidity scale (pK$_a$ values in MeCN)[89–94] for selected achiral acids (blue) and BINOL-based catalysts (black/gray).

exhibit higher Brønsted acidity than corresponding CPAs. Even more acidic, but generally less effective

in inducing stereocontrol, are binaphthyl-2,2'-bis(sulfuryl)imides (JINGLEs)[95] and binaphthyl-2,2'-disulfonic acids (BINSAs)[96–98].

More than a decade ago, List introduced C_2-symmetric *confined* Brønsted acids based on two binaphthol units (Figure 1.8C). Inspired by enzymes, imidodiphosphates (IDPs)—featuring a well-defined chiral environment formed by the two BINOL backbones and four sterically demanding 3,3'-substituents—were developed to enable enantiocontrol over small, structurally unbiased molecules.[99] In contrast to classical CPAs (pK_a(MeCN) ≈ 13)[89], which possess relatively open active sites, these confined catalysts restrict substrate conformational freedom, thereby enhancing enantioselectivity. However, the acidity of IDPs remains moderate (pK_a(MeCN) ≈ 11)[92] limiting their applicability. To address this, the Yagupolskii principle was applied: replacing the catalyst oxygens by one or two *N*-triflyl groups yielded more acidic iminoimidodiphosphates[100] (iIDPs, pK_a(MeCN) ≈ 9)[92] and highly acidic imidodiphosphorimidates[101] (IDPis, pK_a(MeCN) ≈ 7 to < 2)[93,94], respectively. Beyond the backbone and 3,3'-substituents, the incorporation of *N*-perfluoroalkyl or -aryl sulfonyl group(s) into the catalyst core provide(s) an additional handle for fine-tuning steric and electronic properties. These confined Brønsted acids have emerged as highly privileged systems for achieving unprecedented levels of reactivity and selectivity.[102–106] Among these, IDPis—combining spatial confinement with superacidity[2]—are considered some of the most powerful chiral Brønsted acid catalysts developed to date (Figure 1.9).[92,107,108]

A complementary but less widely adopted strategy involves Lewis acid-assisted Brønsted acidity, wherein an achiral Lewis acid transiently enhances the acidity of a chiral Brønsted acid (Figure 1.8D).[109] While this approach can be effective,[110–113] it carries an inherent risk of non-selective background reactivity and has seen more limited application.

Together, these advances have expanded the scope of Brønsted acid catalysis from early hydrogen-bond donors to highly acidic, spatially engineered systems, laying the foundation for reactivity modes that exploit chiral anions as key elements in enantioinduction.

1.4   Asymmetric Counteranion-Directed Catalysis

In 2006, List reported a catalytic transfer hydrogenation reaction of α,β-unsaturated aldehydes using a Hantzsch ester (**28**) as a biomimetic hydrogen source (Figure 1.10).[114] Central to this transformation was

---

[2] A superacid is defined as any acid stronger than pure sulfuric acid.[84,317] This concept was later expanded by Olah, using the Hammett acidity function (H_0), with superacidity typically defined as $H_0 < -12$.[318]

the use of an iminium phosphate salt, formed from a chiral phosphoric acid **15** and an achiral secondary amine **30**, and the underlying catalytic principle. Upon condensation of enal **27** with amine **a**, a cationic iminium intermediate is generated, that forms a tight ion pair with the chiral phosphate anion (Figure 1.11a). During the enantiodetermining hydride transfer from **28**, the stereochemical information is transferred from the chiral counteranion to the substrate, furnishing products with high enantioselectivity.
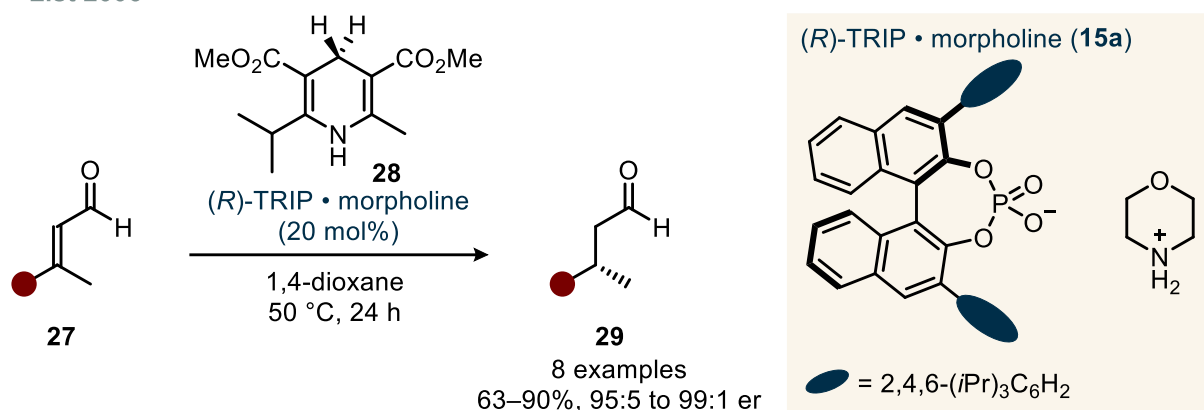
Figure 1.10 Pioneering example of ACDC: Transfer hydrogenation of α,β-unsaturated aldehydes.

This catalytic mode diverged from earlier asymmetric organocatalytic strategies, where enantioinduction typically arose from chiral covalent intermediates formed between catalyst and substrate. In contrast, this reaction featured a near-complete decoupling of reactivity and selectivity: the achiral amine generated the reactive intermediate, while the chiral phosphate anion controlled stereoselectivity via ion pairing. This concept was termed asymmetric counteranion-directed catalysis (ACDC) and later defined as follows:

"*Asymmetric counteranion-directed catalysis refers to the induction of enantioselectivity in a reaction proceeding through a cationic intermediate by means of ion pairing with a chiral, enantiomerically pure anion provided by the catalyst.*"[115]

Although the definition of ACDC centers on ion pairing, the precise nature of the stereodetermining interactions remains complex, and contributions from other noncovalent interactions, such as hydrogen bonding or London dispersion, are typically required.

Shortly after the pioneering report by List, the concept was extended to transition metal catalysis, demonstrating the broad applicability of ACDC. Toste and co-workers reported an intramolecular hydroalkoxylation of allenols using achiral cationic Au(I) complexes in combination with a chiral TRIP counteranion.[116] In contrast to traditional asymmetric transition-metal catalysis, enantioinduction in this system arises not from a chiral ligand bound to the metal, but from the chiral phosphate anion (Figure

1.11b). The concept proved particularly appealing compared to traditional approaches, as the linear coordination geometry of gold typically places chiral ligands in a distal position, limiting their influence on stereocontrol.

Less acidic hydrogen bond donors, such as thioureas, are highly effective at binding small anions and are thus classified as *anion-binding catalysts*.[117] In this role, they can be viewed as supramolecular chiral anions that form ion pairs with cationic intermediates, thereby transferring stereochemical information. An early demonstration of this concept, though not recognized as such at the time, was Jacobsen's acyl-Pictet–Spengler reaction of tryptamine (Figure 1.11c).[118]

With advancements in Brønsted acid catalyst design toward superacidity, a new catalytic strategy emerged. The use of highly acidic disulfonimide (DSI) catalysts in the Mukaiyama aldol reaction of small, unbiased aldehydes introduced *silylium ACDC*—and with it, Lewis acid-type reactivity—into the domain of organocatalysis (Figure 1.11d). Building on this foundation, the development of superacidic BALT and confined IDPi catalysts enabled the rapid expansion of this approach to a range of powerful transformations. The aforementioned conceptual examples illustrate the versatility of ACDC across distinct catalytic platforms, highlighting its broad applicability in asymmetric synthesis.
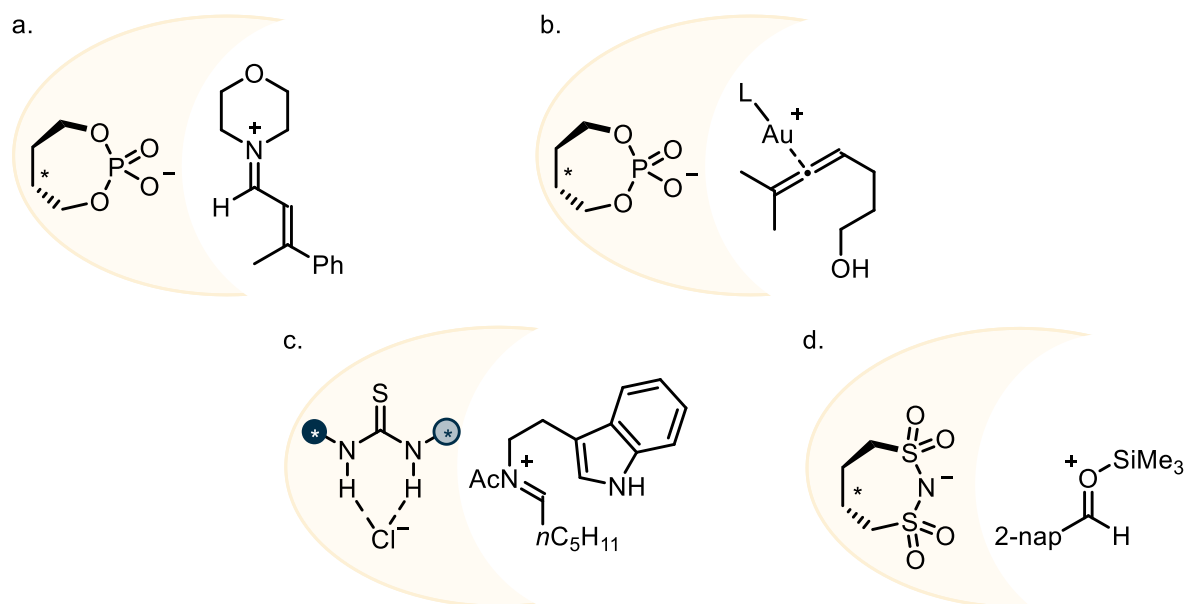
Figure 1.11 Key conceptual advances in ACDC: (a) conceptual introduction using chiral phosphate–iminium ion pairing (List, 2006); (b) extension to metal catalysis via chiral phosphate–gold complex (Toste, 2007); (c) supramolecular chiral anion formation through anion-binding thiourea catalysis (Jacobsen, 2004); (d) Si-ACDC enabled by highly acidic DSI catalysts (List, 2009).

2 DISPERSION–DRIVEN DESIGN OF A TRANSFER HYDRO-GENATION CATALYST

2.1 Background

2.1.1 Asymmetric Organocatalytic Transfer Hydrogenations of C–C π-Bonds

a. Nature
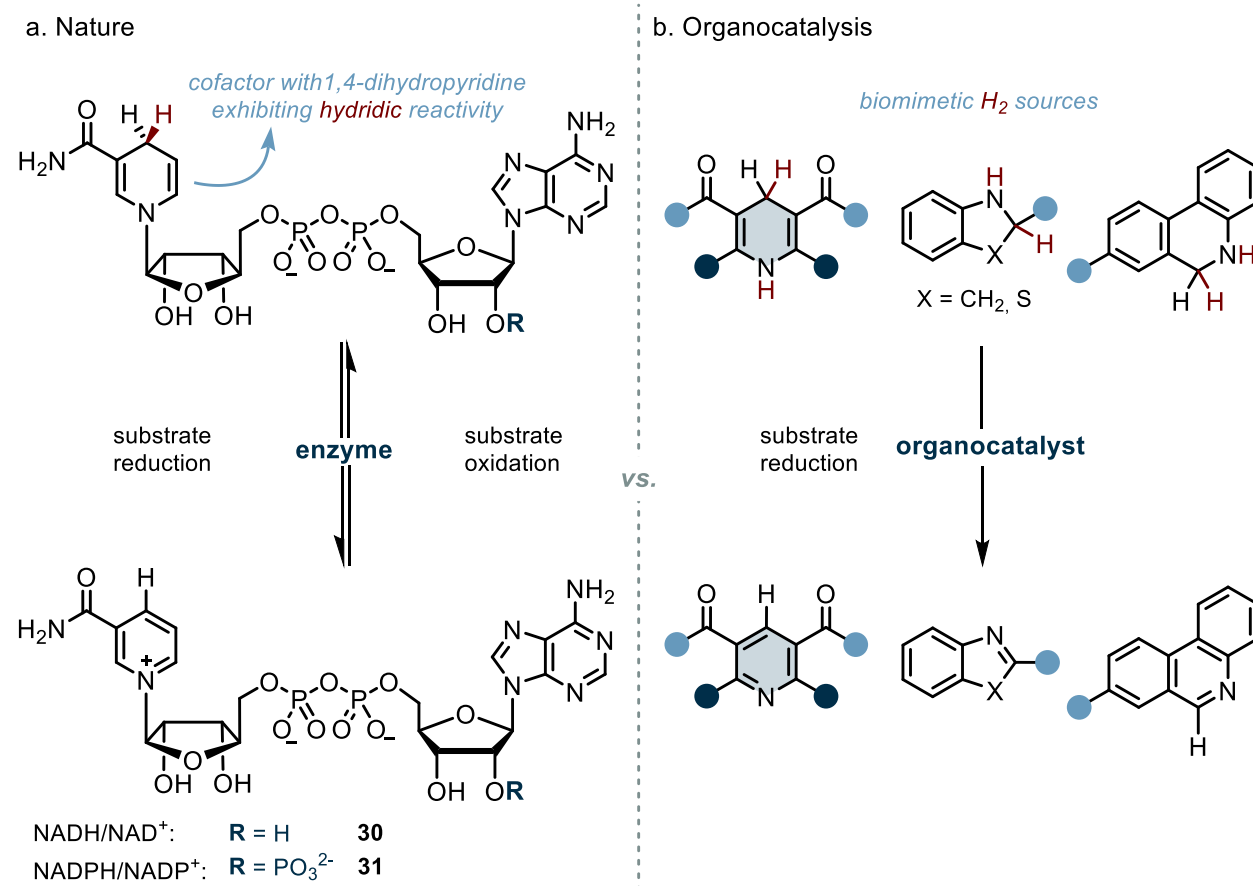
b. Organocatalysis

Figure 2.1 Comparison of transfer hydrogenation strategies: a. Nature's approach using enzymes and cofactors. b. Organocatalytic approach employing small-molecule catalysts and biomimetic dihydrogen surrogates.

The development of asymmetric organocatalytic transfer hydrogenations of unsaturated compounds gained momentum in the early 2000s, coinciding with the emergence of iminium catalysis as a powerful tool for conjugate additions to α,β-unsaturated carbonyl compounds and cycloadditions. Inspired by nature's use of enzymes and organic hydride cofactors such as NAD(P)H (**30**, **31**), chemists adopted biomimetic strategies involving small-molecule catalysts and dihydrogen surrogates that emulate the biological systems. These cofactor mimics, which feature a hydride and a proton, can formally deliver dihydrogen to reduce a variety of unsaturated substrates bearing C=C, C=N or C=O moieties.[25,119] Aromatization of the reducing agents, which occurs upon transfer of both hydride and proton, serves as the thermodynamic driving force of the reaction. Among these surrogates, Hantzsch esters, characterized by a 1,4-dihydropyridine core, have

become the most widely utilized.[27] These often symmetric heterocycles are readily accessible via a one-pot condensation of an aldehyde, two equivalents of a β-ketoester, and ammonia, as first reported by Arthur Rudolf Hantzsch in 1881, after whom they are named.[120,121] Additional, though less commonly employed, surrogates include scaffolds such as indolines[122], benzothiazolines[123,124], and dihydrophenanthridines[125,126] (Figure 2.1).

The first example of an asymmetric organocatalytic transfer hydrogenation was reported by Yang *et al.* in 2004.[127] Using the hydrochloride salt of a chiral MacMillan-type imidazolidinone catalyst **34** and Hantzsch ester **33**, the authors achieved the chemo- and enantioselective 1,4-reduction of an enal via iminium ion activation. The steric environment provided by the substituents of imidazolidinone **34** effectively shields one face of the iminium intermediate, directing the nucleophilic hydride attack from Hantzsch ester **33** to the opposite face and thereby achieving enantiodifferentiation (Figure 2.2).
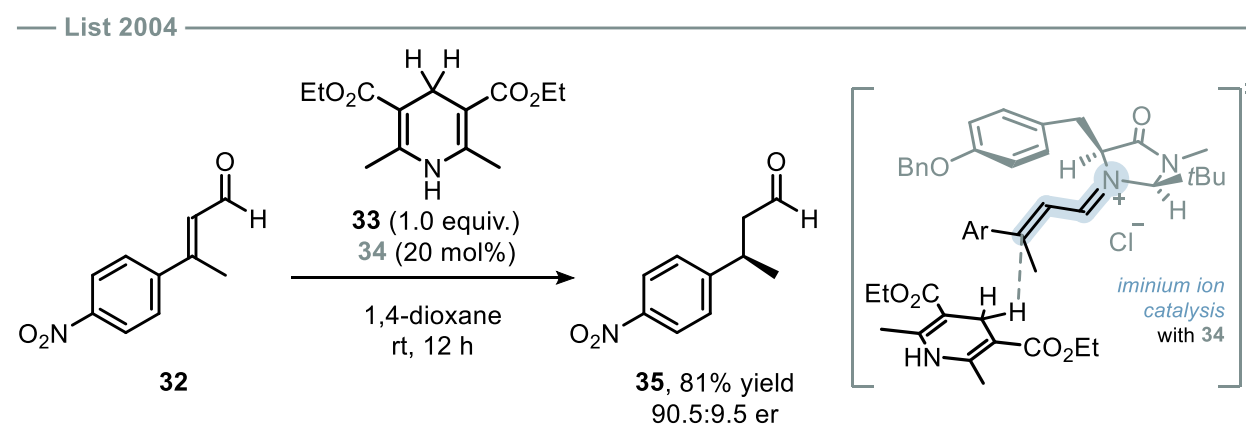
Figure 2.2 The first asymmetric organocatalytic transfer hydrogenation: 1,4-reduction of an α,β-unsaturated aldehyde via iminium activation.

In the following years, a plethora of transfer hydrogenation methods were developed for the reduction of C=C and C=N bonds, heterocycles, and for the application in cascade reactions.[128] In this work, however, we specifically focus on the reduction of C=C double bonds and provide an overview of the various catalytic strategies developed for different substrate classes (Figure 2.3). Electron-poor alkenes, such as enals and enones, are typically activated via iminium ion formation. Depending on the source of chirality, one distinguishes between iminium ion catalysis, which employs chiral amines as catalysts, and ACDC, in which a chiral counteranion forms a stereodefining ion pair with the activated iminium species. Electron-poor nitroolefins are most effectively reduced using chiral thiourea catalysts. Owing to their ability to act as strong hydrogen bond donors to nitro groups, thioureas have proven to be highly effective for this class of Michael acceptors, simultaneously providing a chiral environment for hydride delivery. Electron-rich 1,1-diaryl alkenes, on the other hand, are optimal substrates for chiral phosphoric acid catalysis. Upon

protonation, these substrates form stabilized quinone methide intermediates that can undergo subsequent enantioselective reduction.
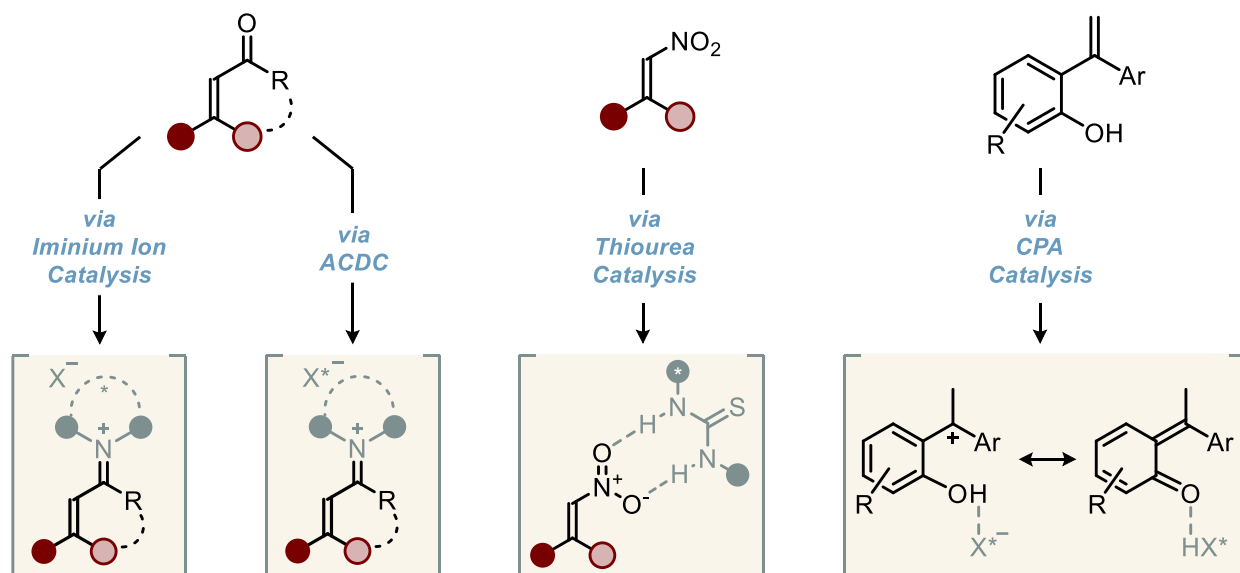
Figure 2.3 Representative substrate classes for different organocatalytic asymmetric transfer hydrogenation strategies.

Iminium-Catalyzed Reduction of Enals and Enones

Shortly after List's pioneering single example, the MacMillan group disclosed a general method for the conjugate reduction of α,β-unsaturated aldehydes using Hantzsch ester **33** and imidazolidinone catalyst **36**.[129] The transfer hydrogenation proved applicable to a broad range of aromatic and aliphatic substrates and was found to be an enantioconvergent process, delivering the same product enantiomer from either the *E*- or *Z*-enal isomer. Around the same time, the List group developed a similar protocol for the enantioconvergent reduction of aromatic enals, employing imidazolidinone **37**, which bears an additional benzyl substituent.[130] Although MacMillan reported that catalyst **37** gave inferior enantioselectivity compared to **36**, the use of an unsymmetrical, more elaborated Hantzsch ester (**28**) enabled the List group to achieve excellent enantioselectivities nonetheless. Compared to enals, enones are sterically and
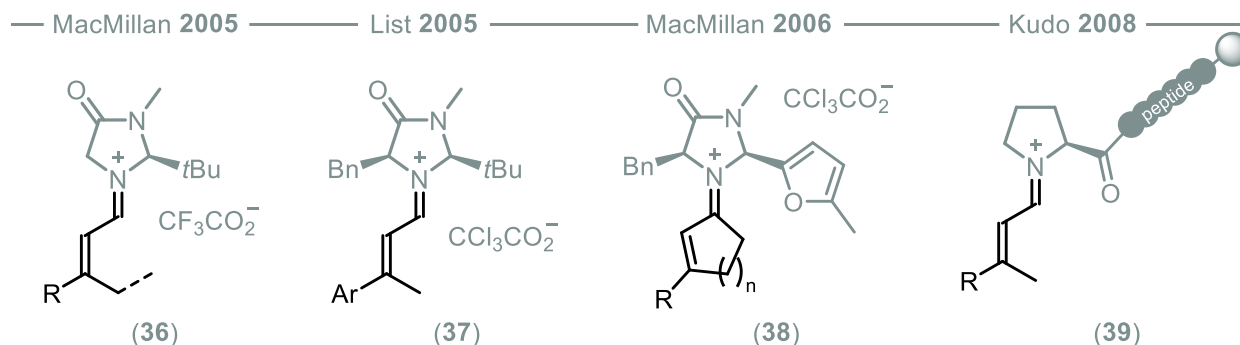
Figure 2.4 Selected chiral amine catalysts for the enantioselective conjugate reduction of α,β-unsaturated carbonyl compounds.

electronically less favorable for iminium ion formation. Consequently, a more reactive catalyst was required to facilitate their transfer hydrogenation. The application of furyl-substituted imidazolidinone **38** ultimately enabled the reduction of cyclic enones with very good yields and excellent enantioselectivities.[131] Further examples of conjugate enal reductions emerged in subsequent years. For instance, the group of Kudo reported a resin-supported peptide catalyst (**39**) effective in aqueous media (Figure 2.4).[132] Tiefenbacher *et al.* demonstrated that proline can induce enantioselectivity, which was further enhanced when the reaction was conducted within a supramolecular capsule.[133] Most recently, in 2024, Appayee synthesized bicyclic secondary amines for the asymmetric transfer hydrogenation of a broad range of α,β-unsaturated aldehydes.[134]

Asymmetric Counteranion-Directed Reduction of Enals

As previously discussed in Section 1.4, the List group demonstrated that ACDC is an effective strategy for the conjugate reduction of enals using the chiral TRIP-derived morpholinium phosphate **15a** and Hantzsch ester **28**.[114] Aromatic enals as well as sterically nonhindered natural products citral and farnesal were efficiently reduced with high enantioselectivity. In contrast, sterically demanding enals bearing a β-*tert*-butyl substituent proved challenging in terms of reactivity. The concept was subsequently extended to the reduction of α,β-unsaturated ketones, which pose a greater activation challenge[135]. Key to overcoming this was the use of a less bulky primary ammonium salt of (*R*)-TRIP. Specifically, the (*S*)-valine ester-derived salt enabled access to both cyclic and acyclic β-chiral ketones with excellent enantioselectivities (Figure 2.5). Notably, the authors observed a pronounced matched/mismatched effect depending on the stereochemical combination of the cation and chiral phosphate counteranion. A different ACDC approach was reported from the field of material science in 2024: (*S*)-TRIP was coupled with an achiral nitrogen-doped carbon dot functionalized with butylenediamine residues, enabling the conjugate reduction of
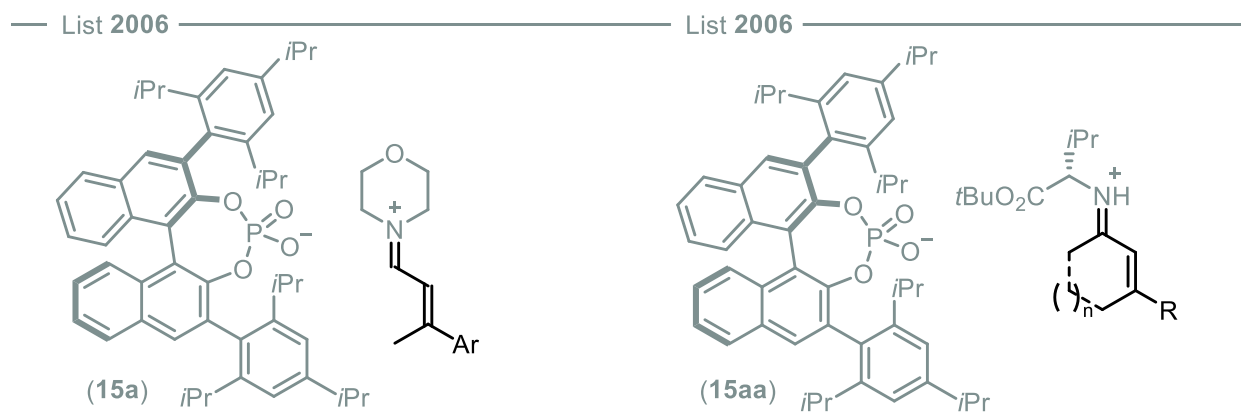
Figure 2.5 Selected chiral ACDC catalysts for the enantioselective conjugate reduction of α,β-unsaturated carbonyl compounds.

aromatic enals.[136] These nanoparticle-sized carbon dots, which play a prominent role in nanotechnology, are gaining attention as emerging platforms for organocatalysis.

Thiourea-Catalyzed Reduction of Nitroolefins

In 2007, the List group identified thiourea **40** as an effective catalyst for the asymmetric transfer hydrogenation of nitroolefins.[137] Shortly thereafter, they demonstrated that the methodology could be extended to more reactive β-nitroacrylates using the same catalyst under reduced reaction temperatures.[138] Notably, the resulting β²-amino acids could be accessed via a simple palladium-catalyzed hydrogenation without erosion of enantiopurity. In an alternative approach, an amino alcohol-derived thiourea was employed for the reduction of nitroolefins.[139] This bifunctional catalyst was proposed to coordinate both the nitroolefin and the Hantzsch ester via hydrogen bonding within a ternary complex. However, only moderate to good enantioselectivities were achieved with this system. In 2015, thiourea-catalyzed reductions were further expanded to include β-CF₃ nitroolefins[140,141] and β-amido nitroolefins[142], enabling downstream transformations into synthetically useful building blocks (Figure 2.6).
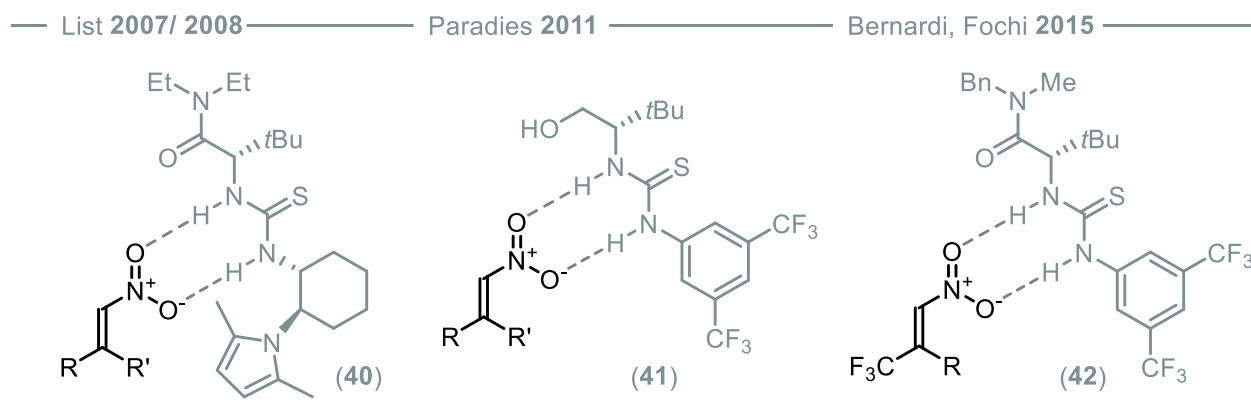
Figure 2.6 Selected chiral thiourea catalysts for the enantioselective conjugate reduction of nitro olefins.

CPA-Catalyzed Reduction of Electron-Rich Styrenes

Zhu, Lin, Sun *et al.* reported a Brønsted acid-catalyzed transfer hydrogenation of 1,1-diaryl alkenes bearing either an *ortho*-hydroxyphenyl or a 3-indolyl substituent.[143] Enantioselective reduction of these electron-rich substrates was achieved using chiral phosphoric acid **43**, proceeding via highly electrophilic *ortho*-quinone methide or 3-indolylmethide intermediates, respectively. Both a Hantzsch ester derivative (**33**) and a benzothiazoline were employed as hydride sources, ultimately affording 1,1-diaryl ethanes with generally high to excellent enantioselectivities (Figure 2.7).
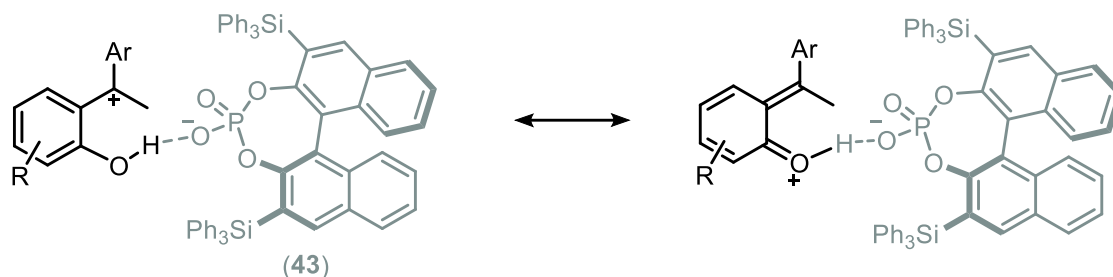
Figure 2.7 Chiral phosphoric acid for the enantioselective conjugate reduction of α-(2-hydroxyaryl) styrenes.

2.1.2 London Dispersion

The remarkable ability of geckos to adhere to various surfaces has intrigued scientists for many years, but is now understood to arise from noncovalent interactions. Among these, van der Waals forces, acting between millions of setae on a gecko's toes and the surface, have been identified as contributors to gecko adhesion.[144,145] Van der Waals interactions occur between uncharged closed shell molecules and are composed of three contributions (Figure 2.8).
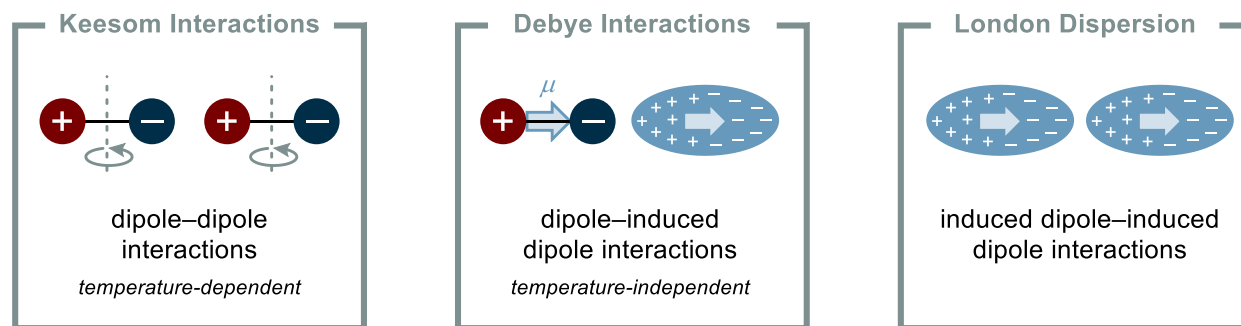
Figure 2.8 Overview of van der Waals interactions.

Keesom interactions describe attractive dipole–dipole interactions between rotating polar molecules and are typically temperature-dependent. Debye interactions, by contrast, are temperature-independent and arise when a permanent dipole induces a dipole in a neighboring polarizable molecule. London dispersion interactions refer to the attractive forces between transiently induced dipoles in nonpolar molecules. They occur due to fluctuations in electron distribution within a molecule, creating an instantaneous dipole moment (μ) and an associated electric field capable of polarizing a nearby molecule. Like Debye interactions, London dispersion forces are essentially insensitive to temperature. Although van der Waals interactions are individually weak compared to ionic or covalent bonds, it is noteworthy that London dispersion dominates among the three types (Figure 2.9a).[146]

Dispersion becomes especially significant for large, polarizable molecules, since the number of pairwise atomic interactions scales superlinearly with molecular size.[147,148] The potential of attractive dispersion interactions can be illustrated by comparing them to electrostatic interactions in simple model systems. Two point charges separated by 5 Å generate the same interaction energy ($\approx$ 60 kcal/mol) as two neutral molecular fragments, each comprising approximately 100 organic atoms, at the same distance (Figure 2.9b).[149] Consequently, dispersion interactions are not to be neglected in molecular chemistry and can influence structures, reactivity, and selectivity.[147,148]

a.

Interaction	Typical energy (kcal/mol)
covalent bond (C–X, σ)	48–120
ion–ion	60
ion–dipole	3.6
Keesom	0.14
Debye	0.19
London dispersion	0.48
H-bonding	4.8

b.

Coulomb interactions between two point charges

5 Å

+ −

$E \approx$ 60 kcal/mol

vs.

London dispersion interactions between two fragments (100 HCNO atoms)

5 Å

$E \approx$ 60 kcal/mol
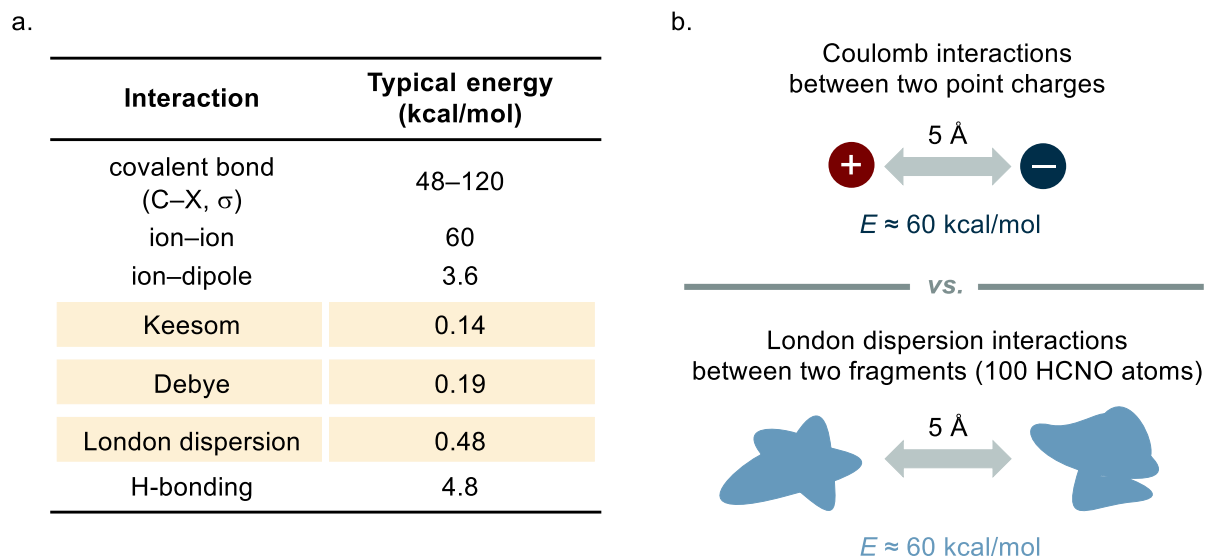
Figure 2.9 a. Interaction potential energies[141] b. Comparison of electrostatic vs. dispersion interactions. Adapted from The Chemical Bond, p. 477[144].

2.1.3 Rethinking Steric Effects Through Dispersion

Even though intermolecular interactions were already defined in 1873 by Johannes Diederik van der Waals[150], and London dispersion was found to contribute to the attractive forces in 1930[151], its importance in practical organic chemistry remained largely underappreciated until the early 2000s. Pauli repulsion, arising from the overlap of electron clouds, was widely accepted as the dominant noncovalent factor guiding reactivity and selectivity. Only with growing experimental evidence and the development of modern density functional theory (DFT) methods, including dispersion corrections,[152,153] did this view begin to shift significantly, enabling the recognition and quantification of attractive dispersion interactions in a broad range of chemical systems. Needless to say, steric repulsion and attractive dispersion are not mutually exclusive; they coexist and can even counterbalance each other. This interplay is well illustrated by the Lennard–Jones potential, a model to approximate the interactions between uncharged closed-shell molecules that are not chemically bonded.[146] The potential energy as a function of the interatomic distance

consists of a repulsive term (Pauli repulsion) and an attractive term (London dispersion), with the energy minimum (ε) occurring *between* the two regimes, not at maximal separation (Figure 2.10).
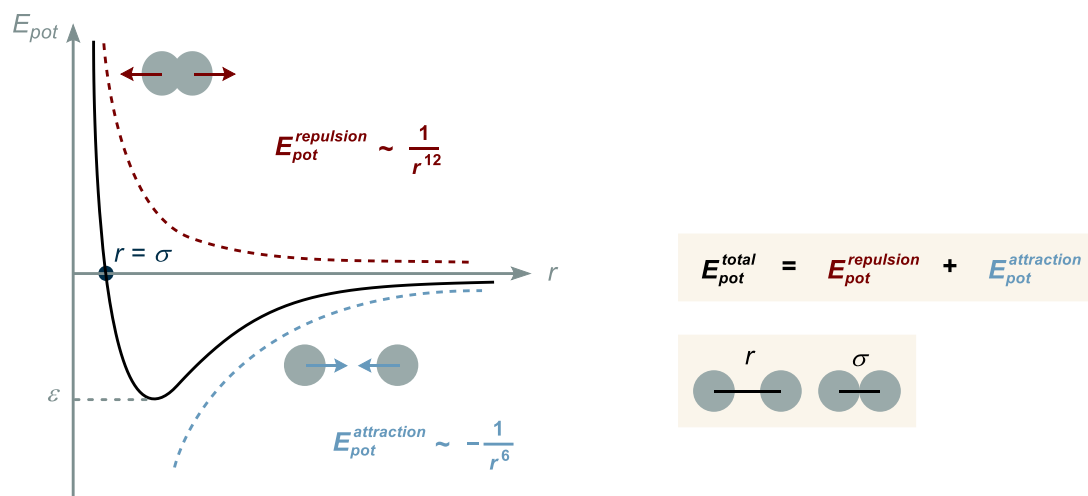
Figure 2.10 Lennard–Jones potential: potential energy (E_{pot}) as a function of the distance (r) between two closed-shell species. The overall curve (black) represents the sum of short-range repulsive interactions (red, dotted) and long-range attractive dispersion forces (blue, dotted).

In this context, several examples illustrate how dispersion has previously been underestimated in systems where sterics were assumed to govern reaction outcomes. One such case is the selectivity model originally proposed for MacMillan's imidazolidinone catalysts[24,154] (see Section 1.2, Figure 1.4), which was later re-evaluated in light of growing awareness of dispersion interactions.[155] Imidazolidinones, primarily used to activate α,β-unsaturated aldehydes or ketones via formation of reactive iminium intermediates, are thought to sterically shield one π-face of the iminium ion, leaving the nucleophile to approach from the opposite side. In the (*S*)-phenylalanine-derived heterocycle **7**, this shielding is attributed to the benzyl group at C(5) (Figure 2.11a, conformer A). However, based on X-ray crystallography and high-level dispersion-corrected computations, an alternative conformer (B)—featuring a stabilizing interaction between the benzyl group and the cis-methyl group at C(2)—was found to be energetically favored by 1–2 kcal/mol, depending on the computational method used. Because of small energy differences and low rotational barriers between these conformers, the steric shielding is better described as dynamic, resembling a *"windshield wiper"*.

Another example is the well-known asymmetric Corey–Bakshi–Shibata (CBS) reduction of ketones, which employs an oxazaborolidine catalyst in combination with BH_3 as the reductant.[156–161] According to Corey's mechanistic rationale, stereoselection is guided solely by steric repulsion, favoring a six-membered boat-like transition state in which the ketone is coordinated to minimize steric interactions between its larger substituent and the boron substituent of the catalyst (Figure 2.11b, top).[162] This stereomodel accounts for most of the observed enantioselectivity outcomes. However, several substrates lead to unexpected results. Trichloroacetophenone, for instance, yields the opposite enantiomer than predicted if the phenyl group is

assumed to be larger than the trichloromethyl group.[163] Similarly, ketones with substituents of similar size, such as 1-cyclopropyl-2-methylpropan-1-one, or 4-methoxy-4'-nitrobenzophenone, afford products with high enantioselectivity, despite the expectation of poor stereodifferentiation.[161] The group of Peter R. Schreiner investigated the origin of enantioselectivity in CBS reductions and found that a comprehensive mechanistic picture requires consideration of all noncovalent interactions.[164] Their detailed computational studies revealed that attractive London dispersion interactions—rather than steric repulsion—determine the enantioselectivity (Figure 2.11b, bottom). On the basis of this revised understanding, they were able to design improved catalysts for the reduction of challenging substrates.
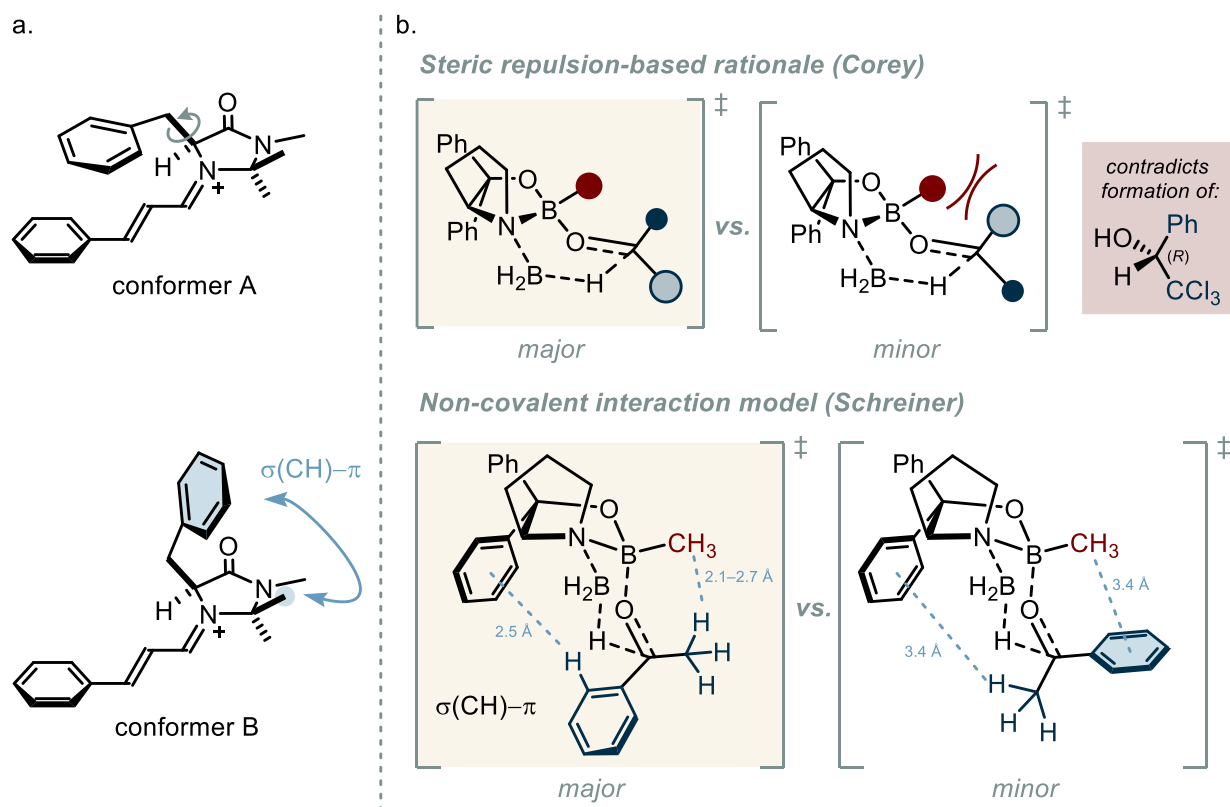
Figure 2.11 Selected examples for reconsidered stereocontrol models: a. The "windshield wiper" effect. b. Transition state models for the CBS reduction: Corey's steric repulsion-based rationale vs. Schreiner's dispersion-stabilized transition states.

2.1.4   Leveraging London Dispersion

Molecular Structures

London dispersion has not only been used retrospectively to explain phenomena that could not be fully accounted for by steric hindrance alone, but has also been increasingly harnessed to stabilize unusual structures and influence chemical reactivity. In this context, polarizable moieties introduced to exploit dispersion have been termed *dispersion energy donors* (DEDs) by Stefan Grimme[165]. Incorporation of such groups into molecular frameworks has pushed the boundaries of structural design by enhancing

thermodynamic stability (Figure 2.12). Hexaphenylethane (HPE, **44**) itself is highly unstable and readily dissociates into trityl radicals, which can rearrange to form the more stable quinoid isomer.[166,167] In contrast, its all-*meta tert*-butyl-substituted derivative **45** forms a stable crystalline solid, stabilized by extensive London dispersion interactions.[168,169] The labile central C–C bond is encapsulated within a dense shell of *tert*-butyl groups—a phenomenon referred to as the "corset effect".[170] Moreover, molecules exhibiting extreme covalent bond lengths have been synthesized, including a diamondoid dimer **46** with a C–C bond of > 1.7 Å[171] and a dispiro[dibenzo-cycloheptatriene]-type HPE derivative **47** with a bond length approaching 1.8 Å.[172] Remarkably, incorporation of *tert*-butyl groups into the latter system (**48**) leads to bond contraction, attributed to attractive intramolecular dispersion contacts.[173] Additionally, the all-*meta tert*-butyl triphenylmethane scaffold (**49**) displays the shortest known intermolecular CH⋯HC contact to date, underscoring the structural consequences of cumulative dispersion forces.[174]
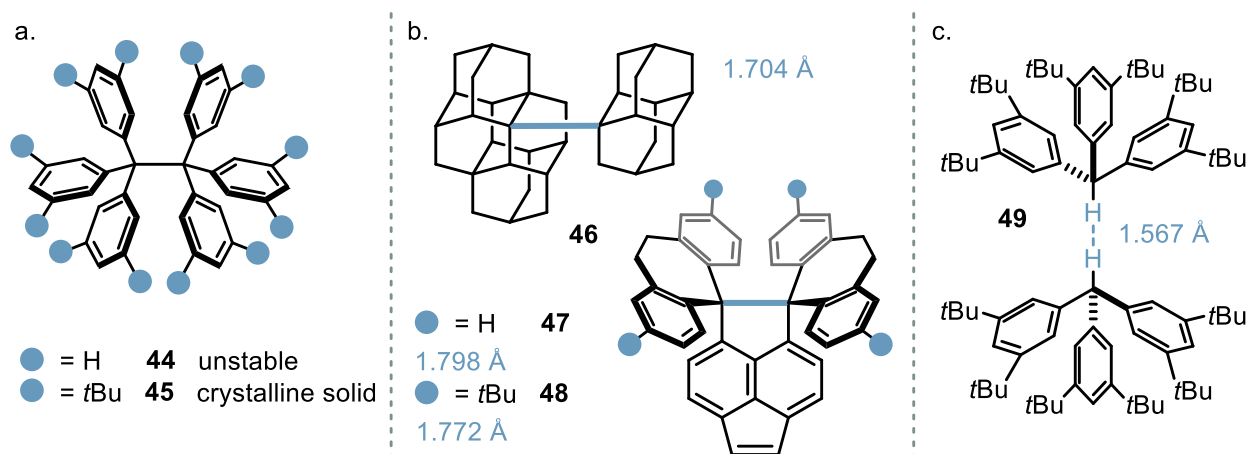
Figure 2.12 Selected examples of unusual structures stabilized by London dispersion: a. Hexaphenylethane (HPE) derivatives. b. Exceptionally long C–C bonds in diamondoid dimers, and dispiro[dibenzocycloheptatriene]-type HPE derivative, with bond contraction observed upon incorporation of DEDs. c. Shortest known intermolecular CH⋯HC contact.

Transition Metal Catalysis

Dispersion interactions have also been shown to modulate transition state geometries and energies. In asymmetric catalysis, where small differences in transition state energies can lead to large effects on selectivity, London dispersion can be particularly influential—especially in polarizable transition states characterized by looser bonding.[147]

In the field of transition metal catalysis, the use of sterically encumbered ligands that bury the active metal center deep within their framework has been correlated with enhanced catalytic activity.[175] However, this increase in reactivity cannot be attributed to Pauli repulsion, which is inherently destabilizing and raises the transition state energy. Instead, the origin of the rate enhancement must lie in stabilizing noncovalent effects. A compelling example of this principle is the enantioselective copper-catalyzed hydroboration of 1,1-disubstituted alkenes utilizing chiral bisphosphine ligands by Liu, Hartwig and co-workers.

Bisphosphines featuring 3,5-bis(trimethyl-germanyl)phenyl groups were found to afford superior catalytic activity and enantioselectivity compared to their silyl or *tert*-butyl analogues. Computational studies attributed this improvement to favorable dispersion interactions between the substituents and the alkene substrate (Figure 2.13a).[176]

A further proof-of-principle was demonstrated by the Fürstner group in a [2+1] cycloaddition catalyzed by a chiral heterobimetallic Bi–Rh paddlewheel complex. In this system, the active conformation of the catalyst was locked in place by attractive dispersion interactions arising from triisopropylsilyl and *tert*-butyl substituents (Figure 2.13b). The new catalyst outperformed other heterobimetallic complexes lacking effective DEDs both in terms of catalytic efficiency and selectivity.[177]
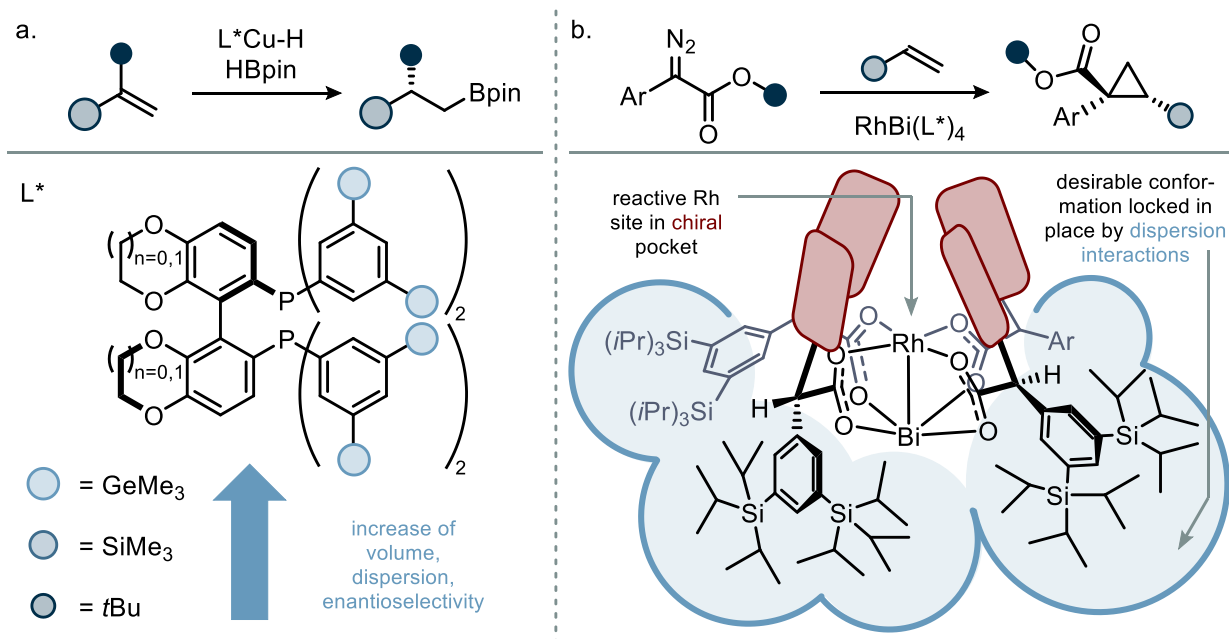
Figure 2.13 Selected examples of asymmetric transition metal catalysis where London dispersion interactions contribute to stereocontrol: a. Cu-catalyzed hydroboration of alkenes, b. Enantioselective [2+1] cycloaddition catalyzed by a heterobimetallic Bi–Rh paddlewheel complex.

Although not exhaustive, the selected examples underscore how dispersion interactions are increasingly leveraged as a strategic design element in metal catalysis. Several other contributions in the field similarly highlight the utility of these interactions.[178–184]

Organocatalysis

Similarly, dispersion interactions have been purposefully leveraged in organocatalytic transformations.[185–193] In the Brønsted acid-catalyzed transfer hydrogenation of imines, the group of Ruth M. Gschwind demonstrated that substrates bearing DEDs, such as 3,5-bis(*tert*-butyl)phenyl groups, shift the *E/Z*-imine equilibrium toward the more sterically congested *Z*-isomer. Using advanced NMR techniques, they showed

that this conformational preference is preserved in both the binary (imine–catalyst) and ternary (imine–catalyst–Hantzsch ester) complexes, and directly correlates with the observed enantioselectivity (Figure 2.14a). Across a set of ten catalysts, a consistent selectivity trend was observed for three imines with varying DED substitution patterns that modulate the population of the Z-isomer.[194]

The Dakin–West reaction enables the synthesis of α-acylamido ketones from primary α-amino acids via reaction with an acid anhydride under basic conditions. Due to the involvement of two achiral intermediates during the reaction pathway, complete racemization is typically observed. Employing peptide catalysis, the Schreiner group reported the first enantioselective variant of the Dakin–West reaction. Stereocontrol in the final reprotonation step was achieved through a dual interaction mechanism: enolate binding between the achiral intermediate and the synthetic tripeptide catalyst, and stabilizing London dispersion interactions between a polarizable cyclohexyl substituent and the α-side chain of the amino acid (Figure 2.14b). Although only moderate enantioselectivity was obtained, this study elegantly demonstrates the catalytic significance of attractive dispersion forces, even in the presence of electrostatic interactions.[195]
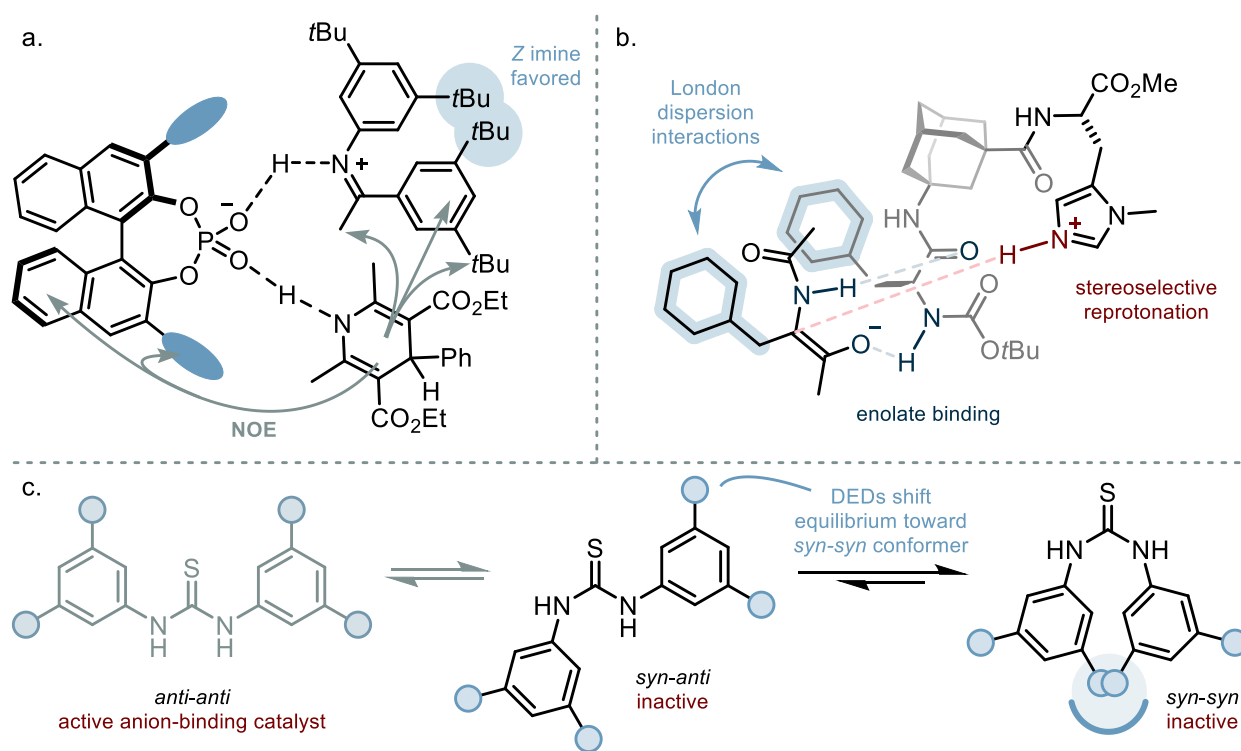
Figure 2.14 Selected examples in organocatalysis where London dispersion interactions influence reactivity or selectivity: a. DED-substituted imines and catalyst enhancing enantioselectivity in Brønsted acid-catalyzed transfer hydrogenation, b. Enantio-selective Dakin–West reaction supported by polarizable cyclohexyl groups facilitating stereoselective reprotonation, c. Dispersion-stabilized inactive conformer in an anion-binding catalyst.

In addition to modulating stereocontrol, London dispersion interactions can also influence catalytic reactivity. A recent study by the Schreiner group revealed that, counterintuitively, such attractive interactions may inhibit rather than promote catalysis. Thioureas are well-established anion-binding

catalysts; effective anion recognition requires adoption of the *anti–anti* conformation out of three possible conformers.[196] Investigation of thioureas bearing DEDs at the 3- and 5-positions of the *N*-aryl substituents showed that the sterically more crowded *syn–anti* and *syn–syn* conformations—both catalytically inactive—were preferentially populated due to stabilizing dispersion forces (Figure 2.14c).[197] These findings are consistent with the observation that such thioureas are typically poor anion binders.[198]

2.2 Objectives

As evident from the examples in Section *Leveraging London Dispersion* (pp. 24–25), dispersion energy donors can serve as powerful elements in catalyst design influencing both reactivity and selectivity.[199] In this context, we have revisited the seminal 2006 report on asymmetric counteranion-directed catalysis: the enantioselective transfer hydrogenation of β,β-disubstituted enals.[114] Utilizing a chiral TRIP-derived morpholinium phosphate, the reaction afforded chiral aldehydes with high enantiopurity (see Figure 1.10, p. 13). However, this method presents several limitations: (I) a narrow substrate scope limited to aromatic and sterically nonhindered aliphatic enals, (II) high catalyst loadings, and (III) the reliance on a sophisticated, commercially unavailable Hantzsch ester **28**. Replacement with the more readily available
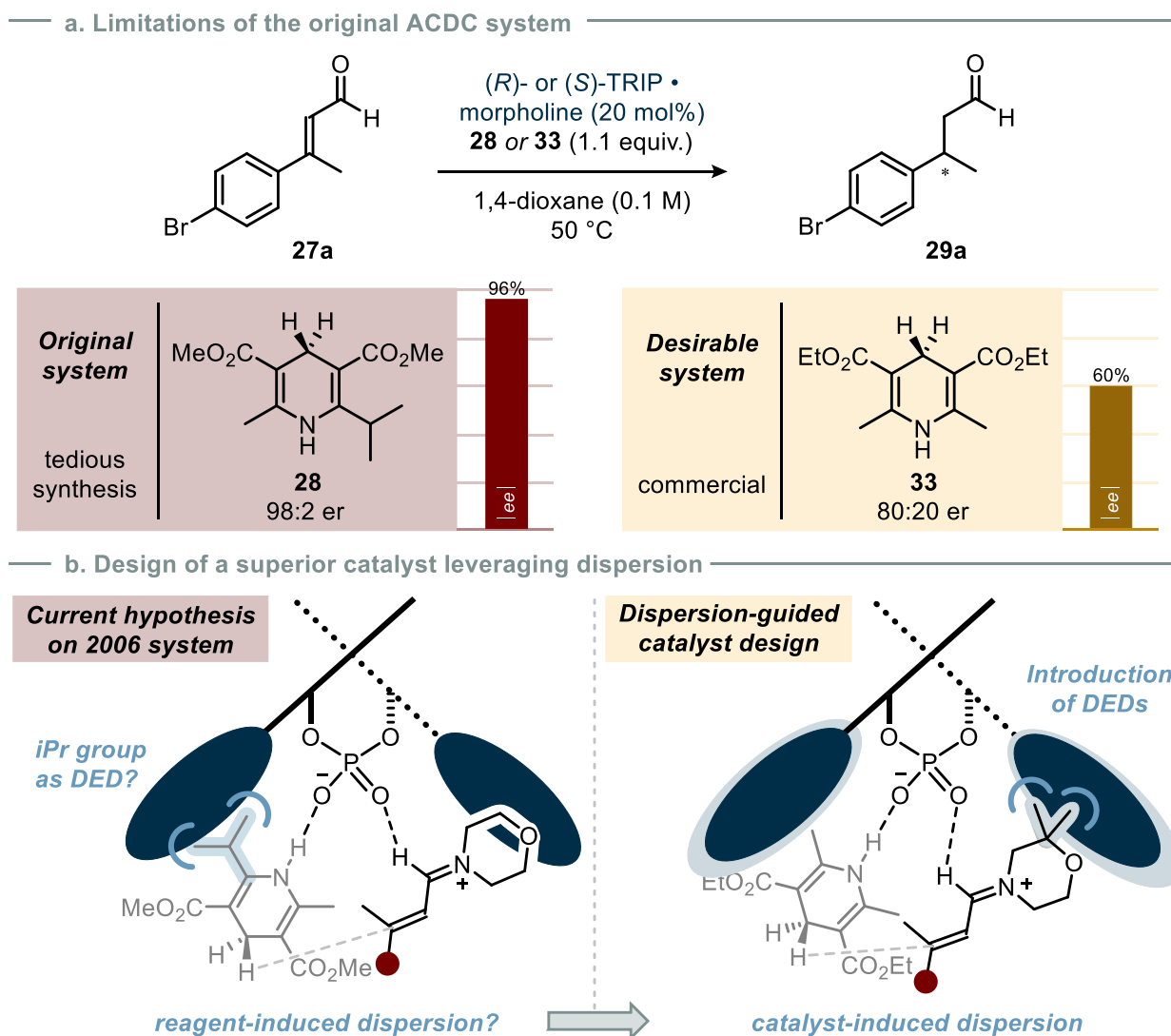
Figure 2.15 a. Comparison of enantioselectivities in the transfer hydrogenation of α,β-unsaturated aldehydes with Hantzsch esters **28** and **37**. b. Objective of this chapter: Exploration of the *i*Pr group as a DED and catalyst design harnessing dispersion interactions.

ester **33** lacking the isopropyl group has resulted in a pronounced drop in enantioselectivity (from 96% ee to 60% ee for **29a**, Figure 2.15a).

This preliminary finding has led to a new hypothesis: the isopropyl group of reagent **28** contributes to stereocontrol through key dispersion interactions. Given the lack of experimental tools to directly probe transition states, we propose to explore the system using computational methods. A qualitative analysis of the full transition state ensemble, including major and minor diastereomeric pathways, is expected to provide mechanistic insight into relevant noncovalent interactions, particularly London dispersion and the stereochemical role of the isopropyl group. To this end, we envision employing Local Energy Decomposition (LED) analysis to break down interfragment interactions into physically meaningful contributions (e.g., electrostatics, dispersion), and the Independent Gradient Model based on Hirshfeld partitioning (IGMH) to distinguish intra- and intermolecular noncovalent interactions. Furthermore, IGMH analysis would allow us to decompose stabilizing interactions into individual atomic pair contributions, offering a means to quantify the influence of the isopropyl group on stereocontrol.

With a deeper understanding of the 2006 system, we aim to overcome its limitations by developing a next-generation transfer hydrogenation method using the commercially available ester **33**. Rather than relying on reagent-induced dispersion effects, our approach proposes the introduction of new DEDs directly into the catalyst scaffold to promote favorable noncovalent interactions (Figure 2.15b). Both the morpholine moiety and the chiral phosphoric acid framework offer multiple sites for structural modification to enable such interactions. By providing an alternative interaction handle, this design is expected to address the key limitations of the original system. A more active catalyst could allow for reduced catalyst loadings, while improved selectivity could enable access to enantiopure β-chiral aldehydes using a readily available Hantzsch ester. Finally, computational analysis of the redesigned system allows us to elucidate the origin of stereocontrol and to evaluate the validity of our dispersion-driven catalyst design hypothesis.

2.3 Results and Discussion

2.3.1 Computational Analysis of the 2006 System

All computational studies presented in this chapter were carried out in collaboration with Dr. Benjamin Mitschke, who performed the calculations and contributed to data analysis.

Transition State Analysis

We initiated our investigations by analyzing the transition states of the 2006 system using density functional theory (DFT) and *ab initio* methods (Figure 2.16). These transition states are derived from ternary complexes comprising the chiral phosphate anion, which binds both the iminium cation, and the nucleophilic Hantzsch ester, positioned to deliver a hydride to the β-position of the activated enal.
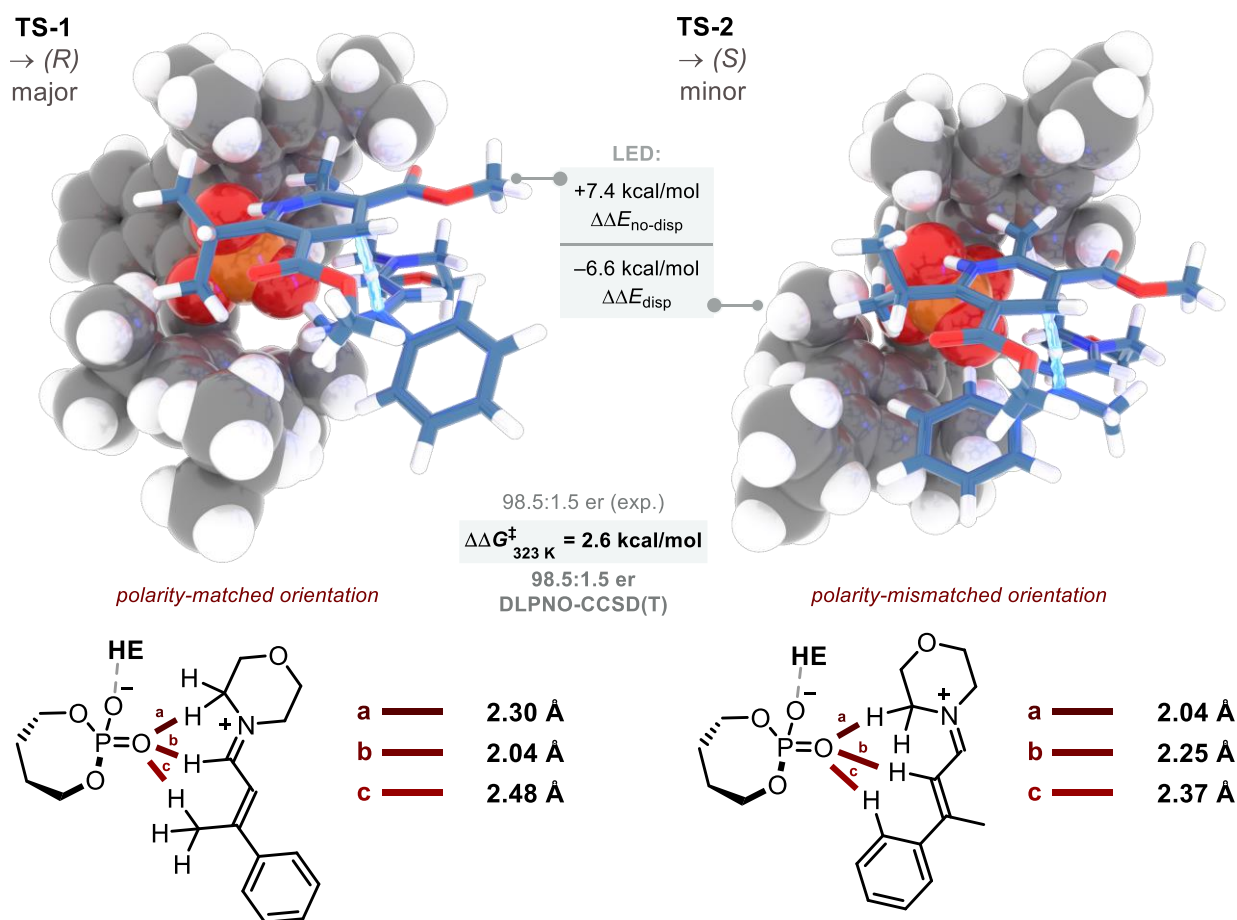
Figure 2.16 Computed transition states leading to the major and minor enantiomers in the 2006 system using (*S*)-TRIP·morpholine (**15**a): DFT transition state evaluation with Gibbs free enthalpies computed at the CPCM(1,4-dioxane)-DLPNO−CCSD(T)/cc-pVTZ//PBE-D3(BJ)/def2-SVP level of theory at 323 K/1 M. Key CH contacts are indicated. Energies are given in kcal/mol.

In the lowest-energy transition state **TS-1**, leading to the major (*R*)-enantiomer, the cationic iminium adopts an *E*-configuration. It coordinates to the phosphate counteranion via three nonclassical CH⋯O hydrogen

bonds, consistent with the interaction mode originally proposed in 2006.[114] This polarity-matched orientation of the iminium likely serves as a substrate-recognition element for the chiral phosphate. Moreover, it aligns with the well-established mechanistic scenario that enables *E*/*Z*-isomerization and thus stereoconvergence via γ-deprotonation to form a dienamine intermediate.[130] In the transition state **TS-2**, leading to the minor (*S*)-enantiomer, the *E*-configured iminium undergoes a complete enantiofacial flip relative to the phosphate counteranion. This polarity-mismatched orientation results in three weaker, less polarized CH···O hydrogen bonds within the chiral ion pair, suggesting diminished electrostatic complementarity. The overall destabilization is partially mitigated by shortened CH···O contacts (a: 2.30 Å in **TS-1** vs. 2.04 Å in **TS-2**, c: 2.48 Å in **TS-1** vs. 2.37 Å in **TS-2**). Furthermore, in contrast to **TS-1**, the β-phenyl substituent in **TS-2** is oriented toward the phosphate counteranion, potentially engaging in attractive noncovalent interactions.

We identified an additional transition state leading to the minor (*S*)-enantiomer (Figure 2.17), which resembles a structure reported in a prior computational study of the 2006 system.[200] In that study, however, the Hantzsch ester nucleophile bearing the isopropyl group was simplified to a symmetric ketone, and the assignment of the resulting product enantiomer appears to be incorrect. **TS-2b** is characterized by a *Z*-configured iminium, which coordinates to the phosphate via two polarized CH···O hydrogen bonds. The β-phenyl substituent is marginally twisted compared to **TS-2**.
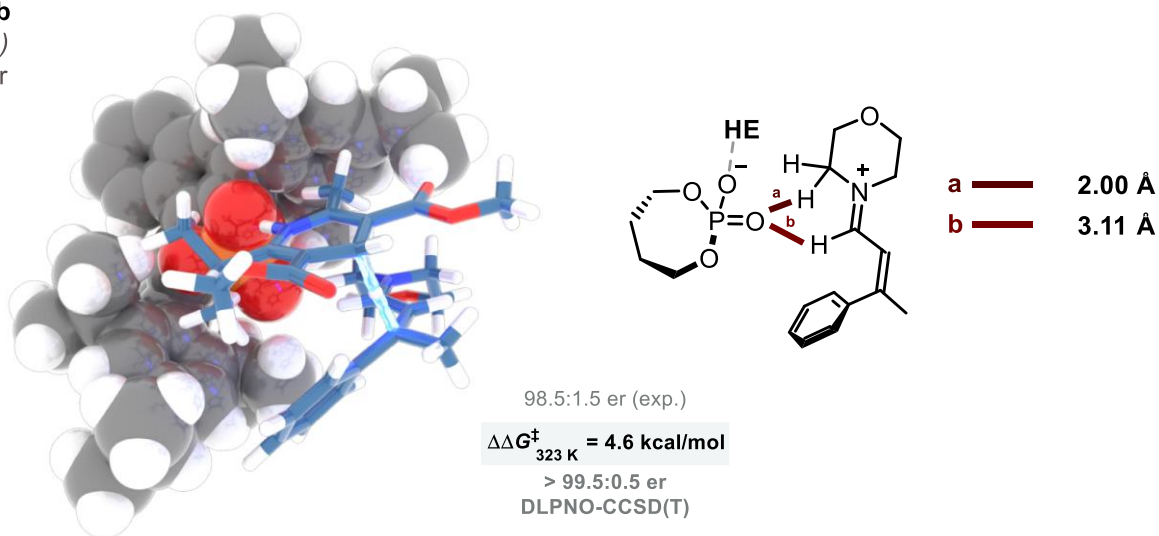
Figure 2.17 Additional, higher-energy transition state leading to the minor enantiomer. Computational details as in Figure 2.16.

Crucially, the experimentally observed enantiomeric ratio (98.5:1.5) is well reproduced by **TS-1** and **TS-2** ($\Delta\Delta G^{\ddagger}$ = 2.6 kcal/mol), while **TS-2b** is energetically disfavored and thus inconsequential ($\Delta\Delta G^{\ddagger}$ = 4.6 kcal/mol), as calculated at the CPCM(1,4-dioxane)-DLPNO−CCSD(T)/cc-pVTZ//PBE-D3(BJ)/def2-SVP level of theory.

Local Energy Decomposition (LED) Analysis

Local energy decomposition analysis enables a breakdown of interfragment interactions into meaningful contributions including repulsive electronic preparation, electrostatics, exchange, dispersion, and nondispersive correlation.[201–209] When applied to the 2006 system, the differential analysis of **TS-1** and **TS-2** reveals that **TS-1** is dominantly stabilized by nondispersion interactions ($\Delta\Delta E_{\text{no-disp}}$ = 7.4 kcal/mol). This relative stabilization mainly arises from stronger electrostatic interactions between Hantzsch ester **28** and the phosphate anion in **TS-1**. Additionally, the polarity-matching orientation of the iminium and phosphate fragments contribute to overall stabilization. In contrast, the transition state energy of **TS-2** benefits more from attractive dispersion interactions ($\Delta\Delta E_{\text{disp}}$ = –6.6 kcal/mol), particularly between the iminium ion and the phosphate counteranion. The proximity of the iminium β-phenyl substituent and the morpholine α-CH$_2$ group to the phosphate 3,3'-substituents likely promotes these favorable dispersion interactions.

IGMH Analysis of Key Noncovalent Interactions

Despite our finding that **TS-2** is stabilized through dispersion interactions to a greater extent than **TS-1**, the specific noncovalent interactions that favor **TS-1** and thus contribute to enantiocontrol, warrant further investigation. In particular, the role of the isopropyl group in Hantzsch ester **28** as a potential DED has not yet been clearly defined, but remains at the center of our design strategy to enable the use of the simplified Hantzsch ester **33**.

To probe this, we employed the Independent Gradient Model based on Hirshfeld partition (IGMH[210]) implemented in the Multiwfn program[211,212] using electron densities derived from B3LYP-D3(BJ)/def2-TZVPP single points of the PBE-D3(BJ)/def2-SVP structures. The IGMH method enables visualization of noncovalent interfragment interactions between the combined Hantzsch ester–iminium ion system and the chiral phosphate counteranion, as well as their quantitative decomposition at the atomic level. Isosurface plots reveal multiple stabilizing contacts in both **TS-1** and **TS-2** (Figure 2.18, top) with no evidence of repulsive contacts. For a more quantitative assessment, atomic contributions to the interfragment interaction are visualized via a color-coded scale (Figure 2.18, bottom).

Consistent with our transition state and LED analysis, the IGMH maps show that stabilizing interactions in **TS-2** are slightly enhanced at the iminium β-phenyl substituent and morpholine α-CH$_2$ group compared to the corresponding β-CH$_3$ and α-CH$_2$ groups in **TS-1**. However, a key differentiator lies in the isopropyl group of the Hantzsch ester: it contributes 21.8% to the interfragment interaction in **TS-1**, but only 11.5% in **TS-2**. This difference substantiates our hypothesis that attractive dispersion between the isopropyl group and the 3,3'-substituents of the phosphate catalyst selectively stabilizes **TS-1**, reinforcing its role as a DED contributing to stereocontrol.
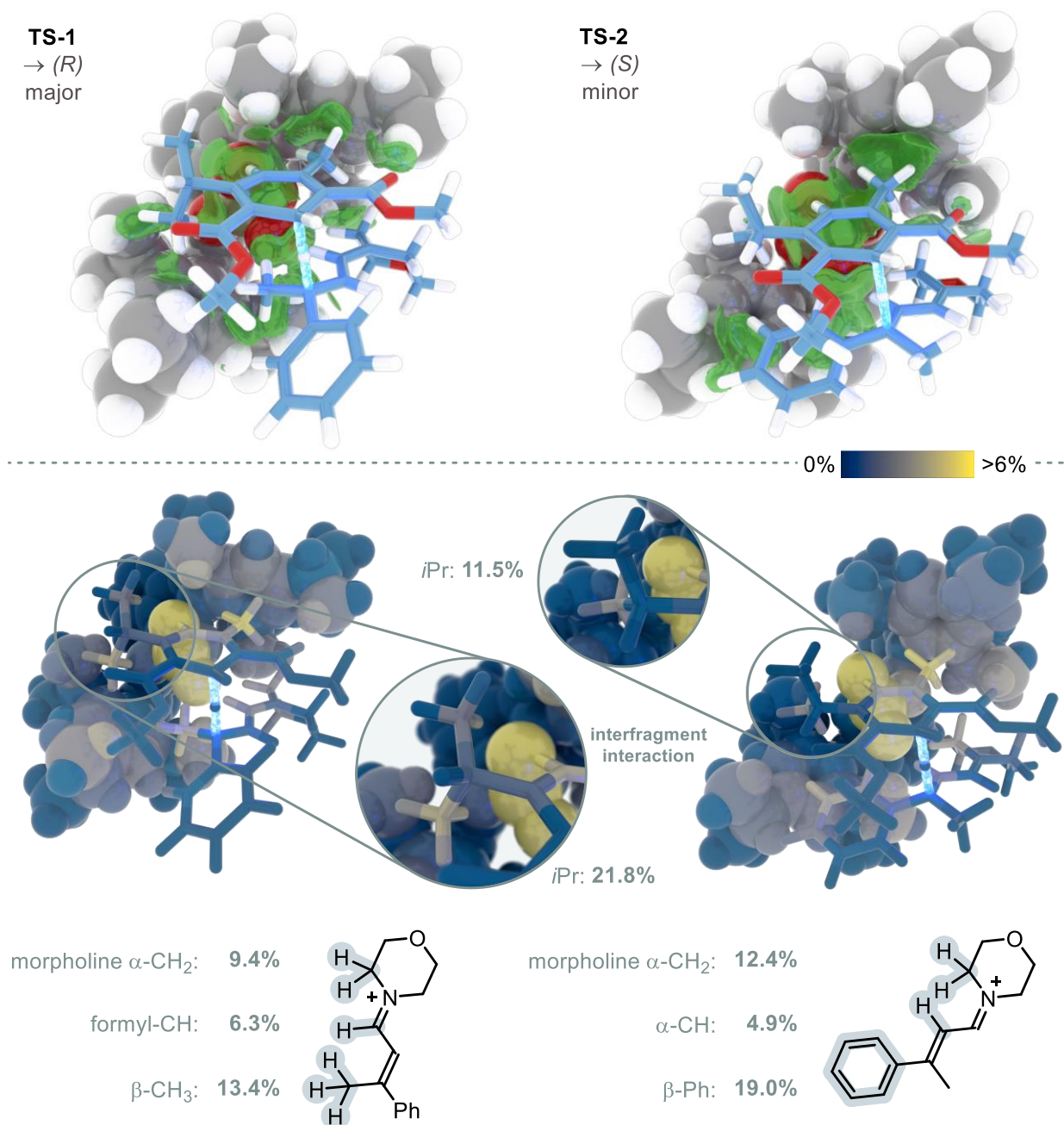
Figure 2.18 IGMH analysis using B3LYP-D3(BJ)/def2-TZVPP densities, highlighting key noncovalent interactions in **TS-1** and **TS-2** as isosurfaces of δg^{inter} with an isovalue of 0.004, with color-coded atoms according to their contribution to the overall interfragment interaction δG^{atom} (%) (bottom).

2.3.2 Development of a Superior Transfer Hydrogenation Catalyst

Reaction Optimization

Table 2.1 Screening catalysts with DED-modified phosphates and morpholines for the transfer hydrogenation of (*E*)-3-(4-bromophenyl)but-2-enal (**27a**) using Hantzsch ester **33**.
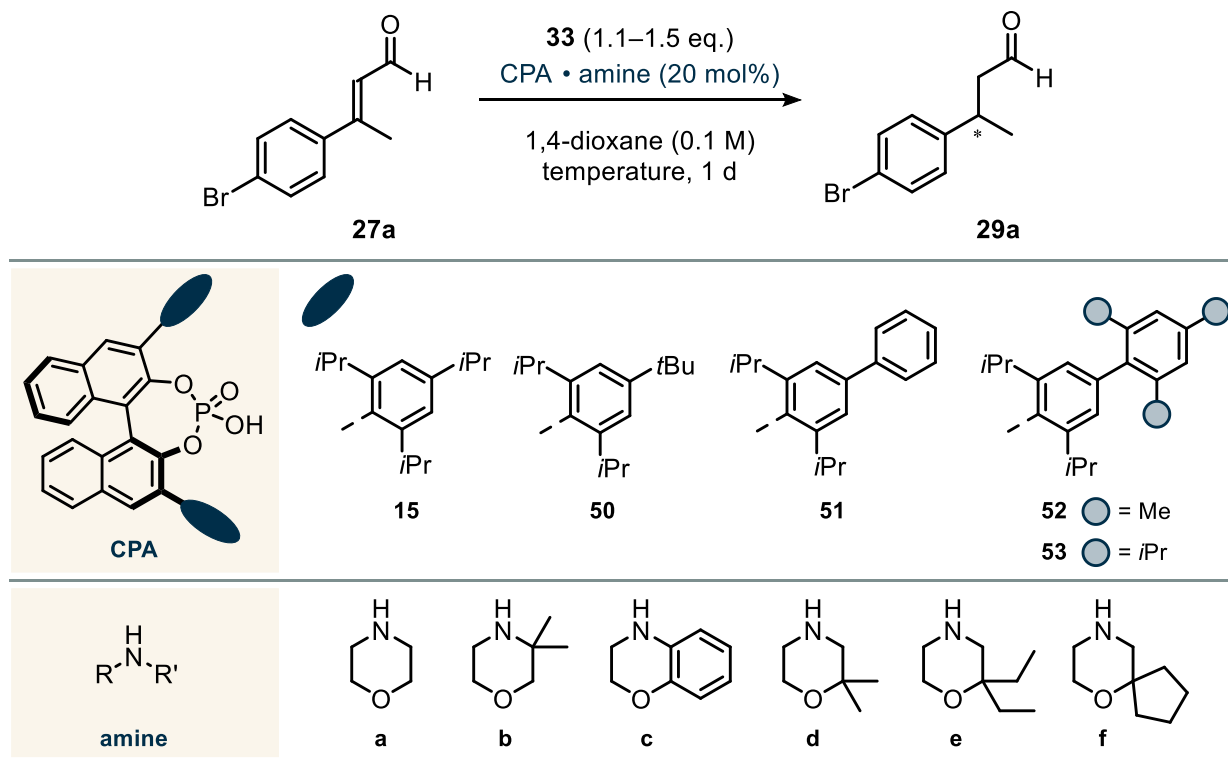
entry	CPA	amine	temperature	conversion	er
1	**15**	**a**	50 °C	100%	80:20
2	**15**	**a**	30 °C	100%	79.5:20.5
3	(*R*)-**50**	**a**	50 °C	100%	21:79
4	(*R*)-**51**	**a**	50 °C	100%	9.5:90.5
5	**52**	**a**	50 °C	100%	91:9
6	**53**	**a**	50 °C	100%	93:7
7	**53**	**b**	50 °C	45%	62:38
8	**53**	**c**	50 °C	100%	83:17
9	**53**	**d**	50 °C	100%	96:4
10	**53**	**e**	50 °C	96%	97.5:2.5
11	**53**	**f**	50 °C	94%	98:2

Following the computational analysis of the 2006 system and confirmation of our hypothesis, we set out to develop an improved transfer hydrogenation method. By incorporating DEDs into the catalyst scaffold, we aimed to enable the selective reduction of α,β-unsaturated aldehydes using the commercially available Hantzsch ester **33**, with the goals of reducing catalyst loadings and expanding the substrate scope to sterically hindered aliphatic enals. We initiated our studies by examining the transfer hydrogenation of (*E*)-3-(4-bromophenyl)but-2-enal (**27a**) as our model substrate, using **33** as the reductant under previously established reaction conditions (Table 2.1). The morpholinium salt of (*S*)-TRIP (**15a**) gave full conversion but only modest enantioselectivity (80:20 er), which remained unchanged upon reducing the temperature (entries 1 and 2). We next explored the influence of different 3,3'-substituents on the phosphoric acid catalyst, aiming to optimize stereoselectivity through noncovalent interactions. Replacing the 4-isopropyl groups of the arene with bulkier *tert*-butyl substituents resulted in slightly lower enantioselectivity (21:79 er, entry 3). In contrast, introducing a second phenyl ring significantly improved the enantiomeric ratio to 9.5:90.5, possibly due to stabilizing CH–π interactions in the stereodetermining transition state **TS-1** (entry 4). Further modification by incorporating alkyl groups at the 2,4,6-positions of the distal aryl ring, which may enhance dispersion interactions as reported in previous studies[185,194], led to additional improvements in enantioselectivity (entries 5 and 6).

Table 2.2 Screening of catalyst loading and solvent for the transfer hydrogenation of (*E*)-3-(4-bromophenyl)but-2-enal (**27a**) using Hantzsch ester **33**.
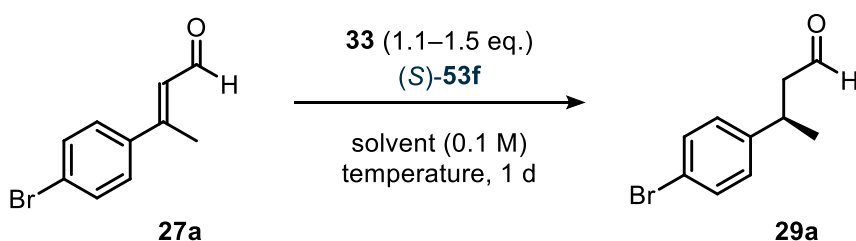
entry	catalyst loading	solvent	temperature	conversion	er
1	20 mol%	1,4-dioxane	50 °C	94%	98:2
2	5 mol%	1,4-dioxane	50 °C	92%	98:2
3	2.5 mol%	1,4-dioxane	50 °C	100%	98:2
4	5 mol%	CHCl$_3$	50 °C	60%	88:12
5	5 mol%	THF	50 °C	92%	93.5:6.5
6	5 mol%	Et$_2$O	rt	100%	97.5:2.5
7	5 mol%	PhMe	50 °C	100%	96.5:3.5
8	5 mol%	CyH	50 °C	100%	97.5:2.5

Next, different morpholine derivatives bearing DEDs were evaluated. Introduction of a *gem*-dimethyl group at the 3-position led to a substantial decrease in reactivity, likely due to steric hindrance impeding iminium ion formation with enal **27a**, and resulted in reduced enantioselectivity (entry 7). Use of benzomorpholine (**c**) in combination with phosphoric acid **53** restored high reactivity, but the enantiomeric ratio was lower than that obtained with unmodified morpholine (entry 8). Remarkably, geminal alkyl substitution at the 2-position significantly improved enantioselectivity (entries 9–11). Ultimately, catalyst **53f** emerged as the optimal system, bearing multiple alkyl-modifications relative to the parent catalyst **15a**.

We next tried to reduce the catalyst loading (Table 2.2). Fortunately, both reactivity and enantioselectivity were maintained upon reducing it from 20 mol% down to 2.5 mol% (entries 1–3). Screening of alternative solvents led to inferior results (entries 4–8). With an efficient and selective system in hand, we next turned to evaluating the substrate scope.

Reaction Scope and Limitations

In 2006, only a few examples of β-aryl-β-methyl disubstituted enals, mostly with *para*-substituents, were shown to be compatible with the transfer hydrogenation protocol. In contrast, our improved catalyst system exhibited a broad substrate scope, tolerating α,β-unsaturated aldehydes with a wide range of electronic and steric features (Figure 2.19).

For example, β-branched aldehydes **27a**−**c** bearing electron-withdrawing groups (Br, CF$_3$) were obtained in very good yields and with exceptional enantioselectivities. β-Aryl enals having electron-neutral or electron-donating groups at the *ortho*, *meta*- or *para*-positions were effectively reduced with excellent enantioselectivities (**27d**−**h**). The styrenyl derivative **27i** also proved to be a compatible substrate for our methodology leaving the benzylic vinyl group fully intact. Furthermore, disubstituted β-aryl enal **27j**, containing both a nitro and a methoxy group, afforded the desired product in high yield and enantioselectivity. Notably, heteroaromatic aldehydes **27k** and **27l** were also well-tolerated, delivering products in excellent yields and enantiomeric ratios.

Although aldehyde **29m** bearing an *ortho*-Cl substituent was obtained with excellent enantioselectivity (99:1 er), the yield was limited to 32%. Reduced reactivity of **27m** was identified as one contributing factor. Additionally, the formation of 1-(2-chlorophenyl)ethan-1-one as a side product suggested that an oxa-Michael–retro-aldol sequence in the presence of water may have occurred as a competing pathway. When boronic acid pinacol ester **27n** was subjected to the reaction conditions, aldehyde **29n** was obtained in 30% yield with excellent enantioselectivity, but was accompanied by the protodeborylated product **29d** as a major side product.
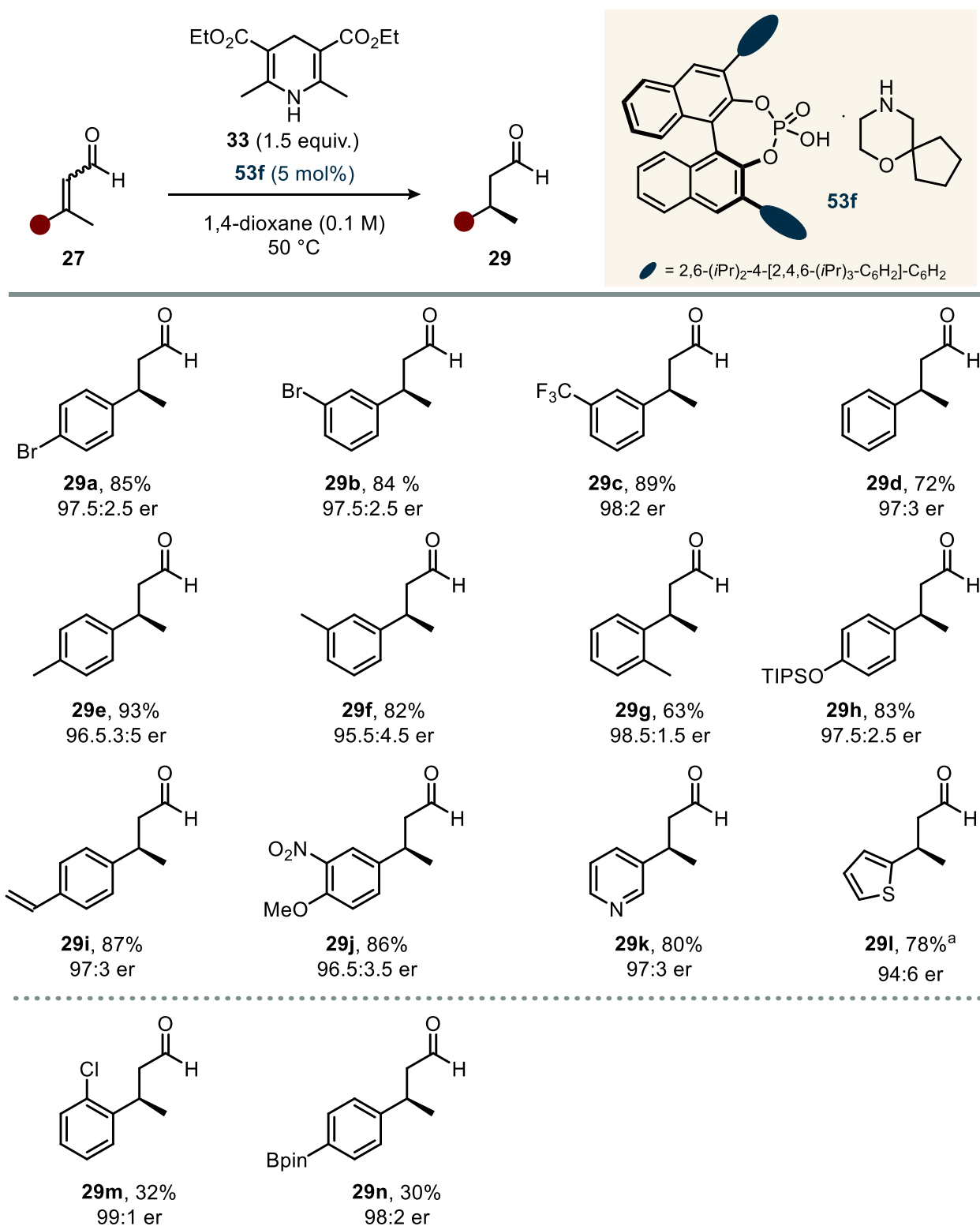
Figure 2.19 Scope of β-aryl-β-methyl-disubstituted enals. All reactions were conducted on a 0.2 mmol scale. Yields are reported as isolated yields after column chromatography. *E/Z* ratios for all starting materials were between 2:1 and >20:1. [a]Reaction was performed in CyH at rt.

Finally, we examined aliphatic α,β-unsaturated aldehydes, including sterically hindered substrates that had previously proven challenging (Figure 2.20). Enals bearing β-cycloalkyl substituents of varying ring sizes were efficiently reduced to aldehydes **29o–q** in very good yields and with excellent enantioselectivities. Sterically demanding substrates **27r** (previously <5%)[114] and **27s** were converted in nearly quantitative yields and similarly high enantioselectivities. Notably, 3-methylpent-2-enal (**27t**), a particularly challenging substrate due to the minimal steric differentiation between methyl and ethyl groups, was reduced to aldehyde **29t** under reoptimized reaction conditions with a very good enantiomeric ratio of 91:9. Extending the β-ethyl chain by one or two methylene units (**29u,v**) restored the excellent enantioselectivity observed for all other aliphatic substrates. Finally, the enals citral (*E/Z* = 3:1) and farnesal underwent smooth reduction to furnish natural products (*S*)-citronellal (**29w**) and (*S*)-dihydrofarnesal (**29x**), each with high yield and excellent enantiomeric excess.
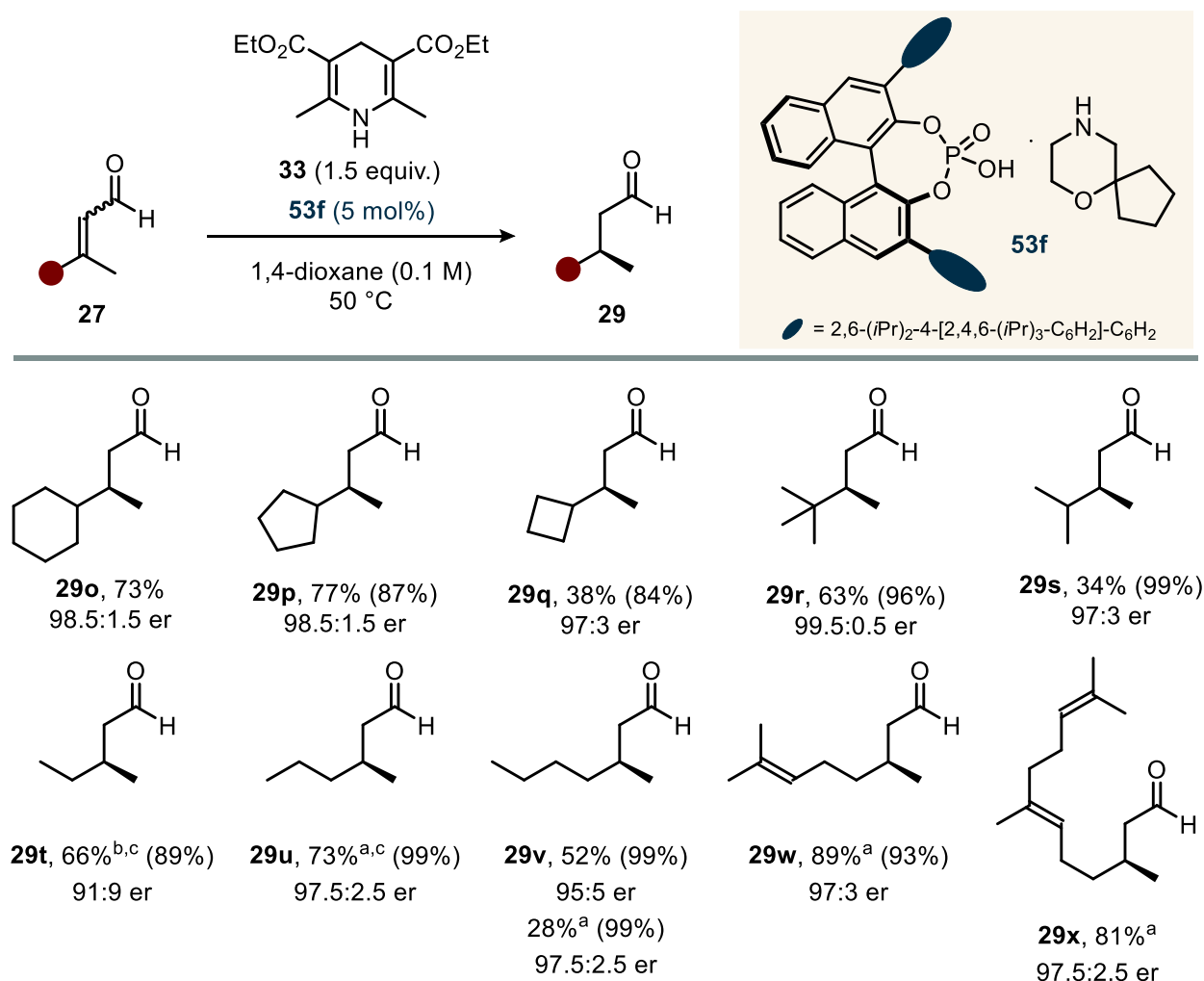
Figure 2.20 Scope of β-alkyl-β-methyl-disubstituted enals. All reactions were conducted on a 0.2 mmol scale. Yields are reported as isolated yields after column chromatography. For some volatile substrates, ¹H NMR yields, reported in parentheses, were determined using mesitylene as an internal standard. *E/Z* ratios for all starting materials were between 2:1 and >20:1. [a]Reaction was performed in CyH at rt. [b]Reaction was performed in CyH/*n*-pentane (9:1) at −10 °C. [c]Product was isolated after *in situ* derivatization with 2,4-dinitrophenylhydrazine as the corresponding hydrazine.

Remarkably, when the transfer hydrogenation of farnesal was scaled to 5 mmol, the catalyst loading could be reduced to 1 mol%, yielding (*S*)-dihydrofarnesal in improved yield of 93% and excellent enantioselectivity (97:3 er, Figure 2.21).
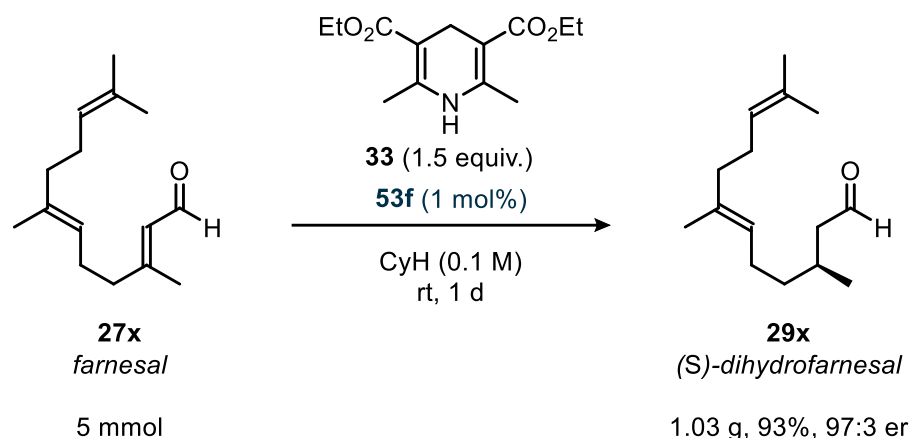
Figure 2.21 Upscaled transfer hydrogenation of farnesal (5 mmol) using 1 mol% catalyst.

The explored substrate scope focused on disubstituted β-methyl enals with both aromatic and aliphatic β-substituents. When the β-methyl group was extended to longer alkyl chains, as in **27y** and **27z**, a pronounced decrease in both reactivity and enantioselectivity was observed (Figure 2.22). Based on our understanding of the 2006 system, this limitation likely stems from weakened interactions between the β-alkyl substituent of the iminium intermediate and the chiral phosphate (cf. Transition State Analysis, p. 30). The reduced performance of the bulkier analogs may arise from weakened CH···O interactions due to lower polarization, or from steric hindrance interfering with close transition state contacts. While the major transition state may be destabilized relative to β-methyl enals, the minor transition state continues to benefit from stabilizing interactions with the β-phenyl group—overall leading to reduced enantioselectivity for these substrates.
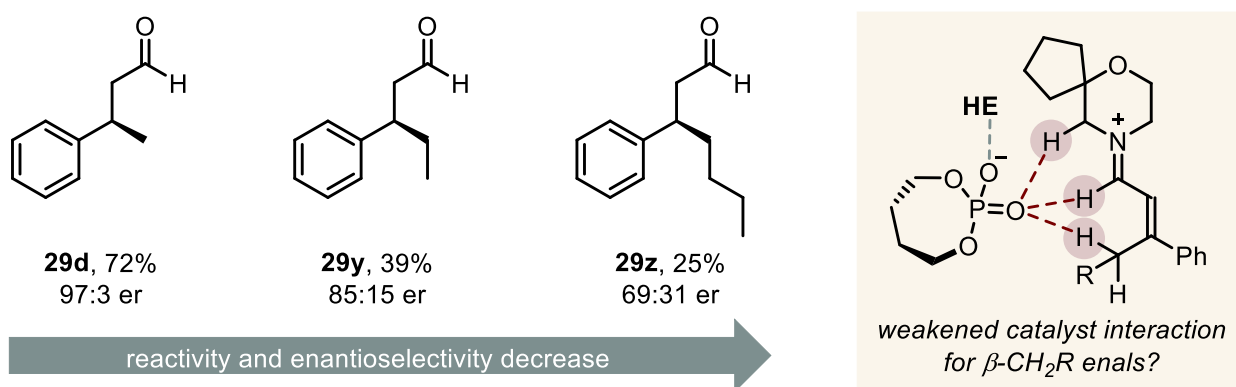
Figure 2.22 Transfer hydrogenation of β-CH₂R cinnamaldehydes under standard conditions, showing reduced reactivity and enantioselectivity with increasing β-substituent size.

In summary, relative to the 2006 catalytic system, the substrate scope of disubstituted β-methyl enals has been significantly broadened—from mostly *para*-substituted aromatic substrates to include diverse

substitution patterns at the *ortho*, *meta* and *para* positions, encompassing functional groups with varied electronic properties as well as heteroaromatic substrates. Both sterically hindered and nonhindered aliphatic enals were efficiently reduced under the new transfer hydrogenation protocol, exceeding previous performance. The effectiveness at reduced catalyst loadings suggests that catalyst **53f** is more reactive than the original catalyst **15a**, a hypothesis that will be further explored in the following sections.

Mechanistic Studies

For organocatalytic transfer hydrogenation reactions of α,β-unsaturated aldehydes that proceed via condensation with an amine to generate the more activated iminium ion intermediate, it is well-established that the same major enantiomer is obtained regardless of the double bond configuration (*E* or *Z*) of the starting enal. This phenomenon, known as enantioconvergence, is attributed to a rapid equilibrium between the *E*- and *Z*-iminium ions via a common dienamine intermediate formed through γ-deprotonation. As
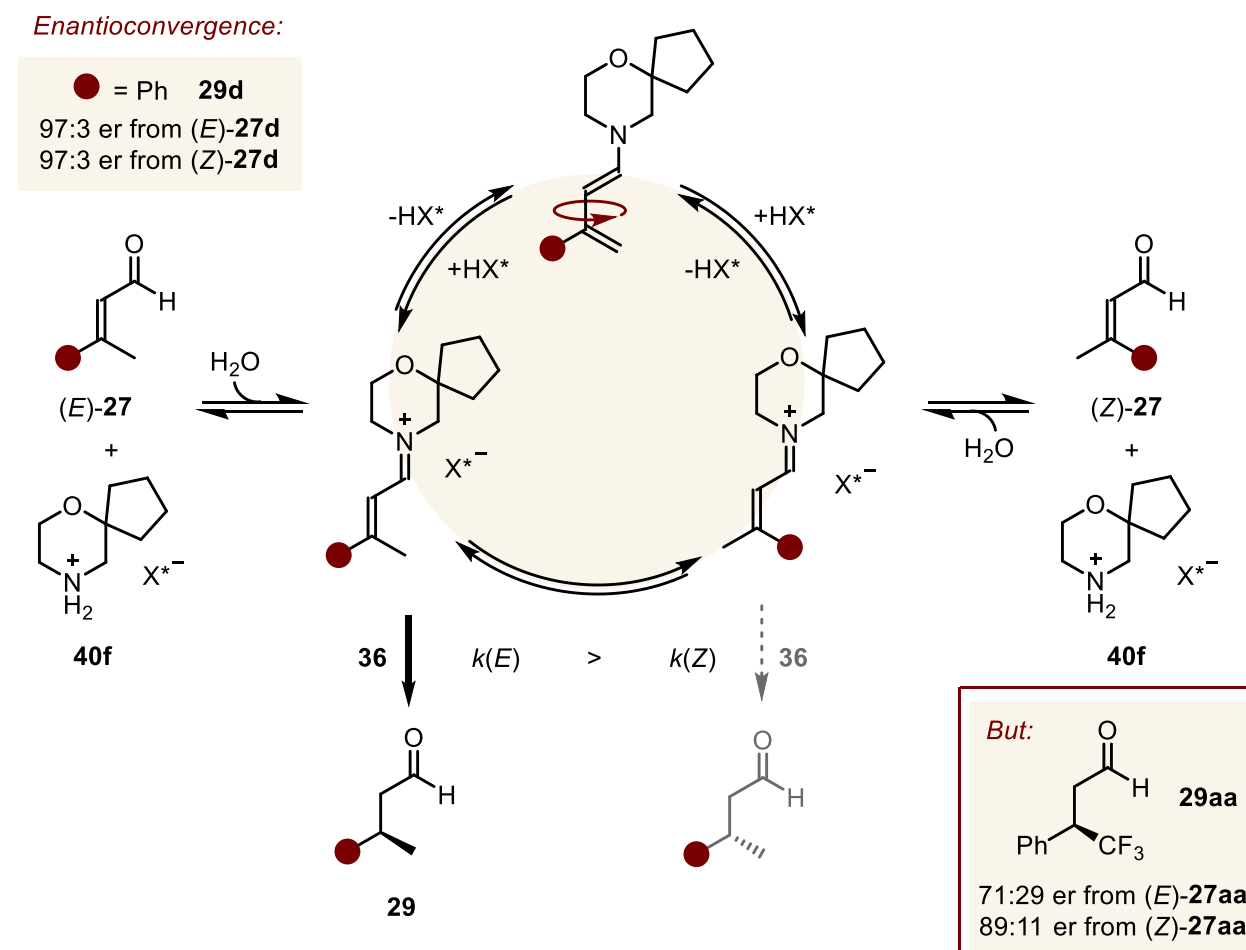
Figure 2.23 Mechanistic rationale for enantioconvergence of β-methyl enals via *E/Z*-iminium ion equilibration and selective hydride transfer.

hydride transfer from the Hantzsch ester typically occurs preferentially with one iminium stereoisomer, the enantiomeric ratio of the product is largely independent of the E/Z ratio of the starting material.[130,213]

To investigate this phenomenon, stereoisomerically pure (*E*)- and (*Z*)-3-phenylbut-2-enal (**27d**) were subjected individually to the reaction conditions. In both cases, product **29d** was obtained with an identical enantiomeric ratio of 97:3, confirming enantioconvergent behavior under the optimized catalytic system (Figure 2.23).

Subjecting the β-CD$_3$ variant of **27d** to the transfer hydrogenation reaction revealed deuterium scrambling between the α- and γ-positions in product **29d'**. This observation is consistent with the formation of a dienamine intermediate, supporting the proposed *E/Z*-iminium equilibration pathway.

Finally, we examined the transfer hydrogenation of 4,4,4-trifluoro-3-phenylbut-2-enal (**27aa**), an enal that lacks γ-protons and is therefore unable to undergo dienamine-mediated *E/Z* isomerization. Pure *E*- and *Z*-isomers of **27aa** were subjected separately to the reaction conditions. In contrast to the enantioconvergent behavior observed for **27d**, the two isomers of **27aa** yielded products with distinct enantiomeric ratios, although the same major enantiomer was obtained in both cases (71:29 er from *E*-**27aa**, 89:11 er from *Z*-**27aa**). In addition, in both cases, incomplete conversion of the starting material was observed and exclusively the *E*-isomer remained unreacted. These observations indicate that a slower, alternative isomerization process is operative under the reaction conditions. One plausible pathway involves a reversible oxa-Michael addition of the chiral phosphate to the iminium ion, followed by bond rotation and subsequent retro-oxa-Michael elimination. While this mechanism may be irrelevant for β-methyl enals, it becomes more likely in the case of enal **27aa** due to its increased electrophilicity. Additionally, each iminium ion could react independently with different levels of facial selectivity.

It is worth noting that in our system, the unsymmetrical nature of the morpholine permits an additional *E/Z*-isomerism about the C=N double bond of the iminium ion. Based on insights from the 2006 system, one can envision two analogous major transition state geometries: one in which the morpholine substituents point toward the chiral phosphate (*endo*-configuration), and another where they are oriented away from it (*exo*-configuration). These scenarios may be rationalized either by attractive dispersion interactions in the *endo* case or by steric repulsion favoring an *exo* arrangement (Figure 2.24, top). To obtain a first indication of which configuration may be preferred, we conducted two comparative experiments: one using unsymmetrical 3-*gem*-dimethyl morpholine (**d**) and the other using symmetrical 3,3,5,5-tetramethylmorpholine (**g**). If the *endo*-configuration with **53d** were favored, a similar transition state geometry would be expected with **53g**, as the additional *gem*-dimethyl group in **g** projects away from the reactive center and should not affect the overall structure. Conversely, if steric repulsion were the dominant

factor favoring an *exo*-orientation in **53d**, the bulkier morpholine **g** would likely lead to a different stereochemical outcome.

Indeed, when the experiments were carried out, the same enantiomeric ratio of product **29a** was obtained in both cases. Although this observation should not be taken as definitive evidence, it provides an indication that the *endo*-configuration may be stabilized by attractive dispersion interactions in unsymmetrical morpholines such as **d**, **e**, and **f** (Table 2.1). This hypothesis will be further evaluated by DFT calculations to probe the underlying transition state geometries.
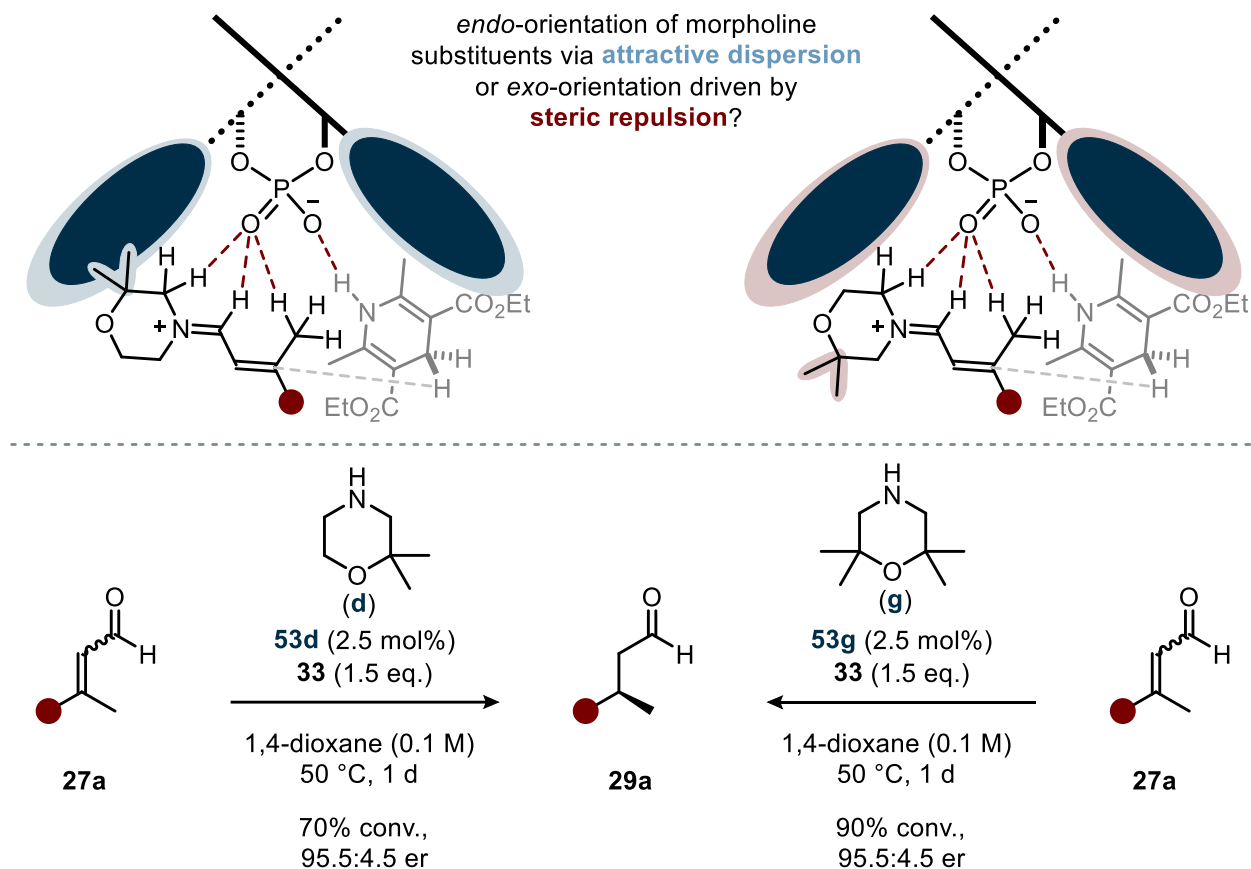
Figure 2.24 Conceptual rationale for *endo* vs. *exo* orientation of unsymmetrical morpholine substituents, guided by either attractive dispersion or steric repulsion (top); transfer hydrogenation of enal **27a** catalyzed by **53d** or **53g**, used to probe the preferred transition state geometry (bottom).

Relative Rate Experiments

The kinetic studies presented in this section were carried out in collaboration with Dr. Markus Leutzsch.

The high reactivity observed across various substrates—including sterically hindered enals such as **27r**—even at reduced catalyst loadings, suggested that the newly developed catalyst **53f** promotes faster reaction rates than the parent catalyst **15a**. To determine whether this enhanced performance arises from structural

modifications to the chiral phosphoric acid or the morpholine component, we conducted a comparative rate analysis. To this end, catalysts **15a** and **53f**, as well as the cross-combinations **15f** and **53a**, were evaluated in the transfer hydrogenation of *E*-**27d** using Hantzsch ester **33**. The reactions were monitored over time by single-scan ¹H NMR spectroscopy (Figure 2.25, left).
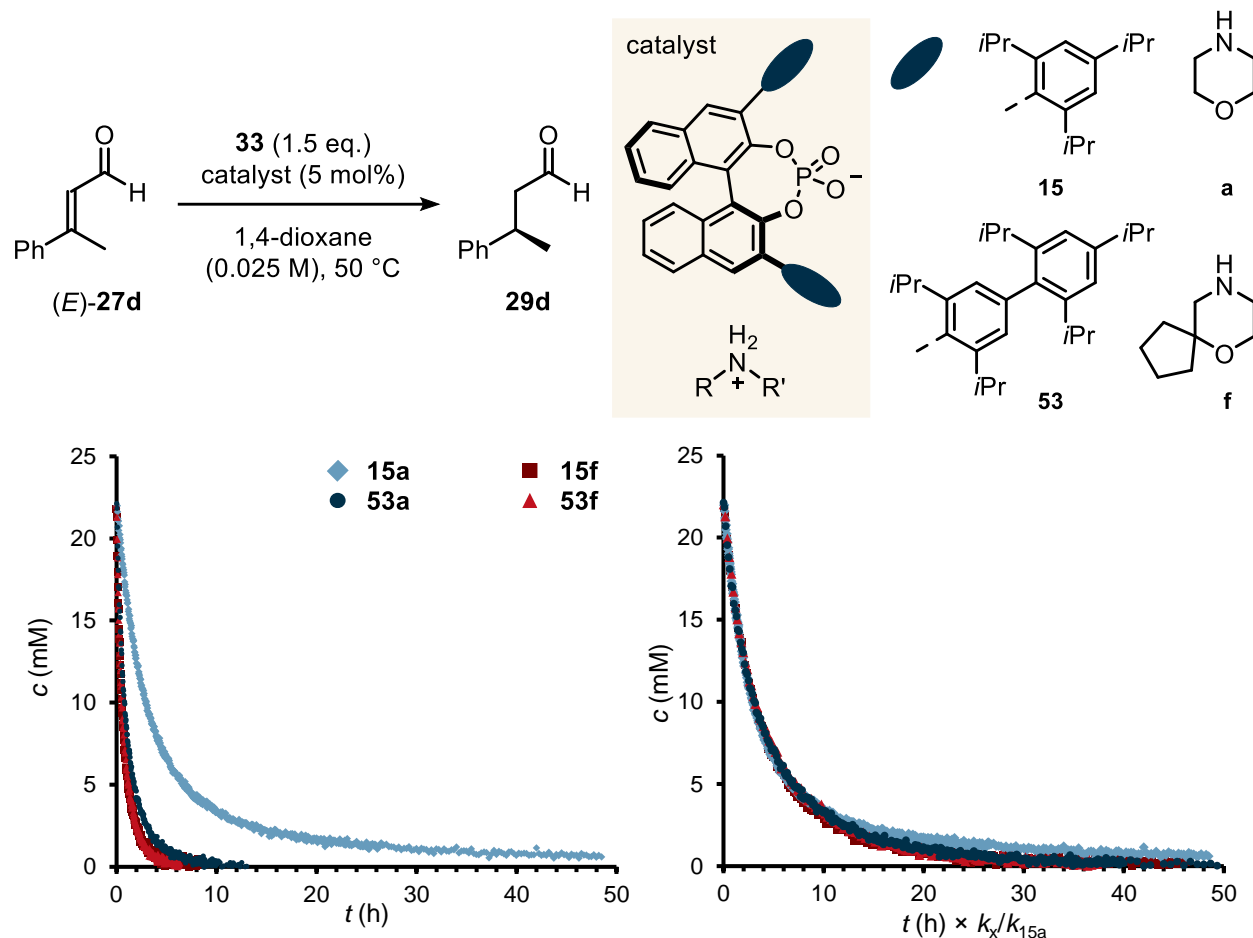
Figure 2.25 Left: conversion of *E*-**27d** over time using different catalysts monitored by single-scan ¹H NMR spectroscopy (0.025 M in 1,4-dioxane-h_8, 50 °C); right: relative rate analysis via variable-time normalization (VTNA), using catalyst salt **15a** as reference ($k_{15a} = 1.0$).

As evident from the plot, the reaction catalyzed by **15a** proceeds the slowest among the catalysts tested. To further compare the reaction profiles without determining detailed reaction orders for this multicomponent system, we employed a variable-time normalization approach (VTNA).[214] In this method, time was scaled by a relative rate constant ($k_{rel} = k_x/k_{ref}$), using the slowest reaction (catalyst **15a**) as the reference. The optimal k_{rel} values were determined by visually identifying the best overlap of each normalized curve with the reference profile (Figure 2.25, right).

We also conducted a second kinetic analysis using the initial rates method. For this, the first 13–15% of conversion was approximated to follow zero-order kinetics, and the slope of the linear region was taken as

the rate constant. To obtain these values, both the consumption of the starting material (**27d**) and the formation of the product (**29d**) were monitored over time for each reaction (**15a**, **15f**, **53a**, **53f**). The resulting slopes were averaged, and standard deviations were calculated (Figure 2.26). Relative rates were then determined with respect to catalyst **15a** as the reference.
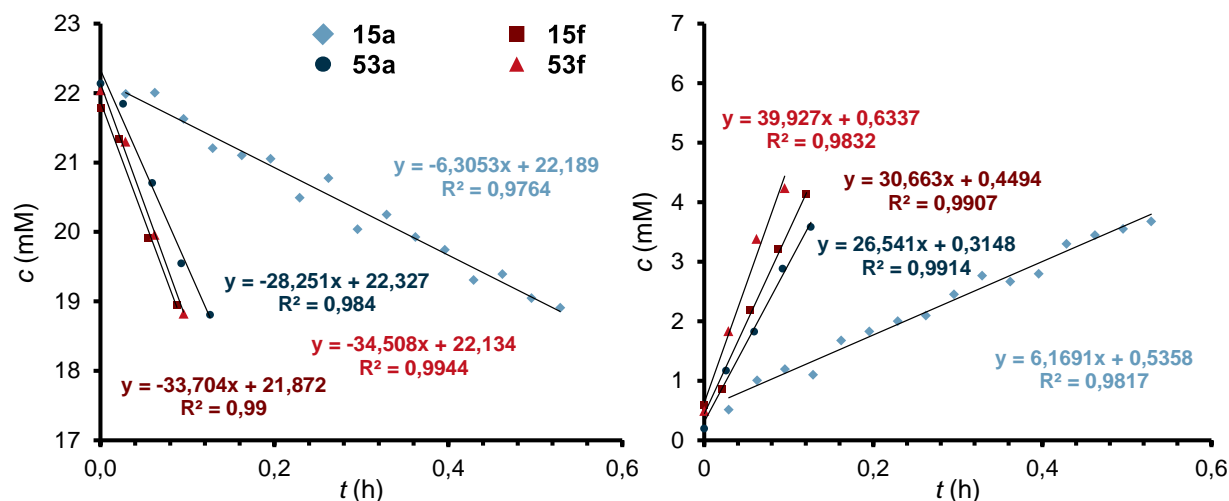
Figure 2.26 Initial rates analysis based on the first 13–15% of conversion for the transfer hydrogenation of *E*-**27d** at 50 °C in 1,4-dioxane-h_8. Left: enal consumption over time; right: product formation over time. Linear fits were used to determine the average rate for each catalyst. Relative rates were extracted with respect to catalyst **15a**.

Table 2.3 Relative reaction rates for different catalysts, obtained from VTNA and initial rates analysis.

catalyst	relative rate $k_{rel} = k_x/k_{15a}$ (VTNA)	relative rate $k_{rel} = k_x/k_{15a}$ (initial rate)
15a	1.0	1.0
15f	5.6	5.4 ± 0.3
53a	4.0	4.5 ± 0.2
53f	6.0	5.6 ± 0.4

The relative rates obtained by the two methods follow the same trend: $k_{15a} < k_{53a} < k_{15f} < k_{53f}$, corresponding to an approximately six-fold increase in rate from catalyst **15a** to **53f** (Table 2.3). Both the phosphoric acid and the morpholine modifications promote faster reaction rates, with the morpholine having the greater impact. Notably, the effects are not additive, suggesting that the two catalyst components influence different elementary steps to varying extents—potentially resulting in a shift of the rate-determining step.

2.3.3   Computational Analysis of the Improved System

All computational studies presented in this chapter were carried out in collaboration with Dr. Benjamin Mitschke, who performed the calculations and contributed to data analysis.

Transition State Analysis
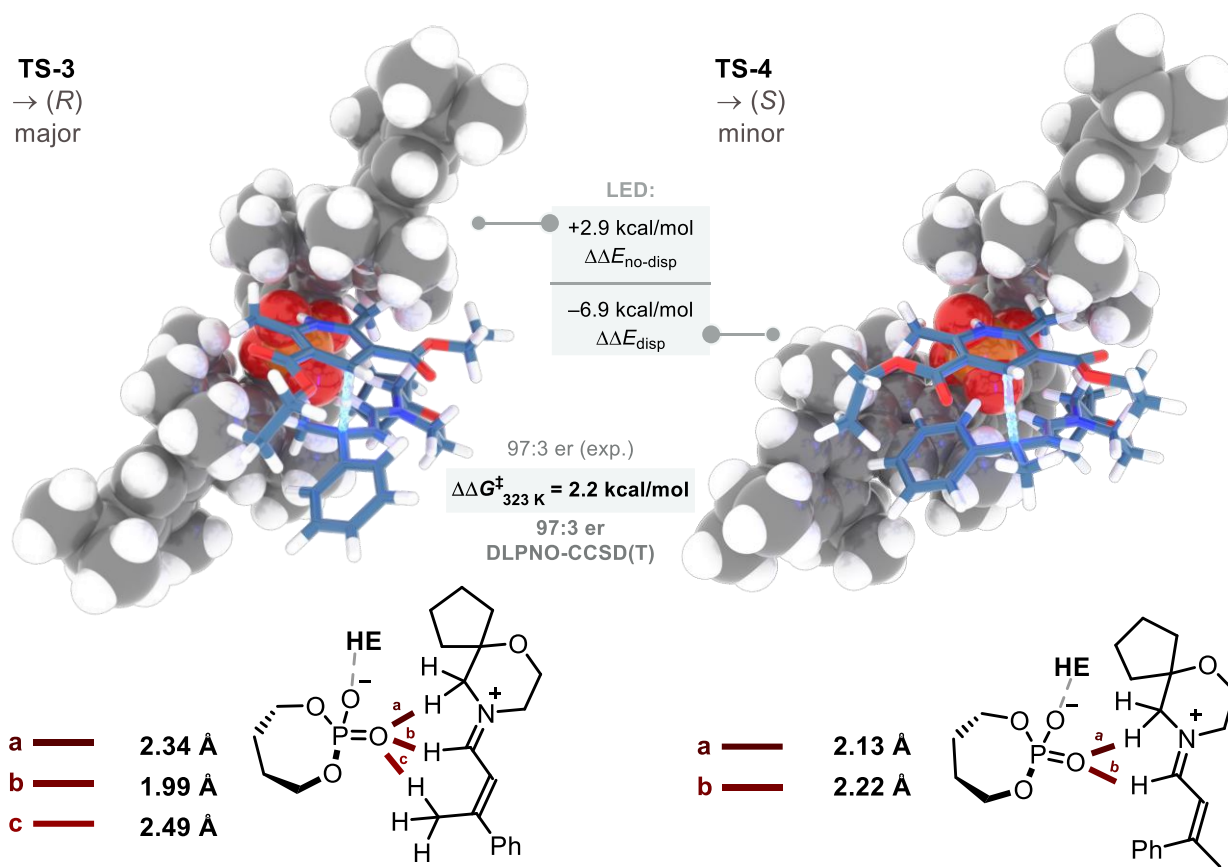
Figure 2.27 Computed transition states leading to the major and minor enantiomers in the improved system using **53f**: DFT transition state evaluation with Gibbs free enthalpies computed at the CPCM(1,4-dioxane)-DLPNO−CCSD(T)/cc-pVTZ//PBE-D3(BJ)/def2-SVP level of theory at 323 K/1 M. Key CH contacts are indicated. Energies are given in kcal/mol.

Following the successful development of a second-generation transfer hydrogenation catalyst, we computationally investigated the origin of its exceptional stereocontrol and the role of London dispersion. DFT calculations identified **TS-3** and **TS-4** as the relevant transition states leading to the major and minor enantiomers, respectively (Figure 2.27). Interestingly, transition states featuring an *endo*-orientation of the spiro functionality were found to be energetically preferred over their *exo*-configured counterparts. This computational result supports our hypothesis that stabilizing attractive interactions, rather than steric repulsion, play a key role in stereocontrol (cf. Figure 2.24, p. 42). The methyl groups of Hantzsch ester **33** are deeply embedded within the chiral phosphate pocket, effectively compensating for the absence of the isopropyl group. Structurally, **TS-3** resembles **TS-1** of the 2006 system: the iminium ion adopts the *E-*

configuration of the C=C double bond, enabling three polarity-matched CH···O contacts. This configuration is consistent with the proposed enantioconvergence via a deprotonated dienamine intermediate (see p. 40).

In contrast, **TS-4**—leading to the minor enantiomer—differs from **TS-2** of the 2006 system and more closely resembles **TS-2b**. The *Z*-configured iminium ion enables two polarity-matched CH···O interactions: one involving the α-CH$_2$ of the morpholine and another from the formyl CH. The β-phenyl group is oriented toward the phosphate pocket, albeit slightly twisted.
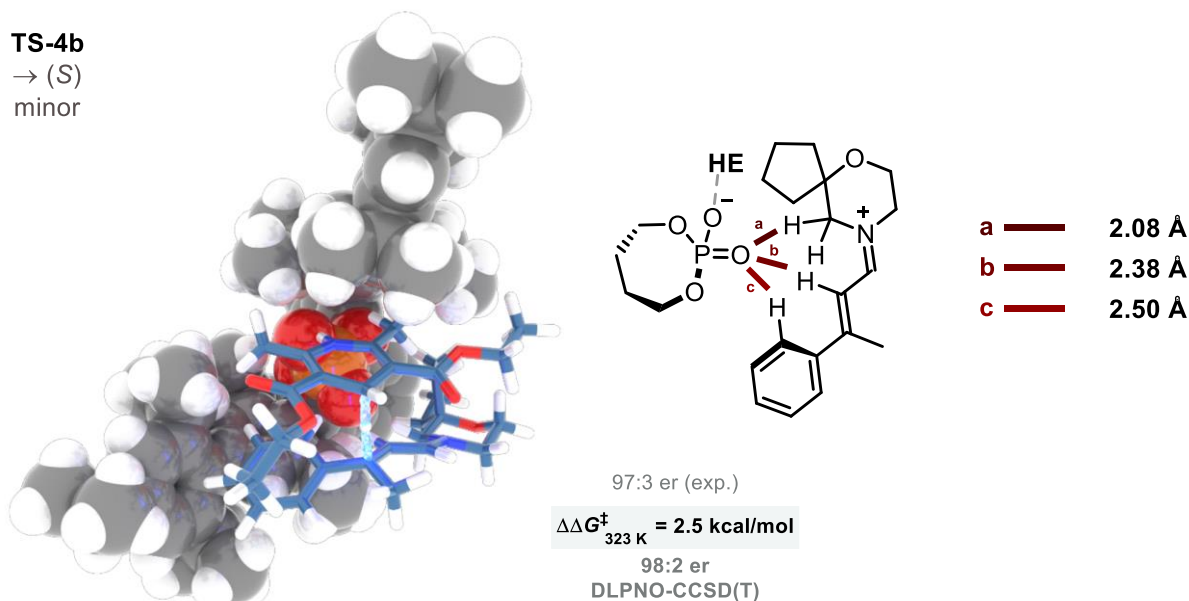
Figure 2.28 Additional, higher-energy transition state leading to the minor enantiomer. Computational details as in Figure 2.26.

An additional low-lying transition state, **TS-4b**, was also located (Figure 2.28). Here, the iminium ion adopts the *E*-configuration and resembles a flipped version of **TS-3** (cf. **TS-2**). However, **TS-4b** is less stabilized than **TS-4** ($\Delta\Delta G^{\ddagger}$ = 2.2 kcal/mol for **TS-4** vs. $\Delta\Delta G^{\ddagger}$ = 2.5 kcal/mol for **TS-4b**), rendering it a less likely pathway.

Local Energy Decomposition Analysis

Differential local energy decomposition analysis of **TS-3** and **TS-4**, allowing the disassembly of the interfragment interactions, revealed **TS-3** to be dominantly stabilized by nondispersion interactions ($\Delta\Delta E_{\text{no-disp}}$ = 2.9 kcal/mol). However, this contribution is not as pronounced as that observed in the 2006 system. This reduction can be attributed to the *Z*-configuration of the iminium in **TS-4**, which enables two favorable electrostatic CH···O interactions with the phosphate, thereby diminishing the difference in electrostatic stabilization between **TS-3** and **TS-4**.

In contrast, **TS-4** experiences greater overall stabilization from dispersion interactions ($\Delta\Delta E_{disp}$ = 6.9 kcal/mol), primarily due to contacts between the iminium and the phosphate. In particular, close spatial proximity of the β-phenyl group to the 3,3'-substituents of the phosphate likely accounts for this enhanced dispersion contribution.

IGMH Analysis of Key Noncovalent Interactions

Visualization of noncovalent interfragment interactions between the combined Hantzsch ester–iminium ion system and the chiral phosphate counteranion reveals multiple stabilizing contacts in **TS-3** and **TS-4** (Figure 2.29, top). The color-coded structures (Figure 2.29, bottom) illustrate the atomic contributions to the overall interfragment interaction. In alignment with the transition state geometries and LED analysis, the IGMH maps indicate enhanced stabilizing interactions in **TS-4** at the iminium β-phenyl substituent compared to the corresponding β-CH₃ group in **TS-3**.

To assess whether the modified catalyst structure **53f**, relative to **15a**, enhances stereocontrol, the additional structural moieties introduced in **53f** were examined with respect to their contributions to transition state stabilization. In **TS-3**, stronger contacts between the morpholine spiro ring and the phosphate counterion result in greater stabilization than observed in **TS-4** (23.9% vs. 19.5% atomic contribution). In **TS-4**, the close contacts between the iminium β-phenyl group and the phosphate displace the spiro-cyclopentyl fragment from the catalyst pocket, likely accounting for the observed difference in stabilization. Regarding the second arene ring of the 3,3′-substituents—the 2,4,6-triisopropylphenyl groups—**TS-3** is more stabilized than **TS-4**, with the two 6-isopropyl groups contributing 13.4% and 12.4% in **TS-3**, versus 11.3% and 8.3% in **TS-4**.

Overall, the new catalyst design preferentially stabilizes **TS-3**, which leads to the major enantiomer, over **TS-4**. Favorable dispersion interactions compensate for the absence of the isopropyl group in the original Hantzsch ester **28**, demonstrating the success of our structural catalyst modifications.
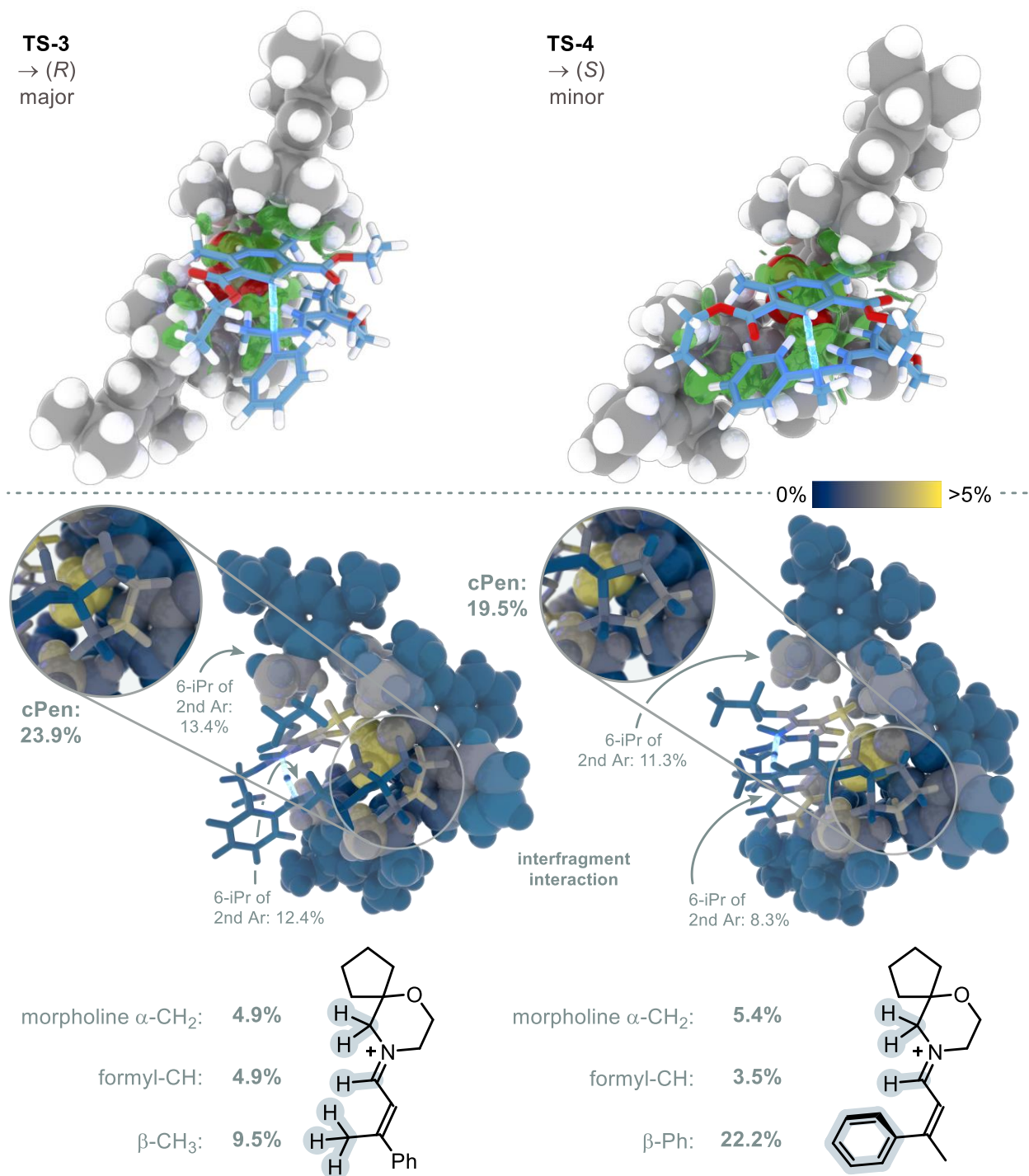
Figure 2.29 IGMH analysis using B3LYP-D3(BJ)/def2-TZVPP densities, highlighting key noncovalent interactions in **TS-3** and **TS-4** as isosurfaces of δg^{inter} with an isovalue of 0.004 (top), and with color-coded atoms according to their contribution to the overall interfragment interaction δG^{atom} (%) (bottom); structures are rotated relative to the top view to enhance visualization of critical interactions.

2.4 Summary and Outlook
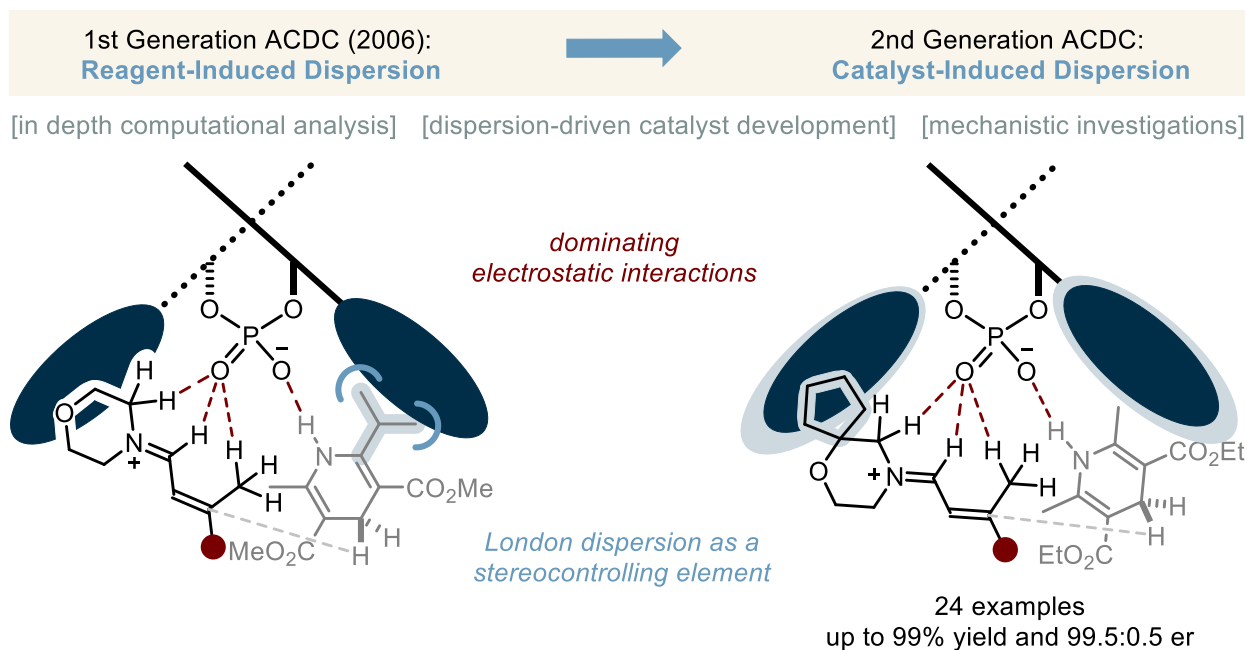
Figure 2.30 Summary of this chapter: Rational design of a general asymmetric catalyst for the transfer hydrogenation of α,β-unsaturated aldehydes by shifting dispersion control from reagent to catalyst through incorporation of DEDs, supported by computational analysis and mechanistic studies.

The pioneering 2006 report on the ACDC-enabled transfer hydrogenation of α,β-unsaturated aldehydes provided access to β-chiral aldehydes with excellent enantioselectivities.[114] However, the transformation faced several limitations, including the reliance on an engineered Hantzsch ester (**28**), a narrow substrate scope, and high catalyst loadings. Notably, replacement of ester **28** with the commercially available Hantzsch ester **33** led to a significant drop in enantioselectivity. This observation prompted a new working hypothesis: that the isopropyl group in ester **28** contributes to stereocontrol via attractive London dispersion interactions. As demonstrated in preceding literature, stabilizing dispersion interactions can significantly influence both reactivity and selectivity.[148,215] Motivated by this insight, we revisited the 2006 system using catalyst **15a** through in-depth computational analysis. The studies revealed that electrostatic interactions dominate the transition state geometry. Remarkably, alongside three key hydrogen bonds between the iminium cation and the chiral phosphate counteranion, dispersion interactions involving the isopropyl group of the Hantzsch ester were found to contribute significantly to transition state stabilization. These findings provided the conceptual foundation for a new design strategy: formally shifting the role of stabilizing dispersion interactions from the reagent to the catalyst itself (Figure 2.30).

By incorporating dispersion energy donors (DEDs) directly into the catalyst, a new catalyst, **53f**, comprising a chiral 2,3′,4,5′,6-pentaisopropyl-1,1′-biphen-4′-yl-substituted phosphate and a spiro-fused cyclopentane–morpholinium scaffold, was developed that overcomes the limitations of the previous system. Application

of **53f** in the transfer hydrogenation of various enals using the commercially available Hantzsch ester **33** enabled a broadened substrate scope, including diversely substituted aromatic enals as well as both sterically hindered and nonhindered examples, all at reduced catalyst loadings. Computational studies of the new system again revealed dominating electrostatic interactions involving hydrogen bonding. Analysis of the newly introduced structural elements confirmed that the DEDs stabilize the transition state leading to the major enantiomer, thereby contributing to stereocontrol as intended. Mechanistic experiments, including probing enantioconvergence, deuterium-labeling studies, and NMR kinetic analysis, further support these findings and demonstrate the extent to which catalyst **53f** exhibits superior activity compared to **15a**.
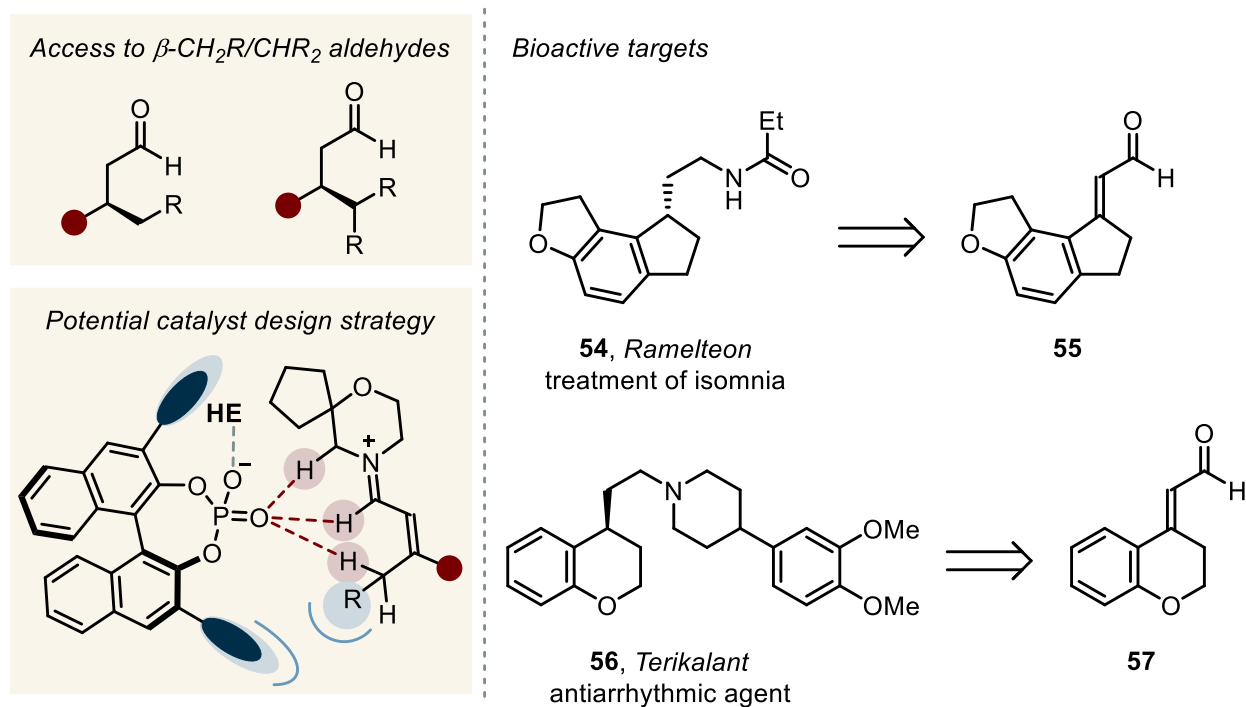
Figure 2.31 Outlook of this chapter: Expanding access to β-CH₂R/CHR₂ aldehydes via a dispersion-driven catalyst design strategy, enabling the synthesis of valuable building blocks for bioactive compounds.

While a broad range of β-methyl enals proved amenable to our transfer hydrogenation protocol, β-CH₂R cinnamaldehydes, such as **27y** and **27z**, presented challenges in achieving high levels of reactivity and enantioselectivity (Figure 2.22). Based on our transition state analysis, this diminished performance may stem from a weakened CH⋯O interaction due to reduced polarization or steric hindrance that interferes with close contacts. Nevertheless, the resulting β-chiral aldehydes are valuable synthetic intermediates for bioactive compounds such as Ramelteon (**54**) and Terikalant (**56**), making them highly desirable targets. Catalyst optimization could potentially unlock access to these scaffolds. Owing to the presence of a γ-proton, a polarity-matched orientation of the iminium intermediate may still be achievable, allowing for the characteristic three hydrogen bonds observed in the original systems. Although electrostatic interactions

may be attenuated by the increased steric bulk at the β-position, this could be compensated by designing catalysts with 3,3'-substituents on the phosphoric acid capable of engaging in stabilizing dispersion interactions with the β-alkyl substituent. Systematically varying the isopropyl substitution pattern on the 3,3'-biaryl backbone may provide a promising starting point for such catalyst optimization. Alternatively, less bulky and more flexible *n*-alkyl groups could be explored as DEDs. In addition to β-CH$_2$R cinnamaldehydes, the methodology may be further extended to include β-CHR$_2$ cinnamaldehydes (Figure 2.31).

Moving beyond the original catalyst class, alternative chiral anions such as more confined IDPs, iIDPs, or IDPis may also be considered. These often enzyme-like Brønsted acids offer multiple tunable structural parameters and may provide tailored solutions for these more demanding enal substrates.

3 CATALYTIC ASYMMETRIC IONIC HYDROGENATION OF α-ALKYL SYTRENES

3.1 Background

3.1.1 Organocatalytic Transfer Hydrogenation: From Activated to Unbiased Alkenes

As previously discussed in Section 2.1.1 (p. 15), various organocatalytic strategies have been developed for the transfer hydrogenation of distinct classes of C=C double bond-containing substrates using biomimetic dihydrogen donors (Figure 3.1). For instance, α,β-unsaturated carbonyl compounds are typically reduced via iminium ion catalysis or ACDC, while nitroolefins are well-suited for thiourea catalysis. In the case of electron-rich 1,1-diaryl alkenes, Brønsted acid catalysis (particularly with chiral phosphoric acids) has proven effective. Across all these transformations, the employed substrates share a common feature: activation of the C=C bond by electron-withdrawing or resonance-stabilizing groups. This activation renders the catalytic intermediates highly electrophilic at the β-position, or at the benzylic position in the case of *ortho*-quinone methide-type systems, facilitating subsequent hydride transfer.
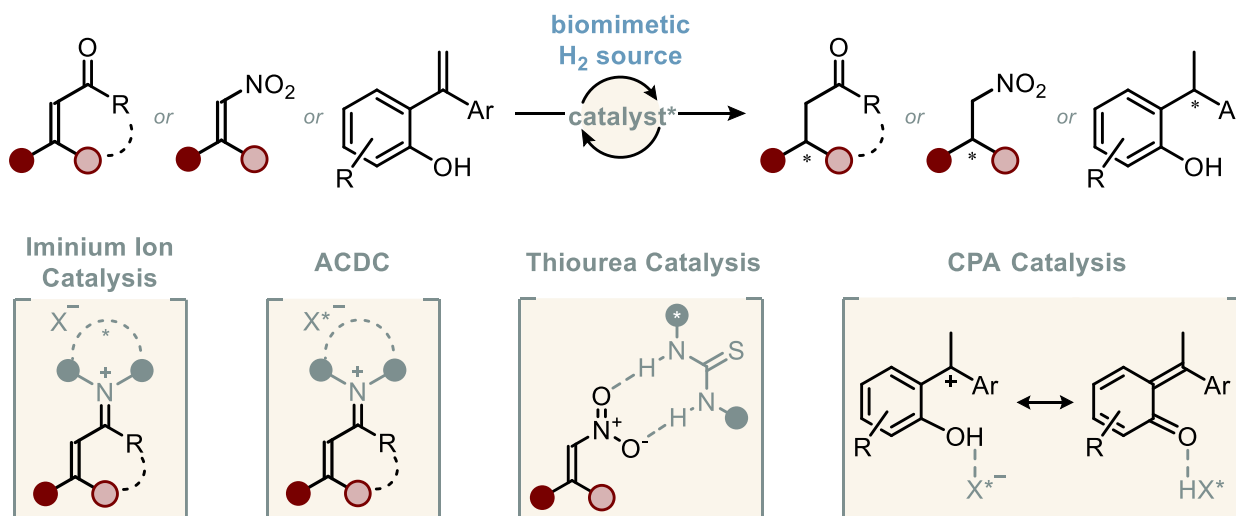
Figure 3.1 Organocatalytic asymmetric transfer hydrogenations of activated C=C double bonds.

On the other hand, stereoselective, metal-free transfer hydrogenations of electronically and structurally unbiased alkenes—such as aliphatic 1,1-disubstituted olefins—remain, to the best of our knowledge, scarce. Styrenes, although somewhat electronically activated through resonance stabilization of the benzylic position, also present a significant challenge in this context. This is particularly true for α-alkyl-substituted styrenes, which are considerably less stabilized than their α-aryl analogues. The absence of additional activating substituents, such as 4-methoxy or -hydroxyl groups, further increases the difficulty, as reflected by the very limited number of reported stereoselective transfer hydrogenations for such substrates.[216–218]

Among potential strategies, Brønsted acid catalysis stands out as a particularly promising approach. Brønsted acids function as broadly applicable catalysts, requiring only the presence of electron density—an inherent feature of (unbiased) alkenes. Upon protonation, such alkenes can generate carbocation intermediates, which may then undergo hydride transfer from a suitable reductant. Two critical challenges must be addressed to realize this transformation asymmetrically: (I) identifying dihydrogen surrogates that are compatible with acidic conditions, and (II) introducing a chiral element capable of exerting stereocontrol during hydride delivery (Figure 3.2).
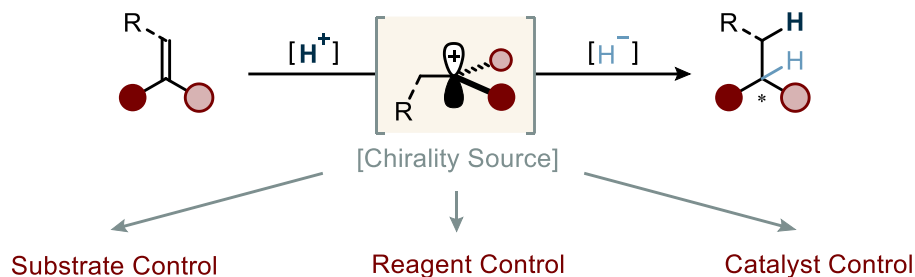
Figure 3.2 Strategic requirements for asymmetric transfer hydrogenation of unactivated alkenes: acid-compatible dihydrogen surrogates and stereocontrol during hydride transfer.

3.1.2 Dihydrogen Surrogates under Acidic Conditions

Biomimetic dihydrogen surrogates (such as Hantzsch esters, benzothiazolines, indolines, and dihydrophenanthridines) bear basic secondary amino groups capable of forming hydrogen bonds, a feature often critical for stereocontrol in the transition states of asymmetric transfer hydrogenations.[142,219–221] However, when applying a Brønsted acid-based strategy to activate electronically or structurally unbiased alkenes, strongly acidic conditions are typically required. Under such conditions, these nitrogen-containing reductants are more likely to interfere with the selective activation of the alkene and undergo protonation themselves. This incompatibility is reflected in the lack of reports on acid-mediated alkene reductions using these types of hydrogen donors.[222] In contrast, acid-tolerant reductants, such as silanes, cyclohexadiene derivatives, ketones, and hydrazine have been successfully employed as hydrogen sources under strongly acidic conditions, albeit predominantly in non-asymmetric transformations (Figure 3.3)[217,218,222–226].
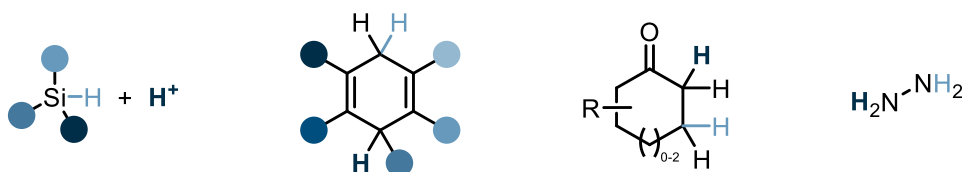
Figure 3.3 Successfully applied dihydrogen surrogates in acid-mediated transfer hydrogenations: silanes, cyclohexadiene derivatives, ketones, and hydrazine.

In the 1960s, Kursanov and Parnes introduced the concept of *ionic hydrogenation* for the reduction of a variety of unsaturated bonds (e.g., C=C, C=O, C=N), as well as single bonds such as C–OH and C–X (with X = halogen). Utilizing hydrosilanes in the presence of excess trifluoroacetic acid (TFA), they demonstrated efficient reduction of several 1,1-disubstituted alkenes.[223,224] The proposed mechanism involves reversible protonation of the unsaturated bond to generate a carbocation intermediate, which may be trapped by trifluoroacetate, forming a transient alkyl trifluoroacetate species. This intermediate can revert to the carbocation, followed by hydride transfer from the silane, ultimately affording the reduced product along with silyl trifluoroacetate as a byproduct (Figure 3.4). Upon neutralization of the reaction mixture, the silyl ester often hydrolyzes to give silanols and disiloxanes.
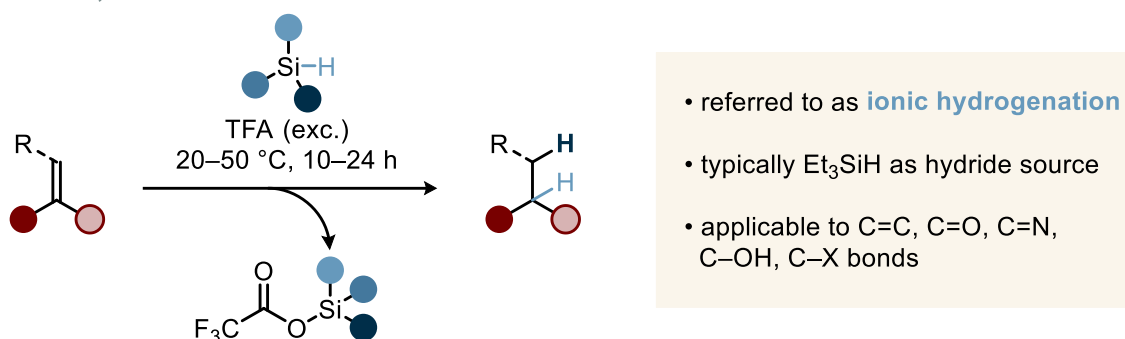
Figure 3.4 Ionic hydrogenation of 1,1-disubstituted alkenes using hydrosilanes and excess trifluoroacetic acid.

This strategy highlights the compatibility of silanes with strong Brønsted acids such as TFA, as no dihydrogen forms under the reaction conditions. Notably, other hydride donors—particularly hydrocarbon-based species—were also investigated. Among them, 1,4-dihydronaphthalene and 9,10-dihydroanthracene emerged as a promising alternative, especially under more acidic conditions where silanes are prone to protolytic degradation. Frank *et al.* recently developed a catalytic ionic hydrogenation using silanes for the selective reduction of furans to 2,5-dihydrofurans or tetrahydrofurans, with the reaction outcome governed by the choice of Brønsted acid catalyst (TFA or TfOH). The utilization of HFIP as the solvent proved crucial in order to suppress undesired polymerization.[227]

The group of Martin Oestreich revisited the concept of hydrocarbon-based dihydrogen surrogates and developed a bistriflimide-catalyzed transfer hydrogenation of alkenes employing 1,3,5-trimethylcyclohexa-1,4-diene (**58**) under ambient conditions (Figure 3.5, left).[222] Analogous to biomimetic hydride donors such as Hantzsch esters, the driving force of this reduction arises from the aromatization to the corresponding benzene derivative. Notably, weaker Brønsted acids such as triflic acid (TfOH) and *p*-toluenesulfonic acid (*p*-TsOH) were also found to be effective catalysts.

More recently, Zhou, Yang, and co-workers disclosed a related TfOH-catalyzed hydrogenation of α-substituted styrenes using ketones as dihydrogen donors.[225] In particular, 1-tetralone (**59**) enabled efficient reduction of a broad range of unbiased styrenes (Figure 3.5, right). However, the transformation required relatively high catalyst loadings and elevated temperatures. Interestingly, the proposed driving force is again aromatization, though not to the expected 1-naphthol. Instead, the reaction proceeds via dimerization to form a dinaphtho[1,2-*b*:1′,2′-*d*]furan structure.
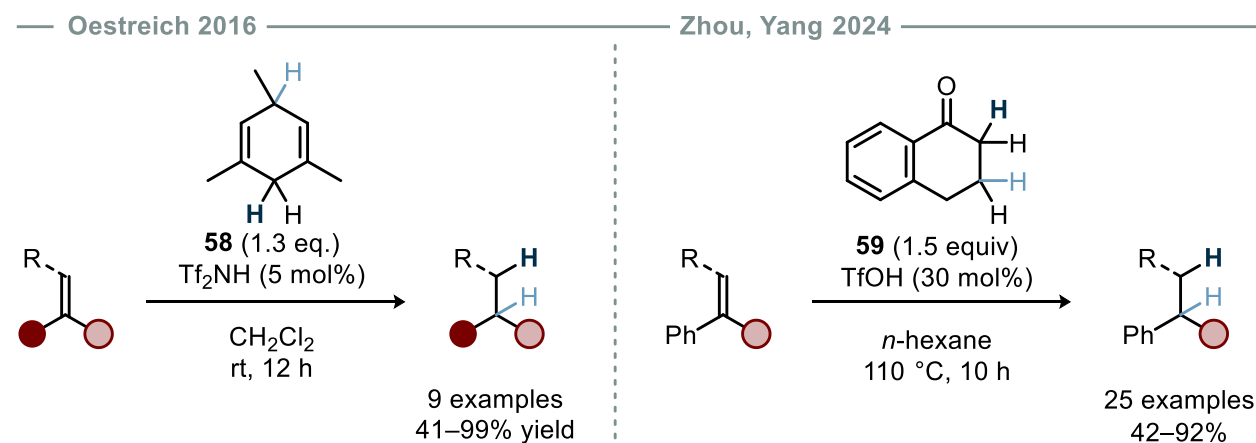
Figure 3.5 Bistriflimide-catalyzed transfer hydrogenation of 1,1-disubstituted alkenes using 1,4-cyclohexadiene as a dihydrogen surrogates (left). Triflic acid-catalyzed transfer hydrogenation of styrenes using 1-tetralone as a dihydrogen surrogate (right).

Additionally, hydrazine has been employed as a reductant for olefins in aerobic transfer hydrogenations. While guanidine- or flavin-derived organocatalysts are commonly used to mediate diimide formation,[228–233] a Brønsted acid-catalyzed variant was reported by the Imada group.[226] *p*-Toluenesulfonic acid reversibly protonates hydrazine, which is irreversibly oxidized to diimide under an oxygen atmosphere. The acid catalyst facilitates isomerization between *trans*- and *cis*-diimide, with the latter serving as the active reducing species. Reduction of the olefin proceeds via a concerted *syn*-addition mechanism. Thus, both mono- and disubstituted olefins were efficiently reduced (15 examples, 74–100% yield), with nitrogen and water as the only non-toxic byproducts.

3.1.3 Strategies for Stereoselective Trapping of Carbocations in Olefin Reductions

Upon protonation of the olefin, a carbocation intermediate is generated. Depending on the origin of chirality, distinct modes of stereocontrol can be distinguished during the subsequent trapping event. In *substrate control*, alkenes bearing an α-stereogenic center enable diastereofacial discrimination of the planar carbocation. In *reagent control*, a chiral *H*-nucleophile facilitates enantioselective hydride delivery. Finally, *catalyst control* involves the use of a chiral catalyst that exerts enantiofacial differentiation through ion-pairing and other noncovalent interactions (Figure 3.6).[234]
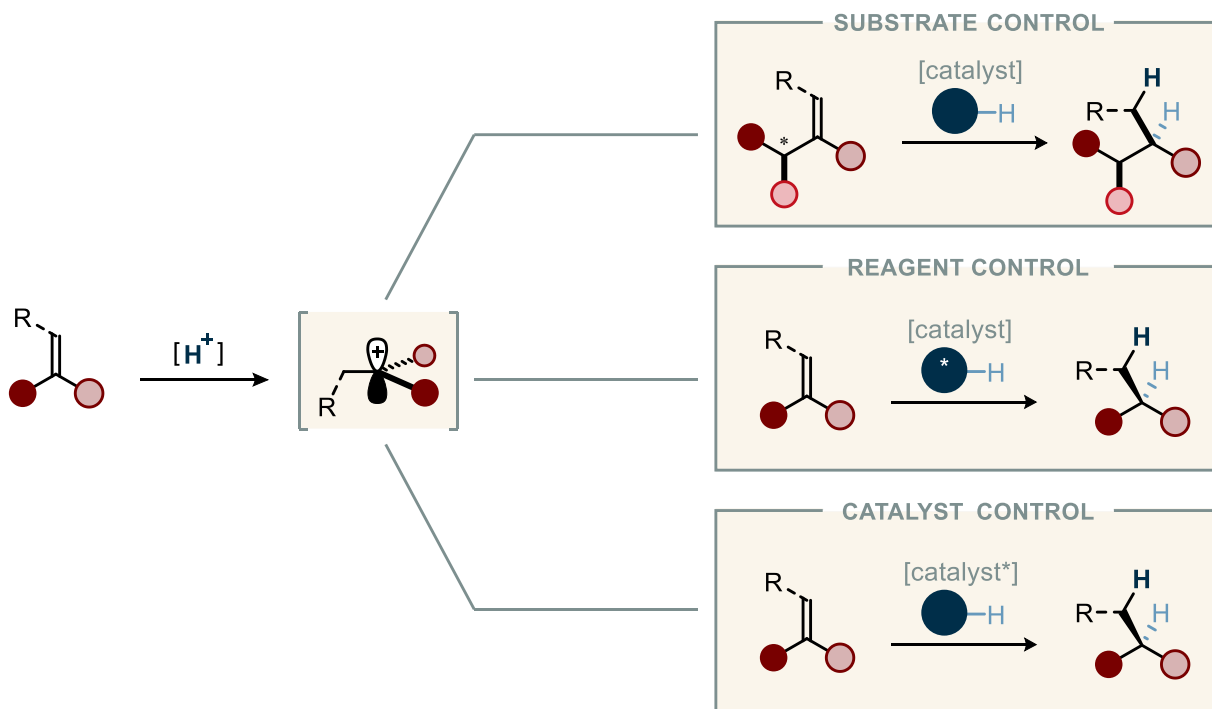
Figure 3.6 Stereoselective reduction strategies using Brønsted acids for unactivated alkenes: Substrate, reagent, and catalyst control.

In 2019, Gagosz, Chiba, and co-workers reported a diastereoselective 1,5-hydride transfer under Brønsted acid catalysis. Using α-stereogenic methyl styrenes (and tertiary alcohols) as precursors, they generated carbocation intermediates that underwent 1,5-hydride delivery from tethered alkyl ethers via a six-membered, chair-like transition state (Figure 3.7).[216] Although the process is formally redox-neutral, it exemplifies a substrate-controlled stereoselective hydride transfer to a carbocation intermediate.
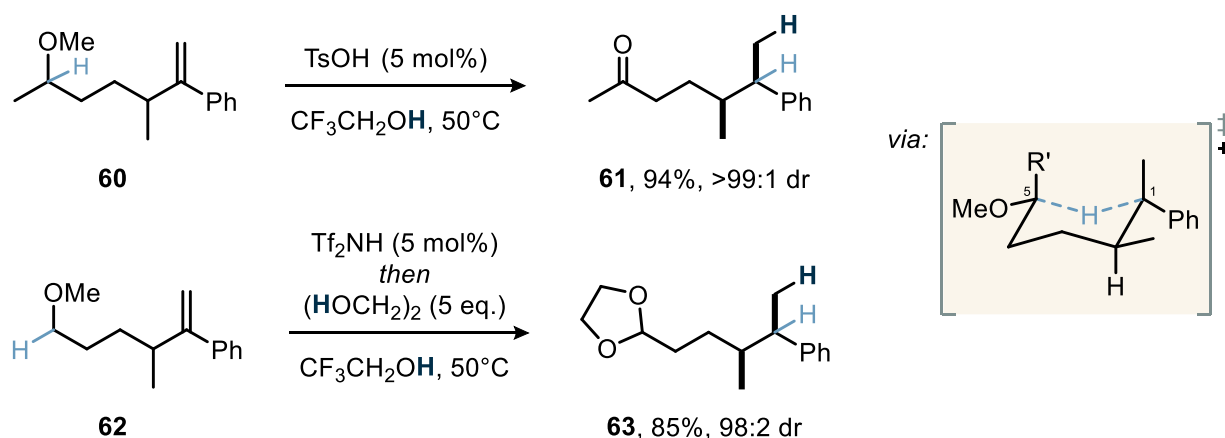
Figure 3.7 Substrate control: Diastereoselective intramolecular 1,5-hydride transfer.

An early example of reagent-controlled enantioselective alkene reduction dates back to the 1970s, when Fry employed a Si-stereogenic hydrosilane (**65**)[235] to reduce α-ethyl styrene (Figure 3.8, top).[218] Although

the enantiomeric excess was close to the detection limit in this ionic hydrogenation (51:49 er), this study likely represents the first of its kind.

More recently, in 2023, Qu, Oestreich, and co-workers advanced this concept by developing an enantioselective transfer hydrogenation of α-alkyl styrenes using chiral cyclohexa-1,4-dienes as dihydrogen surrogates (Figure 3.8, bottom).[217] Building on their previous work with achiral cyclohexadiene derivatives[222,236], they introduced chirality into the hydride donor framework. The reaction is initiated by a trityl salt catalyst, which abstracts a hydride from diene **67** to generate a Wheland intermediate. This cationic arenium species acts as the active Brønsted acid, promoting olefin protonation and setting the stage for stereoselective hydride transfer from the cyclohexadiene. The products are obtained in good yields and moderate to good enantioselectivities. However, the substrate scope is somewhat limited, with most examples containing a *para*-methoxy group, which electronically activates the styrene.
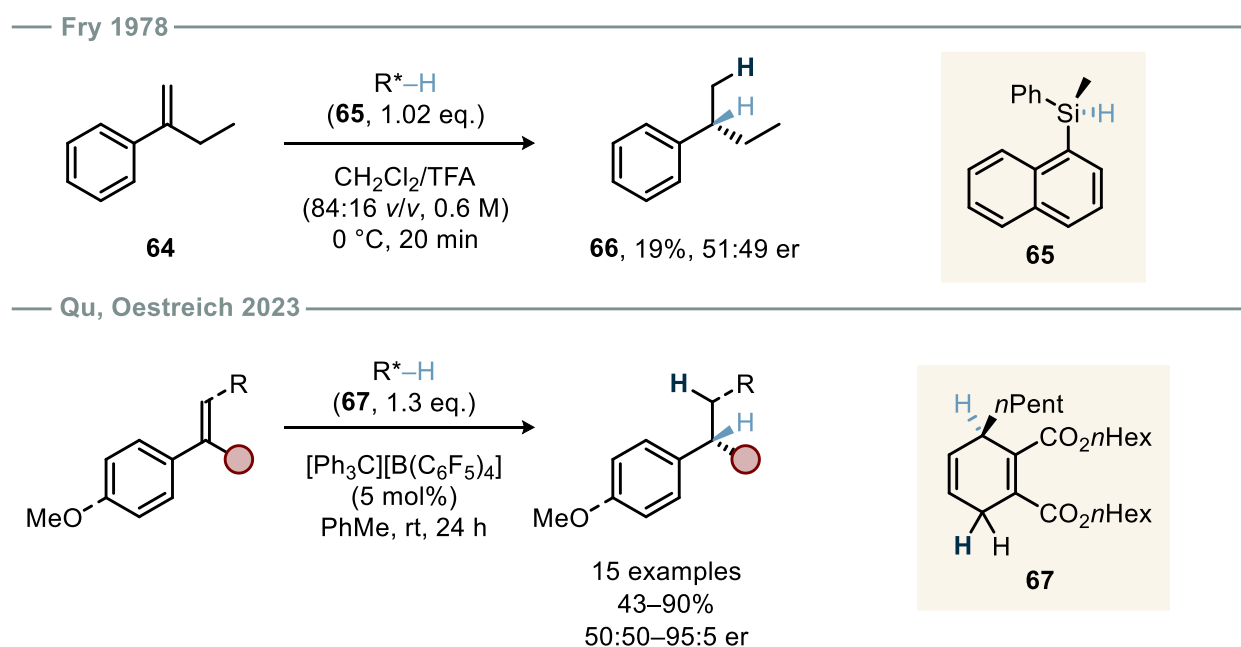
Figure 3.8 Reagent control: Si-stereogenic silanes for the enantioselective ionic hydrogenation of α-ethyl styrene (top). Chiral cyclohexa-1,4-diene for the enantioselective transfer hydrogenation of α-alkyl styrenes (bottom).

To the best of our knowledge, catalyst-controlled enantioselective reductions of unstabilized carbocations generated by olefin protonation have not yet been realized. Nonetheless, a few related transformations involving Brønsted acid activation of olefins and subsequent stereocontrolled trapping by *C-*, *N-* and *O-* nucleophiles have been developed (Figure 3.9).

***O*-nucleophiles:** In 2018, the List group reported a highly enantioselective IDPi-catalyzed intramolecular hydroalkoxylation of terminal olefins. Additionally, a single intermolecular example of styrene and benzyl alcohol was demonstrated, albeit with moderate enantioselectivity (76.5:23.5 er).[237] The same group later reported an intramolecular hydrolactonization under similar conditions.[238]

***C*-nucleophiles:** Terada demonstrated that azlactones serve as effective *C*-nucleophiles in a F_{10}-BINOL-derived NTPA-catalyzed addition to styrenes, enabling the construction of quaternary stereocenters with moderate to high enantioselectivity.[239] In their study about the non-classical 2-norbornyl cation, the List group applied IDPi catalysis to the Friedel–Crafts alkylation of 1,3,5-trimethoxybenzene using norbornene as a substrate.[240] An intramolecular hydroarylation of terminal olefins with tethered indoles was also achieved under IDPi catalysis.[241] Additionally, asymmetric Wagner–Meerwein shifts of alkenyl cycloalkanes to cycloalkenes via acid-catalyzed carbocation intermediates have been disclosed.[105]

***N*-nucleophiles:** A single example of an enantioselective intramolecular CPA-catalyzed hydroamination of a terminal olefin was reported by the Ackermann group, albeit with modest enantioselectivity (58.5:41.5 er).[242] Tan and Liu achieved significantly improved enantioselectivity by employing NTPA catalysis and selecting thioureas as tethered *N*-nucleophiles.[243–245] However, in both cases, the substrates relied on the Thorpe–Ingold effect, limiting the scope. In 2024, Hennecke *et al.* disclosed an IDPi-catalyzed hydroamination of both unbiased terminal and internal alkenes, furnishing pyrrolidines with high enantioselectivity.[246]
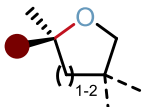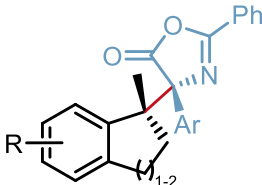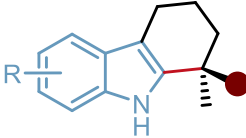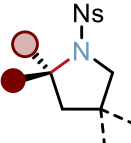
List 2018	Terada 2019	List 2021	Hennecke 2024
tethered *O*-nucleophile	*C*-nucleophile	tethered *C*-nucleophile	tethered *N*-nucleophile
21 examples	16 examples	22 examples	27 examples
41–94% yield	53–92% yield	67–97% yield	20–99% yield
92:8–98.5:1.5 er	76.5:23.5–96.5:3.5 er	84:16–98:2 er	50:50–>99:1 er

Figure 3.9 Selected examples of catalytic enantiofacial control over carbocations formed via olefin protonation with various *C*-, *N*- and *O*-nucleophiles.

These examples highlight the feasibility of catalyst-controlled trapping of carbocation intermediates with various *C*-, *N*-, and *O*-nucleophiles. However, analogous transformations involving hydride donors (i.e., *H*-nucleophiles) remain unprecedented. The predominance of intramolecular variants over intermolecular reactions further illustrates the inherent challenge of achieving high reactivity and selectivity in bimolecular processes.

3.2   Objectives

As outlined in Section 2.1.1 (p. 15), numerous organocatalytic biomimetic strategies have been developed for the enantioselective transfer hydrogenation of olefin substrates. Depending on the alkene subclass, distinct catalytic approaches have proven effective. For electron-deficient alkenes (enals, enones, and nitroolefins) iminium ion catalysis, ACDC, and thiourea catalysis have shown particularly high efficiency. In contrast, electron-rich α-(2-hydroxyaryl) styrenes have been reduced using chiral phosphoric acid catalysis. Despite their diversity, a common feature of these methodologies is their reliance on electronically activated olefin substrates.

Stereoselective, metal-free transfer hydrogenations of electronically or sterically unbiased alkenes remain rare and typically require either *substrate control* through pre-installed stereogenic centers or *reagent control* via the use of chiral *H*-nucleophiles. To the best of our knowledge, no example of an enantioselective, catalyst-controlled transfer hydrogenation has yet been reported for either electronically unactivated 1,1-dialkyl-substituted alkenes or α-alkyl styrenes lacking π-donor substituents.

Motivated by this gap, we envisioned an ionic hydrogenation of simple α-alkyl styrenes enabled by a chiral Brønsted acid catalyst (HX*, Figure 3.10). Although these substrates benefit from some degree of resonance stabilization, the absence of strong π-donating groups and the limited carbocation stabilization relative to
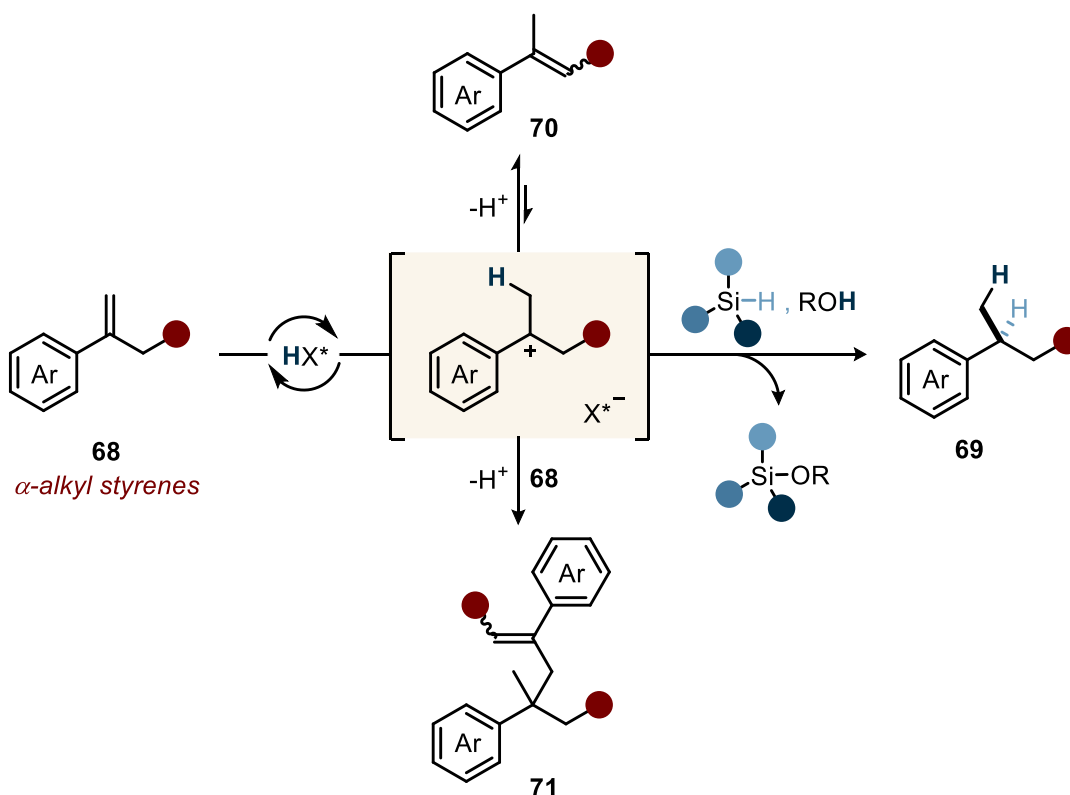
Figure 3.10 Objective of this chapter: Development of a chiral Brønsted acid-catalyzed ionic hydrogenation for the enantioselective reduction of α-alkyl styrenes.

α-aryl analogs make them particularly demanding. We reasoned that developing a successful protocol for these systems could establish a foundation for extending the strategy to fully unbiased alkenes, such as purely aliphatic 1,1-disubstituted olefins.

Upon protonation of an α-alkyl styrene (**68**), a chiral ion pair consisting of a benzylic carbocation and a chiral counteranion may be generated. This intermediate could then undergo nucleophilic attack by a hydrosilane, furnishing a chiral alkylbenzene product (**69**). The use of a stoichiometric oxygen-bound proton source (R–OH) not only ensures catalyst turnover but also provides a thermodynamic driving force through the formation of a strong Si–O bond. A central challenge associated with the proposed carbocationic intermediate lies in its propensity for unproductive side reactions. One major pathway involves the isomerization of the double bond, leading to the thermodynamically more stable trisubstituted styrene **70**. While this transformation may be reversible under certain conditions, re-protonation of the internal alkene is expected to be less favorable due to its reduced reactivity. Additionally, the carbocation can undergo reaction with another equivalent of styrene (**68**), yielding dimer **71**. The formation of higher oligomers cannot be entirely excluded, although it is considered less likely due to sterics and reduced nucleophilicity of the dimer.

The key to achieving an efficient and enantioselective ionic hydrogenation of α-alkyl styrenes lies in the identification of a chiral Brønsted acid catalyst that can both suppress competing isomerization and dimerization pathways and induce enantiocontrol. This control is hypothesized to arise from well-defined noncovalent interactions within the ion pair and the silane during the enantiodetermining hydride transfer step.

3.3   Results and Discussion

3.3.1   Reaction Development

Catalyst Optimization

The synthesis of selected catalysts was carried out in collaboration with Michael Merher.

We initiated our investigations by screening different chiral Brønsted acids for the ionic hydrogenation of the model substrate hex-1-en-2-ylbenene (**68a**) using dimethylphenylsilane as a hydride donor and benzoic acid as a proton source (Table 3.1). As discussed in Section 1.3.2 (p. 9), the selected BINOL-derived catalysts span a range of Brønsted acidities, enabling an assessment of how acid strength influences the reactivity and selectivity of the transformation. After three days at 60 °C with CPA **72** or IDP **73** ($pK_a > 10$, in MeCN)[3], less than 10% conversion exclusively to the undesired isomer **70a** was observed (entries 1, 2). More acidic DSI **19** and NTPA **74**[1] ($8.4 \geq pK_a > 5$, in MeCN) lead to higher conversions (>90%), albeit still only furnishing the double bond isomer (entries 3, 4). Finally, the use of confined IDPi **75a** ($pK_a = -7.4$, in DCE[94]; $4.5 > pK_a > 2$, in MeCN[1]) afforded the reduced alkylbenzene **69a** in 74% yield, with modest enantioselectivity (44.5:55.5 er), along with 15% isomer **70a** and traces of dimer **71a** (entry 5). With the presumably more acidic PADI **76**, the desired product **69a** was obtained in 90% yield. However, the open active site of the catalyst likely impairs enantioselection, resulting in an almost racemic mixture (50.5:49.5 er, entry 6).

Based on the initial Brønsted acid screening, IDPi catalysts emerged as a promising platform for further optimization. Under preliminary conditions, this catalyst class already afforded the desired alkylbenzene **69a** in encouraging yield and enantioselectivity. Furthermore, their structural framework offers tunable steric and electronic properties through variation of the 3,3'-aryl substituents and the *N*-perfluoroalkylsulfonyl moiety.

We next examined a series of IDPi catalysts bearing different substituents (Table 3.2). Although catalyst **75a**, featuring electron-withdrawing 3,5-bis(trifluoromethyl)phenyl groups, already provided **69a** in good yield, several other IDPis exhibited reduced reactivity and preferentially led to the formation of isomer **70a**. Substitution of the *N*-triflyl group with a pentafluorophenylsulfonyl group resulted in a decrease in yield of **69a**, but notably improved enantioselectivity across all tested variants. This trend is consistent with recent findings that IDPi catalysts bearing an $SO_2C_6F_5$ moiety are generally less Brønsted acidic than their SO_2CF_3 analogues, thereby rationalizing the observed reduction in reactivity.[94] Among the catalysts evaluated, we were pleased to find that the highly acidic, electron-rich heteroaromatic IDPis **82a** and **82b** delivered **69a**

---

[3] The exact pK_a values of the acids are not known, but are estimated based on structurally related catalysts (cf. Section 1.3.2, p. 9).

in synthetically useful yields (37% and 19%, respectively), with **82b** achieving a significantly improved enantiomeric ratio of 74:26 (entries 11, 12).

Table 3.1 Initial screening of chiral Brønsted acid catalysts for the asymmetric ionic hydrogenation of hex-1-en-2-ylbenzene (**68a**) using dimethylphenylsilane and benzoic acid.
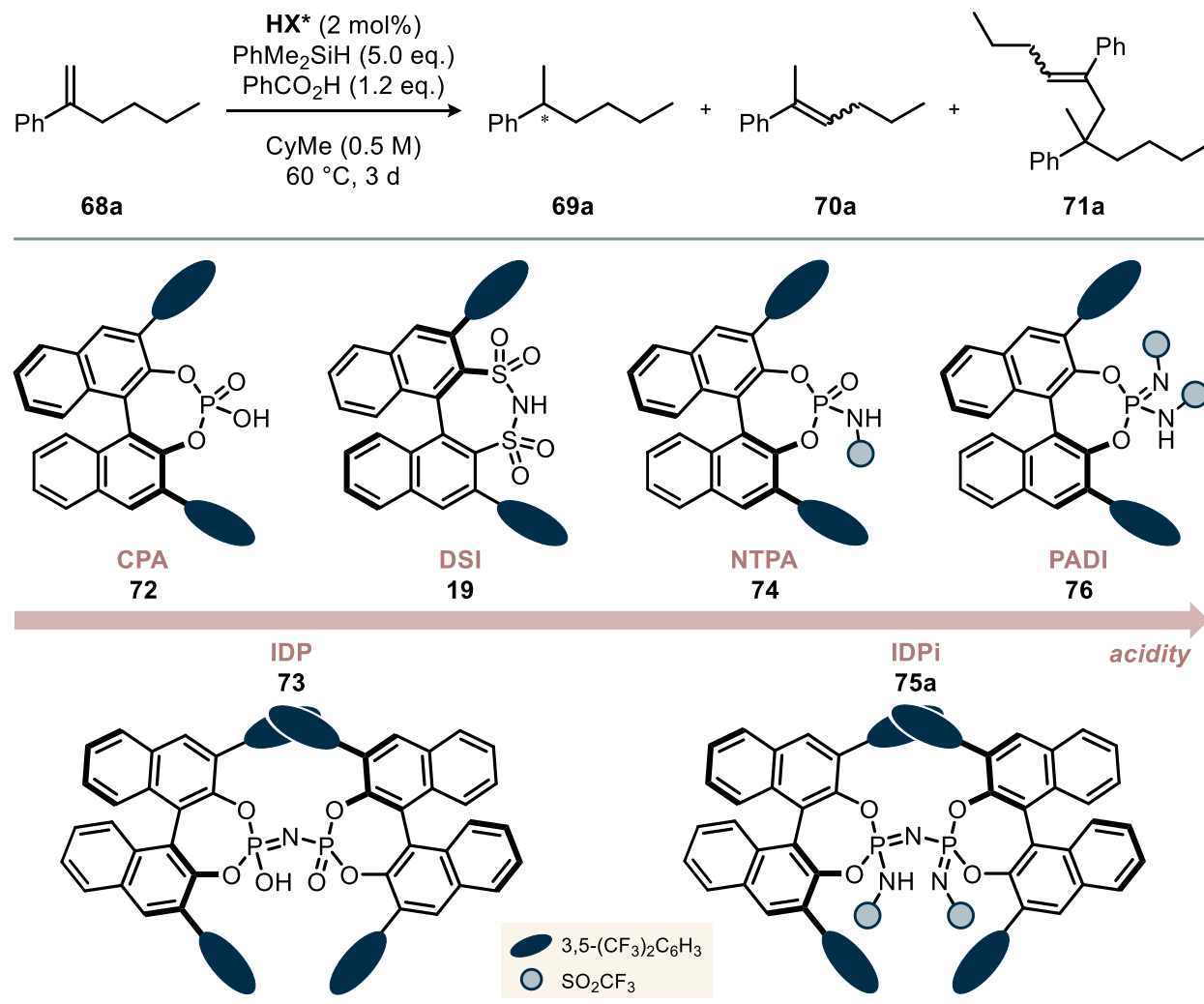
entry	HX*	conversion	yield (69a)	er (69a)	yield (70a)	yield (71a)
1	**CPA 72**	4%	0%	-	4%	0%
2	**IDP 73**	7%	0%	-	7%	0%
3	**DSI 19**	91%	0%	-	91%	0%
4	**NTPA 74**	95%	<1%	n.d.	94%	0%
5	**IDPi 75a**	99%	74%	44.5:55.5	15%	1%
6	**PADI 76**	100%	90%	50.5:49.5	1%	0%

Table 3.2 Screening of (*S,S*)-IDPi catalysts for the asymmetric ionic hydrogenation of hex-1-en-2-ylbenzene (**68a**) using dimethylphenylsilane and benzoic acid.
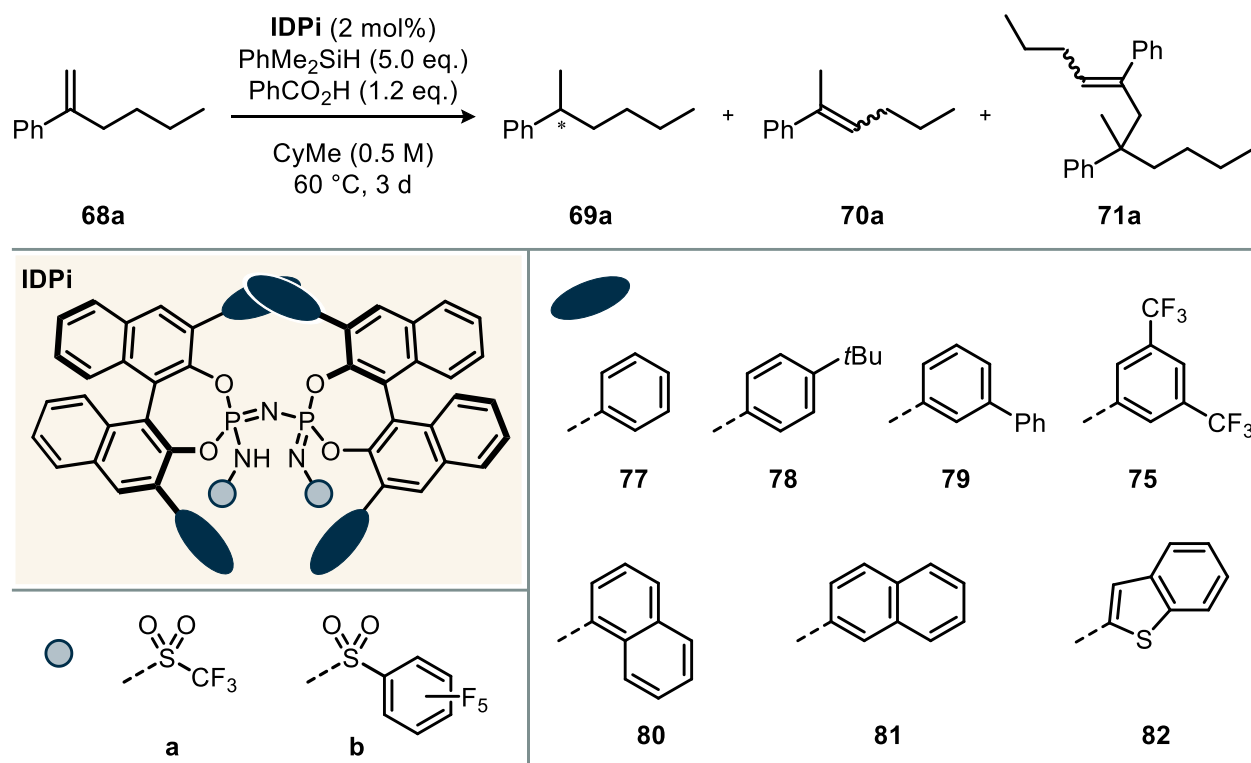
entry	IDPi	conversion	yield (69a)	er (69a)	yield (70a)	yield (71a)
1	**77a**	60%	4%	58:42	55%	0%
2	**78a**	25%	0%	-	21%	0%
3	**78b**	31%	0%	-	31%	0%
4	**79a**	93%	4%	59.5:40.5	89%	0%
5	**79b**	96%	9%	68.5:31.5	87%	0%
6	**75a**	99%	74%	44.5:55.5	15%	1%
7	**75b**	67%	9%	46.5:53.5	58%	0%
8	**80a**	48%	2%	57.5:42.5	46%	0%
9	**81a**	96%	11%	63:37	85%	0%
10	**81b**	66%	2%	67.5:32.5	64%	0%
11	**82a**	98%	**37%**	**57.5:42.5**	60%	1%
12	**82b**	97%	**19%**	**74:26**	77%	0%

With these key findings in mind, we proceeded to explore additional IDPi catalysts bearing heteroaromatic 3,3'-substituents and *N*-pentafluorophenylsulfonyl groups, aiming to further enhance both the yield and

enantioselectivity of the ionic hydrogenation of **68a**. Guided by the insights gained from the previous screening (Table 3.2), our catalyst design focused on two key observations: (I) Polyaromatic 3,3'-substituents appeared to benefit enantioselectivity, as seen in entries 9 and 10 (63:37 er and 67.5:42.5 er, respectively); (II) Electron-withdrawing CF$_3$ groups were associated with higher reactivity and yield (cf. entry 6). Compared to benzothiophen-2-yl substituted IDPi **82b**, its benzofuran-2-yl analogue (pK_a = 4.1 in MeCN[94]) afforded higher yield but lower enantioselectivity (Table 3.3, entry 1). As anticipated, extension of the π-system to naphtho[2,1-*b*]furan-2-yl in **84b** significantly improved the enantiomeric ratio (entry 2).

Table 3.3 Screening of heteroaromatic (*S*,*S*)-IDPi catalysts with *N*-SO$_2$C$_6$F$_5$ core for the asymmetric ionic hydrogenation of hex-1-en-2-ylbenzene (**68a**) using dimethylphenylsilane and benzoic acid.
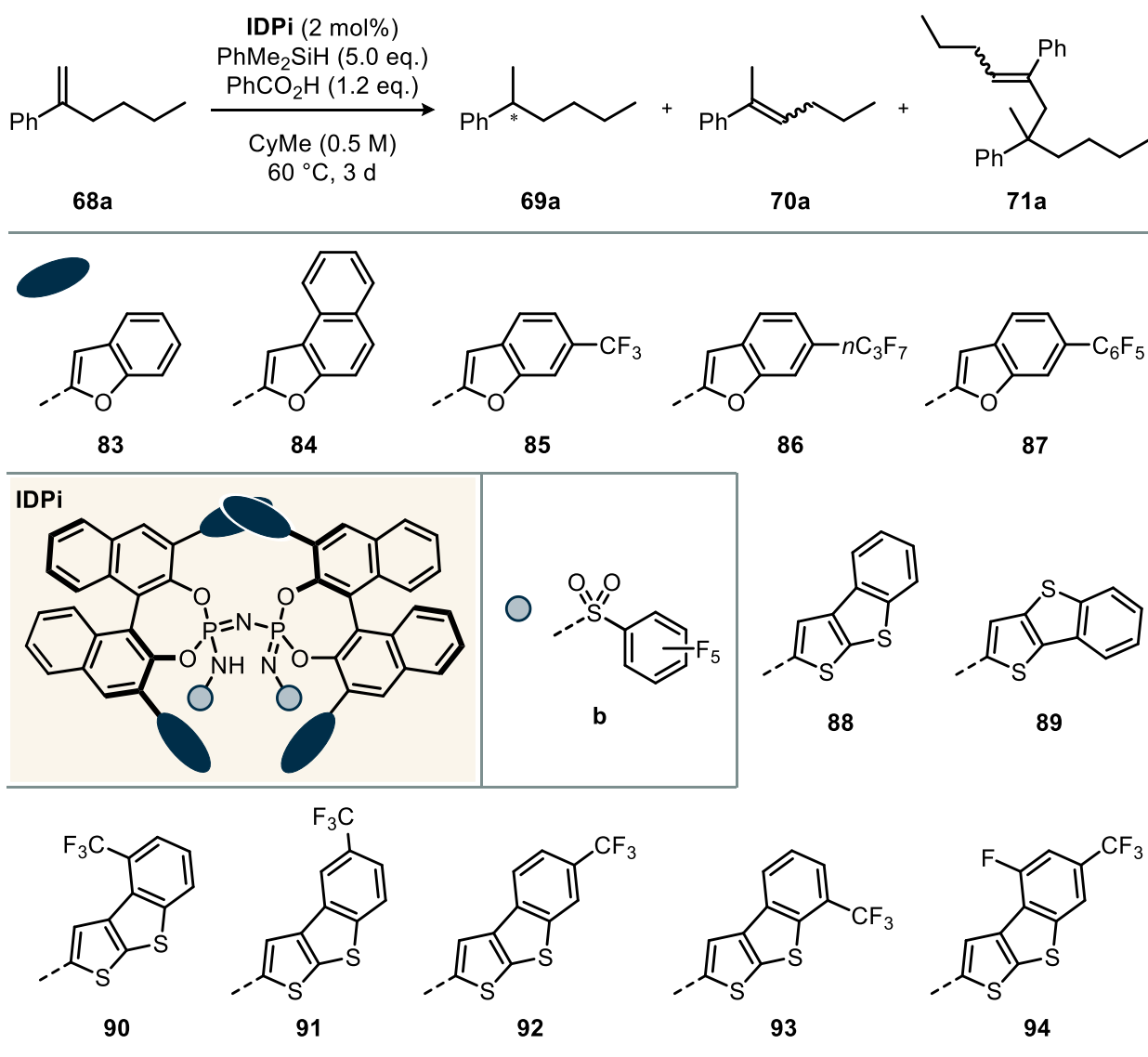
entry	IDPi	conversion	yield (69a)	er (69a)	yield (70a)	yield (71a)
1	**83b**	97%	33%	70:30	64%	0%
2	**84b**	98%	36%	80:20	61%	0%
3	**85b**	100%	98%	73:27	0%	0%
4	**86b**	100%	98%	69:31	0%	0%
5	**87b**	100%	81%	70.5:29.5	18%	1%
6	**88b**	98%	43%	82.5:17.5	54%	1%
7	**89b**	98%	29%	73.5:26.5	69%	1%
8	**90b**	99%	65%	84.5:15.5	33%	1%
9	**91b**	97%	20%	76.5:23.5	75%	1%
10	**92b**	100%	99%	83.5:16.5	<1%	<1%
11	**93b**	96%	8%	70:30	88%	0%
12	**94b**	99%	79%	78:22	20%	1%

Remarkably, introduction of perfluoroalkyl and –aryl groups in the 6-position of benzofuranyl resulted in yields of **69a** exceeding 80%, with IDPi **85b** (bearing a 6-CF$_3$ group) showing a promising enhancement in enantioselectivity (entries 3–5). Given that IDPis containing sulfur-based heteroaromatic substituents had previously shown superior enantiodiscrimination, we next evaluated IDPi variants **88b** and **89b** featuring benzothienothiophen-2-yl groups (entries 6 and 7). The electron-rich IDPi **88b**, bearing a benzo[*b*]thieno[3,2-*d*]thiophen-2-yl moiety, furnished **69a** in a notable enantiomeric ratio of 82.5:17.5, along with a surprisingly high yield of 43%. Finally, additional trifluoromethyl substituents at various positions of the heteroarene were introduced to further improve the yield (entries 8–11). Whereas regioisomers **91b** (5-CF$_3$) and **93b** (7-CF$_3$) delivered the product with reduced yield and selectivity, IDPis **90b** (4-CF$_3$) and **92b** (6-CF$_3$) outperformed all previously tested catalysts. Notably, **92b** furnished **69a** in almost quantitative yield with an enantiomeric ratio of 83.5:16.5 (entry 10). However, further substitution with a fluorine atom at the 4-position (IDPi **95b**, entry 12) resulted in inferior performance in both yield and selectivity.
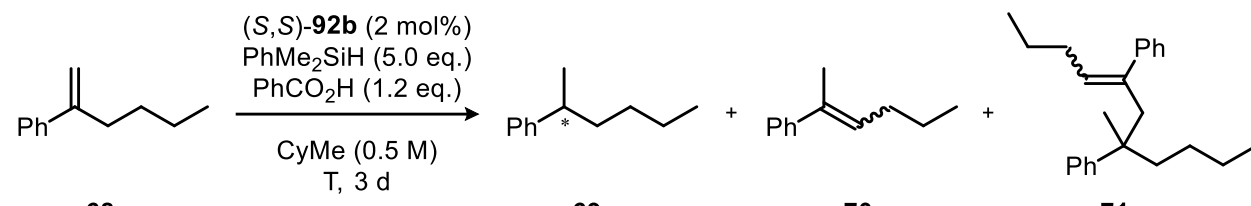
Given that IDPi **92b** furnished alkylbenzene **69a** with a promising balance of yield and enantioselectivity, it was selected for further optimization studies. Key reaction parameters investigated included temperature, the nature and stoichiometry of the silane, the proton source, and the reaction solvent.

Temperature Optimization

We began optimizing additional reaction parameters by incrementally lowering the reaction temperature (Table 3.4). As anticipated, a trend of increasing enantioselectivity was observed at lower temperatures. However, the reactivity decreased in parallel, with enhanced isomerization to **70a** and a corresponding reduction in the yield of **69a** at 20 °C (entries 1–3). Lowering the temperature further to –20 °C led to consistent yields of approximately 80% for **69a**, along with diminished formation of isomer **70a** (entries 3–5). We attribute this trend to a temperature-dependent equilibrium between styrenes **68a** and **70a**, mediated by a carbocation intermediate. At elevated temperatures (e.g., 60 °C), isomerization is rapid and reversible. Reprotonation of the less reactive trisubstituted alkene **70a** remains feasible, allowing for near-quantitative conversion with only trace amounts of unreacted **70a**. In contrast, at 20 °C, the thermodynamically more stable **70a** is less likely to be efficiently reprotonated to form the reactive carbocation intermediate required for hydride transfer. As a result, **70a** accumulates and the formation of **69a** is suppressed. At even lower temperatures (entries 3–6), the isomerization from **68a** to **70a** becomes increasingly disfavored, leading to reduced formation of the isomer.

Interestingly, dimerization is promoted at lower temperatures, with dimer **71a** reaching a maximum of 7% at –40 °C (entry 6). In addition, a pronounced drop in yield of **69a** was observed at –40 °C. Based on these results, –20 °C was selected as the optimal temperature for further optimization studies, furnishing **69a** in 79% yield with 92.5:7.5 er.

Table 3.4 Screening of different temperatures for the asymmetric ionic hydrogenation of hex-1-en-2-ylbenzene (**68a**) using (*S*,*S*)-IDPi **92b** as the catalyst, dimethylphenylsilane and benzoic acid.

entry	temperature	conversion	yield (69a)	er (69a)	yield (70a)	yield (71a)
1	60 °C	100%	99%	83.5:16.5	1%	1%
2	40 °C	100%	84%	86.5:13.5	8%	2%
3	20 °C	100%	79%	89:11	14%	5%
4	0 °C	100%	82%	91:9	9%	5%
5	–20 °C	98%	79%	92.5:7.5	3%	5%
6	–40 °C	62%	48%	94:6	0%	7%

Evaluation of Silane Reductants and Stoichiometry

Next, various silanes were evaluated as hydride donors (Table 3.5). Use of the secondary silane methylphenylsilane resulted in both reduced yield and enantioselectivity, along with significantly increased dimer formation (entry 2). Similarly, methyldiphenylsilane, bearing two aromatic substituents and one methyl group, gave poor results and was therefore excluded from further consideration (entry 3). In contrast, the use of ethyldimethylsilane, a purely aliphatic silane, led to an excellent enantiomeric ratio of 95.5:4.5, albeit with a slightly reduced yield of 62% (entry 4). Further elongation of the alkyl chains, as in triethylsilane, resulted in lower yields due to increased formation of isomer and dimer byproducts, and also diminished enantioselectivity (entry 5).

Based on this outcome, ethyldimethylsilane was selected for further evaluation of silane stoichiometry. A clear trend was observed: reducing the amount of silane led to diminished yields of **69a** and a higher proportion of unproductive dimerization. Notably, the enantioselectivity remained largely unaffected across the tested range (entries 6–9).

Table 3.5 Screening of different silane reductants and their stoichiometry in the asymmetric ionic hydrogenation of hex-1-en-2-ylbenzene (**68a**) using (*S,S*)-IDPi **92b** as the catalyst and benzoic acid as the proton source. The total active concentration was kept constant at 0.5 M ($V_{silane} + V_{solvent} = $ const.).

entry	silane	eq.	conversion	yield (69a)	er (69a)	yield (70a)	yield (71a)
1	PhMe$_2$SiH	5.0 eq.	98%	79%	92.5:7.5	3%	5%
2	PhMeSiH$_2$	5.0 eq.	70%	26%	89.5:10.5	9%	17%
3	Ph$_2$MeSiH	5.0 eq.	85%	43%	88.5:11.5	8%	17%
4	EtMe$_2$SiH	5.0 eq.	62%	51%	95.5:4.5	2%	5%
5	Et$_3$SiH	5.0 eq.	67%	32%	94:6	5%	15%
6	EtMe$_2$SiH	4.0 eq.	73%	57%	95:5	5%	6%
7	EtMe$_2$SiH	3.0 eq.	62%	46%	95.5:4.5	3%	7%
8	EtMe$_2$SiH	2.0 eq	75%	50%	95.5:4.5	5%	10%
9	EtMe$_2$SiH	1.2 eq.	74%	35%	95:5	5%	17%

Effect of Oxygen-Bound Proton Sources

Given the high bond dissociation energy of Si–O bonds (~108 kcal/mol)[247], their formation provides a strong thermodynamic driving force for the reaction. To exploit this, various oxygen-bound proton sources were evaluated, as their conjugate bases are expected to trap the silyl group after hydride transfer (Table 3.6). Since benzoic acid had already delivered promising results (entry 1), acetic acid was tested as a representative aliphatic carboxylic acid. However, it showed poor reactivity, affording **69a** in only 15% yield (entry 2). The use of mesitol gave a comparable yield to benzoic acid (57%), though with slightly reduced enantioselectivity (92.5:7.5 er, entry 3). Aliphatic alcohols were then investigated. Hexafluoroisopropanol (HFIP) led to increased reactivity, affording **69a** in 68% yield along with 12% dimer formation; however, enantioselectivity dropped significantly to 79:21 er (entry 4). In contrast, isopropanol was found to be ineffective as a proton source, with no product formation observed (entry 5). Water similarly failed to promote catalyst turnover (entry 6).

Table 3.6 Screening of different proton sources in the asymmetric ionic hydrogenation of hex-1-en-2-ylbenzene (**68a**) using (*S*,*S*)-IDPi **92b** as the catalyst and ethyldimethylsilane as the hydride donor.

entry	H+ source	conversion	yield (69a)	er (69a)	yield (70a)	yield (71a)
1	PhCO₂H	60%	55%	95.5:4.5	2%	5%
2	AcOH	22%	15%	95:5	1%	3%
3	MesOH	79%	57%	92.5:7.5	4%	8%
4	HFIP	100%	68%	79:21	3%	12%
5	*i*PrOH	traces	traces	-	0%	0%
6	H₂O	traces	traces	-	0%	0%
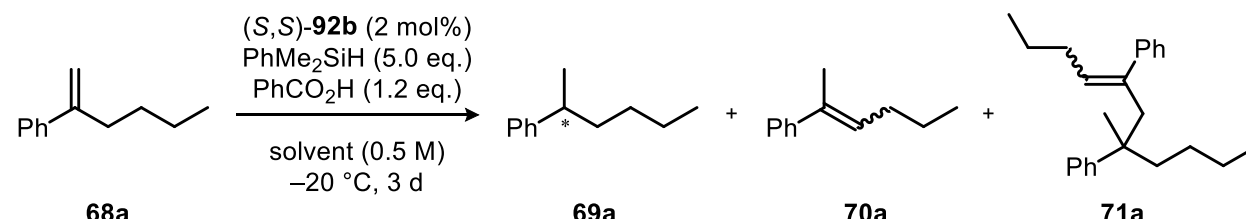
According to our initially proposed mechanism, the proton source is not involved in the enantiodetermining step, serving only to scavenge the silyl group *after* product formation and enable catalyst turnover. However, the variation in enantiomeric ratios of **69a** observed with different proton sources raises the possibility that a trimolecular enantiodetermining transition state—involving the ion pair (carbocation intermediate and IDPi counteranion), the silane, and the proton source—may be operative. Alternatively, the proton source may act as a spectator additive that modulates the reaction medium's polarity or hydrogen-

bonding environment, thereby indirectly influencing enantioselectivity. This question will be investigated in more detail in future studies (see *Influence of a Chiral Proton Source on Stereocontrol*, p. 82).

Solvent and Reaction Concentration Effects

Finally, various solvents were evaluated for the ionic hydrogenation of α-*n*-butylstyrene (Table 3.7). While chlorinated solvents furnished **69a** in comparably good yields, the enantioselectivity was reduced in both $CDCl_3$ and CD_2Cl_2 (entries 1 and 2). Ether-containing solvents showed poor reactivity: THF led to no product formation (entry 3), and diethyl ether afforded **69a** in only 28% yield (entry 4). Aromatic solvents such as toluene and xylene gave moderate yields but with diminished enantioselectivity (entries 5 and 6). Hydrocarbon solvents hexane and pentane provided the highest enantiomeric ratios observed, yet at the expense of increased dimer formation (entries 8 and 9). In contrast, methylcyclohexane suppressed dimerization to just 5% and delivered **69a** in the highest yield observed (51%), along with an excellent enantiomeric ratio of 95.5:4.5 (entry 7). Based on these results, methylcyclohexane was selected as the solvent for subsequent studies.

Table 3.7 Screening of different solvents in the asymmetric ionic hydrogenation of hex-1-en-2-ylbenzene (**68a**) using (*S*,*S*)-IDPi **92b** as the catalyst, ethyldimethylsilane and benzoic acid.

entry	solvent	conversion	yield (69a)	er (69a)	yield (70a)	yield (71a)
1	$CDCl_3$	68%	51%	90.5:9.5	7%	6%
2	CD_2Cl_2	73%	48%	86:14	9%	8%
3	THF	0%	0%	-	0%	0%
4	Et_2O	45%	28%	93.5:6.5	7%	5%
5	PhMe-d_8	58%	38%	92:8	6%	8%
6	*m*-xylene	43%	29%	93.5:6.5	6%	4%
7	CyMe	62%	51%	95.5:4.5	2%	5%
8	hexane	67%	36%	95:5	3%	14%
9	pentane	50%	27%	95.5:4.5	2%	10%

Subsequently, the effect of reaction concentration was investigated (Table 3.8). Decreasing the concentration from 0.5 M to 0.1 M primarily led to reduced reactivity, reflected in lower yields of the desired product **69a** as well as diminished formation of the dimer **71a**. In contrast, isomerization to **70a** and the enantioselectivity remained largely unaffected (entries 1–5). Notably, performing the reaction under neat conditions—using 10 equivalents of ethyldimethylsilane as both reagent and solvent—afforded **69a** in 72% yield with excellent enantioselectivity (95:5 er), while minimizing side product formation (entry 6). With these results, we established optimal reaction conditions and concluded the method development, enabling us to proceed with evaluating the scope and practicality of the transformation.

Table 3.8 Screening of solvent concentrations in the asymmetric ionic hydrogenation of hex-1-en-2-ylbenzene (**68a**) using (*S,S*)-IDPi **92b** as the catalyst, ethyldimethylsilane and benzoic acid.

entry	conc.	conversion	yield (69a)	er (69a)	yield (70a)	yield (71a)
1	0.5 M	62%	51%	95.5:4.5	2%	5%
2	0.4 M	61%	41%	95.5:4.5	2%	7%
3	0.3 M	50%	41%	95.5:4.5	3%	3%
4	0.2 M	53%	36%	96:4	2%	4%
5	0.1 M	34%	24%	96:4	3%	1%
6	neat, in 10 eq. EtMe$_2$SiH	80%	72%	95: 5	3%	3%

3.3.2 Reaction Scope

The synthesis of selected styrene substrates was carried out in collaboration with Michael Merher.

To evaluate the applicability of our ionic hydrogenation protocol, a range of α-alkyl styrenes was examined. Based on structural variations of the model substrate **68a**, we categorized the modifications into two classes: changes to the aryl moiety and changes to the alkyl substituent.

Aryl Modifications

68 → (S,S)-**92b** (2 mol%), EtMe$_2$SiH (10.0 eq.), PhCO$_2$H (1.2 eq.), neat, −20 °C, 3 d → **69** + **70** + **71**

69a
44%, 95:5 er
(67% **69a**, 3% **70a**, 3% **71a**)

69b[a]
62%, 93.5:6.5 er
(76% **69b**, 1% **70b**, 10% **71b**)

69c[b]
76%, 96:4 er
(79% **69c**, 3% **70c**, 6% **71c**)

69d
70%, 96:4 er
(95% **69d**, 4% **70d**, 1% **71d**)

69e*[b]
91.5:8.5 er
(56% **69e**, 4% **70e**, 4% **71e**)

69f*[c]
82:18 er
(84% **69f**, 3% **70f**, 9% **71f**)

69g[b]
69%, 95.5:4.5 er
(88% **69g**, 3% **70g**, 5% **71g**)

69h[c]
89%, 95.5:4.5 er
(90% **69h**, 1% **70h**, 4% **71h**)

69i[d]
72%, 95:5 er
(83% **69i**, 17% **70i**, 0% **71i**)

69j[c]
77%, 97:3 er
(98% **69j**, 2% **70j**, 0% **71j**)

69k
76%, 98:2 er
(82% **69k**, 1% **70k**, 9% **71k**)

69l
63%, 97:3 er
(80% **69l**, 0% **70l**, 11% **71l**)

69m*[b]
89.5:10.5 er
(27% **69m**, 17% **71m**)

Figure 3.11 Substrate scope of the ionic hydrogenation: α-alkyl styrenes bearing aryl modifications. All reactions were conducted on a 0.20 mmol scale. Yields are reported as isolated yields after column chromatography. ^{1}H-NMR yields, reported in parentheses (gray), were determined using CH$_2$Br$_2$ as internal standard. [a]Reaction performed at −50 °C. [b]Using EtMe$_2$SiH (5.0 eq.) in CyMe (0.5 M). [c]Using PhMe$_2$SiH (5.0 eq.) in CyMe (0.5 M). [d]Reaction performed at 10 °C using PhMe$_2$SiH (10.0 eq.) under neat reaction conditions. *Reactions conducted on a 0.025 mmol scale.

The ionic hydrogenation was applied to various aryl-modified α-alkyl styrenes on a 0.20 mmol scale for product isolation (Figure 3.11). In parallel, crude reaction mixtures were analyzed by ^{1}H NMR spectroscopy to determine accurate yields of the desired (sometimes volatile) products **69** and side products **70** and **71**, allowing for a comparative assessment of substrate reactivity.

With model substrate **68a**, the alkylbenzene **69a** was isolated in moderate yield and excellent enantiomeric ratio (95:5 er). Electron-neutral analogues **68b** and **68c**, bearing methyl substituents, afforded improved yields (~80% ^{1}H NMR yield), with the *meta*-substituted derivative **69c** providing excellent enantioselectivity (96:4 er). In contrast, the *para*-substituted compound required adjusted reaction conditions at –50 °C to achieve high enantioselectivity (93.5:6.5 er) and showed more pronounced dimerization (10%).

Increasing the steric bulk of the *meta*-substituent from ethyl (**68d**) to isopropyl (**68e**) and *tert*-butyl (**68f**) led to diminished reactivity and enantioselectivity, with the latter requiring the more reactive dimethylphenylsilane to furnish acceptable yields. This trend suggests that increased steric hindrance may interfere with efficient hydride transfer. Notably, the disubstituted product **69g** was obtained in very good yield and with excellent enantioselectivity.

Halogenated styrenes (**68h** and **68i**) and the *meta*-methoxylated derivative **68j** were also well tolerated using dimethylphenylsilane. The electron-deficient *meta*-bromo substrate required slightly elevated temperature (10 °C) to achieve satisfactory conversion.

Electron-rich polyaromatic substrates also participated well, with the naphthyl derivative **69k** furnishing the product in very good yield (82% NMR yield) and the highest enantioselectivity observed across the series (98:2 er, Figure 3.11). In the case of heteroaromatic styrenes, the position of substitution proved critical: **69l** (from 5-substituted benzofuran) was isolated in very good yield and excellent enantioselectivity (97:3 er), whereas **69m** (from 6-substituted benzofuran) was obtained in lower yield and with reduced selectivity (89.5:10.5 er). Notably, electron-rich substrates (**68k**–**m**) showed increased levels of dimerization, in contrast to electron-deficient styrenes, for which dimer formation was minimal or absent. This observation suggests a possible correlation between electron density and dimerization propensity.

To evaluate the scalability of the method, the ionic hydrogenation of methoxy-substituted styrene **68j** was performed on a 5.0 mmol scale. The catalyst loading could be reduced to 1 mol%, and the reaction was run over seven days, delivering results comparable to those obtained on small scale. The reaction furnished 712 mg of the desired product **69j** in 75% isolated yield with excellent enantioselectivity (97:3 er). Furthermore, catalyst **92b** was recovered after the reaction and reisolated in 88% yield (Figure 3.12, top). For determination of the absolute configuration, **69j** was further derivatized via a two-step sequence: demethylation with BBr₃, followed by reaction with 4-bromophenyl isocyanate to furnish carbamate **95**.

Recrystallization of **95** enabled structure elucidation by single-crystal X-ray diffraction (Figure 3.12, bottom).
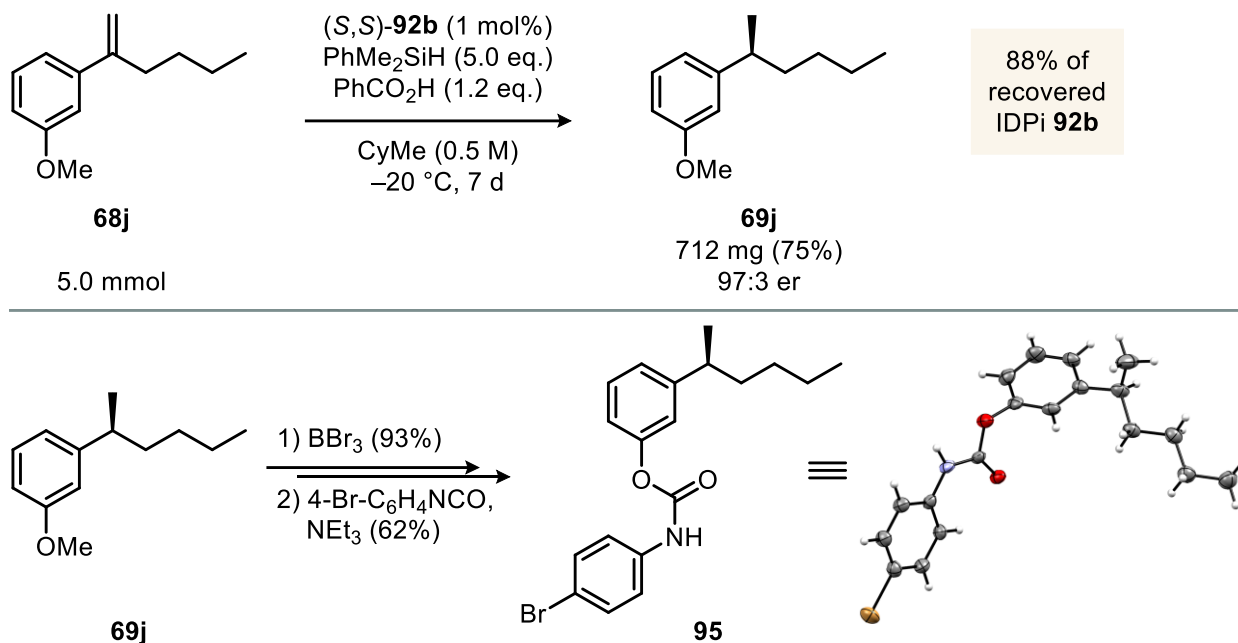
Figure 3.12 Upscaled ionic hydrogenation of styrene **68j** (5 mmol) using 1 mol% catalyst (top). Two-step derivatization of alkylbenzene **69j** to carbamate **95**, enabling unambiguous determination of absolute configuration by X-ray crystallography (bottom).

Alkyl Modifications

We next explored various alkyl substituents and were pleased to find that both shortening the α-alkyl chain to an *n*-propyl group (**68n**) and extending it to *n*-pentyl (**68o**) and *n*-hexyl (**68p**) resulted in comparable reactivity (with higher yields for the larger substrates) and excellent enantioselectivity in all cases (Figure 3.13). The cyclized styrene **68q**, which also serves as an *ortho*-functionalized example, furnished the hydrogenation product in good yield (63%) with slightly reduced but still very good enantioselectivity (92.5:7.5 er), accompanied by more pronounced isomerization (36% NMR yield of **70q**).

Next, we investigated substrates bearing functional groups that are potentially reactive under reductive conditions. Remarkably, the chlorobutyl derivative **69r** was obtained in high yield (76% yield) and good enantioselectivity. Although alkyl halides are often susceptible to reduction under standard ionic hydrogenation conditions,[248] the chloroalkyl group in **69r** remained intact, offering a synthetically useful handle for further derivatization. The methyl ester-containing styrene **68s** was also well tolerated, furnishing **69s** in very good yield (72% yield) and excellent enantioselectivity (97:3 er).

To further assess the chemoselectivity of the ionic hydrogenation, we examined diene substrates **68t** and **68u**. In both cases, selective reduction of the benzylic double bond was observed. However, **68t**, which

contains a terminal olefin, underwent additional undesired cyclization, yielding 1-methyl-1,2,3,4-tetrahydro-1,1′-biphenyl as a side product that could not be separated from **69t**. This side reaction could likely be suppressed by shortening or lengthening the alkyl tether to disfavor the formation of a favorable ring size during cyclization. While **69t** was obtained with high enantioselectivity (93:7 er), the trisubstituted olefin in **68u** led to reduced enantioselectivity in **69u** (82:18 er).
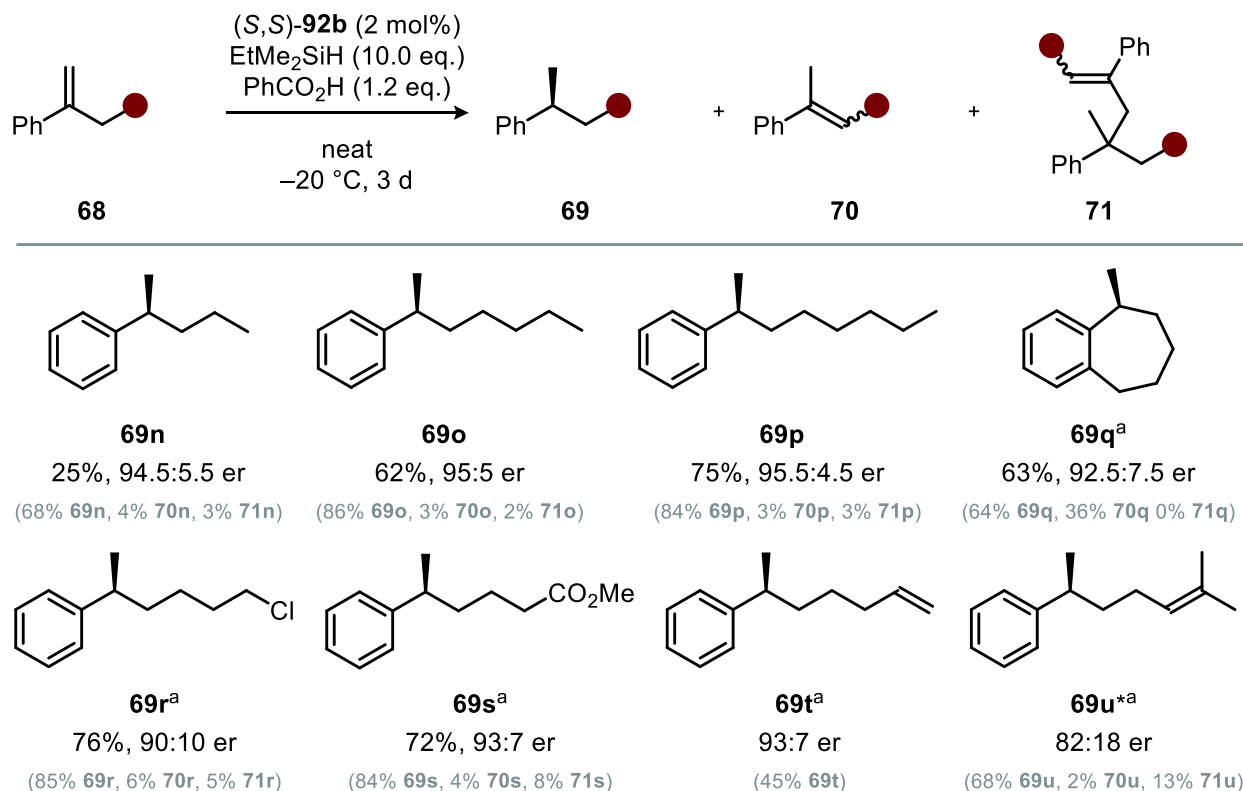
Figure 3.13 Substrate scope of the ionic hydrogenation: α-alkyl styrenes bearing alkyl modifications. All reactions were conducted on a 0.2 mmol scale. Yields are reported as isolated yields after column chromatography. ^{1}H-NMR yields, reported in parentheses (gray), were determined using CH_2Br_2 as internal standard. ^{a}Using $PhMe_2SiH$ (5.0 eq.) in CyMe (0.5 M). *Reactions conducted on a 0.025 mmol scale.

3.3.3 Limitations

During our exploration of various styrenes, we encountered several substrates for which the ionic hydrogenation protocol proved ineffective or suboptimal (Figure 3.14). The electron-rich *para*-methoxy styrene **68v** is one such example. The corresponding alkylbenzene was obtained in moderate yield (44%) due to competing dimerization (19%), and with only modest enantioselectivity (75.5:24.5 er). However, as our approach primarily targets simple styrenes lacking activating π-donors, this limitation may be considered of limited relevance. Moreover, other established methodologies have successfully addressed such electron-rich systems.[217] At the opposite end of the electronic spectrum, the strongly electron-deficient *para*-trifluoromethyl styrene **68w** failed to undergo ionic hydrogenation. Instead, exclusive

isomerization to **70w** was observed (42%). *Ortho*-substituted styrene **68x** bearing a methyl group also proved unreactive under both standard and more forcing conditions using dimethylphenylsilane, despite successful conversion of the structurally related bicyclic **68q**. These observations suggest that steric congestion near the reactive site can critically impair reactivity. An attempt to access the natural product curcumene (**69y**) under optimized conditions gave only moderate enantioselectivity (78:22 er), falling short of synthetic utility.

Reducing the size of the α-alkyl substituent to an ethyl group in **68z** led to a substantial drop in both yield (16%) and enantioselectivity (64.5:35.5 er). Similarly, branched α-substituted styrenes (**68aa** and **68ab**) showed poor enantioselectivity, underscoring the sensitivity of the chiral environment to alkyl substitution patterns.

69v
75.5:24.5 er
(44% **69v**, 0% **70v**, 19% **71v**)

69w[a]
-
(0% **69w**, 42% **70w**, 0% **71w**)

69x[b]
-
(0% conv.)

69y[c]
78:22 er
(65% **69y**, 2% **70y**, 11% **71y**)

69z
64.5:35.5 er
(16% **69z**, 0% **70z**, 1% **71z**)

69aa[d]
65.5:34.5 er
(28% **69aa**)

69ab[b,d]
63:37 er
(92% **69ab**)

69ac[b] (n = 1)
(0% conv.)
69ad[b] (n = 2)
(0% conv.)

69ae[b,d]
-
(0% conv.)

69af[b] (n = 2)
(0% conv.)
69ag[b] (n = 3)
(0% conv.)

69ah[a]
-
(0% conv.)

from purely aliphatic, unbiased 1,1-disubstituted alkene

69ai[a]
≤57:43 er
(<5% **69aj**)
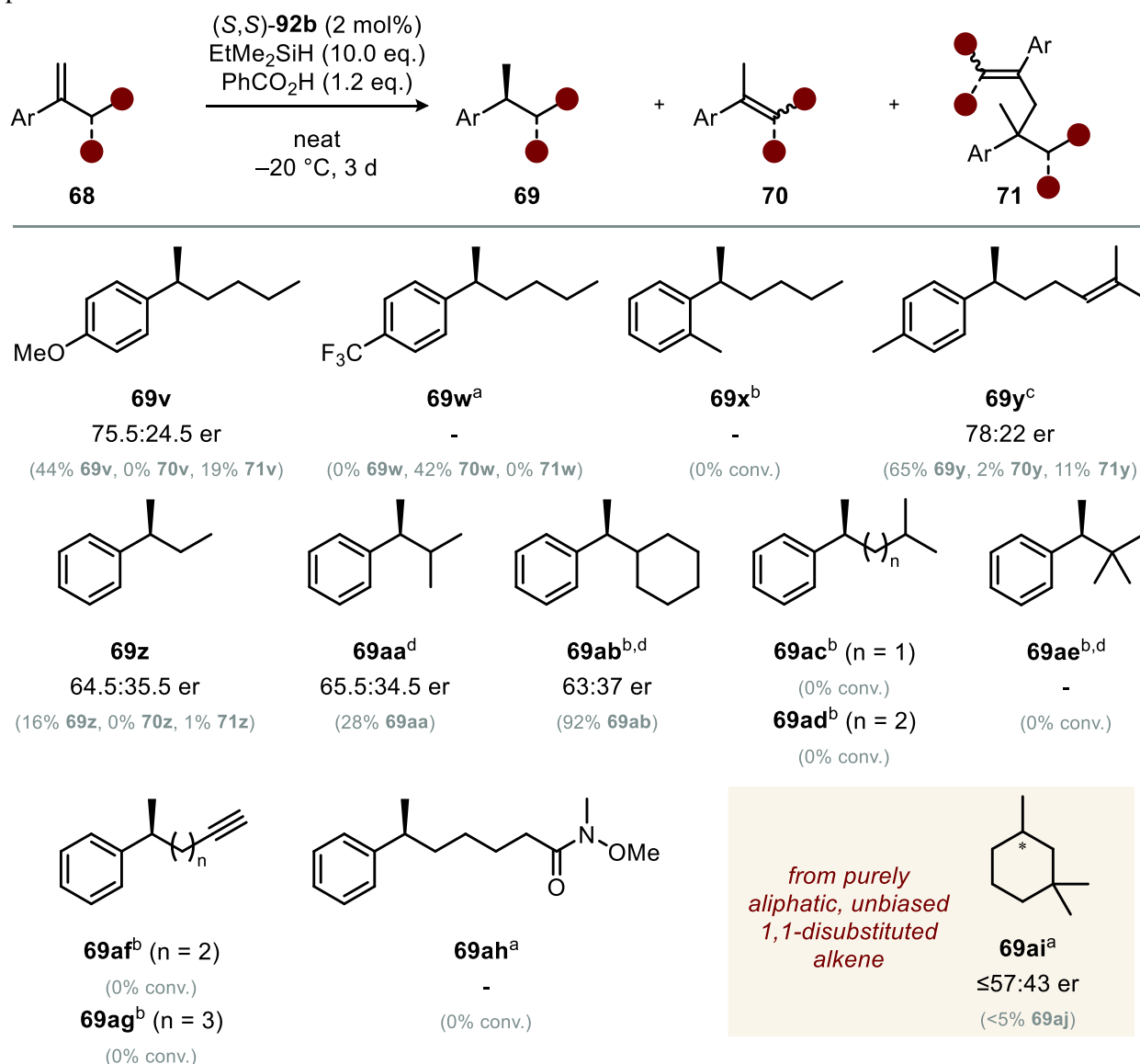
Figure 3.14 Scope limitations: All reactions were conducted on a 0.025 mmol scale. ^{1}H-NMR yields, reported in parentheses (gray), were determined using CH_2Br_2 or mesitylene as internal standard. [a]Using $EtMe_2SiH$ (5.0 eq.) in CyMe (0.5 M). [b]Using $PhMe_2SiH$ (5.0 eq.) in CyMe (0.5 M). [c]Reaction performed at –30 °C. [d]Reaction performed at rt.

Styrenes **68ac–68ag** failed to undergo conversion under the reaction conditions, most likely due to excessive steric hindrance in the case of **68ac–68ae**. Likewise, for the Weinreb amide substrate **68ah**, no conversion was observed. This may be attributed to deactivation of catalyst **92b** by the basic amide moiety. Finally, we subjected a purely aliphatic 1,1-disubstituted alkene (**68ai**) to the ionic hydrogenation protocol to evaluate whether the methodology could be extended beyond aromatic systems. However, only poor reactivity was observed under the reaction conditions, affording less than 5% of the corresponding alkane (**69aj**) with low enantioselectivity (56.5:43.5 er). These results indicate that extension to purely aliphatic alkenes will require a redesigned catalyst and further optimization of the reaction conditions.

In summary, we demonstrated that a broad range of simple α-alkyl styrenes are amenable to our developed ionic hydrogenation protocol. Both electron-rich and electron-deficient substrates, within defined electronic boundaries, were successfully reduced in very good yields and with excellent enantioselectivity in most cases. High chemoselectivity was achieved, with redox-sensitive functional groups such as esters, alkyl chlorides, and aliphatic double bonds remaining intact. Additionally, the limitations of the method were systematically evaluated, revealing key steric and electronic constraints that guide future applications and catalyst design.

3.3.4 Mechanistic Studies

Mechanistically, we envisioned a catalytic cycle initiated by protonation of the styrene substrate by IDPi **92b**, forming an ion pair intermediate comprising a highly reactive benzylic carbocation and the chiral IDPi counteranion (Figure 3.15). This ion pair can follow three distinct pathways:

> (I) Deprotonation to form the isomerized alkene **70**, a process that may be reversible depending on the substrate and reaction conditions;
> (II) Electrophilic addition to another molecule of styrene (**68**), leading to formation of dimer **71**;
> (III) Hydride transfer from the silane, affording the desired alkylarene **69**.

The productive hydride transfer (III) would generate a silylated IDPi species as a catalytic intermediate, which is subsequently protodesilylated by benzoic acid to regenerate IDPi **92b** and form silyl benzoate as a byproduct. Alternatively, the enantiodetermining hydride transfer may proceed via a trimolecular transition state involving the ion pair, the silane, and benzoic acid, directly furnishing product **69**, silyl

benzoate, and regenerated IDPi **92b** in a single step. In this section, we set out to investigate the mechanism of this ionic hydrogenation in greater detail.
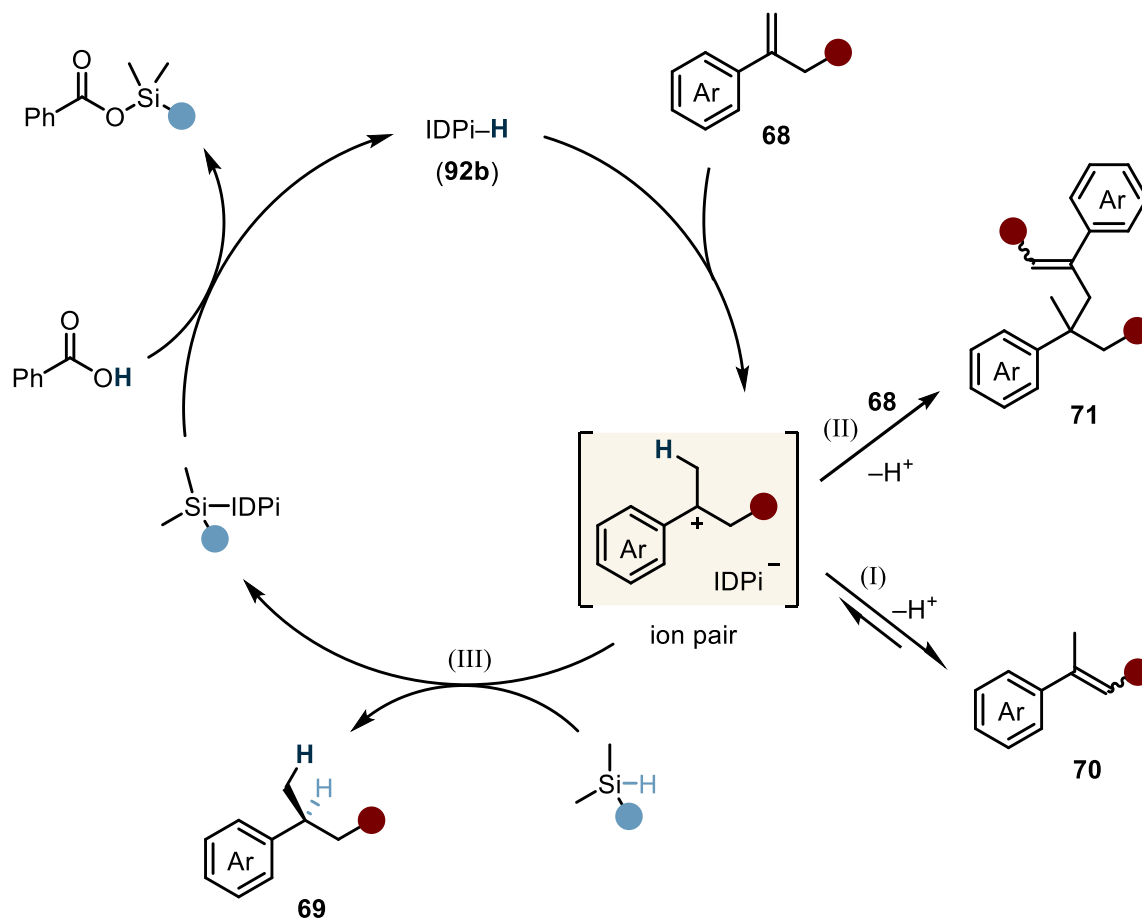
Figure 3.15 Plausible mechanism of the asymmetric catalytic ionic hydrogenation of unbiased styrenes using a silane reductant and benzoic acid as a proton source.

Convergent Reactivity of Styrene Isomers

If the ionic hydrogenation proceeds via a benzylic carbocation intermediate, a similar enantioselective outcome should be expected from both stereoisomers of the styrene *E*-**70** and *Z*-**70**, as the intermediate loses its stereochemical information (Figure 3.16). Moreover, investigating the reactivity of these isomers provides insights into the reversibility of the isomerization between **68** and **70**. To this end, stereochemically pure *E*-**70a** and *Z*-**70a** were synthesized and subjected to the standard reaction conditions over five days at various temperatures (Table 3.9).

A clear trend emerged: the *E*-isomer was significantly more reactive than the *Z*-isomer. At 80 °C, *E*-**70a** furnished **69a** in 95% yield, whereas the *Z*-isomer produced only 49% of the product under identical conditions (entry 1). At 40 °C, neither isomer underwent productive ionic hydrogenation or isomerization,
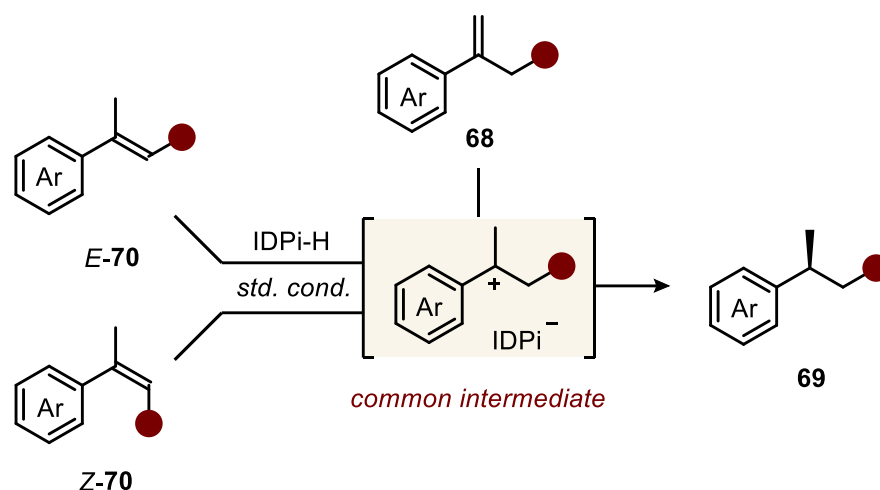
Figure 3.16 Convergent ionic hydrogenation of isomeric styrenes to form alkylarene **69** via a common carbocation intermediate.

indicating that reprotonation of **70a** is no longer feasible at lower temperatures for these trisubstituted alkenes (entry 3). These results suggest that the isomerization from **68a** to **70a** is irreversible under the standard reaction conditions (–20 °C). Notably, the enantiomeric ratios of **69a** obtained from both *E*- and *Z*-**70a** were nearly identical, supporting the involvement of a common carbocation intermediate in the enantiodetermining step.

Table 3.9 Ionic hydrogenation of trisubstituted alkenes *E*- and *Z*-**70a** at elevated temperatures. Reactions were performed on a 0.025 mmol scale.
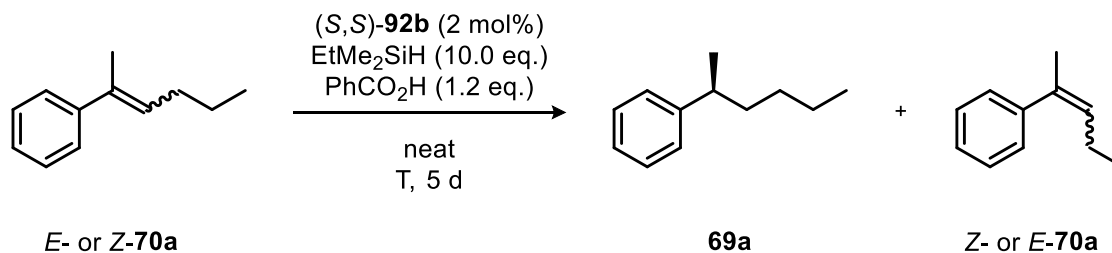
entry	temperature	from *E*-70a			from *Z*-70a		
		yield (69a)	er (69a)	yield (Z-70a)	yield (69a)	er (69a)	yield (E-70a)
1	80 °C	95%	79.5:20.5	0%	49%	79.5:20.5	27%
2	60 °C	64%	81.5:18.5	8%	12%	81:19	12%
3	40 °C	traces	n.d.	traces	traces	n.d.	0%
4	20 °C	traces	n.d.	0%	traces	n.d.	0%

We next turned to an additional, more electron-rich system to obtain more reliable mechanistic insights. Using the naphthyl-derived styrenes **68k**, *E*-**70k**, and *Z*-**70k**, the following results were obtained (Table 3.10). As before, the *E*-isomer displayed higher reactivity than the *Z*-isomer, furnishing **69k** in quantitative yield at 80–40 °C. In contrast, *Z*-**70k** afforded only 43% yield at 40 °C (entries 1–3). At 0 °C, the reactivity of *E*-**70k** decreased significantly, indicating that isomerization from electron-rich **68k** to **70k** is also unlikely to occur under the standard reaction conditions (–20 °C, entry 6). Interestingly, no dimerization was observed for any of the trisubstituted alkenes **70a** or **70k**, likely due to their reduced nucleophilicity and steric hindrance.

Table 3.10 Ionic hydrogenation of trisubstituted alkenes *E*- and *Z*-**70k** at elevated temperatures. Reactions were performed on a 0.025 mmol scale.
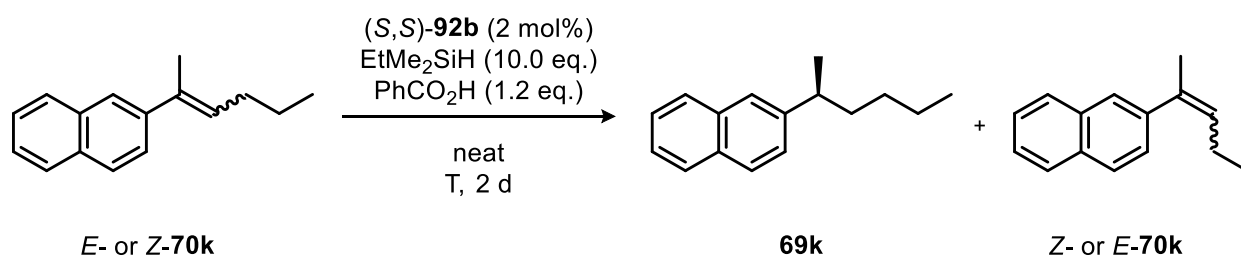
entry	temperature	from *E*-70k			from *Z*-70k		
		yield (69k)	er (69k)	yield (Z-70k)	yield (69k)	er (69k)	yield (E-70k)
1	80 °C	100%	81.5:18.5	0%	100%	82:18	0%
2	60 °C	100%	86:14	0%	94%	86:14	2%
3	40 °C	100%	89:11	0%	43%	89:11	4%
4	20 °C	59%	92.5:7.5	2%	3%	92:8	3%
5	10 °C	8%	94.5:5.5	4%			
6	0 °C	traces	95:5	4%			

The enantioselectivities across all reactions at a defined temperature remained nearly identical, consistently furnishing the same major enantiomer, which further supports the involvement of a common carbocation intermediate. When compared to the enantioselective ionic hydrogenation of terminal olefin **68k** (Table 3.11), these findings further substantiate the convergence of different olefin stereo- and regioisomers through a shared reactive intermediate.

Table 3.11 Ionic hydrogenation of styrene **68k** at elevated temperatures. Reactions were performed on a 0.025 mmol scale.

entry	temperature	yield (69k)	er (69k)	yield (70k)	yield (71k)
1	80 °C	87%	84:16	0%	6%
2	60 °C	83%	86.5:13.5	0%	9%
3	40 °C	79%	90.5:9.5	3%	9%
4	20 °C	78%	94.5:5.5	3%	10%

Beyond the mechanistic insights, these experiments also reveal both a limitation of our current method and a feature that highlights the broader potential of this chemistry. The reduced reactivity of trisubstituted alkenes necessitates elevated temperatures, which typically compromise enantioselectivity. However, the fact that both *E*- and *Z*-isomers converge to the same major enantiomer addresses a key limitation of conventional asymmetric metal-catalyzed hydrogenations. In such cases, the presence of alkene isomers often results in low enantioselectivity due to favored substrate–metal catalyst coordination dictated by the less substituted alkene carbon.[249] In contrast, the ion-pairing mechanism here may override such geometrical constraints. Developing a more strongly acidic chiral Brønsted acid could thus offer a promising strategy for extending ionic hydrogenation to a broader range of unbiased trisubstituted alkenes.

Reversibility of Styrene Protonation

 The NMR-spectroscopic studies presented in this section were carried out in collaboration with Dr. Markus Leutzsch.
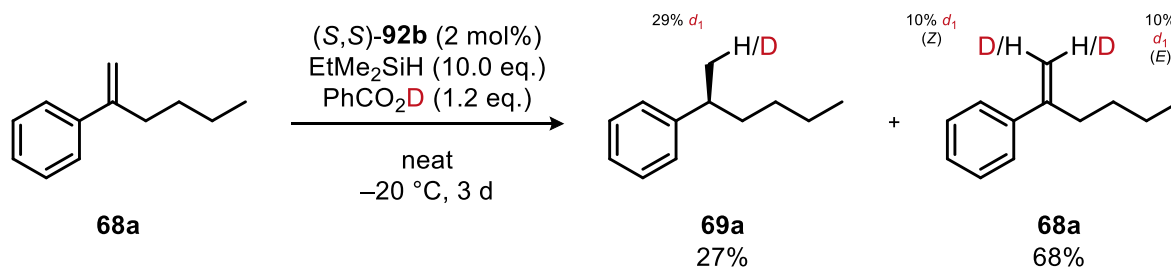
Figure 3.17 Deuterium Scrambling Experiment: Employing benzoic acid-d_1 in the ionic hydrogenation of styrene **68a**. The reaction was performed on a 0.025 mmol scale.

To assess whether the initial protonation by catalyst **92b** is reversible, the ionic hydrogenation of model substrate **68a** was carried out using deuterated benzoic acid (d_1-benzoic acid) as the proton source (Figure 3.17). Analysis of the crude reaction mixture by ^{1}H, ^{2}H, and ^{13}C NMR spectroscopy revealed that the product **69a** was obtained in 27% yield, with partial deuterium incorporation observed in a **69a**-d_1 : **69a**-d_0 ratio of 3:7. In addition to unreacted starting material (54%), partially deuterated styrene **68a**-d_1 was detected in 14%. Notably, the **68a**-d_1 species consisted of both geometric isomers, with an $E : Z : non$-*deuterated* ratio of 1:1:8. This result provides direct evidence that protonation of the alkene is reversible under the reaction conditions.

Influence of a Chiral Proton Source on Stereocontrol

Table 3.12 Control experiments evaluating the influence of enantiopure chiral proton sources on the enantioselectivity of the ionic hydrogenation of styrenes. Reactions were carried out on 0.025 mmol scale using (S,S)-**92b** or (R,R)-**92b** as catalyst and either (R)-, (S)-α-methoxyphenylacetic acid (**96**) or (S)-phenylpropionic acid (**97**) as proton source.

entry	IDPi	H⁺ source	conversion	yield (69a)	er (69a)	yield (70a)	yield (71a)
1	(S,S)-**92b**	(R)-**96**	99%	51%	89.5:10.5	34%	7%
2	(S,S)-**92b**	(S)-**96**	99%	51%	89.5:10.5	34%	7%
3	(S,S)-**92b**	(S)-**97**	99%	54%	90:10	32%	6%
4	(R,R)-**92b**	(S)-**97**	99%	54%	9.5:90.5	33%	6%

To investigate whether benzoic acid, required for catalyst turnover, is possibly involved in the enantiodetermining step, the influence of an enantiopure chiral proton source was examined. If the proton source participates beyond mere catalyst regeneration, one could envision a trimolecular enantiodetermining transition state involving the ion pair, the silane, and the proton source. While such a scenario is kinetically disfavored due to entropic constraints, it cannot be ruled out and should be considered in mechanistic analysis. In such a case, one enantiomer of the proton source might create matched or mismatched scenarios with respect to (*S*,*S*)-**92b**, resulting in two distinct diastereomeric transition states and, consequently, different enantiomeric ratios in product **69a**. Conversely, if the proton source functions solely to regenerate the catalyst after product formation, its absolute configuration should have no impact on enantioselectivity.

To test this, (*R*)- and (*S*)-α-methoxyphenylacetic acid (**96**) were used as proton sources for the ionic hydrogenation of **68a** (Table 3.12). In both cases, the same enantiomeric ratio for **69a** (89.5:10.5) was obtained, indicating that the chiral carboxylic acid does not influence the enantiodetermining step (entries 1 and 2).

In a second experiment, (*S*)-(+)-phenylpropionic acid (**97**) was used as a chiral proton source in the reduction of styrene **68a** with either (*R*,*R*)-**92b** or (*S*,*S*)-**92b** as catalyst. As expected, the absolute configuration of the product was inverted depending on the catalyst enantiomer. Importantly, the enantiomeric excess remained nearly identical across both reactions (entries 3 and 4), excluding a matched/mismatched interaction between the chiral proton source and the catalyst. These results further support the conclusion that the proton source is not involved in the enantiodetermining hydride transfer step.

Formation of Silylated IDPi Species

The NMR-spectroscopic studies presented in this section were carried out in collaboration with Dr. Markus Leutzsch.

To further support our proposed mechanism, we sought to detect the silylated IDPi species as a catalytic intermediate formed after hydride transfer and product formation. For this purpose, the model reaction was conducted using 22 mol% IDPi **75a** under homogeneous conditions in an NMR tube, in the absence of benzoic acid (Figure 3.18a). Reaction progress was monitored over 40 hours by ^{1}H and ^{31}P NMR spectroscopy, and the resulting concentration profiles of key species were plotted (Figure 3.18b). As anticipated, we observed a gradual decrease in the concentration of styrene **68a** (red crosses) accompanied by the formation of the hydrogenation product **69a** (dark blue crosses), isomer **70a** (gray crosses), and trace amounts of dimer **71a** (not shown).
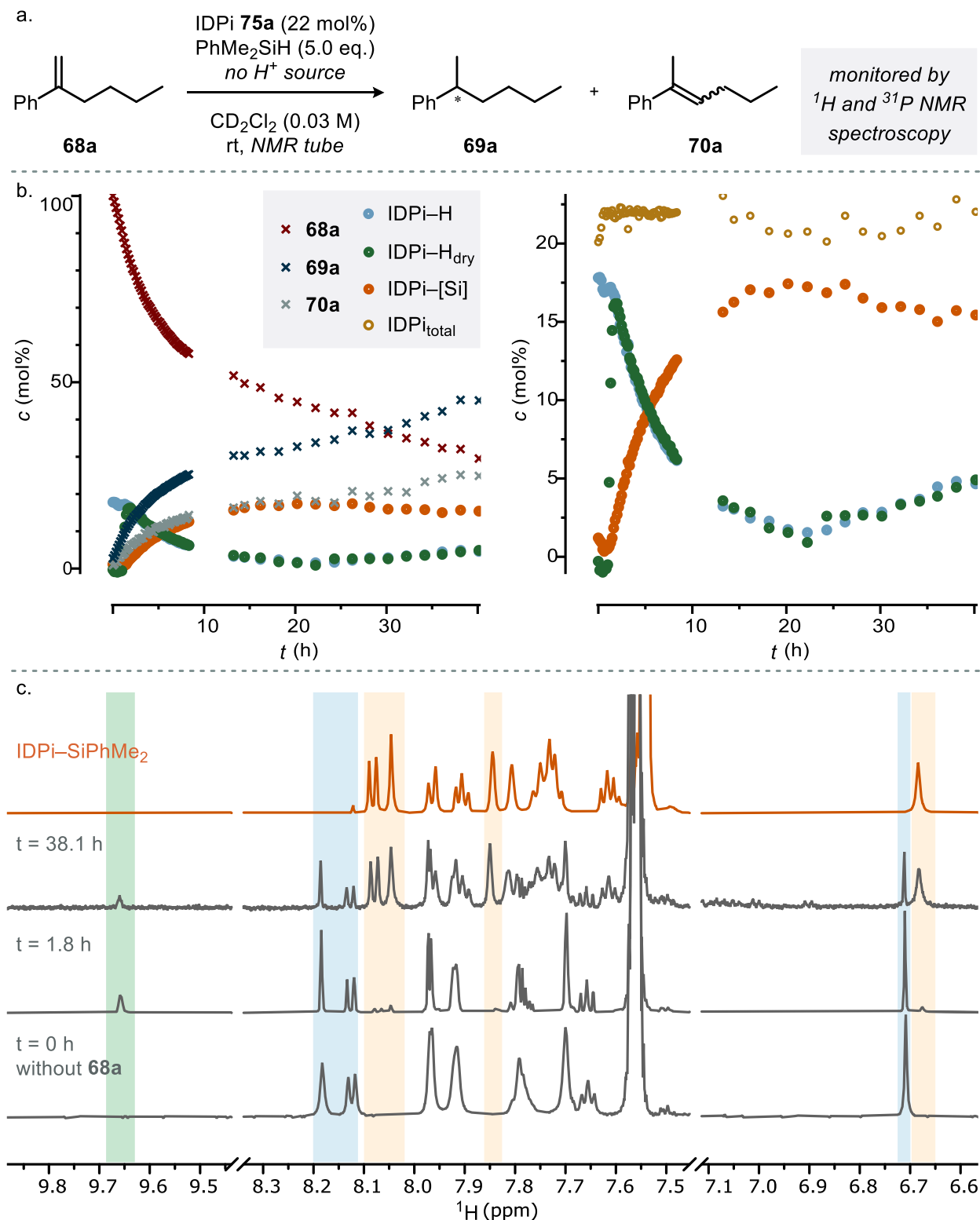
Figure 3.18 a: Ionic hydrogenation of **68a** using IDPi **75a** under homogeneous conditions in the absence of an external proton source, monitored *in situ* by ^{1}H NMR spectroscopy in an NMR tube; b: Reaction progress plot showing the concentration of different reaction components over time, derived from ^{1}H NMR spectra; c: stacked ^{1}H NMR spectra recorded during reaction, along with reference spectrum of silylated IDPi **75a** (top trace, orange), with selected highlighted signals corresponding to IDPi–H (blue), IDPi–H$_{dry}$ (green), IDPi–[Si] (orange).

The signal corresponding to the protic form of IDPi (IDPi–H, light blue circles) remained constant during the first hour, then steadily declined. During this same initial period, a new species (green circles) was absent but began to appear after ~1 hour, increasing to match the concentration of the original IDPi–H. Beyond 2 hours, the concentration of the two species overlapped and decreased in parallel. This newly appearing signal corresponds to the fully dried catalyst (IDPi–H$_{dry}$, as confirmed by a ^{1}H–^{31}P HMBC correlation), whose acidic proton becomes visible in the ^{1}H NMR spectrum only once residual water has been removed (Figure 3.18c, green highlight). This behavior reflects a self-drying cycle in which the IDPi catalyst is gradually desolvated by reaction of residual water with silyl groups (Figure 3.19, left). In this process, silanol is formed as a transient proton source, which in turn generates disiloxane upon further silylation. As [IDPi–H] = [IDPi–H$_{dry}$] + [IDPi–H$_{wet}$], the convergence of the light blue and green traces in Figure 3.18 after two hours indicates complete conversion to the dry form.

Figure 3.19 Left: Self-drying catalytic cycle in the presence of residual water. No accumulation of silylated IDPi observed due to continuous formation of silanol and disiloxane. Right: Accumulation of silylated IDPi once all available proton sources are consumed.

As the concentration of the protic IDPi (IDPi–H) decreases, a new catalytic species (orange circles) emerges, increasing at the same rate as IDPi–H declines. The ^{1}H NMR spectrum of this species corresponds exactly to that of independently prepared silylated IDPi (Figure 3.18c, orange trace), confirming its identity. The observed accumulation of the silylated IDPi species can be attributed to the absence of available proton

sources (such as water or silanol). Without a proton donor to enable protodesilylation, the silylated intermediate persists and accumulates in solution (Figure 3.19, right).

The continued increase in product formation and the observed fluctuations in the concentrations of IDPi–H and IDPi–[Si] are likely due to slow exchange with atmospheric moisture over time.

Additionally, analysis of the recorded ^{31}P NMR spectra over time provided a comparable reaction progress plot for the catalytic species (Figure 3.20), showing the evolution of the protic IDPi (IDPi–H, blue circles) and the silylated IDPi (IDPi–[Si], orange circles). The protic IDPi displays a sharp singlet in the ^{31}P spectrum, consistent with its C_2 symmetry. In contrast, the silylated species loses this symmetry upon silylation of one of the diastereotopic sulfonamide oxygen atoms, generating two diastereomers, (S,S,R) and (S,S,S), that are likely in equilibrium (IDPi–[Si]$_O$). In principle, this should give rise to four doublets in the ^{31}P NMR spectrum, as reported in previous studies.[250,251]
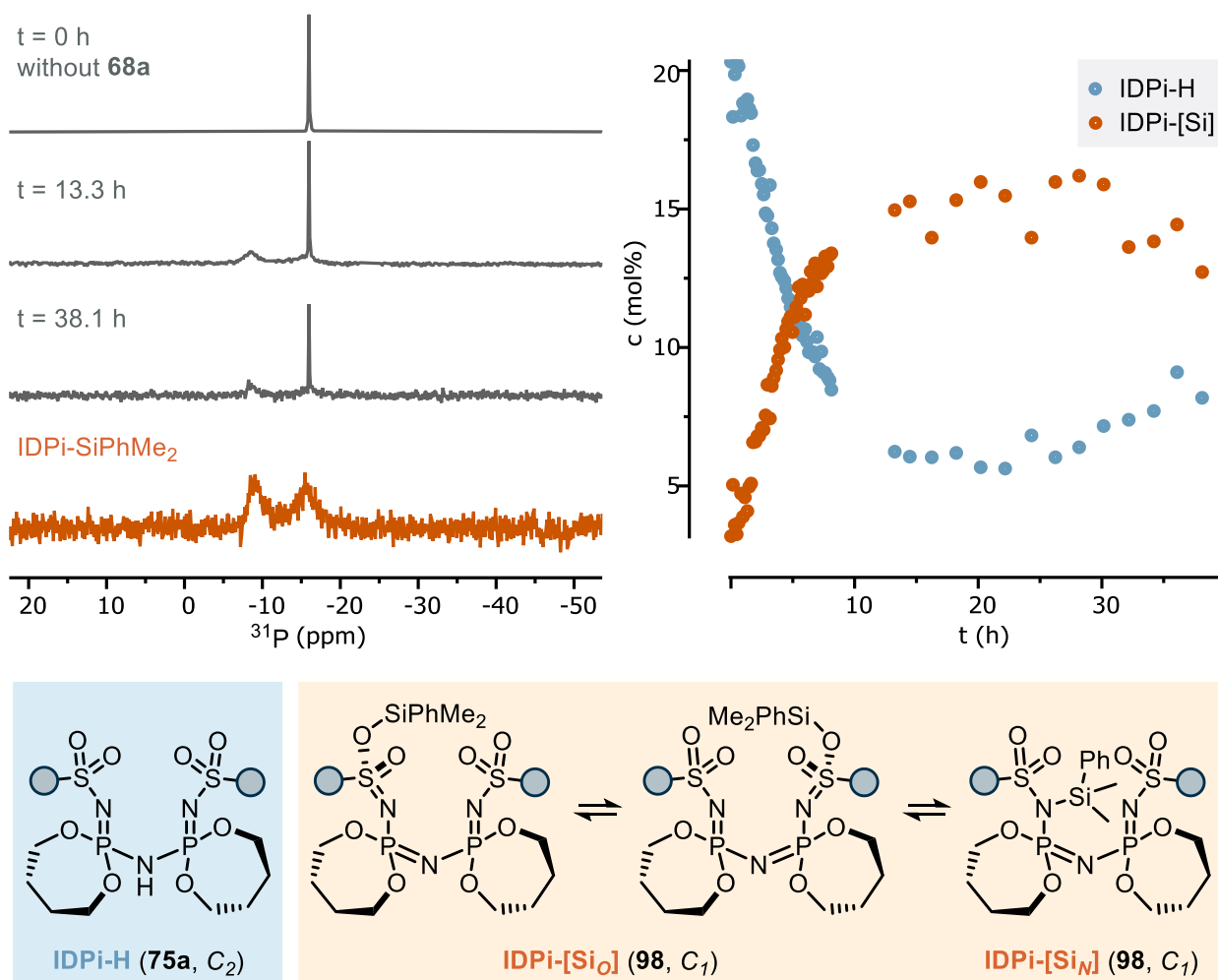
Figure 3.20 Stacked ^{31}P NMR spectra recorded at different time points during the ionic hydrogenation, along with reference spectrum of silylated IDPi **75a** (top trace, orange); reaction progress plot showing the concentrations of IDPi–H and silylated IDPi–[Si] over time, derived from ^{31}P NMR spectra.

However, under the present conditions, no distinct doublets are observed. Instead, two broad signals appear for the silylated IDPi, which likely reflect a fast exchange process between the diastereomers. Additionally, an *N*-silylated IDPi (IDPi–[Si]$_N$) isomer is possibly involved in the dynamic equilibrium, facilitated by the relatively small size of the silyl group (SiPhMe$_2$). This would give rise to two further doublets. In prior reports, sharp signals were observed at reduced temperature when bulkier silyl groups (e.g., Si*t*BuMe$_2$) were employed, presumably due to slower exchange and improved resolution of the individual species.

Catalyst Turnover and Regeneration

The NMR-spectroscopic studies presented in this section were carried out in collaboration with Dr. Markus Leutzsch.
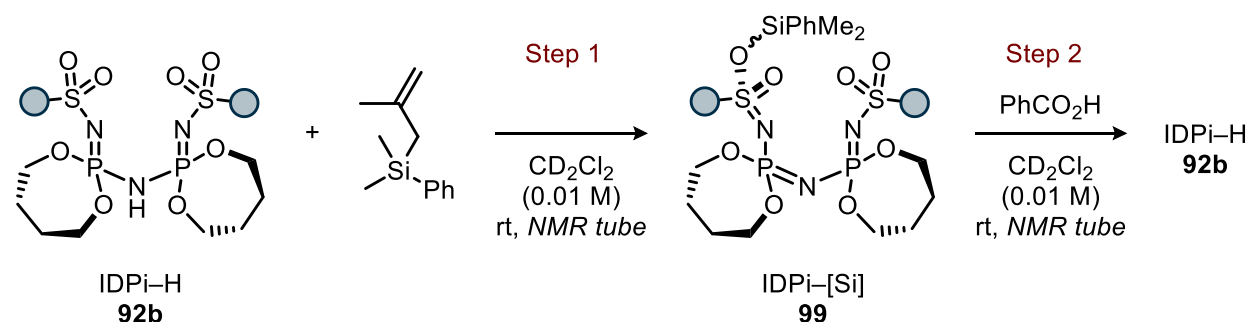
Figure 3.21 Silylation of IDPi **92b** using dimethyl(2-methylallyl)(phenyl)silane (step 1), and subsequent protodesilylation using benzoic acid (step 2).

To further investigate the final step of the catalytic cycle—catalyst regeneration via protodesilylation of the silylated IDPi species by benzoic acid—we conducted a model study using independently prepared silylated IDPi. For this purpose, IDPi **92b** was treated with increasing amounts of dimethyl(2-methylallyl)(phenyl)silane and monitored by both ^{1}H and ^{31}P NMR spectroscopy (Figure 3.21, step 1). As evident from the recorded spectra, the first 2.0 equivalents of silane were consumed by residual water in the sample and did not lead to silylation of the catalyst (Figure 3.22). Concurrently, the characteristic ^{1}H NMR signal corresponding to the acidic IDPi proton (δ = 9.87 ppm)—only visible under dry conditions (see previous section)—emerged, indicating successful water scavenging and effective "drying" of the catalyst. Upon addition of a third equivalent of silane, the signals for the protic IDPi disappeared, and broad new signals emerged in both the ^{1}H and ^{31}P NMR spectra. These observations suggest the formation of a new catalytic species, consistent with silylated IDPi. The sharp singlet in the ^{31}P NMR spectrum was replaced by three broad signals. As discussed previously (p. 86), four doublets would be expected for the *O*-silylated IDPi due to the formation of C_1-symmetrical diastereomeric species. The broadness of the observed signals likely stems from a fast exchange process between these diastereomers and a possibly involved *N*-silylated IDPi species.
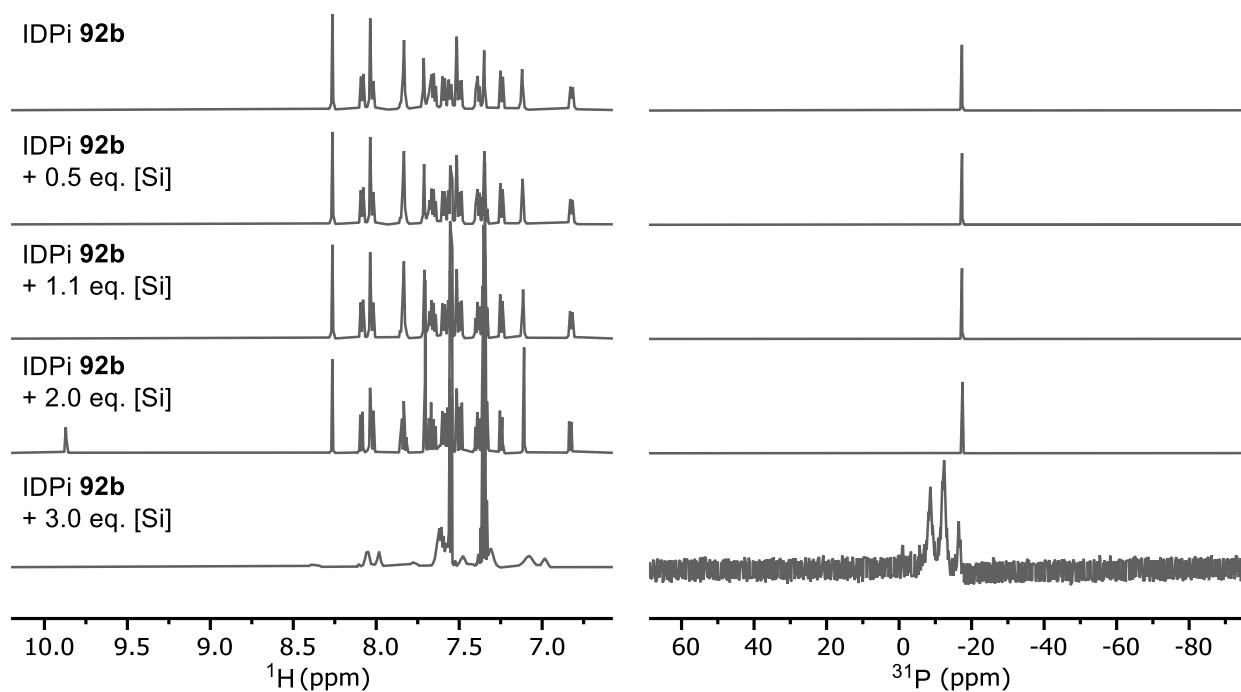
Figure 3.22 Stacked 1H and 31P NMR spectra of IDPi **92b** upon sequential addition of increasing amounts of dimethyl(2-methylallyl)(phenyl)silane at room temperature.

To gain further insight, the sample was cooled to 233 K. At 253 K, partial resolution was achieved, revealing a pattern consisting of one broad signal and two partially resolved doublets (Figure 3.23).
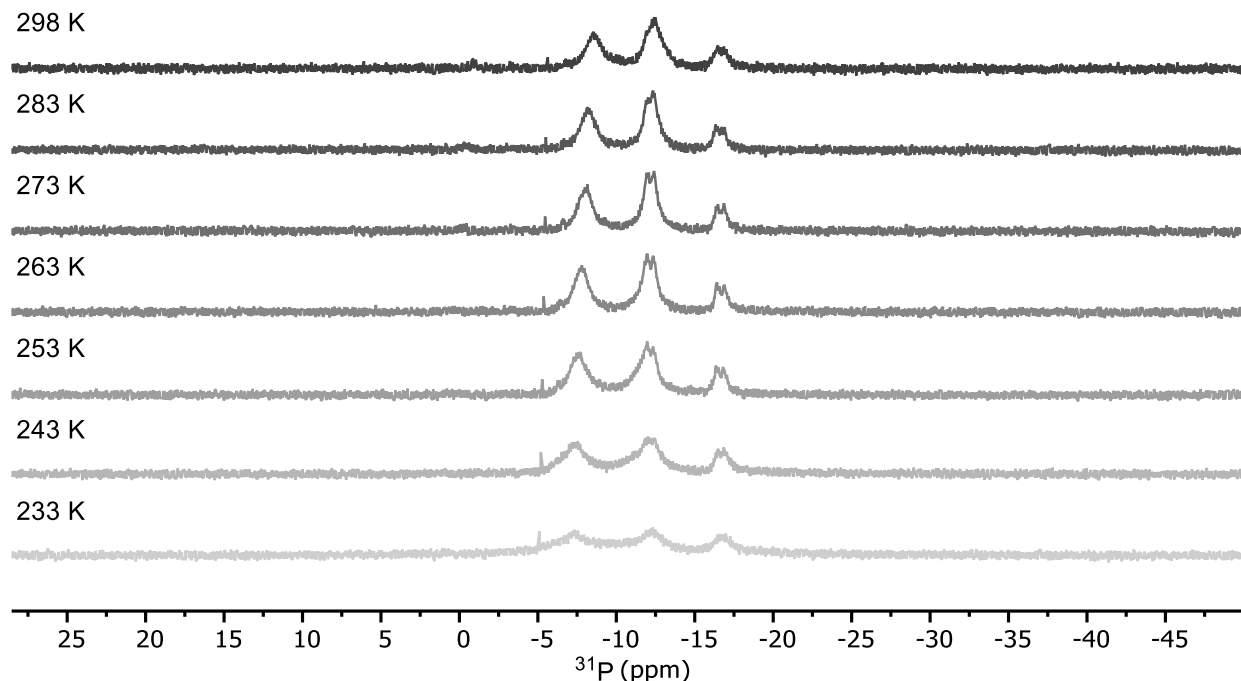
Figure 3.23 Stacked ^{31}P NMR spectra of silylated IDPi **92b** recorded at progressively lower temperatures, reaching 233 K.

Repeating the experiment in PhMe-d_8 and performing additional temperature variations (both cooling and heating) did not lead to improved signal resolution (data not shown).

Finally, sequential addition of benzoic acid to the silylated IDPi mixture (Figure 3.21, step 2) immediately restored the signals of the protic catalyst in both the ^{1}H and ^{31}P spectra, supporting rapid and efficient protodesilylation and regeneration of the active Brønsted acid catalyst under reaction conditions (Figure 3.24). Concurrently, dimethyl(phenyl)silyl benzoate was formed as the corresponding silyl ester byproduct. This scenario is reminiscent of a previously reported IDPi-catalyzed cyclization of bis(methallyl)silanes, in which a covalent silylated IDPi intermediate was observed and turnover required acetic acid to promote protodesilylation and regenerate the active Brønsted acid catalyst.[251]
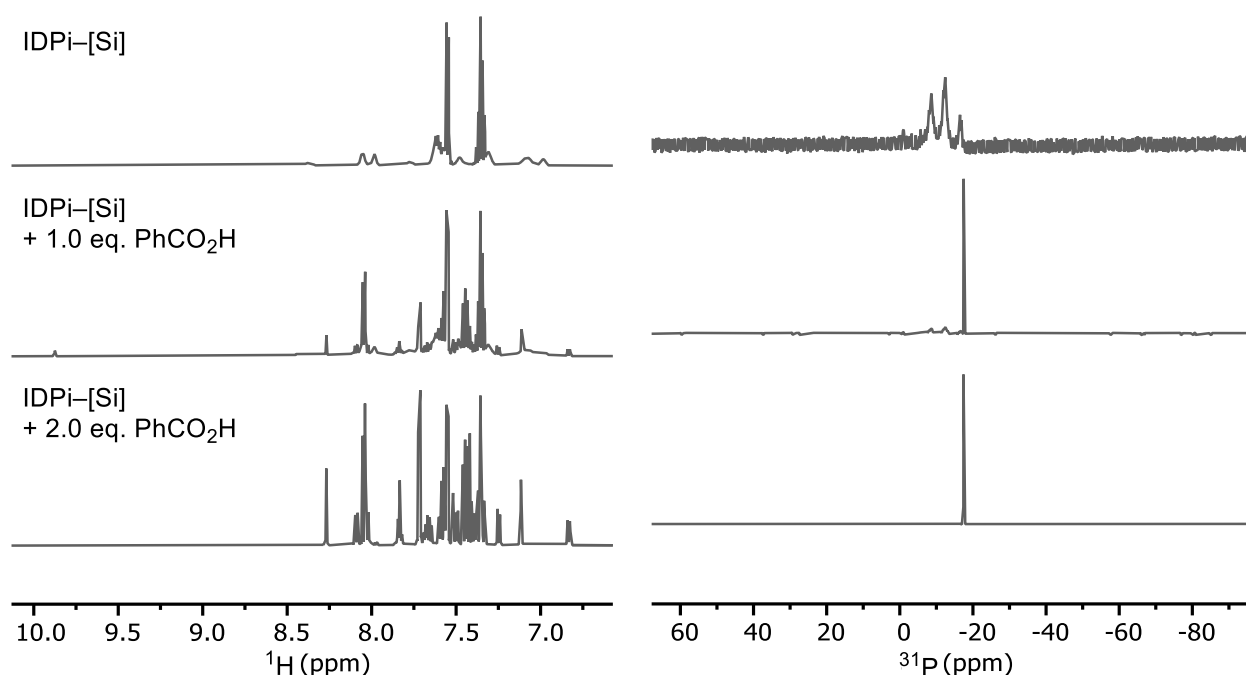
Figure 3.24 Stacked ^{1}H and ^{31}P NMR spectra of silylated IDPi **92b** upon sequential addition of increasing amounts of benzoic acid at room temperature.

Computational Studies

The computational studies presented in this section were carried out in collaboration with Prof. Dr. Nobuya Tsuji.

To gain deeper insight into the mechanism of the ionic hydrogenation and the origin of enantioselectivity, we performed computational studies involving alkene **68a**, silane EtMe$_2$SiH, and catalyst IDPi **92b**. The resulting free energy profile for the protonation and hydride transfer steps (SMD(methylcyclohexane)-ωB97X-V/def2-TZVPP//r2SCAN-3c level of theory[252–254]) is in good agreement with experimental

observations (Figure 3.25). In the pre-transition state complex **I**, alkene **68a** is preorganized for protonation by IDPi **92b**. Proton transfer via transition state **TS-5** furnishes the ion pair **II**. The endergonic nature of this step corroborates the reversible protonation process observed experimentally (cf. *Reversibility of Styrene Protonation*, p. 81). In the presence of the silane (complex **III**), the enantiodetermining hydride transfer proceeds via **TS-6** or **TS-7**, affording post-transfer complexes **IV** and **IV'**, which ultimately release the products (*S*)-**69a** and (*R*)-**69a**, respectively. The computed free energy difference between **TS-6** and **TS-7** ($\Delta\Delta G^{\ddagger} = 1.7$ kcal/mol) aligns closely with the experimentally observed enantioselectivity ($\Delta\Delta G^{\ddagger} = 1.6$ kcal/mol).
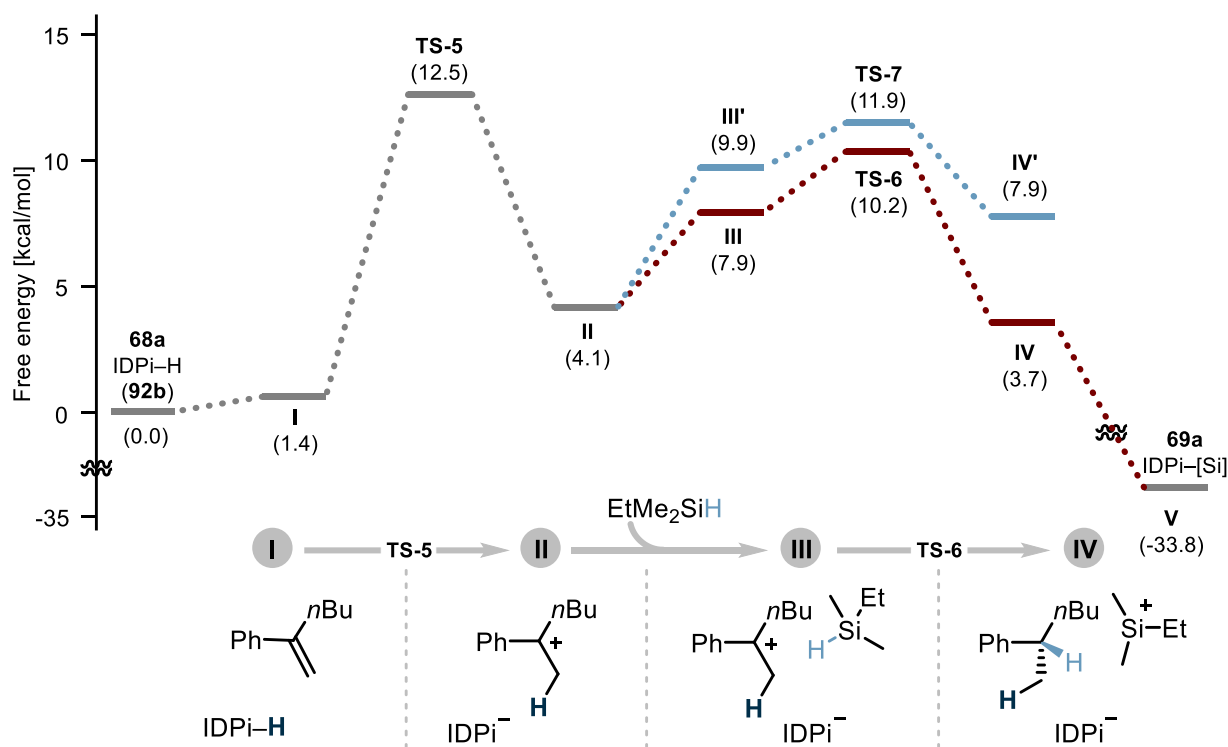
Figure 3.25 Free energy diagram leading to product **69a** at SMD(methylcyclohexane)-ωB97X-V/def2-TZVPP//r^{2}SCAN-3c level of theory (253 K). **TS-6** represents the transition state leading to the major (*S*)-**69a**, while **TS-7** leads to the minor (*R*)-**69a**.

We performed a distortion–interaction analysis, which highlights the dominant role of noncovalent interactions between the chiral IDPi counteranion and the substrate–silane complex.[255] In the favored transition state **TS-6**, the phenyl group of the benzylic carbocation points forward, while the *n*-butyl chain is directed backward (Figure 3.26). Hydride delivery from EtMe$_2$SiH occurs from the top. In contrast, in **TS-7**, the carbocation is flipped—its phenyl substituent is directed backward and the alkyl chain forward— resulting in less favorable interactions. To further visualize these differences and rationalize the origin of enantioselectivity, we employed the Independent Gradient Model based on Hirshfeld partitioning (IGMH)[210] using the Multiwfn program[211,212] (Figure 3.27). The system was partitioned into the catalyst anion and the substrate–silane fragment. The IGMH surfaces highlight noncovalent interactions between

the two fragments, including interactions between polarized C–H bonds of the substrate and the Lewis-basic residues of the IDPi core. Most strikingly, a cation–π interaction is observed in **TS-6** between the phenyl group of the substrate and the heteroaromatic substituent of the IDPi anion. This interaction is absent in **TS-7**, which likely accounts for the observed enantiodifferentiation.
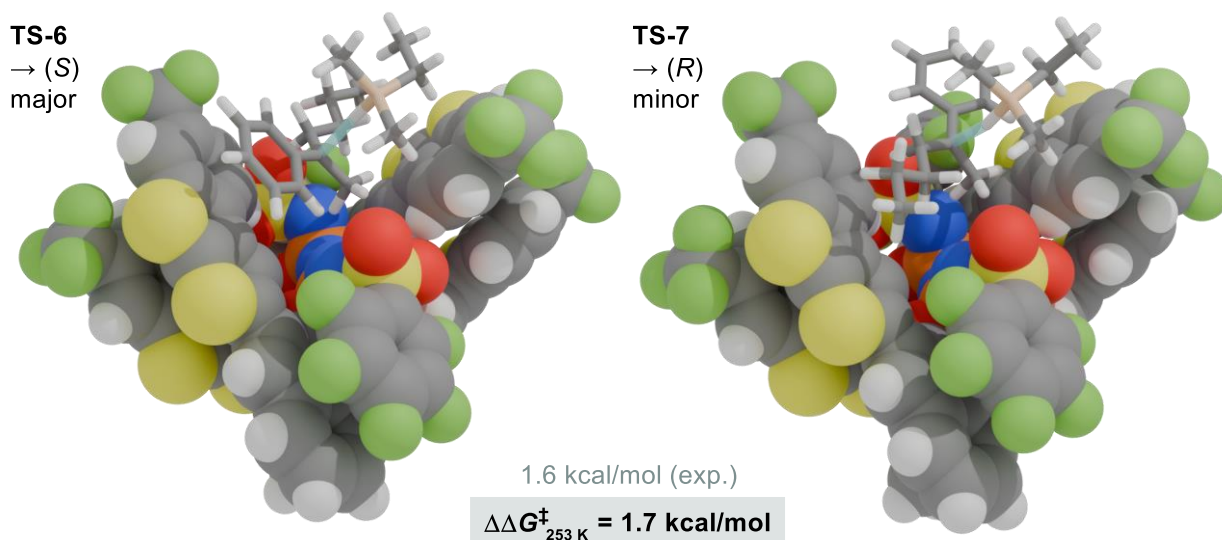
Figure 3.26 Visualization of **TS-6** leading to (*S*)-**69a** (major) and **TS-7** leading to (*R*)-**69a** (minor).

Interestingly, the geometries of the IDPi counteranion remain largely conserved across both transition states. This conformational rigidity is maintained by a network of intramolecular noncovalent interactions
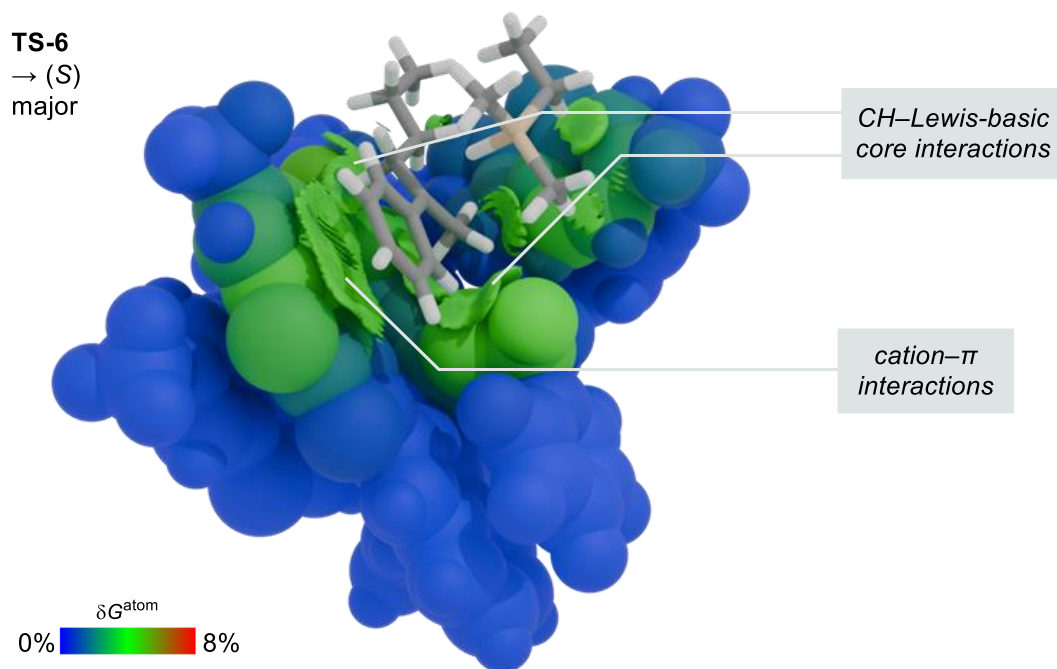
Figure 3.27 Visualization of noncovalent interactions between substrates and the catalyst in **TS-6** using IGMH analysis. The $sign(\lambda_2)\rho$-colored isosurface corresponds to a $\delta g^{inter} = 0.004$ a.u., with a color scale range from -0.05 to 0.05 a.u. The atoms of the anion are colored by δG^{atom} (%) using a scale from 0 to 8% to highlight their relative contributions.

that help preserve a well-defined chiral environment during the reaction.[94] Visualization of these interactions reveals multiple π–π stacking contacts between the heteroaromatic 3,3'-substituents, the BINOL backbone, and the C_6F_5 groups within the catalyst core. In addition, polarized aromatic C–H bonds of the thienothiophene moieties engage in favorable contacts with the sulfonyl oxygen atoms, further stabilizing the conformation of the IDPi anion. This enhanced anion stabilization may contribute to the high reactivity—and likely increased Brønsted acidity—of **92b** compared to other tested IDPi catalysts (cf. *Catalyst Optimization*, p. 62). Notably, the trifluoromethyl groups introduced in **92b** are expected to strengthen the polarization of these CH···O=S interactions relative to IDPi **88b** (which lacks CF_3 groups), thereby reinforcing the intramolecular hydrogen-bonding network and leading to increased yields of hydrogenation product **69**.

Nonlinear Effect Study

ee (92b)	yield (69a)	ee (69a)
2%	1%	23%
4%	1%	34%
14%	10%	79%
21%	15%	84%
37%	33%	88%
61%	53%	89%
80%	65%	90%
99%	59%	90%
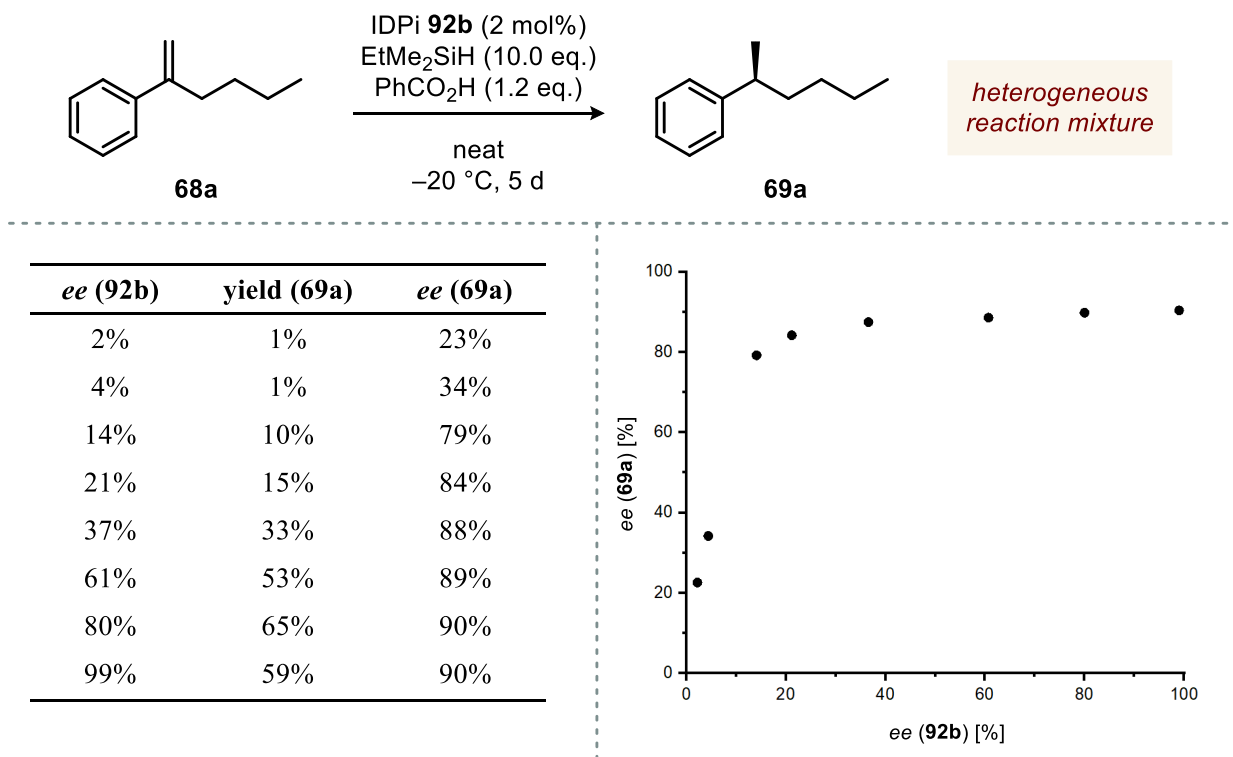
Figure 3.28 Investigation of non-linear effects in the heterogeneous catalytic reaction of **68a** with scalemic mixtures of **92b**.

In an asymmetric catalytic reaction, the enantiomeric excess (*ee*) of the product is generally expected to correlate linearly with that of the chiral catalyst, provided that a single catalyst molecule is involved in the enantiodetermining transition state. Deviations from this linear correlation—known as nonlinear effects (NLEs)—can arise from various mechanistic phenomena, including catalyst aggregation, autocatalysis, or solubility-dependent speciation.[256] In our ionic hydrogenation of α-alkyl styrene **68a**, we observed a

pronounced positive nonlinear effect ((+)-NLE) between the enantiomeric purity of catalyst **92b** and that of the product **69a** (Figure 3.28). Notably, the reaction is heterogeneous under standard conditions. Additionally, a progressive decrease in reactivity was observed with decreasing catalyst *ee*, further supporting the involvement of higher-order catalyst species or solubility-related effects.
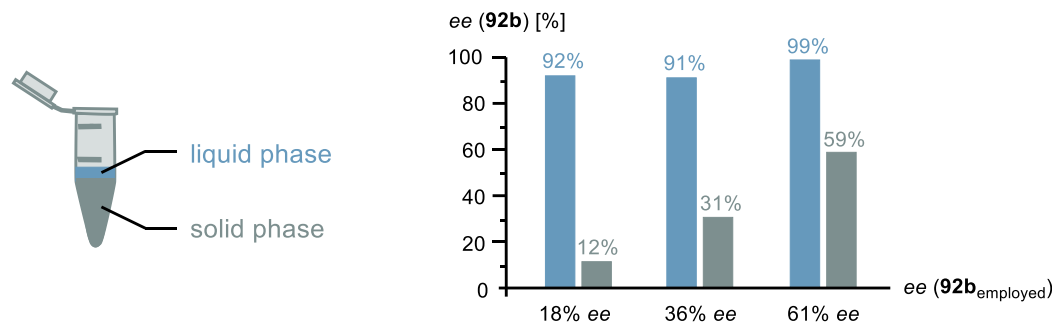
Figure 3.29 Analysis of the enantiomeric excess of **92b** in solution and solid phases.

This nonlinear effect can be attributed to differential solubility between homo- and heterochiral IDPi aggregates, as evidenced by distinct enantiomeric ratios measured in the solid and liquid phases of the reaction mixture. Across catalyst samples with varying enantiopurities (18%, 36%, and 61% *ee*), the enantiomeric excess of **92b** in solution consistently exceeds 90% *ee*, whereas the solid phase exhibits significantly reduced *ee* values. These findings suggest that homochiral aggregates possess greater solubility, leading to enrichment of the solution phase with enantiomerically pure **92b** and concomitant depletion of heterochiral material via preferential precipitation (Figure 3.29). As a result, when catalyst

ee (**92b**)	yield (**69a**)	*ee* (**69a**)
5%	41%	11%
9%	51%	18%
35%	53%	31%
62%	51%	44%
83%	53%	59%
99%	51%	71%
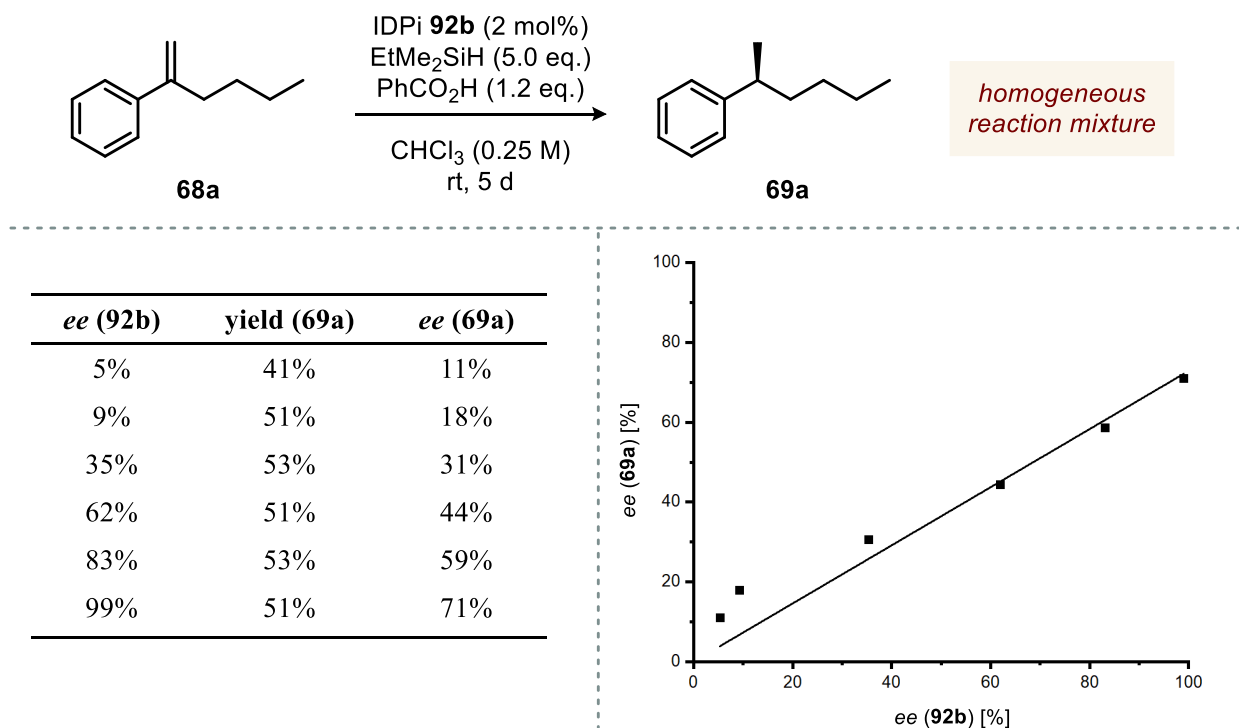
Figure 3.30 Investigation of non-linear effects in the homogeneous catalytic reaction of **68a** with scalemic mixtures of **92b**.

samples of lower initial enantiopurity are used, a larger fraction of heterochiral aggregates is removed from the reactive phase, reducing the effective concentration of catalytically active, enantiopure IDPi. This accounts for the diminished yields of product **69a** under such conditions.

In contrast, under homogeneous conditions a nearly linear relationship between catalyst and product enantiomeric excess was observed (Figure 3.30), further supporting the solubility-based origin of the observed positive nonlinear effect. Moreover, yields remained largely constant across all tested enantiopurities, indicating that catalyst *ee* does not influence reactivity in the absence of phase separation. Similar behavior has been reported in systems involving amino acids[257,258] and chiral phosphoric acids.[259] The exact nature of the homo- and heterochiral aggregates formed between IDPi molecules remains unknown. However, given the sterically encumbered nature of the IDPi scaffold, the formation of hydrogen bonds between catalytic cores appears unlikely. Instead, π–π stacking interactions between the aromatic components of the catalyst may contribute to the proposed aggregation behavior.

Proposed Catalytic Cycle
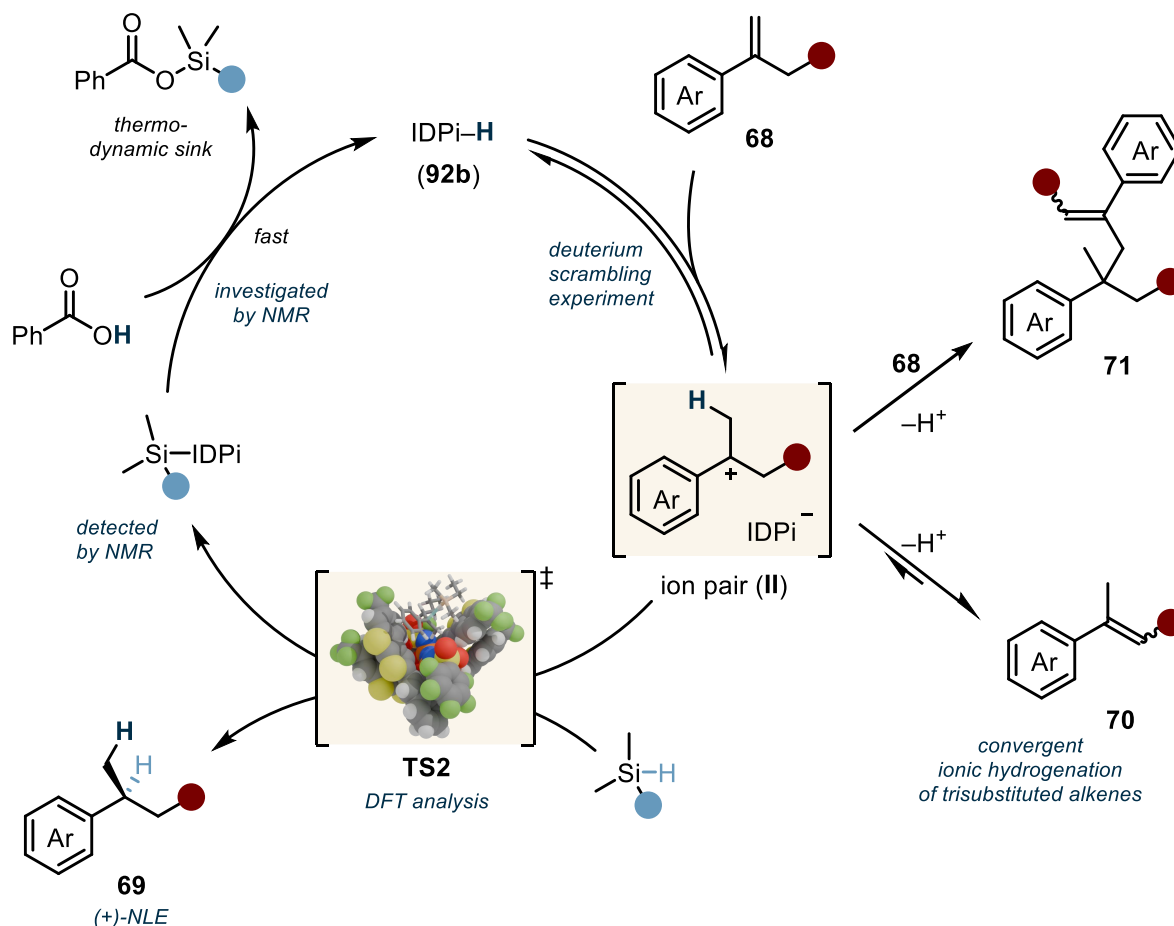
Figure 3.31 Proposed catalytic cycle for the IDPi-catalyzed ionic hydrogenation of α-alkyl styrenes using a silane and benzoic acid as a protic additive, based on conducted mechanistic studies.

Based on our experimental and computational findings, we propose the following catalytic cycle for the IDPi-catalyzed ionic hydrogenation of α-alkyl styrenes (Figure 3.31). The reaction is initiated by reversible protonation of styrene **68** by the highly acidic and confined IDPi **92b**, generating a chiral ion pair (**II**) comprising a benzylic carbocation intermediate. From this key intermediate, two unproductive pathways can compete: nucleophilic attack by another styrene molecule leads to dimer **71** after deprotonation, while β-deprotonation yields the isomeric alkene **70**. Although reprotonation of **70** is theoretically possible, it is unlikely under the optimized reaction conditions for most α-alkyl styrenes employed in this study. Productive hydride transfer from RMe₂SiH via transition state **TS2** furnishes enantioenriched alkyl arene (*S*)-**69** and a silylated IDPi species. This intermediate is, however, extremely short-lived in the presence of a proton donor and is rapidly protodesilylated by benzoic acid to regenerate the active Brønsted acid catalyst **92b** and form silyl benzoate. The formation of the strong Si–O bond in this final step serves as the thermodynamic driving force of the overall transformation.

3.4   Summary and Outlook

The landscape of asymmetric organocatalytic transfer hydrogenations of alkenes is dominated by substrate classes bearing activating groups. Depending on the nature of these groups, tailored catalytic strategies have enabled highly enantioselective C=C bond reductions. In contrast, when shifting focus to structurally or electronically unactivated alkenes, such as α-alkyl styrenes or aliphatic 1,1-disubstituted olefins, reports of stereoselective methods become scarce. For α-alkyl styrenes, only a limited number of *substrate-* or *reagent-controlled* approaches have been developed, and to the best of our knowledge, no stereoselective methods exist for purely aliphatic substrates.

Addressing this gap, we developed a *catalyst-controlled*, chemo- and enantioselective ionic hydrogenation of α-alkyl styrenes with minimal electronic bias using a silane in combination with benzoic acid as a protic additive. Central to enantiocontrol and suppressing competing isomerization and dimerization pathways was the use of a highly acidic, confined IDPi catalyst. Under these conditions, a broad range of α-alkyl styrenes—bearing diverse aryl and alkyl substitutions, including redox-sensitive functional groups—were efficiently reduced in up to 95% yield and 98:2 er (Figure 3.32).
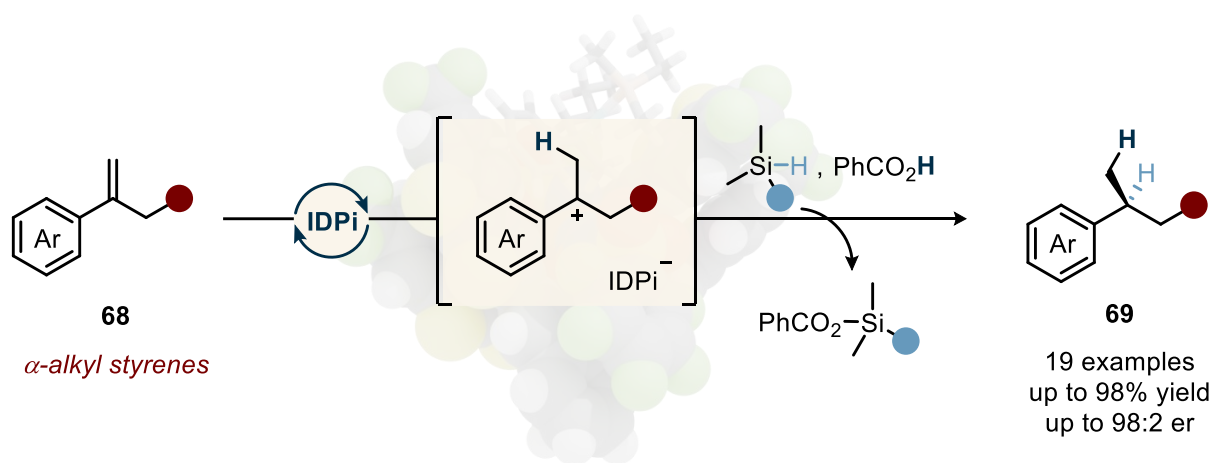
Figure 3.32 Summary of this chapter: Brønsted acid-catalyzed asymmetric ionic hydrogenation of α-alkyl styrenes using a silane and benzoic acid.

Experimental and computational investigations support the formation of a benzylic carbocation intermediate stabilized by multiple noncovalent interactions with the chiral IDPi counteranion, including key cation–π interactions with the benzothienothiophenyl moieties. NMR kinetic studies further revealed the transient formation of a silylated IDPi species, with turnover facilitated by the protic additive. Remarkably, a pronounced positive nonlinear effect was observed, enabling high enantioselectivities even at low catalyst enantiopurity. This phenomenon was attributed to solubility differences between homo- and heterochiral IDPi aggregates.

While the stereoconvergent reduction of a trisubstituted alkene remains only partially resolved, it highlights the promise of organocatalytic strategies in overcoming longstanding limitations of traditional metal-catalyzed hydrogenations. Future efforts may focus on the design of even more strongly acidic chiral Brønsted acids to enable efficient activation of less reactive α,β-disubstituted styrenes and potentially tetrasubstituted alkene derivatives. In addition, our studies have shown that fully aliphatic 1,1-disubstituted alkenes remain a key challenge in terms of both reactivity and stereoselectivity. Developing a general catalytic system for such electronically unbiased substrates remains a highly desirable goal (Figure 3.33, top).

Reduction of challenging substrates: tri-, tetrasubstituted, and aliphatic alkenes
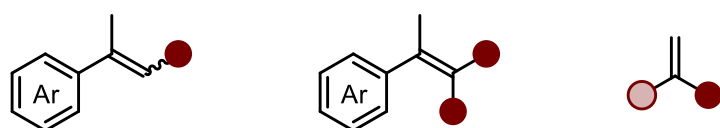
Hydrofunctionalization of Styrenes
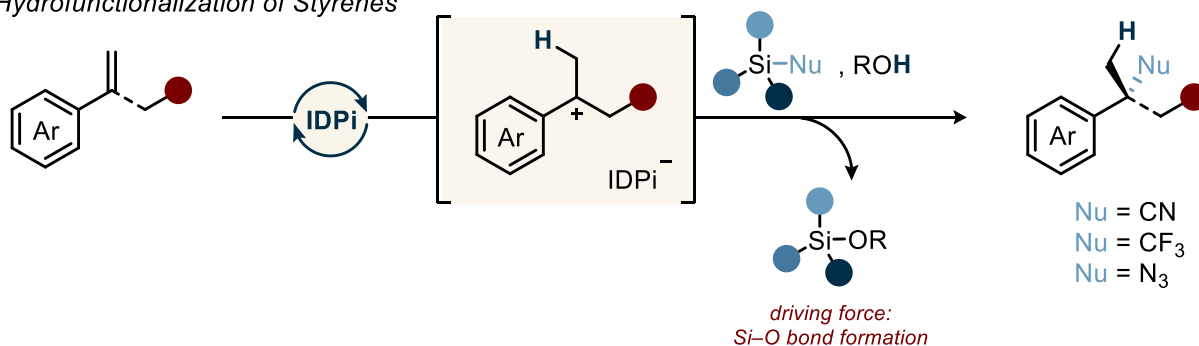
Kinetic resolution of carboxylic esters
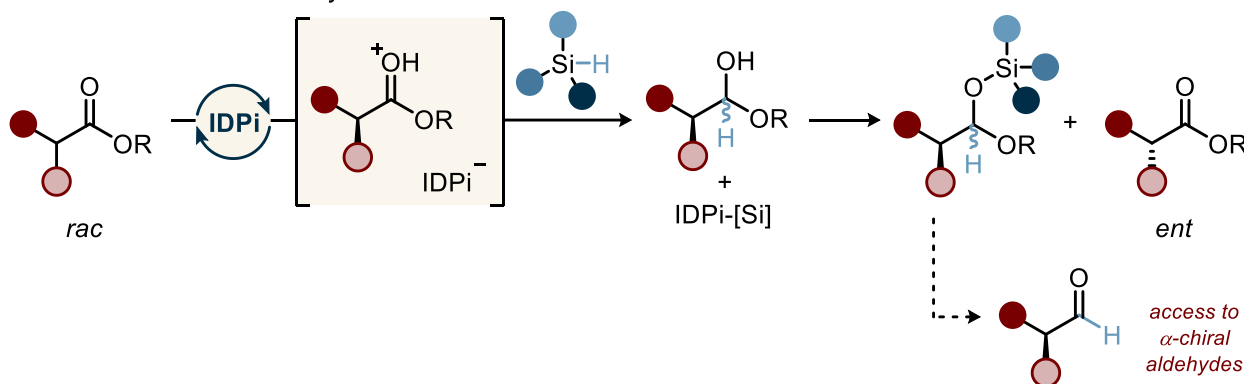
Figure 3.33 Outlook of this chapter: Expanding the substrate scope to tri- and tetrasubstituted aromatic alkenes, and aliphatic 1,1-disubstituted alkenes (top); Enabling hydrofunctionalization of styrenes via *Si*-bound nucleophiles, leveraging Si–O bond formation as the thermodynamic driving force (middle); Selective reduction of carboxylic acids to α-chiral aldehydes via kinetic resolution (bottom).

On the other hand, capitalizing on Si–O bond formation as the thermodynamic driving force opens new avenues for hydrofunctionalizations of styrenes. By employing alternative silicon-based nucleophiles (e.g.,

silyl cyanide, silyl azide, or silyl trifluoromethyl), this approach may enable access to chiral α-functionalized alkyl arenes (Figure 3.33, middle).

Moving beyond alkene substrates, a selective Brønsted acid-catalyzed reduction of carboxylic esters to aldehydes can be envisioned. In this scenario, no external protic additive is required. Instead, the substrate itself—through formation of a hemiacetal intermediate following hydride transfer—can facilitate protodesilylation of the *in situ* generated silylated catalyst species. This strategy grants access to silyl acetals, and when bulky silanes are employed, these reactive intermediates may be rendered incompatible with a confined IDPi catalyst due to a size-exclusion effect, and therefore remain intact without undergoing overreduction. If chiral (racemic) esters are employed, a kinetic resolution may become operative, furnishing both chiral aldehydes—following conversion from the silyl acetals—and unreacted esters in high enantiopurity. (Figure 3.33, bottom).

4 EXPERIMENTAL PART

4.1 General Information

Unless otherwise stated, reactions were carried out under an argon atmosphere in oven- or flame-dried glassware with magnetic stirring. Solvents and liquid reagents, as well as reagent solutions, were added via syringes or stainless steel/polyethylene cannulas through rubber septa or under a weak argon counterflow. Solid reagents were added under a weak argon counterflow. Reactions conducted below room temperature were cooled using appropriate cooling baths or cryostats. Cooling baths were prepared in Dewar vessels containing ice/water (0 °C), ice/NaCl (–20 °C), or dry ice/acetone (–78 °C). For reactions at elevated temperatures, heated oil baths were employed. Solvents were removed under reduced pressure at 40 °C using a rotary evaporator, and the resulting residues were dried under high vacuum (10^{-3} mbar) at room temperature or under an argon stream. All reported yields refer to NMR-spectroscopically pure materials unless otherwise stated.

All reagents were purchased from commercial suppliers (abcr, Alfa Aesar, Acros Organics, BLDpharm, Fluorochem, Sigma-Aldrich, TCI) and used without further purification. Solvents used in the reactions (Et_2O, THF, 1,4-dioxane, CyH, pentane, DCM, $CHCl_3$, PhH, PhMe) were distilled from appropriate drying agents and stored under argon. Other solvents (CyMe, hexanes, xylene) were obtained from commercial suppliers and stored under an argon atmosphere in a Schlenk flask.

Reactions were monitored by thin layer chromatography (TLC) on silica gel pre-coated plastic sheets (0.2 mm, Macherey-Nagel). Visualization was performed by irradiation with UV light at 254 nm and/or phosphomolybdic acid (PMA) or $KMnO_4$ staining. Preparative thin-layer chromatography was performed on silica gel pre-coated glass plates SIL G-100, with fluorescent indicator UV_{254} (Macherey-Nagel).

Column chromatography was conducted using Merck silica gel (60 Å, 230–400 mesh, particle size 0.040–0.063 mm) using technical grade solvents. Elution was accelerated using compressed air. Automated column chromatography was conducted on a Biotage® Isolera™ ISO-4SW instrument, using SNAP Ultra HP-Sphere™ 25 μm chromatography cartridges. All fractions containing a desired substance were combined and concentrated in vacuo, then redissolved in an appropriate solvent and filtered through cotton to remove silica residues.

^{1}H, ^{13}C, ^{19}F, and ^{31}P NMR spectra were recorded on a Bruker Avance III 500 MHz or Bruker NEO 600 MHz (equipped with a BBO CryoProbe) spectrometer in deuterated solvents. All spectra were recorded at 298 K unless otherwise noted, processed with the program MestReNova 15.0.0. ^{1}H chemical shifts (δ) are reported in ppm relative to the protonated solvent resonance employed as the internal standard ($CDCl_3$ δ = 7.26,

CD_2Cl_2 δ = 5.32, C_6D_6 δ = 7.16, $(CD_3)_2CO$) δ = 2.05). Data are reported as follows: chemical shift, multiplicity (s = singlet, d = doublet, t = triplet, q = quartet, p = pentet, h = heptet, m = multiplet), coupling constants (Hz) and integration. All X-nuclei spectra were acquired proton decoupled unless otherwise noted. When data from a mixture of *E/Z* isomers were reported, signals of the minor isomer were assigned only if they were unambiguously resolved. ^{13}C chemical shifts are reported in ppm with the solvent resonance as the internal standard ($CDCl_3$ δ = 77.16, CD_2Cl_2 δ = 54.00, C_6D_6 δ = 128.06, $(CD_3)_2CO$ δ = 29.84).

Electron impact (EI) mass spectrometry (MS) was performed on a Finnigan MAT 8200 (70 eV) or MAT 8400 (70 eV) spectrometer. Electrospray ionization (ESI) mass spectrometry was conducted on a Bruker ESQ 3000 spectrometer. High-resolution mass spectrometry (HRMS) was performed on a Finnigan MAT 95 (EI) or Bruker APEX III FTMS (7T magnet, ESI). The ionization method and mode of detection employed are indicated for the respective experiment and all masses are reported in atomic units per elementary charge (*m/z*) with an intensity normalized to the most intense peak.

Optical rotations were determined with an Autopol IV polarimeter (Rudolph Research Analytical) at 589 nm (sodium D line) and 25 °C. Data are reported as follows: $[\alpha]_D^T$, concentration *c* (g/100 mL) and solvent.

Enantiomeric ratios (er) were determined by GC or HPLC analysis using a chiral stationary phase column, indicated in each experiment, by comparing the samples with the corresponding racemic mixtures.

Language corrections have been conducted with the assistance of the ChatGPT language model (GPT-5, OpenAI). Suggested corrections were carefully reviewed and selectively integrated to improve clarity and readability.

4.2 Experimental Procedures for Chapter 2

4.2.1 Reaction Optimization

An oven-dried GC vial under argon, equipped with a magnetic stirring bar, was charged with the chiral phosphoric acid (CPA) and the amine of choice (2.5–20 mol%). Substrate **27** (0.025–0.03 mmol) was added and dissolved in the respective dry solvent. The reaction mixture was stirred for five minutes at room temperature. After addition of Hantzsch ester **33** (1.1–1.5 eq.) the reaction mixture was heated to the desired temperature and stirred overnight (for reduced temperatures the reaction was set up at –78°C and warmed to the reaction temperature). The reaction was quenched by addition of NEt$_3$ (10 µL) followed by addition of Ph$_3$CH (1.0 M in PhMe) or mesitylene as internal standard. An aliquot of the mixture was taken and diluted with CDCl$_3$ for subsequent ^{1}H NMR analysis. The remaining solution was used for preparative thin layer chromatography to purify the chiral product **29**. Chiral GC analysis was performed to give the corresponding enantiomeric ratio.
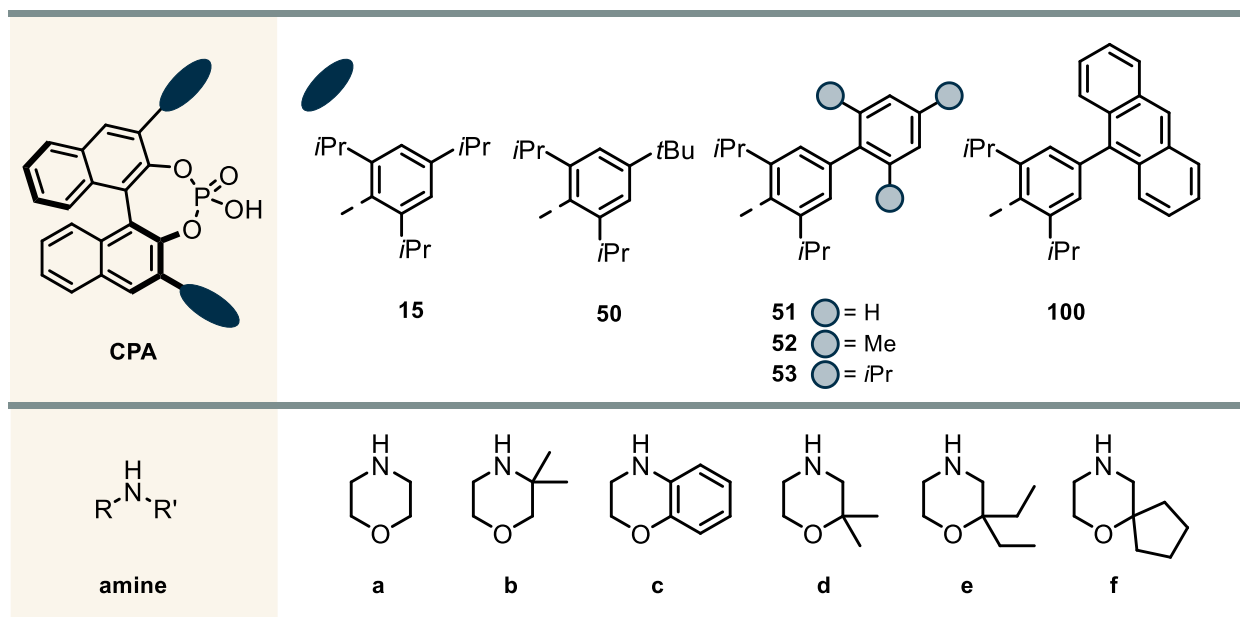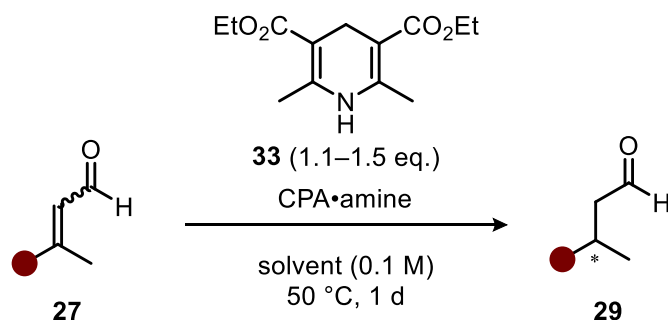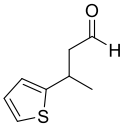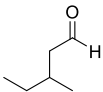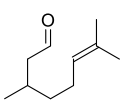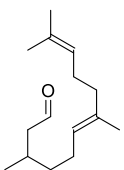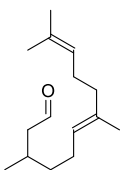
Table 4.1 Reaction Optimization for ● = 4-Br-C$_6$H$_4$ (**27a/29a**).

entry	CPA	amine	catalyst loading [mol%]	solvent	temperature	conversion	yield	er
1	**15**	**a**	20	1,4-dioxane	50 °C	100%	73%	80:20
2	**15**	**a**	20	1,4-dioxane	30 °C	92%	68%	79.5:20.5
3	**15**	**a**	10	1,4-dioxane	50 °C	100%	70%	80:20
4	**15**	**a**	5	1,4-dioxane	50 °C	100%	82%	80:20
5	**15**	**a**	2.5	1,4-dioxane	50 °C	100%	78%	80:20
6	**15**	**b**	20	1,4-dioxane	50 °C	22%	7%	57:43
7	**15**	**c**	20	1,4-dioxane	50 °C	100%	72%	53.5:46.5
8	(*R*)-**50**	**a**	20	1,4-dioxane	50 °C	100%	69%	21:79
9	(*R*)-**51**	**a**	20	1,4-dioxane	50 °C	100%	74%	9.5:90.5
10	**53**	**a**	20	1,4-dioxane	50 °C	100%	58%	93:7
11	**53**	**b**	20	1,4-dioxane	50 °C	45%	28%	62:38
12	**53**	**c**	20	1,4-dioxane	50 °C	100%	68%	83:17
13	**53**	**d**	20	1,4-dioxane	50 °C	100%	58%	96:4
14	**53**	**e**	20	1,4-dioxane	50 °C	96%	78%	97.5:2.5
15	**53**	**f**	20	1,4-dioxane	50 °C	94%	66%	98:2
16	**53**	**f**	5	1,4-dioxane	50 °C	92%	57%	98:2
17	**53**	**f**	2.5	1,4-dioxane	50 °C	100%	81%	98:2
18	**53**	**f**	5	CHCl$_3$	50 °C	60%	n.d.	88:12
19	**53**	**f**	5	THF	50 °C	92%	n.d.	93.5:6.5
20	**53**	**f**	5	Et$_2$O	rt	100%	n.d.	97.5:2.5
21	**53**	**f**	5	PhMe	50 °C	100%	n.d.	96.5:3.5
22	**53**	**f**	5	CyH	50 °C	100%	n.d.	97.5:2.5

Table 4.2 Reoptimization for other substrates.

CPA	amine	catalyst loading [mol%]	solvent	temperature	conversion	yield	er
53	**f**	2.5	1,4-dioxane	50 °C	95%	51%	92:8
(*R*)-**50**	**f**	2.5	1,4-dioxane	50 °C	85%	40%	31.5:68.5
(*R*)-**51**	**f**	2.5	1,4-dioxane	50 °C	87%	52%	27:73
(*R*)-**100**	**f**	2.5	1,4-dioxane	50 °C	86%	31%	16:84
53	**f**	2.5	Et$_2$O	rt	88%	72%	92:8
53	**f**	2.5	PhMe	rt	100%	87%	93:7
53	**f**	2.5	*n*-pentane	rt	100%	70%	92:8
53	**f**	2.5	CyH	rt	92%	72%	95:5
53	**f**	2.5	CyMe	rt	64%	30%	93.5:6.5
53	**f**	2.5	1,4-dioxane	50 °C	100%	57%	86.5:13.5
(*R*)-S1	**f**	2.5	1,4-dioxane	50 °C	100%	67%	18:82
(*R*)-**5**	**f**	2.5	1,4-dioxane	50 °C	97%	67%	17.5:82.5
(*R*)-S2	**f**	2.5	1,4-dioxane	50 °C	97%	62%	17:83
53	**f**	2.5	Et$_2$O	rt	100%	84%	86:14
53	**f**	2.5	PhMe	rt	100%	87%	86.5:13.5
53	**f**	2.5	*n*-pentane	rt	100%	83%	88:12
53	**f**	2.5	CyH	rt	100%	84%	90.5:9.5
53	**f**	2.5	CyMe	rt	100%	85%	89.5:10.5
53	**f**	2.5	CyH/*n*-pentane 9:1	0	75%[4]	59%	92:8
53	**f**	2.5	CyH/*n*-pentane	−10	67%[4]	39%	92.5:7.5

---

[4] Reaction was run for 2 days.

CPA	amine	catalyst loading [mol%]	solvent	temperature	conversion	yield	er
			9:1				
53	f	2.5	CyH/n-pentane 9:1	−20	35%[4]	20%	93.5:6.5
53	f	2.5	1,4-dioxane	50 °C	100%	83%	94:6
(R)-S1	f	2.5	1,4-dioxane	50 °C	100%	40%	10:90
(R)-5	f	2.5	1,4-dioxane	50 °C	98%	58%	9.5:90.5
(R)-S2	f	2.5	1,4-dioxane	50 °C	80%	43%	11:89
53	f	2.5	CyH	rt	100%	88%	97:3
53	f	2.5	1,4-dioxane	50 °C	100%	56%	94.5:5.5
53	f	2.5	CyH	rt	100%	61%	97.5:2.5

4.2.2 Synthesis of α,β-Unsaturated Esters
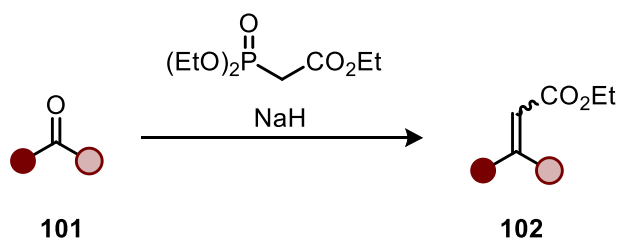
General procedure 1 (GP1)

In a flame-dried Schlenk flask under argon, NaH (60% in mineral oil, 1.5 eq.) was suspended in dry THF (0.2 M). After dropwise addition of triethyl phosphonoacetate (1.7 eq.) at 0 °C, the reaction mixture was allowed to reach room temperature. The respective ketone (**101**, 1.0 eq.) was then slowly added and the resulting mixture was stirred at room temperature overnight. The reaction was quenched by the addition of

water and extracted with DCM (3x). The combined organic layers were washed with water (2x), dried over anhydrous Na_2CO_3 and concentrated under reduced pressure. The residue was purified via flash chromatography on silica gel to obtain the corresponding α,β-unsaturated ester.

ethyl 3-(4-bromophenyl)but-2-enoate (102a)
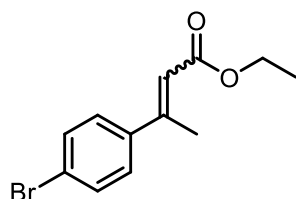
Following GP1 the reaction was performed using 4'-bromoacetophenone (2.00 g, 10.0 mmol, 1.00 eq.). Purification by silica gel flash chromatography (5% Et_2O in pentane) afforded the product as a mixture of E/Z isomers (2.63 g, 9.78 mmol, 97%, $E/Z \approx 76:24$) as a colorless oil. The NMR-spectroscopic data are in agreement with the literature.[260]

¹H NMR (501 MHz, CDCl₃): δ = 7.52–7.48 (m, 2H$_{maj}$), 7.47 (d, J = 8.4 Hz, 2H$_{min}$), 7.37–7.32 (m, 2H$_{maj}$), 7.11–7.05 (m, 2H$_{min}$), 6.11 (q, J = 1.3 Hz, 1H$_{maj}$), 5.92 (q, J = 1.5 Hz, 1H$_{min}$), 4.22 (q, J = 7.1 Hz, 2H$_{maj}$), 4.01 (q, J = 7.2 Hz, 2H$_{min}$), 2.54 (d, J = 1.3 Hz, 3H$_{maj}$), 2.15 (d, J = 1.5 Hz, 3H$_{min}$), 1.32 (t, J = 7.1 Hz, 3H$_{maj}$), 1.12 (t, J = 7.1 Hz, 3H$_{min}$).

ethyl 3-(3-bromophenyl)but-2-enoate (102b)
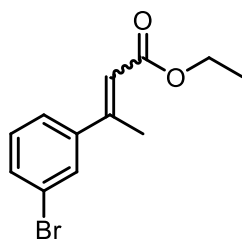
Following GP1 the reaction was performed using 3'-bromoacetophenone (2.0 mL, 15 mmol, 1.0 eq.). Purification by silica gel flash chromatography (5% Et_2O in pentane) afforded the product as a mixture of E/Z isomers (3.87 g, 14.4 mmol, 96%, $E/Z \approx 89:11$) as a colorless oil. The NMR-spectroscopic data are in agreement with the literature.[261]

¹H NMR (501 MHz, CDCl₃): δ = 7.61 (t, J = 1.9 Hz, 1H$_{maj}$), 7.48 (ddd, J = 7.9, 2.0, 1.0 Hz, 1H$_{maj}$), 7.43 (ddd, J = 8.0, 2.0, 1.1 Hz, 1H$_{min}$), 7.39 (ddd, J = 7.8, 1.8, 1.0 Hz, 1H$_{maj}$), 7.34 (t, J = 1.8 Hz, 1H$_{min}$), 7.26 (d, J = 0.9 Hz, 1H$_{maj}$), 7.24 (s, 1H$_{min}$), 7.13 (dt, J = 7.7, 1.3 Hz, 1H$_{min}$), 6.11 (q, J = 1.3 Hz, 1H$_{maj}$), 5.92 (q, J = 1.5 Hz, 1H$_{min}$), 4.22 (q, J = 7.1 Hz, 2H$_{maj}$), 4.01 (q, J = 7.1 Hz, 2H$_{min}$), 2.54 (d, J = 1.4 Hz, 3H$_{maj}$), 2.15 (d, J = 1.4 Hz, 3H$_{min}$), 1.32 (t, J = 7.1 Hz, 3H$_{maj}$), 1.09 (t, J = 7.1 Hz, 3H$_{min}$).

ethyl 3-(3-(trifluoromethyl)phenyl)but-2-enoate (102c)

Following GP1 the reaction was performed using 3'-(trifluoromethyl)acetophenone (1.0 mL, 6.6 mmol, 1.0 eq.). Purification by silica gel flash chromatography (10% Et_2O in pentane) afforded the product as a mixture of E/Z isomers (1.41 g, 5.47 mmol, 83%, $E/Z \approx 97:3$) as a light yellow oil.
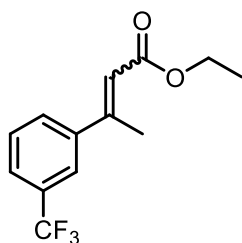
¹H NMR (501 MHz, CDCl$_3$): δ = 7.70 (d, J = 1.9 Hz, 1H$_{maj}$), 7.67–7.59 (m, 2H$_{maj}$), 7.50 (t, J = 7.8 Hz, 1H$_{maj}$), 6.15 (q, J = 1.3 Hz, 1H$_{maj}$), 4.23 (q, J = 7.1 Hz, 2H$_{maj}$), 2.59 (d, J = 1.3 Hz, 3H$_{maj}$), 1.33 (t, J = 7.1 Hz, 3H$_{maj}$).

¹⁹F NMR (471 MHz, CDCl$_3$): δ = –62.6 (s, 3F$_{min}$), –62.73 (s, 3F$_{maj}$).

(*E*)- and (*Z*)-ethyl 3-phenylbut-2-enoate (*E*-102d, *Z*-102d)
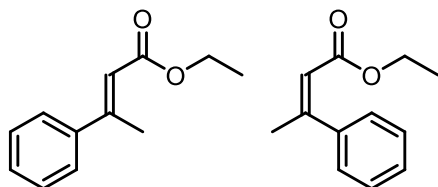
Following GP1 the reaction was performed using acetophenone (2.0 mL, 17 mmol, 1.0 eq.). Purification by silica gel flash chromatography (10% Et$_2$O in pentane) afforded the separated *E*- (2.50 g, 13.2 mmol, 77%) and *Z*-isomer (0.45 g, 2.4 mmol, 14%) of the product as light yellow oils. The NMR-spectroscopic data are in agreement with the literature.[260]

E-isomer: **¹H NMR** (501 MHz, CDCl$_3$): δ = 7.51–7.43 (m, 2H), 7.41–7.33 (m, 3H), 6.13 (q, J = 1.4 Hz, 1H), 4.22 (q, J = 7.1 Hz, 2H), 2.58 (d, J = 1.3 Hz, 3H), 1.32 (t, J = 7.1 Hz, 3H).

Z-isomer: **¹H NMR** (501 MHz, CDCl$_3$): δ = 7.38–7.28 (m, 3H), 7.23–7.17 (m, 2H), 5.91 (q, J = 1.5 Hz, 1H), 4.00 (q, J = 7.1 Hz, 2H), 2.18 (d, J = 1.5 Hz, 3H), 1.08 (t, J = 7.1 Hz, 3H).

ethyl 3-(*p*-tolyl)but-2-enoate (102e)
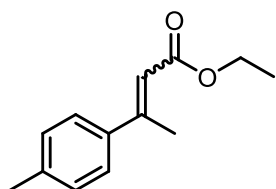
Following GP1 the reaction was performed using 4'-methylacetophenone (2.2 mL, 16 mmol, 1.0 eq.). Purification by silica gel flash chromatography (10% Et$_2$O in pentane) afforded the product as a mixture of *E*/*Z* isomers (3.15 g, 15.4 mmol, 94%, *E*/*Z* ≈ 83:17) as a colorless oil. The NMR-spectroscopic data are in agreement with the literature.[260]

¹H NMR (501 MHz, CDCl$_3$): δ = 7.39 (d, J = 8.3 Hz, 2H$_{maj}$), 7.20–7.10 (m, 2H$_{maj}$, 4H$_{min}$), 6.13 (q, J = 1.4 Hz, 1H$_{maj}$), 5.89 (q, J = 1.5 Hz, 1H$_{min}$), 4.21 (q, J = 7.1 Hz, 2H$_{maj}$), 4.02 (q, J = 7.1 Hz, 1H$_{min}$), 2.57 (d, J = 1.3 Hz, 3H$_{maj}$), 2.16 (d, J = 1.5 Hz, 1H$_{min}$), 1.32 (t, J = 7.1 Hz, 3H$_{maj}$), 1.12 (t, J = 7.1 Hz, 3H$_{min}$).

ethyl 3-(*m*-tolyl)but-2-enoate (102f)

Following GP1 the reaction was performed using 3'-methylacetophenone (3.0 mL, 22 mmol, 1.0 eq.). Purification by silica gel flash chromatography (10% Et$_2$O in pentane) afforded the product as a mixture of
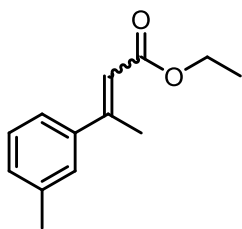
E/*Z* isomers (4.42 g, 21.6 mmol, 98%, *E*/*Z* ≈ 85:15) as a colorless oil. The NMR-spectroscopic data are in agreement with the literature.[262]

¹H NMR (501 MHz, CDCl₃): δ = 7.30–7.25 (m, 3H_maj), 7.25–7.21 (m, 1H_min), 7.20–7.15 (m, 1H_maj), 7.13–7.10 (m, 1H_min), 7.02–6.98 (m, 2H_min), 6.12 (d, *J* = 1.4 Hz, 1H_maj), 5.89 (d, *J* = 1.4 Hz, 1H_min), 4.22 (q, *J* = 7.1 Hz, 2H_maj), 4.00 (q, *J* = 7.1 Hz, 2H_min), 2.57 (d, *J* = 1.4 Hz, 3H_maj), 2.16 (d, *J* = 1.4 Hz, 3H_min), 1.32 (t, *J* = 7.1 Hz, 3H_maj), 1.08 (t, *J* = 7.1 Hz, 1H_min).

ethyl (*E*)-3-(o-tolyl)but-2-enoate (102g)
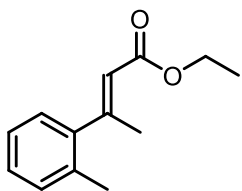
Following GP1 the reaction was performed using 2'-methylacetophenone (1.0 mL, 7.6 mmol, 1.0 eq.). Purification by silica gel flash chromatography (10–50% DCM in hexanes) afforded the product (612 mg, 3.00 mmol, 39%, *E*/*Z*>99:1) as a colorless oil. The NMR-spectroscopic data are in agreement with the literature.[263]

¹H NMR (501 MHz, CDCl₃): δ = 7.23–7.13 (m, 3H), 7.07 (dd, *J* = 7.4, 1.5 Hz, 1H), 5.76 (q, *J* = 1.4 Hz, 1H), 4.22 (q, *J* = 7.1 Hz, 2H), 2.45 (d, *J* = 1.4 Hz, 3H), 2.29 (s, 3H), 1.31 (t, *J* = 7.1 Hz, 3H).

ethyl 3-(4-((triisopropylsilyl)oxy)phenyl)but-2-enoate (102h)
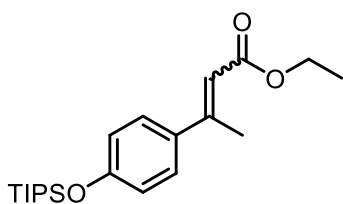
Following GP1 the reaction was performed using ethyl 3-(4-((triisopropylsilyl)oxy)phenyl)but-2-enoate² (4.59 g, 15.7 mmol, 1.00 eq.). The reaction mixture was additionally stirred at 80 °C overnight. Purification by silica gel flash chromatography (10% Et₂O in pentane) afforded the product (3.70 g, 10.2 mmol, 65%, *E*/*Z* ≈ 98:2) as a colorless oil. The NMR-spectroscopic data are in agreement with the literature.[264]

¹H NMR (501 MHz, CD₂Cl₂): δ = 7.43–7.38 (m, 2H_maj), 6.90–6.85 (m, 2H_maj), 6.09 (q, *J* = 1.3 Hz, 1H_maj), 4.17 (q, *J* = 7.1 Hz, 2H_maj), 2.53 (d, *J* = 1.2 Hz, 3H_maj), 1.31–1.24 (m, 6H_maj), 1.11 (d, *J* = 7.4 Hz, 18H_maj).

ethyl 3-(4-methoxy-3-nitrophenyl)but-2-enoate (102j)

Following GP1 the reaction was performed using 4'-methoxy-3'-nitroacetophenone (2.00 g, 10.2 mmol, 1.00 eq.). Purification by silica gel flash chromatography (30% Et₂O in pentane) afforded the product as a mixture of *E*/*Z* isomers (1.99 g, 7.48 mmol, 73%, *E*/*Z* ≈ 74:26) as an off-white solid.
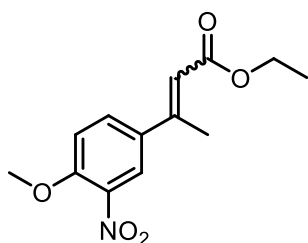
¹H NMR (501 MHz, CDCl₃): δ = 7.99 (d, J = 2.5 Hz, 1H$_{maj}$), 7.76 (d, J = 2.3 Hz, 1H$_{min}$), 7.67 (dd, J = 8.8, 2.4 Hz, 1H$_{maj}$), 7.44 (dd, J = 8.7, 2.2 Hz, 1H$_{min}$), 7.09 (d, J = 8.8 Hz, 1H$_{maj}$), 7.06 (d, J = 8.7 Hz, 1H$_{min}$), 6.14 (q, J = 1.3 Hz, 1H$_{maj}$), 5.95 (q, J = 1.5 Hz, 1H$_{min}$), 4.22 (q, J = 7.1 Hz, 2H$_{maj}$), 4.04 (q, J = 7.1 Hz, 2H$_{min}$), 3.99 (s, 3H$_{maj}$), 3.97 (s, 3H$_{min}$), 2.56 (d, J = 1.3 Hz, 3H$_{maj}$), 2.18 (d, J = 1.5 Hz, 3H$_{min}$), 1.32 (t, J = 7.1 Hz, 3H$_{maj}$), 1.15 (t, J = 7.1 Hz, 3H$_{min}$).

¹³C NMR (126 MHz, CDCl₃): δ = 166.5, 165.5, 153.4, 152.8, 152.4, 152.1, 139.6, 139.1, 134.4, 133.6, 132.7, 131.9, 124.9, 123.7, 119.0, 117.7, 113.7, 113.0, 60.2, 60.2, 56.8, 56.7, 26.9, 17.6, 14.4, 14.2.

HRMS m/z (GC-EI): calcd. for $C_{13}H_{15}N_1O_5$ ([M]⁺): 265.094474; found: 265.094600.

ethyl 3-(pyridin-3-yl)but-2-enoate (102k)
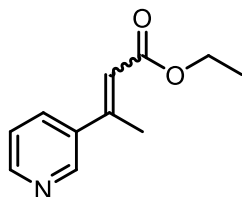
Following GP1 the reaction was performed using 3-acetylpyridine (2.0 mL, 18 mmol, 1.0 eq.). Purification by silica gel flash chromatography (5–30% EtOAc in hexanes) afforded the product as a mixture of E/Z isomers (1.68 g, 8.77 mmol, 48%, E/Z ≈ 97:3) as a yellow oil. The NMR-spectroscopic data are in agreement with the literature.[260]

¹H NMR (501 MHz, CDCl₃): δ = 8.72 (d, J = 2.4 Hz, 1H$_{maj}$), 8.59 (dd, J = 4.8, 1.6 Hz, 1H$_{maj}$), 7.75 (dt, J = 7.9, 2.2 Hz, 1H$_{maj}$), 7.30 (dd, J = 8.0, 4.8 Hz, 1H$_{maj}$), 6.14 (q, J = 1.4 Hz, 1H$_{maj}$), 4.22 (qd, J = 7.1, 1.1 Hz, 2H$_{maj}$), 2.58 (d, J = 1.4 Hz, 3H$_{maj}$), 1.32 (td, J = 7.2, 1.1 Hz, 3H$_{maj}$).

ethyl 3-(thiophen-2-yl)but-2-enoate (102l)
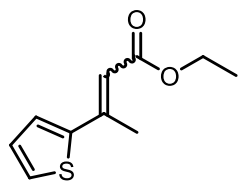
Following GP1 the reaction was performed using 2-acetylthiophene (2.0 mL, 19 mmol, 1.0 eq.). Purification by silica gel flash chromatography (2–5% EtOAc in hexanes) afforded the product as a mixture of E/Z isomers (3.64 g, 16.3 mmol, 88%, E/Z ≈ 87:13) as a light yellow oil. The NMR-spectroscopic data are in agreement with the literature.[260]

¹H NMR (501 MHz, CDCl₃): δ = 7.49–7.44 (m, 1H$_{min}$), 7.38 (d, J = 4.8 Hz, 1H$_{min}$), 7.34–7.29 (m, 2H$_{maj}$), 7.07–7.01 (m, 1H$_{maj}$, 1H$_{min}$), 6.27–6.24 (m, 1H$_{maj}$), 5.89–5.82 (m, 1H$_{min}$), 4.20 (q, J = 2.4 Hz, 2H$_{maj}$), 4.16–4.07 (m, 2H$_{min}$), 2.61 (s, 3H$_{maj}$), 2.29 (s, 3H$_{min}$), 1.31 (t, J = 7.2 Hz, 3H$_{maj}$), 1.25 (t, J = 7.2 Hz, 3H$_{min}$).

ethyl 3-(2-chlorophenyl)but-2-enoate (102m)
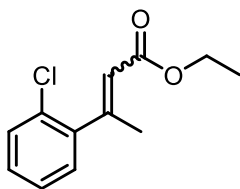
Following GP1 the reaction was performed using 1-(2-chlorophenyl)ethan-1-one (2.0 mL, 15 mmol, 1.0 eq.). Purification by silica gel flash chromatography (10% EtOAc in pentane) afforded the product as a mixture of E/Z isomers (2.03 g, 7.72 mmol, 85%, $E/Z \approx 62{:}38$) as a light yellow oil. The NMR-spectroscopic data are in agreement with the literature.[133]

¹H NMR (501 MHz, CDCl₃): δ = 7.42–7.38 (m, 1H$_{maj}$, 1H$_{min}$), 7.30–7.23 (m, 2H$_{maj}$, 2H$_{min}$), 7.21–7.17 (m, 1H$_{maj}$), 7.13–7.06 (m, 1H$_{min}$), 6.03 (q, J = 1.5 Hz, 1H$_{min}$), 5.85 (q, J = 1.4 Hz, 1H$_{maj}$), 4.25 (q, J = 7.1 Hz, 2H$_{maj}$), 4.00 (q, J = 7.1 Hz, 2H$_{min}$), 2.51 (d, J = 1.5 Hz, 3H$_{maj}$), 2.18 (d, J = 1.5 Hz, 3H$_{min}$), 1.34 (t, J = 7.1 Hz, 3H$_{maj}$), 1.07 (t, J = 7.1 Hz, 3H$_{min}$).

ethyl 3-(4-(4,4,5,5-tetramethyl-1,3,2-dioxaborolan-2-yl)phenyl)but-2-enoate (102n)
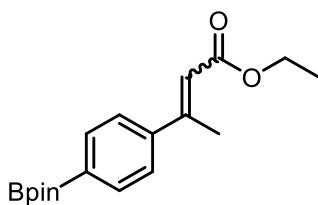
Following GP1 the reaction was performed using 1-(2-chlorophenyl)ethan-1-one (2.0 mL, 15 mmol, 1.0 eq.). Purification by silica gel flash chromatography (10% EtOAc in pentane) afforded the product as a mixture of E/Z isomers (2.03 g, 7.72 mmol, 85%, $E/Z \approx 62{:}38$) as a light yellow oil.

¹H NMR (501 MHz, CDCl₃): δ = 7.80 (t, J = 7.7 Hz, 2H$_{maj}$, 2H$_{min}$), 7.49–7.45 (m, 2H$_{maj}$), 7.22–7.17 (m, 2H$_{min}$), 6.16 (t, J = 1.4 Hz, 1H$_{maj}$), 5.91 (q, J = 1.5 Hz, 1H$_{min}$), 4.22 (q, J = 7.1 Hz, 2H$_{maj}$), 3.99 (q, J = 7.1 Hz, 2H$_{min}$), 2.57 (d, J = 1.3 Hz, 3H$_{maj}$), 2.16 (d, J = 1.4 Hz, 3H$_{min}$), 1.35 (s, 12H$_{maj}$), 1.34 (s, 12H$_{min}$).

ethyl 3-cyclohexylbut-2-enoate (102o)
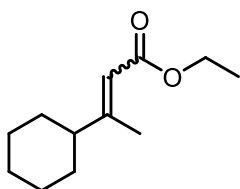
Following GP1 the reaction was performed using cyclohexyl methyl ketone (1.8 mL, 13 mmol, 1.0 eq.). Purification by silica gel flash chromatography (20–30% DCM in hexanes) afforded the product as a mixture of E/Z isomers (1.64 g, 8.37 mmol, 64%, $E/Z \approx 89{:}11$) as a colorless oil. The NMR-spectroscopic data are in agreement with the literature.[265]

¹H NMR (501 MHz, CDCl₃): δ = 5.64 (d, J = 1.5 Hz, 1H$_{maj}$), 5.57 (d, J = 1.5 Hz, 1H$_{min}$), 4.13 (q, J = 7.1 Hz, 2H$_{maj}$, 2H$_{min}$), 3.60 (tt, J = 11.5, 3.5 Hz, 1H$_{min}$), 2.13 (d, J = 1.1 Hz, 3H$_{maj}$), 1.96 (tt, J = 11.3, 3.2 Hz, 1H$_{maj}$), 1.82–1.51 (m, 8H$_{min}$, 5H$_{maj}$), 1.41–1.10 (m, 8H$_{maj}$, 8H$_{min}$).

ethyl 3-cyclopentylbut-2-enoate (102p)
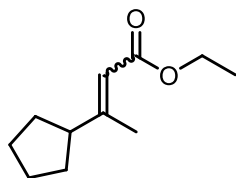
Following GP1 the reaction was performed using cyclopentyl methyl ketone (2.0 mL, 16 mmol, 1.0 eq.). Purification by silica gel flash chromatography (5% Et$_2$O in pentane) afforded the product as a mixture of E/Z isomers (2.75 g, 15.1 mmol, 93%, E/Z ≈ 86:14) as a colorless oil. The NMR-spectroscopic data are in agreement with the literature.[266]

¹H NMR (501 MHz, CDCl$_3$): δ = 5.70 (s, 1H$_{maj}$), 5.64 (s, 1H$_{min}$), 4.14 (q, J = 7.2 Hz, 2H$_{maj}$, 2H$_{min}$), 4.07–3.98 (m, 1H$_{min}$), 2.59–2.46 (m, 1H$_{maj}$), 2.15 (d, J = 1.2 Hz, 3H$_{maj}$), 1.87–1.77 (m, 2H$_{maj}$, 5H$_{min}$), 1.74–1.55 (m, 4H$_{maj}$, 4H$_{min}$), 1.49–1.39 (m, 2H$_{maj}$, 2H$_{min}$), 1.31–1.23 (m, 3H$_{maj}$, 3H$_{min}$).

ethyl 3-cyclobutylbut-2-enoate (102q)
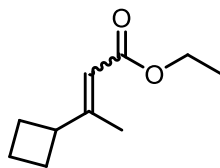
Following GP1 the reaction was performed using cyclobutyl methyl ketone (2.5 mL, 23 mmol, 1.0 eq.). Purification by silica gel flash chromatography (4% Et$_2$O in pentane) afforded the product (3.33 g, 19.8 mmol, 86%) as a colorless oil. The exact E/Z ratio could not be determined by NMR analysis due to significant signal overlap.

¹H NMR (501 MHz, CDCl$_3$): δ = 5.59 (t, J = 1.5 Hz, 1H), 4.18–4.09 (m, 2H), 3.05–2.94 (m, 1H), 2.17–2.09 (m, 2H), 2.08–2.05 (m, 3H), 1.99–1.85 (m, 3H), 1.75–1.67 (m, 1H), 1.28 (t, J = 7.2 Hz, 3H).

¹³C NMR (126 MHz, CDCl$_3$): δ = 167.4, 162.8, 113.2, 59.6, 44.3, 27.3, 17.6, 16.4, 14.5. (Signals of major E-isomer given.)

HRMS m/z (GC-EI): calcd. for C$_{10}$H$_{16}$O$_2$ ([M]$^+$): 168.114480; found: 168.114550.

ethyl (E)-3,4,4-trimethylpent-2-enoate (102r)
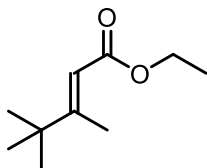
Following GP1 the reaction was performed using 3,3-dimethylbutan-2-one (3.7 mL, 30 mmol, 1.0 eq.). Purification by silica gel flash chromatography (20% DCM in pentane) afforded the product (2.42 g, 14.2 mmol, 48%) as a colorless oil. The NMR-spectroscopic data are in agreement with the literature.[267]

¹H NMR (501 MHz, CDCl$_3$): δ = 5.73 (d, J = 1.5 Hz, 1H), 4.14 (q, J = 7.1 Hz, 2H), 2.16 (d, J = 1.1 Hz, 3H), 1.28 (t, J = 7.1 Hz, 3H), 1.10 (s, 9H).

ethyl 3,4-dimethylpent-2-enoate (102s)
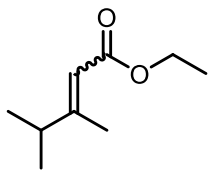
Following GP1 the reaction was performed using 3-methylbutan-2-one (5.0 mL, 47 mmol, 1.0 eq.). Purification by silica gel flash chromatography (1–5% Et$_2$O in pentane) afforded the product as a mixture of E/Z isomers (6.81 g, 43.6 mmol, 93%, E/$Z \approx$ 85:15) as a colorless oil. The NMR-spectroscopic data are in agreement with the literature.[268]

¹H NMR (501 MHz, CDCl$_3$): δ = 5.67 (s, 1H$_{maj}$), 5.58 (d, J = 1.6 Hz, 1H$_{min}$), 4.14 (q, J = 7.2 Hz, 2H$_{maj}$, 2H$_{min}$), 3.97 (h, J = 7.1 Hz, 1H$_{min}$), 2.35 (h, J = 6.7 Hz, 1H$_{maj}$), 2.13 (d, J = 1.3 Hz, 3H$_{maj}$), 1.79 (d, J = 1.4 Hz, 3H$_{min}$), 1.27 (t, J = 7.2 Hz, 3H$_{maj}$, 3H$_{min}$), 1.06 (d, J = 6.8 Hz, 6H$_{maj}$), 1.03 (d, J = 6.8 Hz, 6H$_{min}$).

ethyl 3-methylpent-2-enoate (102t)
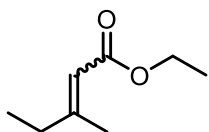
Following GP1 the reaction was performed using butan-2-one (3.7 mL, 41 mmol, 1.0 eq.). Purification by silica gel flash chromatography (1–5% Et$_2$O in pentane) afforded the product as a mixture of E/Z isomers (5.28 g, 37.1 mmol, 90%, E/$Z \approx$ 75:25) as a colorless oil. The NMR-spectroscopic data are in agreement with the literature.[269]

¹H NMR (501 MHz, CDCl$_3$): δ = 5.66–5.63 (m, 1H$_{maj}$), 5.62–5.60 (m, 1H$_{min}$), 4.18–4.07 (m, 2H$_{maj}$, 2H$_{min}$), 2.62 (q, J = 7.6 Hz, 2H$_{min}$), 2.18–2.11 (m, 5H$_{maj}$), 1.86 (s, 3H$_{min}$), 1.29–1.23 (m, 3H$_{maj}$, 3H$_{min}$), 1.03–1.08 (m, 3H$_{maj}$, 3H$_{min}$).

ethyl 3-methylhex-2-enoate (102u)
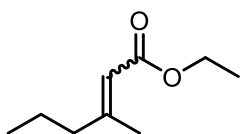
Following GP1 the reaction was performed using pentan-2-one (2.0 mL, 19 mmol, 1.0 eq.). Purification by silica gel flash chromatography (2% Et$_2$O in pentane) afforded the product as a mixture of E/Z isomers (2.58 g, 16.5 mmol, 88%, E/$Z \approx$ 73:27) as a colorless oil. The NMR-spectroscopic data are in agreement with the literature.[270]

¹H NMR (501 MHz, CDCl$_3$): δ = 5.65 (q, J = 1.3 Hz, 1H$_{maj}$, 1H$_{min}$), 4.17–4.11 (m, 2H$_{maj}$, 2H$_{min}$), 2.63–2.57 (m, 2H$_{min}$), 2.14 (d, J = 1.2 Hz, 3H$_{maj}$), 2.11 (td, J = 7.4, 1.2 Hz, 2H$_{maj}$), 1.87 (s, 3H$_{min}$), 1.55–1.46 (m, 2H$_{maj}$, 2H$_{min}$), 1.29–1.25 (m, 3H$_{maj}$, 3H$_{min}$), 0.95 (t, J = 7.4 Hz, 3H$_{min}$), 0.91 (t, J = 7.4 Hz, 3H$_{maj}$).

ethyl 3-methylhept-2-enoate (102v)
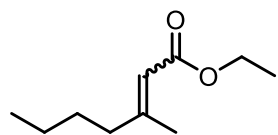
Following GP1 the reaction was performed using hexan-2-one (2.0 mL, 16 mmol, 1.0 eq.). Purification by silica gel flash chromatography (2% Et_2O in pentane) afforded the product as a mixture of E/Z isomers (2.46 g, 14.5 mmol, 89%, $E/Z \approx$ 78:22) as a colorless oil. The NMR-spectroscopic data are in agreement with the literature.[271]

^{1}H NMR (501 MHz, CDCl$_3$): δ = 5.66 (q, J = 1.3 Hz, 1H$_{maj}$),), 5.64 (d, J = 1.5 Hz, 1H$_{min}$), 4.17–4.11 (m, 2H$_{maj}$, 2H$_{min}$), 2.65–2.59 (m, 2H$_{min}$), 2.15 (d, J = 1.4 Hz, 3H$_{maj}$), 2.14–2.11 (m, 2H$_{maj}$), 1.88 (s, 3H$_{min}$), 1.47–1.42 (m, 2H$_{maj}$, 2H$_{min}$), 1.38–1.22 (m, 5H$_{maj}$, 5H$_{min}$), 0.94–0.89 (m, 3H$_{maj}$, 3H$_{min}$).

ethyl 3-phenylpent-2-enoate (102y)
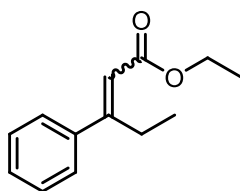
Following GP1 the reaction was performed using propiophenone (3.0 mL, 37 mmol, 1.0 eq.). Purification by silica gel flash chromatography (4% EtOAc in hexanes) afforded the product as a mixture of E/Z isomers (1.38 g, 4.37 mmol, 64%, $E/Z \approx$ 78:22) as a colorless oil. The NMR-spectroscopic data are in agreement with the literature.[272]

^{1}H NMR (501 MHz, CDCl$_3$): δ = 7.45–7.29 (m, 5H$_{maj}$, 5H$_{min}$), 7.17–7.12 (m, 2H$_{min}$), 6.02 (s, 1H$_{maj}$), 5.87 (s, 1H$_{min}$), 4.22 (q, J = 7.1 Hz, 2H$_{maj}$), 3.98 (q, J = 7.2 Hz, 2H$_{min}$), 3.11 (q, J = 7.4 Hz, 2H$_{maj}$), 2.46 (qd, J = 7.4, 1.5 Hz, 2H$_{min}$), 1.32 (t, J = 7.1 Hz, 3H$_{maj}$), 1.10–1.04 (m, 6H$_{maj}$, 3H$_{min}$).

(*E*)- and (*Z*)-ethyl 3-phenylhept-2-enoate (*E*-102z, *Z*-102z)
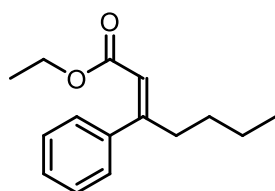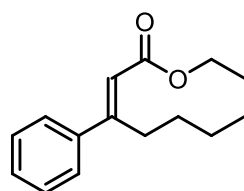
Following GP1 the reaction was performed using 1-phenylpentan-1-one (5.1 mL, 31 mmol, 1.0 eq.). Purification by silica gel flash chromatography (1–5% Et_2O in pentane) afforded the separated *E*- (3.8 g, 16 mmol, 53%) and *Z*-isomer (3.3 g, 14 mmol, 46%) of the product as colorless oils. The NMR-spectroscopic data are in agreement with the literature.[260]

E-isomer: **^{1}H NMR** (501 MHz, CDCl$_3$): δ = 7.45–7.40 (m, 2H), 7.40–7.33 (m, 3H), 6.01 (s, 1H), 4.21 (q, J = 7.1 Hz, 2H), 3.13–3.05 (m, 2H), 1.44–1.34 (m, 4H), 1.31 (t, J = 7.1 Hz, 3H), 0.88 (t, J = 7.0 Hz, 3H).

Z-isomer: **¹H NMR** (501 MHz, CDCl₃): δ 7.36–7.27 (m, 3H), 7.17–7.13 (m, 2H), 5.87 (s, 1H), 3.98 (q, *J* = 7.1 Hz, 2H), 2.44 (ddd, *J* = 8.2, 6.9, 1.3 Hz, 2H), 1.41–1.28 (m, 4H), 1.06 (t, *J* = 7.1 Hz, 3H), 0.87 (t, *J* = 7.1 Hz, 3H).

(*E*)- and (*Z*)-ethyl 4,4,4-trifluoro-3-phenylbut-2-enoate (*E*-102aa, *Z*-102aa)
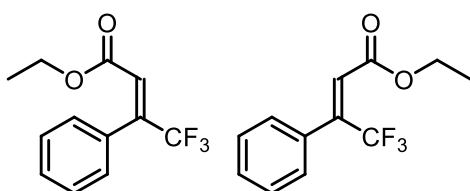
Following GP1 the reaction was performed using trifluoroacetyl benzene (560 µL, 4.0 mmol, 1.0 eq.). Purification by silica gel flash chromatography (5% Et₂O in pentane) afforded the separated *E*- (761 mg, 3.12 mmol, 78%) and *Z*-isomer (70.0 mg, 0.287 mmol, 7%) of the product as light yellow oils. The NMR-spectroscopic data are in agreement with the literature.[260]

E-isomer: **¹H NMR** (501 MHz, CDCl₃): δ = 7.44–7.38 (m, 3H), 7.30–7.27 (m, 2H), 6.61 (q, *J* = 1.4 Hz, 1H), 4.04 (q, *J* = 7.1 Hz, 2H), 1.06 (t, *J* = 7.1 Hz, 3H).

Z-isomer: **¹H NMR** (501 MHz, CDCl₃): δ = 7.41–7.41 (m, 5H), 6.34 (s, 1H), 4.31 (q, *J* = 7.1 Hz, 2H), 1.35 (t, *J* = 7.1 Hz, 3H).

4.2.3   Synthesis of α,β-Unsaturated Aldehydes
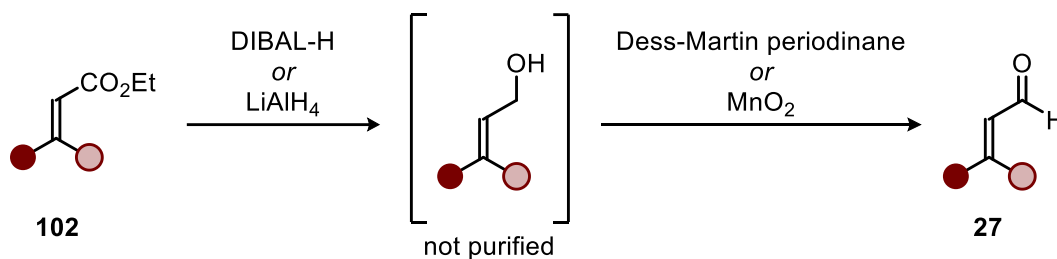
General procedure 2 (GP2)

a: In a flame-dried Schlenk flask under argon, the respective unsaturated ester (**102**, 1.0 eq.) dissolved in dry DCM (0.2 M) was cooled to –78 °C. Then a solution of DIBAL-H (1 M in DCM, 2.5–3.0 eq.) was added dropwise. The reaction mixture was stirred at that temperature overnight until the reaction was judged to be complete by TLC. After warming the mixture to 0 °C, water was added dropwise to quench the reaction, followed by aqueous NaOH (10%). After separation of the organic layer, the aqueous phase was extracted with DCM (3x). The combined organic layers were washed with water, dried over anhydrous

Na$_2$SO$_4$ and concentrated under reduced pressure. The residue was taken on to the next step without further purification.

b: In a flame-dried Schlenk flask under argon, the respective unsaturated ester (**102**, 1.0 eq.) dissolved in dry THF (0.4 M) was cooled to 0 °C. Then a solution of LiAlH$_4$ (1 M in THF, 1.0 eq.) was added dropwise. The reaction mixture was stirred at that temperature for 1–3 h until the reaction was judged to be complete by TLC. After warming the mixture to 0 °C, water was added dropwise to quench the reaction, followed by aqueous NaOH (10%). After separation of the organic layer, the aqueous phase was extracted with DCM (3x). The combined organic layers were washed with water, dried over anhydrous Na$_2$SO$_4$ and concentrated under reduced pressure. The residue was taken on to the next step without further purification.

General procedure 3 (GP3)

a: A flame-dried Schlenk flask under argon, was charged with the crude allylic alcohol (1.0 eq.) dissolved in dry DCM (0.2 M). After cooling down to 0 °C, Dess-Martin periodinane (1.1 eq.) was added in one portion. The reaction mixture was stirred at room temperature for 3–6 h, until TLC analysis indicated complete conversion of the starting material. Subsequent addition of aqueous NaHCO$_3$ was followed by extraction of the aqueous phase with DCM (3x). The combined organic layers were washed with water, dried over anhydrous Na$_2$SO$_4$ and concentrated under reduced pressure. The residue was purified via flash chromatography on silica gel to obtain an *E/Z*-mixture of the corresponding α,β-unsaturated aldehyde.

b: A flame-dried Schlenk flask under argon was charged with the crude allylic alcohol (1.0 eq.) dissolved in dry DCM (0.4 M). MnO$_2$ (10 eq.) was added and the resulting reaction mixture was stirred at room temperature for 1–3 days until TLC analysis indicated complete conversion of the starting material. The suspension was filtered over a short pad of Celite and washed with DCM. Subsequently, the filtrate was concentrated under reduced pressure. The residue was purified via flash chromatography on silica gel to obtain an *E/Z*-mixture of the corresponding α,β-unsaturated aldehyde.

3-(4-bromophenyl)but-2-enal (27a)
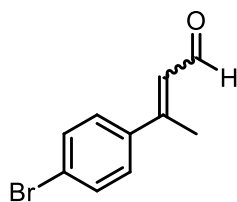
Preparation according to GP2a and GP3a followed by silica gel flash chromatography (10% Et$_2$O in pentane) afforded the product as a mixture of *E/Z* isomers as a yellow oil (1.23 g, 5.48 mmol, 72%, *E/Z* ≈ 77:23).

¹H NMR (501 MHz, CD₂Cl₂): δ = 10.15 (d, J = 7.7 Hz, 1H$_{maj}$), 9.44 (d, J = 8.2 Hz, 1H$_{min}$), 7.58–7.50 (m, 2H$_{maj}$, 2H$_{min}$), 7.47–7.39 (m, 2H$_{maj}$), 7.20 (d, J = 8.4 Hz, 2H$_{min}$), 6.32 (dq, J = 7.8, 1.4 Hz, 1H$_{maj}$), 6.10 (dd, J = 8.1, 1.4 Hz, 1H$_{min}$), 2.52 (d, J = 1.4 Hz, 3H$_{maj}$), 2.27 (d, J = 1.4 Hz, 3H$_{min}$).

¹³C NMR (126 MHz, CD₂Cl₂): δ = 192.7, 191.2, 160.7, 156.2, 139.9, 137.8, 132.1, 131.9, 130.4, 129.8, 128.2, 127.7, 124.5, 123.5, 26.4, 16.4.

HRMS m/z (GC-EI): calcd. for C₁₀H₉O₁Br₁ ([M]⁺): 223.983140; found: 223.983140.

3-(3-bromophenyl)but-2-enal (27b)

Preparation according to GP2a and GP3a followed by silica gel flash chromatography (20% Et₂O in pentane) afforded the product as a white solid (571 mg, 2.54 mmol, 77%, E/Z>99:1).

¹H NMR (501 MHz, CD₂Cl₂): δ = 10.16 (d, J = 7.7 Hz, 1H), 7.70 (t, J = 1.9 Hz, 1H), 7.56 (ddd, J = 8.0, 2.0, 1.0 Hz, 1H), 7.50 (ddd, J = 7.9, 1.9, 1.0 Hz, 1H), 7.31 (t, J = 7.9 Hz, 1H), 6.31 (dq, J = 7.7, 1.3 Hz, 1H), 2.53 (d, J = 1.3 Hz, 3H).

¹³C NMR (126 MHz, CD₂Cl₂): δ = 191.2, 156.0, 143.4, 133.1, 130.7, 129.7, 128.3, 125.4, 123.2, 16.6.

HRMS m/z (GC-EI): calcd. for C₁₀H₉O₁Br₁ ([M]⁺): 223.983140; found: 223.983160.

(*E*)-3-(3-(trifluoromethyl)phenyl)but-2-enal (27c)
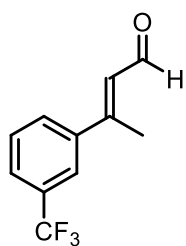
Preparation according to GP2a and GP3a followed by silica gel flash chromatography (15% Et₂O in pentane) afforded the product as a mixture of E/Z isomers as a light yellow oil (358 mg, 1.67 mmol, 89%, E/Z ≈ 99:1).

¹H NMR (501 MHz, CD₂Cl₂): δ = 10.18 (d, J = 7.6 Hz, 1H), 7.80 (d, J = 1.9 Hz, 1H), 7.76 (dt, J = 7.9, 1.5 Hz, 1H), 7.71–7.66 (m, 1H), 7.58 (t, J = 7.8 Hz, 1H), 6.36 (dt, J = 7.6, 1.3 Hz, 1H), 2.58 (d, J = 1.3 Hz, 3H).

¹³C NMR (126 MHz, CD₂Cl₂): δ = 191.2, 156.0, 142.1, 131.3 (q, J = 32.4 Hz), 130.1, 129.8, 128.7, 126.8 (q, J = 3.7 Hz), 124.5 (q, J = 272.4 Hz), 123.5 (q, J = 3.9 Hz), 16.7.

¹⁹F NMR (471 MHz, CD₂Cl₂): δ = –63.1.

HRMS m/z (GC-CI): calcd. for C₁₁H₁₀O₁F₃ ([M+H]⁺): 215.067826; found: 215.067890.

(*E*)-3-phenylbut-2-enal (*E*-27d)
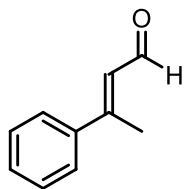
Preparation according to GP2a and GP3a followed by silica gel flash chromatography (5–10% Et$_2$O in pentane) afforded the product as a light yellow oil (728 mg, 4.98 mmol, 88%, *E*/*Z*>99:1).

^{1}H NMR (501 MHz, CD$_2$Cl$_2$): δ = 10.17 (d, *J* = 7.8 Hz, 1H), 7.61–7.54 (m, 2H), 7.47–7.39 (m, 2H), 6.36 (dd, *J* = 7.8, 1.3 Hz, 1H), 2.56 (d, *J* = 1.3 Hz, 3H).

^{13}C NMR (126 MHz, CD$_2$Cl$_2$): δ = 191.4, 157.9, 141.1, 130.3, 129.1, 127.6, 126.7, 16.6.

HRMS *m*/*z* (GC-EI): calcd. for C$_{10}$H$_{10}$O$_1$ ([M]$^+$): 146.072615; found: 146.072690.

(*Z*)-3-phenylbut-2-enal (*Z*-27d)
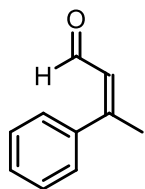
Preparation according to GP2a and GP3a followed by silica gel flash chromatography (5–10% Et$_2$O in pentane) afforded the product as a light yellow oil (339 mg, 2.32 mmol, 65%, *E*/*Z*<1:99).

^{1}H NMR (501 MHz, CD$_2$Cl$_2$): δ = 9.45 (d, *J* = 8.1 Hz, 1H), 7.46–7.38 (m, 3H), 7.36–7.29 (m, 2H), 6.10 (dq, *J* = 8.2, 1.4 Hz, 1H), 2.31 (d, *J* = 1.4 Hz, 3H).

^{13}C NMR (126 MHz, CD$_2$Cl$_2$): δ = 193.4, 162.5, 139.0, 129.5, 129.4, 128.8, 128.7, 26.6.

HRMS *m*/*z* (GC-EI): calcd. for C$_{10}$H$_{10}$O$_1$ ([M]$^+$): 146.072615; found: 146.072740.

(*E*)-3-(p-tolyl)but-2-enal (27e)
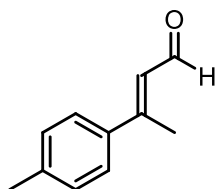
Preparation according to GP2a and GP3a followed by silica gel flash chromatography (10% Et$_2$O in pentane) afforded the product as a light yellow oil (364 mg, 2.27 mmol, 59%, *E*/*Z*>99:1).

^{1}H NMR (501 MHz, CD$_2$Cl$_2$): δ = 10.16 (d, *J* = 7.9 Hz, 1H), 7.52–7.45 (m, 2H), 7.26–7.20 (m, 3H), 6.35 (dt, *J* = 7.9, 1.3 Hz, 1H), 2.54 (d, *J* = 1.3 Hz, 3H), 2.38 (s, 3H).

^{13}C NMR (126 MHz, CD$_2$Cl$_2$): δ = 191.4, 157.7, 141.0, 138.0, 129.8, 126.8, 126.6, 21.4, 16.4.

HRMS *m*/*z* (GC-EI): calcd. for C$_{11}$H$_{13}$O$_1$ ([M+H]$^+$): 161.096090; found: 161.096250.

(*E*)-3-(m-tolyl)but-2-enal (27f)
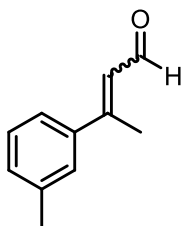
Preparation according to GP2a and GP3b followed by silica gel flash chromatography (20% Et$_2$O in pentane) afforded the product as a mixture of *E/Z* isomers as a light yellow oil (736 mg, 4.59 mmol, 69%, *E/Z* ≈ 94:6).

^{1}H NMR (501 MHz, CD$_2$Cl$_2$): δ = 10.16 (d, *J* = 7.9 Hz, 1H$_{maj}$), 9.45 (d, *J* = 8.1 Hz, 1H$_{min}$), 7.40–7.34 (m, 2H$_{maj}$), 7.30 (t, *J* = 7.6 Hz, 1H$_{maj}$, 1H$_{min}$), 7.26–7.21 (m, 1H$_{maj}$, 1H$_{min}$), 7.15–7.10 (m, 2H$_{min}$), 6.34 (dq, *J* = 7.9, 1.3 Hz, 1H$_{maj}$), 6.08 (dq, *J* = 8.1, 1.4 Hz, 1H$_{min}$), 2.55 (d, *J* = 1.3 Hz, 3H$_{maj}$), 2.39 (d, *J* = 0.8 Hz, 3H$_{maj}$, 3H$_{min}$), 2.29 (d, *J* = 1.4 Hz, 3H$_{min}$).

^{13}C NMR (126 MHz, CD$_2$Cl$_2$): δ = 193.5, 191.5, 158.1, 141.1, 138.9, 131.1, 130.1, 129.4, 129.3, 128.9, 128.6, 127.5, 127.3, 125.9, 123.8, 26.7, 21.6, 21.5, 16.6.

HRMS *m/z* (EI): calcd. for C$_{11}$H$_{12}$O$_1$ ([M]$^+$): 160.088265; found: 160.088310.

(*E*)-3-(o-tolyl)but-2-enal (27g)
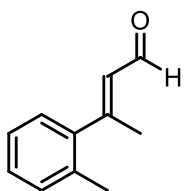
Preparation according to GP2b and GP3a followed by silica gel flash chromatography (5% Et$_2$O in pentane) afforded the product as a light yellow oil (377 mg, 2.35 mmol, 62%, *E/Z*>99:1).

^{1}H NMR (501 MHz, CD$_2$Cl$_2$): δ = 10.15 (d, *J* = 7.9 Hz, 1H), 7.29–7.15 (m, 3H), 7.11 (dd, *J* = 7.3, 1.2 Hz, 1H), 5.90 (dq, *J* = 7.9, 1.4 Hz, 1H), 2.45 (d, *J* = 1.4 Hz, 3H), 2.31 (s, 3H).

^{13}C NMR (126 MHz, CD$_2$Cl$_2$): δ = 191.3, 161.2, 143.3, 134.2, 131.0, 130.5, 128.5, 127.1, 126.2, 19.9, 19.5.

HRMS *m/z* (GC-EI): calcd. for C$_{11}$H$_{12}$O$_1$ ([M]$^+$): 160.088265; found: 160.088540.

(*E*)-3-(4-((triisopropylsilyl)oxy)phenyl)but-2-enal (27h)
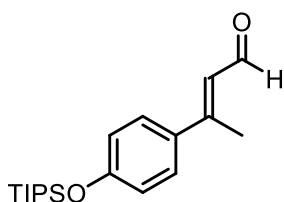
Preparation according to GP2b and GP3a followed by silica gel flash chromatography (10% Et$_2$O in pentane) afforded the product as a yellow solid (354 mg, 1.11 mmol, 65%, *E/Z* ≈ 99:1).

^{1}H NMR (501 MHz, CD$_2$Cl$_2$): δ = 10.14 (d, *J* = 7.9 Hz, 1H), 7.54–7.47 (m, 2H), 6.95–6.88 (m, 2H), 6.34 (dq, *J* = 7.9, 1.2 Hz, 1H), 2.53 (d, *J* = 1.2 Hz, 3H), 1.35–1.21 (m, 3H), 1.11 (d, *J* = 7.4 Hz, 18H).

^{13}C NMR (126 MHz, CD$_2$Cl$_2$): δ = 191.4, 158.6, 157.2, 133.2, 128.2, 125.9, 120.4, 18.1, 16.2, 13.1.

HRMS *m/z* (ESI): calcd. for $C_{19}H_{30}O_2Si_1Na_1$ ([M+Na]$^+$): 341.19073; found: 341.19064.

3-(4-vinylphenyl)but-2-enal (27i)
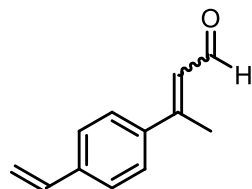
A flame-dried Schlenk flask under argon was charged with 3-(4-bromophenyl)but-2-enal (504 mg, 2.24 mmol, 1.00 eq.), trimethyl orthoformate (0.29 mL, 2.69 mmol, 1.20 eq.), anhydrous camphorsulfonic acid (5.2 mg, 22 μmol, 1.0 mol%) and anhydrous methanol (2 mL). The reaction mixture was stirred overnight until TLC analysis indicated full conversion of the starting material. Addition of aqueous NaHCO$_3$ (20 mL) was followed by extraction with Et$_2$O (3x 20 mL). The combined organic phases were dried over anhydrous Na$_2$SO$_4$ and concentrated under reduced pressure. The residue was transferred into a flame-dried flask under argon and dissolved in dry toluene (7.5 mL). After addition of tributylvinyltin (1.07 g, 3.36 mmol, 1.50 eq.) and tetrakis(triphenylphosphine)palladium(0) (52 mg, 45 μmol, 2.0 mol%) the reaction mixture was heated to 120 °C and stirred for 22 h. Subsequent cooling down to ambient temperature was followed by addition of a saturated KF solution (5 mL). The formed precipitate was filtered off over a short pad of Celite. The aqueous phase was extracted with DCM (4 x 30 mL). The combined organic phases were washed with water (2 x 20 mL), dried over anhydrous Na$_2$SO$_4$ and concentrated under reduced pressure. The crude oil was then dissolved in 4 mL THF and 2 mL HCl (10%) and stirred for 1 h. Dilution with water (30 mL) was followed by extraction with DCM (3 x 30 mL). The combined organic phases were dried over anhydrous Na$_2$SO$_4$ and concentrated under reduced pressure. After purification via column chromatography (60% DCM, hexanes) an *E/Z* mixture of the product (262 mg, 2.24 mmol, 68%, *E/Z* ≈ 84:16) was obtained as a yellow creamy solid.

^{1}H NMR (501 MHz, CD$_2$Cl$_2$): δ = 10.17 (d, *J* = 7.8 Hz, 1H$_{maj}$), 9.48 (d, *J* = 8.2 Hz, 1H$_{min}$), 7.59–7.52 (m, 2H$_{maj}$), 7.51–7.44 (m, 2H$_{maj}$, 2H$_{min}$), 7.32–7.27 (m, 2H$_{min}$), 6.80–6.71 (m, 1H$_{maj}$, 1H$_{min}$), 6.38 (dq, *J* = 7.9, 1.3 Hz, 1H$_{maj}$), 6.09 (dq, *J* = 8.2, 1.4 Hz, 1H$_{min}$), 5.88–5.79 (m, 1H$_{maj}$, 1H$_{min}$), 5.37–5.31 (m, 1H$_{maj}$, 1H$_{min}$), 2.55 (d, *J* = 1.2 Hz, 3H$_{maj}$), 2.30 (d, *J* = 1.4 Hz, 3H$_{min}$).

^{13}C NMR (126 MHz, CD$_2$Cl$_2$): δ = 193.3, 191.4, 161.9, 157.1, 140.2, 139.7, 138.8, 138.4, 136.4, 136.4, 129.5, 129.2, 127.2, 126.9, 126.8, 126.5, 115.5, 115.3, 26.4, 16.4.

HRMS *m/z* (EI): calcd. for $C_{12}H_{12}O_1$ ([M]$^+$): 172.088265; found: 172.088440.

3-(4-methoxy-3-nitrophenyl)but-2-enal (27j)
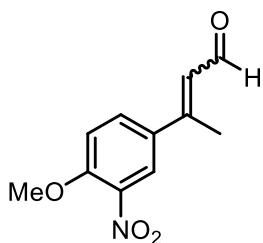
Preparation according to GP2a and GP3b followed by silica gel flash chromatography (3% Et$_2$O in DCM) afforded the product as a mixture of *E/Z* isomers as a yellow solid (145 mg, 0.66 mmol, 33%, *E/Z* ≈ 82:18).

^{1}H NMR (501 MHz, CD$_2$Cl$_2$): δ = 10.16 (d, *J* = 7.6 Hz, 1H$_{maj}$), 9.48 (d, *J* = 8.1 Hz, 1H$_{maj}$), 8.06 (d, *J* = 2.5 Hz, 1H$_{maj}$), 7.83–7.76 (m, 1H$_{maj}$, 1H$_{min}$), 7.52 (dd, *J* = 8.6, 2.3 Hz, 1H$_{min}$), 7.17 (d, *J* = 9.0 Hz, 1H$_{maj}$, 1H$_{min}$), 6.37 (d, *J* = 1.3 Hz, 1H$_{maj}$), 6.14 (dq, *J* = 8.1, 1.5 Hz, 1H$_{min}$), 4.00 (d, *J* = 1.4 Hz, 3H$_{maj}$, 3H$_{min}$), 2.55 (d, *J* = 1.3 Hz, 3H$_{maj}$), 2.30 (d, *J* = 1.5 Hz, 3H$_{min}$).

^{13}C NMR (126 MHz, CD$_2$Cl$_2$): δ = 192.4, 191.1, 158.9, 154.3, 153.7, 140.0, 134.7, 133.1, 132.2, 131.0, 130.3, 127.5, 125.6, 123.9, 114.3, 114.1, 57.2, 57.2, 26.3, 16.3.

HRMS *m/z* (GC-EI): calcd. for C$_{11}$H$_{11}$O$_4$N$_1$ ([M]$^+$): 221.068259; found: 221.068310.

(*E*)-3-(pyridin-3-yl)but-2-enal (27k)
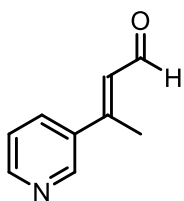
Preparation according to GP2a and GP3a followed by silica gel flash chromatography (70% EtOAc, hexanes) afforded the product as a yellow solid (1046 mg, 7.11 mmol, 81%, *E/Z* ≈ 98:2).

^{1}H NMR (501 MHz, CD$_2$Cl$_2$): δ = 10.18 (d, *J* = 7.7 Hz, 1H), 8.61 (dd, *J* = 4.8, 1.6 Hz, 1H), 7.84 (ddd, *J* = 8.0, 2.5, 1.6 Hz, 1H), 7.35 (ddd, *J* = 8.0, 4.8, 0.9 Hz, 1H), 6.35 (dq, *J* = 7.6, 1.3 Hz, 1H), 2.57 (d, *J* = 1.3 Hz, 3H).

^{13}C NMR (126 MHz, CD$_2$Cl$_2$): δ = 191.0, 154.7, 151.2, 147.9, 136.6, 133.8, 128.5, 123.8, 16.4.

HRMS *m/z* (GC-EI): calcd. for C$_9$H$_9$O$_1$N$_1$ ([M]$^+$): 147.067864; found: 147.067810.

(*E*)-3-(thiophen-2-yl)but-2-enal (27l)
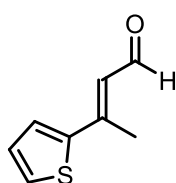
Preparation according to GP2b and GP3b followed by silica gel flash chromatography (10% EtOAc, hexanes) afforded the product as a yellow oil (414 mg, 2.72 mmol, 42%, *E/Z* ≈ 98:2).

^{1}H NMR (501 MHz, CD$_2$Cl$_2$): δ = 10.11 (d, *J* = 7.8 Hz, 1H), 7.50–7.44 (m, 2H), 7.12 (dd, *J* = 4.9, 4.0 Hz, 1H), 6.42 (dd, *J* = 7.7, 1.2 Hz, 1H), 2.57 (d, *J* = 1.2 Hz, 3H).

^{13}C NMR (126 MHz, CD$_2$Cl$_2$): δ = 190.8, 150.1, 145.0, 129.2, 128.7, 128.3, 124.8, 16.3.

HRMS m/z (GC-EI): calcd. for $C_8H_8O_1S_1$ ([M]$^+$): 152.029037; found: 152.029150.

3-(2-chlorophenyl)but-2-enal (27m)
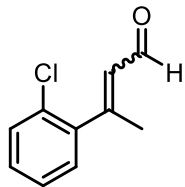
Preparation according to GP2a and GP3a followed by silica gel flash chromatography (20% Et$_2$O, pentane) afforded the product as a colorless oil (1.48 g, 8.18 mmol, 90%, E/Z ≈ 65:35).

^{1}H NMR (501 MHz, CD$_2$Cl$_2$): δ = 10.15 (d, J = 7.8 Hz, 1H$_{maj}$), 9.23 (d, J = 8.2 Hz, 1H$_{min}$), 7.49–7.39 (m, 1H$_{maj}$,1H$_{min}$), 7.39–7.27 (m, 2H$_{maj}$, 2H$_{min}$), 7.26–7.18 (m, 1H$_{maj}$, 1H$_{min}$), 6.14 (dq, J = 8.4, 1.5 Hz, 1H$_{min}$), 5.96 (dq, J = 7.8, 1.4 Hz, 1H$_{maj}$), 2.50 (d, J = 1.5 Hz, 3H$_{maj}$), 2.27 (d, J = 1.5 Hz, 3H$_{min}$).

^{13}C NMR (126 MHz, CD$_2$Cl$_2$): δ = 192.7, 191.2, 160.3, 158.5, 142.1, 138.1, 132.0, 131.3, 131.1, 130.6, 130.4, 130.2, 130.2, 130.1, 130.0, 129.2, 127.5, 127.3, 26.0, 18.8.

HRMS m/z (ESI): calcd. for $C_{10}H_9O_1Cl_1Na_1$ ([M+Na]$^+$): 203.023412; found: 203.023510.

3-(4-(4,4,5,5-tetramethyl-1,3,2-dioxaborolan-2-yl)phenyl)but-2-enal (27n)
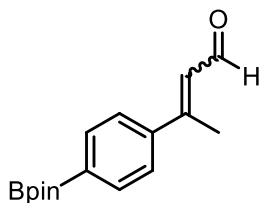
Preparation according to GP2a and GP3a followed by silica gel flash chromatography (20% Et$_2$O, pentane) afforded the product as a white solid (250 mg, 0.92 mmol, 42%, E/Z ≈ 89:11).

^{1}H NMR (501 MHz, CD$_2$Cl$_2$): δ = 10.17 (d, J = 7.8 Hz, 1H$_{maj}$), 9.43 (d, J = 8.2 Hz, 1H$_{min}$), 7.80 (d, J = 7.9 Hz, 2H$_{maj}$, 2H$_{min}$), 7.56 (d, J = 8.1 Hz, 2H$_{maj}$), 7.32 (d, J = 7.6 Hz, 2H$_{min}$), 6.41–6.33 (m, 1H$_{maj}$), 6.10 (d, J = 8.2 Hz, 1H$_{min}$), 2.60–2.53 (m, 3H$_{maj}$), 2.30 (d, J = 1.4 Hz, 3H$_{min}$), 1.34 (s, 12H$_{maj}$, 12H$_{min}$).

^{13}C NMR (126 MHz, CD$_2$Cl$_2$): δ = 193.3, 191.4, 157.7, 143.6, 135.3, 135.0, 129.6, 128.1, 128.0, 125.9, 84.4, 25.1, 16.5.

HRMS m/z (GC-EI): calcd. for $C_{16}H_{21}O_3B_1$ ([M]$^+$): 272.157825; found: 272.158170.

(*E*)-3-cyclohexylbut-2-enal (27o)

Preparation according to GP2a and GP3a followed by silica gel flash chromatography (10% Et$_2$O in pentane) afforded the product as a light yellow oil (546 mg, 3.69 mmol, 43%, *E/Z*>99:1).
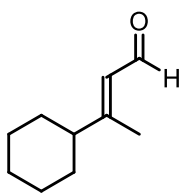
¹**H NMR** (501 MHz, CD$_2$Cl$_2$): δ = 10.00 (d, *J* = 8.0 Hz, 1H), 5.82 (ddq, *J* = 8.0, 1.3, 1.3 Hz, 1H), 2.14 (d, *J* = 1.3 Hz, 3H), 2.04 (tt, *J* = 11.3, 3.2 Hz, 1H), 1.86–1.65 (m, 5H), 1.38–1.13 (m, 5H).

¹³**C NMR** (126 MHz, CD$_2$Cl$_2$): δ = 191.9, 169.2, 126.0, 48.8, 31.6, 26.7, 26.5, 16.2.

HRMS *m/z* (GC-EI): calcd. for C$_{10}$H$_{16}$O$_1$ ([M]$^+$): 152.119565; found: 152.119540.

3-cyclopentylbut-2-enal (27p)
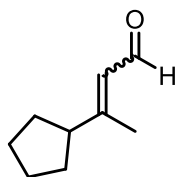
Preparation according to GP2a and GP3a followed by silica gel flash chromatography (5% Et$_2$O in pentane) afforded the product as a mixture of *E/Z* isomers as a light yellow oil (430 mg, 3.11 mmol, 38%, *E/Z* ≈ 85:15).

¹**H NMR** (501 MHz, CD$_2$Cl$_2$): δ = 10.03 (d, *J* = 8.2 Hz, 1H$_{min}$), 10.00 (d, *J* = 8.0 Hz, 1H$_{maj}$), 5.86 (ddq, *J* = 8.0, 1.2, 1.2 Hz, 1H$_{maj}$), 5.83–5.79 (m, 1H$_{min}$), 3.71–3.62 (m, 1H$_{min}$), 2.63–2.53 (m, 1H$_{maj}$), 2.15 (d, *J* = 1.2 Hz, 3H$_{maj}$), 1.91 (d, *J* = 1.2 Hz, 3H$_{min}$), 1.90–1.82 (m, 2H$_{maj}$), 1.76–1.68 (m, 2H$_{maj}$), 1.68–1.60 (m, 2H$_{maj}$), 1.53–1.43 (m, 2H$_{maj}$).

¹³**C NMR** (126 MHz, CD$_2$Cl$_2$): δ = 191.8, 190.4, 167.6, 129.1, 125.9, 50.2, 41.6, 32.2, 31.4, 26.5, 25.7, 20.5, 16.3.

HRMS *m/z* (GC-EI): calcd. for C$_9$H$_{14}$O$_1$ ([M]$^+$): 138.103915; found: 138.104000.

3-cyclobutylbut-2-enal (27q)
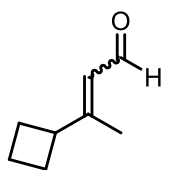
Preparation according to GP2a and GP3a followed by silica gel flash chromatography (10% Et$_2$O in pentane) afforded the product as a mixture of *E/Z* isomers as a light yellow oil (766 mg, 6.17 mmol, 67%, *E/Z* ≈ 92:8).

¹**H NMR** (501 MHz, CD$_2$Cl$_2$): δ = 9.99 (d, *J* = 8.1 Hz, 1H$_{maj}$), 9.93 (d, *J* = 8.4 Hz, 1H$_{min}$), 5.78 (ddq, *J* = 8.2, 1.3, 1.3 Hz, 1H$_{maj}$), 5.72 (ddq, *J* = 8.3, 1.4, 1.4 Hz, 1H$_{min}$), 3.93 (p, *J* = 9.0 Hz, 1H$_{min}$), 3.07 (p, *J* = 8.5 Hz, 1H$_{maj}$), 2.25–2.10 (m, 2H$_{maj}$), 2.08–2.05 (m, 3H$_{maj}$), 2.04–1.89 (m, 3H$_{maj}$), 1.82–1.69 (m, 1H$_{maj}$).

¹³**C NMR** (126 MHz, CD$_2$Cl$_2$): δ = 191.7, 190.9, 167.1, 127.8, 124.9, 44.4, 38.3, 28.8, 27.5, 22.0, 19.2, 17.9, 15.2.

HRMS *m/z* (GC-CI): calcd. for C$_8$H$_{13}$O$_1$ ([M+H]$^+$): 125.096090; found: 125.096180.

(*E*)-3,4,4-trimethylpent-2-enal (27r)
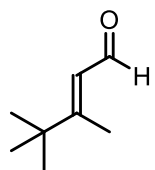
Preparation according to GP2a and GP3b followed by silica gel flash chromatography (5% Et$_2$O in pentane) afforded the product as a light yellow oil (468 mg, 3.71 mmol, 26%, *E/Z*>99:1).

^{1}H NMR (501 MHz, CD$_2$Cl$_2$): δ = 10.04 (d, *J* = 7.8 Hz, 1H), 5.91 (dq, *J* = 7.7, 1.2 Hz, 1H), 2.17 (d, *J* = 1.2 Hz, 3H), 1.13 (s, 9H).

^{13}C NMR (126 MHz, CD$_2$Cl$_2$): δ = 192.7, 171.4, 124.9, 38.1, 28.5, 13.9.

HRMS *m/z* (ESI): calcd. for C$_8$H$_{15}$O$_1$ ([M+H]$^+$): 127.111740; found: 127.111900.

3,4-dimethylpent-2-enal (27s)
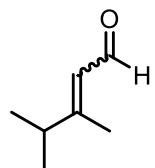
Preparation according to GP2a and GP3b followed by silica gel flash chromatography (5% Et$_2$O in pentane) afforded the product as a mixture of *E/Z* isomers as a light yellow oil (617 mg, 5.50 mmol, 52%, *E/Z* ≈ 87:13).

^{1}H NMR (501 MHz, CD$_2$Cl$_2$): δ = 10.04 (d, *J* = 8.2 Hz, 1H$_{min}$), 10.00 (d, *J* = 8.0 Hz, 1H$_{min}$), 5.84 (dq, *J* = 8.0, 1.1 Hz, 1H$_{maj}$), 5.74 (dq, *J* = 8.2, 1.4 Hz, 1H$_{min}$), 3.63 (h, *J* = 6.8 Hz, 1H$_{min}$), 2.41 (h, *J* = 6.9 Hz, 1H$_{maj}$), 2.14 (d, *J* = 1.3 Hz, 3H$_{maj}$), 1.88 (d, *J* = 1.3 Hz, 3H$_{min}$), 1.13 (d, *J* = 6.9 Hz, 6H$_{min}$), 1.10 (d, *J* = 6.9 Hz, 6H$_{maj}$).

^{13}C NMR (126 MHz, CD$_2$Cl$_2$): δ = 191.9, 190.1, 169.8, 127.8, 125.6, 38.3, 29.8, 21.2, 20.9, 19.5, 15.4.

HRMS *m/z* (ESI): calcd. for C$_7$H$_{13}$O$_1$ ([M+H]$^+$): 113.096090; found: 113.096230.

3-methylpent-2-enal (27t)
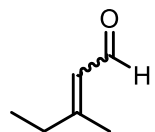
Preparation according to GP2a and GP3a followed by silica gel flash chromatography (5% Et$_2$O in pentane) afforded the product as a mixture of *E/Z* isomers as a colorless oil (517 mg, 5.27 mmol, 38%, *E/Z* ≈ 78:22).

^{1}H NMR (501 MHz, CD$_2$Cl$_2$): δ = 9.99 (d, *J* = 8.0 Hz, 1H$_{maj}$), 9.95 (d, *J* = 8.2 Hz, 1H$_{min}$), 5.83 (dp, *J* = 8.1, 1.4 Hz, 1H$_{maj}$), 5.79 (dd, *J* = 8.1, 1.4 Hz, 1H$_{min}$), 2.59 (q, *J* = 7.6 Hz, 2H$_{min}$), 2.24 (qd, *J* = 7.4, 1.3 Hz, 2H$_{maj}$), 2.16 (d, *J* = 1.3 Hz, 3H$_{maj}$), 1.97 (d, *J* = 1.3 Hz, 3H$_{min}$), 1.16 (t, *J* = 7.6 Hz, 3H$_{min}$), 1.10 (t, *J* = 7.4 Hz, 3H$_{maj}$).

^{13}C NMR (126 MHz, CD$_2$Cl$_2$): δ = 191.6, 190.8, 166.7, 166.0, 127.8, 126.5, 33.8, 26.1, 24.6, 17.6, 13.8, 11.8.

HRMS *m/z* (ESI): calcd. for $C_6H_{11}O_1$ ([M+H]$^+$): 99.080440; found: 99.080550.

3-methylhex-2-enal (27u)
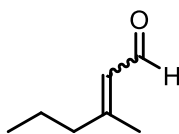
Preparation according to GP2a and GP3b followed by silica gel flash chromatography (5% Et$_2$O in pentane) afforded the product as a mixture of *E/Z* isomers as a light yellow oil (347 mg, 3.09 mmol, 47%, *E/Z* ≈ 75:25).

¹H NMR (501 MHz, CD$_2$Cl$_2$): δ = 9.98 (d, *J* = 8.0 Hz, 1H$_{maj}$), 9.94 (d, *J* = 8.3 Hz, 1H$_{min}$), 5.87–5.79 (m, 1H$_{maj}$, 1H$_{min}$), 2.58–2.53 (m, 2H$_{min}$), 2.19 (td, *J* = 7.6, 1.2 Hz, 2H$_{maj}$), 2.14 (d, *J* = 1.3 Hz, 3H$_{maj}$), 1.96 (d, *J* = 1.3 Hz, 3H$_{min}$), 1.64–1.49 (m, 2H$_{maj}$, 2H$_{min}$), 0.99–0.89 (m, 3H$_{maj}$, 3H$_{min}$).

¹³C NMR (126 MHz, CD$_2$Cl$_2$): δ = 191.5, 190.9, 164.9, 164.5, 128.9, 127.7, 43.0, 34.7, 25.0, 22.3, 20.8, 17.6, 13.9, 13.8.

HRMS *m/z* (ESI): calcd. for $C_7H_{13}O_1$ ([M+H]$^+$): 113.096090; found: 113.096150.

3-methylhept-2-enal (27v)
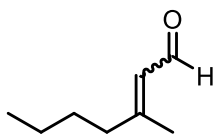
Preparation according to GP2a and GP3b followed by silica gel flash chromatography (5% Et$_2$O in pentane) afforded the product as a mixture of *E/Z* isomers as a light yellow oil (599 mg, 4.74 mmol, 62%, *E/Z* ≈ 74:26).

¹H NMR (501 MHz, CD$_2$Cl$_2$): δ = 9.97 (d, *J* = 8.1 Hz, 1H$_{maj}$), 9.94 (d, *J* = 8.2 Hz, 1H$_{min}$), 5.86–5.79 (m, 1H$_{maj}$, 1H$_{min}$), 2.61–2.54 (m, 2H$_{min}$), 2.24–2.18 (m, 2H$_{maj}$), 2.15 (d, *J* = 1.3 Hz, 3H$_{maj}$), 1.96 (d, *J* = 1.3 Hz, 3H$_{min}$), 1.58–1.44 (m, 2H$_{maj}$, 2H$_{min}$), 1.43–1.28 (m, 2H$_{maj}$, 2H$_{min}$), 0.97–0.88 (m, 3H$_{maj}$, 3H$_{min}$).

¹³C NMR (126 MHz, CD$_2$Cl$_2$): δ = 191.5, 190.9, 165.3, 164.8, 128.6, 127.5, 40.7, 32.7, 31.4, 29.7, 25.1, 23.0, 22.7, 17.6, 14.0.

HRMS *m/z* (ESI): calcd. for $C_8H_{15}O_1$ ([M+H]$^+$): 127.111740; found: 127.111880.

(*E*)-4,4,4-trifluoro-3-phenylbut-2-enal (*E*-27aa)
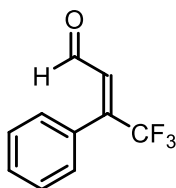
Preparation according to GP2a and GP3a followed by silica gel flash chromatography (5% Et$_2$O in pentane) afforded the product as a light yellow oil (562 mg, 2.81 mmol, 90%, *E/Z* ≈ 98:2).

¹H NMR (501 MHz, CD$_2$Cl$_2$): δ = 9.55 (dd, J = 7.5, 0.7 Hz, 1H), 7.58–7.48 (m, 3H), 7.45–7.40 (m, 2H), 6.64 (dq, J = 7.6, 1.3 Hz, 1H).

¹⁹F NMR (471 MHz, CD$_2$Cl$_2$): δ = –67.69.

¹³C NMR (126 MHz, CD$_2$Cl$_2$): δ = 192.0, 147.9 (q, J = 31.6 Hz), 131.5 (q, J = 4.9 Hz), 130.9, 130.4, 129.2, 123.34 (q, J = 274.7 Hz).

HRMS m/z (GC-EI): calcd. for C$_{10}$H$_7$O$_1$F$_3$ ([M]$^+$): 200.044351; found: 200.044270.

(Z)-4,4,4-trifluoro-3-phenylbut-2-enal (Z-27aa)
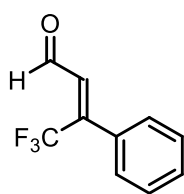
Preparation according to GP2a and GP3a followed by silica gel flash chromatography (5% Et$_2$O in pentane) afforded the product as a light yellow oil (48 mg, 0.24 mmol, 84%, E/Z ≈ 4:96).

¹H NMR (501 MHz, CD$_2$Cl$_2$): δ = 10.20 (dq, J = 7.4, 2.2 Hz, 1H), 7.53–7.42 (m, 5H), 6.38 (d, J = 7.4 Hz, 1H).

¹⁹F NMR (471 MHz, CD$_2$Cl$_2$): δ = –55.61.

¹³C NMR (126 MHz, CD$_2$Cl$_2$): δ = 190.0, 135.4, 135.4, 133.6, 130.8, 129.2, 128.3.

HRMS m/z (GC-EI): calcd. for C$_{10}$H$_7$O$_1$F$_3$ ([M]$^+$): 200.044351; found: 200.044440.

3-phenylpent-2-enal (27y)
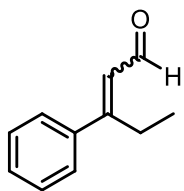
Preparation according to GP2a and GP3b followed by silica gel flash chromatography (5% Et$_2$O in pentane) afforded the product as a light yellow oil (693 mg, 4.33 mmol, 65%, E/Z ≈ 82:18). The NMR-spectroscopic data are in agreement with the literature.[273]

¹H NMR (501 MHz, CDCl$_3$): δ = 10.16 (d, J = 8.0 Hz, 1H$_{maj}$), 9.45 (d, J = 8.1 Hz, 1H$_{min}$), 7.55–7.25 (m, 5H$_{maj,}$ 5H$_{maj}$), 6.25 (d, J = 8.0 Hz, 1H$_{maj}$), 6.11 (dt, J = 8.0, 1.4 Hz, 1H$_{min}$), 3.07 (q, J = 7.6 Hz, 2H$_{maj}$), 2.60 (qd, J = 7.4, 1.4 Hz, 2H$_{min}$), 1.18 (t, J = 7.6 Hz, 3H$_{maj}$), 1.11 (t, J = 7.4 Hz, 3H$_{min}$).

HRMS m/z (EI): calcd. for C$_{11}$H$_{12}$O$_1$ ([M]$^+$): 160.088265; found: 160.088360.
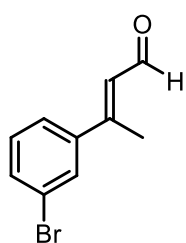
(*E*)-3-phenylhept-2-enal (27z)
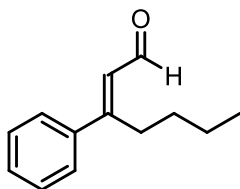
Preparation according to GP2a and GP3b followed by silica gel flash chromatography (2–5% Et$_2$O in pentane) afforded the product as a light yellow oil (1.40 g, 7.43 mmol, 86%, *E/Z*>99:1).The NMR-spectroscopic data are in agreement with the literature.[274]

^{1}H NMR (501 MHz, CDCl$_3$): δ = 10.15 (d, *J* = 8.0 Hz, 1H), 7.52–7.46 (m, 2H), 7.44–7.38 (m, 3H), 6.28 (d, *J* = 8.0 Hz, 1H), 3.08–3.00 (m, 2H), 1.54–1.45 (m, 2H), 1.44–1.31 (m, 2H), 0.90 (t, *J* = 7.3 Hz, 3H).

HRMS *m/z* (ESI): calcd. for C$_{13}$H$_{16}$O$_1$Na$_1$ ([M+Na]$^+$): 211.109334; found: 211.109550.

(*E*)-3-phenylbut-2-enal-4,4,4-*d*$_3$ (*E*-27d')
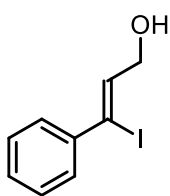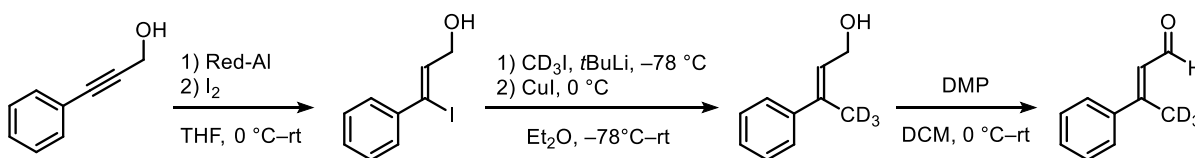
In a flame-dried Schlenk under argon 3-phenylprop-2-yn-1-ol (0.93 mL, 7.5 mmol, 1.0 eq.) was dissolved in dry THF (30 mL) and cooled to 0 °C. After dropwise addition of Red-Al (2.7 mL, 8.2 mmol, 1.1 eq., 60% in toluene) the reaction mixture was stirred for 4 h at 0 °C. Then iodine (2.08 g, 8.21 mmol, 1.10 eq.) was added and the reaction mixture was stirred for 15 minutes while slowly warming to room temperature. The reaction was terminated by addition of an aqueous Rochelle's salt solution followed by saturated Na$_2$SO$_3$ solution. After separation of the organic phase, the aqueous layer was extracted with EtOAc (3x). The combined organic phases were washed with water, dried over anhydrous Na$_2$SO$_4$ and then concentrated under reduced pressure. Purification via column chromatography (10–20% EtOAc in hexanes) furnished (*Z*)-3-iodo-3-phenylprop-2-en-1-ol (1.54 g, 5.91 mmol, 79%). The NMR-spectroscopic data are in agreement with the literature.[275]

^{1}H NMR (501 MHz, CDCl$_3$): δ = 7.49–7.45 (m, 2H), 7.34–7.27 (m, 3H), 6.26 (t, *J* = 5.7 Hz, 1H), 4.40 (d, *J* = 5.7 Hz, 2H), 1.71 (s, 1H).
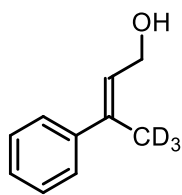
In a flame-dried Schlenk under argon CD$_3$I (0.68 mL, 11 mmol, 5.0 eq.) was dissolved in dry Et$_2$O (20 mL) and cooled to –78 °C. After dropwise addition of *t*BuLi (12.9 mL, 21.9 mmol, 10.0 eq.) the solution was stirred for 30 minutes and then warmed to 0 °C. CuI (1.04 g, 5.48 mmol, 2.50 eq.) was added and the reaction mixture was stirred for additional 30 minutes and then cooled down to –78 °C. (*Z*)-3-iodo-3-phenylprop-2-en-1-ol (570 mg, 2.19 mmol, 1.00 eq.) dissolved in dry Et$_2$O (7 mL) was added dropwise. The reaction was gradually warmed to 0 °C and stirred for 1 h. Saturated NH$_4$Cl solution was added, followed by extraction with EtOAc (3x). The combined organic phases were washed with water, dried over anhydrous Na$_2$SO$_4$ and concentrated under reduced pressure. Purification via column chromatography (10–20% EtOAc in hexanes) yielded the product as an inseparable mixture of desired (*E*)-3-phenylbut-2-en-4,4,4-*d$_3$*-1-ol (85% purity, 283 mg, 1.59 mmol, 73%) and deiodinated side product (*E*)-3-phenylprop-2-en-1-ol. The NMR-spectroscopic data are in agreement with the literature.[276]

^{1}H NMR (501 MHz, CDCl$_3$): δ = 7.43–7.38 (m, 2H), 7.36–7.31 (m, 2H), 7.28–7.24 (m, 1H), 5.99 (t, *J* = 6.7 Hz, 1H), 4.37 (d, *J* = 6.5 Hz, 2H).
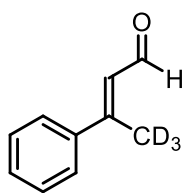
In a flame-dried Schlenk under argon (*E*)-3-phenylbut-2-en-4,4,4-*d$_3$*-1-ol (85% purity, 283 mg, 1.59 mmol, 1.00 eq.) was dissolved in dichloromethane (9 mL) and cooled to 0 °C. Dess-Martin periodinane (873 mg, 2.06 mmol, 1.29 eq.) was added in one portion and the reaction mixture was stirred overnight while warming to room temperature. The organic phase was sequentially washed with saturated NaHCO$_3$ solution and water (2x). The organic layer was dried over anhydrous Na$_2$SO$_4$ and concentrated under reduced pressure. Purification via column chromatography (3–5% Et$_2$O, hexanes) furnished the desired (*E*)-3-phenylbut-2-enal-4,4,4-*d$_3$* (68 mg, 0.456 mmol, 29%). The NMR-spectroscopic data are in agreement with the literature.[277]

^{1}H NMR (501 MHz, CD$_2$Cl$_2$): δ = 10.16 (d, *J* = 7.9 Hz, 1H), 7.61–7.52 (m, 2H), 7.45–7.39 (m, 3H), 6.36 (d, *J* = 7.8 Hz, 1H).

4.2.4 Transfer Hydrogenation of α,β-Unsaturated Aldehydes
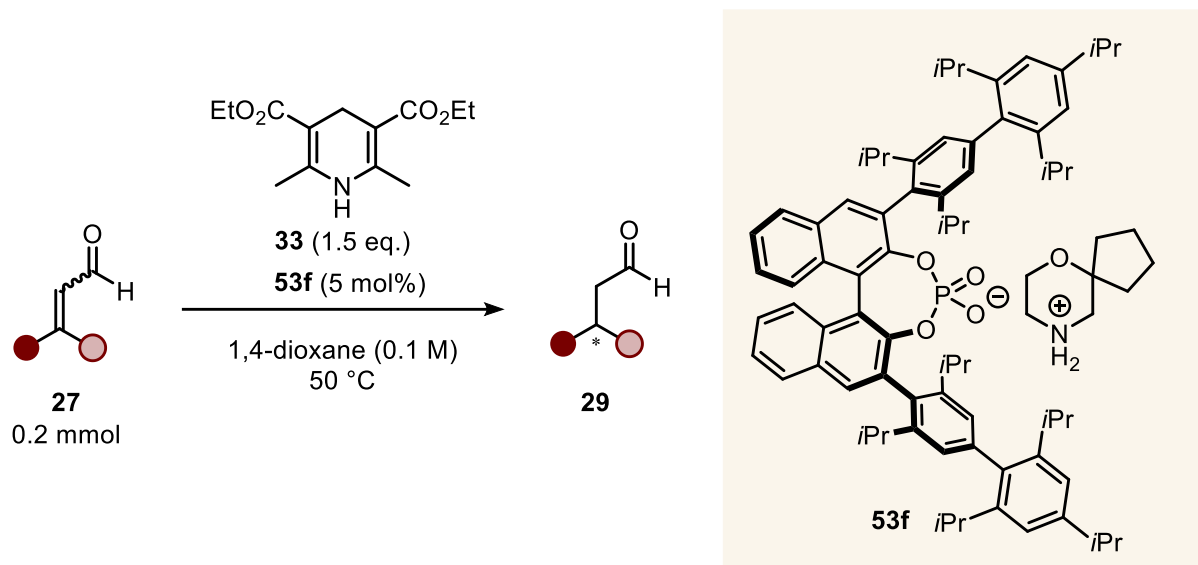
General Procedure 4 (GP4)

In a flame-dried Schlenk flask under argon the respective α,β-unsaturated aldehyde (**27**, 1.00 eq., 0.20 mmol) and the preformed catalyst **53f** (5 mol%, 0.01 mmol) were dissolved in dry 1,4-dioxane (2 mL) and heated to 50 °C. After five minutes Hantzsch ester **33** (1.5 eq., 0.30 mmol) was added and the resulting reaction mixture was stirred at 50 °C for 24 h. After cooling to ambient temperature, the mixture was directly loaded onto a column packed with silica and eluted with DCM/pentane to give the β-chiral aldehyde products (**29**). For deviations from the general procedure, see the respective entries.

Racemate syntheses

For the racemate syntheses, the respective α,β-unsaturated aldehyde (**27**, 0.03 mmol, 1.00 eq.) was reacted with Hantzsch ester **33** (45.0 µmol, 1.50 eq.) and morpholinium diphenyl phosphate (20 mol%, 6 µmol) in dry 1,4-dioxane (0.3 mL) at 50 °C for 10–24 h. Subsequent thin-layer chromatography gave the isolated racemic products that were used for the determination of the enantiomeric ratio by GC-analysis.

(*R*)-3-(4-bromophenyl)butanal (29a)
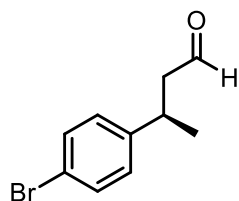
Following GP4 the reaction was performed using enal **27a** (45.2 mg, 0.20 mmol, 1.00 eq.). Purification by silica gel flash chromatography (20–50% DCM in pentane) afforded the product **29a** (38.7 mg, 0.17 mmol, 85%) as a light yellow oil.

¹H NMR (501 MHz, CD₂Cl₂): δ = 9.67 (t, J = 1.8 Hz, 1H), 7.47–7.40 (m, 2H), 7.16–7.09 (m, 2H), 3.32 (h, J = 7.1 Hz, 1H), 2.72 (ddd, J = 16.9, 7.1, 1.8 Hz, 1H), 2.65 (ddd, J = 17.0, 7.4, 1.9 Hz, 1H), 1.28 (d, J = 7.0 Hz, 3H).

¹³C NMR (126 MHz, CD₂Cl₂): δ = 201.5, 145.3, 132.0, 129.1, 120.3, 51.9, 34.1, 22.2.

HRMS m/z (EI): calcd. for C₁₀H₁₁O₁Br₁ ([M]⁺): 225.998790; found: 225.998770.

GC (30 m Ivadex-1, injection temperature: 220 °C, 110 °C iso 5 min, 2 °C/min, 150 °C iso 5 min, 5 °C/min, 200 °C iso 30 min, 5 °C/min, 220 °C iso 5 min, 0.5 bar H₂): t_{R1} = 30.1 min (major), t_{R2} = 30.6 min (minor), er = 97.5:2.5 (95% ee).

$[\alpha]_D^{25}$ = –28.5 (c= 0.20, CHCl₃)

(*R*)-3-(3-bromophenyl)butanal (29b)
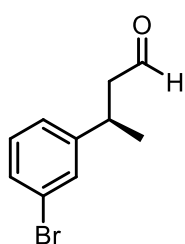
Following GP4 the reaction was performed using enal **27b** (44.9 mg, 0.20 mmol, 1.00 eq.). Purification by silica gel flash chromatography (20–50% DCM in pentane) afforded the product **29b** (38.0 mg, 0.17 mmol, 84%) as a yellow oil.

¹H NMR (501 MHz, CD₂Cl₂): δ = 9.68 (t, J = 1.8 Hz, 1H), 7.39 (t, J = 1.8 Hz, 1H), 7.35 (dt, J = 7.1, 2.0 Hz, 1H), 7.23–7.15 (m, 2H), 3.33 (h, J = 7.0 Hz, 1H), 2.74 (ddd, J = 17.0, 7.0, 1.7 Hz, 1H), 2.66 (ddd, J = 17.0, 7.4, 1.9 Hz, 1H), 1.28 (d, J = 7.0 Hz, 3H).

¹³C NMR (126 MHz, CD₂Cl₂): δ = 201.4, 148.7, 130.6, 130.4, 129.9, 126.1, 122.9, 51.8, 34.3, 22.2.

HRMS m/z (EI): calcd. for C₁₀H₁₁O₁Br₁ ([M]⁺): 225.998790; found: 225.998640.

GC (30 m Ivadex-1, injection temperature: 220 °C, 110 °C iso 5 min, 2 °C/min, 150 °C iso 5 min, 8 °C/min, 220 °C iso 5 min, 0.5 bar H₂): t_{R1} = 26.8 min (major), t_{R2} = 27.2 min (minor), er = 97.5:2.5 (95% ee).

$[\alpha]_D^{25}$ = –25.3 (c= 0.17, CHCl₃)

(*R*)-3-(3-(trifluoromethyl)phenyl)butanal (29c)

Following GP4 the reaction was performed using enal **27c** (35 µL, 0.20 mmol, 1.00 eq.). Purification by silica gel flash chromatography (20–50% DCM in pentane) afforded the product **29c** (38.5 mg, 0.18 mmol, 89%) as a light yellow oil.
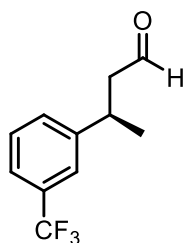
¹H NMR (501 MHz, CD$_2$Cl$_2$): δ = 9.70 (t, J = 1.7 Hz, 1H), 7.52–7.41 (m, 4H), 3.44 (h, J = 7.1 Hz, 1H), 2.78 (ddd, J = 17.1, 6.9, 1.7 Hz, 1H), 2.71 (ddd, J = 17.1, 7.4, 1.8 Hz, 1H), 1.32 (d, J = 7.0 Hz, 3H).

¹³C NMR (126 MHz, CD$_2$Cl$_2$): δ = 201.2, 147.3, 131.0 (q, J = 32.0 Hz), 131.0, 129.6, 128.0, 125.8, 124.8 (q, J = 274.7 Hz), 124.0 (q, J = 3.9 Hz), 123.7 (q, J = 3.9 Hz), 51.8, 34.4, 22.2.

¹⁹F NMR (471 MHz, CD$_2$Cl$_2$): δ = –62.9.

HRMS m/z (EI): calcd. for C$_{11}$H$_{11}$O$_1$F$_3$ ([M]$^+$): 216.075650; found: 216.075790.

GC (30 m Ivadex-1, injection temperature: 220 °C, 110 °C iso 5 min, 2 °C/min, 150 °C iso 5 min, 8 °C/min, 220 °C iso 5 min, 0.5 bar H$_2$): t$_{R1}$ = 10.9 min (major), t$_{R2}$ = 11.3 min (minor), er = 98:2 (96% ee).

$[\boldsymbol{\alpha}]_D^{25}$ = –24.3 (c= 0.32, CHCl$_3$)

(*R*)-3-phenylbutanal (29d)
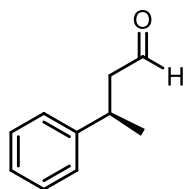
Following GP4 the reaction was performed using enal **27d** (28 µL, 0.20 mmol, 1.00 eq.). Purification by silica gel flash chromatography (20–50% DCM in pentane) afforded the product **29d** (21.6 mg, 0.15 mmol, 72%) as a light yellow oil.

¹H NMR (501 MHz, CD$_2$Cl$_2$): δ = 9.68 (t, J = 2.0 Hz, 1H), 7.33–7.28 (m, 2H), 7.26–7.18 (m, 3H), 3.35 (h, J = 7.1 Hz, 1H), 2.74 (ddd, J = 16.7, 7.1, 1.9 Hz, 1H), 2.65 (ddd, J = 16.7, 7.5, 2.1 Hz, 1H), 1.30 (d, J = 7.0 Hz, 3H).

¹³C NMR (126 MHz, CD$_2$Cl$_2$): δ = 202.0, 146.2, 129.0, 127.2, 126.8, 52.1, 34.7, 22.4.

HRMS m/z (GC-EI): calcd. for C$_{10}$H$_{12}$O$_1$ ([M]$^+$): 148.088265; found: 148.088520.

GC (30 m Ivadex-1, injection temperature: 220 °C, 110 °C iso 5 min, 2 °C/min, 150 °C iso 5 min, 8 °C/min, 220 °C iso 5 min, 0.5 bar H$_2$): t$_{R1}$ = 11.5 min (major), t$_{R2}$ = 12.0 min (minor), er = 97:3 (94% ee).

$[\boldsymbol{\alpha}]_D^{25}$ = –37.0 (c= 0.15, CHCl$_3$)

The absolute configuration was determined by comparison with the previously reported optical rotation $[\boldsymbol{\alpha}]_D^{20}$ = –33.2 (c= 0.74, CHCl$_3$) of the (*R*) enantiomer (90% ee).[278] The absolute stereochemistry of further substrates was assigned as (*R*) by analogy.

(*R*)-3-(p-tolyl)butanal (29e)
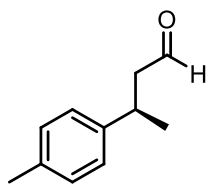
Following GP4 the reaction was performed using enal **27e** (32 μL, 0.20 mmol, 1.00 eq.). Purification by silica gel flash chromatography (20–50% DCM in pentane) afforded the product **29e** (30.6 mg, 0.19 mmol, 93%) as a light yellow oil.

^{1}H NMR (501 MHz, CD$_2$Cl$_2$): δ = 9.67 (t, *J* = 2.1 Hz, 1H), 7.12 (s, 4H), 3.30 (h, *J* = 7.1 Hz, 1H), 2.70 (ddd, *J* = 16.6, 7.2, 2.0 Hz, 1H), 2.62 (ddd, *J* = 16.6, 7.4, 2.2 Hz, 1H), 2.31 (s, 3H), 1.28 (d, *J* = 7.0 Hz, 4H).

^{13}C NMR (126 MHz, CD$_2$Cl$_2$): δ = 202.2, 143.1, 136.4, 129.6, 127.0, 52.1, 34.3, 22.5, 21.1.

HRMS *m/z* (EI): calcd. for C$_{11}$H$_{14}$O$_1$ ([M]$^+$): 162.103915; found: 162.104070.

GC (30 m Ivadex-1, injection temperature: 220 °C, 110 °C iso 5 min, 2 °C/min, 150 °C iso 5 min, 8 °C/min, 220 °C iso 5 min, 0.5 bar H$_2$): t_{R1} = 15.9 min (major), t_{R2} = 16.3 min (minor), er = 96.5:3.5 (93% ee).

$[\alpha]_D^{25}$ = –33.1 (c= 0.33, CHCl$_3$)

(*R*)-3-(m-tolyl)butanal (29f)
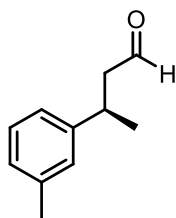
Following GP4 the reaction was performed using enal **27f** (31 μL, 0.20 mmol, 1.00 eq.). Purification by silica gel flash chromatography (20–50% DCM in pentane) afforded the product **29f** (26.7 mg, 0.17 mmol, 82%) as a light yellow oil.

^{1}H NMR (501 MHz, CD$_2$Cl$_2$): δ = 9.67 (t, *J* = 2.0 Hz, 1H), 7.19 (t, *J* = 7.5 Hz, 1H), 7.06–6.99 (m, 3H), 3.30 (h, *J* = 7.1 Hz, 1H), 2.72 (ddd, *J* = 16.6, 7.1, 1.9 Hz, 1H), 2.63 (ddd, *J* = 16.6, 7.5, 2.1 Hz, 1H), 2.33 (s, 3H), 1.28 (d, *J* = 7.0 Hz, 4H).

^{13}C NMR (126 MHz, CD$_2$Cl$_2$): δ = 202.2, 146.1, 138.7, 128.8, 128.0, 127.5, 124.2, 52.0, 34.7, 22.5, 21.6.

HRMS *m/z* (EI): calcd. for C$_{11}$H$_{14}$O$_1$ ([M]$^+$): 162.103915; found: 162.104170.

GC (30 m Ivadex-1, injection temperature: 220 °C, 110 °C iso 5 min, 2 °C/min, 150 °C iso 5 min, 8 °C/min, 220 °C iso 5 min, 0.5 bar H$_2$): t_{R1} = 15.0 min (major), t_{R2} = 15.3 min (minor), er = 95.5:4.5 (91% ee).

$[\alpha]_D^{25}$ = –31.9 (c= 0.18, CHCl$_3$)

(R)-3-(o-tolyl)butanal (29g)
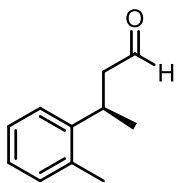
Following GP4 the reaction was performed using enal **27g** (32 µL, 0.20 mmol, 1.00 eq.). Purification by silica gel flash chromatography (20–50% DCM in pentane) afforded the product **29g** (20.6 mg, 0.13 mmol, 63%) as a light yellow oil.

^{1}H NMR (501 MHz, CD$_2$Cl$_2$): δ = 9.69 (t, J = 1.9 Hz, 1H), 7.19–7.13 (m, 3H), 7.12–7.07 (m, 1H), 3.64–3.54 (m, 1H), 2.76 (ddd, J = 16.8, 6.7, 1.8 Hz, 1H), 2.66 (ddd, J = 16.8, 7.8, 2.1 Hz, 1H), 2.37 (s, 3H), 1.25 (d, J = 6.9 Hz, 3H).

^{13}C NMR (126 MHz, CD$_2$Cl$_2$): δ = 202.0, 144.3, 135.6, 130.8, 126.7, 126.5, 125.6, 51.5, 29.6, 21.8, 19.6.

HRMS m/z (EI): calcd. for C$_{11}$H$_{14}$O$_1$ ([M]$^+$): 162.103915; found: 162.103960.

GC (30 m Ivadex-1, injection temperature: 220 °C, 110 °C iso 30 min, 2 °C/min, 130 °C iso 2 min, 8 °C/min, 220 °C iso 5 min, 0.5 bar H$_2$): t_{R1} = 19.8 min (major), t_{R2} = 20.5 min (minor), er = 98.5:1.5 (97% ee).

$[\alpha]_D^{25}$ = –35.3 (c= 0.17, CHCl$_3$)

(R)-3-(4-((triisopropylsilyl)oxy)phenyl)butanal (29h)
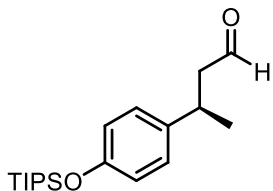
Following GP4 the reaction was performed using enal **27h** (63.4 mg, 0.20 mmol, 1.00 eq.). Purification by silica gel flash chromatography (20–50% DCM in pentane) afforded the product **29h** (52.8 mg, 0.17 mmol, 83%) as a light yellow oil.

^{1}H NMR (501 MHz, CD$_2$Cl$_2$): δ = 9.66 (t, J = 2.1 Hz, 1H), 7.10–7.03 (m, 2H), 6.85–6.78 (m, 2H), 3.28 (h, J = 7.1 Hz, 1H), 2.67 (ddd, J = 16.5, 7.0, 2.0 Hz, 1H), 2.59 (ddd, J = 16.5, 7.5, 2.3 Hz, 1H), 1.28–1.19 (m, 6H), 1.09 (d, J = 7.4 Hz, 18H).

^{13}C NMR (126 MHz, CD$_2$Cl$_2$): δ = 202.3, 154.9, 138.5, 128.0, 120.2, 52.3, 34.0, 22.5, 18.1, 13.1.

HRMS m/z (GC-EI): calcd. for C$_{19}$H$_{32}$O$_2$Si$_1$ ([M]$^+$): 320.216609; found: 320.216360.

GC (25 m Ivadex-1, injection temperature: 220 °C, 140 °C iso 150 min, 8 °C/min, 220 °C iso 3 min, 0.5 bar H$_2$): t_{R1} = 135.9 min (major), t_{R2} = 137.8 min (minor), er = 97.5:2.5 (95% ee).

$[\alpha]_D^{25}$ = –10.2 (c= 0.20, CHCl$_3$)

(*R*)-3-(4-vinylphenyl)butanal (29i)
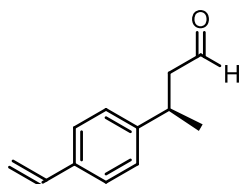
Following GP4 the reaction was performed using enal **27i** (34.2 mg, 0.20 mmol, 1.00 eq.). Purification by silica gel flash chromatography (20–50% DCM in pentane) afforded the product **29i** (30.1 mg, 0.17 mmol, 87%) as a light yellow oil.

^{1}H NMR (501 MHz, CD$_2$Cl$_2$): δ = 9.68 (t, *J* = 2.0 Hz, 1H), 7.40–7.33 (m, 2H), 7.23–7.16 (m, 2H), 6.70 (dd, *J* = 17.6, 10.9 Hz, 1H), 5.72 (dd, *J* = 17.5, 0.9 Hz, 1H), 5.21 (dd, *J* = 11.0, 0.9 Hz, 1H), 3.34 (h, *J* = 7.1 Hz, 1H), 2.73 (ddd, *J* = 16.7, 7.1, 1.9 Hz, 1H), 2.65 (ddd, *J* = 16.7, 7.5, 2.1 Hz, 1H), 1.29 (d, *J* = 7.0 Hz, 3H).

^{13}C NMR (126 MHz, CD$_2$Cl$_2$): δ = 201.9, 145.9, 136.9, 136.3, 127.4, 126.8, 113.5, 52.0, 34.4, 22.3.

HRMS *m/z* (EI): calcd. for C$_{12}$H$_{14}$O$_1$ ([M]$^+$): 174.103915; found: 174.104050.

GC (30 m Ivadex-1, injection temperature: 220 °C, 110 °C iso 5 min, 2 °C/min, 150 °C iso 5 min, 8 °C/min, 220 °C iso 5 min, 0.5 bar H$_2$): t_{R1} = 24.2 min (major), t_{R2} = 24,6 min (minor), er = 97:3 (94% ee).

$[\alpha]_D^{25}$ = –45.5 (c= 0.22, CHCl$_3$)

(*R*)-3-(4-methoxy-3-nitrophenyl)butanal (29j)
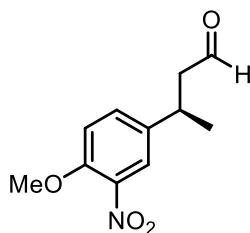
Following GP4 the reaction was performed using enal **27j** (44.0 mg, 0.20 mmol, 1.00 eq.). Purification by silica gel flash chromatography (5–20% EtOAc in hexanes) afforded the product **29j** (38.2 mg, 0.17 mmol, 86%) as a yellow oil.

^{1}H NMR (501 MHz, CD$_2$Cl$_2$): δ = 9.69 (t, *J* = 1.7 Hz, 1H), 7.69 (d, *J* = 2.4 Hz, 1H), 7.43 (dd, *J* = 8.7, 2.4 Hz, 1H), 7.06 (d, *J* = 8.7 Hz, 1H), 3.92 (s, 3H), 3.38 (h, *J* = 7.1 Hz, 1H), 2.75 (ddd, *J* = 17.2, 7.1, 1.6 Hz, 1H), 2.69 (ddd, *J* = 17.2, 7.2, 1.7 Hz, 1H), 1.30 (d, *J* = 7.0 Hz, 3H).

^{13}C NMR (126 MHz, CD$_2$Cl$_2$): δ = 201.1, 151.8, 140.0, 138.6, 133.2, 124.0, 114.3, 57.0, 51.9, 33.4, 22.2.

HRMS *m/z* (GC-EI): calcd. for C$_{11}$H$_{13}$N$_1$O$_4$ ([M]$^+$): 223.083909; found: 223.083860.

GC (30 m BGB-176, injection temperature: 220 °C, 130 °C iso 410 min, 8 °C/min, 240 °C, 0.6 bar H$_2$): t_{R1} = 380.8 min (major), t_{R2} = 390.5 min (minor), er = 96.5:3.5 (93% ee).

$[\alpha]_D^{25}$ = –18.2 (c= 0.20, CHCl$_3$)

(*R*)-3-(pyridin-3-yl)butanal (29k)
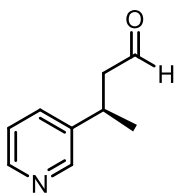
Following GP4 the reaction was performed using enal **27k** (30.4 mg, 0.21 mmol, 1.00 eq.). Purification by silica gel flash chromatography (20–50% EtOAc in hexanes) afforded the product **29k** (24.7 mg, 0.17 mmol, 80%) as a light yellow oil.

^{1}H NMR (501 MHz, CD$_2$Cl$_2$): δ = 9.70 (t, *J* = 1.7 Hz, 1H), 8.49 (d, *J* = 2.4 Hz, 1H), 8.43 (dd, *J* = 4.8, 1.7 Hz, 1H), 7.55 (dt, *J* = 7.8, 2.0 Hz, 1H), 7.24 (ddd, *J* = 7.9, 4.8, 0.9 Hz, 1H), 3.38 (h, *J* = 7.1 Hz, 1H), 2.77 (ddd, *J* = 17.2, 7.0, 1.6 Hz, 1H), 2.71 (ddd, *J* = 17.2, 7.4, 1.8 Hz, 1H), 1.32 (d, *J* = 7.0 Hz, 3H).

^{13}C NMR (126 MHz, CD$_2$Cl$_2$): δ = 201.1, 149.2, 148.2, 141.4, 134.5, 123.9, 51.7, 32.1, 22.1.

HRMS *m*/*z* (ESI): calcd. for C$_9$H$_{12}$N$_1$O$_1$ ([M+H]$^+$): 150.091339; found: 150.091310.

GC (30 m Ivadex-1, injection temperature: 220 °C, 110 °C iso 5 min, 2 °C/min, 150 °C iso 5 min, 8 °C/min, 220 °C iso 5 min, 0.5 bar H$_2$): t$_{R1}$ = 19.0 min (major), t$_{R2}$ = 19.5 min (minor), er = 97:3 (94% ee).

$[\alpha]_D^{25}$ = –15.8 (c= 0.20, CHCl$_3$)

(*R*)-3-(thiophen-2-yl)butanal (29l)
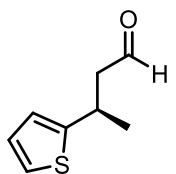
Following GP4 the reaction was performed using enal **27l** (26 µL, 0.20 mmol, 1.00 eq.) in CyH at room temperature for 4 days. Purification by silica gel flash chromatography (50% DCM in pentane) afforded the product **29l** (24.2 mg, 0.16 mmol, 78%) as a yellow oil.

^{1}H NMR (501 MHz, CD$_2$Cl$_2$): δ = 9.71 (t, *J* = 1.8 Hz, 1H), 7.16 (dd, *J* = 5.1, 1.2 Hz, 1H), 6.93 (dd, *J* = 5.1, 3.5 Hz, 1H), 6.85 (dt, *J* = 3.5, 1.1 Hz, 1H), 3.67 (hd, *J* = 7.0, 0.8 Hz, 1H), 2.79 (ddd, *J* = 16.9, 6.9, 1.8 Hz, 1H), 2.68 (ddd, *J* = 17.0, 7.2, 1.9 Hz, 1H), 1.38 (d, *J* = 7.0 Hz, 4H).

^{13}C NMR (126 MHz, CD$_2$Cl$_2$): δ = 201.4, 150.2, 127.1, 123.5, 123.4, 52.7, 30.2, 23.2.

HRMS *m*/*z* (GC-EI): calcd. for C$_8$H$_{10}$O$_1$S$_1$ ([M]$^+$): 154.044687; found: 154.044850.

GC (30 m Ivadex-1, injection temperature: 220 °C, 110 °C iso 5 min, 2 °C/min, 150 °C iso 5 min, 8 °C/min, 220 °C iso 5 min, 0.5 bar H$_2$): t$_{R1}$ = 11.7 min (major), t$_{R2}$ = 12.1 min (minor), er = 94:6 (88% ee).

$[\alpha]_D^{25}$ = –27.8 (c= 0.23, CHCl$_3$)

(*R*)-3-(2-chlorophenyl)butanal (29m)
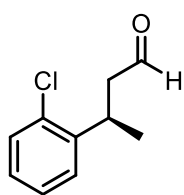
Following GP4 the reaction was performed using enal **27m** (31 μL, 0.20 mmol, 1.00 eq.) in 1,4-dioxane at 50 °C for 24 h. Purification by silica gel flash chromatography (0–50% DCM in pentane) afforded the product **29m** (11.7 mg, 0.06 mmol, 32%) as a colorless oil.

^{1}H NMR (501 MHz, CD$_2$Cl$_2$): δ = 9.70 (t, *J* = 2.0 Hz, 1H), 7.37 (dd, *J* = 8.1, 1.0 Hz, 1H), 7.29–7.24 (m, 2H), 7.20–7.15 (m, 1H), 3.86 (dt, *J* = 14.0, 7.0 Hz, 1H), 2.78 (ddd, *J* = 16.9, 6.3, 1.7 Hz, 1H), 2.65 (ddd, *J* = 16.7, 8.1, 2.1 Hz, 1H), 1.30 (d, *J* = 6.9 Hz, 3H).

^{13}C NMR (126 MHz, CD$_2$Cl$_2$): δ = 201.5, 143.1, 133.7, 130.1, 128.0, 127.7, 127.7, 50.8, 30.7, 20.8.

HRMS *m/z* (EI): calcd. for C$_{10}$H$_{11}$O$_1$Cl$_1$ ([M]$^+$): 182.049293; found: 182.049190.

GC (25 m Lipodex-G, injection temperature: 220 °C, 90 °C iso 60 min, 8 °C/min, 220 °C, 0.6 bar H$_2$): t_{R1} = 39.8 min (minor), t_{R2} = 40.1 min (major), er = 99:1 (98% ee).

(*R*)-3-(4-(4,4,5,5-tetramethyl-1,3,2-dioxaborolan-2-yl)phenyl)butanal (29n)
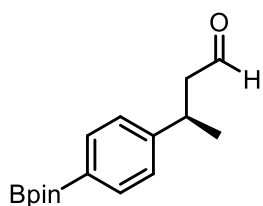
Following GP4 the reaction was performed using enal **27n** (54.6 mg, 0.20 mmol, 1.00 eq.) in 1,4-dioxane at 50 °C for 24 h. Purification by silica gel flash chromatography (20–50% DCM in pentane) afforded the product **29n** (16.3 mg, 0.06 mmol, 30%) as a white solid.

^{1}H NMR (501 MHz, CD$_2$Cl$_2$): δ = 9.67 (t, *J* = 2.0 Hz, 1H), 7.71–7.68 (m, 2H), 7.25–7.22 (m, 2H), 3.35 (dt, J = 7.1, 7.1 Hz, 1H), 2.74 (ddd, J = 16.7, 7.0, 1.9 Hz, 1H), 2.65 (ddd, J = 16.7, 7.5, 2.1 Hz, 1H), 1.32 (s, 12H), 1.29 (d, J = 7.0 Hz, 3H).

^{13}C NMR (126 MHz, CD$_2$Cl$_2$): δ = 201.9, 149.4, 135.4, 126.7, 84.1, 51.9, 34.8, 25.1, 22.3.

HRMS *m/z* (EI): calcd. for C$_{16}$H$_{23}$O$_3$B$_1$ ([M]$^+$): 274.173475; found: 274.173530.

GC (22 m Ivadex-1, injection temperature: 220 °C, 120 °C iso 500 min, 8 °C/min, 220 °C iso 3 min, 0.5 bar H$_2$): t_{R1} = 310.8 min (major), t_{R2} = 318.0 min (minor), er = 98:2 (96% ee).

(*R*)-3-cyclohexylbutanal (29o)
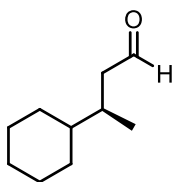
Following GP4 the reaction was performed using enal **27o** (31 μL, 0.20 mmol, 1.00 eq.). Purification by silica gel flash chromatography (20–50% DCM in pentane) afforded the product **29o** (22.9 mg, 0.15 mmol, 73%) as a colorless oil.

¹H NMR (501 MHz, CD$_2$Cl$_2$): δ = 9.72 (dd, *J* = 2.9, 1.8 Hz, 1H), 2.44 (ddd, *J* = 16.0, 4.8, 1.9 Hz, 1H), 2.16 (ddd, *J* = 16.0, 8.9, 2.9 Hz, 1H), 1.99–1.88 (m, 1H), 1.80–1.70 (m, 2H), 1.69–1.59 (m, 3H), 1.29–1.07 (m, 4H), 1.07–0.93 (m, 2H), 0.90 (d, *J* = 6.9 Hz, 3H).

¹³C NMR (126 MHz, CD$_2$Cl$_2$): δ = 203.6, 48.9, 43.2, 33.5, 30.7, 29.6, 27.1, 27.1, 27.0, 17.0.

HRMS *m/z* (ESI): calcd. for C$_{10}$H$_{18}$Na$_1$O$_1$ ([M+Na]$^+$): 177.12499; found: 177.12493.

GC (30 m Ivadex-1, injection temperature: 220 °C, 110 °C iso 5 min, 2 °C/min, 150 °C iso 5 min, 8 °C/min, 220 °C iso 5 min, 0.5 bar H$_2$): t$_{R1}$ = 11.3 min (major), t$_{R2}$ = 11.6 min (minor), er = 98.5:1.5 (97% ee).

$[\alpha]_D^{25}$ = –20.6 (c= 0.24, CHCl$_3$)

(*R*)-3-cyclopentylbutanal (29p)
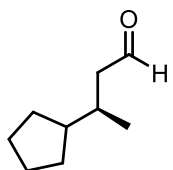
Following GP4 the reaction was performed using enal **27p** (30 μL, 0.20 mmol, 1.00 eq.). ¹H NMR yield was determined to be 87% using mesitylene as internal standard. Purification by silica gel flash chromatography (20–50% DCM in pentane) afforded the product **29p** (21.8 mg, 0.16 mmol, 77%) as a light yellow oil.

¹H NMR (501 MHz, CD$_2$Cl$_2$): δ = 9.73 (dd, *J* = 3.0, 1.8 Hz, 1H), 2.48 (ddd, *J* = 15.9, 4.3, 1.7 Hz, 1H), 2.19 (ddd, *J* = 16.0, 9.0, 3.0 Hz, 1H), 1.95–1.85 (m, 1H), 1.80–1.70 (m, 2H), 1.70–1.57 (m, 3H), 1.57–1.49 (m, 2H), 1.20–1.08 (m, 2H), 0.95 (d, *J* = 6.8 Hz, 3H).

¹³C NMR (126 MHz, CD$_2$Cl$_2$): δ = 203.5, 50.6, 46.7, 33.9, 31.2, 30.6, 25.8, 18.9.

HRMS *m/z* (ESI): calcd. for C$_9$H$_{17}$O$_1$ ([M+H]$^+$): 141.127390; found: 141.127310.

GC (30 m Ivadex-1, injection temperature: 220 °C, 40 °C, 1 °C/min, 80 °C iso 5 min, 8 °C/min, 220 °C iso 5 min, 0.5 bar H$_2$): t$_{R1}$ = 49.1 min (major), t$_{R2}$ = 49.5 min (minor), er = 98.5:1.5 (97% ee).

$[\alpha]_D^{25}$ = –17.7 (c= 0.23, CHCl$_3$)

(*R*)-3-cyclobutylbutanal (29q)
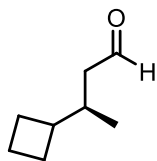
Following GP4 the reaction was performed using enal **27q** (27 μL, 0.20 mmol, 1.00 eq.). ^{1}H NMR yield was determined to be 84% using mesitylene as internal standard. Purification by silica gel flash chromatography (20–50% DCM in pentane) afforded the product **29q** (9.7 mg, 0.08 mmol, 38%) as a light yellow oil.

^{1}H NMR (501 MHz, CD$_2$Cl$_2$): δ = 9.72 (dd, *J* = 2.9, 2.0 Hz, 1H), 2.34 (ddd, *J* = 15.8, 4.5, 1.9 Hz, 1H), 2.10–2.02 (m, 2H), 2.02–1.87 (m, 3H), 1.85–1.76 (m, 1H), 1.75–1.60 (m, 3H), 0.85 (d, *J* = 6.6 Hz, 3H).

^{13}C NMR (126 MHz, CD$_2$Cl$_2$): δ = 203.3, 48.9, 42.5, 35.4, 27.4, 27.1, 17.7, 17.1.

HRMS *m/z* (ESI): calcd. for C$_8$H$_{14}$Na$_1$O$_1$ ([M+Na]$^+$): 149.09369; found: 149.09376.

GC (30 m Ivadex-1, injection temperature: 220 °C, 40 °C, 1 °C/min, 80 °C iso 5 min, 8 °C/min, 220 °C iso 5 min, 0.5 bar H$_2$): t$_{R1}$ = 31.5 min (major), t$_{R2}$ = 32.9 min (minor), er = 97:3 (94% ee).

$[\alpha]_D^{25}$ = –28.6 (c= 0.14, CHCl$_3$)

(*R*)-3,4,4-trimethylpentanal (29r)
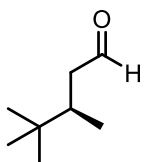
Following GP4 the reaction was performed using enal **27r** (29 μL, 0.20 mmol, 1.00 eq.). ^{1}H NMR yield was determined to be 96% using mesitylene as internal standard. Purification by silica gel flash chromatography (20–50% DCM in pentane) afforded the product **29r** (16.1 mg, 0.13 mmol, 63%) as a colorless oil.

^{1}H NMR (501 MHz, CD$_2$Cl$_2$): δ = 9.72 (dd, *J* = 3.3, 1.3 Hz, 1H), 2.57–2.50 (m, 1H), 2.06 (ddd, *J* = 16.0, 10.2, 3.3 Hz, 1H), 1.93–1.81 (m, 1H), 0.89–0.87 (m, 12H).

^{13}C NMR (126 MHz, CD$_2$Cl$_2$): δ = 203.7, 47.4, 37.8, 33.0, 27.3, 15.5.

HRMS *m/z* (GC-EI): calcd. for C$_8$H$_{16}$O$_1$ ([M]$^+$): 128.119565; found: 128.119770.

GC (30 m Ivadex-1, injection temperature: 220 °C, 40 °C, 1 °C/min, 80 °C iso 5 min, 8 °C/min, 220 °C iso 5 min, 0.5 bar H$_2$): t$_{R1}$ = 21.9 min (major), t$_{R2}$ = 24.0 min (minor), er = 99.5:0.5 (99% ee).

$[\alpha]_D^{25}$ = –30.1 (c= 0.07, CHCl$_3$)

(*R*)-3,4-dimethylpentanal (29s)
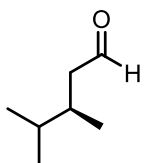
Following GP4 the reaction was performed using enal **27s** (26 μL, 0.20 mmol, 1.00 eq.). ^{1}H NMR yield was determined to be 84% using mesitylene as internal standard. Purification by silica gel flash chromatography (20–50% DCM in pentane) afforded the product **29s** (7.7 mg, 0.07 mmol, 34%) as a colorless oil.

^{1}H NMR (501 MHz, CD$_2$Cl$_2$): δ = 9.73 (dd, *J* = 2.9, 1.8 Hz, 1H), 2.41 (ddd, *J* = 16.0, 4.8, 1.9 Hz, 1H), 2.16 (ddd, *J* = 16.0, 9.0, 2.9 Hz, 1H), 2.01–1.90 (m, 1H), 1.64–1.55 (m, 1H), 0.89 (d, *J* = 6.8 Hz, 6H), 0.86 (d, *J* = 6.9 Hz, 3H).

^{13}C NMR (126 MHz, CD$_2$Cl$_2$): δ = 203.5, 48.8, 34.0, 32.7, 19.8, 18.7, 16.4.

HRMS *m/z* (GC-CI): calcd. for C$_7$H$_{15}$O$_1$ ([M+H]$^+$): 115.111740; found: 115.111850.

GC (30 m Ivadex-1, injection temperature: 220 °C, 40 °C, 1 °C/min, 80 °C iso 5 min, 8 °C/min, 220 °C iso 5 min, 0.5 bar H$_2$): t_{R1} = 14.9 min (major), t_{R2} = 16.1 min (minor), er = 97:3 (94% ee).

$[\alpha]_D^{25}$ = –9.2 (c= 0.06, CHCl$_3$)

(*S*)-3-methylpentanal (29t), (*S*)-1-(2,4-dinitrophenyl)-2-(3-methylpentylidene)hydrazine (29ta)
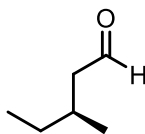
Following GP4 the reaction was performed using enal **27t** (22μL, 0.20 mmol, 1.00 eq.) in CyH/*n*-pentane (9:1) at –10 °C for 8 days. After addition of mesitylene as an internal standard ^{1}H NMR analysis of the crude reaction mixture showed 89% yield of product **29t**.

^{1}H NMR (501 MHz, CD$_2$Cl$_2$): δ 9.73 (t, *J* = 2.3 Hz, 1H), 2.38 (ddd, *J* = 16.1, 5.8, 2.1 Hz, 1H), 2.19 (ddd, *J* = 16.1, 7.9, 2.5 Hz, 1H), 2.01–1.91 (m, 1H), 1.42–1.31 (m, 1H), 1.31–1.21 (m, 1H), 0.94 (d, *J* = 6.8 Hz, 3H), 0.90 (t, *J* = 7.4 Hz, 3H).
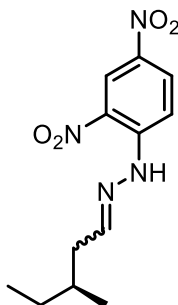
For *in situ* derivatization of the volatile aldehyde **29t**, 2,4-dinitrophenylhydrazine (43 mg, 0.22 mmol, 1.10 eq.), 1 mL EtOH and a drop of concentrated H$_2$SO$_4$ were added to the crude mixture. The reaction was stirred at room temperature for 1 h. Subsequent silica gel flash chromatography (0–10% EtOAc in hexanes) afforded an *E/Z* mixture of the corresponding hydrazone **29ta** (36.3 mg, 0.13 mmol, 66%, *E/Z* ≈ 77:23) as an orange solid.

^{1}H NMR (501 MHz, CDCl$_3$): δ = 11.20 (s, 1H$_{min}$), 11.03 (s, 1H$_{maj}$), 9.13 (d, *J* = 2.6 Hz, 1H$_{min}$), 9.12 (d, *J* = 2.6 Hz, 1H$_{maj}$), 8.33 (dd, *J* = 9.6, 2.6 Hz, 1H$_{min}$), 8.29 (dd, *J* = 9.6, 2.6 Hz, 1H$_{maj}$), 7.96 (d, *J* = 9.5 Hz, 1H$_{min}$),

7.93 (d, J = 9.6 Hz, 1H$_{maj}$), 7.53 (t, J = 5.8 Hz, 1H$_{maj}$), 7.00 (t, J = 5.6 Hz, 1H$_{min}$), 2.48–2.32 (m, 1H$_{maj}$, 1H$_{min}$), 2.32–2.17 (m, 1H$_{maj}$, 1H$_{min}$), 1.87–1.69 (m, 1H$_{maj}$, 1H$_{min}$), 1.54–1.39 (m, 1H$_{maj}$, 1H$_{min}$), 1.38–1.23 (m, 1H$_{maj}$, 1H$_{min}$), 1.04 (d, J = 6.7 Hz, 3H$_{min}$), 0.99 (d, J = 6.7 Hz, 3H$_{maj}$), 0.98–0.92 (m, 3H$_{maj}$, 3H$_{min}$).

^{13}C NMR (126 MHz, CDCl$_3$): δ = 152.3, 150.8, 145.4, 145.3, 137.9, 130.2, 130.1, 128.9, 123.7, 123.5, 116.7, 116.6, 39.3, 34.4, 33.2, 33.0, 29.6, 29.5, 19.7, 19.4, 11.6, 11.5.

HRMS m/z (GC-EI): calcd. for C$_{12}$H$_{16}$N$_4$O$_4$ ([M]$^+$): 280.116605; found: 280.116700.

HPLC (OD-3, n-heptane/i-PrOH 95:5, 298 K, 340 nm): t_{R1} = 13.273 min (major), t_{R2} = 15.590 min (minor), er = 91:9 (82% ee).

$[\alpha]_D^{25}$ = 2.4 (c= 0.17, CHCl$_3$)

(S)-3-methylhexanal (29u), (S)-1-(2,4-dinitrophenyl)-2-(3-methylhexylidene)hydrazine (29ua)
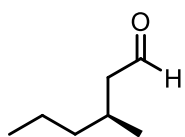
Following GP4 the reaction was performed using enal **27u** (26μL, 0.20 mmol, 1.00 eq.) in CyH at room temperature for 17 h. After addition of mesitylene as an internal standard ^{1}H NMR analysis of the crude reaction mixture showed 99% yield of product **29u**.

^{1}H NMR (501 MHz, CD$_2$Cl$_2$): δ = 9.72 (t, J = 2.3 Hz, 1H), 2.37 (ddd, J = 16.0, 5.7, 2.1 Hz, 1H), 2.19 (ddd, J = 16.0, 7.8, 2.6 Hz, 1H), 2.09–2.01 (m, 1H), 1.37–1.20 (m, 4H), 0.94 (d, J = 6.7 Hz, 3H), 0.90 (t, J = 7.1 Hz, 3H).
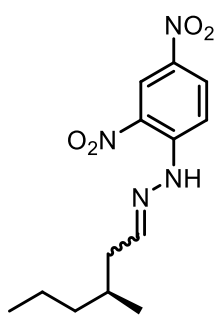
For *in situ* derivatization of the volatile aldehyde **29u**, 2,4-dinitrophenylhydrazine (44 mg, 0.22 mmol, 1.10 eq.), 1 mL EtOH and a drop of concentrated H$_2$SO$_4$ were added to the crude mixture. The reaction was stirred at room temperature for 1 h. Subsequent silica gel flash chromatography (0–10% EtOAc in hexanes) afforded an E/Z mixture of the corresponding hydrazone **29ua** (43.9 mg, 0.15 mmol, 73%, $E/Z ≈$ 77:23) as an orange solid.

^{1}H NMR (501 MHz, CDCl$_3$): δ = 11.19 (s, 1H$_{min}$), 11.02 (s, 1H$_{maj}$), 9.12 (d, J = 2.6 Hz, 1H$_{min}$), 9.10 (d, J = 2.6 Hz, 1H$_{maj}$), 8.32 (dd, J = 9.6, 2.6 Hz, 1H$_{min}$), 8.29 (dd, J = 9.6, 2.6 Hz, 1H$_{maj}$), 7.95 (d, J = 9.6 Hz, 1H$_{min}$), 7.93 (d, J = 9.7 Hz, 1H$_{maj}$), 7.53 (t, J = 5.8 Hz, 1H$_{maj}$), 6.99 (t, J = 5.6 Hz, 1H$_{min}$), 2.42 (dt, J = 14.6, 5.7 Hz, 1H$_{maj}$), 2.36 (dt, J = 16.1, 5.7 Hz, 1H$_{min}$), 2.31–2.17 (m, 1H$_{maj}$, 1H$_{min}$), 1.94–1.88 (m, 1H$_{min}$), 1.83 (h, J = 6.8 Hz, 1H$_{maj}$), 1.46–1.17 (m, 4H$_{maj}$, 4H$_{min}$), 1.04 (d, J = 6.7 Hz, 3H$_{min}$), 0.99 (d, J = 6.7 Hz, 3H$_{maj}$), 0.95–0.88 (m, 3H$_{maj}$, 3H$_{min}$).

13C NMR (126 MHz, CDCl$_3$): δ = 152.3, 150.8, 145.4, 145.3, 138.4, 137.9, 130.2, 130.1, 129.6, 128.9, 123.6, 123.5, 116.7, 116.6, 39.7, 39.2, 39.1, 34.7, 31.3, 31.1, 20.2, 20.2, 20.0, 19.8, 14.3, 14.3.

HRMS m/z (GC-EI): calcd. for C$_{13}$H$_{18}$N$_4$O$_4$ ([M]$^+$): 294.132255; found: 294.132420.

HPLC (OD-3, n-heptane/i-PrOH 95:5, 298 K, 340 nm): t_{R1} = 12.716 min (major), t_{R2} = 15.413 min (minor), er = 97.5:2.5 (95% ee).

$[α]_D^{25}$ = –1.4 (c= 0.14, CHCl$_3$)

(S)-3-methylheptanal (29v)
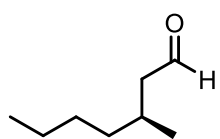
Following GP4 the reaction was performed using enal **27v** (29 μL, 0.20 mmol, 1.00 eq.). ^{1}H NMR yield was determined to be 84% using mesitylene as internal standard. Purification by silica gel flash chromatography (20–50% DCM in pentane) afforded the product **29v** (13.4 mg, 0.11 mmol, 52%) as a colorless oil.

1H NMR (501 MHz, CD$_2$Cl$_2$): δ = 9.73 (t, J = 2.4 Hz, 1H), 2.37 (ddd, J = 16.1, 5.7, 2.1 Hz, 1H), 2.20 (ddd, J = 16.1, 7.9, 2.6 Hz, 1H), 2.07–1.98 (m, 1H), 1.32–1.23 (m, 6H), 0.94 (d, J = 6.7 Hz, 3H), 0.91–0.87 (m, 3H).

13C NMR (126 MHz, CD$_2$Cl$_2$): δ = 203.3, 51.4, 37.0, 29.5, 28.5, 23.2, 20.1, 14.2.

HRMS m/z (ESI): calcd. for C$_8$H$_{16}$Na$_1$O$_1$ ([M+Na]$^+$): 151.10934; found: 151.10946.

GC (30 m Ivadex-1, injection temperature: 220 °C, 45 °C iso 40 min, 1 °C/min, 65 °C, 8 °C/min, 220 °C iso 5 min, 0.5 bar H$_2$): t_{R1} = 44.3 min (major), t_{R2} = 46.4 min (minor), er = 95:5 (90% ee).

$[α]_D^{25}$ = –17.4 (c= 0.23, CHCl$_3$)

Following GP4 the reaction was performed using enal **27v** (29 μL, 0.20 mmol, 1.00 eq.) in CyH at room temperature. ^{1}H NMR yield was determined to be 84% using mesitylene as internal standard. Purification by silica gel flash chromatography (20–50% DCM in pentane) afforded the product **29v** (7.1 mg, 0.06 mmol, 28%) as a colorless oil.

GC (25 m Hydrodex-beta-TBDAc-CD, injection temperature: 220 °C, 70 °C iso 44 min, 8 °C/min, 220 °C, 0.5 bar H$_2$): t_{R1} = 37.5 min (major), t_{R2} = 40.6 min (minor), er = 97.5:2.5 (95% ee).

$[α]_D^{25}$ = –23.5 (c= 0.03, CHCl$_3$)

(*S*)-3,7-dimethyloct-6-enal/ (*S*)-citronellal (29w)
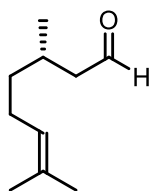
Following GP4 the reaction was performed using citral (34 μL, 0.20 mmol, 1.00 eq.) in CyH at room temperature. ^{1}H NMR yield was determined to be 84% using mesitylene as internal standard. Purification by silica gel flash chromatography (20–50% DCM in pentane) afforded the product **29w** (27.3 mg, 0.18 mmol, 89%) as a light yellow oil.

^{1}H NMR (501 MHz, CD$_2$Cl$_2$): δ = 9.72 (t, *J* = 2.3 Hz, 1H), 5.13–5.07 (m, 1H), 2.38 (ddd, *J* = 16.1, 5.6, 2.0 Hz, 1H), 2.20 (ddd, *J* = 16.1, 8.0, 2.6 Hz, 1H), 2.10–1.92 (m, 3H), 1.68 (d, *J* = 1.4 Hz, 3H), 1.60 (d, *J* = 1.3 Hz, 3H), 1.41–1.30 (m, 1H), 1.30–1.22 (m, 1H), 0.95 (d, *J* = 6.7 Hz, 3H).

^{13}C NMR (126 MHz, CD$_2$Cl$_2$): δ = 203.2, 132.0, 124.5, 51.4, 37.3, 28.2, 25.8, 20.0, 17.7.

HRMS *m/z* (ESI): calcd. for C$_{10}$H$_{19}$O$_1$ ([M+H]$^+$): 155.143040; found: 155.143110.

GC (30 m BGB-174, injection temperature: 220 °C, 70 °C iso 120 min, 8 °C/min, 240 °C iso 3 min, 0.6 bar H$_2$): t_{R1} = 95.0 min (major), t_{R2} = 102.3 min (minor), er = 97:3 (94% ee).

[α]$_D^{25}$ = –19.1 (c= 0.34, CHCl$_3$)

(*S,E*)-3,7,11-trimethyldodeca-6,10-dienal/ (*S,E*)-dihydrofarnesal (29x)
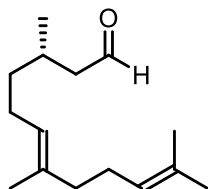
Following GP4 the reaction was performed using farnesal (96%, 50 μL, 0.20 mmol, 1.00 eq.) in CyH at room temperature for 7 days. Purification by silica gel flash chromatography (20–50% DCM in pentane) afforded the product **29x** (35.4 mg, 0.16 mmol, 81%) as a colorless oil.

^{1}H NMR (501 MHz, CD$_2$Cl$_2$): δ = 9.72 (t, *J* = 2.2 Hz, 1H), 5.14–5.07 (m, 2H), 2.39 (ddd, *J* = 16.0, 5.6, 2.1 Hz, 1H), 2.20 (ddd, *J* = 16.0, 8.0, 2.6 Hz, 1H), 2.11–1.93 (m, 8H), 1.67 (d, *J* = 1.4 Hz, 3H), 1.60 (d, *J* = 1.3 Hz, 6H), 1.41–1.23 (m, 3H), 0.96 (d, *J* = 6.7 Hz, 3H).

^{13}C NMR (126 MHz, CD$_2$Cl$_2$): δ = 203.2, 135.7, 131.7, 124.7, 124.5, 51.4, 40.1, 37.3, 28.1, 27.1, 25.8, 25.7, 20.0, 17.8, 16.1.

HRMS *m/z* (ESI): calcd. for C$_{15}$H$_{26}$O$_1$ ([M]$^+$): 222.197815; found: 222.197800.

GC (30 m BGB-174, injection temperature: 220 °C, 110 °C iso 160 min, 8 °C/min, 220 °C iso 3 min, 0.6 bar H$_2$): t_{R1} = 123.8 min (major), t_{R2} = 127.2 min (minor), er = 97.5:2.5 (95% ee).

[α]$_D^{25}$ = –14.3 (c= 0.27, CHCl$_3$)

5 mmol scale (29x)

Following GP4 the reaction was performed using farnesal (96%, 1.15 g, 5.00 mmol, 1.00 eq.) in CyH at room temperature for 19 h. Cyclohexane was removed under reduced pressure prior to purification by silica gel flash chromatography (20–50% DCM in pentane). Product **29x** (1.03 g, 4.63 mmol, 93%) was obtained as a colorless oil.

GC (30 m BGB-174, injection temperature: 220 °C, 110 °C iso 160 min, 8 °C/min, 220 °C iso 3 min, 0.6 bar H_2): t_{R1} = 123.6 min (major), t_{R2} = 127.1 min (minor), er = 97:3 (94% ee).

$[\alpha]_D^{25}$ = –14.7 (c= 0.37, CHCl$_3$)

3-phenylpentanal (29y)
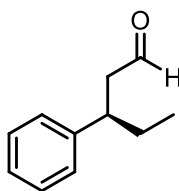
An oven-dried GC vial under argon, equipped with a magnetic stirring bar, was charged with the chiral catalyst **53f** (2.5 mol%). Substrate **27y** (0.03 mmol) was added and dissolved in dry 1,4-dioxane (0.1 M). The reaction mixture was stirred for five minutes at room temperature. After addition of Hantzsch ester **33** (1.1 eq.) the reaction mixture was heated to 50 °C and stirred for 24 h. The reaction was quenched by addition of NEt$_3$ (10 µL) followed by addition of Ph$_3$CH (1.0 M in PhMe) as internal standard. An aliquot of the mixture was taken and diluted with CDCl$_3$ for subsequent ^{1}H NMR analysis. The remaining solution was used for preparative thin layer chromatography to purify the chiral product **29y**. Chiral GC analysis was performed to give the corresponding enantiomeric ratio.

^{1}H NMR analysis of the crude: 39% yield.

^{1}H NMR (501 MHz, CD$_2$Cl$_2$): δ = 9.64 (t, J = 2.1 Hz, 1H), 7.30 (t, J = 7.6 Hz, 2H), 7.24–7.17 (m, 3H), 3.12–3.03 (m, 1H), 2.71 (d, J = 2.1 Hz, 1H), 2.71–2.69 (m, 1H), 1.75–1.57 (m, 2H), 0.80 (t, J = 7.4 Hz, 3H).

HRMS m/z (EI): calcd. for C$_{11}$H$_{14}$O$_1$ ([M]$^+$): 162.103915; found: 162.104130.

GC (30 m Ivadex-1, injection temperature: 220 °C, 110 °C, 2 °C/min, 150 °C iso 5 min, 5 °C/min, 200 °C iso 30 min, 5 °C/min 220 °C iso 5 min, 0.5 bar H_2): t_{R1} = 14.5 min (major), t_{R2} = 14.7 min (minor), er = 85:15 (70% ee).

3-phenylheptanal (29z)
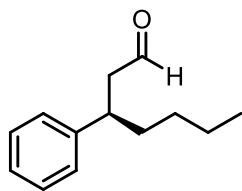
An oven-dried GC vial under argon, equipped with a magnetic stirring bar, was charged with the chiral catalyst **53f** (2.5 mol%). Substrate **27z** (0.03 mmol) was added and dissolved in dry 1,4-dioxane (0.1 M). The reaction mixture was stirred for five minutes at room temperature. After addition of Hantzsch ester **33** (1.1 eq.) the reaction mixture was heated to 50 °C and stirred for 24 h. The reaction was quenched by addition of NEt$_3$ (10 µL) followed by addition of Ph$_3$CH (1.0 M in PhMe) as internal standard. An aliquot of the mixture was taken and diluted with CDCl$_3$ for subsequent ^{1}H NMR analysis. The remaining solution was used for preparative thin layer chromatography to purify the chiral product **29z**. Chiral GC analysis was performed to give the corresponding enantiomeric ratio.

^{1}H NMR analysis of the crude: 25% yield.

^{1}H NMR (501 MHz, CD$_2$Cl$_2$): δ = 9.63 (t, J = 2.1 Hz, 1H), 7.33–7.26 (m, 2H), 7.23–7.17 (m, 3H), 3.19–3.11 (m, 1H), 2.70 (d, J = 2.1 Hz, 1H), 2.69 (d, J = 2.1 Hz, 1H), 1.71–1.57 (m, 2H), 1.35–1.04 (m, 4H), 0.83 (t, J = 7.2 Hz, 3H).

HRMS m/z (ESI): calcd. for C$_{13}$H$_{18}$O$_1$Na$_1$ ([M+Na]$^+$): 213.124984; found: 213.125310.

GC (30 m Ivadex-1, injection temperature: 220 °C, 110 °C, 2 °C/min, 150 °C iso 5 min, 5 °C/min, 200 °C iso 30 min, 5 °C/min 220 °C iso 5 min, 0.5 bar H$_2$): t$_{R1}$ = 22.4 min (major), t$_{R2}$ = 22.6 min (minor), er = 69:31 (38% ee).

4.2.5 Catalyst Characterization
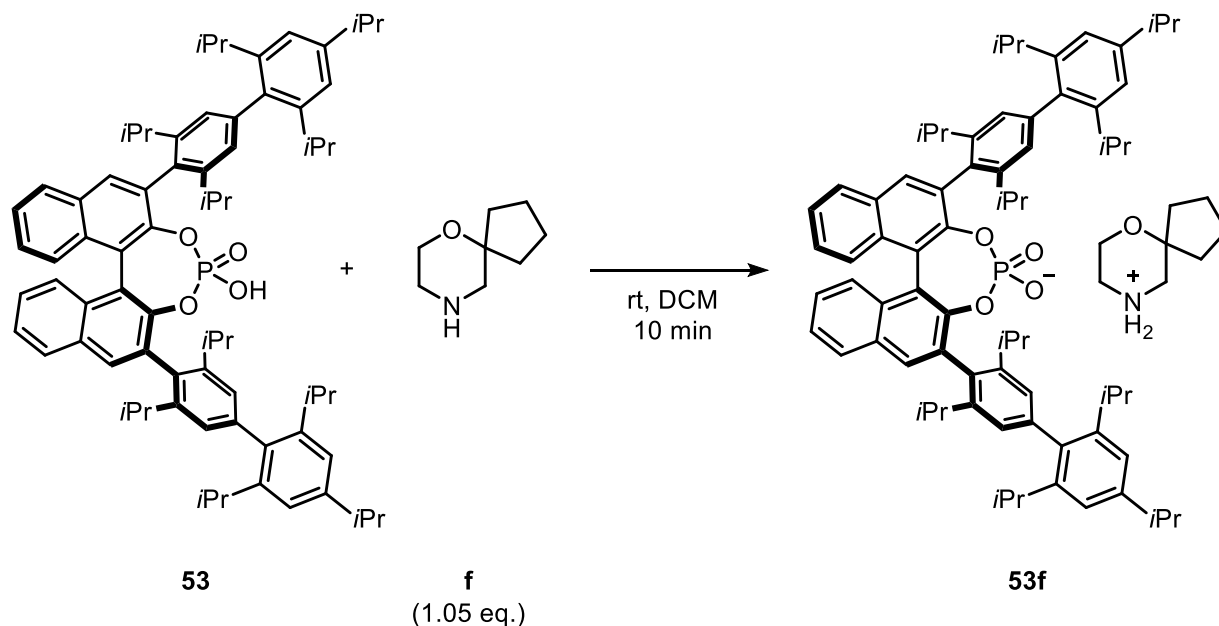
An oven-dried vial, equipped with a magnetic stirring bar, was charged with chiral phosphoric acid **53** (790 mg, 0.74 mmol, 1.00 eq.) and amine **f** (109 mg, 0.77 mmol, 1.05 eq.). After addition of DCM (2 mL), the reaction mixture was stirred for ten minutes at room temperature. The solvent was removed under reduced pressure. The remaining salt was washed four times with *n*-pentane and then dried under high vacuum overnight to afford **53f** as an off-white solid (881 mg, 0.73 mmol, 99%).

^{1}H NMR (501 MHz, CD$_2$Cl$_2$): δ = 7.94 (d, *J* = 8.2 Hz, 2H), 7.84 (s, 2H), 7.46 (ddd, *J* = 8.0, 6.3, 1.4 Hz, 2H), 7.36–7.28 (m, 4H), 7.15–7.09 (m, 6H), 7.03 (d, *J* = 1.7 Hz, 2H), 3.69–3.44 (m, 2H), 3.13–3.03 (m, 2H), 3.01–2.94 (m, 2H), 2.93–2.86 (m, 2H), 2.86–2.77 (m, 3H), 2.76–2.61 (m, 5H), 1.80–1.61 (m, 4H), 1.55–1.42 (m, 4H), 1.34 (d, *J* = 6.9 Hz, 12H), 1.25–1.12 (m, 42H), 0.92 (d, *J* = 6.8 Hz, 6H).

^{31}P NMR (203 MHz, CDCl$_3$): δ = 6.1.

^{13}C NMR (126 MHz, CD$_2$Cl$_2$): δ = 148.2, 147.8, 147.4, 147.3, 146.2, 140.0, 138.1, 133.0, 132.8, 132.5, 130.7, 128.2, 127.5, 126.0, 125.0, 123.8, 123.0, 121.0, 120.7, 81.3, 58.9, 49.7, 42.5, 35.7, 34.4, 31.0, 30.8, 30.6, 30.4, 26.3, 25.1, 24.9, 24.6, 24.6, 24.5, 24.3, 24.3, 24.0, 23.9, 23.8, 23.7.

HRMS *m/z* (ESI): calcd. for C$_8$H$_{16}$N$_1$O$_1$ ([M– C$_{74}$H$_{88}$O$_1$P$_1$]$^+$): 142.12264; found: 142.12263.

HRMS *m/z* (ESI): calcd. for C$_{74}$H$_{88}$O$_1$P$_1$ ([M– C$_8$H$_{16}$N$_1$O$_1$]$^-$): 1071.64257; found: 1071.64271.

4.2.6 Mechanistic experiments

Enantioconvergence Experiment
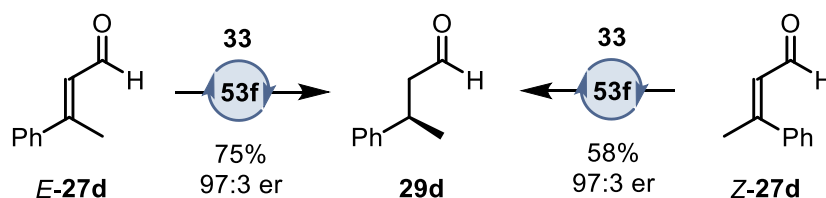
An oven-dried GC vial under argon, equipped with a magnetic stirring bar, was charged with the chiral catalyst **53f** (2.5 mol%). The respective *E*- or *Z*-isomer of **27d** (0.03 mmol) was added and dissolved in dry 1,4-dioxane (0.1 M). The reaction mixture was stirred for five minutes at room temperature. After addition of Hantzsch ester **33** (1.1 eq.) the reaction mixture was heated to 50 °C and stirred for 24 h. The reaction was quenched by addition of NEt$_3$ (10 μL) followed by addition of Ph$_3$CH (1.0 M in PhMe) as internal standard. An aliquot of the mixture was taken and diluted with CDCl$_3$ for subsequent ^{1}H NMR analysis. The remaining solution was used for preparative thin layer chromatography to purify the chiral product **29d**. Chiral GC analysis was performed to give the corresponding enantiomeric ratio.

Regardless of which geometric isomer was used as the starting material, the same enantiomeric ratio of the product (97:3 er) was obtained.

Deuterium Scrambling Experiment
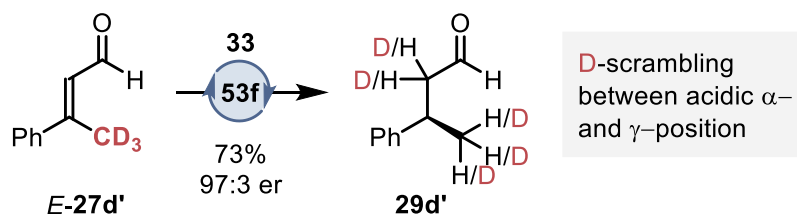
An oven-dried GC vial under argon, equipped with a magnetic stirring bar, was charged with the chiral catalyst **53f** (2.5 mol%). The *E*-isomer of the deuterated substrate **27d'** (0.03 mmol) was added and dissolved in dry 1,4-dioxane (0.1 M). The reaction mixture was stirred for five minutes at room temperature. After addition of Hantzsch ester **33** (1.1 eq.) the reaction mixture was heated to 50 °C and stirred for 24 h. The reaction was quenched by addition of NEt$_3$ (10 μL) followed by addition of Ph$_3$CH (1.0 M in PhMe) as internal standard. An aliquot of the mixture was taken and diluted with CDCl$_3$ for subsequent ^{1}H NMR analysis. The remaining solution was used for preparative thin layer chromatography to purify the chiral product **29d'**. Chiral GC analysis was performed to give the corresponding enantiomeric ratio.

Mass spectrometry as well as ^{1}H and ^{2}H NMR analyses (in CD$_2$Cl$_2$) were performed. Based on the C**H**O NMR signal, **29d'** was found to be a mixture of isotopomers with the following average D distribution:
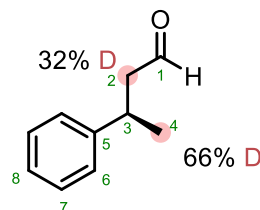
1H{off},1D, 600.20 MHz,CD2Cl2,298.0K, pulse sequence: zg30
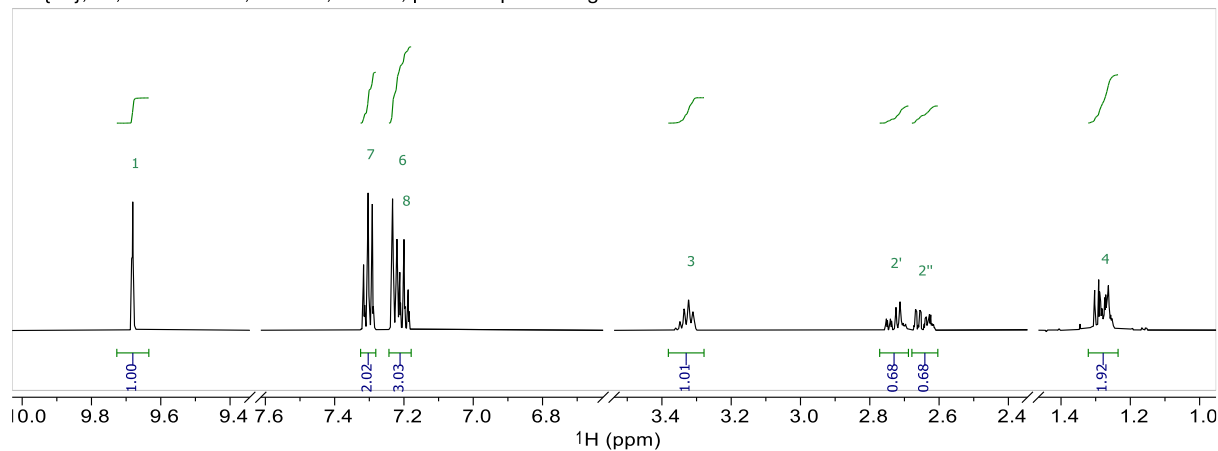
Figure 4.1 ^{1}H NMR spectrum of the reaction crude.

2H{off},1D, 92.13 MHz,CD2Cl2,298.0K, pulse sequence: zg2h.2
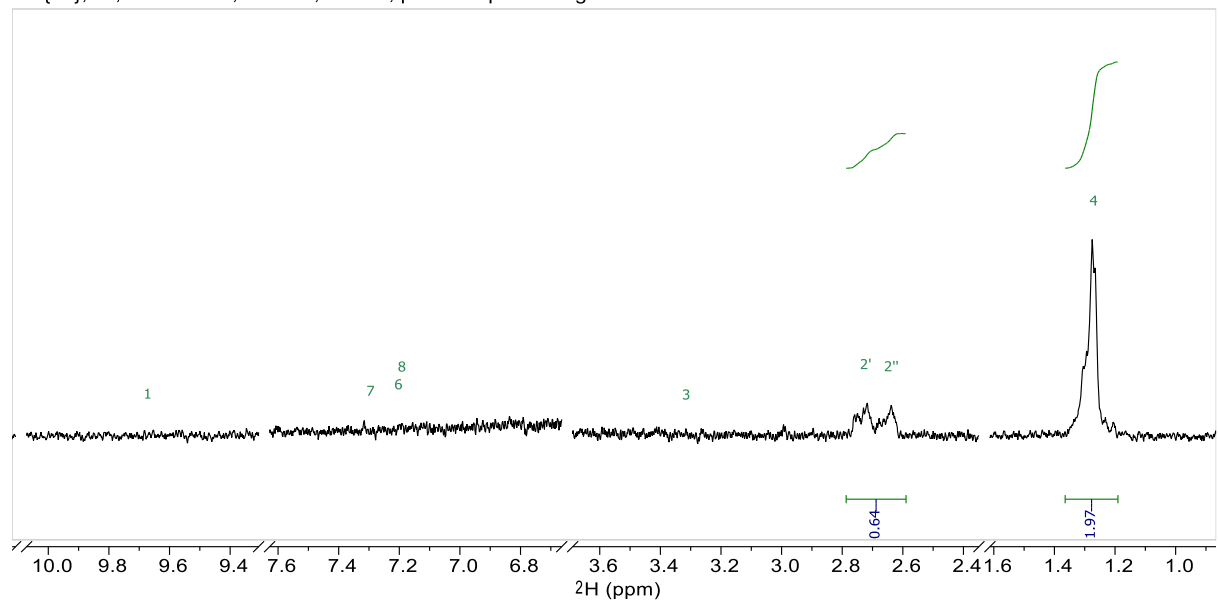
Figure 4.2 ^{2}H NMR spectrum of the reaction crude.

GC-EI-MS analysis revealed the presence of D0 to D5 species with the following D distribution:

D0	**4.5% ± 0.6%**
D1	13.9% ± 0.8%
D2	23.5% ± 0.8%
D3	31.2% ± 0.8%
D4	21.6% ± 0.8%
D5	5.0% ± 0.6%
	99.7%

Transfer Hydrogenation of 4,4,4-trifluoro-3-phenylbut-2-enal
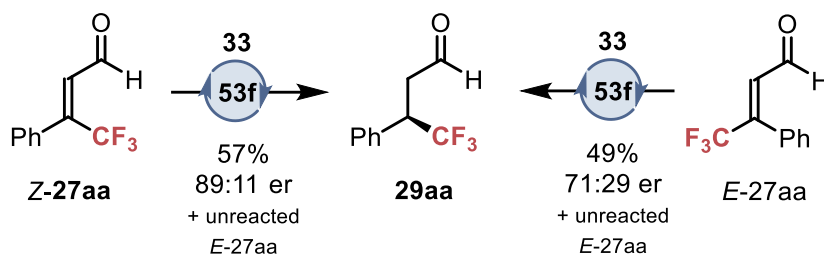
An oven-dried GC vial under argon, equipped with a magnetic stirring bar, was charged with the chiral catalyst **53f** (2.5 mol%). The respective *E*- or *Z*-isomer of **27aa** (0.03 mmol) was added and dissolved in dry 1,4-dioxane (0.1 M). The reaction mixture was stirred for five minutes at room temperature. After addition of Hantzsch ester **33** (1.1 eq.) the reaction mixture was heated to 50 °C and stirred for 24 h. The reaction was quenched by addition of NEt₃ (10 µL) followed by addition of Ph₃CH (1.0 M in PhMe) as internal standard. An aliquot of the mixture was taken and diluted with CDCl₃ for subsequent ¹H NMR analysis. The remaining solution was used for preparative thin layer chromatography to purify the chiral product **29aa**. Chiral GC analysis was performed to give the corresponding enantiomeric ratio.

Regardless of which isomer was reacted, the same product enantiomer is favored and exclusively the *E*-isomer remains unreacted. However, different enantiomeric ratios are obtained depending on the geometrical purity of the starting material. These observations indicate a different and slower isomerization pathway taking place.

From *Z*-**27aa**: **GC** (30 m Ivadex-1, injection temperature: 220 °C, 110 °C iso 5 min, 2 °C/min, 150 °C iso 5 min, 5 °C/min, 200 °C iso 30 min, 5 °C/min 220 °C iso 5 min, 0.5 bar H_2): t_{R1} = 7.7 min (major), t_{R2} = 7.9 min (minor), er = 89:11 (78% ee).

From *E*-**27aa**: **GC** (30 m Ivadex-1, injection temperature: 220 °C, 110 °C iso 5 min, 2 °C/min, 150 °C iso 5 min, 5 °C/min, 200 °C iso 30 min, 5 °C/min 220 °C iso 5 min, 0.5 bar H_2): t_{R1} = 7.7 min (major), t_{R2} = 7.8 min (minor), er = 71:29 (42% ee).

Effect of Morpholine Symmetry on Stereochemical Outcome
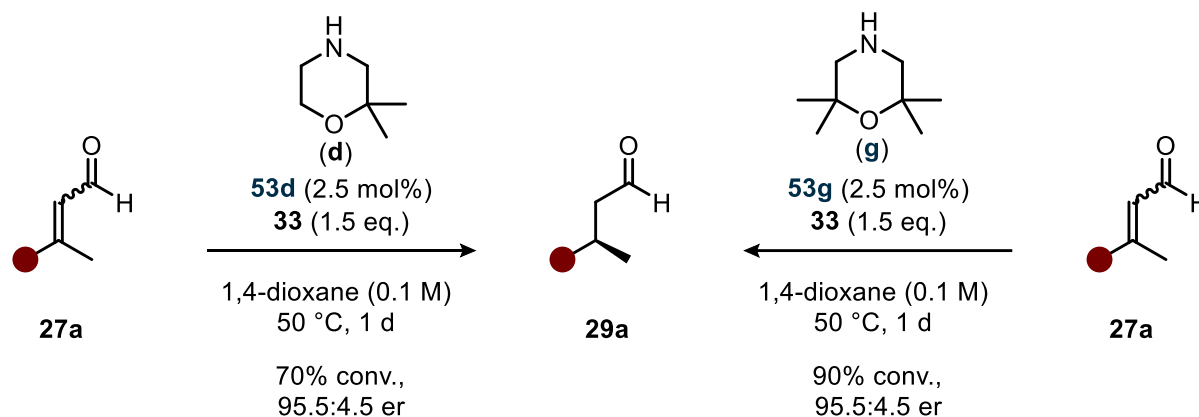
An oven-dried GC vial under argon, equipped with a magnetic stirring bar, was charged with the chiral catalyst **53d** or **53g** (2.5 mol%). Substrate **27a** (0.025 mmol) was added and dissolved in dry 1,4-dioxane (0.1 M). The reaction mixture was stirred for five minutes at room temperature. After addition of Hantzsch ester **33** (1.5 eq.) the reaction mixture was heated to 50 °C and stirred for 24 h. The reaction was quenched by addition of NEt$_3$ (10 µL) followed by addition of Ph$_3$CH (1.0 M in PhMe) as internal standard. An aliquot of the mixture was taken and diluted with CDCl$_3$ for subsequent ^{1}H NMR analysis. The remaining solution was used for preparative thin layer chromatography to purify the chiral product **29a**. Chiral GC analysis was performed to give the corresponding enantiomeric ratio.

4.2.7   Computational Details

All computational studies were carried out in collaboration with Dr. Benjamin Mitschke, who performed the calculations and contributed to data analysis.

Preliminary transition state structures were generated at the GFN2-xTB[279] level using the xtb program version 6.6.0, followed by exploration of the conformational landscape at the same level of theory using

Grimme's Conformer–Rotamer Ensemble Sampling Tool (CREST)[280], version 2.12 with the `mdlen = 50` setting. All resulting conformers were subsequently optimized using constraints at the GFN2-xTB level. Following structure reduction through RMSD evaluation, conformers that met the elimination criteria were subsequently subjected to constrained optimizations using DFT. All DFT calculations were conducted using ORCA version 5.0.3.[281] The GFN2-xTB conformers were optimized using the PBE exchange-correlation functional[282] and Grimme's DFT-D3[283] scheme with Becke–Johnson damping[284] along with the def2-SVP[285] basis set (verytightscf convergence criterion). This computational protocol for geometry optimization has proven successful in the literature.[102,286] The Resolution of Identity (RI) approximation[287] in the Split-RI-J[288] variant using a corresponding auxiliary basis set[289] was used. After successful constrained geometry optimizations, another round of RMSD elimination was performed (see below for exact criteria), followed by transition state optimizations (OptTS keyword). True transition state structures were verified by subsequent vibrational frequency calculation at the same level of theory. Solvent effect were included implicitly with the CPCM model[290] in 1,4-dioxane (`epsilon 2.25` and `refrac 1.42` options in the `%cpcm` block). Gibbs free energies were calculated using refined electronic energies at various levels of theory in combination with thermochemical corrections from the vibrational frequency calculations acquired by using Duarte's `otherm.py`[291] in a 1 M solution standard state at 323 K.

Non-covalent interactions were studied using the Independent Gradient Model based on Hirshfeld partition (IGMH)[210] in conjunction with the Multiwfn program, version 3.8.[211,212]

The following input was used for the DLPNO-CCSD(T) calculations:

```
! DLPNO-CCSD(T) cc-pVTZ cc-pVTZ/C cc-pVTZ/JK verytightscf TightPNO
keepdens
```

a. 2006 System: Transition State Overview
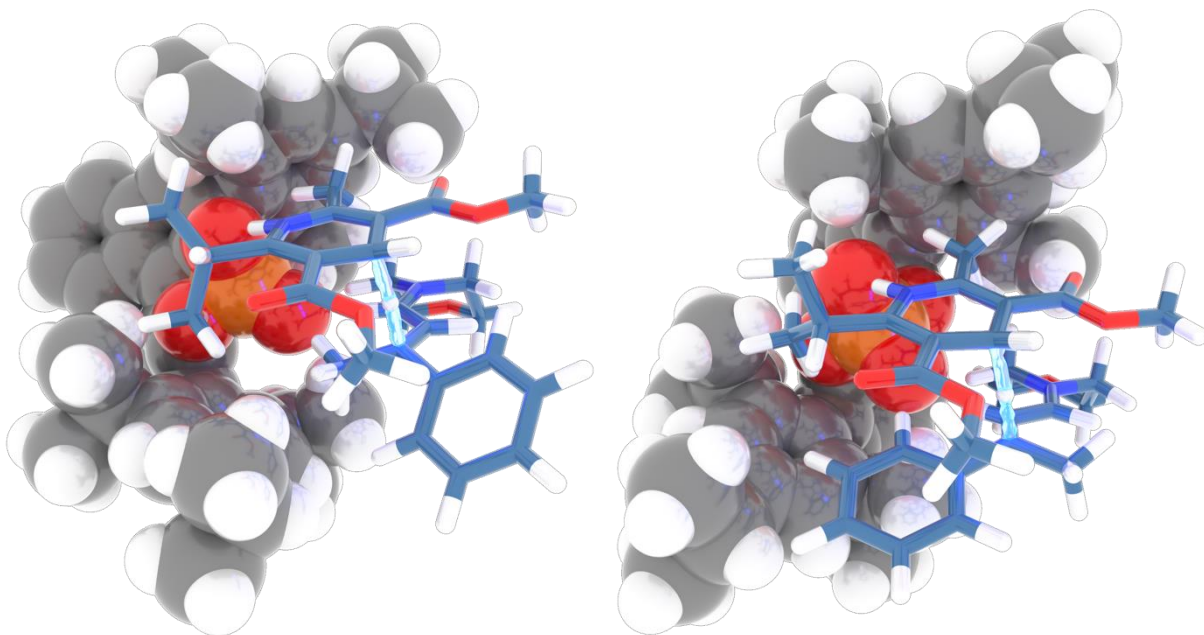
Figure 4.3 Structural overview of **TS-1** (left) and **TS-2** (right).
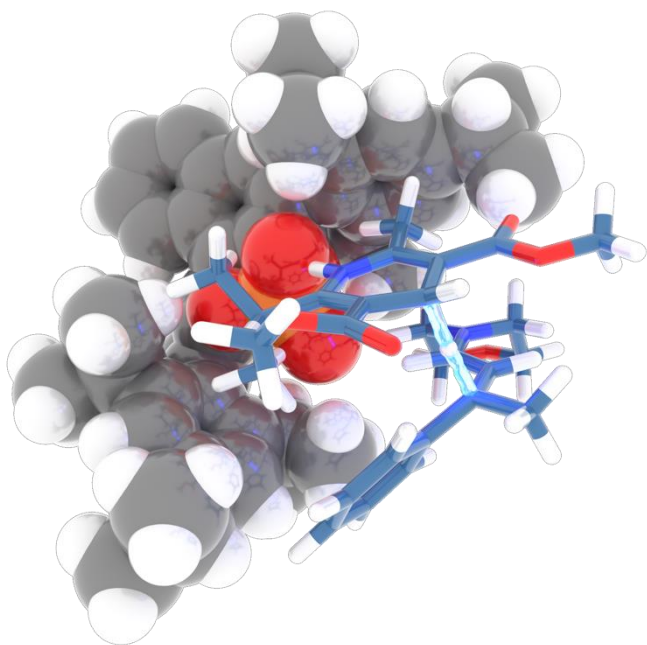
Figure 4.4 Structural overview of **TS-2b**.

b. Method Screening

In order to gain access to a computationally verifiable data point, we conducted the transfer hydrogenation of enal **27d** according to the following procedure:
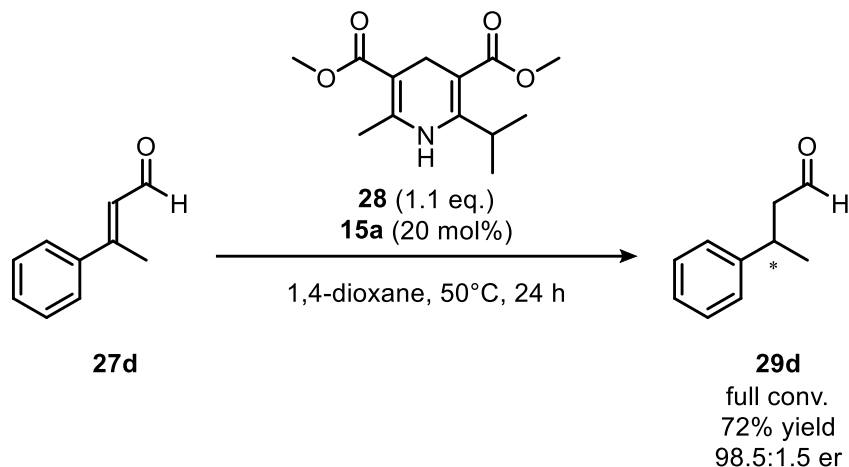
27d

28 (1.1 eq.)
15a (20 mol%)

1,4-dioxane, 50°C, 24 h

29d
full conv.
72% yield
98.5:1.5 er

An oven dried GC vial under argon, equipped with a magnetic stirring bar, was charged with the chiral phosphoric acid (*S*)-**15** and morpholine **a** (20 mol%). Substrate **27d** (0.025 mmol) was added and dissolved in dry 1,4-dioxane (0.1 M). The reaction mixture was stirred for five minutes at room temperature. After addition of Hantzsch ester **28** (1.1 eq.) the reaction mixture was heated to 50 °C and stirred overnight. The reaction was terminated by addition of NEt$_3$ (10 µL) followed by addition of mesitylene as internal standard. An aliquot of the mixture was taken and diluted with CDCl$_3$ for subsequent ^{1}H NMR analysis. The remaining solution was used for preparative thin layer chromatography to purify the chiral product **29d**. Chiral GC analysis was performed to give the corresponding enantiomeric ratio (98.5:1.5).

According to the following equation, this enantiomeric ratio at 323 K corresponds to an energy difference of 2.7 kcal/mol.

$$ee = \frac{e^{\frac{-\Delta\Delta G^{\ddagger}}{RT}} - 1}{e^{\frac{-\Delta\Delta G^{\ddagger}}{RT}} + 1}$$

Subsequently, the three transition states **TS-1**, **TS-2**, and **TS-2b** were evaluated by single point calculation using distinct functionals, and eventually the corresponding Gibbs energies were compared by comparing with the thermochemical corrections obtained at the PBE-D3(BJ)/def2-SVP level of theory.

The same protocol was followed for catalyst **53f** (97:3 er in the reaction to form **29d**), corresponding to an energy difference of 2.2 kcal/mol.

Table 4.3 Gibbs energies (in kcal/mol) of the transition states (double bond configurations below) as calculated by combining single point energies of different functionals and basis sets with the PBE-D3(BJ)/def2-SVP thermochemical corrections; solvent effects taken into account by using the CPCM model (epsilon = 2.25, refrac = 1.42).

	B3LYP-D3(BJ)/def2-TZVPP[292,293]	B3LYP-D3(BJ)/def2-TZVPPD[292,293]	B3LYP/def2-TZVPP[292,293]	M06-2X/def2-TZVPP[294]	B2PLYP-D3(BJ)/def2-TZVPP[295]	ωB97X-V/def2-TZVPP[252]	ωB97M-D3(BJ)/def2-TZVPP[296]	ωB97M-V/def2-TZVPP[296]	DLPNO-CCSD(T)/cc-pVTZ[201,204–209,297]
TS-1 (*E*)	0.0	0.0	0.0	0.0	0.0	0.0	0.0	0.0	**0.0**
TS-2 (*E*)	2.7	3.3	8.7	2.1	2.2	3.9	3.2	2.7	**2.6**
TS-2b (*Z*)	3.8	4.0	2.1	4.2	4.0	5.5	5.2	5.6	**4.6**
TS-3 (*E,E*)	0.0	–	0.0	0.0	–	0.0	0.0	0.0	**0.0**
TS-4 (*E,Z*)	2.5	–	9.0	2.7	–	3.9	2.8	3.0	**2.2**
TS-4b (*Z,E*)	1.2	–	8.8	3.5	–	3.2	2.6	2.5	**2.5**
TS-3b (*Z,E*)	4.1	–	–5.5	3.3	0.0	4.5	4.1	4.7	**3.7**
TS-4c (*Z,Z*)	6.5	–	5.7	4.6	1.9	8.1	6.6	7.2	**5.8**
TS-4d (*E,E*)	6.0	–	5.4	4.4	1.3	8.3	6.6	7.2	**6.1**

In light of the good agreement between the experimental values and computational benchmark, the DLPNO-CCSD(T) method in conjunction with a cc-pVTZ basis set was used for all further calculations reported in this study, unless stated otherwise.

c. 2006 System: Distortion–Interaction Analysis

Table 4.4 Overview of the transition states at the CPCM(1,4-dioxane)-DLPNO-CCSD(T)/cc-pVTZ//PBE-D3(BJ)def2-SVP level of theory as well as computed enantiomeric ratios at 323 K.

	$\Delta\Delta G^{\ddagger}$ (323 K)	Computed er (323 K)
TS-1	0.0 kcal/mol	–
TS-2	2.6 kcal/mol	98.5:1.5
TS-2b	4.6 kcal/mol	>99.5:0.5

In addition to the Gibbs free energy comparison of the lowest-lying transition states, Distortion–Interaction Analysis of the final single point energies was conducted[298]:

Table 4.5 Distortion–Interaction analysis between **TS-1**, **TS-2**, and **TS-2b** at the DLPNO-CCSD(T)/cc-pVTZ//PBE-D3(BJ)def2-SVP level of theory. Positive values: favored in **TS-1**, negative values: favored in **TS-2** or **TS-2b**.

Component	ΔE(SP), TS-2 – TS-1	ΔE(SP), TS-2b – TS-1
total	1.7 kcal/mol	4.4 kcal/mol
IM + H	–1.5 kcal/mol	–0.8 kcal/mol
P	1.1 kcal/mol	–1.1 kcal/mol
distortion	–0.4 kcal/mol	–1.8 kcal/mol
interaction	2.1 kcal/mol	6.2 kcal/mol

Table 4.5 shows that the substrates in **TS-1** undergo a significant amount of distortion, most likely due to maximized electrostatic interactions of the iminium to the phosphate fragment. However, the phosphate in **TS-2** experiences a higher degree of distortion, which might be related to the increased dispersion

interactions. For further discussion, please see the LED calculations (Table 4.9, Table 4.10). The comparison between **TS-1** and **TS-2b** highlights the dominance of interaction as a stereodetermining element. Not only are electrostatic interactions due to an unfavorable orientation of the iminium in **TS-2b** expected to contribute to this observation, but further dispersion interactions between the fragments as well.

d. 2006 System: Local Energy Decomposition

In order to calculate the interaction between the three fragments within the system, we chose to perform a Local Energy Decomposition analysis at the DLPNO-CCSD(T)/cc-pVTZ level of theory for **TS-1**, **TS-2** and **TS-2b**.[201,204–209,297]

The resulting terms, corresponding to the decomposition of the HF interaction energy as well as the correlation interaction energy, can be found below. The sum of the individual elements is given at the top left corner of each matrix. The overall non-dispersion fragment interaction was calculated by adding the non-dispersion correlation contribution to the sum of electrostatic E_{elstat} and exchange E_{exch} interactions. All energies are given in kcal/mol.

Table 4.6 Results of the LED analysis of **TS-1** at the DLPNO-CCSD(T)/cc-pVTZ level of theory.

Electronic Preparation and Binding Energy

−149.9	H	IM	P
H	584.6	−793.2	−204.8
IM	−	307.7	−163.1
P	−	−	118.9

Overall Non-Dispersion

−75.2	H	IM	P
H	565.5	−714.3	−169.7
IM	−	272.7	−140.6
P	−	−	111.1

Electrostatics

82.6	H	IM	P
H	565.5	−594.5	−144.3
IM	−	272.7	−127.9
P	−	−	111.1

Exchange

−157.8	H	IM	P
H	−	−119.8	−25.4
IM	−	−	−12.7
P	−	−	−

Dispersion

−78.5	H	IM	P
H	−	−35.1	−25.4
IM	−	−	−18.0
P	−	−	−

The non-dispersion correlation contribution was found to be 3.6 kcal/mol, resulting in a total $\Delta E_{\text{non-disp}}$ of –71.7 kcal/mol.

Table 4.7 Results of the LED analysis of **TS-2** at the DLPNO-CCSD(T)/cc-pVTZ level of theory.

Electronic Preparation and Binding Energy

–149.0	H	IM	P
H	590.1	–824.0	–177.3
IM	–	327.4	–177.4
P	–	–	112.1

Overall Non-Dispersion

–66.6	H	IM	P
H	571.2	–741.6	–144.4
IM	–	292.0	–148.0
P	–	–	104.3

Electrostatics

95.4	H	IM	P
H	571.2	–617.8	–122.4
IM	–	292.0	–131.9
P	–	–	104.3

Exchange

–162.0	H	IM	P
H	–	–123.8	–22.1
IM	–	–	–16.1
P	–	–	–

Dispersion

–85.1	H	IM	P
H	–	–37.4	–24.2
IM	–	–	–23.5
P	–	–	–

The non-dispersion correlation contribution was found to be 2.3 kcal/mol, resulting in a total $\Delta E_{\text{non-disp}}$ of –64.3 kcal/mol.

Table 4.8 Results of the LED analysis of **TS-2b** at the DLPNO-CCSD(T)/cc-pVTZ level of theory.

Electronic Preparation and Binding Energy

–142.2	H	IM	P
H	510.4	–678.4	–217.0
IM	–	261.2	–132.3
P	–	–	113.9

Overall Non-Dispersion

–69.1	H	IM	P
H	492.0	–602.4	–182.5
IM	–	229.9	–112.7
P	–	–	106.6

Electrostatics

79.0	H	IM	P
H	492.0	–490.6	–156.6
IM	–	229.9	–102.3
P	–	–	106.6

Exchange

–148.2	H	IM	P
H	–	–111.9	–25.9
IM	–	–	–10.4
P	–	–	–

Dispersion

–74.9	H	IM	P
H	–	–34.1	–24.7
IM	–	–	–16.2
P	–	–	–

The non-dispersion correlation contribution was found to be 2.1 kcal/mol, resulting in a total $\Delta E_{\text{non-disp}}$ of –67.0 kcal/mol.

Ultimately, we used the individual LED analyses of **TS-1**, **TS-2**, and **TS-2b** to calculate their corresponding difference.

Table 4.9 Difference of LED analyses between **TS-1** and **TS-2** at the DLPNO-CCSD(T)/cc-pVTZ level of theory. Positive values: favored in **TS-1**, negative values: favored in **TS-2**.

Electronic Preparation and Binding Energy

0.8	H	IM	P
H	5.5	−30.8	27.5
IM	–	19.7	−14.3
P	–	–	−6.8

Overall Non-Dispersion

8.6	H	IM	P
H	5.7	−27.3	25.2
IM	–	19.3	−7.4
P	–	–	−6.8

Electrostatics

12.8	H	IM	P
H	5.7	−23.3	21.9
IM	–	19.3	−4.0
P	–	–	−6.8

Exchange

−4.2	H	IM	P
H	–	−4.1	3.3
IM	–	–	−3.4
P	–	–	–

Dispersion

−6.6	H	IM	P
H	–	−2.3	1.1
IM	–	–	−5.5
P	–	–	–

Taking into account the individual non-dispersion correlation contributions, an overall difference in $\Delta E_{\text{non-disp}}$ between both transition states of 7.4 kcal/mol was obtained.

Table 4.10 Difference of LED analyses between **TS-1** and **TS-2b** at the DLPNO-CCSD(T)/cc-pVTZ level of theory. Positive values: favored in **TS-1**, negative values: favored in **TS-2b**.

Electronic Preparation and Binding Energy

7.6	H	IM	P
H	−74.2	114.8	−12.2
IM	–	−46.6	30.8
P	–	–	−5.0

Overall Non-Dispersion

6.1	H	IM	P
H	−73.5	111.8	−12.9
IM	–	−42.8	28.0
P	–	–	−4.5

Electrostatics

−3.6	H	IM	P
H	−73.5	104.0	−12.3
IM	–	−42.8	25.6
P	–	–	−4.5

Exchange

9.7	H	IM	P
H	–	7.9	−0.6
IM	–	–	2.4
P	–	–	–

Dispersion

3.5	H	IM	P
H	–	1.1	0.7
IM	–	–	1.8
P	–	–	–

Taking into account the individual non-dispersion correlation contributions, an overall difference in $\Delta E_{\text{non-disp}}$ between both transition states of 4.7 kcal/mol was obtained.

e. 2006 System: IGMH Analysis

An analysis according to the Independent Gradient Model based on Hirshfeld partition[210] was conducted with the Multiwfn program, version 3.8, using the B3LYP-D3(BJ)/def2-TZVPP densities.[211] Non-covalent interactions were subsequently plotted as an isosurface of δg^{inter} with an isovalue of 0.004. In a direct comparison, the atoms were colored by their respective $\delta G^{\text{atom}}(\%)$.

0% >6%

Figure 4.5 δg^{inter} isosurface (left) and color-coded atoms according to their contribution to the overall interfragment interaction $\delta G^{\text{atom}}(\%)$ for **TS-1**.

0% >6%

Figure 4.6 δg^{inter} isosurface (left) and color-coded atoms according to their contribution to the overall interfragment interaction $\delta G^{\text{atom}}(\%)$ for **TS-2**.

0% >6%

Figure 4.7 δg^{inter} isosurface (left) and color-coded atoms according to their contribution to the overall interfragment interaction $\delta G^{\text{atom}}(\%)$ for **TS-2b**

Visual inspection reveals three hotspots for non-covalent interaction: the isopropyl group of the Hantzsch ester, the methyl group of the Hantzsch ester, as well as the α-CH_2 group of the morpholine fragment. The following quantitative analysis was made based on the percentage contribution of the individual atoms $\delta G^{atom}(\%)$ of these groups to the overall interfragment interaction:

Table 4.11 Comparison of $\delta G^{atom}(\%)$ of the Hantzsch ester's isopropyl fragment between **TS-1**, **TS-2**, and **TS-2b**.

TS-1		TS-2		TS-2b	
#	$\delta G^{atom}(\%)$	#	$\delta G^{atom}(\%)$	#	$\delta G^{atom}(\%)$
62 (C)	1.15%	62 (C)	0.63%	62 (C)	1.43%
179 (H)	0.22%	179 (H)	0.26%	179 (H)	0.38%
178 (C)	4.28%	178 (C)	3.04%	178 (C)	5.20%
180 (H)	3.12%	180 (H)	2.97%	180 (H)	5.17%
181 (H)	4.37%	181 (H)	2.76%	181 (H)	2.16%
182 (H)	2.65%	182 (H)	1.32%	182 (H)	5.21%
174 (C)	1.87%	174 (C)	0.19%	174 (C)	2.30%
175 (H)	0.39%	175 (H)	0.23%	175 (H)	1.55%
176 (H)	2.94%	176 (H)	0.02%	176 (H)	3.28%
177 (H)	0.80%	177 (H)	0.07%	177 (H)	0.39%
Σ	**21.79%**	Σ	**11.49%**	Σ	**27.07%**

Table 4.12 Comparison of $\delta G^{atom}(\%)$ of the Hantzsch ester's methyl fragment between **TS-1**, **TS-2**, and **TS-2b**.

TS-1		TS-2		TS-2b	
#	$\delta G^{atom}(\%)$	#	$\delta G^{atom}(\%)$	#	$\delta G^{atom}(\%)$
63 (C)	5.92%	63 (C)	7.81%	63 (C)	6.16%
64 (H)	6.87%	64 (H)	5.04%	64 (H)	2.76%

65 (H)	2.54%	65 (H)	4.87%	65 (H)	4.13%
66 (H)	3.26%	66 (H)	6.96%	66 (H)	6.71%
Σ	**18.59%**	Σ	**24.68%**	Σ	**19.76%**

Table 4.13 Comparison of δG^{atom}(%) of the α-CH$_2$ morpholine fragment between **TS-1**, **TS-2**, and **TS-2b**.

TS-1		**TS-2**		**TS-2b**	
#	δG^{atom}(%)	#	δG^{atom}(%)	#	δG^{atom}(%)
21 (C)	3.17%	29 (C)	4.01%	21 (C)	3.78%
23 (H)	2.36%	30 (H)	3.98%	23 (H)	3.44%
24 (H)	3.90%	31 (H)	4.36%	24 (H)	3.66%
Σ	**9.43%**	Σ	**12.35%**	Σ	**11.88%**

Table 4.14 Comparison of δG^{atom}(%) of the iminium formyl CH fragment between **TS-1**, **TS-2**, and **TS-2b**.

TS-1		**TS-2**		**TS-2b**	
#	δG^{atom}(%)	#	δG^{atom}(%)	#	δG^{atom}(%)
20 (C)	2.41%	20 (C)	0.72%	20 (C)	0.64%
33 (H)	3.92%	33 (H)	0.10%	33 (H)	1.00%
Σ	**6.33%**	Σ	**0.82%**	Σ	**1.64%**

Table 4.15 Comparison of δG^{atom}(%) of the iminium α-CH fragment between **TS-1**, **TS-2**, and **TS-2b**.

TS-1		**TS-2**		**TS-2b**	
#	δG^{atom}(%)	#	δG^{atom}(%)	#	δG^{atom}(%)
32 (C)	0.77%	32 (C)	1.85%	32 (C)	0.10%
42 (H)	0.11%	42 (H)	3.05%	42 (H)	0.04%

Σ	0.88%	Σ	4.90%	Σ	0.14%

Table 4.16 Comparison of δG^{atom}(%) of the iminium β-CH$_3$ fragment between **TS-1**, **TS-2**, and **TS-2b**.

TS-1		TS-2		TS-2b	
#	δG^{atom}(%)	#	δG^{atom}(%)	#	δG^{atom}(%)
35 (C)	3.82%	35 (C)	0.09%	35 (C)	0.00%
36 (H)	2.13%	36 (H)	0.06%	36 (H)	0.00%
37 (H)	4.24%	37 (H)	0.01%	37 (H)	0.00%
38 (H)	3.17%	38 (H)	0.02%	38 (H)	0.00%
Σ	13.36%	Σ	0.18%	Σ	0.00%

Table 4.17 Comparison of δG^{atom}(%) of the iminium phenyl fragment between **TS-1**, **TS-2**, and **TS-2b**.

TS-1		TS-2		TS-2b	
#	δG^{atom}(%)	#	δG^{atom}(%)	#	δG^{atom}(%)
39 (C)	0.27%	39 (C)	1.03%	39 (C)	0.22%
40 (C)	0.03%	40 (C)	2.99%	40 (C)	1.06%
41 (C)	0.62%	41 (C)	0.31%	41 (C)	0.21%
43 (C)	0.17%	43 (C)	0.36%	43 (C)	0.91%
44 (C)	0.01%	44 (C)	3.76%	44 (C)	2.48%
45 (C)	0.02%	45 (C)	1.74%	45 (C)	2.40%
46 (H)	1.25%	46 (H)	0.04%	46 (H)	0.03%
47 (H)	0.11%	47 (H)	0.07%	47 (H)	0.49%
48 (H)	0.00%	48 (H)	1.31%	48 (H)	2.42%

49 (H)	0.01%	49 (H)	3.16%	49 (H)	0.65%
50 (H)	0.00%	50 (H)	4.24%	50 (H)	2.52%
Σ	**2.49%**	Σ	**19.01%**	Σ	**13.39%**

Table 4.18 Comparison of δG^{atom}(%) of the western 2-isopropyl fragment between **TS-1**, **TS-2**, and **TS-2b**.

TS-1		**TS-2**		**TS-2b**	
#	δG^{atom}(%)	#	δG^{atom}(%)	#	δG^{atom}(%)
133 (C)	0.63%	133 (C)	0.56%	133 (C)	0.63%
139 (H)	0.24%	139 (H)	0.29%	139 (H)	0.37%
134 (C)	2.87%	134 (C)	3.11%	134 (C)	2.42%
135 (H)	1.35%	135 (H)	3.89%	135 (H)	1.18%
136 (H)	1.56%	136 (H)	1.16%	136 (H)	1.55%
137 (H)	3.99%	137 (H)	2.27%	137 (H)	3.14%
138 (C)	0.10%	138 (C)	0.10%	138 (C)	0.10%
140 (H)	0.04%	140 (H)	0.01%	140 (H)	0.01%
141 (H)	0.01%	141 (H)	0.06%	141 (H)	0.05%
142 (H)	0.05%	142 (H)	0.04%	142 (H)	0.05%
Σ	**10.84%**	Σ	**11.49%**	Σ	**9.51%**

Table 4.19 Comparison of δG^{atom}(%) of the western 4-isopropyl fragment between **TS-1**, **TS-2**, and **TS-2b**.

TS-1		**TS-2**		**TS-2b**	
#	δG^{atom}(%)	#	δG^{atom}(%)	#	δG^{atom}(%)
153 (C)	1.19%	153 (C)	1.40%	153 (C)	1.41%
168 (H)	1.05%	168 (H)	1.55%	168 (H)	1.47%

#	$\delta G^{atom}(\%)$	#	$\delta G^{atom}(\%)$	#	$\delta G^{atom}(\%)$
163 (C)	2.37%	163 (C)	1.42%	163 (C)	2.11%
164 (H)	0.65%	164 (H)	2.10%	164 (H)	0.60%
165 (H)	0.94%	165 (H)	0.37%	165 (H)	0.51%
166 (H)	3.84%	166 (H)	0.28%	166 (H)	3.26%
167 (C)	0.13%	167 (C)	0.14%	167 (C)	0.16%
169 (H)	0.04%	169 (H)	0.04%	169 (H)	0.06%
170 (H)	0.04%	170 (H)	0.03%	170 (H)	0.04%
171 (H)	0.03%	171 (H)	0.05%	171 (H)	0.04%
Σ	**10.28%**	Σ	**7.38%**	Σ	**9.66%**

Table 4.20 Comparison of $\delta G^{atom}(\%)$ of the western 6-isopropyl fragment between **TS-1**, **TS-2**, and **TS-2b**.

TS-1		TS-2		TS-2b	
#	$\delta G^{atom}(\%)$	#	$\delta G^{atom}(\%)$	#	$\delta G^{atom}(\%)$
143 (C)	0.42%	143 (C)	0.16%	143 (C)	0.31%
149 (H)	0.09%	149 (H)	0.04%	149 (H)	0.07%
144 (C)	0.06%	144 (C)	0.02%	144 (C)	0.05%
145 (H)	0.04%	145 (H)	0.00%	145 (H)	0.03%
146 (H)	0.01%	146 (H)	0.01%	146 (H)	0.01%
147 (H)	0.01%	147 (H)	0.00%	147 (H)	0.01%
148 (C)	1.42%	148 (C)	0.48%	148 (C)	1.10%
150 (H)	1.22%	150 (H)	0.06%	150 (H)	0.84%
151 (H)	0.18%	151 (H)	0.82%	151 (H)	0.18%
152 (H)	1.68%	152 (H)	0.34%	152 (H)	1.56%
Σ	**5.14%**	Σ	**1.93%**	Σ	**4.16%**

Table 4.21 Comparison of $\delta G^{\text{atom}}(\%)$ of the eastern 2-isopropyl fragment between **TS-1**, **TS-2**, and **TS-2b**.

TS-1		TS-2		TS-2b	
#	$\delta G^{\text{atom}}(\%)$	#	$\delta G^{\text{atom}}(\%)$	#	$\delta G^{\text{atom}}(\%)$
104 (C)	0.32%	104 (C)	1.66%	104 (C)	0.42%
110 (H)	0.08%	110 (H)	1.74%	110 (H)	0.10%
105 (C)	1.73%	105 (C)	2.98%	105 (C)	2.13%
106 (H)	0.57%	106 (H)	2.56%	106 (H)	1.86%
107 (H)	0.42%	107 (H)	3.50%	107 (H)	0.48%
108 (H)	1.89%	108 (H)	0.39%	108 (H)	2.39%
109 (C)	0.06%	109 (C)	0.22%	109 (C)	0.07%
111 (H)	0.01%	111 (H)	0.04%	111 (H)	0.01%
112 (H)	0.02%	112 (H)	0.06%	112 (H)	0.02%
113 (H)	0.04%	113 (H)	0.14%	113 (H)	0.04%
Σ	5.14%	Σ	13.29%	Σ	7.51%

Table 4.22 Comparison of $\delta G^{\text{atom}}(\%)$ of the eastern 4-isopropyl fragment between **TS-1**, **TS-2**, and **TS-2b**.

TS-1		TS-2		TS-2b	
#	$\delta G^{\text{atom}}(\%)$	#	$\delta G^{\text{atom}}(\%)$	#	$\delta G^{\text{atom}}(\%)$
124 (C)	0.73%	124 (C)	0.49%	124 (C)	0.84%
159 (H)	0.37%	159 (H)	0.09%	159 (H)	0.42%
154 (C)	0.07%	154 (C)	0.08%	154 (C)	0.08%
155 (H)	0.02%	155 (H)	0.01%	155 (H)	0.02%
156 (H)	0.03%	156 (H)	0.01%	156 (H)	0.02%

157 (H)	0.01%	157 (H)	0.05%	157 (H)	0.03%
158 (C)	1.64%	158 (C)	1.16%	158 (C)	2.21%
160 (H)	0.80%	160 (H)	0.13%	160 (H)	0.45%
161 (H)	3.02%	161 (H)	1.29%	161 (H)	1.15%
162 (H)	0.30%	162 (H)	1.10%	162 (H)	3.94%
Σ	**6.99%**	Σ	**4.41%**	Σ	**9.16%**

Table 4.23 Comparison of $\delta G^{atom}(\%)$ of the eastern 6-isopropyl fragment between **TS-1**, **TS-2**, and **TS-2b**.

TS-1		TS-2		TS-2b	
#	$\delta G^{atom}(\%)$	#	$\delta G^{atom}(\%)$	#	$\delta G^{atom}(\%)$
114 (C)	0.87%	114 (C)	0.50%	114 (C)	0.66%
120 (H)	0.47%	120 (H)	0.23%	120 (H)	0.20%
115 (C)	2.15%	115 (C)	0.76%	115 (C)	1.85%
116 (H)	0.82%	116 (H)	1.46%	116 (H)	0.30%
117 (H)	0.54%	117 (H)	0.14%	117 (H)	1.12%
118 (H)	3.63%	118 (H)	0.22%	118 (H)	2.80%
119 (C)	0.09%	119 (C)	0.05%	119 (C)	0.08%
121 (H)	0.01%	121 (H)	0.01%	121 (H)	0.02%
122 (H)	0.03%	122 (H)	0.02%	122 (H)	0.01%
123 (H)	0.03%	123 (H)	0.01%	123 (H)	0.05%
Σ	**8.64%**	Σ	**3.40%**	Σ	**7.09%**

f. 2006 System: Activation Energies

In order to investigate the activation energy computationally, we optimized the structure of the pre-transition state complex (**1d2a4a**).
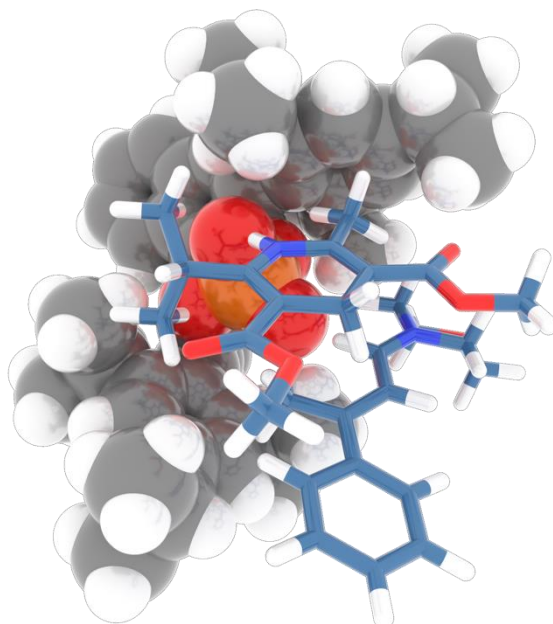
Figure 4.8 Structure of the pre-transition state complex **1d2a4a**, obtained by relaxation of **TS-1**

Table 4.24 Obtained thermochemical corrections at the PBE-D3(BJ)/def2-SVP level (323 K, 1 M) as well as single point energies for the pre-transition state complex **1d2a4a**; Gibbs free energies were calculated with respect to **TS-1**.

TC 1.380282790774	E^{SP} / a.u.	$\Delta\Delta G$(323 K)
B3LYP-D3(BJ)/def2-TZVPP	–4117.81165	10.1 kcal/mol
B3LYP/def2-TZVPP	–4117.29809	12.1 kcal/mol
ωB97M-V/def2-TZVPP	–4118.27199	12.7 kcal/mol

We additionally conducted an IGMH analysis with the B3LYP-D3(BJ)/def2-TZVPP densities.

0% ▮▮▮▮▮▮▮▮ >6%
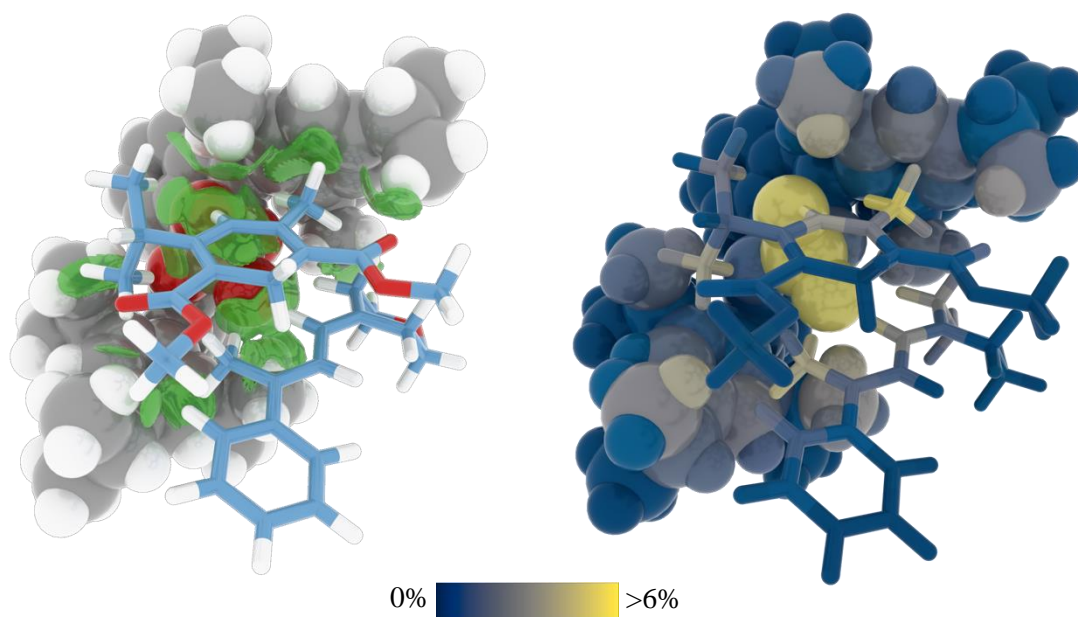
Figure 4.9 δg^{inter} isosurface (left) and color-coded atoms according to their contribution to the overall interfragment interaction $\delta G^{atom}(\%)$ for pre-transition state complex **1d2a4a**.

Table 4.25 Comparison of $\delta G^{atom}(\%)$ of the Hantzsch ester's isopropyl fragment between **1d2a4a** and **TS-1**.

1d2a4a		TS-2	
#	$\delta G^{atom}(\%)$	#	$\delta G^{atom}(\%)$
62 (C)	1.04%	62 (C)	1.15%
179 (H)	0.19%	179 (H)	0.22%
178 (C)	3.79%	178 (C)	4.28%
180 (H)	2.68%	180 (H)	3.12%
181 (H)	4.02%	181 (H)	4.37%
182 (H)	2.32%	182 (H)	2.65%
174 (C)	1.88%	174 (C)	1.87%
175 (H)	0.38%	175 (H)	0.39%
176 (H)	2.98%	176 (H)	2.94%

177 (H)	0.87%	177 (H)	0.80%
Σ	**20.15%**	Σ	**21.79%**

Table 4.26 Comparison of δG^{atom}(%) of the Hantzsch ester's methyl fragment between **1d2a4a** and **TS-1**.

1d2a4a		TS-1	
#	δG^{atom}(%)	#	δG^{atom}(%)
63 (C)	5.90%	63 (C)	5.92%
64 (H)	3.55%	64 (H)	6.87%
65 (H)	6.69%	65 (H)	2.54%
66 (H)	2.52%	66 (H)	3.26%
Σ	**18.66%**	Σ	**18.59%**

Table 4.27 Comparison of δG^{atom}(%) of the α-CH$_2$ morpholine fragment between **1d2a4a** and **TS-1**.

1d2a4a		TS-1	
#	δG^{atom}(%)	#	δG^{atom}(%)
21 (C)	3.03%	21 (C)	3.17%
23 (H)	1.96%	23 (H)	2.36%
24 (H)	3.96%	24 (H)	3.90%
Σ	**8.95%**	Σ	**9.43%**

Table 4.28 Comparison of $\delta G^{atom}(\%)$ of the iminium phenyl fragment between **1d2a4a** and **TS-1**.

1d2a4a		TS-1	
#	$\delta G^{atom}(\%)$	#	$\delta G^{atom}(\%)$
39 (C)	0.49%	39 (C)	0.49%
40 (C)	0.12%	40 (C)	0.12%
41 (C)	0.95%	41 (C)	0.95%
43 (C)	0.34%	43 (C)	0.34%
44 (C)	0.03%	44 (C)	0.03%
45 (C)	0.05%	45 (C)	0.05%
46 (H)	1.46%	46 (H)	1.46%
47 (H)	0.21%	47 (H)	0.21%
48 (H)	0.01%	48 (H)	0.01%
49 (H)	0.05%	49 (H)	0.05%
50 (H)	0.00%	50 (H)	0.00%
Σ	**3.71%**	Σ	**3.71%**

Table 4.29 Comparison of $\delta G^{atom}(\%)$ of the western 2-isopropyl fragment between **1d2a4a** and **TS-1**.

1d2a4a		TS-1	
#	$\delta G^{atom}(\%)$	#	$\delta G^{atom}(\%)$
133 (C)	0.57%	133 (C)	0.63%
139 (H)	0.19%	139 (H)	0.24%
134 (C)	3.00%	134 (C)	2.87%
135 (H)	1.25%	135 (H)	1.35%
136 (H)	2.02%	136 (H)	1.56%

137 (H)	3.79%	137 (H)	3.99%
138 (C)	0.10%	138 (C)	0.10%
140 (H)	0.04%	140 (H)	0.04%
141 (H)	0.01%	141 (H)	0.01%
142 (H)	0.06%	142 (H)	0.05%
Σ	**11.03%**	Σ	**10.84%**

Table 4.30 Comparison of δG^{atom}(%) of the western 4-isopropyl fragment between **1d2a4a** and **TS-1**.

1d2a4a		TS-1	
#	δG^{atom}(%)	#	δG^{atom}(%)
153 (C)	1.38%	153 (C)	1.19%
168 (H)	1.23%	168 (H)	1.05%
163 (C)	2.36%	163 (C)	2.37%
164 (H)	0.69%	164 (H)	0.65%
165 (H)	0.72%	165 (H)	0.94%
166 (H)	3.86%	166 (H)	3.84%
167 (C)	0.14%	167 (C)	0.13%
169 (H)	0.04%	169 (H)	0.04%
170 (H)	0.04%	170 (H)	0.04%
171 (H)	0.05%	171 (H)	0.03%
Σ	**10.51%**	Σ	**10.28%**

Table 4.31 Comparison of $\delta G^{\text{atom}}(\%)$ of the western 6-isopropyl fragment between **1d2a4a** and **TS-1**.

1d2a4a		TS-1	
#	$\delta G^{\text{atom}}(\%)$	#	$\delta G^{\text{atom}}(\%)$
143 (C)	0.37%	143 (C)	0.42%
149 (H)	0.08%	149 (H)	0.09%
144 (C)	0.05%	144 (C)	0.06%
145 (H)	0.03%	145 (H)	0.04%
146 (H)	0.01%	146 (H)	0.01%
147 (H)	0.01%	147 (H)	0.01%
148 (C)	1.38%	148 (C)	1.42%
150 (H)	0.18%	150 (H)	1.22%
151 (H)	1.73%	151 (H)	0.18%
152 (H)	1.17%	152 (H)	1.68%
Σ	**5.01%**	Σ	**5.14%**

Table 4.32 Comparison of $\delta G^{\text{atom}}(\%)$ of the eastern 2-isopropyl fragment between **1d2a4a** and **TS-1**.

1d2a4a		TS-1	
#	$\delta G^{\text{atom}}(\%)$	#	$\delta G^{\text{atom}}(\%)$
104 (C)	0.30%	104 (C)	0.32%
110 (H)	0.07%	110 (H)	0.08%
105 (C)	1.63%	105 (C)	1.73%
106 (H)	1.55%	106 (H)	0.57%
107 (H)	0.40%	107 (H)	0.42%
108 (H)	1.71%	108 (H)	1.89%

109 (C)	0.06%	109 (C)	0.06%
111 (H)	0.01%	111 (H)	0.01%
112 (H)	0.02%	112 (H)	0.02%
113 (H)	0.04%	113 (H)	0.04%
Σ	**5.79%**	Σ	**5.14%**

Table 4.33 Comparison of δG^{atom}(%) of the eastern 4-isopropyl fragment between **1d2a4a** and **TS-1**.

1d2a4a		TS-1	
#	δG^{atom}(%)	#	δG^{atom}(%)
124 (C)	0.70%	124 (C)	0.73%
159 (H)	0.36%	159 (H)	0.37%
154 (C)	0.06%	154 (C)	0.07%
155 (H)	0.01%	155 (H)	0.02%
156 (H)	0.01%	156 (H)	0.03%
157 (H)	0.02%	157 (H)	0.01%
158 (C)	1.60%	158 (C)	1.64%
160 (H)	0.73%	160 (H)	0.80%
161 (H)	3.00%	161 (H)	3.02%
162 (H)	0.28%	162 (H)	0.30%
Σ	**6.77%**	Σ	**6.99%**

Table 4.34 Comparison of $\delta G^{atom}(\%)$ of the eastern 6-isopropyl fragment between **1d2a4a** and **TS-1**.

1d2a4a		TS-1	
#	$\delta G^{atom}(\%)$	#	$\delta G^{atom}(\%)$
114 (C)	0.91%	114 (C)	0.87%
120 (H)	0.52%	120 (H)	0.47%
115 (C)	2.33%	115 (C)	2.15%
116 (H)	1.00%	116 (H)	0.82%
117 (H)	0.55%	117 (H)	0.54%
118 (H)	3.87%	118 (H)	3.63%
119 (C)	0.10%	119 (C)	0.09%
121 (H)	0.03%	121 (H)	0.01%
122 (H)	0.03%	122 (H)	0.03%
123 (H)	0.02%	123 (H)	0.03%
Σ	**9.36%**	Σ	**8.64%**
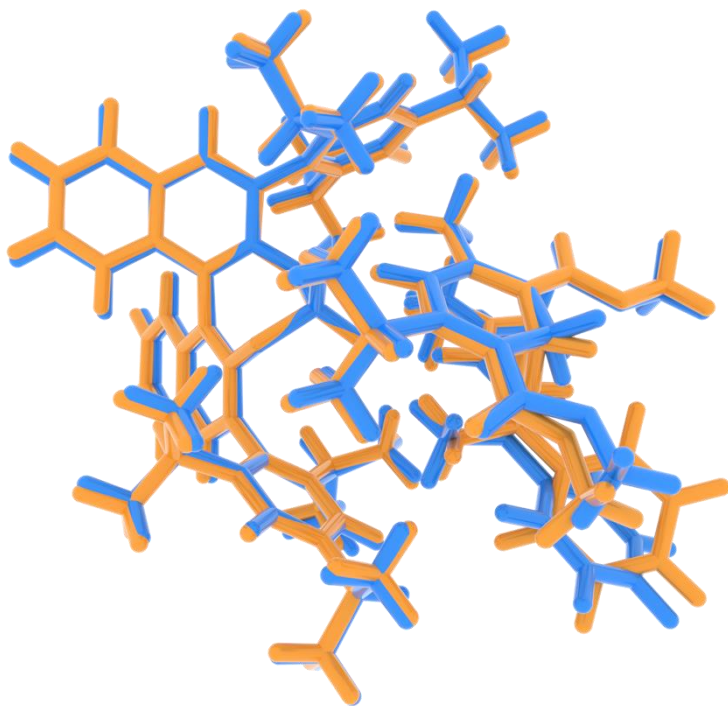
Figure 4.10 Structural comparison between **1d2a4a** (blue) and **TS-1** (orange).

Structural comparison of **1d2a4a** and **TS-1** indicates no observable qualitative differences.

g. Improved System: Transition State Overview
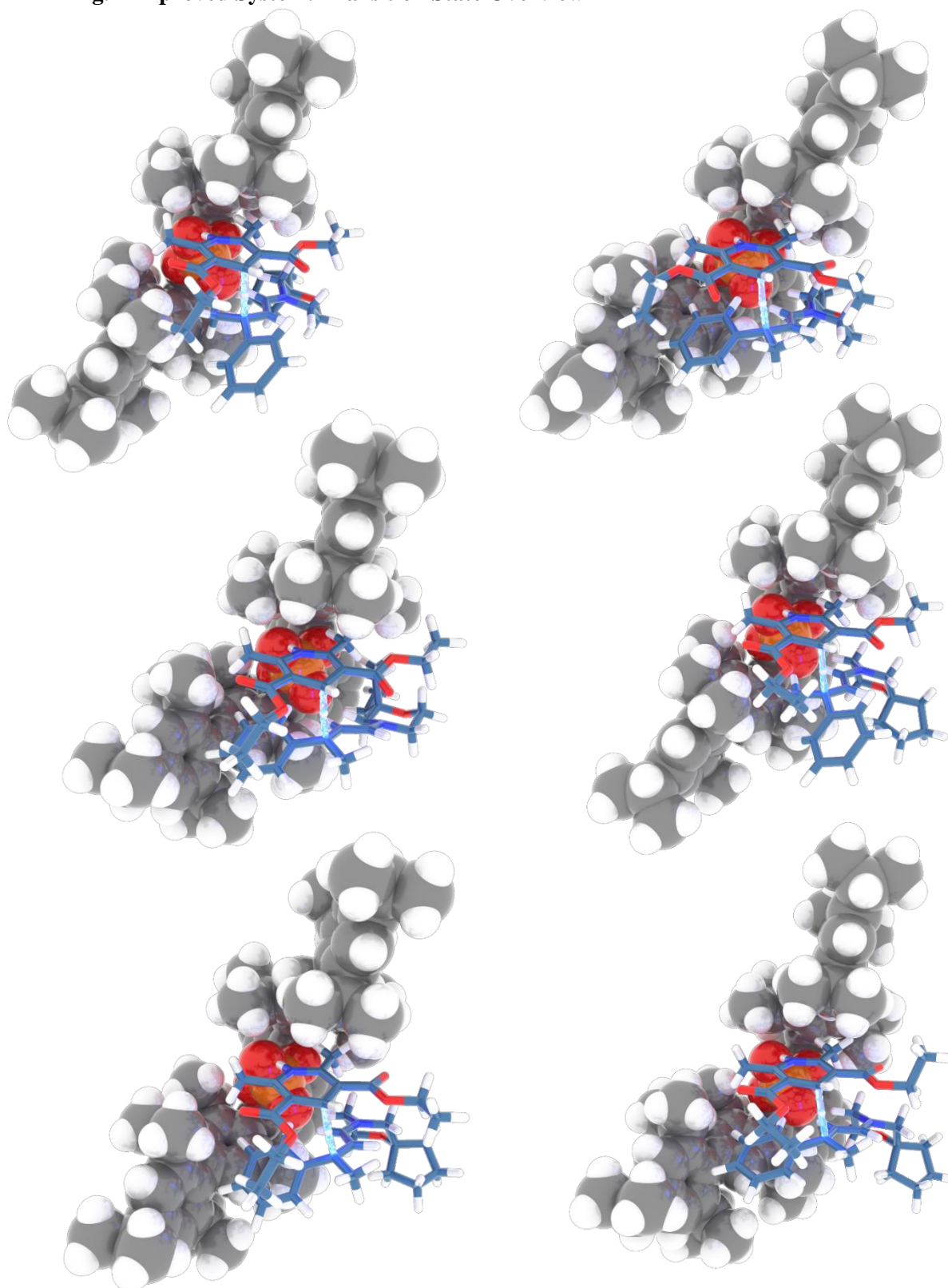
Figure 4.11 Structural overview of **TS-3** (top left), **TS-4** (top right), **TS-4b** (middle left), **TS-3b** (middle right), **TS-4c** (bottom left), and **TS-4d** (bottom right).

h. Improved System: Distortion–Interaction Analysis

Table 4.35 Overview of the transition states at the CPCM(1,4-dioxane)-DLPNO-CCSD(T)/cc-pVTZ//PBE-D3(BJ)def2-SVP level of theory as well as computed enantiomeric ratios at 323 K.

	$\Delta\Delta G^{\ddagger}$ (323 K)	Computed er (323 K)
TS-3	0.0 kcal/mol	–
TS-4	2.2 kcal/mol	97:3
TS-4b	2.5 kcal/mol	98:2
TS-3b	3.7 kcal/mol	>99:1
TS-4c	5.8 kcal/mol	>99:1
TS-4d	6.1 kcal/mol	>99:1

In analogy to the 2006 system, we could also locate transition states leading to the minor enantiomer similar to **TS-2** (**TS-4b** and **TS-4d**). However, it appears as though the extended size of the phosphate (**53**) stabilizes both phenyl fragments of the iminium ion in **TS-4** and **TS-4b** (and **TS-4c** and **TS-4d**, respectively) to a similar extent, eventually resulting in an energetic preference of **TS-4** over **TS-4b** (and **TS-4c** and **TS-4d**, respectively; please also see the LED calculations).

In addition to the Gibbs free energy comparison of the lowest-lying transition states, Distortion–Interaction Analysis[298] of the final single point energies was conducted:

Table 4.36 Distortion–Interaction analysis between **TS-3**, **TS-4**, and **TS-4b** at the DLPNO-CCSD(T)/cc-pVTZ//PBE-D3(BJ)def2-SVP level of theory. Positive values: favored in **TS-3**, negative values: favored in **TS-4** or **TS-4b**.

Component	ΔE(SP), TS-4 −TS-3	ΔE(SP), TS-4b − TS-3
total	0.6 kcal/mol	2.1 kcal/mol
IM + H	–1.3 kcal/mol	–1.7 kcal/mol
P	3.0 kcal/mol	4.2 kcal/mol

distortion	1.7 kcal/mol	2.5 kcal/mol
interaction	–1.1 kcal/mol	–0.4 kcal/mol

As has already been discussed for **TS-1** vs **TS-2** (Table 4.5), the same arguments are valid for the improved system (catalyst distorted in the minor transition state to maximize London dispersion interactions leading to a lack of electrostatic interactions). Whereas interaction was found the driving force in the DIA between **TS-1** and **TS-2**, we now find distortion to be the main contributor for stereodifferentiation. It is plausible that, in order to maximize the London dispersion interactions, the phosphate anion in **TS-4** adapts a higher-energy conformation.

Table 4.37 Distortion–Interaction analysis between **TS-3b**, **TS-4c**, and **TS-4d** at the DLPNO-CCSD(T)/cc-pVTZ//PBE-D3(BJ)def2-SVP level of theory. Positive values: favored in **TS-3**, negative values: favored in **TS-4** or **TS-4b**.

Component	ΔE(SP), TS-4c –TS-3b	ΔE(SP), TS-4d – TS-3b
total	0.6 kcal/mol	1.4 kcal/mol
IM + H	–0.2 kcal/mol	–0.6 kcal/mol
P	2.6 kcal/mol	3.9 kcal/mol
distortion	2.4 kcal/mol	3.3 kcal/mol
interaction	–1.7 kcal/mol	–1.9 kcal/mol

For the sake of completeness, the same analysis was conducted for the three transition states corresponding to an *exo*-orientation of the spiro fragment (Table 4.37).

i. Improved System: Local Energy Decomposition

In order to calculate the interaction between the three fragments within the system, we chose to perform a Local Energy Decomposition analysis at the DLPNO-CCSD(T)/cc-pVTZ level of theory for all transition states.[201,204–209,297]

The resulting terms, corresponding to the decomposition of the HF interaction energy as well as the correlation interaction energy, can be found below. The sum of the individual elements is given at the top

left corner of each matrix. The overall non-dispersion fragment interaction was calculated by adding the non-dispersion correlation contribution to the sum of electrostatic E_{elstat} and exchange E_{exch} interactions. All energies are given in kcal/mol.

Table 4.38 Results of the LED analysis of **TS-3** at the DLPNO-CCSD(T)/cc-pVTZ level of theory.

Electronic Preparation and Binding Energy

−157.8	H	IM	P
H	587.9	−769.9	−207.3
IM	−	322.9	−198.5
P	−	−	134.1

Overall Non-Dispersion

−66.7	H	IM	P
H	568.8	−717.7	−166.8
IM	−	286.3	−162.1
P	−	−	124.8

Electrostatics

97.0	H	IM	P
H	568.8	−599.3	−140.5
IM	−	286.3	−143.1
P	−	−	124.8

Exchange

−163.7	H	IM	P
H	−	−118.4	−26.3
IM	−	−	−19.0
P	−	−	−

Dispersion

−95.8	H	IM	P
H	−	−36.0	−30.4
IM	−	−	−29.4
P	−	−	−

The non-dispersion correlation contribution was found to be 4.2 kcal/mol, resulting in a total $\Delta E_{non\text{-}disp}$ of −62.6 kcal/mol.

Table 4.39 Results of the LED analysis of **TS-4** at the DLPNO-CCSD(T)/cc-pVTZ level of theory.

Electronic Preparation and Binding Energy

−161.9	H	IM	P
H	577.7	−800.1	−202.6
IM	−	335.0	−208.9
P	−	−	136.9

Overall Non-Dispersion

−63.7	H	IM	P
H	557.9	−717.0	−164.0
IM	−	297.5	−165.2
P	−	−	127.1

Electrostatics

106.3	H	IM	P
H	557.9	−594.5	−138.2
IM	−	297.5	−143.5
P	−	−	127.1

Exchange

−170.0	H	IM	P
H	−	−122.5	−25.9
IM	−	−	−21.7
P	−	−	−

Dispersion

−102.7	H	IM	P
H	−	−38.3	−28.7
IM	−	−	−35.6
P	−	−	−

The non-dispersion correlation contribution was found to be 4.0 kcal/mol, resulting in a total $\Delta E_{non\text{-}disp}$ of −59.7 kcal/mol.

Table 4.40 Results of the LED analysis of **TS-4b** at the DLPNO-CCSD(T)/cc-pVTZ level of theory.

Electronic Preparation and Binding Energy

−155.2	H	IM	P
H	501.4	−680.7	−196.7
IM	–	298.4	−211.4
P	–	–	133.8

Overall Non-Dispersion

−56.6	H	IM	P
H	483.7	−604.3	−158.3
IM	–	264.1	−165.6
P	–	–	123.8

Electrostatics

102.4	H	IM	P
H	483.7	−493.1	−133.2
IM	–	264.1	−143.0
P	–	–	123.8

Exchange

−158.9	H	IM	P
H	–	−111.2	−25.1
IM	–	–	−22.6
P	–	–	–

Dispersion

−101.5	H	IM	P
H	–	−35.5	−28.7
IM	–	–	−37.2
P	–	–	–

The non-dispersion correlation contribution was found to be 2.5 kcal/mol, resulting in a total $\Delta E_{\text{non-disp}}$ of −54.1 kcal/mol.

Table 4.41 Results of the LED analysis of **TS-3b** at the DLPNO-CCSD(T)/cc-pVTZ level of theory.

Electronic Preparation and Binding Energy

−149.4	H	IM	P
H	572.1	−782.7	−202.6
IM	–	310.8	−168.6
P	–	–	121.5

Overall Non-Dispersion

−69.6	H	IM	P
H	553.0	−703.7	−162.3
IM	–	275.3	−145.6
P	–	–	113.3

Electrostatics

88.6	H	IM	P
H	553.0	−584.9	−136.1
IM	–	275.3	−132.1
P	–	–	113.3

Exchange

−158.5	H	IM	P
H	–	−118.8	−26.2
IM	–	–	−13.5
P	–	–	–

Dispersion

−84.2	H	IM	P
H	–	−35.6	−30.3
IM	–	–	−18.3
P	–	–	–

The non-dispersion correlation contribution was found to be 4.2 kcal/mol, resulting in a total $\Delta E_{\text{non-disp}}$ of −65.7 kcal/mol.

Table 4.42 Results of the LED analysis of **TS-4c** at the DLPNO-CCSD(T)/cc-pVTZ level of theory.

Electronic Preparation and Binding Energy

−150.6	H	IM	P
H	543.5	−748.2	−196.0
IM	−	311.6	−188.6
P	−	−	127.0

Overall Non-Dispersion

−61.6	H	IM	P
H	525.1	−667.9	−157.5
IM	−	276.2	−155.4
P	−	−	118.0

Electrostatics

100.5	H	IM	P
H	525.1	−549.1	−132.1
IM	−	276.2	−137.6
P	−	−	118.0

Exchange

−162.1	H	IM	P
H	−	−118.9	−25.5
IM	−	−	−17.8
P	−	−	−

Dispersion

−92.0	H	IM	P
H	−	−36.8	−28.7
IM	−	−	−26.6
P	−	−	−

The non-dispersion correlation contribution was found to be 2.9 kcal/mol, resulting in a total $\Delta E_{\text{non-disp}}$ of −58.8 kcal/mol.

Table 4.43 Results of the LED analysis of **TS-4d** at the DLPNO-CCSD(T)/cc-pVTZ level of theory

Electronic Preparation and Binding Energy

−149.8	H	IM	P
H	556.2	−766.1	−192.9
IM	−	318.2	−192.0
P	−	−	126.7

Overall Non-Dispersion

−58.9	H	IM	P
H	538.0	−685.8	−154.8
IM	−	283.0	−156.8
P	−	−	117.5

Electrostatics

105.2	H	IM	P
H	538.0	−565.5	−129.8
IM	−	283.0	−138.0
P	−	−	117.5

Exchange

−164.1	H	IM	P
H	−	−120.3	−25.0
IM	−	−	−18.8
P	−	−	−

Dispersion

−93.0	H	IM	P
H	−	−36.4	−28.4
IM	−	−	−28.2
P	−	−	−

The non-dispersion correlation contribution was found to be 1.9 kcal/mol, resulting in a total $\Delta E_{\text{non-disp}}$ of −57.0 kcal/mol.

Table 4.44 Difference of LED analyses between **TS-3** and **TS-4** at the DLPNO-CCSD(T)/cc-pVTZ level of theory. Positive values: favored in **TS-3**, negative values: favored in **TS-4**.

Electronic Preparation and Binding Energy

−4.1	H	IM	P
H	−10.2	−3.2	4.7
IM	–	12.1	−10.4
P	–	–	2.9

Overall Non-Dispersion

3.0	H	IM	P
H	−10.9	0.7	2.7
IM	–	11.2	−3.1
P	–	–	2.3

Electrostatics

9.4	H	IM	P
H	−10.9	4.8	2.3
IM	–	11.2	−0.4
P	–	–	2.3

Exchange

−6.3	H	IM	P
H	–	−4.1	0.4
IM	–	–	−2.7
P	–	–	–

Dispersion

−6.9	H	IM	P
H	–	−2.3	1.7
IM	–	–	−6.3
P	–	–	–

Taking into account the individual non-dispersion correlation contributions, an overall difference in $\Delta E_{\text{non-disp}}$ between both transition states of 2.9 kcal/mol was obtained.

Table 4.45 Difference of LED analyses between **TS-3** and **TS-4b** at the DLPNO-CCSD(T)/cc-pVTZ level of theory. Positive values: favored in **TS-3**, negative values: favored in **TS-4b**.

Electronic Preparation and Binding Energy

2.7	H	IM	P
H	−86.6	116.2	10.6
IM	–	−24.5	−12.9
P	–	–	−0.3

Overall Non-Dispersion

10.2	H	IM	P
H	−85.0	113.4	8.5
IM	–	−22.2	−3.5
P	–	–	−1.0

Electrostatics

5.4	H	IM	P
H	−85.0	106.2	7.3
IM	–	−22.2	0.1
P	–	–	−1.0

Exchange

4.8	H	IM	P
H	–	7.2	1.2
IM	–	–	−3.6
P	–	–	–

Dispersion

−5.7	H	IM	P
H	–	0.5	1.7
IM	–	–	−7.9
P	–	–	–

Taking into account the individual non-dispersion correlation contributions, an overall difference in $\Delta E_{\text{non-disp}}$ between both transition states of 8.5 kcal/mol was obtained.

Table 4.46 Difference of LED analyses between **TS-3b** and **TS-4c** at the DLPNO-CCSD(T)/cc-pVTZ level of theory. Positive values: favored in **TS-3b**, negative values: favored in **TS-4c**.

Electronic Preparation and Binding Energy

−1.2	H	IM	P
H	−28.6	34.5	6.6
IM	−	0.8	−20.0
P	−	−	5.5

Overall Non-Dispersion

8.3	H	IM	P
H	−27.9	35.7	4.7
IM	−	0.9	−9.7
P	−	−	4.6

Electrostatics

11.9	H	IM	P
H	−27.9	35.8	4.0
IM	−	0.9	−5.5
P	−	−	4.6

Exchange

−3.6	H	IM	P
H	−	−0.1	0.7
IM	−	−	−4.3
P	−	−	−

Dispersion

−7.9	H	IM	P
H	−	−1.1	1.7
IM	−	−	−8.4
P	−	−	−

Taking into account the individual non-dispersion correlation contributions, an overall difference in $\Delta E_{\text{non-disp}}$ between both transition states of 6.9 kcal/mol was obtained.

Table 4.47 Difference of LED analyses between **TS-3b** and **TS-4d** at the DLPNO-CCSD(T)/cc-pVTZ level of theory. Positive values: favored in **TS-3b**, negative values: favored in **TS-4d**.

Electronic Preparation and Binding Energy

−0.4	H	IM	P
H	−16.0	16.6	9.7
IM	−	7.4	−23.4
P	−	−	5.3

Overall Non-Dispersion

11.0	H	IM	P
H	−15.0	17.9	7.5
IM	−	7.7	−11.2
P	−	−	4.2

Electrostatics

16.6	H	IM	P
H	−15.0	19.4	6.3
IM	−	7.7	−5.9
P	−	−	4.2

Exchange

−5.6	H	IM	P
H	−	−1.5	1.2
IM	−	−	−5.3
P	−	−	−

Dispersion

−8.8	H	IM	P
H	−	−0.8	1.9
IM	−	−	−9.9
P	−	−	−

Taking into account the individual non-dispersion correlation contributions, an overall difference in $\Delta E_{\text{non-disp}}$ between both transition states of 8.7 kcal/mol was obtained.

j. Improved System: IGMH Analysis

An analysis according to the Independent Gradient Model based on Hirshfeld partition[210] was conducted with the Multiwfn program, version 3.8, using the B3LYP-D3(BJ)/def2-TZVPP densities.[211,212] Non-covalent interactions were subsequently plotted as an isosurface of δg^{inter} with an isovalue of 0.004. In a direct comparison, the atoms were colored by their respective $\delta G^{\text{atom}}(\%)$.

0%   >5%
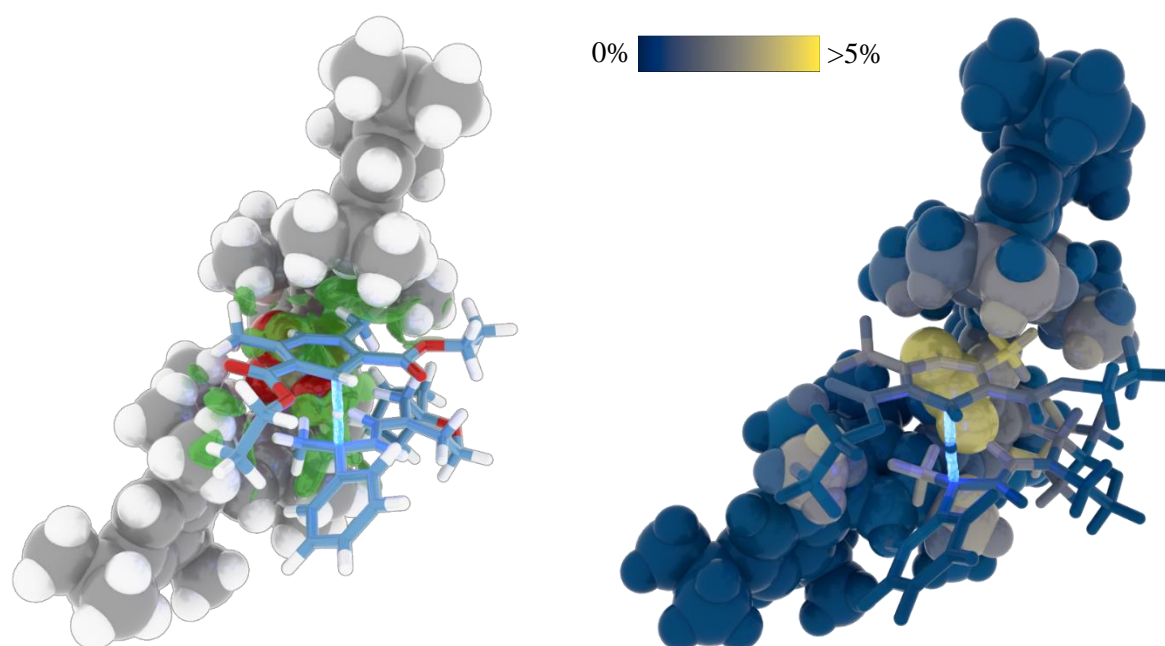
Figure 4.12 δg^{inter} isosurface (left) and color-coded atoms according to their contribution to the overall interfragment interaction $\delta G^{\text{atom}}(\%)$ for **TS-3**.
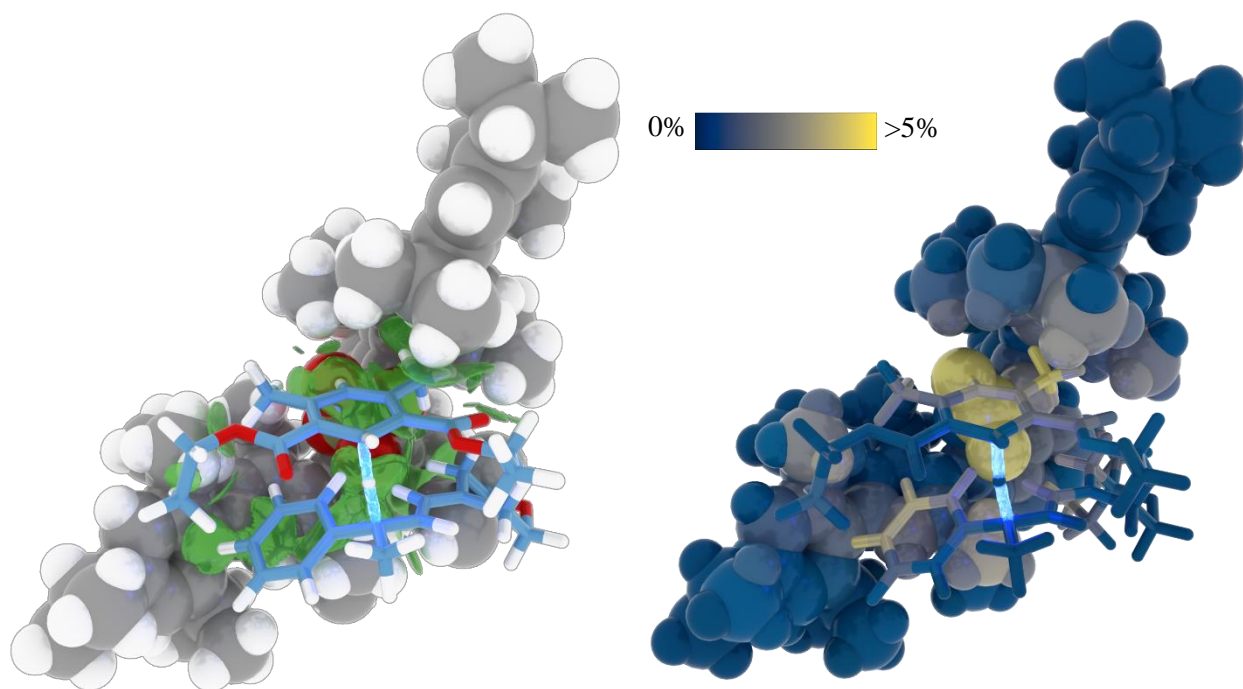
Figure 4.13 δg^{inter} isosurface (left) and color-coded atoms according to their contribution to the overall interfragment interaction $\delta G^{\text{atom}}(\%)$ for **TS-4**.
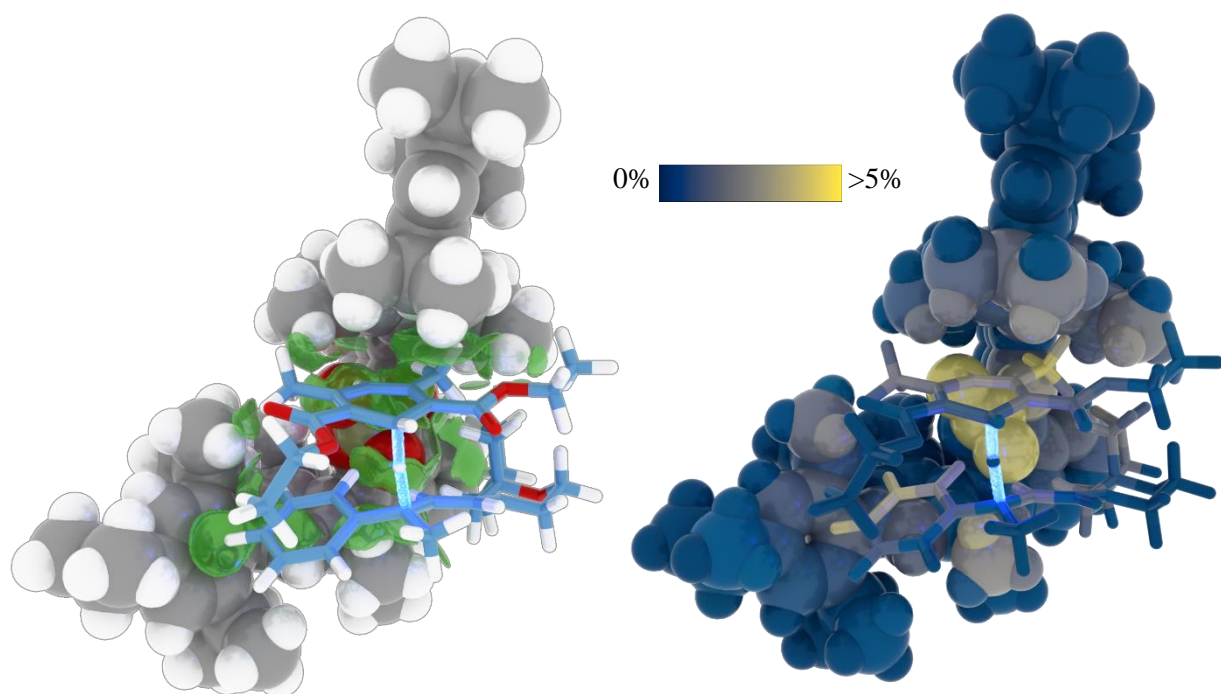
Figure 4.14 δg^{inter} isosurface (left) and color-coded atoms according to their contribution to the overall interfragment interaction $\delta G^{\text{atom}}(\%)$ for **TS-4b**
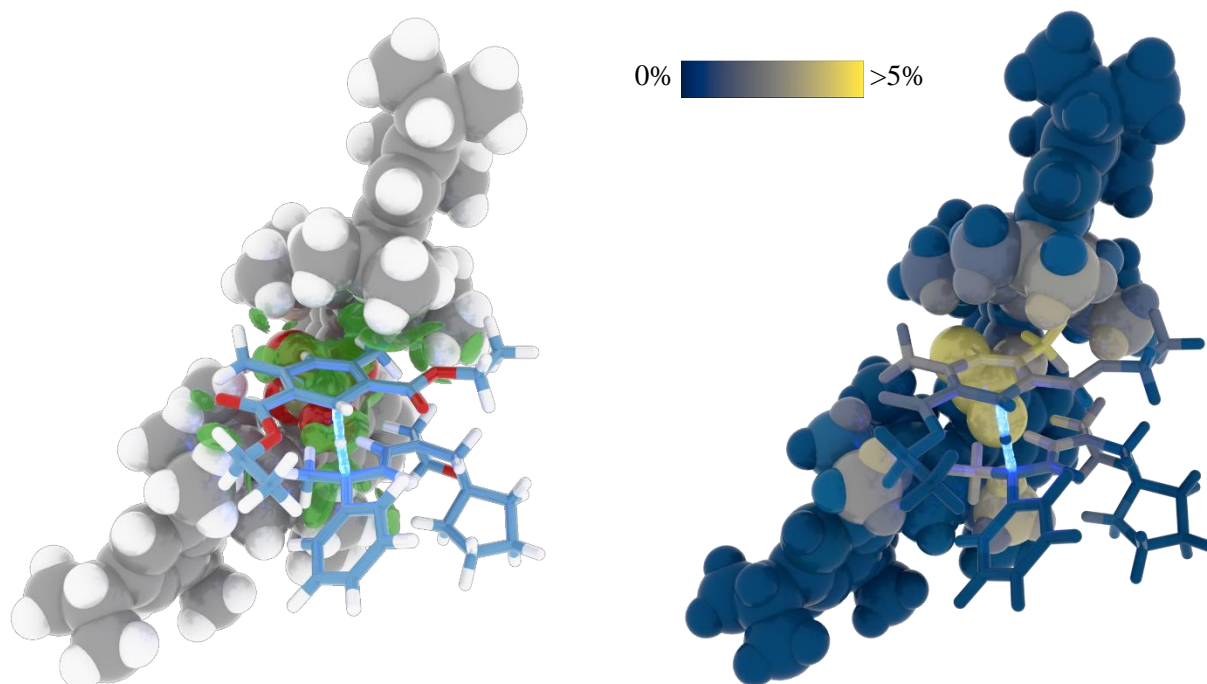
Figure 4.15 δg^{inter} isosurface (left) and color-coded atoms according to their contribution to the overall interfragment interaction $\delta G^{atom}(\%)$ for **TS-3b**.
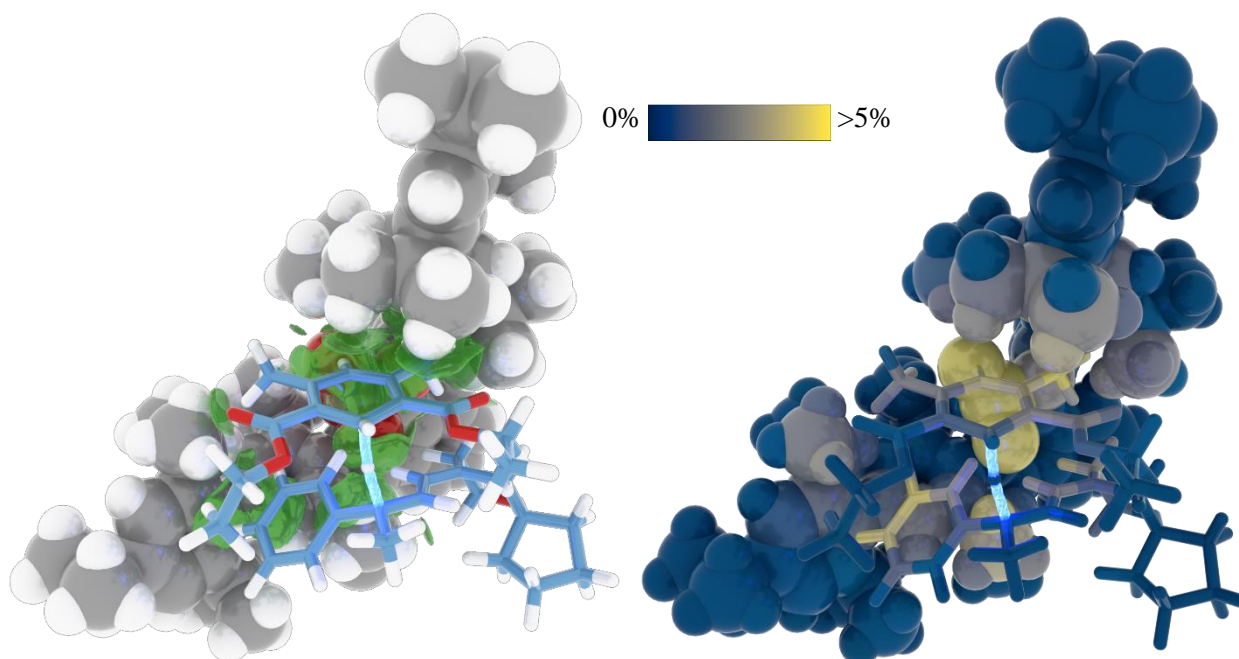
Figure 4.16 δg^{inter} isosurface (left) and color-coded atoms according to their contribution to the overall interfragment interaction $\delta G^{atom}(\%)$ for **TS-4c**.
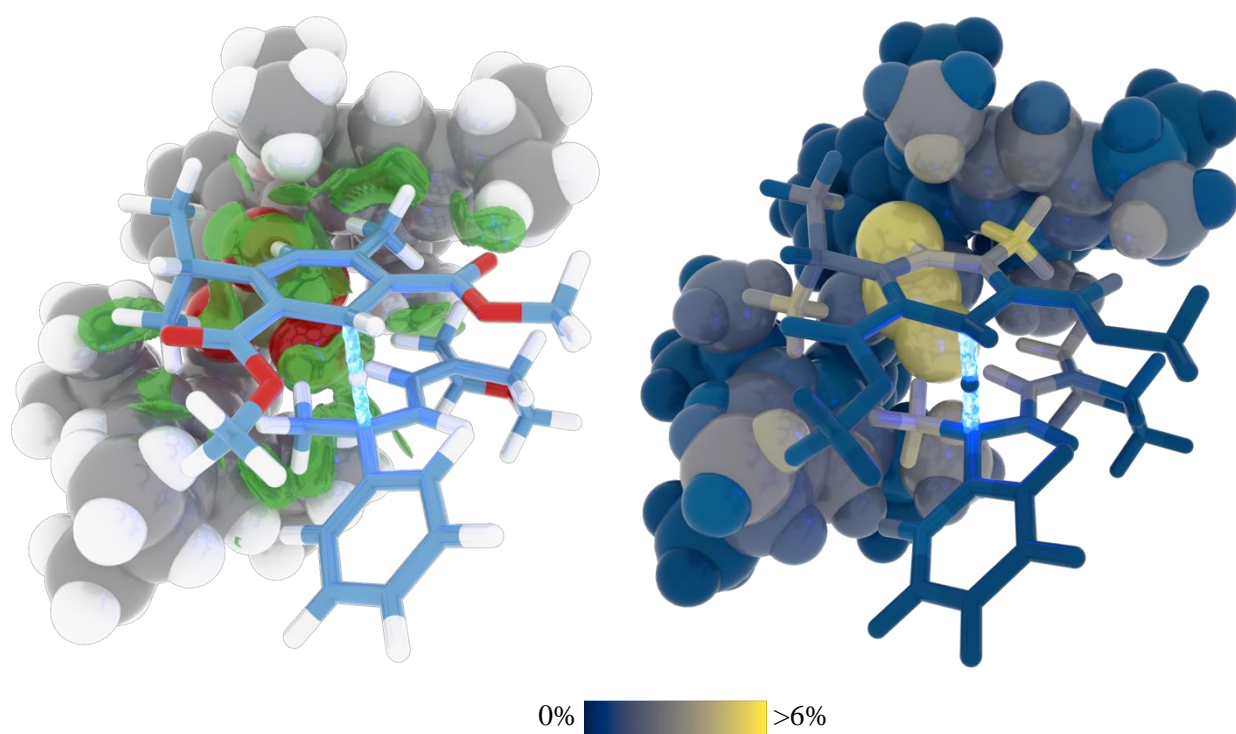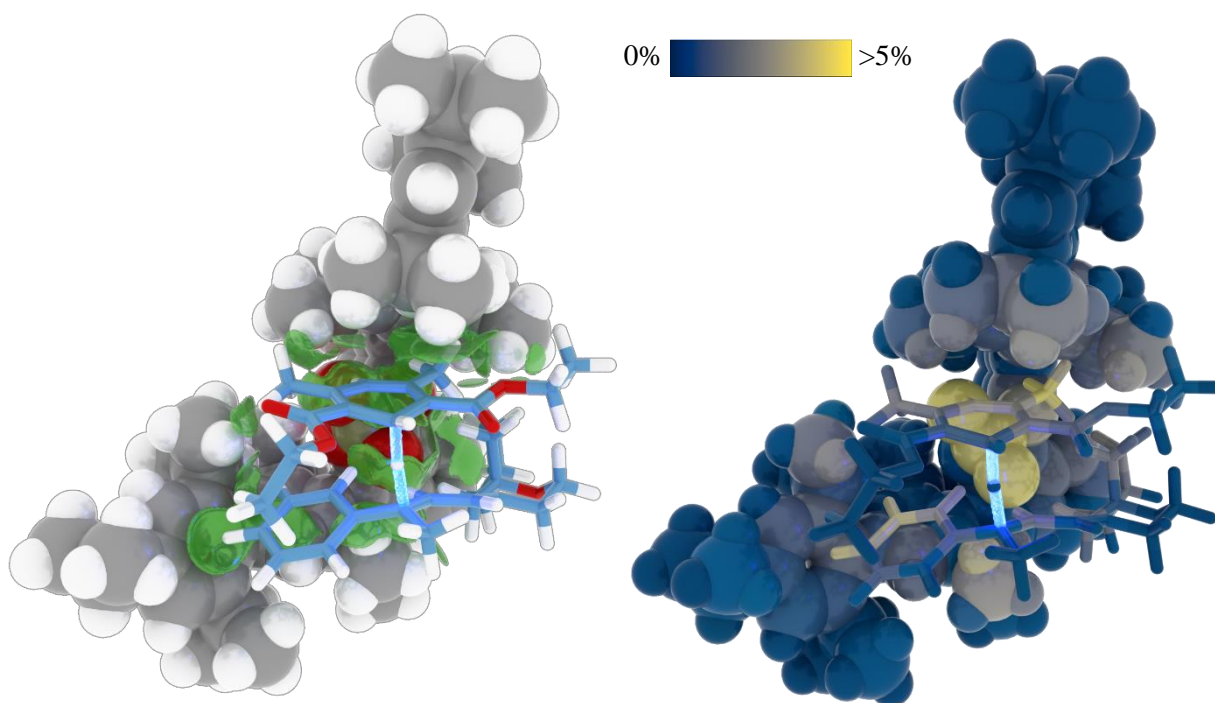
Figure 4.17 δg^{inter} isosurface (left) and color-coded atoms according to their contribution to the overall interfragment interaction $\delta G^{\text{atom}}(\%)$ for **TS-4d**.
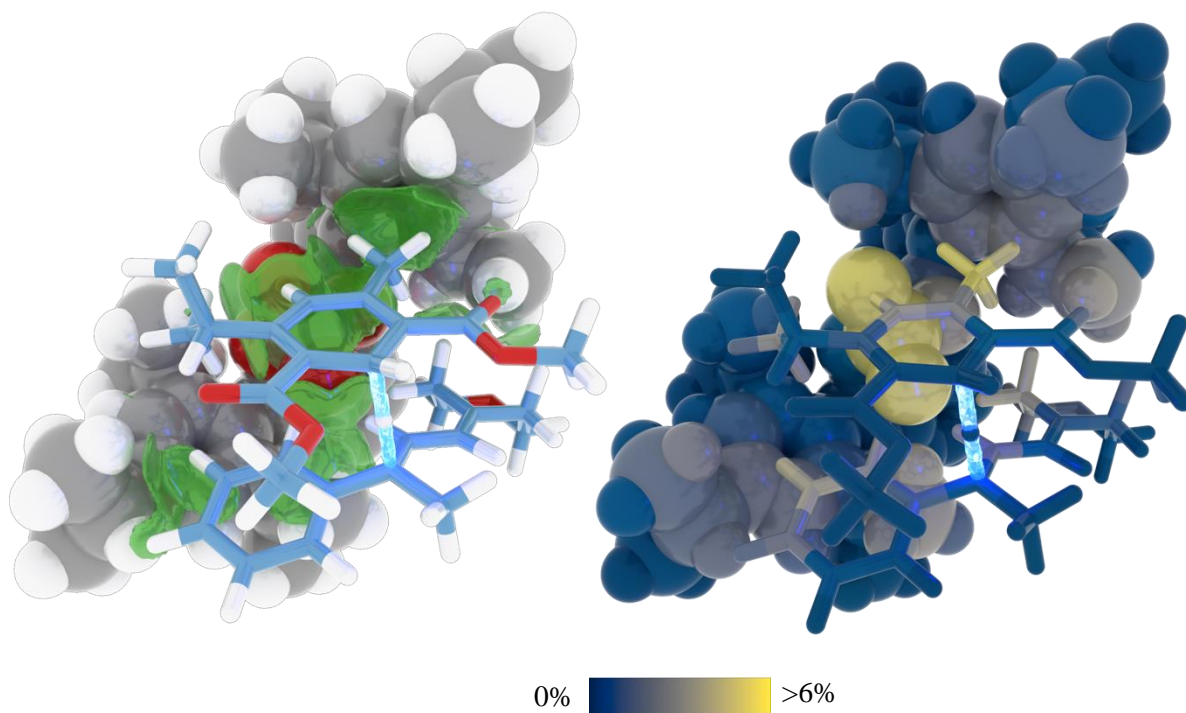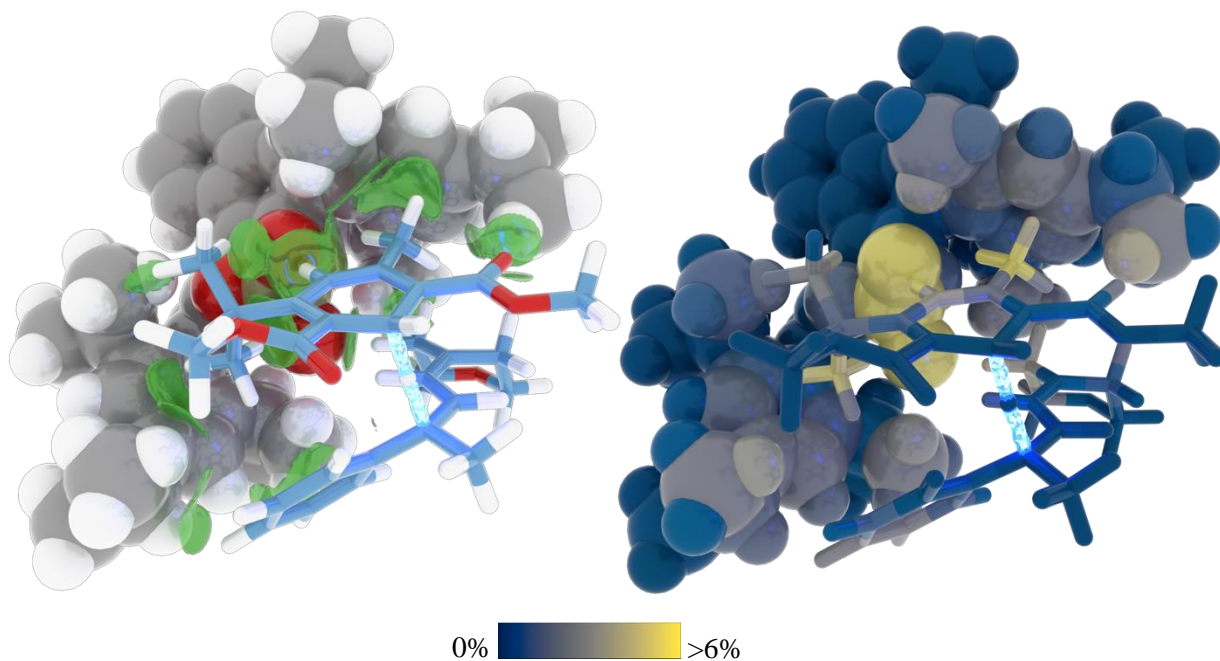
Visual inspection reveals three hotspots for non-covalent interaction: the two methyl groups of the Hantzsch ester, the α-CH$_2$ group, as well as the spirocyclopentane ring of the morpholine fragment. The following quantitative analysis was made based on the percentage contribution of the individual atoms $\delta G^{\text{atom}}(\%)$ of these groups to the overall interfragment interaction:

Table 4.48 Comparison of $\delta G^{\text{atom}}(\%)$ of the Hantzsch ester's western methyl fragment between **TS-3**, **TS-4**, and **TS-4b**.

TS-3		TS-4		TS-4b	
#	$\delta G^{\text{atom}}(\%)$	#	$\delta G^{\text{atom}}(\%)$	#	$\delta G^{\text{atom}}(\%)$
58 (C)	2.06%	59 (C)	1.76%	59 (C)	2.08%
59 (H)	1.95%	60 (H)	1.82%	60 (H)	0.88%
60 (H)	1.07%	61 (H)	0.51%	61 (H)	2.30%
61 (H)	1.19%	62 (H)	1.58%	62 (H)	1.08%
Σ	**6.27%**	Σ	**5.67%**	Σ	**6.34%**

Table 4.49 Comparison of δG^{atom}(%) of the Hantzsch ester's eastern methyl fragment between **TS-3**, **TS-4**, and **TS-4b**.

TS-3		TS-4		TS-4b	
#	δG^{atom}(%)	#	δG^{atom}(%)	#	δG^{atom}(%)
62 (C)	5.85%	63 (C)	5.89%	63 (C)	5.16%
63 (H)	2.36%	64 (H)	3.17%	64 (H)	3.54%
64 (H)	3.53%	65 (H)	2.94%	65 (H)	5.41%
65 (H)	6.03%	66 (H)	6.05%	66 (H)	1.74%
Σ	**17.07%**	Σ	**18.05%**	Σ	**15.85%**

Table 4.50 Comparison of δG^{atom}(%) of the α-CH₂ morpholine fragment between **TS-3**, **TS-4**, and **TS-4b**.

TS-3		TS-4		TS-4b	
#	δG^{atom}(%)	#	δG^{atom}(%)	#	δG^{atom}(%)
21 (C)	1.51%	29 (C)	1.83%	29 (C)	1.65%
23 (H)	1.01%	30 (H)	1.43%	30 (H)	2.66%
24 (H)	2.34%	31 (H)	2.81%	31 (H)	1.05%
Σ	**4.86%**	Σ	**5.36%**	Σ	**6.07%**

Table 4.51 Comparison of δG^{atom}(%) of the spiro-cyclopentane morpholine fragment between **TS-3**, **TS-4**, and **TS-4b**.

TS-3		TS-4		TS-4b	
#	δG^{atom}(%)	#	δG^{atom}(%)	#	δG^{atom}(%)
238 (C)	1.26%	233 (C)	1.24%	233 (C)	2.12%
247 (H)	1.71%	239 (H)	0.54%	239 (H)	1.19%
248 (H)	0.25%	240 (H)	1.81%	240 (H)	2.73%
242 (C)	3.74%	238 (C)	1.81%	238 (C)	2.32%

245 (H)	2.67%	241 (H)	0.35%	241 (H)	0.99%
246 (H)	4.33%	242 (H)	2.76%	242 (H)	3.01%
239 (C)	2.74%	235 (C)	2.85%	235 (C)	1.60%
243 (H)	1.75%	243 (H)	3.59%	243 (H)	2.45%
244 (H)	3.11%	244 (H)	1.72%	244 (H)	0.21%
237 (C)	0.88%	234 (C)	1.12%	234 (C)	1.42%
240 (H)	0.15%	236 (H)	1.51%	236 (H)	2.26%
241 (H)	1.29%	237 (H)	0.20%	237 (H)	0.42%
Σ	**23.88%**	Σ	**19.50%**	Σ	**20.72%**

Table 4.52 Comparison of δG^{atom}(%) of the iminium formyl CH fragment between **TS-3**, **TS-4**, and **TS-4b**.

TS-3		**TS-4**		**TS-4b**	
#	δG^{atom}(%)	#	δG^{atom}(%)	#	δG^{atom}(%)
20 (C)	1.97%	20 (C)	1.31%	20 (C)	0.45%
31 (H)	2.96%	248 (H)	2.23%	248 (H)	0.05%
Σ	**4.93%**	Σ	**3.54%**	Σ	**0.50%**

Table 4.53 Comparison of δG^{atom}(%) of the iminium α-CH fragment between **TS-3**, **TS-4**, and **TS-4b**.

TS-3		**TS-4**		**TS-4b**	
#	δG^{atom}(%)	#	δG^{atom}(%)	#	δG^{atom}(%)
30 (C)	0.72%	32 (C)	0.34%	32 (C)	1.42%
40 (H)	0.10%	41 (H)	0.04%	41 (H)	2.30%
Σ	**0.82%**	Σ	**0.38%**	Σ	**3.72%**

Table 4.54 Comparison of $\delta G^{atom}(\%)$ of the iminium β-CH$_3$ fragment between **TS-3**, **TS-4**, and **TS-4b**.

TS-3		TS-4		TS-4b	
#	$\delta G^{atom}(\%)$	#	$\delta G^{atom}(\%)$	#	$\delta G^{atom}(\%)$
33 (C)	2.74%	34 (C)	0.03%	34 (C)	0.09%
34 (H)	2.04%	35 (H)	0.01%	35 (H)	0.06%
35 (H)	2.43%	36 (H)	0.01%	36 (H)	0.01%
36 (H)	2.27%	37 (H)	0.01%	37 (H)	0.02%
Σ	**9.48%**	Σ	**0.06%**	Σ	**0.18%**

Table 4.55 Comparison of $\delta G^{atom}(\%)$ of the iminium phenyl fragment between **TS-3**, **TS-4**, and **TS-4b**.

TS-3		TS-4		TS-4b	
#	$\delta G^{atom}(\%)$	#	$\delta G^{atom}(\%)$	#	$\delta G^{atom}(\%)$
37 (C)	0.27%	38 (C)	0.71%	38 (C)	1.01%
38 (C)	0.51%	39 (C)	2.30%	39 (C)	2.58%
42 (C)	0.14%	43 (C)	3.96%	43 (C)	3.99%
43 (C)	0.02%	44 (C)	3.72%	44 (C)	3.35%
41 (C)	0.01%	42 (C)	1.01%	42 (C)	0.92%
39 (C)	0.04%	40 (C)	0.40%	40 (C)	0.44%
47 (H)	0.73%	48 (H)	1.93%	48 (H)	2.27%
48 (H)	0.07%	49 (H)	3.27%	49 (H)	3.80%
46 (H)	0.00%	47 (H)	4.36%	47 (H)	3.95%
45 (H)	0.00%	46 (H)	0.49%	46 (H)	0.42%
44 (H)	0.01%	45 (H)	0.06%	45 (H)	0.07%
Σ	**1.80%**	Σ	**22.21%**	Σ	**22.80%**

Table 4.56 Comparison of $\delta G^{atom}(\%)$ of the western 2-isopropyl fragment (first arene) between **TS-3**, **TS-4**, and **TS-4b**.

TS-3		TS-4		TS-4b	
#	$\delta G^{atom}(\%)$	#	$\delta G^{atom}(\%)$	#	$\delta G^{atom}(\%)$
140 (C)	1.11%	141 (C)	1.22%	141 (C)	1.05%
146 (H)	1.56%	147 (H)	3.05%	147 (H)	2.69%
141 (C)	2.91%	142 (C)	3.48%	142 (C)	3.86%
142 (H)	3.60%	143 (H)	1.67%	143 (H)	1.67%
143 (H)	1.80%	144 (H)	1.59%	144 (H)	0.66%
144 (H)	1.10%	145 (H)	0.33%	145 (H)	40.26%
145 (C)	0.25%	146 (C)	1.63%	146 (C)	1.35%
147 (H)	0.06%	245 (H)	0.25%	245 (H)	0.09%
148 (H)	0.05%	246 (H)	0.09%	246 (H)	0.04%
149 (H)	0.18%	247 (H)	7.00%	247 (H)	0.22%
Σ	**12.62%**	Σ	**20.31%**	Σ	**11.89%**

Table 4.57 Comparison of $\delta G^{atom}(\%)$ of the western 6-isopropyl fragment (first arene) between **TS-3**, **TS-4**, and **TS-4b**.

TS-3		TS-4		TS-4b	
#	$\delta G^{atom}(\%)$	#	$\delta G^{atom}(\%)$	#	$\delta G^{atom}(\%)$
150 (C)	0.02%	148 (C)	0.02%	148 (C)	0.01%
156 (H)	0.01%	154 (H)	0.00%	154 (H)	0.00%
151 (C)	0.00%	149 (C)	0.00%	149 (C)	0.00%
152 (H)	0.00%	150 (H)	0.00%	150 (H)	0.00%
153 (H)	0.00%	151 (H)	0.00%	151 (H)	0.00%

154 (H)	0.00%	152 (H)	0.03%	152 (H)	0.01%
155 (C)	0.04%	153 (C)	0.01%	153 (C)	0.01%
157 (H)	0.02%	155 (H)	0.00%	155 (H)	0.00%
158 (H)	0.01%	156 (H)	0.08%	156 (H)	0.02%
159 (H)	0.12%	157 (H)	0.02%	157 (H)	0.01%
Σ	**0.22%**	Σ	**0.16%**	Σ	**0.06%**

Table 4.58 Comparison of δG^{atom}(%) of the western 2-isopropyl fragment (second arene) between **TS-3**, **TS-4**, and **TS-4b**.

TS-3		TS-4		TS-4b	
#	δG^{atom}(%)	#	δG^{atom}(%)	#	δG^{atom}(%)
205 (C)	0.00%	203 (C)	0.14%	203 (C)	0.17%
211 (H)	0.00%	209 (H)	0.01%	209 (H)	0.02%
206 (C)	0.00%	204 (C)	0.00%	204 (C)	0.01%
207 (H)	0.00%	205 (H)	0.00%	205 (H)	0.00%
208 (H)	0.00%	206 (H)	0.00%	206 (H)	0.00%
209 (H)	0.00%	207 (H)	0.16%	207 (H)	0.28%
210 (C)	0.00%	208 (C)	0.06%	208 (C)	0.06%
212 (H)	0.00%	210 (H)	0.01%	210 (H)	0.02%
213 (H)	0.00%	211 (H)	0.06%	211 (H)	0.12%
214 (H)	0.01%	212 (H)	0.29%	212 (H)	0.49%
Σ	**0.01%**	Σ	**0.73%**	Σ	**1.17%**

Table 4.59 Comparison of $\delta G^{\text{atom}}(\%)$ of the western 4-isopropyl fragment (second arene) between **TS-3**, **TS-4**, and **TS-4b**.

TS-3		TS-4		TS-4b	
#	$\delta G^{\text{atom}}(\%)$	#	$\delta G^{\text{atom}}(\%)$	#	$\delta G^{\text{atom}}(\%)$
225 (C)	0.00%	223 (C)	0.13%	223 (C)	0.20%
231 (H)	0.00%	229 (H)	0.40%	229 (H)	0.03%
226 (C)	0.00%	224 (C)	0.27%	224 (C)	0.02%
227 (H)	0.00%	225 (H)	0.07%	225 (H)	0.00%
228 (H)	0.00%	226 (H)	0.71%	226 (H)	0.01%
229 (H)	0.00%	227 (H)	0.02%	227 (H)	0.38%
230 (C)	1.00%	228 (C)	0.04%	228 (C)	0.05%
232 (H)	0.01%	230 (H)	0.00%	230 (H)	0.51%
233 (H)	0.00%	231 (H)	0.00%	231 (H)	0.04%
234 (H)	0.02%	232 (H)	0.01%	232 (H)	0.27%
Σ	**1.03%**	Σ	**1.65%**	Σ	**1.51%**

Table 4.60 Comparison of $\delta G^{\text{atom}}(\%)$ of the western 6-isopropyl fragment (second arene) between **TS-3**, **TS-4**, and **TS-4b**.

TS-3		TS-4		TS-4b	
#	$\delta G^{\text{atom}}(\%)$	#	$\delta G^{\text{atom}}(\%)$	#	$\delta G^{\text{atom}}(\%)$
215 (C)	0.93%	213 (C)	0.86%	213 (C)	0.78%
221 (H)	1.02%	219 (H)	2.02%	219 (H)	1.43%
216 (C)	2.60%	214 (C)	1.03%	214 (C)	0.62%
217 (H)	0.73%	215 (H)	3.04%	215 (H)	2.29%
218 (H)	3.30%	216 (H)	0.52%	216 (H)	0.25%

219 (H)	2.00%	217 (H)	0.10%	217 (H)	0.08%
220 (C)	0.56%	218 (C)	0.64%	218 (C)	0.54%
222 (H)	0.12%	220 (H)	0.03%	220 (H)	0.02%
223 (H)	1.00%	221 (H)	0.02%	221 (H)	0.02%
224 (H)	0.11%	222 (H)	0.04%	222 (H)	0.03%
Σ	**12.37%**	Σ	**8.30%**	Σ	**6.06%**

Table 4.61 Comparison of δG^{atom}(%) of the eastern 2-isopropyl fragment (first arene) between **TS-3**, **TS-4**, and **TS-4b**.

TS-3		TS-4		TS-4b	
#	δG^{atom}(%)	#	δG^{atom}(%)	#	δG^{atom}(%)
111 (C)	0.86%	112 (C)	0.91%	112 (C)	1.16%
117 (H)	0.74%	118 (H)	1.44%	118 (H)	2.03%
112 (C)	2.04%	113 (C)	2.02%	113 (C)	0.49%
113 (H)	0.68%	114 (H)	0.21%	114 (H)	1.15%
114 (H)	1.10%	115 (H)	0.92%	115 (H)	2.74%
115 (H)	2.92%	116 (H)	0.12%	116 (H)	0.18%
116 (C)	0.12%	117 (C)	0.90%	117 (C)	1.28%
118 (H)	0.02%	119 (H)	0.02%	119 (H)	0.11%
119 (H)	0.06%	120 (H)	0.03%	120 (H)	0.04%
120 (H)	0.03%	121 (H)	0.07%	121 (H)	0.05%
Σ	**8.57%**	Σ	**6.64%**	Σ	**9.23%**

Table 4.62 Comparison of $\delta G^{\text{atom}}(\%)$ of the eastern 6-isopropyl fragment (first arene) between **TS-3**, **TS-4**, and **TS-4b**.

TS-3		TS-4		TS-4b	
#	$\delta G^{\text{atom}}(\%)$	#	$\delta G^{\text{atom}}(\%)$	#	$\delta G^{\text{atom}}(\%)$
121 (C)	0.41%	122 (C)	0.45%	122 (C)	0.40%
127 (H)	0.24%	128 (H)	0.76%	128 (H)	0.86%
122 (C)	0.81%	123 (C)	1.43%	123 (C)	1.68%
123 (H)	0.24%	124 (H)	0.21%	124 (H)	0.26%
124 (H)	0.19%	125 (H)	0.15%	125 (H)	0.20%
125 (H)	1.58%	126 (H)	0.04%	126 (H)	0.03%
126 (C)	0.04%	127 (C)	0.26%	127 (C)	0.25%
128 (H)	0.01%	129 (H)	0.01%	129 (H)	0.01%
129 (H)	0.01%	130 (H)	0.01%	130 (H)	0.01%
130 (H)	0.01%	131 (H)	0.01%	131 (H)	0.01%
Σ	**3.54%**	Σ	**3.33%**	Σ	**3.71%**

Table 4.63 Comparison of $\delta G^{\text{atom}}(\%)$ of the eastern 2-isopropyl fragment (second arene) between **TS-3**, **TS-4**, and **TS-4b**.

TS-3		TS-4		TS-4b	
#	$\delta G^{\text{atom}}(\%)$	#	$\delta G^{\text{atom}}(\%)$	#	$\delta G^{\text{atom}}(\%)$
170 (C)	0.01%	168 (C)	0.01%	168 (C)	0.01%
176 (H)	0.01%	174 (H)	0.00%	174 (H)	0.00%
171 (C)	0.00%	169 (C)	0.00%	169 (C)	0.00%
172 (H)	0.00%	170 (H)	0.00%	170 (H)	0.00%
173 (H)	0.00%	171 (H)	0.00%	171 (H)	0.00%

174 (H)	0.00%	172 (H)	0.00%	172 (H)	0.00%
175 (C)	0.00%	173 (C)	0.01%	173 (C)	0.01%
177 (H)	0.00%	175 (H)	0.00%	175 (H)	0.01%
178 (H)	0.01%	176 (H)	0.00%	176 (H)	0.00%
179 (H)	0.00%	177 (H)	0.01%	177 (H)	0.00%
Σ	**0.03%**	Σ	**0.03%**	Σ	**0.03%**

Table 4.64 Comparison of δG^{atom}(%) of the eastern 4-isopropyl fragment (second arene) between **TS-3**, **TS-4**, and **TS-4b**.

TS-3		**TS-4**		**TS-4b**	
#	δG^{atom}(%)	#	δG^{atom}(%)	#	δG^{atom}(%)
190 (C)	0.00%	188 (C)	0.00%	188 (C)	0.00%
196 (H)	0.00%	194 (H)	0.00%	194 (H)	0.00%
191 (C)	0.00%	189 (C)	0.00%	189 (C)	0.00%
192 (H)	0.00%	190 (H)	0.00%	190 (H)	0.00%
193 (H)	0.00%	191 (H)	0.00%	191 (H)	0.00%
194 (H)	0.00%	192 (H)	0.00%	192 (H)	0.00%
195 (C)	0.00%	193 (C)	0.00%	193 (C)	0.00%
197 (H)	0.00%	195 (H)	0.00%	195 (H)	0.00%
198 (H)	0.00%	196 (H)	0.00%	196 (H)	0.00%
199 (H)	0.00%	197 (H)	0.00%	197 (H)	0.00%
Σ	**0.00%**	Σ	**0.00%**	Σ	**0.00%**

Table 4.65 Comparison of $\delta G^{atom}(\%)$ of the eastern 6-isopropyl fragment (second arene) between **TS-3**, **TS-4**, and **TS-4b**.

TS-3		TS-4		TS-4b	
#	$\delta G^{atom}(\%)$	#	$\delta G^{atom}(\%)$	#	$\delta G^{atom}(\%)$
180 (C)	1.55%	178 (C)	1.31%	178 (C)	1.40%
186 (H)	2.35%	184 (H)	0.71%	184 (H)	1.11%
181 (C)	1.04%	179 (C)	0.24%	179 (C)	0.13%
182 (H)	0.38%	180 (H)	0.07%	180 (H)	1.77%
183 (H)	0.12%	181 (H)	0.96%	181 (H)	0.41%
184 (H)	1.57%	182 (H)	1.90%	182 (H)	1.88%
185 (C)	2.09%	183 (C)	2.12%	183 (C)	2.09%
187 (H)	2.76%	185 (H)	0.22%	185 (H)	2.53%
188 (H)	0.23%	186 (H)	1.19%	186 (H)	0.20%
189 (H)	1.32%	187 (H)	2.55%	187 (H)	1.17%
Σ	**13.41%**	Σ	**11.27%**	Σ	**12.69%**

Table 4.66 Comparison of $\delta G^{atom}(\%)$ of the Hantzsch ester's western methyl fragment between **TS-3b**, **TS-4c**, and **TS-4d**.

TS-3b		TS-4c		TS-4d	
#	$\delta G^{atom}(\%)$	#	$\delta G^{atom}(\%)$	#	$\delta G^{atom}(\%)$
60 (C)	2.38%	59 (C)	1.96%	59 (C)	2.00%
61 (H)	1.09%	60 (H)	2.17%	60 (H)	2.08%
62 (C)	1.40%	61 (C)	0.64%	61 (C)	0.61%
63 (H)	2.47%	62 (H)	1.40%	62 (H)	1.67%
Σ	**7.34%**	Σ	**6.17%**	Σ	**6.36%**

Table 4.67 Comparison of δG^{atom}(%) of the Hantzsch ester's eastern methyl fragment between **TS-3b**, **TS-4c**, and **TS-4d**.

TS-3b		TS-4c		TS-4d	
#	δG^{atom}(%)	#	δG^{atom}(%)	#	δG^{atom}(%)
64 (C)	7.46%	63 (C)	7.13%	63 (C)	7.11%
65 (H)	5.42%	64 (H)	4.24%	64 (H)	3.55%
66 (H)	7.57%	65 (H)	7.26%	65 (H)	3.88%
67 (H)	2.62%	66 (H)	3.04%	66 (H)	6.99%
Σ	**23.07%**	Σ	**21.67%**	Σ	**21.53%**

Table 4.68 Comparison of δG^{atom}(%) of the α-CH$_2$ morpholine fragment between **TS-3b**, **TS-4c**, and **TS-4d**.

TS-3b		TS-4c		TS-4d	
#	δG^{atom}(%)	#	δG^{atom}(%)	#	δG^{atom}(%)
21 (C)	2.69%	21 (C)	2.87%	21 (C)	2.62%
23 (H)	1.66%	23 (H)	2.10%	23 (H)	2.12%
24 (H)	4.00%	24 (H)	4.01%	24 (H)	3.62%
Σ	**8.35%**	Σ	**8.98%**	Σ	**8.36%**

Table 4.69 Comparison of δG^{atom}(%) of the spiro-cyclopentane morpholine fragment between **TS-3b**, **TS-4c**, and **TS-4d**.

TS-3b		TS-4c		TS-4d	
#	δG^{atom}(%)	#	δG^{atom}(%)	#	δG^{atom}(%)
237 (C)	0.65%	233 (C)	0.18%	233 (C)	0.18%
244 (H)	1.05%	240 (H)	0.31%	240 (H)	0.27%
243 (H)	0.42%	239 (H)	0.10%	239 (H)	0.15%
245 (H)	0.04%	238 (C)	0.02%	238 (C)	0.02%

246 (H)	0.03%	241 (H)	0.01%	241 (H)	0.01%
242 (C)	0.08%	242 (H)	0.01%	242 (H)	0.00%
239 (C)	0.02%	235 (C)	0.00%	235 (C)	0.00%
247 (H)	0.00%	243 (H)	0.00%	243 (H)	0.00%
248 (H)	0.01%	244 (H)	0.00%	244 (H)	0.00%
238 (C)	0.03%	234 (C)	0.02%	234 (C)	0.02%
240 (H)	0.01%	236 (H)	0.01%	236 (H)	0.01%
241 (H)	0.01%	237 (H)	0.01%	237 (H)	0.02%
Σ	**2.35%**	Σ	**0.67%**	Σ	**0.68%**

Table 4.70 Comparison of δG^{atom}(%) of the iminium phenyl fragment between **TS-3b**, **TS-4c**, and **TS-4d**.

TS-3b		TS-4c		TS-4d	
#	δG^{atom}(%)	#	δG^{atom}(%)	#	δG^{atom}(%)
39 (C)	0.22%	38 (C)	0.97%	38 (C)	1.24%
40 (C)	0.36%	39 (C)	2.77%	39 (C)	3.11%
41 (C)	0.03%	40 (C)	0.55%	40 (C)	0.50%
43 (C)	0.01%	42 (C)	1.11%	42 (C)	0.88%
44 (C)	0.08%	43 (C)	4.76%	43 (C)	4.96%
45 (C)	0.01%	44 (C)	4.22%	44 (C)	3.68%
46 (H)	0.02%	45 (H)	0.08%	45 (H)	0.08%
47 (H)	0.00%	46 (H)	0.40%	46 (H)	0.32%
48 (H)	0.00%	47 (H)	4.59%	47 (H)	4.06%
49 (H)	0.60%	48 (H)	2.18%	48 (H)	2.81%

50 (H)	0.04%	49 (H)	3.92%	49 (H)	5.06%
Σ	**1.37%**	Σ	**25.55%**	Σ	**26.70%**

Table 4.71 Comparison of δG^{atom}(%) of the western 2-isopropyl fragment (first arene) between **TS-3b**, **TS-4c**, and **TS-4d**.

TS-3b		TS-4c		TS-4d	
#	δG^{atom}(%)	#	δG^{atom}(%)	#	δG^{atom}(%)
142 (C)	0.76%	141 (C)	0.93%	141 (C)	0.79%
148 (H)	0.63%	147 (H)	0.76%	147 (H)	0.61%
143 (C)	3.56%	142 (C)	3.48%	142 (C)	3.37%
144 (H)	1.35%	143 (H)	1.48%	143 (H)	1.69%
145 (H)	4.33%	144 (H)	4.65%	144 (H)	1.78%
146 (H)	2.88%	145 (H)	2.09%	145 (H)	4.37%
147 (C)	0.17%	146 (C)	0.18%	146 (C)	0.15%
149 (H)	0.15%	245 (H)	0.03%	245 (H)	0.02%
150 (H)	0.02%	246 (H)	0.06%	246 (H)	0.06%
151 (H)	0.05%	247 (H)	0.15%	247 (H)	0.10%
Σ	**13.90%**	Σ	**13.81%**	Σ	**12.94%**

Table 4.72 Comparison of δG^{atom}(%) of the western 6-isopropyl fragment (first arene) between **TS-3b**, **TS-4c**, and **TS-4d**.

TS-3b		TS-4c		TS-4d	
#	δG^{atom}(%)	#	δG^{atom}(%)	#	δG^{atom}(%)
152 (C)	0.01%	148 (C)	0.02%	148 (C)	0.02%
158 (H)	0.01%	154 (H)	0.01%	154 (H)	0.01%
153 (C)	0.00%	149 (C)	0.00%	149 (C)	0.00%

153 (H)	0.00%	150 (H)	0.00%	150 (H)	0.00%
155 (H)	0.00%	151 (H)	0.00%	151 (H)	0.00%
156 (H)	0.00%	152 (H)	0.00%	152 (H)	0.00%
157 (C)	0.05%	153 (C)	0.04%	153 (C)	0.04%
159 (H)	0.02%	155 (H)	0.02%	155 (H)	0.02%
160 (H)	0.01%	156 (H)	0.00%	156 (H)	0.00%
161 (H)	0.14%	157 (H)	0.09%	157 (H)	0.09%
Σ	**0.24%**	Σ	**0.18%**	Σ	**0.18%**

Table 4.73 Comparison of $\delta G^{atom}(\%)$ of the western 2-isopropyl fragment (second arene) between **TS-3b**, **TS-4c**, and **TS-4d**.

TS-3b		**TS-4c**		**TS-4d**	
#	$\delta G^{atom}(\%)$	#	$\delta G^{atom}(\%)$	#	$\delta G^{atom}(\%)$
207 (C)	0.00%	203 (C)	0.13%	203 (C)	0.16%
213 (H)	0.00%	209 (H)	0.06%	209 (H)	0.06%
208 (C)	0.00%	204 (C)	0.01%	204 (C)	0.01%
209 (H)	0.00%	205 (H)	0.00%	205 (H)	0.00%
210 (H)	0.00%	206 (H)	0.00%	206 (H)	0.00%
211 (H)	0.00%	207 (H)	0.00%	207 (H)	0.00%
212 (C)	0.00%	208 (C)	0.15%	208 (C)	0.20%
214 (H)	0.00%	210 (H)	0.28%	210 (H)	0.01%
215 (H)	0.00%	211 (H)	0.01%	211 (H)	0.07%
216 (H)	0.00%	212 (H)	0.05%	212 (H)	0.36%
Σ	**0.00%**	Σ	**0.69%**	Σ	**0.87%**

Table 4.74 Comparison of δG^{atom}(%) of the western 4-isopropyl fragment (second arene) between **TS-3b**, **TS-4c**, and **TS-4d**.

TS-3b		TS-4c		TS-4d	
#	δG^{atom}(%)	#	δG^{atom}(%)	#	δG^{atom}(%)
227 (C)	0.00%	223 (C)	0.06%	223 (C)	0.14%
233 (H)	0.00%	229 (H)	0.01%	229 (H)	0.03%
228 (C)	0.00%	221 (C)	0.03%	221 (C)	0.03%
229 (H)	0.00%	225 (H)	0.01%	225 (H)	0.01%
230 (H)	0.00%	226 (H)	0.00%	226 (H)	0.00%
231 (H)	0.00%	227 (H)	0.00%	227 (H)	0.00%
232 (C)	0.00%	228 (C)	0.12%	228 (C)	0.24%
234 (H)	0.00%	230 (H)	0.16%	230 (H)	0.32%
235 (H)	0.00%	231 (H)	0.01%	231 (H)	0.02%
236 (H)	0.00%	232 (H)	0.09%	232 (H)	0.18%
Σ	**0.00%**	Σ	**0.49%**	Σ	**0.97%**

Table 4.75 Comparison of δG^{atom}(%) of the western 6-isopropyl fragment (second arene) between **TS-3b**, **TS-4c**, and **TS-4d**.

TS-3b		TS-4c		TS-4d	
#	δG^{atom}(%)	#	δG^{atom}(%)	#	δG^{atom}(%)
217 (C)	0.85%	213 (C)	1.05%	213 (C)	1.26%
223 (H)	0.90%	219 (H)	0.90%	219 (H)	1.04%
218 (C)	2.37%	214 (C)	1.84%	214 (C)	1.96%
219 (H)	0.52%	215 (H)	0.28%	215 (H)	1.01%
220 (H)	3.53%	216 (H)	1.09%	216 (H)	2.76%

221 (H)	1.61%	217 (H)	2.62%	217 (H)	0.28%
222 (C)	0.65%	218 (C)	0.12%	218 (C)	0.14%
224 (H)	1.26%	220 (H)	0.03%	220 (H)	0.05%
225 (H)	0.13%	221 (H)	0.03%	221 (H)	0.03%
226 (H)	0.14%	222 (H)	0.06%	222 (H)	0.03%
Σ	**11.96%**	Σ	**8.02%**	Σ	**8.56%**

Table 4.76 Comparison of δG^{atom}(%) of the eastern 2-isopropyl fragment (first arene) between **TS-3b**, **TS-4c**, and **TS-4d**.

TS-3b		TS-4c		TS-4d	
#	δG^{atom}(%)	#	δG^{atom}(%)	#	δG^{atom}(%)
113 (C)	0.89%	112 (C)	0.57%	112 (C)	0.54%
119 (H)	0.48%	118 (H)	0.12%	118 (H)	0.12%
114 (C)	2.13%	113 (C)	2.00%	113 (C)	2.05%
115 (H)	0.64%	114 (H)	1.55%	114 (H)	1.62%
116 (H)	3.36%	115 (H)	0.52%	115 (H)	0.55%
117 (H)	0.98%	116 (H)	2.37%	116 (H)	2.36%
118 (C)	0.09%	117 (C)	0.10%	117 (C)	0.10%
120 (H)	0.03%	119 (H)	0.02%	119 (H)	0.02%
121 (H)	0.04%	120 (H)	0.07%	120 (H)	0.02%
122 (H)	0.02%	121 (H)	0.02%	121 (H)	0.07%
Σ	**8.66%**	Σ	**7.34%**	Σ	**7.45%**

Table 4.77 Comparison of δG^{atom}(%) of the eastern 6-isopropyl fragment (first arene) between **TS-3b**, **TS-4c**, and **TS-4d**.

TS-3b		TS-4c		TS-4d	
#	δG^{atom}(%)	#	δG^{atom}(%)	#	δG^{atom}(%)
123 (C)	0.55%	122 (C)	0.54%	122 (C)	0.48%
129 (H)	0.35%	128 (H)	0.35%	128 (H)	0.30%
124 (C)	1.01%	123 (C)	0.82%	123 (C)	0.66%
125 (H)	0.31%	124 (H)	1.56%	124 (H)	0.18%
126 (H)	0.21%	125 (H)	0.24%	125 (H)	0.11%
127 (H)	1.95%	126 (H)	0.14%	126 (H)	1.28%
128 (C)	0.05%	127 (C)	0.05%	127 (C)	0.04%
130 (H)	0.01%	129 (H)	0.01%	129 (H)	0.01%
131 (H)	0.01%	130 (H)	0.01%	130 (H)	0.01%
132 (H)	0.01%	131 (H)	0.01%	131 (H)	0.01%
Σ	**4.46%**	Σ	**3.73%**	Σ	**3.08%**

Table 4.78 Comparison of δG^{atom}(%) of the eastern 2-isopropyl fragment (second arene) between **TS-3b**, **TS-4c**, and **TS-4d**.

TS-3b		TS-4c		TS-4d	
#	δG^{atom}(%)	#	δG^{atom}(%)	#	δG^{atom}(%)
172 (C)	0.01%	168 (C)	0.01%	168 (C)	0.01%
178 (H)	0.02%	174 (H)	0.02%	174 (H)	0.01%
173 (C)	0.00%	169 (C)	0.00%	169 (C)	0.00%
174 (H)	0.00%	170 (H)	0.00%	170 (H)	0.00%
175 (H)	0.00%	171 (H)	0.00%	171 (H)	0.00%

176 (H)	0.00%	172 (H)	0.00%	172 (H)	0.00%
177 (C)	0.01%	173 (C)	0.00%	173 (C)	0.00%
179 (H)	0.02%	175 (H)	0.00%	175 (H)	0.01%
180 (H)	0.00%	176 (H)	0.00%	176 (H)	0.00%
181 (H)	0.00%	177 (H)	0.01%	177 (H)	0.00%
Σ	**0.06%**	Σ	**0.04%**	Σ	**0.03%**

Table 4.79 Comparison of $\delta G^{\text{atom}}(\%)$ of the eastern 4-isopropyl fragment (second arene) between **TS-3b**, **TS-4c**, and **TS-4d**.

TS-3b		TS-4c		TS-4d	
#	$\delta G^{\text{atom}}(\%)$	#	$\delta G^{\text{atom}}(\%)$	#	$\delta G^{\text{atom}}(\%)$
192 (C)	0.00%	188 (C)	0.00%	188 (C)	0.00%
198 (H)	0.00%	194 (H)	0.00%	194 (H)	0.00%
193 (C)	0.00%	189 (C)	0.00%	189 (C)	0.00%
194 (H)	0.00%	190 (H)	0.00%	190 (H)	0.00%
195 (H)	0.00%	191 (H)	0.00%	191 (H)	0.00%
196 (H)	0.00%	192 (H)	0.00%	192 (H)	0.00%
197 (C)	0.00%	193 (C)	0.00%	193 (C)	0.00%
199 (H)	0.00%	195 (H)	0.00%	195 (H)	0.00%
200 (H)	0.00%	196 (H)	0.00%	196 (H)	0.00%
201 (H)	0.00%	197 (H)	0.00%	197 (H)	0.00%
Σ	**0.00%**	Σ	**0.00%**	Σ	**0.00%**

Table 4.80 Comparison of $\delta G^{\text{atom}}(\%)$ of the eastern 6-isopropyl fragment (second arene) between **TS-3b**, **TS-4c**, and **TS-4d**.

TS-3b		TS-4c		TS-4d	
#	$\delta G^{\text{atom}}(\%)$	#	$\delta G^{\text{atom}}(\%)$	#	$\delta G^{\text{atom}}(\%)$
182 (C)	1.91%	178 (C)	1.85%	178 (C)	1.70%
188 (H)	3.01%	184 (H)	2.79%	184 (H)	2.64%
183 (C)	1.07%	179 (C)	1.55%	179 (C)	1.18%
184 (H)	0.11%	180 (H)	0.59%	180 (H)	0.13%
185 (H)	1.52%	181 (H)	0.17%	181 (H)	1.73%
186 (H)	0.38%	182 (H)	2.33%	182 (H)	0.41%
187 (C)	2.63%	183 (C)	2.25%	183 (C)	2.30%
189 (H)	3.28%	185 (H)	0.26%	185 (H)	0.34%
190 (H)	0.28%	186 (H)	1.12%	186 (H)	1.37%
191 (H)	1.88%	187 (H)	3.23%	187 (H)	3.07%
Σ	**16.07%**	Σ	**16.14%**	Σ	**14.87%**

k. Improved System: Activation Energies

In order to investigate the activation energy computationally, we optimized the structure of the pre-transition state complex (**1d2a6a**).
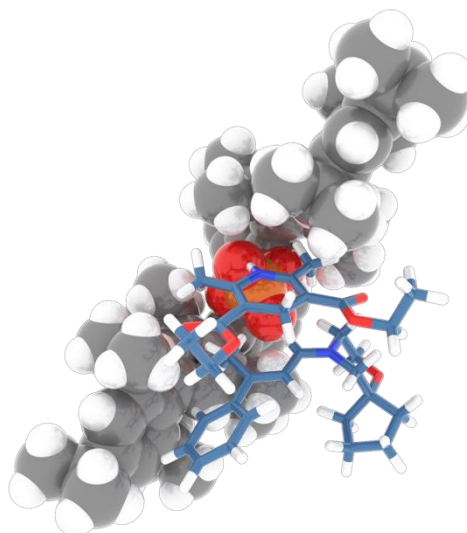
Figure 4.18 Structure of the pre-transition state complex **1d2b6e**, obtained by relaxation of **TS-3b**.

Table 4.81 Obtained thermochemical corrections at the PBE-D3(BJ)/def2-SVP level (323 K, 1 M) as well as single point energies for the pre-transition state complex **1d2b6e**; Gibbs free energies were calculated with respect to **TS-3**.

TC 1.921211795535	E^{SP} / a.u.	$\Delta\Delta G$(323 K)
B3LYP-D3(BJ)/def2-TZVPP	–5207.54815	11.0 kcal/mol
B3LYP/def2-TZVPP	–5206.85244	6.5 kcal/mol
ωB97M-V/def2-TZVPP	–5208.11048	14.7 kcal/mol

We additionally conducted an IGMH analysis with the B3LYP-D3(BJ)/def2-TZVPP densities.
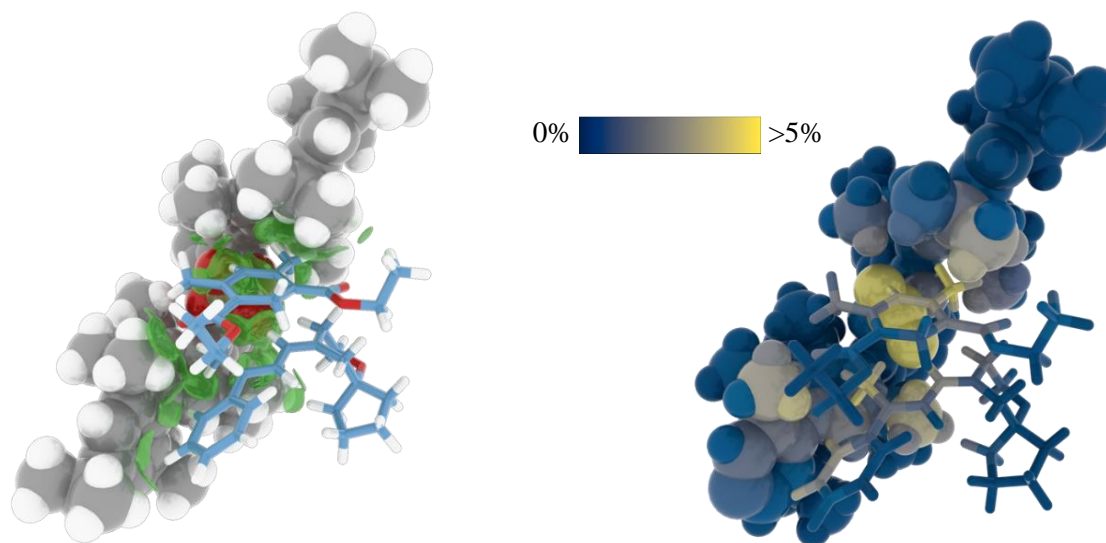
Figure 4.19 δg^{inter} isosurface (left) and color-coded atoms according to their contribution to the overall interfragment interaction $\delta G^{\text{atom}}(\%)$ for pre-transition state complex **1d2b4e**.

Table 4.82 Comparison of $\delta G^{\text{atom}}(\%)$ of the Hantzsch ester's western methyl fragment between **1d2b6e** and **TS-3b**.

1d2b6e		TS-3b	
#	#	#	$\delta G^{\text{atom}}(\%)$
60 (C)	1.85%	60 (C)	2.38%
61 (H)	1.19%	61 (H)	1.09%
62 (C)	1.86%	62 (C)	1.40%
63 (H)	0.99%	63 (H)	2.47%
Σ	5.89%	Σ	7.34%

Table 4.83 Comparison of $\delta G^{\text{atom}}(\%)$ of the Hantzsch ester's eastern methyl fragment between **1d2b6e** and **TS-3b**.

1d2b6e		TS-3b	
#	$\delta G^{\text{atom}}(\%)$	#	$\delta G^{\text{atom}}(\%)$
64 (C)	6.31%	64 (C)	7.46%
65 (H)	3.00%	65 (H)	5.42%

66 (H)	6.50%	66 (H)	7.57%
67 (H)	3.65%	67 (H)	2.62%
Σ	**19.46%**	Σ	**23.07%**

Table 4.84 Comparison of δG^{atom}(%) of the α-CH$_2$ morpholine fragment between **1d2b6e** and **TS-3b**.

1d2b6e		TS-3b	
#	δG^{atom}(%)	#	δG^{atom}(%)
21 (C)	1.66%	21 (C)	2.69%
23 (H)	0.66%	23 (H)	1.66%
24 (H)	2.55%	24 (H)	4.00%
Σ	**4.87%**	Σ	**8.35%**

Table 4.85 Comparison of δG^{atom}(%) of the spiro-cyclopentane morpholine fragment between **1d2b6e** and **TS-3b**.

1d2b6e		TS-3b	
#	δG^{atom}(%)	#	δG^{atom}(%)
237 (C)	0.66%	237 (C)	0.65%
244 (H)	1.33%	244 (H)	1.05%
243 (H)	0.27%	243 (H)	0.42%
245 (H)	0.04%	245 (H)	0.04%
246 (H)	0.07%	246 (H)	0.03%
242 (C)	0.11%	242 (C)	0.08%
239 (C)	0.02%	239 (C)	0.02%
247 (H)	0.00%	247 (H)	0.00%
248 (H)	0.00%	248 (H)	0.01%

238 (C)	0.02%	238 (C)	0.03%
240 (H)	0.00%	240 (H)	0.01%
241 (H)	0.01%	241 (H)	0.01%
Σ	**2.53%**	Σ	**2.35%**

Table 4.86 Comparison of $\delta G^{\text{atom}}(\%)$ of the iminium phenyl fragment between **1d2b6e** and **TS-3b**.

1d2b6e		TS-3b	
#	$\delta G^{\text{atom}}(\%)$	#	$\delta G^{\text{atom}}(\%)$
39 (C)	0.98%	39 (C)	0.22%
40 (C)	3.00%	40 (C)	0.36%
41 (C)	0.21%	41 (C)	0.03%
43 (C)	0.14%	43 (C)	0.01%
44 (C)	2.41%	44 (C)	0.08%
45 (C)	0.55%	45 (C)	0.01%
46 (H)	0.03%	46 (H)	0.02%
47 (H)	0.01%	47 (H)	0.00%
48 (H)	0.27%	48 (H)	0.00%
49 (H)	3.84%	49 (H)	0.60%
50 (H)	3.09%	50 (H)	0.04%
Σ	**14.53%**	Σ	**1.37%**

Table 4.87 Comparison of δG^{atom}(%) of the western 2-isopropyl fragment (first arene) between **1d2b6e** and **TS-3b**.

1d2b6e		TS-3b	
#	δG^{atom}(%)	#	δG^{atom}(%)
142 (C)	0.64%	142 (C)	0.76%
148 (H)	0.23%	148 (H)	0.63%
143 (C)	3.52%	143 (C)	3.56%
144 (H)	2.10%	144 (H)	1.35%
145 (H)	3.82%	145 (H)	4.33%
146 (H)	2.21%	146 (H)	2.88%
147 (C)	0.14%	147 (C)	0.17%
149 (H)	0.07%	149 (H)	0.15%
150 (H)	0.02%	150 (H)	0.02%
151 (H)	0.07%	151 (H)	0.05%
Σ	**12.62%**	Σ	**13.90%**

Table 4.88 Comparison of δG^{atom}(%) of the western 6-isopropyl fragment (first arene) between **1d2b6e** and **TS-3b**.

1d2b6e		TS-3b	
#	δG^{atom}(%)	#	δG^{atom}(%)
152 (C)	0.05%	152 (C)	0.01%
158 (H)	0.01%	158 (H)	0.01%
153 (C)	0.00%	153 (C)	0.00%
153 (H)	0.00%	153 (H)	0.00%
155 (H)	0.00%	155 (H)	0.00%
156 (H)	0.00%	156 (H)	0.00%

157 (C)	0.11%	157 (C)	0.05%
159 (H)	0.07%	159 (H)	0.02%
160 (H)	0.01%	160 (H)	0.01%
161 (H)	0.24%	161 (H)	0.14%
Σ	**0.49%**	Σ	**0.24%**

Table 4.89 Comparison of δG^{atom}(%) of the western 2-isopropyl fragment (second arene) between **1d2b6e** and **TS-3b**.

1d2b6e		TS-3b	
#	δG^{atom}(%)	#	δG^{atom}(%)
207 (C)	0.11%	207 (C)	0.00%
213 (H)	0.05%	213 (H)	0.00%
208 (C)	0.01%	208 (C)	0.00%
209 (H)	0.00%	209 (H)	0.00%
210 (H)	0.00%	210 (H)	0.00%
211 (H)	0.00%	211 (H)	0.00%
212 (C)	0.11%	212 (C)	0.00%
214 (H)	0.04%	214 (H)	0.00%
215 (H)	0.17%	215 (H)	0.00%
216 (H)	0.01%	216 (H)	0.00%
Σ	**0.50%**	Σ	**0.00%**

Table 4.90 Comparison of $\delta G^{atom}(\%)$ of the western 4-isopropyl fragment (second arene) between **1d2b6e** and **TS-3b**.

1d2b6e		TS-3b	
#	$\delta G^{atom}(\%)$	#	$\delta G^{atom}(\%)$
227 (C)	0.29%	227 (C)	0.00%
233 (H)	0.06%	233 (H)	0.00%
228 (C)	0.04%	228 (C)	0.00%
229 (H)	0.02%	229 (H)	0.00%
230 (H)	0.01%	230 (H)	0.00%
231 (H)	0.01%	231 (H)	0.00%
232 (C)	0.75%	232 (C)	0.00%
234 (H)	0.62%	234 (H)	0.00%
235 (H)	0.87%	235 (H)	0.00%
236 (H)	0.09%	236 (H)	0.00%
Σ	**2.76%**	Σ	**0.00%**

Table 4.91 Comparison of $\delta G^{atom}(\%)$ of the western 6-isopropyl fragment (second arene) between **1d2b6e** and **TS-3b**.

1d2b6e		TS-3b	
#	$\delta G^{atom}(\%)$	#	$\delta G^{atom}(\%)$
217 (C)	1.45%	217 (C)	0.85%
223 (H)	1.38%	223 (H)	0.90%
218 (C)	3.01%	218 (C)	2.37%
219 (H)	0.56%	219 (H)	0.52%
220 (H)	2.01%	220 (H)	3.53%

221 (H)	3.98%	221 (H)	1.61%
222 (C)	0.19%	222 (C)	0.65%
224 (H)	0.13%	224 (H)	1.26%
225 (H)	0.04%	225 (H)	0.13%
226 (H)	0.04%	226 (H)	0.14%
Σ	**12.79%**	Σ	**11.96%**

Table 4.92 Comparison of δG^{atom}(%) of the eastern 2-isopropyl fragment (first arene) between **1d2b6e** and **TS-3b**.

1d2b6e		TS-3b	
#	δG^{atom}(%)	#	δG^{atom}(%)
113 (C)	0.42%	113 (C)	0.89%
119 (H)	0.11%	119 (H)	0.48%
114 (C)	1.35%	114 (C)	2.13%
115 (H)	0.30%	115 (H)	0.64%
116 (H)	1.88%	116 (H)	3.36%
117 (H)	0.91%	117 (H)	0.98%
118 (C)	0.06%	118 (C)	0.09%
120 (H)	0.03%	120 (H)	0.03%
121 (H)	0.01%	121 (H)	0.04%
122 (H)	0.01%	122 (H)	0.02%
Σ	**5.08%**	Σ	**8.66%**

Table 4.93 Comparison of $\delta G^{atom}(\%)$ of the eastern 6-isopropyl fragment (first arene) between **1d2b6e** and **TS-3b**.

1d2b6e		TS-3b	
#	$\delta G^{atom}(\%)$	#	$\delta G^{atom}(\%)$
123 (C)	0.47%	123 (C)	0.55%
129 (H)	0.26%	129 (H)	0.35%
124 (C)	1.03%	124 (C)	1.01%
125 (H)	0.34%	125 (H)	0.31%
126 (H)	0.21%	126 (H)	0.21%
127 (H)	1.98%	127 (H)	1.95%
128 (C)	0.04%	128 (C)	0.05%
130 (H)	0.01%	130 (H)	0.01%
131 (H)	0.01%	131 (H)	0.01%
132 (H)	0.01%	132 (H)	0.01%
Σ	**4.36%**	Σ	**4.46%**

Table 4.94 Comparison of $\delta G^{atom}(\%)$ of the eastern 2-isopropyl fragment (second arene) between **1d2b6e** and **TS-3b**.

1d2b6e		TS-3b	
#	$\delta G^{atom}(\%)$	#	$\delta G^{atom}(\%)$
172 (C)	0.01%	172 (C)	0.01%
178 (H)	0.02%	178 (H)	0.02%
173 (C)	0.00%	173 (C)	0.00%
174 (H)	0.00%	174 (H)	0.00%
175 (H)	0.00%	175 (H)	0.00%
176 (H)	0.00%	176 (H)	0.00%

177 (C)	0.00%	177 (C)	0.01%
179 (H)	0.01%	179 (H)	0.02%
180 (H)	0.00%	180 (H)	0.00%
181 (H)	0.00%	181 (H)	0.00%
Σ	**0.04%**	Σ	**0.06%**

Table 4.95 Comparison of δG^{atom}(%) of the eastern 4-isopropyl fragment (second arene) between **1d2b6e** and **TS-3b**.

1d2b6e		**TS-3b**	
#	δG^{atom}(%)	#	δG^{atom}(%)
192 (C)	0.00%	192 (C)	0.00%
198 (H)	0.00%	198 (H)	0.00%
193 (C)	0.00%	193 (C)	0.00%
194 (H)	0.00%	194 (H)	0.00%
195 (H)	0.00%	195 (H)	0.00%
196 (H)	0.00%	196 (H)	0.00%
197 (C)	0.00%	197 (C)	0.00%
199 (H)	0.00%	199 (H)	0.00%
200 (H)	0.00%	200 (H)	0.00%
201 (H)	0.00%	201 (H)	0.00%
Σ	**0.00%**	Σ	**0.00%**

Table 4.96 Comparison of $\delta G^{atom}(\%)$ of the eastern 6-isopropyl fragment (second arene) between **1d2b6e** and **TS-3b**.

1d2b6e		TS-3b	
#	$\delta G^{atom}(\%)$	#	$\delta G^{atom}(\%)$
182 (C)	1.53%	182 (C)	1.91%
188 (H)	2.41%	188 (H)	3.01%
183 (C)	0.68%	183 (C)	1.07%
184 (H)	0.08%	184 (H)	0.11%
185 (H)	0.86%	185 (H)	1.52%
186 (H)	0.20%	186 (H)	0.38%
187 (C)	2.78%	187 (C)	2.63%
189 (H)	3.43%	189 (H)	3.28%
190 (H)	0.49%	190 (H)	0.28%
191 (H)	2.03%	191 (H)	1.88%
Σ	**14.49%**	Σ	**16.07%**
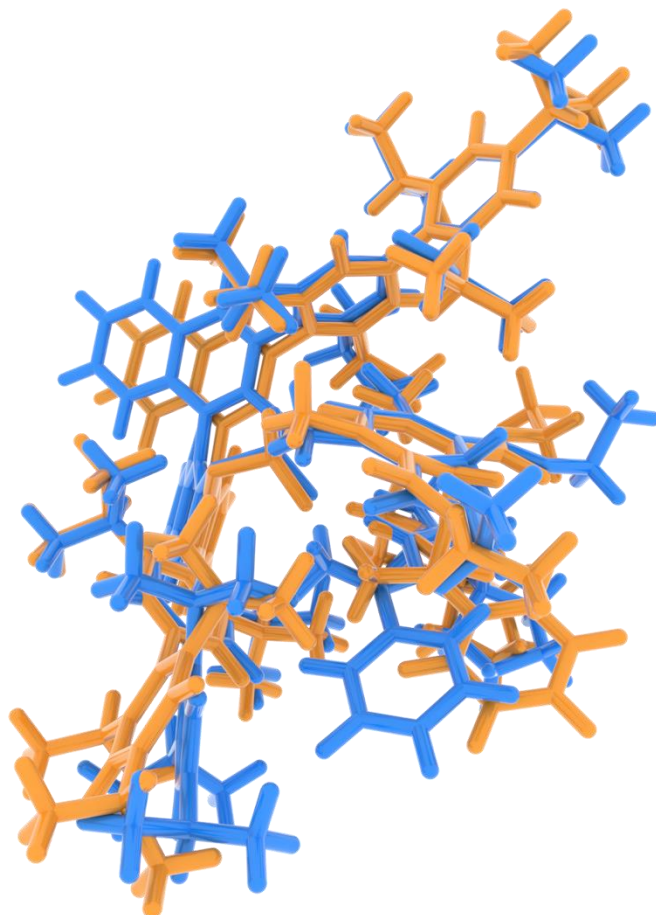
Figure 4.20 Structural comparison between **1d2b6e** (blue) and **TS-3b** (orange).

The structural overlay of both **1d2b6e** and **TS-3b** indicates a substantial difference, most of which is being caused by a closer orientation of the phenyl fragment to the phosphate anion. This eventually leads to the calculated difference in activation energies with and without dispersion correction (11.0 kcal/mol vs. 6.5 kcal/mol), and is further supported by the larger contribution to the interfragment interaction as calculated by the IGMH analysis. These effects are expected to be transposable to the *endo*-rotated **TS-3**.

4.2.8 Kinetic Studies of catalysts 15a, 15f, 53a, and 53f

The kinetic studies were carried out in collaboration with Dr. Markus Leutzsch.

A flame-dried NMR tube under argon was filled with 5 mol% of the respective catalyst salt **15a**, **15f**, **53a** or **53f**, 1.5 eq. Hantzsch ester **33** (5.5 mg, 21.7 μmol), 1.0 eq. mesitylene (2 μL, 14.4 μmol) as internal standard and 0.58 mL 1,4-dioxane-h_8. The mixture was sonicated for approximately 20 min until complete dissolution. Subsequently, 1.0 eq. *E*-enal **27d** (2 μL, 14.4 μmol) was added, and the tube was inverted one time to ensure thorough mixing. The reaction was monitored by single scan ^{1}H NMR spectroscopy at 50 °C. The data was then imported into MNOVA 15.0.0 with the Reaction Monitoring plugin and processed therein (phasing, multi point baseline correction, integration and referencing).

Note: The reaction concentration was adjusted from 0.1 M to 0.025 M to ensure complete dissolution of all reagents yielding a homogeneous solution. Furthermore, 1,4-dioxane-h_8 was used as a solvent instead of the d_8 variant, as deuteration at the acidic α-position had been observed (likely due to the presence of D_2O). The solvent signal was suppressed using a WET pulse sequence (Bruker pulse sequence: wet) to enhance the signal-to-noise ratio of the reactants for the single scan measurements. (See the following review as a reference[299]).
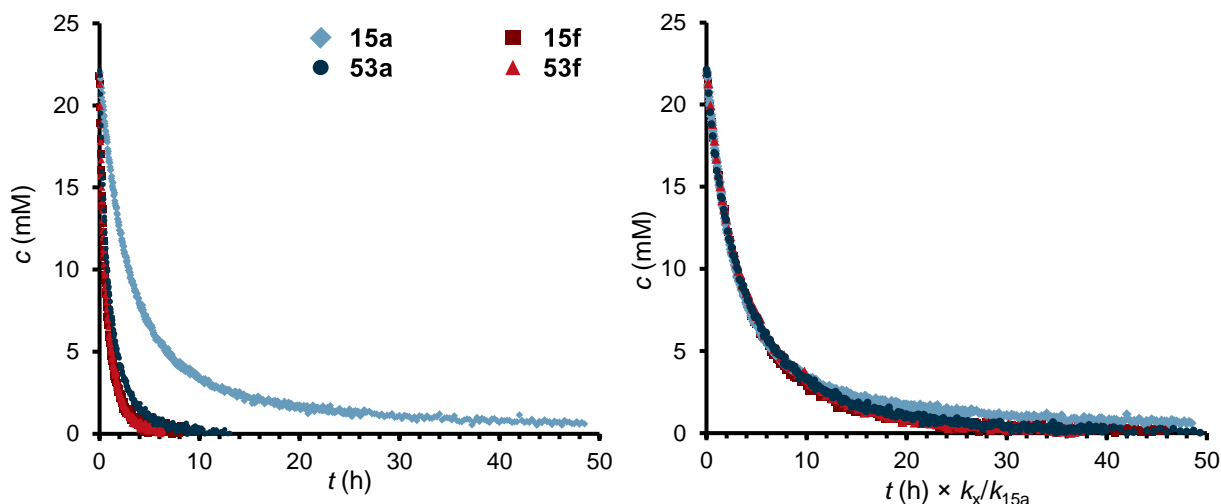
Figure 4.21 Left: conversion of *E*-**27d** over time using different catalysts monitored by single-scan ^{1}H NMR spectroscopy (0.025 M in 1,4-dioxane-h_8, 50 °C); right: relative rate analysis via variable-time normalization (VTNA), using catalyst salt **15a** as reference ($k_{15a} = 1.0$).

In order to compare the reactions without investigating reaction orders of this multiple component reaction in detail, we determined the relative rates of the reaction by using a variable-time-normalization approach.[214] Therefore, the time was multiplied with a relative rate ($k_{rel} = k_x/k_{ref}$), whereas the slowest

reaction was used as reference reaction (**15a**). The value was obtained by visually searching the best graphical overlap to the reference reaction. This data was then converted to the respective relative energies using the following equation:

$$k = A \times e^{-\frac{\Delta E_A}{RT}} \qquad \text{Arrhenius Equation} \quad (1)$$

$$k_{rel} = \frac{k_x}{k_{ref}} = \frac{A_x \times e^{-\frac{E_{A,x}}{RT}}}{A_{ref} \times e^{-\frac{E_{A,ref}}{RT}}} \qquad (2)$$

Assuming that A_x and A_{ref} are similar we obtain:

$$k_{rel} = e^{-\frac{(E_{A,x} - E_{A,ref})}{RT}} = e^{-\frac{\Delta E_A}{RT}} \qquad (3)$$

$$\Delta E_A = -\ln(k_{rel}) \times R \times T \qquad (4)$$

Table 4.97 Relative reaction rates for different catalysts, obtained from VTNA.

CPA	Amine	Relative Rate k_x/k_{4a}	Relative Energy ΔE_A (kcal/mol)
53	**a**	4.0	−0.89
53	**f**	6.0	−1.15
15	**f**	5.6	−1.11
15	**a**	1.0	0

We performed a second kinetic analysis using the initial rates method, where the first 13–15% of conversion was approximated to follow zero-order kinetics, and the slope of the curve was taken as the rate constant. To achieve this, we monitored both the consumption of the starting material (enal) and the formation of the product over time, determining the slope for each reaction (**15a**, **15f**, **53a**, **53f**). After averaging the values and calculating the standard deviation, we extracted the relative rates with respect to catalyst **15a**. As previously described, relative energies were then obtained using the Arrhenius equation.
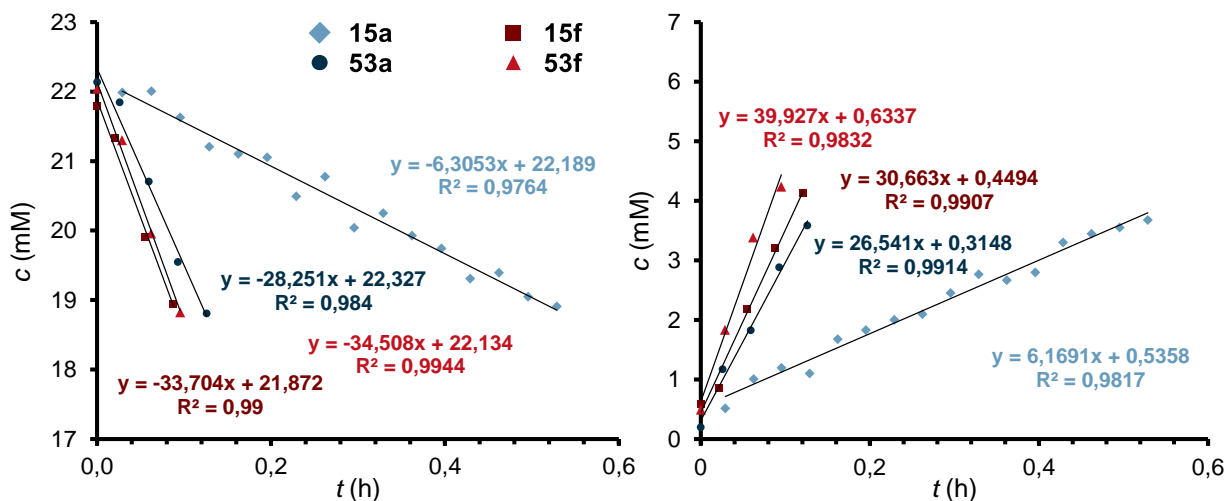
Figure 4.22 Initial rates analysis based on the first 13–15% of conversion for the transfer hydrogenation of *E*-**27d** at 50 °C in 1,4-dioxane-h_8. Left: enal consumption over time; right: product formation over time. Linear fits were used to determine the average rate for each catalyst. Relative rates were extracted with respect to catalyst **15a**.

Table 4.98 Relative reaction rates for different catalysts, obtained from initial rates analysis.

CPA	Amine	Enal Conv. (mM/h)	Product Formation (mM/h)	Average Rate (mM/h)	Relative Rate k_x/k_{4a} (initial rate)		Relative Energy ΔE_A (kcal/mol)	
53	**a**	28.3	26.5	27.4	4.5	± 0.2	−0.96	± 0.04
53	**f**	35.5	40.0	37.7	5.6	± 0.4	−1.11	± 0.08
15	**f**	33.7	30.7	32.2	5.4	± 0.3	−1.08	± 0.06
15	**a**	6.3	6.2	6.2	1.0		0.0	

4.3 Experimental Procedures for Chapter 3

4.3.1 Reaction Development

General procedure 5 (GP5)

A 2 mL GC vial, equipped with a magnetic stirring bar, was charged with the chiral catalyst (2 mol%) and the proton source (0.030 mmol, 1.2 eq.) and then placed under argon. The respective solvent and hydrosilane (0.125 mmol, 5.0 eq.) were added sequentially, followed by the styrene (**68**, 0.025 mmol, 1.0 eq.). The reaction was stirred at the indicated temperature for three days (for reactions at temperatures below 20 °C, the vial was cooled to –78 °C before substrate addition and then warmed to the respective temperature). The reaction was quenched by addition of pyridine (5 μL) followed by addition of mesitylene (3 μL) as internal standard. An aliquot of the mixture was taken and diluted with C_6D_6 for subsequent ^1H NMR analysis. The remaining solution was used for preparative thin layer chromatography (pentane) to purify the chiral product. Chiral GC analysis was performed to give the corresponding enantiomeric ratio.

4.3.2 Synthesis of Styrenes

*Styrenes **68d**, **68g**, **68h**, **68j**, **68u**, **68v**, **68ab**, **68ae**, **68af**, and **68ag**, as well as precursors **111** and **103u** were synthesized by Michael Merher.*

General Procedure 6 (GP6)

$$103 \qquad 68$$
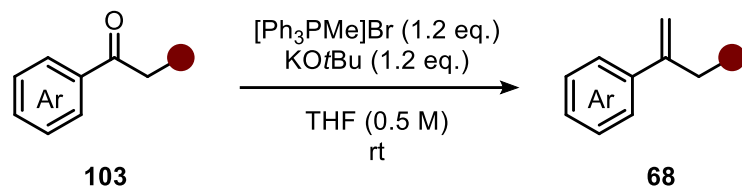
A flame-dried Schlenk flask under argon was charged with KOtBu (1.2 eq.) and dry THF (0.5 M). [Ph$_3$PMe]Br (1.2 eq.) was added to the suspension, and it was subsequently stirred at room temperature for 1 h. The corresponding ketone (1.0 eq.) was added and the resulting mixture was stirred for 1–18 h until TLC indicated full consumption of the starting material. The reaction was quenched by addition of water, followed by extraction of the aqueous phase with DCM (3x). The combined organic layers were washed with water, dried over anhydrous Na_2SO_4, filtered, and concentrated under reduced pressure. The crude was purified via flash column chromatography on silica gel.

hex-1-en-2-ylbenzene (68a)
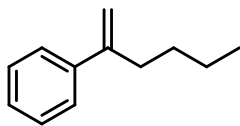
Prepared according to **GP6**, stirred for for 1 h, eluent: pentane, 1.86 g (96%), colorless oil.

R_F (100% hexanes) = 0.63.

¹H NMR (501 MHz, CDCl₃): δ = 7.43–7.39 (m, 2H), 7.36–7.30 (m, 2H), 7.26 (tt, *J* = 6.5, 1.4 Hz, 1H), 5.26 (d, *J* = 1.5 Hz, 1H), 5.06 (d, *J* = 1.4 Hz, 1H), 2.51 (td, *J* = 7.5, 1.3 Hz, 2H), 1.49–1.40 (m, 2H), 1.40–1.32 (m, 2H), 0.90 (t, *J* = 7.3 Hz, 3H).

¹³C NMR (126 MHz, CDCl₃): δ = 148.9, 141.7, 128.4, 127.4, 126.3, 112.1, 35.2, 30.6, 22.6, 14.1.

HRMS *m/z* (GC-EI): calcd. For $C_{12}H_{16}$ ([M]⁺): 160.124650; found: 160.124710.

1-(hex-1-en-2-yl)-4-methylbenzene (68b)
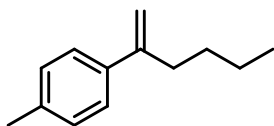
Prepared according to **GP6**, stirred for 18 h, eluent: pentane, 889 mg (97%), colorless oil.

R_F (100% hexanes) = 0.59.

¹H NMR (501 MHz, CDCl₃): δ = 7.34–7.29 (m, 2H), 7.14 (d, *J* = 7.9 Hz, 2H), 5.24 (d, *J* = 1.7 Hz, 1H), 5.01 (d, *J* = 1.5 Hz, 1H), 2.49 (td, *J* = 7.5, 1.4 Hz, 2H), 2.35 (s, 3H), 1.49–1.39 (m, 2H), 1.39–1.31 (m, 2H), 0.90 (t, *J* = 7.3 Hz, 3H).

¹³C NMR (126 MHz, CDCl₃): δ = 148.7, 138.7, 137.1, 129.1, 126.1, 111.4, 35.2, 30.7, 22.6, 21.2, 14.1.

HRMS *m/z* (GC-EI): calcd. For $C_{13}H_{18}$ ([M]⁺): 174.140300; found: 174.140300.

1-(hex-1-en-2-yl)-3-methylbenzene (68c)
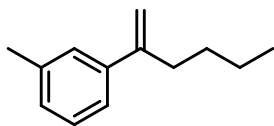
Prepared according to **GP6**, stirred for 18 h, eluent: pentane, 358 mg (99%), colorless oil.

R_F (100% hexanes) = 0.59.

¹H NMR (501 MHz, CDCl₃): δ = 7.24–7.18 (m, 3H), 7.08 (ddd, *J* = 5.9, 2.7, 1.3 Hz, 1H), 5.24 (d, *J* = 1.6 Hz, 1H), 5.03 (q, *J* = 1.4 Hz, 1H), 2.53–2.46 (m, 2H), 2.36 (s, 3H), 1.48–1.39 (m, 2H), 1.39–1.30 (m, 2H), 0.90 (t, *J* = 7.2 Hz, 3H).

¹³C NMR (126 MHz, CDCl₃): δ = 149.1, 141.7, 137.8, 128.2, 128.1, 127.0, 123.4, 111.9, 35.3, 30.6, 22.6, 21.7, 14.1.

HRMS *m/z* (GC-EI): calcd. For $C_{13}H_{18}$ ([M]⁺): 174.140300; found: 174.140450.

1-ethyl-3-(hex-1-en-2-yl)benzene (68d)
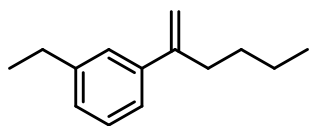
Prepared according to **GP6**, stirred for 18 h, eluent: pentane, 1.08 g (96%), colorless oil.

R_F (100% hexanes) = 0.59.

¹H NMR (501 MHz, CD₂Cl₂): δ = 7.26–7.19 (m, 3H), 7.10 (dt, *J* = 6.7, 2.0 Hz, 1H), 5.24 (d, *J* = 1.7 Hz, 1H), 5.03 (q, *J* = 1.5 Hz, 1H), 2.65 (q, *J* = 7.6 Hz, 2H), 2.53–2.47 (m, 2H), 1.52 (s, 2H), 1.46–1.38 (m, 2H), 1.38–1.31 (m, 2H), 1.23 (t, *J* = 7.6 Hz, 3H), 0.90 (t, *J* = 7.2 Hz, 3H).

¹³C NMR (126 MHz, CD₂Cl₂): δ = 149.5, 144.7, 141.9, 128.5, 127.2, 126.1, 123.8, 111.8, 35.4, 31.0, 29.3, 22.8, 15.9, 14.1.

HRMS *m/z* (GC-EI): calcd. For $C_{14}H_{20}$ ([M]⁺): 188.155950; found: 188.155860.

1-(hex-1-en-2-yl)-3-isopropylbenzene (68e)
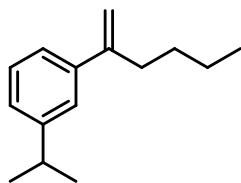
Prepared according to **GP6**, stirred for 3 h, eluent: pentane, 257 mg (>99%), colorless oil.

¹H NMR (501 MHz, CDCl₃): δ = 7.27–7.26 (m, 1H), 7.25 (d, *J* = 7.1 Hz, 1H), 7.22 (dt, *J* = 7.7, 1.7 Hz, 1H), 7.14 (dt, *J* = 7.3, 1.7 Hz, 1H), 5.26 (d, *J* = 1.7 Hz, 1H), 5.04 (q, *J* = 1.4 Hz, 1H), 2.91 (h, *J* = 7.0 Hz, 1H), 2.54–2.47 (m, 2H), 1.49–1.41 (m, 2H), 1.41–1.31 (m, 2H), 1.27 (d, *J* = 6.9 Hz, 6H), 0.91 (t, *J* = 7.3 Hz, 3H).

¹³C NMR (126 MHz, CDCl₃): δ = 149.2, 148.9, 141.7, 128.3, 125.4, 124.5, 123.8, 111.8, 35.2, 34.3, 30.6, 24.2, 22.6, 14.1.

HRMS *m/z* (GC-EI): calcd. For $C_{15}H_{22}$ ([M]⁺): 202.171600; found: 202.171730.

1-(*tert*-butyl)-3-(hex-1-en-2-yl)benzene (68f)

Prepared according to **GP6**, stirred for 3 h, eluent: pentane, 1.35 g (91%), colorless oil.
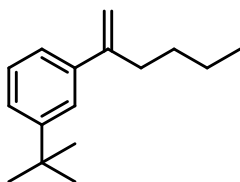
¹H NMR (501 MHz, CDCl₃): δ = 7.43 (t, *J* = 1.9 Hz, 1H), 7.31 (dt, *J* = 7.7, 1.7 Hz, 1H), 7.26 (t, *J* = 7.5 Hz, 1H), 7.22 (dt, *J* = 7.4, 1.6 Hz, 1H), 5.26 (d, *J* = 1.7 Hz, 1H), 5.05 (q, *J* = 1.4 Hz, 1H), 2.55–2.48 (m, 2H), 1.49–1.41 (m, 2H), 1.40–1.35 (m, 2H), 1.34 (s, 9H), 0.91 (t, *J* = 7.2 Hz, 3H).

¹³C NMR (126 MHz, CDCl₃): δ = 151.1, 149.4, 141.4, 128.0, 124.4, 123.5, 123.3, 111.8, 35.3, 34.8, 31.5, 30.6, 22.6, 14.1.

HRMS *m/z* (GC-EI): calcd. For C₁₆H₂₄ ([M]⁺): 216.187250; found: 216.187000.

1-(hex-1-en-2-yl)-3,5-dimethylbenzene (68g)
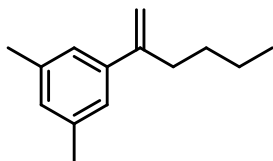
Prepared according to **GP6**, stirred for 18 h, eluent: pentane, 873 mg (94%), colorless oil.

*R*ᶠ (100% hexanes) = 0.56.

¹H NMR (501 MHz, CD₂Cl₂): δ = 7.03–6.99 (m, 2H), 6.91 (dt, *J* = 1.7, 0.9 Hz, 1H), 5.20 (d, *J* = 1.8 Hz, 1H), 5.00 (q, *J* = 1.4 Hz, 1H), 2.51–2.44 (m, 2H), 2.30 (d, *J* = 0.8 Hz, 6H), 1.46–1.37 (m, 2H), 1.37–1.30 (m, 2H), 0.89 (t, *J* = 7.2 Hz, 3H).

¹³C NMR (126 MHz, CD₂Cl₂): δ = 149.6, 141.8, 138.0, 129.2, 124.3, 111.7, 35.5, 31.0, 22.8, 21.5, 14.1.

HRMS *m/z* (GC-EI): calcd. For C₁₄H₂₀ ([M]⁺): 188.155950; found: 188.155830.

1-fluoro-4-(hex-1-en-2-yl)benzene (68h)
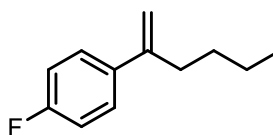
Prepared according to **GP6**, stirred for 18 h, eluent: pentane, 1.73 g (84%), colorless oil.

*R*ᶠ (100% hexanes) = 0.57.

¹H NMR (501 MHz, CDCl₃): δ = 7.39–7.33 (m, 2H), 7.03–6.97 (m, 2H), 5.20 (d, *J* = 1.4 Hz, 1H), 5.03 (q, *J* = 1.4 Hz, 1H), 2.50–2.44 (m, 2H), 1.45–1.38 (m, 2H), 1.38–1.30 (m, 2H), 0.90 (t, *J* = 7.2 Hz, 3H).

¹⁹F NMR (471 MHz, CDCl₃): δ = –115.7 (s, 1F).

¹³C NMR (126 MHz, CDCl₃): δ = 162.2 (d, *J* = 245.9 Hz), 147.7, 137.5 (d, *J* = 3.3 Hz), 127.6 (d, *J* = 7.9 Hz), 115.0 (d, *J* = 21.3 Hz), 111.9, 35.2, 30.3, 22.3, 13.9.

HRMS *m/z* (GC-EI): calcd. For C₁₂H₁₅F₁ ([M]⁺): 178.115228; found: 178.115410.

1-bromo-3-(hex-1-en-2-yl)benzene (68i)
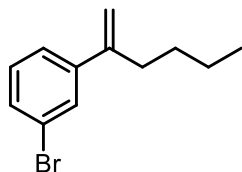
Prepared according to **GP6**, stirred for 18 h, eluent: pentane, 1.32 g (96%), colorless oil.

R_F (100% hexanes) = 0.82.

1H NMR (501 MHz, CDCl3): δ = 7.54 (t, J = 1.9 Hz, 1H), 7.39 (ddd, J = 7.9, 2.1, 1.1 Hz, 1H), 7.34–7.29 (m, 1H), 7.19 (t, J = 7.8 Hz, 1H), 5.25 (d, J = 1.4 Hz, 1H), 5.08 (q, J = 1.4 Hz, 1H), 2.49–2.43 (m, 2H), 1.46–1.38 (m, 2H), 1.38–1.30 (m, 2H), 0.90 (t, J = 7.2 Hz, 3H).

13C NMR (126 MHz, CDCl3): δ = 147.7, 143.9, 130.3, 129.9, 129.4, 124.9, 122.6, 113.4, 35.1, 30.4, 22.5, 14.0.

HRMS *m/z* (GC-EI): calcd. For $C_{12}H_{15}Br_1$ ([M]$^+$): 238.035175; found: 238.035510.

1-(hex-1-en-2-yl)-3-methoxybenzene (68j)
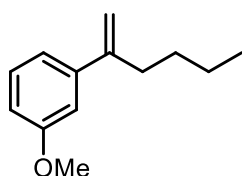
Prepared according to **GP6**, stirred for 18 h, eluent: pentane, 508 mg (72%), light yellow oil.

R_F (20% DCM, hexanes) = 0.42.

1H NMR (501 MHz, CDCl3): δ = 7.28–7.22 (m, 1H), 7.03–6.98 (m, 1H), 6.95 (q, J = 2.0 Hz, 1H), 6.82 (dt, J = 8.4, 2.2 Hz, 1H), 5.26 (d, J = 1.8 Hz, 1H), 5.07–5.01 (m, 1H), 3.83 (d, J = 1.7 Hz, 3H), 2.52–2.44 (m, 2H), 1.48–1.40 (m, 2H), 1.40–1.30 (m, 2H), 0.90 (td, J = 7.3, 1.7 Hz, 3H).

13C NMR (126 MHz, CDCl3): δ = 159.7, 148.8, 143.3, 129.3, 118.9, 112.5, 112.3, 112.3, 55.4, 35.3, 30.6, 22.6, 14.1.

HRMS *m/z* (GC-EI): calcd. For $C_{13}H_{15}O_1$ ([M]$^+$): 190.135215; found: 190.135120.

2-(hex-1-en-2-yl)naphthalene (68k)
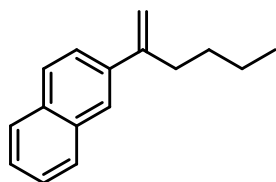
Prepared according to **GP6**, stirred for 18 h, eluent: pentane, 614 mg (99%), colorless oil.

R_F (100% hexanes) = 0.51.

1H NMR (501 MHz, CDCl3): δ = 7.86–7.78 (m, 4H), 7.59 (dd, J = 8.6, 1.8 Hz, 1H), 7.50–7.42 (m, 2H), 5.41 (d, J = 1.5 Hz, 1H), 5.17 (q, J = 1.4 Hz, 1H), 2.63 (td, J = 7.6, 1.3 Hz, 2H), 1.56–1.46 (m, 2H), 1.44–1.32 (m, 2H), 0.92 (t, J = 7.3 Hz, 3H).

¹³C NMR (126 MHz, CDCl₃): δ = 148.7, 138.9, 133.6, 132.9, 128.3, 127.9, 127.7, 126.2, 125.8, 124.9, 124.8, 112.8, 35.2, 30.7, 22.6, 14.1.

HRMS *m/z* (GC-EI): calcd. For $C_{16}H_{18}$ ([M]⁺): 210.140300; found: 210.140170.

Synthesis of 5-(hex-1-en-2-yl)benzofuran (68l)
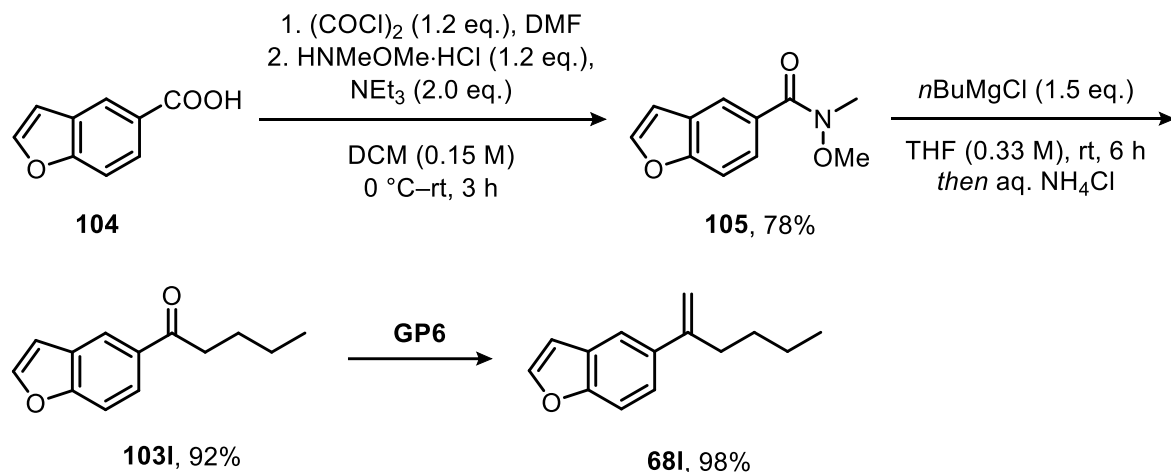
N-methoxy-*N*-methylbenzofuran-5-carboxamide (105)

In a flame-dried Schlenk flask under argon, benzofuran-5-carboxylic acid (**104**, 760 mg, 4.69 mmol, 1.00 eq.) was suspended in dry DCM (10 mL), cooled to 0 °C, and one drop of DMF was added. Oxalyl chloride (0.49 mL, 5.62 mmol, 1.20 eq.) was then added slowly at 0 °C. The reaction mixture was stirred at room temperature for 2 h until the suspension turned into a solution. The mixture was transferred to a 100 mL round-bottom flask and concentrated under reduced pressure. The resulting crude acid chloride was redissolved in dry DCM (5 mL, plus 5 mL for rinsing) and added to a second flame-dried Schlenk flask containing *N,O*-dimethylhydroxylamine hydrochloride (549 mg, 5.62 mmol, 1.20 eq.) in DCM (20 mL) at 0 °C. Et₃N (1.3 mL, 9.37 mmol, 2.00 eq.) was added dropwise at 0 °C, after which the mixture was warmed to room temperature and stirred overnight. The reaction was quenched with saturated NH₄Cl (30 mL) solution and extracted with DCM (3 x 20 mL). The combined organic layers were washed with water, dried over anhydrous Na₂SO₄, and concentrated. Purification by flash column chromatography on silica gel (30% EtOAc, cyclohexane) afforded the product as a yellow oil (754 mg, 78%).

¹H NMR (501 MHz, CDCl₃): δ = 7.99 (d, *J* = 1.7 Hz, 1H), 7.67 (td, *J* = 4.0, 1.7 Hz, 2H), 7.51 (dt, *J* = 8.6, 0.8 Hz, 1H), 6.82 (dd, *J* = 2.2, 1.0 Hz, 1H), 3.56 (s, 3H), 3.39 (s, 3H).

^{13}**C NMR** (126 MHz, CDCl$_3$): δ = 170.2, 156.1, 146.1, 129.0, 127.2, 125.1, 122.2, 111.1, 107.1, 61.1, 34.1.

HRMS *m/z* (GC-EI): calcd. For C$_{11}$H$_{11}$O$_3$N$_1$Na$_1$ ([M+Na]$^+$): 228.063113; found: 228.063100.

1-(benzofuran-5-yl)pentan-1-one (103l)
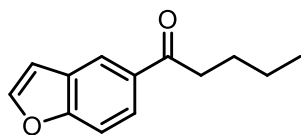
Weinreb amide **105** (754 mg, 3.67 mmol, 1.00 eq.) was dissolved in dry THF (11 mL) and cooled to 0 °C. *n*-Butylmagnesium chloride (2 M in THF, 2.8 mL, 5.6 mmol, 1.52 eq.) was added dropwise at 0 °C, and the reaction mixture was then warmed to room temperature and stirred for 6 h. After completion, as monitored by TLC, saturated NH$_4$Cl solution was added, and the mixture was stirred at room temperature for 1 h. The aqueous phase was extracted with DCM (3 x 20 mL), and the combined organic layers were dried over anhydrous Na$_2$SO$_4$ and concentrated under reduced pressure. Purification by flash column chromatography on silica gel (0–4% MTBE in pentane) afforded the product as a white solid (682 mg, 92%).

^{1}**H NMR** (501 MHz, CDCl$_3$): δ = 8.26 (d, *J* = 1.8 Hz, 1H), 7.97 (dd, *J* = 8.7, 1.8 Hz, 1H), 7.69 (d, *J* = 2.2 Hz, 1H), 7.54 (dt, *J* = 8.7, 0.9 Hz, 1H), 6.86 (dd, *J* = 2.2, 0.9 Hz, 1H), 3.06–2.99 (m, 2H), 1.80–1.71 (m, 2H), 1.48–1.39 (m, 2H), 0.97 (t, *J* = 7.3 Hz, 3H).

^{13}**C NMR** (126 MHz, CDCl$_3$): δ = 200.3, 157.5, 146.5, 132.8, 127.6, 125.0, 122.4, 111.6, 107.4, 38.6, 26.9, 22.7, 14.1.

HRMS *m/z* (GC-EI): calcd. For C$_{13}$H$_{14}$O$_2$ ([M]$^+$): 202.098830; found: 202.098770.

5-(hex-1-en-2-yl)benzofuran (68l)
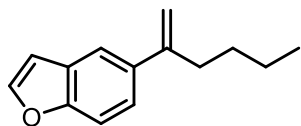
Prepared according to **GP6**, stirred for 18 h, eluent: pentane, 664 mg (98%), colorless oil.

R_F (100% hexanes) = 0.43.

^{1}**H NMR** (501 MHz, CDCl$_3$): δ = 7.61 (dt, *J* = 2.1, 1.2 Hz, 2H), 7.45 (d, *J* = 8.6 Hz, 1H), 7.36 (d, *J* = 8.5 Hz, 1H), 6.76 (dt, *J* = 2.1, 1.0 Hz, 1H), 5.24 (s, 1H), 5.06 (s, 1H), 2.55 (t, *J* = 7.5 Hz, 2H), 1.49–1.41 (m, 2H), 1.41–1.30 (m, 2H), 0.90 (td, *J* = 7.3, 1.1 Hz, 3H).

^{13}**C NMR** (126 MHz, CDCl$_3$): δ = 154.6, 149.2, 145.4, 136.8, 127.5, 123.1, 118.8, 111.8, 111.1, 106.9, 35.8, 30.6, 22.6, 14.1.

HRMS *m/z* (GC-EI): calcd. For C$_{14}$H$_{16}$O$_1$ ([M]$^+$): 200.119565; found: 200.119510.

Synthesis of 6-(hex-1-en-2-yl)benzofuran (68m)
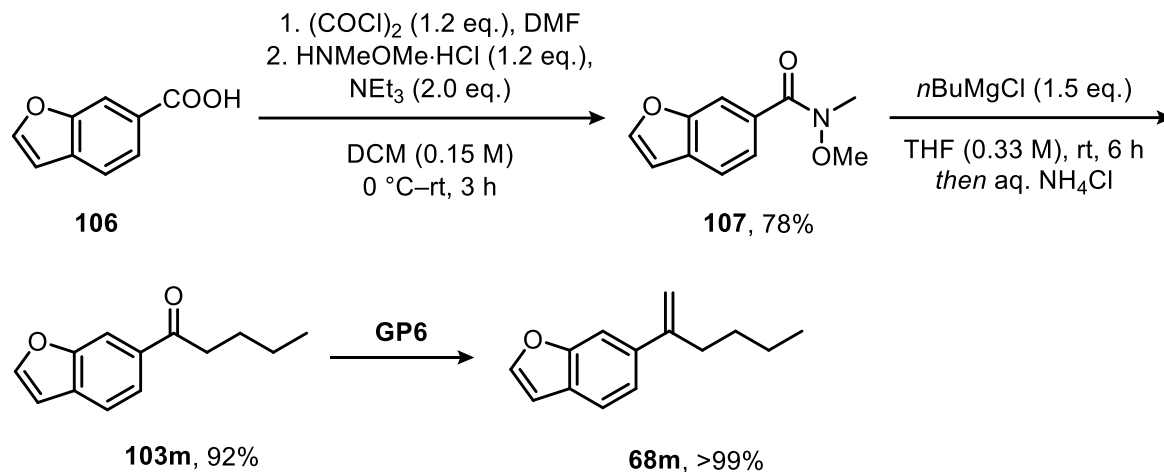
N-methoxy-*N*-methylbenzofuran-6-carboxamide (107)
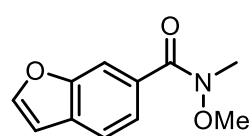
In a flame-dried Schlenk flask under argon, benzofuran-6-carboxylic acid (**106**, 1.53 mg, 9.43 mmol, 1.00 eq.) was suspended in dry DCM (10 mL), cooled to 0 °C, and one drop of DMF was added. Oxalyl chloride (0.99 mL, 11.3 mmol, 1.20 eq.) was then added slowly at 0 °C. The reaction mixture was stirred at room temperature for 2 h until the suspension turned into a solution. The mixture was transferred to a 100 mL round-bottom flask and concentrated under reduced pressure. The resulting crude acid chloride was redissolved in dry DCM (5 mL, plus 5 mL for rinsing) and added to a second flame-dried Schlenk flask containing *N,O*-dimethylhydroxylamine hydrochloride (1.10 g, 11.3 mmol, 1.20 eq.) in DCM (20 mL) at 0 °C. Et₃N (2.6 mL, 18.9 mmol, 2.00 eq.) was added dropwise at 0 °C, after which the mixture was warmed to room temperature and stirred overnight. The reaction was quenched with saturated NH₄Cl (30 mL) solution and extracted with DCM (3 x 20 mL). The combined organic layers were washed with water, dried over anhydrous Na₂SO₄, and concentrated. The crude (brown oil) was used without further purification for the next step (1.91 g, 99%).

^{1}H NMR (501 MHz, CDCl$_3$): δ = 7.90 (t, *J* = 1.1 Hz, 1H), 7.72 (d, *J* = 2.2 Hz, 1H), 7.62 (d, *J* = 0.9 Hz, 2H), 6.81 (dd, *J* = 2.1, 1.0 Hz, 1H), 3.57 (s, 3H), 3.39 (s, 3H).

^{13}C NMR (126 MHz, CDCl$_3$): δ = 169.9, 154.2, 147.1, 130.1, 129.8, 123.4, 120.8, 112.1, 106.8, 61.2, 34.1.

HRMS *m/z* (GC-EI): calcd. For C$_{11}$H$_{11}$O$_3$N$_1$Na$_1$ ([M+Na]$^+$): 228.06311; found: 228.063106292.

1-(benzofuran-6-yl)pentan-1-one (103m)
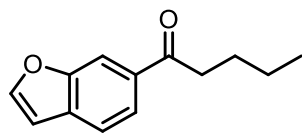
Weinreb amide **107** (1.45 gg, 7.05 mmol, 1.00 eq.) was dissolved in dry THF (21 mL) and cooled to 0 °C. *n*-Butylmagnesium chloride (2 M in THF, 5.3 mL, 10.6 mmol, 1.50 eq.) was added dropwise at 0 °C, and the reaction mixture was then warmed to room temperature and stirred for 2 h. After completion, as monitored by TLC, saturated NH₄Cl solution was added, and the mixture was stirred at room temperature for 1 h. The aqueous phase was extracted with DCM (3 x 20 mL), and the combined organic layers were dried over anhydrous Na₂SO₄ and concentrated under reduced pressure. Purification by flash column chromatography on silica gel (2.5% MTBE in pentane) afforded the product as a white solid (1.19 g, 83%).

¹H NMR (501 MHz, CDCl₃): δ = 8.14–8.11 (m, 1H), 7.90 (dd, *J* = 8.2, 1.5 Hz, 1H), 7.78 (d, *J* = 2.2 Hz, 1H), 7.65 (d, *J* = 8.1 Hz, 1H), 6.83 (dd, *J* = 2.2, 1.0 Hz, 1H), 3.06–2.98 (m, 2H), 1.76 (p, *J* = 7.5 Hz, 2H), 1.49–1.38 (m, 2H), 0.97 (t, *J* = 7.3 Hz, 3H).

¹³C NMR (126 MHz, CDCl₃): δ = 200.2, 154.9, 148.3, 133.9, 131.8, 123.0, 121.1, 111.7, 106.9, 38.7, 26.9, 22.7, 14.1.

HRMS *m/z* (GC-EI): calcd. For $C_{13}H_{14}O_2$ ([M]⁺): 202.098830; found: 202.098930.

6-(hex-1-en-2-yl)benzofuran (68m)

Prepared according to **GP6**, stirred for 18 h, eluent: pentane, 1.15 g (>99%), colorless oil.
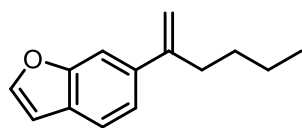
¹H NMR (501 MHz, CDCl₃): δ = 7.61 (d, *J* = 2.2 Hz, 1H), 7.56–7.51 (m, 2H), 7.34 (dd, *J* = 8.1, 1.5 Hz, 1H), 6.75 (dd, *J* = 2.2, 1.0 Hz, 1H), 5.31 (d, *J* = 1.5 Hz, 1H), 5.09 (q, *J* = 1.4 Hz, 1H), 2.60–2.52 (m, 2H), 1.50–1.42 (m, 2H), 1.41–1.32 (m, 2H), 0.90 (t, *J* = 7.3 Hz, 3H).

¹³C NMR (126 MHz, CDCl₃): δ) 155.4, 148.9, 145.4, 138.4, 126.7, 121.5, 120.7, 112.3, 109.1, 106.6, 35.6, 30.7, 22.6, 14.1.

HRMS *m/z* (GC-EI): calcd. For $C_{14}H_{16}O_1$ ([M]⁺): 200.119565; found: 200.1196.

pent-1-en-2-ylbenzene (68n)
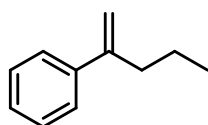
Prepared according to **GP6**, stirred for 18 h, eluent: pentane, 737 mg (82%), colorless oil.

R_F (100% hexanes) = 0.63.

¹H NMR (501 MHz, CDCl₃): δ = 7.43–7.39 (m, 2H), 7.35–7.30 (m, 2H), 7.29–7.24 (m, 1H), 5.28 (d, J = 1.6 Hz, 1H), 5.06 (q, J = 1.4 Hz, 1H), 2.49 (td, J = 7.5, 1.3 Hz, 2H), 1.55–1.43 (m, 2H), 0.93 (t, J = 7.4 Hz, 3H).

¹³C NMR (126 MHz, CDCl₃): δ = 148.7, 141.6, 128.4, 127.4, 126.3, 126.3, 112.3, 37.6, 21.5, 13.9.

HRMS *m/z* (GC-EI): calcd. For $C_{11}H_{14}$ ([M]⁺): 146.109000; found: 146.109020.

hept-1-en-2-ylbenzene (68o)
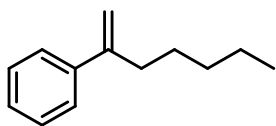
Prepared according to **GP6**, stirred for 18 h, eluent: pentane, 1.43 g (95%), colorless oil.

R_F (100% hexanes) = 0.63.

¹H NMR (501 MHz, CDCl₃): δ = 7.43–7.39 (m, 2H), 7.35–7.30 (m, 2H), 7.26 (tt, J = 6.9, 1.4 Hz, 1H), 5.26 (d, J = 1.6 Hz, 1H), 5.06 (q, J = 1.4 Hz, 1H), 2.50 (td, J = 7.6, 1.3 Hz, 2H), 1.50–1.41 (m, 2H), 1.36–1.24 (m, 4H), 0.94–0.84 (m, 3H).

¹³C NMR (126 MHz, CDCl₃): δ = 149.0, 141.7, 128.4, 127.4, 126.3, 112.1, 35.5, 31.7, 28.1, 22.6, 14.2.

HRMS *m/z* (GC-EI): calcd. For $C_{13}H_{18}$ ([M]⁺): 174.140300; found: 174.140370.

oct-1-en-2-ylbenzene (68p)

Prepared according to **GP6**, stirred for 18 h, eluent: pentane, 893 mg (79%), colorless oil.
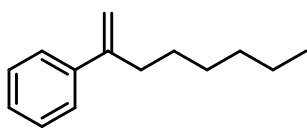
R_F (100% hexanes) = 0.63.

¹H NMR (501 MHz, CDCl₃): δ = 7.42–7.36 (m, 2H), 7.34–7.27 (m, 2H), 7.27–7.21 (m, 1H), 5.24 (d, J = 1.5 Hz, 1H), 5.04 (q, J = 1.4 Hz, 1H), 2.48 (td, J = 7.5, 1.3 Hz, 2H), 1.48–1.38 (m, 2H), 1.36–1.29 (m, 2H), 1.29–1.19 (m, 4H), 0.89–0.82 (m, 3H).

¹³C NMR (126 MHz, CDCl₃) δ 148.8, 141.5, 128.2, 127.2, 126.1, 111.9, 35.3, 31.6, 29.0, 28.2, 22.6, 14.0.

HRMS *m/z* (GC-EI): calcd. For $C_{14}H_{20}$ ([M]⁺): 188.155950; found: 188.155900.

5-methylene-6,7,8,9-tetrahydro-5*H*-benzo[7]annulene (68q)

Prepared according to **GP6**, stirred for 18 h, eluent: pentane, 649 mg (88%), colorless oil.

R_F (100% hexanes) = 0.60.
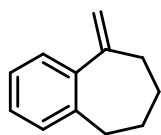
¹H NMR (501 MHz, CDCl₃): δ = 7.23–7.19 (m, 1H), 7.19–7.13 (m, 2H), 7.12–7.07 (m, 1H), 5.11 (dt, *J* = 2.1, 1.0 Hz, 1H), 4.99 (d, *J* = 2.2 Hz, 1H), 2.80–2.75 (m, 2H), 2.43–2.36 (m, 2H), 1.84 (td, *J* = 7.4, 4.5 Hz, 2H), 1.78–1.72 (m, 2H).

¹³C NMR (126 MHz, CDCl₃): δ = 153.0, 144.3, 140.4, 129.1, 128.3, 127.2, 126.2, 113.8, 36.7, 36.5, 31.6, 27.5.

HRMS *m/z* (GC-EI): calcd. For C₁₂H₁₄ ([M]⁺): 158.109000; found: 158.109170.

Synthesis of (6-chlorohex-1-en-2-yl)benzene (68r)
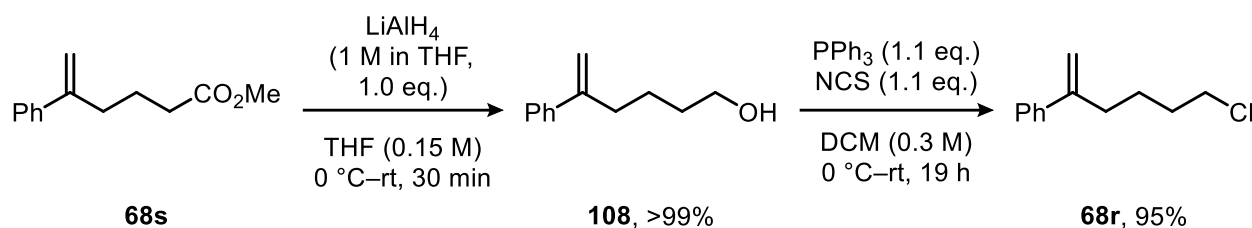
5-phenylhex-5-en-1-ol (108)
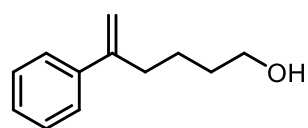
In a flame-dried Schlenk flask under argon methyl 5-phenylhex-5-enoate (**68s**, 806 mg, 3.95 mmol, 1.00 eq.) was dissolved in THF (26 mL) and cooled to 0 °C. LiAlH₄ (1 M in THF, 3.9 mL, 3.9 mmol, 0.99 eq.) was added dropwise and the resulting mixture was stirred at room temperature for 30 min. The reaction was quenched by the addition of 5% NaOH solution at 0 °C and subsequently extracted with DCM (3 x 30 mL). The combined organic layers were washed with water, dried over anhydrous Na₂SO₄ and concentrated under reduced pressure. The colorless oil (695 mg, >99%) was used without further purification.

¹H NMR (501 MHz, CDCl₃): δ = 7.42–7.37 (m, 2H), 7.36–7.29 (m, 2H), 7.29–7.24 (m, 1H), 5.27 (d, *J* = 1.5 Hz, 1H), 5.07 (q, *J* = 1.4 Hz, 1H), 3.63 (t, *J* = 6.5 Hz, 2H), 2.54 (td, *J* = 7.4, 1.3 Hz, 2H), 1.64–1.57 (m, 2H), 1.57–1.47 (m, 2H), 1.34 (s, 1H).

¹³C NMR (126 MHz, CDCl₃): δ = 148.5, 141.4, 128.4, 127.5, 126.3, 112.6, 63.0, 35.2, 32.5, 24.5.

HRMS *m/z* (GC-EI): calcd. For C₁₂H₁₆O₁ ([M]⁺): 176.119565; found: 176.119470.

(6-chlorohex-1-en-2-yl)benzene (68r)
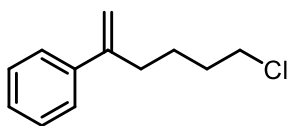
A flame-dried Schlenk flask under argon was charged with 5-phenylhex-5-en-1-ol (**108**, 438 mg, 2.49 mmol, 1.00 eq.) and dry DCM (8.3 mL). At 0 °C PPh$_3$ (708 mg, 2.70 mmol, 1.09 eq.) and NCS (361 mg, 2.70 mmol, 1.09 eq.) were added and the mixture was subsequently stirred at room temperature for 19 h. After addition of water the aqueous phase was extracted with DCM (3 x 20 mL). The combined organic layers were washed with water, dried over anhydrous Na$_2$SO$_4$ and concentrated under reduced pressure. Purification via flash column chromatography on silica gel (100% pentane) furnished the title compound as a colorless oil (459 mg, 95%).

R_F (100% hexanes) = 0.29.

1H NMR (501 MHz, CDCl$_3$): δ = 7.44–7.38 (m, 2H), 7.37–7.31 (m, 2H), 7.31–7.25 (m, 1H), 5.29 (s, 1H), 5.14–5.05 (m, 1H), 3.58–3.47 (m, 2H), 2.55 (t, J = 7.5 Hz, 2H), 1.87–1.75 (m, 2H), 1.69–1.56 (m, 2H).

13C NMR (126 MHz, CDCl$_3$): δ = 148.1, 141.2, 128.5, 127.6, 126.3, 112.8, 45.0, 34.7, 32.3, 25.5.

HRMS m/z (GC-EI): calcd. For C$_{12}$H$_{15}$Cl$_1$ ([M]$^+$): 194.085678; found: 194.085630.

methyl 5-phenylhex-5-enoate (68s)
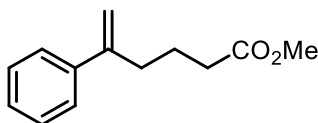
Prepared according to **GP6**, stirred for 4 h, eluent: 2% MTBE, pentane, 1.34 g (95%), colorless oil.

R_F (5% EtOAc, hexanes) = 0.29.

1H NMR (501 MHz, CDCl$_3$): δ = 7.42–7.38 (m, 2H), 7.36–7.30 (m, 2H), 7.29–7.24 (m, 1H), 5.30 (d, J = 1.4 Hz, 1H), 5.07 (q, J = 1.3 Hz, 1H), 3.66 (s, 3H), 2.55 (td, J = 7.5, 1.3 Hz, 2H), 2.34 (t, J = 7.4 Hz, 2H), 1.79 (p, J = 7.5 Hz, 2H).

13C NMR (126 MHz, CDCl$_3$): δ = 174.1, 147.6, 141.0, 128.5, 127.6, 126.2, 113.1, 51.6, 34.7, 33.5, 23.5.

HRMS m/z (GC-EI): calcd. For C$_{13}$H$_{16}$O$_2$ ([M]$^+$): 204.114480; found: 204.114500.

Synthesis of hepta-1,6-dien-2-ylbenzene (68t)

109, 77%   **103t**, 77%   **68t**, 91%
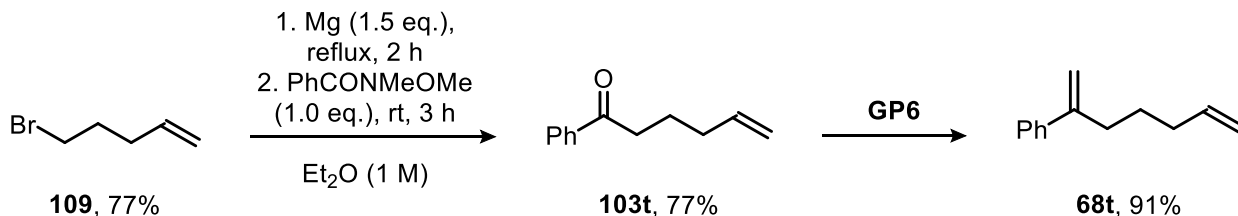
1-phenylhex-5-en-1-one (103t)
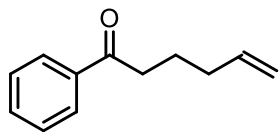
A flame-dried flask equipped with a reflux condenser under argon was charged with Mg (221 mg, 9.08 mmol, 1.50 eq.), Et$_2$O (8 mL), and a small crystal of I$_2$. The mixture was heated to reflux for 15 min until decolorized. 5-Bromopent-1-ene (**109**, 0.93 mL, 7.87 mmol, 1.30 eq.) was added dropwise at room temperature, and the reaction was heated to reflux for 2 h. After cooling to room temperature, N-methoxy-N-methylbenzamide (1.00 g, 6.05 mmol, 1.00 eq.) was added, and the mixture was stirred at ambient temperature for an additional 3 h. The reaction was quenched with 10% HCl (x mL) and stirred for 30 min. The aqueous layer was extracted with DCM (3 × 30 mL), and the combined organic layers were washed with water, dried over anhydrous Na$_2$SO$_4$, and concentrated under reduced pressure. Purification by flash column chromatography on silica gel (1% MTBE in pentane) afforded the title compound as a colorless oil (811 mg, 77%).

^{1}H NMR (501 MHz, CD$_2$Cl$_2$) δ 7.97–7.92 (m, 2H), 7.60–7.53 (m, 1H), 7.50–7.44 (m, 2H), 5.85 (ddt, J = 17.0, 10.2, 6.7 Hz, 1H), 5.05 (dq, J = 17.2, 1.7 Hz, 1H), 4.99 (ddt, J = 10.2, 2.3, 1.3 Hz, 1H), 2.98 (t, J = 7.3 Hz, 2H), 2.19–2.12 (m, 2H), 1.82 (p, J = 7.4 Hz, 2H).

^{13}C NMR (126 MHz, CD$_2$Cl$_2$): δ = 200.3, 138.7, 137.6, 133.2, 128.9, 128.3, 115.2, 38.1, 33.6, 23.7.

HRMS *m/z* (GC-EI): calcd. For C$_{12}$H$_{14}$O$_1$ ([M]$^+$): 174.103915; found: 174.103970.

hepta-1,6-dien-2-ylbenzene (68t)
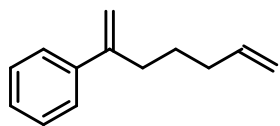
Prepared according to **GP6**, stirred for 4 h, eluent: pentane, 175 mg (91%), colorless oil.

R_F (100% hexanes) = 0.51.

^{1}H NMR (501 MHz, CDCl$_3$): δ = 7.43–7.38 (m, 2H), 7.36–7.30 (m, 2H), 7.29–7.24 (m, 1H), 5.81 (ddt, J = 17.0, 10.2, 6.7 Hz, 1H), 5.28 (d, J = 1.5 Hz, 1H), 5.07 (q, J = 1.4 Hz, 1H), 5.01 (dq, J = 17.2, 1.7 Hz, 1H), 4.96 (ddt, J = 10.2, 2.3, 1.2 Hz, 1H), 2.55–2.50 (m, 2H), 2.13–2.06 (m, 2H), 1.60–1.52 (m, 2H).

^{13}C NMR (126 MHz, CDCl$_3$): δ = 148.6, 141.5, 138.8, 128.4, 127.4, 126.3, 114.8, 112.5, 34.9, 33.5, 27.6.

HRMS *m/z* (GC-EI): calcd. For C$_{13}$H$_{16}$ ([M]$^+$): 172.124650; found: 172.124590.

Synthesis of (6-methylhepta-1,5-dien-2-yl)benzene (68u)
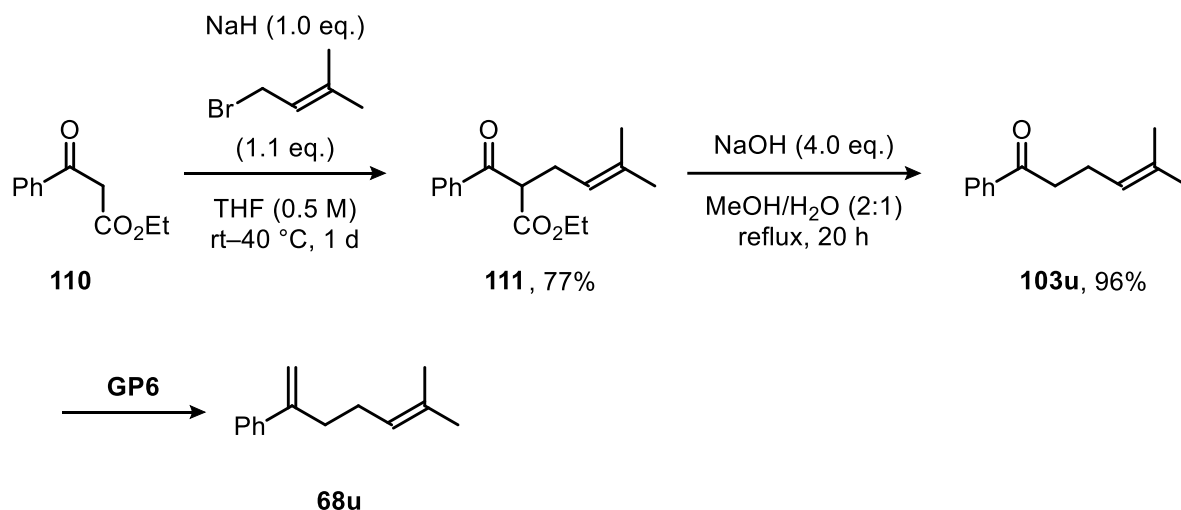
ethyl 2-benzoyl-5-methylhex-4-enoate (111)
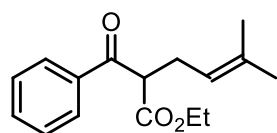
In a 100 mL two-neck flask under argon, β-ketoester **110** (2.00 g, 10.4 mmol, 1.00 eq.) was dissolved in dry THF (20 mL). NaH (60% in mineral oil, 416 mg, 10.4 mmol, 1.00 eq.) was added portionwise and the resulting mixture was stirred at room temperature for 1 h. 1-Bromo-3-methylbut-2-ene (1.32 mL, 11.4 mmol, 1.10 eq.) was added via syringe, and after 15 min of stirring, the mixture was heated to 40 °C and stirred overnight. After cooling to room temperature, the reaction was quenched by slow addition of saturated NaCl solution. The aqueous layer was extracted with EtOAc (3 × 30 mL), and the combined organic layers were dried over anhydrous Na$_2$SO$_4$, and concentrated under reduced pressure. Purification by flash column chromatography on silica gel (2–5% MTBE in pentane) afforded the title compound (2.10 g, 77%).

^{1}H NMR (501 MHz, CD$_2$Cl$_2$): δ = 7.98–7.93 (m, 2H), 7.62–7.57 (m, 1H), 7.51–7.47 (m, 2H), 5.10 (ddq, *J* = 8.8, 5.9, 1.5 Hz, 1H), 4.31 (dd, *J* = 7.8, 6.8 Hz, 1H), 4.13–4.09 (m, 2H), 2.72–2.60 (m, 2H), 1.65 (d, *J* = 1.4 Hz, 3H), 1.62 (d, *J* = 1.3 Hz, 3H), 1.16 (t, *J* = 7.1 Hz, 3H).

5-methyl-1-phenylhex-4-en-1-one (103u)
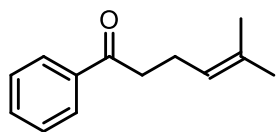
A one-neck flask was charged with ester **111** (2.00 g, 7.68 mmol, 1.00 eq.), NaOH (1.23 g, 30.7 mmol, 4.00 eq.), water (25 mL) and MeOH (50 mL). The reaction mixture was heated to reflux and stirred for 20 h. After cooling down to room temperature, MeOH was removed under reduced pressure, and the aqueous phase was extracted with

EtOAc. The combined organic layers were dried over anhydrous Na_2SO_4, and concentrated under reduced pressure. The crude (colorless oil) was used for the next step without further purification (1.39 g, 96%).

^{1}H NMR (501 MHz, CD_2Cl_2): δ = 7.96–7.92 (m, 2H), 7.59–7.54 (m, 1H), 7.49–7.44 (m, 2H), 5.18 (th, J = 7.3, 1.5 Hz, 1H), 3.02–2.96 (m, 2H), 2.43–2.34 (m, 2H), 1.69 (q, J = 1.4 Hz, 3H), 1.64 (d, J = 1.3 Hz, 3H), 1.53 (s, 2H).

(6-methylhepta-1,5-dien-2-yl)benzene (68u)
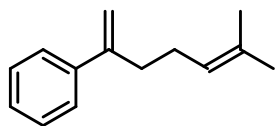
Prepared according to GP6, stirred for 1 h, eluent: pentane, colorless oil.

^{1}H NMR (501 MHz, CD_2Cl_2): δ = 7.43–7.39 (m, 2H), 7.34–7.30 (m, 2H), 7.28–7.23 (m, 1H), 5.27 (d, J = 1.6 Hz, 1H), 5.17–5.13 (m, 1H), 5.06 (q, J = 1.4 Hz, 1H), 2.55–2.49 (m, 2H), 2.13 (q, J = 7.5 Hz, 2H), 1.67 (d, J = 1.4 Hz, 3H), 1.54 (d, J = 1.2 Hz, 3H).

HRMS m/z (GC-EI): calcd. for $C_{14}H_{19}$ ([M]$^+$): 187.14813; found: 187.14812.

1-(hex-1-en-2-yl)-4-methoxybenzene (68v)
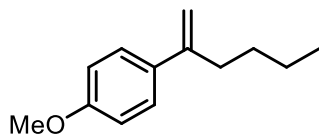
Prepared according to GP6, stirred for 1.5 h, eluent: 100% hexanes to 10% MTBE in hexanes, 1.77 g (92%), colorless oil.

^{1}H NMR (501 MHz, $CDCl_3$): δ = 7.39–7.32 (m, 2H), 6.89–6.83 (m, 2H), 5.19 (d, J = 1.7 Hz, 1H), 4.97 (d, J = 1.4 Hz, 1H), 3.81 (s, 3H), 2.51–2.43 (m, 2H), 1.43 (ddt, J = 8.6, 7.2, 5.4 Hz, 2H), 1.39–1.27 (m, 2H), 0.90 (t, J = 7.3 Hz, 3H).

^{13}C NMR (126 MHz, $CDCl_3$): δ = 159.1, 148.2, 134.0, 127.3, 113.7, 110.6, 55.4, 35.3, 30.7, 22.6, 14.1.

HRMS m/z (GC-EI): calcd. For $C_{13}H_{18}O$ ([M]$^+$): 190.135215, found: 190.135210.

1-(hex-1-en-2-yl)-4-(trifluoromethyl)benzene (68w)
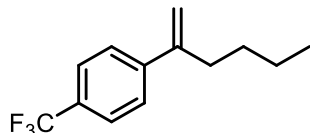
Prepared according to GP6, stirred for 18 h, eluent: hexanes, 528 mg (58%), colorless oil.

^{1}H NMR (501 MHz, $CDCl_3$): δ = 7.58 (d, J = 8.2 Hz, 2H), 7.49 (d, J = 8.2 Hz, 2H), 5.32 (d, J = 1.3 Hz, 1H), 5.15 (q, J = 1.3 Hz, 1H), 2.55–2.48 (m, 2H), 1.47–1.38 (m, 2H), 1.38–1.30 (m, 2H), 0.90 (t, J = 7.2 Hz, 3H).

^{19}F NMR (471 MHz, $CDCl_3$): δ = –62.5.

HRMS *m/z* (GC-EI): calcd. For $C_{13}H_{15}F_3$ ([M]$^+$): 228.112036, found: 228.112060.

1-(hex-1-en-2-yl)-2-methylbenzene (68x)
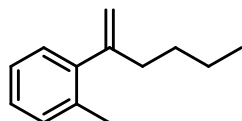
Prepared according to GP6, stirred for 3 h, eluent: pentane, 214 mg (>99%), colorless oil.

^{1}H NMR (501 MHz, CDCl$_3$): δ = 7.19–7.11 (m, 3H), 7.09–7.05 (m, 1H), 5.17 (q, *J* = 1.5 Hz, 1H), 4.87–4.82 (m, 1H), 2.36–2.30 (m, 2H), 2.30 (s, 3H), 1.43–1.29 (m, 4H), 0.89 (t, *J* = 7.1 Hz, 3H).

^{13}C NMR (126 MHz, CDCl$_3$): δ = 150.4, 143.5, 134.9, 130.2, 128.5, 126.8, 125.4, 113.6, 37.7, 30.2, 22.6, 20.0, 14.1.

HRMS *m/z* (GC-EI): calcd. For $C_{13}H_{18}$ ([M]$^+$): 174.140300, found: 174.140180.

Synthesis of 1-methyl-4-(6-methylhepta-1,5-dien-2-yl)benzene (68y)
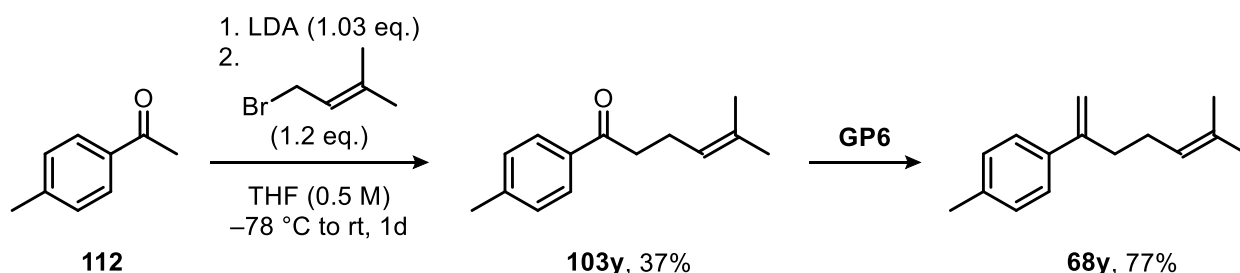
5-methyl-1-(p-tolyl)hex-4-en-1-one (103y)
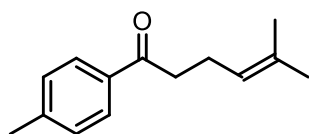
n-Butyllithium (2.5 M in heptane, 4.22 mL, 10.6 mmol, 1.03 eq.) was slowly added to a solution of diisopropylamine (1.54 mL, 11.0 mmol, 1.07 eq.) in anhydrous THF (20 mL) at –78 °C. The mixture was stirred for 1 h. After addition of ketone **112** (1.38 mL, 10.3 mmol, 1.00 eq.) and another hour of stirring at –78 °C, 1-bromo-3-methylbut-2-ene (1.41 mL, 12.2 mmol, 1.18 eq.) was added. The reaction mixture was stirred overnight slowly reaching room temperature. The reaction was quenched by addition of 0.5 M HCl, the aqueous layer was extracted with MTBE (3 x 30 mL), and the combined organic phases were washed with brine, dried over anhydrous Na$_2$SO$_4$, and concentrated under reduced pressure. Purification by flash column chromatography on silica gel (1% MTBE in pentane) afforded the title compound as a colorless oil (771 mg, 37%).

¹H NMR (501 MHz, CDCl₃): δ = 7.89–7.83 (m, 2H), 7.27–7.22 (m, 2H), 5.17 (tp, *J* = 7.3, 1.5 Hz, 1H), 2.96 (dd, *J* = 8.0, 7.0 Hz, 2H), 2.44–2.37 (m, 5H), 1.69 (d, *J* = 1.4 Hz, 3H), 1.63 (d, *J* = 1.3 Hz, 3H).

¹³C NMR (126 MHz, CDCl₃): δ = 199.9, 143.8, 134.7, 132.8, 129.4, 128.3, 123.2, 38.8, 25.8, 23.2, 21.8, 17.8.

HRMS *m/z* (GC-EI): calcd. For $C_{14}H_{18}O_1$ ([M]⁺): 202.135215, found: 202.135070.

1-methyl-4-(6-methylhepta-1,5-dien-2-yl)benzene (68y)
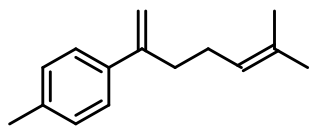
Prepared according to GP6, stirred for 4 h, eluent: pentane, 588 mg (77%), colorless oil.

¹H NMR (501 MHz, CDCl₃): δ = 7.31 (d, *J* = 8.2 Hz, 2H), 7.14 (d, *J* = 7.9 Hz, 2H), 5.26 (d, *J* = 1.5 Hz, 1H), 5.18–5.13 (m, 1H), 5.02 (d, *J* = 1.4 Hz, 1H), 2.53–2.47 (m, 2H), 2.35 (s, 3H), 2.14 (q, *J* = 7.5 Hz, 2H), 1.69 (d, *J* = 1.3 Hz, 3H), 1.56 (d, *J* = 1.3 Hz, 3H).

¹³C NMR (126 MHz, CDCl₃): δ = 148.3, 138.5, 137.1, 131.9, 129.1, 126.1, 124.1, 111.5, 35.6, 27.2, 25.8, 21.2, 17.9.

HRMS *m/z* (GC-EI): calcd. For $C_{15}H_{20}$ ([M]⁺): 200.155950, found: 200.156120.

but-1-en-2-ylbenzene (68z)
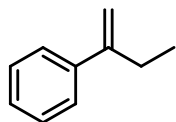
Prepared according to GP6, stirred for 1 h, eluent: pentane, 1.90 g (95%), colorless oil.

¹H NMR (501 MHz, CDCl₃): δ = 7.46–7.39 (m, 2H), 7.37–7.31 (m, 2H), 7.30–7.25 (m, 1H), 5.28 (s, 1H), 5.07 (s, 1H), 2.58–2.48 (m, 2H), 1.12 (t, *J* = 7.4 Hz, 3H).

(1-cyclohexylvinyl)benzene (68ab)
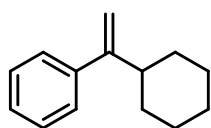
Prepared according to GP6, stirred for 1 h, eluent: hexanes, 962 mg (57%), colorless oil.

¹H-NMR (501 MHz, CD₂Cl₂): δ = 7.4–7.3 (m, 4H), 7.3–7.2 (m, 1H), 5.1 (d, *J* = 1.3 Hz, 1H), 5.0 (t, *J* = 1.4 Hz, 1H), 2.5–2.4 (m, 1H), 1.8 (ddt, *J* = 22.0, 12.8, 2.8 Hz, 4H), 1.7 (dddd, *J* = 11.4, 5.1, 3.3, 1.7 Hz, 1H), 1.3 (qt, *J* = 12.8, 3.1 Hz, 2H), 1.3–1.1 (m, 3H).

¹³C NMR (126 MHz, CD₂Cl₂): δ = 155.2, 142.9, 128.1, 126.9, 126.5, 110.0, 42.5, 32.7, 26.8, 26.4.

HRMS *m/z* (GC-EI): calcd. For $C_{14}H_{18}$ ([M]$^+$): 186.140300, found: 186.140530.

(4-methylpent-1-en-2-yl)benzene (68ac)
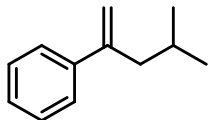
Prepared according to GP6, stirred for 4 h, eluent: pentane, 1.13 g (77%), colorless oil.

¹H NMR (501 MHz, CDCl$_3$): δ = 7.42–7.38 (m, 2H), 7.35–7.30 (m, 2H), 7.28–7.24 (m, 1H), 5.26 (d, *J* = 1.8 Hz, 1H), 5.03 (q, *J* = 1.3 Hz, 1H), 2.39 (dd, *J* = 7.2, 1.2 Hz, 2H), 1.72–1.62 (m, 1H), 0.89 (s, 3H), 0.87 (s, 3H).

¹³C NMR (126 MHz, CDCl$_3$): δ = 148.0, 141.6, 128.3, 127.3, 126.4, 113.6, 45.3, 26.5, 22.5.

HRMS *m/z* (GC-EI): calcd. For $C_{12}H_{16}$ ([M]$^+$): 160.12465, found: 160.12443.

(5-methylhex-1-en-2-yl)benzene (68ad)
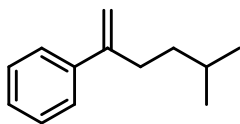
Prepared according to GP6, stirred for 4 h, eluent: pentane, 923 mg (86%), colorless oil.

¹H NMR (501 MHz, CDCl$_3$): δ = 7.43–7.39 (m, 2H), 7.35–7.31 (m, 2H), 7.29–7.24 (m, 1H), 5.26 (d, *J* = 1.5 Hz, 1H), 5.06 (q, *J* = 1.4 Hz, 1H), 2.54–2.48 (m, 2H), 1.65–1.55 (m, 1H), 1.38–1.31 (m, 2H), 0.91 (s, 3H), 0.90 (s, 3H).

¹³C NMR (126 MHz, CDCl$_3$): δ = 149.2, 141.7, 128.4, 127.4, 126.2, 112.0, 37.7, 33.4, 28.0, 22.7.

HRMS *m/z* (GC-EI): calcd. For $C_{13}H_{18}$ ([M]$^+$): 174.140300, found: 174.140360.

(3,3-dimethylbut-1-en-2-yl)benzene (68ae)
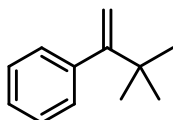
Prepared according to GP6, stirred for 16 h, eluent: hexanes, 1.42 g (85%), colorless oil.

¹H NMR (501 MHz, CD$_2$Cl$_2$): δ = 7.3–7.2 (m, 3H), 7.1–7.1 (m, 2H), 5.2 (d, *J* = 1.6 Hz, 1H), 4.7 (d, *J* = 1.7 Hz, 1H), 1.1 (s, 9H).

¹³C NMR (126 MHz, CD2Cl2): δ = 160.4, 144.0, 129.4, 127.7, 126.6, 111.7, 36.4, 29.9.

HRMS *m/z* (GC-EI): calcd. For $C_{12}H_{16}$ ([M]$^+$): 160.124650, found: 160.124530.

hex-1-en-5-yn-2-ylbenzene (68af), hept-1-en-6-yn-2-ylbenzene (68ag)

n = 1 **113**
n = 2 **114**

n = 1 **115**
n = 2 **116**

n = 1 **103af**, 71% *o2s*
n = 2 **103ag**, 85% *o2s*

n = 1 **68af**, 91%
n = 2 **68ag**, 92%
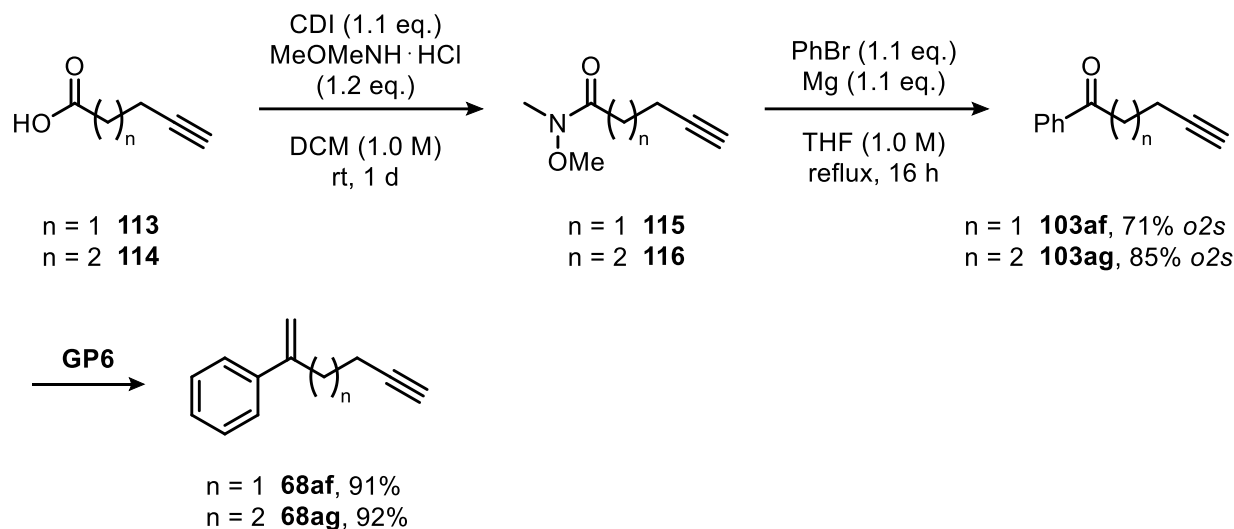
Hex-1-en-5-yn-2-ylbenzene (**68af**) and hept-1-en-6-yn-2-ylbenzene (**68ag**) were synthesized according to a three step literature procedure starting from pent-4-ynoic acid and hex-5-ynoic acid, respectively.[300] The NMR-spectroscopic data were in agreement with the literature reports.[300,301]

Synthesis of *N*-methoxy-*N*-methyl-6-phenylhept-6-enamide (68ah)

117

103ah, 66%

68ah, 78%
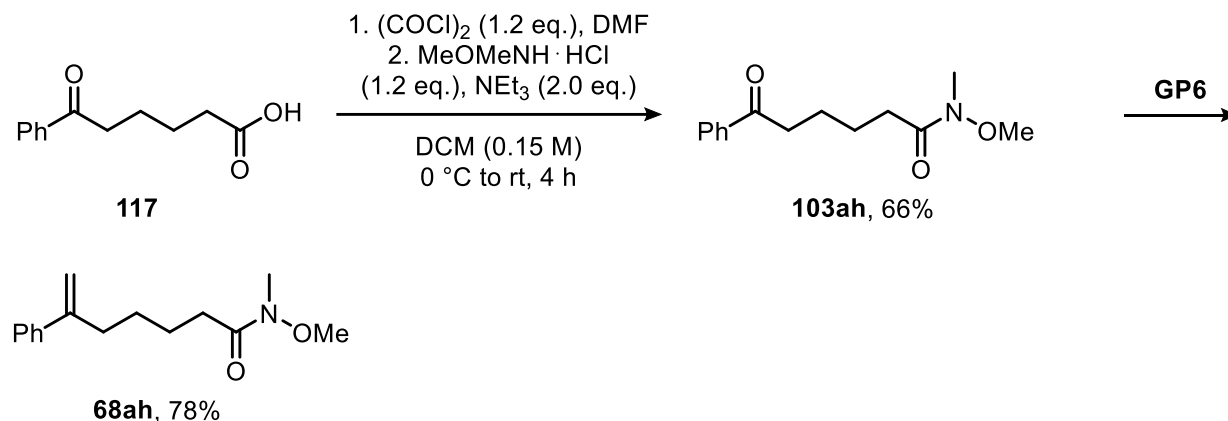
_N_-methoxy-_N_-methyl-6-oxo-6-phenylhexanamide (103ah)
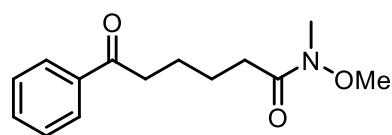
In a flame-dried Schlenk flask under argon, carboxylic acid **117** (1.01 g, 4.90 mmol, 1.00 eq.) was suspended in dry DCM (10 mL), cooled to 0 °C, and one drop of DMF was added. Oxalyl chloride (0.51 mL, 5.88 mL, 1.20 eq.) was then added slowly at 0 °C. The reaction mixture

was stirred at room temperature for 1 h. The mixture was transferred to a 100 mL round-bottom flask and concentrated under reduced pressure. The resulting crude acid chloride was redissolved in dry DCM (5 mL, plus 5 mL for rinsing) and added to a second flame-dried Schlenk flask containing N,O-dimethylhydroxylamine hydrochloride (574 mg, 5.88 mmol, 1.20 eq.) in DCM (20 mL) at 0 °C. Et$_3$N (1.4 mL, 9.8 mmol, 2.0 eq.) was added dropwise at 0 °C, after which the mixture was warmed to room temperature and stirred for 3 h. The reaction was quenched with saturated NH$_4$Cl (30 mL) solution and extracted with DCM (3 x 20 mL). The combined organic layers were washed with water, dried over anhydrous Na$_2$SO$_4$, and concentrated. Purification by flash column chromatography on silica gel (20–30% EtOAc in CyH) afforded the title compound as a yellow oil (807 mg, 66%).

^{1}H NMR (501 MHz, CDCl$_3$): δ = 7.97–7.93 (m, 2H), 7.58–7.53 (m, 1H), 7.49–7.43 (m, 2H), 3.68 (s, 3H), 3.18 (s, 3H), 3.01 (t, J = 7.1 Hz, 2H), 2.49 (t, J = 7.2 Hz, 2H), 1.85–1.70 (m, 4H).

HRMS m/z (GC-ESI): calcd. For C$_{14}$H$_{19}$N$_1$Na$_1$O$_3$ ([M+Na]$^+$): 272.12571, found: 272.12581.

N-methoxy-N-methyl-6-phenylhept-6-enamide (68ah)
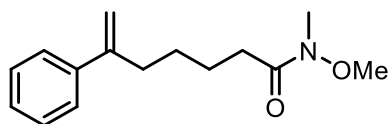
Prepared according to GP6, stirred for 6 h, eluent: 5–30% MTBE in pentane, 465 mg (78%), colorless oil.

^{1}H NMR (501 MHz, CDCl$_3$): δ = 7.41–7.38 (m, 2H), 7.34–7.30 (m, 2H), 7.28–7.24 (m, 1H), 5.26 (d, J = 1.4 Hz, 1H), 5.07 (q, J = 1.4 Hz, 1H), 3.65 (s, 3H), 3.16 (s, 3H), 2.54 (td, J = 7.5, 1.3 Hz, 2H), 2.41 (t, J = 7.6 Hz, 2H), 1.73–1.63 (m, 2H), 1.56–1.46 (m, 2H).

^{13}C NMR (126 MHz, CDCl$_3$): δ = 148.4, 141.4, 128.4, 127.4, 126.3, 112.5, 61.3, 35.3, 31.9, 28.1, 24.4.

HRMS m/z (GC-EI): calcd. For C$_{15}$H$_{21}$N$_1$O$_2$ ([M]$^+$): 247.156679, found: 247.156770.

1,1-dimethyl-3-methylenecyclohexane (68ai)
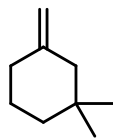
Prepared according to GP6, stirred for 3 h, eluent: pentane, 764 mg (78%), colorless oil.

**^{1}H NMR** (501 MHz, CDCl$_3$): δ = 4.67–4.64 (m, 1H), 4.56–4.53 (m, 1H), 2.06 (tt, J = 6.5, 1.0 Hz, 2H), 1.89 (d, J = 1.2 Hz, 2H), 1.57–1.51 (m, 2H), 1.34–1.31 (m, 2H), 0.88 (s, 6H).

^{13}C NMR (126 MHz, CDCl$_3$): δ = 148.2, 108.2, 48.8, 39.2, 35.0, 28.6, 23.8, 22.5, 14.2.

HRMS m/z (GC-EI): calcd. For C$_9$H$_{16}$ ([M]$^+$): 124.124650, found: 124.124800.

(*E*)- and (*Z*)-2-(hex-2-en-2-yl)naphthalene (70k)
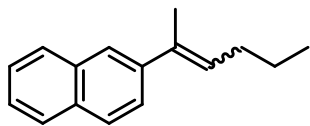
A flame-dried Schlenk flask under argon was charged with *n*-butyltriphenylphosphonium bromide (1.70 g, 4.26 mmol, 1.00 eq.) and anhydrous THF (8.5 mL). The suspension was cooled to 0 °C, and *n*-BuLi (2.5 M in heptane, 1.7 mL, 4.26 mmol, 1.00 eq.) was added dropwise. After stirring the resulting solution at 0 °C for 15 min, 1-(naphthalen-2-yl)ethan-1-one (1.01 g, 5.11 mmol, 1.20 eq.) dissolved in 4 mL THF was added. The reaction was then warmed to room temperature and stirred overnight (18 h). By addition of saturated ammonium chloride solution, the reaction was quenched. The aqueous phase was extracted with Et$_2$O (3 x 30 mL), and the combined organic layers were washed with brine, dried over anhydrous Na$_2$SO$_4$ and concentrated under reduced pressure. Purification by flash column chromatography on silica gel (100% pentane) yielded the pure *E*-isomer (69 mg, 8%) and *Z*-isomer (82 mg, 9%) of **70k**, along with a mixed fraction (*E/Z* = 39:61, 222 mg, 25%), all as colorless oils.

E-isomer:

^{1}H NMR (501 MHz, CDCl$_3$): δ = 7.85–7.75 (m, 4H), 7.60 (dd, *J* = 8.6, 1.9 Hz, 1H), 7.49–7.39 (m, 2H), 5.97 (td, *J* = 7.2, 1.4 Hz, 1H), 2.25 (qd, *J* = 7.3, 1.0 Hz, 2H), 2.15 (q, *J* = 1.0 Hz, 3H), 1.54 (h, *J* = 7.4 Hz, 2H), 1.00 (t, *J* = 7.4 Hz, 3H).

^{13}C NMR (126 MHz, CDCl$_3$): δ = 141.4, 134.7, 133.7, 132.5, 129.4, 128.1, 127.7, 127.6, 126.1, 125.5, 124.6, 124.0, 31.2, 23.0, 16.0, 14.1.

HRMS *m/z* (GC-EI): calcd. For C$_{16}$H$_{18}$ ([M]$^+$): 210.140300; found: 210.140110.

Z-isomer:

^{1}H NMR (501 MHz, CDCl$_3$): δ = 7.86–7.78 (m, 3H), 7.63 (d, *J* = 1.7 Hz, 1H), 7.51–7.42 (m, 2H), 7.34 (dd, *J* = 8.4, 1.7 Hz, 1H), 5.56 (ddt, *J* = 7.4, 5.9, 1.5 Hz, 1H), 2.12 (q, *J* = 1.4 Hz, 3H), 2.01 (qd, *J* = 7.3, 1.3 Hz, 2H), 1.38 (h, *J* = 7.4 Hz, 2H), 0.85 (t, *J* = 7.4 Hz, 3H).

^{13}C NMR (126 MHz, CDCl$_3$): δ = 140.0, 136.2, 133.5, 132.3, 128.4, 128.0, 127.7, 127.6, 126.9, 126.6, 126.0, 125.6, 31.4, 25.8, 23.4, 14.0.

HRMS *m/z* (GC-EI): calcd. For C$_{16}$H$_{18}$ ([M]$^+$): 210.140300; found: 210.140400.

4.3.3 Asymmetric Ionic Hydrogenation of α-Alkyl Styrenes

Racemate Syntheses

For the racemate syntheses of compounds **69a–69g**, **69i**, **69n–69q**, **69s**, **69v**, **69z**, **69aa**, **69ab**, **69ai** the respective styrene (0.030 mmol, 1.00 eq.) was added to a GC vial filled with TFA (0.1 mL) and Et₃SiH (0.033 mmol, 1.10 eq.) and stirred at room temperature for 90 min to 24 h until TLC indicated full consumption of the starting material. Subsequent preparative thin-layer chromatography furnished the isolated racemic products that were used for the determination of the enantiomeric ratio by GC analysis.

For racemic compounds **69h**, **69j** and **69k** the respective styrene (0.030 mmol, 1.00 eq.) was added to a GC vial filled with $HNTf_2$ (0.2 M in DCM, 5 mol%), benzoic acid (0.036 mmol, 1.20 eq.), Et_3SiH (0.036 mmol, 1.20 eq.) and DCM (0.15 mL) and stirred at rt for 90 min to 24 h until TLC indicated full consumption of the starting material. Subsequent preparative thin-layer chromatography furnished the isolated racemic products that were used for the determination of the enantiomeric ratio by GC analysis.

For the racemate synthesis of compounds **69l** and **69m**, the respective styrene (0.030 mmol, 1.00 eq.) was added to a GC vial filled with a 1:1 mixture of (*S*,*S*)- and (*R*,*R*)-IDPi **75a** (2 mol%), benzoic acid (0.036 mmol, 1.20 eq.), $PhMe_2SiH$ (0.15 mmol, 5.0 eq.) and CyMe (0.06 mL) and stirred at rt for 24 h. Subsequent preparative thin-layer chromatography furnished the isolated racemic products that were used for the determination of the enantiomeric ratio by GC analysis.

To obtain racemic compound **69t** a literature procedure starting from 3-phenylbutanal was followed.[302]

For racemic compound **69r** the respective styrene (0.030 mmol, 1.00 eq.) was dissolved in dry THF (0.6 mL) in a GC vial. Pd/C (10%, 5 mol%) was added and the reaction mixture was stirred at room temperature under a H_2 atmosphere for 3 h. The mixture was filtered over Celite and concentrated to furnish the racemic product for subsequent GC analysis.

For racemic compound **69u** and **69y** the respective styrene (0.030 mmol, 1.00 eq.) was dissolved in dry THF (0.6 mL) in a GC vial. $Pd/BaSO_4$ (10%, 5 mol%) was added and the reaction mixture was stirred at room temperature under a H_2 atmosphere for 30 min. The mixture was filtered over Celite and concentrated to furnish the racemic product for subsequent GC analysis.

General Procedure 7 (GP7)
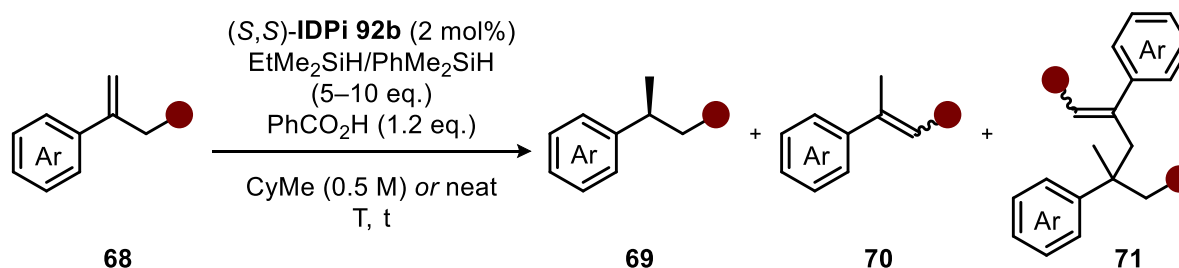
A 2 mL GC vial equipped with a magnetic stirring bar was charged with (*S,S*)-**IDPi 92b** (2 mol%), benzoic acid (0.24 mmol, 1.20 eq.) and then placed under argon. CyMe (0.4 mL) and the respective silane, EtMe₂SiH or PhMe₂SiH (1.0–2.0 mmol, 5.0–10 eq.), were added. After cooling the reaction mixture to –78 °C, the corresponding styrene (**68**, 0.20 mmol, 1.00 eq.) was added via syringe. The cap was replaced under argon, and the reaction vial was stirred at the specified temperature for the indicated duration. The reaction was quenched by adding pyridine (5 µL), followed by the addition of dibromomethane (7 µL, 0.10 mmol, 0.50 eq.) as an internal standard. The composition of the reaction mixture was analyzed via ^{1}H NMR spectroscopy of an aliquot in C₆D₆. The crude reaction mixture was then directly purified by flash column chromatography on AgNO₃-impregnated silica gel.

Note: AgNO₃-impregnated silica gel was prepared by adding a solution of AgNO₃ (10 g in 10 mL of Millipore water) to 100 g of silica gel (Merck, 60 Å, 230−400 mesh, particle size 0.040−0.063 mm) suspended in 200 mL of Millipore water, yielding a 10% AgNO₃ on silica gel mixture. The suspension was shaken, and the water was evaporated under reduced pressure using a rotary evaporator at 55 °C in a dark environment. The resulting material was further dried in an oven at 100 °C for 48 hours.

General Procedure 8 (GP8)

A 2 mL GC vial equipped with a magnetic stirring bar was charged with (*S,S*)-**IDPi 92b** (2 mol%), benzoic acid (0.030 mmol, 1.2 eq.) and then placed under argon. CyMe (0.05 mL) and the respective silane, EtMe₂SiH or PhMe₂SiH (0.125–0.250 mmol, 5.0–10 eq.), were added. After cooling the reaction mixture to –78 °C, the corresponding styrene (**68**, 0.025 mmol, 1.0 eq.) was added via syringe. The cap was replaced under argon, and the reaction vial was stirred at the specified temperature for the indicated duration. The reaction was quenched by adding pyridine (5 µL), followed by the addition of mesitylene (3 µL, 0.022 mmol, 0.86 eq.) as an internal standard. An aliquot of the mixture was taken and diluted with C₆D₆ for subsequent ^{1}H NMR analysis. The remaining solution was used for preparative thin layer chromatography (pentane) to purify the chiral product. Chiral GC analysis was performed to give the corresponding enantiomeric ratio.

For the spectral identification of desired product **69**, isomer **70**, and dimer **71** in the ^{1}H NMR spectra of the individual reaction crudes, these species were characterized in C_6D_6 using the model substrate hex-1-en-2-ylbenzene (**68a**) and subsequently assigned by analogy for other substrates.

hexan-2-ylbenzene (69a)
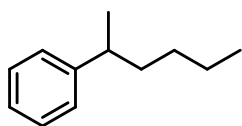
^{1}**H NMR** (501 MHz, C_6D_6): δ = 7.22–7.17 (m, 2H), 7.11–7.07 (m, 3H), 2.59–2.48 (m, 1H), 1.58–1.49 (m, 1H), 1.49–1.41 (m, 1H), 1.27–1.07 (m, 7H), 0.81 (t, J = 7.1 Hz, 3H).

^{13}**C NMR** (126 MHz, C_6D_6): δ = 148.0, 128.7, 127.3, 126.2, 40.4, 38.5, 30.3, 23.2, 22.7, 14.2.

HRMS m/z (GC-EI): calcd. For $C_{12}H_{18}$ ([M]$^+$): 162.140300; found: 162.140400.

hex-2-en-2-ylbenzene (70a)
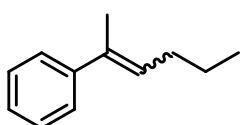
E-isomer:

^{1}**H NMR** (501 MHz, C_6D_6): δ = 7.37–7.33 (m, 2H), 7.21–7.17 (m, 2H), 7.13–7.08 (m, 1H), 5.79 (tq, J = 7.2, 1.4 Hz, 1H), 2.06 (qd, J = 7.2, 1.0 Hz, 2H), 1.91 (s, 3H), 1.43–1.34 (m, 2H), 0.89 (t, J = 7.3 Hz, 3H).

^{13}**C NMR** (126 MHz, C_6D_6): δ = 144.5, 135.4, 128.5, 128.5, 126.8, 126.1, 31.1, 23.2, 15.9, 14.1.

Z-isomer:

^{1}**H NMR** (501 MHz, C_6D_6): δ = 7.18 (d, J = 5.7 Hz, 4H), 7.12–7.05 (m, 1H), 5.45 (tq, J = 7.3, 1.4 Hz, 1H), 2.05–1.97 (m, 5H), 1.36–1.27 (m, 2H), 0.79 (t, J = 7.4 Hz, 3H).

^{13}**C NMR** (126 MHz, C_6D_6): δ = 142.7, 136.6, 128.4, 128.4, 126.8, 31.6, 25.8, 23.7, 14.0.

HRMS m/z (GC-EI): calcd. For $C_{12}H_{16}$ ([M]$^+$): 160.124650; found: 160.124810.

(7-methylundec-4-ene-5,7-diyl)dibenzene (71a)

The dimer was isolated as a mixture of isomers with a ratio of *E/Z* ≈ 1:2.

^{1}**H NMR** (600 MHz, C_6D_6): δ = 7.24–7.21 (m, 2H$_{min}$), 7.21–7.17 (m, 2H$_{min}$, 2H$_{maj}$), 7.15–7.08 (m, 4H$_{min}$, 4H$_{maj}$), 7.07–6.99 (m, 2H$_{min}$, 4H$_{maj}$), 5.57 (t, J = 7.2 Hz, 1H$_{min}$), 5.26 (t, J = 7.4 Hz, 1H$_{maj}$), 2.87 (d, J = 13.7 Hz, 1H$_{min}$), 2.82 (d, J = 13.7 Hz, 1H$_{min}$), 2.80 (d, J = 13.5 Hz, 1H$_{maj}$), 2.72 (d, J = 13.5 Hz, 1H$_{maj}$), 1.92 (q,
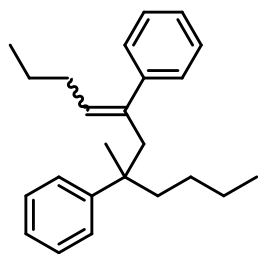
J = 7.4 Hz, 2H$_{maj}$), 1.91–1.81 (m, 2H$_{min}$), 1.77 (td, J = 13.8, 4.2 Hz, 1H$_{min}$), 1.68 (td, J = 13.8, 4.4 Hz, 1H$_{maj}$), 1.49–1.41 (m, 1H$_{min}$, 1H$_{maj}$), 1.30–1.17 (m, 5H$_{min}$, 5H$_{maj}$), 1.15–0.99 (m, 3H$_{min}$, 3H$_{maj}$), 0.95–0.89 (m, 1H$_{min}$, 1H$_{maj}$), 0.84 (t, J = 7.4 Hz, 3H$_{min}$), 0.74 (t, J = 7.2 Hz, 3H$_{maj}$), 0.73 (t, J = 7.4 Hz, 3H$_{maj}$), 0.72 (t, J = 7.2 Hz, 3H$_{min}$).

^{13}C NMR (151 MHz, C$_6$D$_6$): δ = 148.0, 148.0, 146.7, 142.8, 138.7, 138.3, 133.9, 132.1, 129.1, 128.1, 128.0, 127.3, 127.0, 126.9, 126.3, 126.3, 125.7, 125.5, 53.2, 44.5, 43.1, 43.1, 42.5, 42.3, 31.6, 31.3, 26.9, 26.8, 24.6, 24.5, 23.8, 23.8, 23.6, 23.2, 14.2, 14.1, 14.1, 13.9.

HRMS *m/z* (GC-CI): calcd. For C$_{24}$H$_{36}$N$_1$ ([M+NH$_4$]$^+$): 338.284224; found: 338.284550.

(*S*)-hexan-2-ylbenzene (69a)
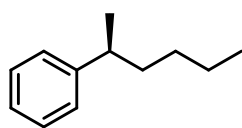
Prepared according to GP7 using EtMe$_2$SiH (10 eq.) under neat reaction conditions at –20 °C for 4 d, eluent: pentane, 14.5 mg (44%), colorless oil.

^{1}H NMR analysis of the crude: 76% conv., 67% **69a**, 3% **70a**, 3% **71a**.

R_F (100% hexanes) = 0.72.

^{1}H NMR (501 MHz, CD$_2$Cl$_2$): δ = 7.27 (t, J = 7.6 Hz, 2H), 7.20–7.13 (m, 3H), 2.67 (qt, J = 7.1, 7.1 Hz, 1H), 1.63–1.53 (m, 2H), 1.33–1.21 (m, 6H), 1.19–1.08 (m, 1H), 0.85 (t, J = 7.0 Hz, 2H).

^{13}C NMR (126 MHz, CD$_2$Cl$_2$): δ = 148.5, 128.6, 127.4, 126.1, 40.3, 38.5, 30.4, 23.2, 22.6, 14.2.

HRMS *m/z* (GC-EI): calcd. For C$_{12}$H$_{18}$ ([M]$^+$): 162.140300; found: 162.140400.

GC (30 m Cyclosil B, injection temperature: 220 °C, 90 °C iso 30 min, 1 °C/min, 100 °C iso 5 min, 8 °C/min, 220 °C iso 5 min, 0.5 bar H$_2$): t$_{R1}$ = 38.6 min (major), t$_{R2}$ = 39.5 min (minor), er = 95:5 (90% ee).

$[\alpha]_D^{25}$ = +18.7 (c = 0.27, CHCl$_3$). Literature data for (*S*) enantiomer[303]: (89% ee) $[\alpha]_D^{20}$ = +20.6 (c = 0.01, hexane).

(*S*)-1-(hexan-2-yl)-4-methylbenzene (69b)
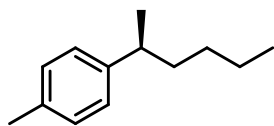
Prepared according to GP7 using EtMe$_2$SiH (10 eq.) under neat reaction conditions at –50 °C for 5 d, eluent: pentane, 21.8 mg (62%), colorless oil.

^{1}H NMR analysis of the crude: 98% conv., 76% **69b**, 1% **70b**, 10% **71b**.

R_F (100% hexanes) = 0.71.

¹H NMR (501 MHz, CD₂Cl₂): δ = 7.11–7.04 (m, 4H), 2.63 (qt, *J* = 7.0, 7.0 Hz, 1H), 2.30 (s, 3H), 1.58–1.50 (m, 2H), 1.33–1.18 (m, 6H), 1.16–1.06 (m, 1H), 0.85 (t, *J* = 7.2 Hz, 3H).

¹³C NMR (126 MHz, CD₂Cl₂): δ = 145.4, 135.5, 129.2, 127.2, 39.9, 38.6, 30.4, 23.2, 22.7, 21.1, 14.2.

HRMS *m/z* (GC-EI): calcd. For $C_{13}H_{20}$ ([M]⁺): 176.155950; found: 176.156030.

GC (30 m Cyclosil B, injection temperature: 220 °C, 90 °C iso 30 min, 1 °C/min, 100 °C iso 5 min, 8 °C/min, 220 °C iso 5 min, 0.5 bar H₂): t_{R1} = 51.1 min (major), t_{R2} = 51.4 min (minor), er = 93.5:6.5 (87% ee).

$[\alpha]_D^{25}$ = +18.9 (c = 0.27, CHCl₃).

(*S*)-1-(hexan-2-yl)-3-methylbenzene (69c)
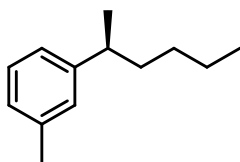
Prepared according to GP7 using EtMe₂SiH (5 eq.) in CyMe (0.5 M) at –20 °C for 3 d, eluent: pentane, 26.9 mg (76%), colorless oil.

¹H NMR analysis of the crude: 93% conv., 79% **69c**, 3% **70c**, 6% **71c**.

R_F (100% hexanes) = 0.72.

¹H NMR (501 MHz, CD₂Cl₂): δ = 7.15 (t, *J* = 7.5 Hz, 1H), 7.01–6.94 (m, 3H), 2.62 (qt, *J* = 7.1, 7.1 Hz, 1H), 2.32 (s, 3H), 1.58–1.52 (m, 2H), 1.33–1.17 (m, 6H), 1.17–1.08 (m, 1H), 0.85 (t, *J* = 7.1 Hz, 3H).

¹³C NMR (126 MHz, CD₂Cl₂): δ = 148.5, 138.2, 128.5, 128.2, 126.8, 124.4, 40.3, 38.5, 30.4, 23.2, 22.6, 21.6, 14.2.

HRMS *m/z* (GC-EI): calcd. For $C_{13}H_{20}$ ([M]⁺): 176.155950; found: 176.155980.

GC (25 m Lipodex-G, injection temperature: 220 °C, 80 °C iso 20 min, 8 °C/min, 220 °C iso 3 min, 0.6 bar H₂): t_{R1} = 16.7 min (minor), t_{R2} = 17.9 min (major), er = 96:4 (92% ee).

$[\alpha]_D^{25}$ = +19.0 (c = 0.26, CHCl₃).

(*S*)-1-ethyl-3-(hexan-2-yl)benzene (69d)
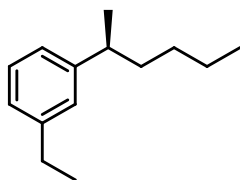
Prepared according to GP7 using EtMe₂SiH (10 eq.) under neat reaction conditions at –20 °C for 3 d, eluent: pentane, 26.5 mg (70%), colorless oil.

¹H NMR analysis of the crude: >99% conv., 95% **69d**, 4% **70d**, 1% **71d**.

R_F (100% hexanes) = 0.72.

¹H NMR (501 MHz, CD₂Cl₂): δ = 7.18 (t, *J* = 7.4 Hz, 1H), 7.03–6.97 (m, 3H), 2.68–2.57 (m, 3H), 1.61–1.53 (m, 2H), 1.33–1.19 (m, 9H), 1.17–1.10 (m, 1H), 0.85 (t, *J* = 7.1 Hz, 3H).

¹³C NMR (126 MHz, CD₂Cl₂): δ = 148.5, 144.7, 128.5, 127.1, 125.6, 124.6, 40.3, 38.5, 30.4, 29.3, 23.2, 22.6, 15.9, 14.2.

HRMS *m/z* (GC-EI): calcd. For $C_{14}H_{22}$ ([M]⁺): 190.171600; found: 190.171460.

GC (25 m Lipodex-G, injection temperature: 220 °C, 75 °C iso 45 min, 8 °C/min, 220 °C iso 3 min, 0.6 bar H₂): t_{R1} = 35.6 min (minor), t_{R2} = 37.5 min (major), er = 96:4 (92% ee).

$[\alpha]_D^{25}$ = +18.1 (c = 0.38, CHCl₃).

(*S*)-1-(hexan-2-yl)-3,5-dimethylbenzene (69e)
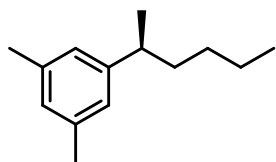
Prepared according to GP7 using EtMe₂SiH (5 eq.) in CyMe (0.5 M) at –20 °C for 3 d, eluent: pentane, 26.2 mg (69%), colorless oil.

¹H NMR analysis of the crude: 99% conv., 88% **69e**, 3% **70e**, 5% **71e**.

R_F (100% hexanes) = 0.74.

¹H NMR (501 MHz, CD₂Cl₂): δ = 6.82–6.77 (m, 3H), 2.58 (qt, *J* = 7.1, 7.1 Hz, 1H), 2.27 (s, 6H), 1.59–1.49 (m, 2H), 1.33–1.09 (m, 7H), 0.86 (t, *J* = 7.2 Hz, 3H).

¹³C NMR (126 MHz, CD₂Cl₂): δ = 148.4, 138.0, 127.6, 125.2, 40.2, 38.5, 30.5, 23.2, 22.6, 21.5, 14.2.

HRMS *m/z* (GC-EI): calcd. For $C_{14}H_{22}$ ([M]⁺): 190.171600; found: 190.171750.

GC (25 m Lipodex-G, injection temperature: 220 °C, 70 °C iso 53 min, 8 °C/min, 220 °C iso 3 min, 0.6 bar H₂): t_{R1} = 45.7 min (minor), t_{R2} = 47.8 min (major), er = 95.5:4.5 (91% ee).

$[\alpha]_D^{25}$ = +17.7 (c = 0.37, CHCl₃).

(*S*)-1-fluoro-4-(hexan-2-yl)benzene (69h)
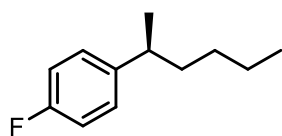
Prepared according to GP7 using PhMe₂SiH (5 eq.) in CyMe (0.5 M) at –20 °C for 3 d, eluent: pentane, 31.8 mg (89%), colorless oil.

¹H NMR analysis of the crude: 99% conv., 90% **69h**, 1% **70h**, 4% **71h**.

R_F (100% hexanes) = 0.85.

¹H NMR (501 MHz, CD₂Cl₂): δ = 7.18–7.11 (m, 2H), 7.00–6.94 (m, 2H), 2.67 (qt, *J* = 7.1, 7.1 Hz, 1H), 1.59–1.49 (m, 2H), 1.33–1.16 (m, 6H), 1.15–1.06 (m, 1H), 0.85 (t, *J* = 7.2 Hz, 3H).

¹⁹F{H} NMR (471 MHz, CD₂Cl₂): δ = -118.9.

¹³C NMR (126 MHz, CD₂Cl₂): δ = 161.04 (d, *J* = 241.7 Hz), 143.76 (d, *J* = 3.1 Hz), 128.25 (d, *J* = 7.8 Hz), 114.67 (d, *J* = 20.9 Hz), 39.2, 38.1, 29.8, 22.7, 22.2, 13.7.

HRMS *m/z* (GC-EI): calcd. For $C_{12}H_{17}F$ ([M]⁺): 180.130879; found: 180.130580.

GC (30 m Cyclosil B, injection temperature: 220 °C, 90 °C iso 30 min, 1 °C/min, 100 °C iso 5 min, 8 °C/min, 220 °C iso 5 min, 0.5 bar H₂): t_{R1} = 44.4 min (major), t_{R2} = 45.9 min (minor), er = 95.5:4.5 (91% ee).

$[\alpha]_D^{25}$ = +16.6 (c = 0.37, CHCl₃).

(*S*)-1-bromo-3-(hexan-2-yl)benzene (69i)
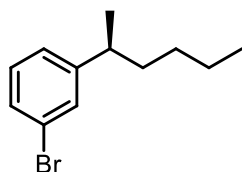
Prepared according to GP7 using PhMe₂SiH (10 eq.) under neat reaction conditions at 10 °C for 4 d, eluent: pentane, 34.5 mg (72%), colorless oil.

¹H NMR analysis of the crude: 99% conv., 83% **69i**, 17% **70i**, 0% **71i**.

R_F (100% hexanes) = 0.79.

¹H NMR (501 MHz, CD₂Cl₂): δ = 7.34 (t, *J* = 1.8 Hz, 1H), 7.31 (ddd, *J* = 7.7, 2.0, 1.3 Hz, 1H), 7.19–7.11 (m, 2H), 2.65 (qt, *J* = 7.1, 7.1 Hz, 1H), 1.58–1.53 (m, 2H), 1.33–1.18 (m, 6H), 1.17–1.07 (m, 1H), 0.85 (t, *J* = 7.2 Hz, 3H).

¹³C NMR (126 MHz, CD₂Cl₂): δ = 151.1, 130.5, 130.3, 129.1, 126.3, 122.6, 40.2, 38.3, 30.2, 23.1, 22.4, 14.2.

HRMS *m/z* (GC-EI): calcd. For $C_{12}H_{17}Br_1$ ([M]⁺): 240.050825; found: 240.050860.

GC (25 m Lipodex-G, injection temperature: 220 °C, 85 °C iso 55 min, 8 °C/min, 220 °C iso 3 min, 0.6 bar H₂): t_{R1} = 47.6 min (minor), t_{R2} = 49.8 min (major), er = 95:5 (90% ee).

$[\alpha]_D^{25}$ = +18.2 (c = 0.39, CHCl₃).

(*S*)-1-(hexan-2-yl)-3-methoxybenzene (69j)
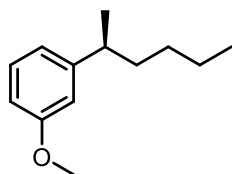
Prepared according to GP7 using PhMe$_2$SiH (5 eq.) in CyMe (0.5 M) at –20 °C for 3 d, eluent: pentane → 5% DCM, pentane, 29.8 mg (77%), colorless oil.

^{1}H NMR analysis of the crude: >99% conv., 98% **69j**, 2% **70j**, 0% **71j**.

***R*$_F$** (20% DCM, hexanes) = 0.38.

^{1}H NMR (501 MHz, CD$_2$Cl$_2$): δ = 7.19 (t, *J* = 7.8 Hz, 1H), 6.78 (dt, *J* = 7.6, 1.4 Hz, 1H), 6.74–6.68 (m, 2H), 3.78 (s, 3H), 2.64 (qt, *J* = 7.0, 7.0 Hz, 1H), 1.58–1.53 (m, 2H), 1.33–1.18 (m, 6H), 1.18–1.09 (m, 1H), 0.85 (t, *J* = 7.2 Hz, 3H).

^{13}C NMR (126 MHz, CD$_2$Cl$_2$): δ = 160.1, 150.3, 129.5, 119.8, 113.3, 111.1, 55.4, 40.4, 38.4, 30.4, 23.2, 22.5, 14.2.

HRMS *m/z* (GC-EI): calcd. For C$_{13}$H$_{20}$O$_1$ ([M]$^+$): 192.150865; found: 192.150990.

GC (25 m Lipodex-G, injection temperature: 220 °C, 90 °C iso 35 min, 8 °C/min, 220 °C iso 3 min, 0.6 bar H$_2$): t$_{R1}$ = 30.4 min (minor), t$_{R2}$ = 31.8 min (major), er = 97:3 (94% ee).

$[\alpha]_D^{25}$ = +20.3 (c = 0.33, CHCl$_3$).

(*S*)-2-(hexan-2-yl)naphthalene (69k)
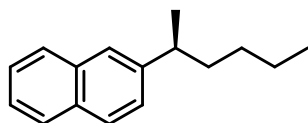
Prepared according to GP7 using EtMe$_2$SiH (10 eq.) under neat reaction conditions at –20 °C for 3 d, eluent: pentane, 32.1 mg (76%), colorless oil.

^{1}H NMR analysis of the crude: 99% conv., 82% **69k**, 1% **70k**, 9% **71k**.

***R*$_F$** (100% hexanes) = 0.59.

^{1}H NMR (501 MHz, CD$_2$Cl$_2$): δ = 7.82–7.76 (m, 3H), 7.62 (d, *J* = 1.7 Hz, 1H), 7.43 (dddd, *J* = 17.7, 8.1, 6.8, 1.4 Hz, 2H), 7.37 (dd, *J* = 8.5, 1.8 Hz, 1H), 2.86 (qt, *J* = 7.0, 7.0 Hz, 1H), 1.73–1.60 (m, 2H), 1.35–1.23 (m, 6H), 1.21–1.10 (m, 1H), 0.85 (t, *J* = 7.1 Hz, 3H).

^{13}C NMR (126 MHz, CD$_2$Cl$_2$): δ = 146.0, 134.1, 132.6, 128.1, 127.9, 127.8, 126.3, 126.1, 125.5, 125.4, 40.5, 38.4, 30.4, 23.2, 22.5, 14.2.

HRMS *m/z* (GC-EI): calcd. For C$_{16}$H$_{20}$ ([M]$^+$): 212.155950; found: 212.155840.

GC (24 m Cyclodextrin-H, injection temperature: 220 °C, 100 °C iso 112 min, 8 °C/min, 180 °C iso 3 min, 0.5 bar H$_2$): t$_{R1}$ = 98.8 min (major), t$_{R2}$ = 104.1 min (minor), er = 98:2 (96% ee).

$[\boldsymbol{\alpha}]_D^{25}$ = +29.7 (c = 0.17, CHCl$_3$).

(*S*)-5-(hexan-2-yl)benzofuran (69l)
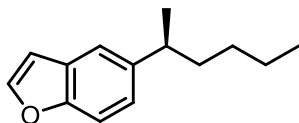
Prepared according to GP7 using EtMe$_2$SiH (10 eq.) under neat reaction conditions at –20 °C for 3 d, eluent: pentane, 25.8 mg (63%), colorless oil.

^{1}H NMR analysis of the crude: >99% conv., 80% **69l**, 0% **70l**, 11% **71l**.

$\boldsymbol{R}_F$ (100% hexanes) = 0.50.

^{1}**H NMR** (501 MHz, CD$_2$Cl$_2$): δ = 7.61 (d, *J* = 2.2 Hz, 1H), 7.43–7.37 (m, 2H), 7.13 (dd, *J* = 8.5, 1.8 Hz, 1H), 6.74 (dd, *J* = 2.2, 1.0 Hz, 1H), 2.78 (qt, *J* = 7.1, 7.1 Hz, 1H), 1.61 (q, *J* = 7.3 Hz, 2H), 1.32–1.20 (m, 6H), 1.16–1.08 (m, 1H), 0.84 (t, *J* = 7.2 Hz, 3H).

^{13}**C NMR** (126 MHz, CD$_2$Cl$_2$): δ = 154.0, 145.5, 143.1, 127.8, 124.0, 119.4, 111.1, 106.9, 40.3, 39.0, 30.4, 23.2, 23.1, 14.2.

HRMS *m/z* (GC-EI): calcd. For C$_{14}$H$_{18}$O ([M]$^+$): 202.135215; found: 202.135430.

GC (24 m Cyclodextrin-H, injection temperature: 220 °C, 100 °C iso 45 min, 8 °C/min, 180 °C iso 3 min, 0.5 bar H$_2$): t$_{R1}$ = 34.0 min (major), t$_{R2}$ = 38.7 min (minor), er = 97:3 (94% ee).

$[\boldsymbol{\alpha}]_D^{25}$ = +20.4 (c = 0.28, CHCl$_3$).

(*S*)-6-(hexan-2-yl)benzofuran (69m)
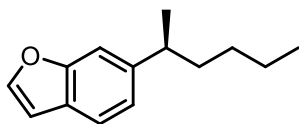
Prepared according to GP8 using EtMe$_2$SiH (10 eq.) in CyMe (0.5 M) at –20 °C for 2 d, eluent: pentane.

^{1}H NMR analysis of the crude: >99% conv., 27% **69n**, 0% **70n**, 17% **71n**.

^{1}**H NMR** (501 MHz, C$_6$D$_6$): δ = 7.38 (d, *J* = 8.0 Hz, 1H), 7.35 (s, 1H), 7.16–7.16 (m, 1H), 7.02 (dd, *J* = 7.9, 1.5 Hz, 1H), 6.38 (dd, *J* = 2.2, 0.9 Hz, 1H), 2.62 (h, *J* = 6.9 Hz, 1H), 1.58–1.50 (m, 1H), 1.49–1.43 (m, 1H), 1.24–1.07 (m, 7H), 0.80 (t, *J* = 7.1 Hz, 3H).

GC (30 m Cyclosil B, injection temperature: 220 °C, 80 °C, 1 °C/min, 220 °C iso 5 min, 0.5 bar H$_2$): t$_{R1}$ = 76.2 min (major), t$_{R2}$ = 76.6 min (minor), er = 89.5:10.5 (79% ee).

(*S*)-pentan-2-ylbenzene (69n)
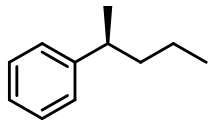
Prepared according to GP7 using EtMe$_2$SiH (5 eq.) under neat reaction conditions at –20 °C for 4 d, eluent: pentane, 7.2 mg (25%), colorless oil.

^{1}H NMR analysis of the crude: 79% conv., 68% **69n**, 4% **70n**, 3% **71n**.

R$_F$ (100% hexanes) = 0.69.

^{1}H NMR (501 MHz, CD$_2$Cl$_2$): δ = 7.30–7.24 (m, 2H), 7.20–7.13 (m, 3H), 2.69 (qt, *J* = 7.0, 7.0 Hz, 1H), 1.59–1.49 (m, 2H), 1.29–1.14 (m, 5H), 0.87 (t, *J* = 7.4 Hz, 3H).

^{13}C NMR (126 MHz, CD$_2$Cl$_2$): δ = 148.5, 128.6, 127.4, 126.1, 41.0, 40.0, 22.5, 21.2, 14.3.

HRMS *m/z* (GC-EI): calcd. For C$_{11}$H$_{16}$ ([M]$^+$): 148.124650; found: 148.124700.

GC (30 m Cyclosil B, injection temperature: 220 °C, 80 °C iso 30 min, 1 °C/min, 95 °C iso 5 min, 8 °C/min, 220 °C iso 5 min, 0.5 bar H$_2$): t$_{R1}$ = 34.4 min (major), t$_{R2}$ = 35.2 min (minor), er = 94.5:5.5 (89% ee).

[α]$_D^{25}$ = +11.3 (c = 0.11, CHCl$_3$). Literature data for (*S*) enantiomer[304]: (2.5% ee) **[α]$_D^{20}$** = +0.49 (c = 3.51, hexane).

(*S*)-heptan-2-ylbenzene (69o)
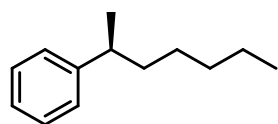
Prepared according to GP7 using EtMe$_2$SiH (10 eq.) under neat reaction conditions at –20 °C for 4 d, eluent: pentane, 21.9 mg (62%), colorless oil.

^{1}H NMR analysis of the crude: 92% conv., 86% **69o**, 3% **70o**, 2% **71o**.

R$_F$ (100% hexanes) = 0.69.

^{1}H NMR (501 MHz, CD$_2$Cl$_2$): δ = 7.30–7.25 (m, 2H), 7.20–7.13 (m, 3H), 2.67 (qt, *J* = 7.1, 7.1 Hz, 1H), 1.62–1.50 (m, 2H), 1.30–1.20 (m, 8H), 1.20–1.07 (m, 1H), 0.92–0.80 (m, 3H).

^{13}C NMR (126 MHz, CD$_2$Cl$_2$): δ = 148.5, 128.6, 127.4, 126.1, 40.3, 38.8, 32.4, 27.8, 23.0, 22.6, 14.2.

HRMS *m/z* (GC-EI): calcd. For C$_{13}$H$_{20}$ ([M]$^+$): 176.1155950; found: 176.156030.

GC (29.5 m BGB-178/BGB-15, injection temperature: 220 °C, 65 °C iso 142 min, 8 °C/min, 230 °C iso 3 min, 0.6 bar H$_2$): t$_{R1}$ = 128.4 min (major), t$_{R2}$ = 133.3 min (minor), er = 95:5 (90% ee).

[α]$_D^{25}$ = +19.0 (c = 0.30, CHCl$_3$). Literature data for (*R*) enantiomer[305]: (99% ee) **[α]$_D^{20}$** = –7.0 (c = 1.25, CHCl$_3$).

(*S*)-octan-2-ylbenzene (69p)
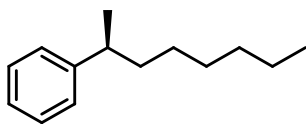
Prepared according to GP7 using EtMe$_2$SiH (10 eq.) under neat reaction conditions at –20 °C for 4 d, eluent: pentane, 28.2 mg (75%), colorless oil.

^{1}H NMR analysis of the crude: 94% conv., 84% **69p**, 3% **70p**, 3% **71p**.

R_F (100% hexanes) = 0.69.

^{1}H NMR (501 MHz, CD$_2$Cl$_2$): δ = 7.30–7.24 (m, 2H), 7.20–7.13 (m, 3H), 2.67 (qt, *J* = 7.1, 7.1 Hz, 1H), 1.61–1.53 (m, 2H), 1.30–1.18 (m, 10H), 1.18–1.10 (m, 1H), 0.86 (t, *J* = 7.0 Hz, 3H).

^{13}C NMR (126 MHz, CD$_2$Cl$_2$): δ = 148.6, 128.6, 127.4, 126.1, 40.3, 38.8, 32.2, 29.8, 28.1, 23.1, 22.6, 14.3.

HRMS *m/z* (GC-EI): calcd. For C$_{14}$H$_{22}$ ([M]$^+$): 190.171600; found: 190.171700.

GC (24 m Cyclodextrin-H, injection temperature: 220 °C, 90 °C iso 25 min, 8 °C/min, 180 °C, 0.5 bar H$_2$): t_{R1} = 19.0 min (major), t_{R2} = 20.5 min (minor), er = 95.5:4.5 (91% ee).

$[\alpha]_D^{25}$ = +20.3 (c = 0.39, CHCl$_3$).

(*S*)-5-methyl-6,7,8,9-tetrahydro-5*H*-benzo[7]annulene (69q)
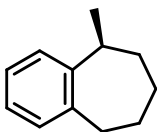
Prepared according to GP7 using PhMe$_2$SiH (5 eq.) in CyMe (0.5 M) at –20 °C for 4 d, eluent: pentane, 20.3 mg (63%), colorless oil.

^{1}H NMR analysis of the crude: >99% conv., 64% **69q**, 36% **70q**, 0% **71q**.

R_F (100% hexanes) = 0.65.

^{1}H NMR (501 MHz, CD$_2$Cl$_2$): δ = 7.17 (dd, *J* = 7.6, 1.2 Hz, 1H), 7.14–7.09 (m, 1H), 7.08–7.03 (m, 2H), 3.09–3.00 (m, 1H), 2.92–2.83 (m, 1H), 2.83–2.74 (m, 1H), 1.95–1.87 (m, 1H), 1.80–1.71 (m, 2H), 1.47–1.32 (m, 5H), 1.30–1.21 (m, 1H).

^{13}C NMR (126 MHz, CD$_2$Cl$_2$): δ = 147.1, 143.3, 129.6, 126.3, 126.0, 36.6, 36.5, 30.1, 28.4, 20.6.

HRMS *m/z* (GC-EI): calcd. For C$_{12}$H$_{16}$ ([M]$^+$): 160.124650; found: 160.124930.

GC (30 m Cyclosil B, injection temperature: 220 °C, 90 °C iso 30 min, 1 °C/min, 100 °C iso 5 min, 8 °C/min, 220 °C iso 5 min, 0.5 bar H$_2$): t_{R1} = 55.0 min (minor), t_{R2} = 55.6 min (major), er = 92.5:7.5 (85% ee).

$[\alpha]_D^{25}$ = –6.9 (c = 0.20, CHCl$_3$). Literature data for (*S*) enantiomer[306]: (85% ee) **$[\alpha]_D^{23}$** = –9.4 (c = 5, CHCl$_3$).

(S)-(6-chlorohexan-2-yl)benzene (69r)
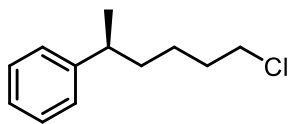
Prepared according to GP7 using PhMe$_2$SiH (5 eq.) in CyMe (0.5 M) at –20 °C for 4 d, eluent: pentane → 1% MTBE, pentane, 29.7 mg (76%), colorless oil.

^{1}H NMR analysis of the crude: >99% conv., 85% **69r**, 6% **70r**, 5% **71r**.

R_F (100% hexanes) = 0.41.

^{1}**H NMR** (501 MHz, CD$_2$Cl$_2$): δ = 7.31–7.26 (m, 2H), 7.20–7.15 (m, 3H), 3.49 (t, J = 6.8 Hz, 2H), 2.69 (qt, J = 7.1, 7.1 Hz, 1H), 1.81–1.64 (m, 2H), 1.66–1.56 (m, 2H), 1.43–1.33 (m, 1H), 1.31–1.25 (m, 2H), 1.23 (d, J = 6.9 Hz, 3H).

^{13}**C NMR** (126 MHz, CD$_2$Cl$_2$): δ = 148.0, 128.7, 127.4, 126.2, 45.6, 40.2, 37.9, 33.1, 25.5, 22.5.

HRMS m/z (GC-EI): calcd. For C$_{12}$H$_{17}$Cl$_1$ ([M]$^+$): 196.101328; found: 196.101320.

GC (25 m Hydrodex-beta-TBDAc-CD, injection temperature: 220 °C, 90 °C iso 220 min, 8 °C/min, 220 °C iso 3 min, 0.6 bar H$_2$): t$_{R1}$ = 194.2 min (major), t$_{R2}$ = 204.2 min (minor), er = 90:10 (80% ee).

$[\alpha]_D^{25}$ = +17.4 (c = 0.25, CHCl$_3$).

methyl (S)-5-phenylhexanoate (69s)
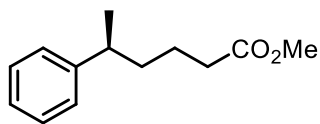
Prepared according to GP7 using PhMe$_2$SiH (5 eq.) in CyMe (0.5 M) at –20 °C for 4 d, eluent: pentane → 3% MTBE, pentane, 30.0 mg (72%), colorless oil.

^{1}H NMR analysis of the crude: >99% conv., 84% **69s**, 4% **70s**, 8% **71s**.

R_F (5% EtOAc, hexanes) = 0.49.

^{1}**H NMR** (501 MHz, CD$_2$Cl$_2$): δ = 7.31–7.25 (m, 2H), 7.20–7.15 (m, 3H), 3.61 (s, 3H), 2.69 (qt, J = 7.0, 7.0 Hz, 1H), 2.28–2.23 (m, 2H), 1.63–1.51 (m, 4H), 1.51–1.40 (m, 1H), 1.23 (d, J = 7.0 Hz, 3H).

^{13}**C NMR** (126 MHz, CD$_2$Cl$_2$): δ = 174.2, 147.8, 128.7, 127.4, 126.3, 51.6, 40.1, 38.0, 34.4, 23.6, 22.5.

HRMS m/z (API-ES): calcd. For C$_{13}$H$_{18}$O$_2$Na$_1$ ([M+Na]$^+$): 229.119899; found: 229.119960.

GC (25 m Ivadex-7/PS086, injection temperature: 220 °C, 100 °C iso 62 min, 8 °C/min, 220 °C, 0.6 bar H$_2$): t$_{R1}$ = 53.4 min (major), t$_{R2}$ = 56.8 min (minor), er = 93:7 (86% ee).

$[\alpha]_D^{25}$ = +14.8 (c = 0.26, CHCl$_3$).

(*S*)-hept-6-en-2-ylbenzene (69t)
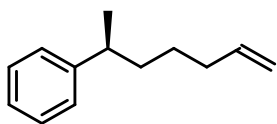
Prepared according to GP7 using PhMe$_2$SiH (5 eq.) in CyMe (0.5 M) at –20 °C for 4 d, eluent: pentane, 2.8 mg (8%), colorless oil.

Note: The reaction resulted in the formation of a cyclized side product (1-methyl-1,2,3,4-tetrahydro-1,1'-biphenyl)[307] that could not be separated from the desired compound. Consequently, the isolated sample contains approximately 10% of the cyclized species. The optical rotation reported below corresponds to this mixture.
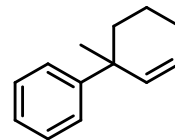
^{1}H NMR analysis of the crude: >99% conv., 45% **69t**.

R$_F$ (100% hexanes) = 0.65.

^{1}H NMR (501 MHz, CD$_2$Cl$_2$): δ = 7.32–7.26 (m, 2H), 7.22–7.15 (m, 3H), 5.79 (ddt, *J* = 16.9, 10.2, 6.7 Hz, 1H), 4.98 (ddt, *J* = 17.1, 1.7, 1.7 Hz, 1H), 4.92 (ddt, *J* = 10.2, 2.3, 1.2 Hz, 1H), 2.70 (qt, *J* = 7.0, 7.0 Hz, 1H), 2.11–1.98 (m, 2H), 1.65–1.55 (m, 2H), 1.41–1.30 (m, 1H), 1.30–1.23 (m, 4H).

^{1}H NMR (501 MHz, C$_6$D$_6$): δ = 7.21–7.17 (m, 2H), 7.11–7.05 (m, 3H), 5.69 (ddt, *J* = 17.0, 10.2, 6.7 Hz, 1H), 5.02–4.91 (m, 2H), 2.56–2.46 (m, 1H), 1.96–1.85 (m, 2H), 1.55–1.37 (m, 2H), 1.31–1.16 (m, 2H), 1.14 (d, *J* = 6.9 Hz, 3H).

^{13}C NMR (126 MHz, CD$_2$Cl$_2$): δ = 148.3, 139.5, 128.7, 127.4, 126.2, 114.4, 40.3, 38.3, 34.2, 27.5, 22.5.

HRMS *m/z* (API-ES): calcd. For C$_{13}$H$_{18}$ ([M]$^+$): 174.140300; found: 174.140330.

GC (30 m Cyclosil B, injection temperature: 220 °C, 110 °C iso 60 min, 8 °C/min, 220 °C iso 5 min, 0.5 bar H$_2$): t$_{R1}$ = 33.6 min (major), t$_{R2}$ = 34.3 min (minor), er = 93:7 (86% ee).

$[\alpha]_D^{25}$ = +14.3 (c = 0.14, CHCl$_3$).

(*S*)-(6-methylhept-5-en-2-yl)benzene (69u)
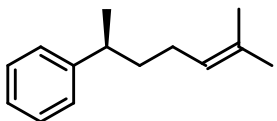
Prepared according to GP8 using PhMe$_2$SiH (5 eq.) in CyMe (0.5 M) at –20 °C for 3 d, eluent: pentane.

^{1}H NMR analysis of the crude: 98% conv., 68% **69u**, 2% **70u**, 13% **71u**.

GC (30 m Cyclosil B, injection temperature: 220 °C, 90 °C iso 30 min, 1 °C/min, 100 °C iso 5 min, 8 °C/min, 220 °C iso 5 min, 0.5 bar H$_2$): t$_{R1}$ = 55.1 min (major), t$_{R2}$ = 55.2 min (minor), er = 82:18 (64% ee).

(*S*)-1-(hexan-2-yl)-4-methoxybenzene (69v)
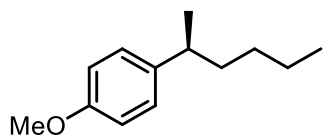
Prepared according to GP8 using EtMe₂SiH (10 eq.) under neat reaction conditions at –20 °C for 3 d, eluent: 5% DCM, pentane.

^{1}H NMR analysis of the crude: >99% conv., 44% **69v**, 0% **70v**, 19% **71v**.

GC (30 m BGB-176/BGB-15, injection temperature: 220 °C, 80 °C iso 220 min, 8 °C/min, 240 °C, 0.6 bar H₂): t_{R1} = 201.6 min (major), t_{R2} = 208.0 min (minor), er = 75.5:24.5 (51% ee).

(*S*)-1-methyl-4-(6-methylhept-5-en-2-yl)benzene (69y)
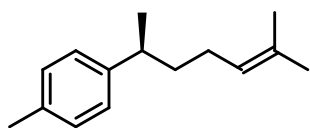
Prepared according to GP8 using EtMe₂SiH (10 eq.) under neat reaction conditions at –30 °C for 3 d, eluent: pentane.

^{1}H NMR analysis of the crude: 96% conv., 65% **69y**, 2% **70y**, 11% **71y**.

GC (30 m Cyclosil B, injection temperature: 220 °C, 60 °C, 1 °C/min, 130 °C iso 5 min, 8 °C/min, 220 °C iso 3 min, 0.5 bar H₂): t_{R1} = 83.6 min (major), t_{R2} = 84.5 min (minor), = 78:22 (56% ee).

(*S*)-sec-butylbenzene (69z)
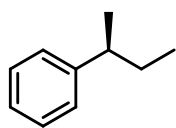
Prepared according to GP8 using EtMe₂SiH (10 eq.) under neat reaction conditions at –20 °C for 3 d, eluent: pentane.

^{1}H NMR analysis of the crude: 19% conv., 16% **69z**, 0% **70z**, 1% **71z**.

GC (25 m Hydrodex-beta-TBDAc-CD, injection temperature: 220 °C, 40 °C, iso 65 min, 8 °C/min, 220 °C, 0.5 bar H₂): t_{R1} = 52.7 min (major), t_{R2} = 57.1 min (minor), = 64.5:35.5 (29% ee).

(*S*)-(3-methylbutan-2-yl)benzene (69aa)
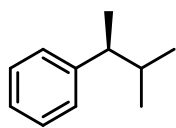
Prepared according to GP8 using EtMe₂SiH (10 eq.) under neat reaction conditions at –20 °C for 3 d, eluent: pentane.

^{1}H NMR analysis of the crude: 50% conv., 28% **69aa**.

GC (30 m Cyclosil B, injection temperature: 220 °C, 80 °C, 1 °C/min, 103 °C, 8 °C/min, 220 °C iso 3 min, 0.5 bar H₂): t_{R1} = 21.8 min (major), t_{R2} = 22.5 min (minor), er = 65.5:34.5 (31% ee).

(*S*)-(1-cyclohexylethyl)benzene (69ab)
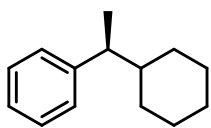
Prepared according to GP8 using PhMe$_2$SiH (5 eq.) in CyMe (0.5 M) at –20 °C for 3 d, eluent: pentane.

^{1}H NMR analysis of the crude: >99% conv., 92% **69ab**.

GC (30 m Cyclosil B, injection temperature: 220 °C, 90 °C iso 30 min, 1 °C/min, 100 °C iso 5 min, 8 °C/min, 220 °C iso 5 min, 0.5 bar H$_2$): t_{R1} = 57.7 min (major), t_{R2} = 57.8 min (minor), er = 63:37 (26% ee).

1,1,3-trimethylcyclohexane (69ai)
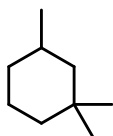
Prepared according to GP8 using EtMe$_2$SiH (5 eq.) in CyMe (0.5 M) at –20 °C for 3 d, eluent: pentane.

^{1}H NMR analysis of the crude: 10% conv., <5% **69ai**.

GC (24.5 m Ivadex-1, injection temperature: 220 °C, 40 °C iso 12 min, 8 °C/min, 230 °C, 0.6 bar H$_2$): t_{R1} = 7.5 min (major), t_{R2} = 8.1 min (minor), er = 56.5:43.5 (13% ee).

4.3.4   Scale-Up Experiment and Derivatization for Absolute Configuration Assignment

92b (1 mol%)
PhMe$_2$SiH (5.0 eq.)
PhCOOH (1.2 eq.)

CyMe (0.5 M)
–20 °C, 7 d

68j
5 mmol

69j, 712 mg
75%, **97:3 er**
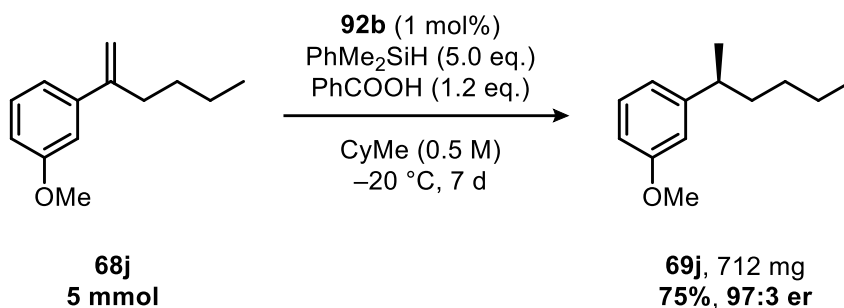
An oven-dried Schlenk flask under argon atmosphere was charged with IDPi **92b** (106.5 mg, 1 mol%), benzoic acid (722 mg, 5.91 mmol, 1.19 eq.), and CyMe (9.9 mL), then cooled to –20 °C. PhMe$_2$SiH (3.8 mL, 25 mmol, 5.0 eq.) was added, followed by the dropwise addition of styrene **68j** (945 mg, 4.97 mmol, 1.00 eq.). The reaction mixture was stirred at –20 °C for 7 d, and then quenched by adding pyridine (40 µL) while maintaining –20 °C for an additional 15 min. The crude mixture was directly loaded onto a silica column. The product **69j** was eluted first (100% pentane to 5% DCM, pentane) and obtained as a colorless oil (712 mg, 75%, 97:3 er), followed by the catalyst (100% DCM). To remove residual

benzoic acid, a basic extraction with 3% NaOH and DCM was performed. Acidification via filtration over DOWEX 50WX8 (H-form, eluted with DCM) furnished the recovered catalyst **92b** (94 mg, 88%) as a beige solid.

Derivatization of 69j
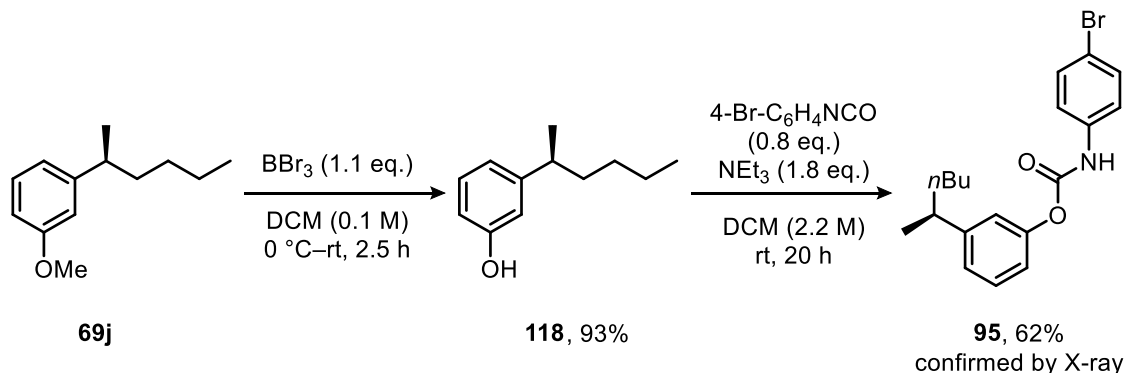
(S)-3-(hexan-2-yl)phenol (118)
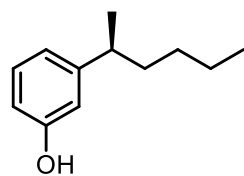
In a flame-dried Schlenk flask under argon, **69j** (449 mg, 2.33 mmol, 1.00 eq.) was dissolved in dry DCM (20 mL) and cooled to 0 °C. BBr$_3$ (1 M in DCM, 2.6 mL, 2.6 mmol, 1.11 eq.) was added dropwise and the resulting solution was then stirred at room temperature for 2.5 h until TLC indicated full consumption of the starting material. The reaction was quenched by adding water (20 mL) at 0 °C. The aqueous layer was subsequently extracted with DCM (2 x 20 mL), the combined organic phases were washed with water, dried over anhydrous Na$_2$SO$_4$, and concentrated under reduced pressure. Purification via flash column chromatography on silica gel (5–10% EtOAc, pentane) furnished the title compound **118** (386 mg, 93%) as a light yellow oil.

^{1}H NMR (501 MHz, CD$_2$Cl$_2$): δ = 7.13 (t, J = 7.8 Hz, 1H), 6.75 (dt, J = 7.5, 1.3 Hz, 1H), 6.66 (t, J = 2.1 Hz, 1H), 6.63 (ddd, J = 8.0, 2.6, 1.0 Hz, 1H), 4.83 (s, 1H), 2.62 (qt, J = 7.0, 7.0 Hz, 1H), 1.57–1.49 (m, 2H), 1.34–1.18 (m, 6H), 1.18–1.07 (m, 1H), 0.85 (t, J = 7.2 Hz, 3H).

^{13}C NMR (126 MHz, CD$_2$Cl$_2$) δ 156.1, 150.6, 129.7, 119.9, 114.2, 112.9, 40.2, 38.4, 30.3, 23.2, 22.5, 14.2.

HRMS *m/z* (GC-EI): calcd. For C$_{12}$H$_{18}$O$_1$ ([M]$^+$): 178.135215; found: 178.135460.

(*S*)-3-(hexan-2-yl)phenyl (4-bromophenyl)carbamate (95)
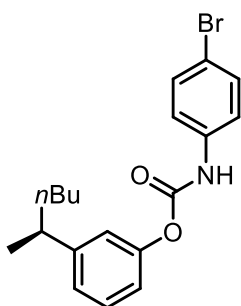
A GC vial was charged with phenol **118** (47.5 mg, 0.266 mmol, 1.25 eq.), DCM (0.1 mL) and NEt$_3$ (54 µL, 0.39 mmol, 1.8 eq.). 4-Bromophenylisocyanate (42.2 mg, 0.213 mmol, 1.00 eq.) was added, and the resulting mixture was stirred at room temperature for 20 h. The crude material was directly loaded onto a silica column and eluted (2–10% EtOAc, pentane) to furnish carbamate **95** (50.0 mg, 62%) as a white solid.

^{1}H NMR (501 MHz, CD$_2$Cl$_2$): δ = 7.48–7.43 (m, 2H), 7.40–7.34 (m, 2H), 7.34–7.29 (m, 1H), 7.14–7.08 (m, 2H), 7.04–6.98 (m, 2H), 2.71 (qt, *J* = 7.0, 7.0 Hz, 1H), 1.65–1.50 (m, 2H), 1.36–1.22 (m, 6H), 1.22–1.10 (m, 1H), 0.87 (t, *J* = 7.1 Hz, 3H).

^{13}C NMR (126 MHz, CD$_2$Cl$_2$) δ 152.0, 151.0, 150.5, 137.3, 132.4, 129.5, 125.0, 120.5, 119.3, 40.2, 38.4, 30.3, 23.1, 22.3, 14.2.

HRMS *m/z* (GC-EI): calcd. For C$_{19}$H$_{22}$O$_2$N$_1$Na$_1$Br$_1$ ([M+Na]$^+$): 398.072623; found: 398.072280.

Recrystallization for X-ray crystallography: The white solid was suspended in hexanes and heated to reflux. Additional hexanes were added dropwise until complete dissolution. The solution was then allowed to cool slowly to room temperature. Crystals suitable for X-ray analysis were obtained, and the (*S*)-configuration was assigned based on the data.
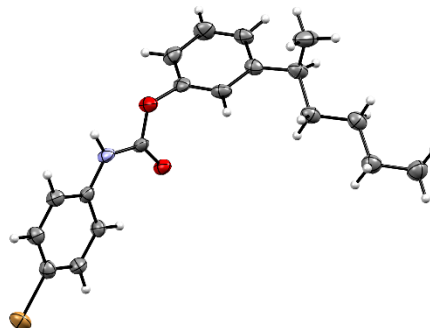
Validation of Absolute Configuration through Comparison with Reported $[\alpha]_D^{25}$ Values

The measured $[\alpha]_D^{25}$ values for products **69a**, **69n**, and **69q** align with literature values for the corresponding (*S*)-enantiomers. For substrate **69o**, the literature reports the specific optical rotation of the (*R*)-enantiomer, which is opposite to the value measured in this work for the (*S*)-enantiomer (see characterization in Section 4.3.3).

For **69b**, literature data contradict our assigned (*S*)-configuration:

$[\alpha]_D^{25}$ = +18.9 (c = 0.27, CHCl$_3$, 87% ee). Literature data for (*R*) enantiomer[308]: (85% ee) $[\alpha]_D^{24}$ = +4.9 (c = 1.0, CHCl$_3$).

However, based on our X-Ray analysis and consistent optical rotation measurements across four compounds, we conclude that our assignment is correct.

4.3.5 Synthesis of IDPi catalysts

Synthesis of 2-iodo-6-(perfluorophenyl)benzofuran (119)
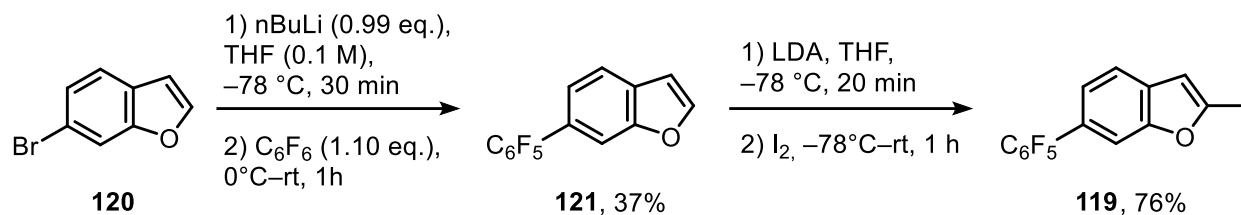
6-(perfluorophenyl)benzofuran (121)
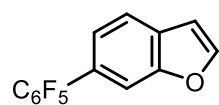
In a flame-dried Schlenk flask under argon, 6-bromobenzofuran (**120**, 965 mg, 4.90 mmol, 1.00 eq.) was dissolved in anhydrous THF (7.3 mL) and cooled to –78 °C. *n*-BuLi (2.7 M in heptane, 1.78 mL, 4.85 mmol, 0.99 eq.) was added dropwise, and the mixture was stirred for 30 min at –78 °C. The resulting green solution was transferred via cannula to a precooled solution of hexafluorobenzene (0.62 mL, 5.39 mmol, 1.10 eq.) in THF (10 mL) at 0 °C. The reaction mixture was stirred for 1 h while gradually warming to room temperature. The reaction was quenched with water (20 mL), and the aqueous phase was extracted with DCM (3×25 mL). The combined organic layers were washed with water (15 mL), dried over anhydrous Na_2SO_4, filtered, and concentrated under reduced pressure. Purification by silica gel flash chromatography (100% hexanes) afforded the title compound as a white solid (589 mg, 88% purity, 1.82 mmol, 37%). Minor amounts of 2,6-bis(perfluorophenyl)benzofuran were present but did not interfere with subsequent steps.

^{1}H NMR (501 MHz, CD_2Cl_2): δ = 7.77–7.72 (m, 2H), 7.61 (d, J = 1.6 Hz, 1H), 7.31 (dq, J = 7.9, 1.4 Hz, 1H), 6.88 (dd, J = 2.2, 1.0 Hz, 1H).

^{19}F NMR (471 MHz, CD_2Cl_2): δ = –143.8 (dd, J = 22.9, 8.0 Hz, 2F), –156.7 (t, J = 21.0 Hz, 1F), –163.15––163.39 (m, 2H).

HRMS *m/z* (GC-EI): calcd. for $C_{14}H_4O_1F_5$ ([M]$^+$): 284.025508; found: 284.025780.

2-iodo-6-(perfluorophenyl)benzofuran (119)
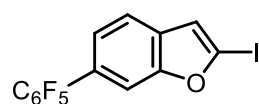
n-BuLi (2.7 M in heptane, 0.21 mL, 0.57 mmol, 1.00 eq.) was slowly added to a solution of diisopropylamine (84 µL, 0.60 mmol, 1.05 eq.) in anhydrous THF (0.4 mL) at –78 °C. The mixture was warmed to 0 °C, stirred for 15 min, and then cooled to –78 °C. After addition of benzofuran **121** (184 mg, 88% purity, 0.57 mmol, 1.00 eq.) in THF (0.9 mL) and another 20 min of stirring at –78 °C, iodine (159 mg, 0.63 mmol, 1.10 eq.) in THF (0.5 mL) was added. The reaction mixture was stirred at –78 °C for 15 min, warmed to 0 °C and stirred for 1 h. The

reaction was quenched by addition of saturated NH_4Cl and Na_2SO_3 solution, the aqueous layer was extracted with DCM (3 x 15 mL), and the combined organic phases were washed with Na_2SO_3 solution, dried over anhydrous Na_2SO_4, and concentrated under reduced pressure. Purification by flash column chromatography on silica gel (100% hexanes) afforded the title compound as a white solid (177 mg, 76%).

^{1}H NMR (501 MHz, CD_2Cl_2): δ = 7.66 (d, J = 8.1 Hz, 1H), 7.58 (s, 1H), 7.29 (dq, J = 8.1, 1.5 Hz, 1H), 7.08 (d, J = 0.9 Hz, 1H).

^{19}F NMR (471 MHz, CD_2Cl_2): δ = –143.7– –143.9 (m, 2F), –156.3 (t, J = 20.8 Hz, 1F), –163.1 (td, J = 22.6, 8.0 Hz, 2F).

^{13}C NMR (126 MHz, CD_2Cl_2): δ = 158.3, 147.1, 130.5, 125.6, 120.3, 117.8, 113.0, 98.5.

HRMS m/z (GC-EI): calcd. for $C_{14}H_4O_1I_1F_5$ ([M]$^+$): 409.922155; found: 409.923100.

2-bromobenzo[*b*]thieno[3,2-*d*]thiophene (122)
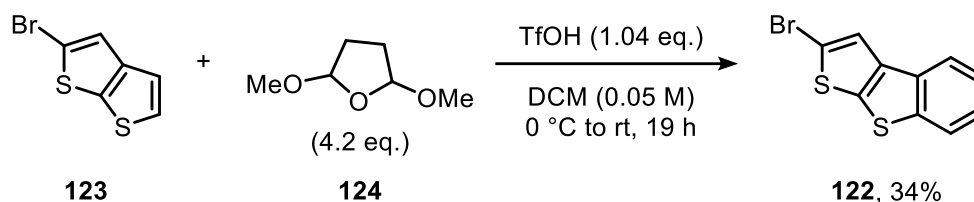
The synthesis was carried out following a modified procedure reported by Rafiq *et al.*[309] In a flame-dried Schlenk flask under argon, 2-bromothieno[2,3-*b*]thiophene (**123**, 1.24 g, 5.65 mmol, 1.00 eq.) was dissolved in dry DCM (115 mL) and 2,5-dimethoxytetrahydrofuran (**124**, 1.6 mL, 12.4 mmol, 2.20 eq.). The solution was cooled to 0 °C, and TfOH (0.52 mL, 5.88 mmol, 1.04 eq.) was added dropwise. After stirring for 15 min at 0 °C, the reaction mixture was warmed to room temperature and stirred for an additional 2.5 h. 2,5-Dimethoxyfuran (1.5 mL, 11.3 mmol, 2.00 eq.) was then added, and the reaction was stirred for a further 16 h. The reaction was quenched by the addition of aqueous $NaHCO_3$ solution (60 mL). The aqueous layer was extracted with DCM (3 × 40 mL), and the combined organic layers were washed with water, dried over anhydrous Na_2SO_4, and concentrated under reduced pressure. Purification by flash column chromatography on silica gel (100% hexanes) afforded the title compound (516 mg, 5.65 mmol, 34%) as a white solid.

R_F (100% hexanes) = 0.61.

^{1}H NMR (501 MHz, CD_2Cl_2): δ = 7.89 (d, J = 7.8 Hz, 1H), 7.84 (d, J = 8.0 Hz, 1H), 7.57 (s, 1H), 7.46–7.41 (m, 1H), 7.37 (ddd, J = 8.4, 7.2, 1.3 Hz, 1H).

^{13}C NMR (126 MHz, CD_2Cl_2): δ = 143.2, 141.3, 137.3, 132.5, 125.2, 125.0, 123.5, 122.9, 121.9, 112.9.

HRMS *m/z* (GC-EI): calcd. for $C_{10}H_5S_2Br_1$ ([M]$^+$): 267.901070; found: 267.901440.

2-bromobenzo[b]thieno[2,3-d]thiophene (125)
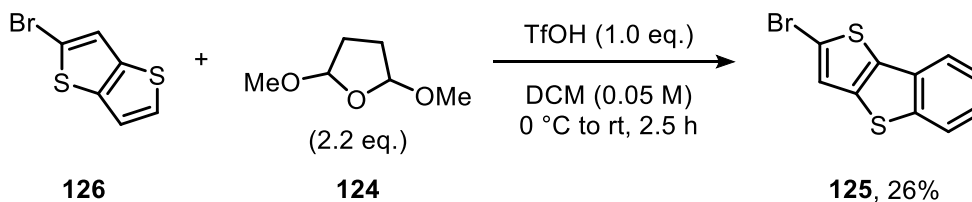
The synthesis was carried out following a modified procedure reported by Rafiq *et al*.[309] In a flame-dried Schlenk flask under argon, 2-bromothieno[3,2-*b*]thiophene (**123**, 480 mg, 2.19 mmol, 1.00 eq.) was dissolved in dry DCM (44 mL) and 2,5-dimethoxytetrahydrofuran (**124**, 0.62 mL, 4.82 mmol, 2.20 eq.). The solution was cooled to 0 °C, and TfOH (0.19 mL, 2.19 mmol, 1.00 eq.) was added dropwise. After stirring for 15 min at 0 °C, the reaction mixture was warmed to room temperature and stirred for an additional 2 h. The reaction was quenched by the addition of aqueous NaHCO₃ solution (30 mL). The aqueous layer was extracted with DCM (3 × 30 mL), and the combined organic layers were washed with water, dried over anhydrous Na₂SO₄, and concentrated under reduced pressure. Purification by flash column chromatography on silica gel (100% hexanes) afforded the title compound (153 mg, 0.57 mmol, 26%) as a white solid.

¹H NMR (501 MHz, CDCl₃): δ = 7.86–7.80 (m, 1H), 7.75 (ddd, *J* = 7.9, 1.4, 0.7 Hz, 1H), 7.41 (ddd, *J* = 7.9, 7.2, 1.2 Hz, 1H), 7.36 (ddd, *J* = 8.4, 7.2, 1.3 Hz, 1H), 7.31 (s, 1H).

¹³C NMR (126 MHz, CDCl₃): δ = 141.6, 136.8, 135.0, 132.4, 125.0, 124.8, 123.9, 123.2, 120.9, 114.3.

HRMS *m/z* (GC-EI): calcd. for $C_{10}H_5S_2Br_1$ ([M]$^+$): 267.901070; found: 267.901570.

Synthesis of 2-bromo-5-(trifluoromethyl)benzo[*b*]thieno[3,2-*d*]thiophene (127)
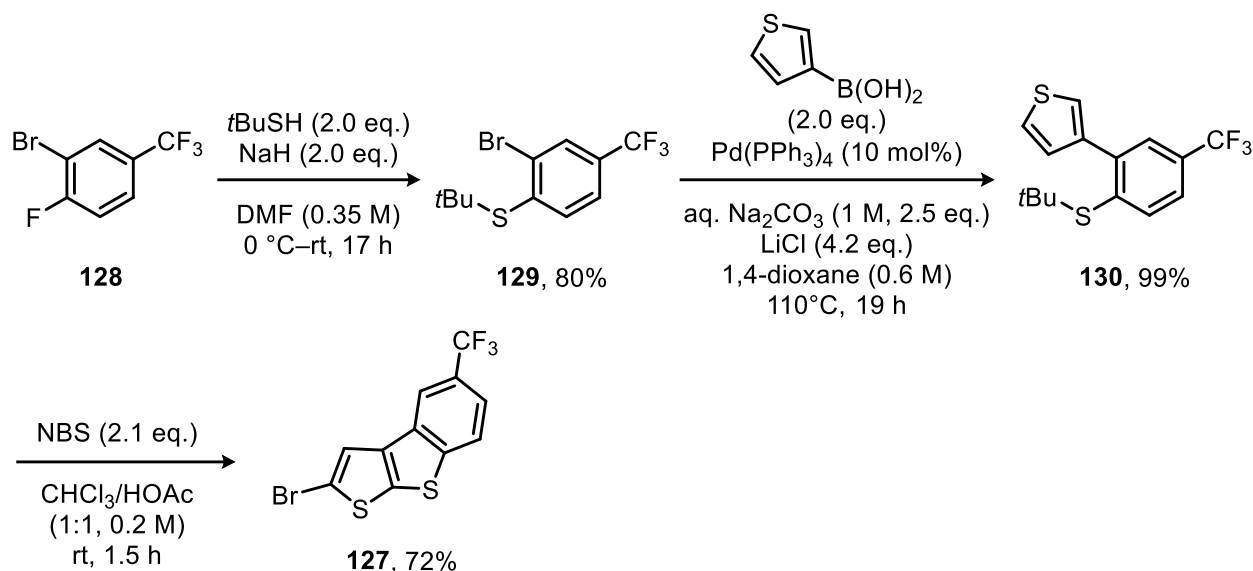
(2-bromo-4-(trifluoromethyl)phenyl)(*tert*-butyl)sulfane (129)
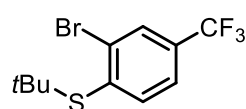
A flame-dried Schlenk flask under argon was charged with NaH (60% in mineral oil, 329 mg, 8.23 mmol, 2.00 eq.) and dry DMF (12 mL), and cooled to 0 °C. After dropwise addition of *tert*-butylthiol (0.93 mL, 8.23 mmol, 2.00 eq.) the reaction mixture was stirred for 1 h. 2-Bromo-1-fluoro-4-(trifluoromethyl)benzene (**128**, 1.00 g, 4.12 mmol, 1.00 eq.) was added in one portion at 0 °C. The reaction was allowed to warm to room temperature and stirred for 17 h until TLC indicated full consumption of the starting material. It was then diluted with MTBE and quenched with 10% HCl. The aqueous layer was extracted with MTBE (2 x 50 mL), and the combined organic phases were washed with brine (4 x 50 mL), dried over anhydrous Na_2SO_4 and concentrated under reduced pressure. Purification via flash column chromatography on silica gel (100% hexanes) furnished the title compound as a colorless oil (991 mg, 3.16 mmol, 77%).

¹H NMR (501 MHz, CD_2Cl_2): δ = 7.94 (d, *J* = 1.9 Hz, 1H), 7.78 (d, *J* = 8.1 Hz, 1H), 7.54 (dd, *J* = 8.1, 2.0 Hz, 1H), 1.38 (s, 9H).

¹⁹F NMR (471 MHz, CD_2Cl_2): δ = −63.23 (s, 3F).

HRMS *m/z* (GC-EI): calcd. For $C_{11}H_{12}S_1F_3Br_1$ ([M]⁺): 311.978983; found: 311.979050.

3-(2-(*tert*-butylthio)-5-(trifluoromethyl)phenyl)thiophene (130)
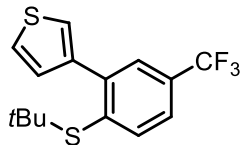
A Schlenk flask was charged with (2-bromo-4-(trifluoromethyl)phenyl)(*tert*-butyl)sulfane (**129**, 750 mg, 2.39 mmol, 1.00 eq.), 3-thienylboronic acid (613 mg, 4.79 mmol, 2.00 eq.), LiCl (425 mg, 10.0 mmol, 4.19 eq.), aqueous Na_2CO_3 (2 M, 3.0 mL, 6.0 mmol, 2.5 eq.) and 1,4-dioxane (4 mL). Subsequently the suspension was sparged with argon for 30 min, $Pd(PPh_3)_4$ (5 mol%, 277 mg) was added under argon, and the mixture was heated to 110 °C for 19 h. After addition of water the aqueous phase was extracted with DCM (3 x 30 mL). The combined organic layers were washed with water, dried over anhydrous Na_2SO_4 and concentrated under reduced pressure. Purification via flash column chromatography on silica gel (100% hexanes) furnished the title compound as a colorless oil (753 mg, 99%).

^{1}H NMR (501 MHz, CD_2Cl_2): δ = 7.80 (d, J = 8.1 Hz, 1H), 7.70 (d, J = 2.1 Hz, 1H), 7.55–7.51 (m, 1H), 7.46 (dd, J = 3.0, 1.3 Hz, 1H), 7.36 (dd, J = 5.0, 3.0 Hz, 1H), 7.31 (dd, J = 5.0, 1.3 Hz, 1H), 1.12 (s, 9H).

^{19}F NMR (471 MHz, CD_2Cl_2): δ = –63.1 (s, 3F).

HRMS *m/z* (GC-EI): calcd. For $C_{15}H_{15}S_2F_3$ ([M]$^+$): 316.056181; found: 316.056620.

2-bromo-5-(trifluoromethyl)benzo[*b*]thieno[3,2-*d*]thiophene (127)
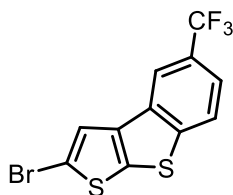
In a flame-dried Schlenk flask under argon 3-(2-(*tert*-butylthio)-5-(trifluoromethyl)phenyl)thiophene (**130**, 1.02 g, 3.21 mmol, 1.00 eq.) was dissolved in dry $CHCl_3$ (8 mL) and AcOH (8 mL). *N*-Bromosuccinimide (1.20 g, 6.74 mmol, 2.1 eq.) was added, and the reaction mixture was stirred at room temperature for 1.5 h. The reaction was then quenched with water, and the aqueous phase was extracted with DCM (3 x 40 mL). The combined organic layers were washed with 3% NaOH solution and water, dried over anhydrous Na_2SO_4 and concentrated under reduced pressure. Purification by flash column chromatography on silica gel (100% hexanes) afforded a white solid containing 87% of the desired title compound (890 mg, 87% purity, 72% yield). The material was suitable for use in the subsequent Suzuki coupling without significantly affecting the reaction outcome. Alternatively, recrystallization from hexanes/DCM provided the pure title compound as a white solid.

^{1}H NMR (501 MHz, CD_2Cl_2): δ = 8.15 (s, 1H), 7.97 (d, J = 8.5 Hz, 1H), 7.64–7.56 (m, 2H).

^{19}F NMR (471 MHz, CD_2Cl_2): δ = –61.9 (s, 3F).

^{13}C NMR (126 MHz, CD_2Cl_2): δ = 146.5, 140.9, 138.9, 132.2, 129.6, 129.2, 127.7, 127.4, 126.3, 126.1, 124.1, 122.8, 121.2 (q, J = 3.5 Hz), 118.9 (q, J = 4.2 Hz), 114.1.

HRMS *m/z* (ESI): calcd. For $C_{11}H_4S_2F_3Br_1$ ([M]$^+$): 335.888456; found: 335.888040.

Synthesis of 2-bromo-6-(trifluoromethyl)benzo[*b*]thieno[3,2-*d*]thiophene (131)
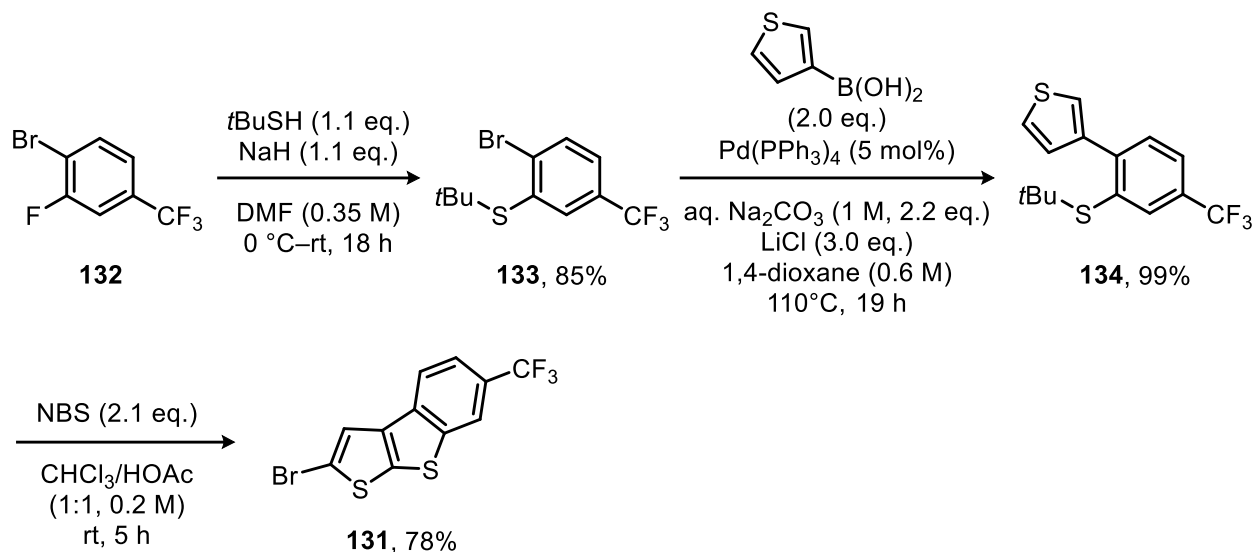
(2-bromo-5-(trifluoromethyl)phenyl)(*tert*-butyl)sulfane (133)
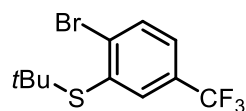
A flame-dried Schlenk flask under argon was charged with NaH (60% in mineral oil, 905 mg, 22.6 mmol, 1.10 eq.) and dry DMF (60 mL), and cooled to 0 °C. After dropwise addition of *tert*-butylthiol (2.5 mL, 23 mmol, 1.1 eq.) the reaction mixture was stirred for 1 h. 1-Bromo-2-fluoro-4-(trifluoromethyl)benzene (**132**, 4.99 g, 20.5 mmol, 1.00 eq.) was added in one portion at 0 °C. The reaction was allowed to warm to room temperature and stirred for 18 h until TLC indicated full consumption of the starting material. It was then diluted with MTBE and quenched with 10% HCl. The aqueous layer was extracted with MTBE (2 x 100 mL), and the combined organic phases were washed with brine (4 x 100 mL), dried over anhydrous Na_2SO_4 and concentrated under reduced pressure. Purification via flash column chromatography on silica gel (100% hexanes) furnished the title compound as a colorless oil (5.44 g, 85%).

R_F (100% hexanes) = 0.51.

^{1}H NMR (501 MHz, CD_2Cl_2): δ = 7.91 (dd, *J* = 2.3, 0.8 Hz, 1H), 7.84 (dd, *J* = 8.4, 0.9 Hz, 1H), 7.45 (ddd, *J* = 8.4, 2.4, 0.8 Hz, 1H), 1.36 (s, 9H).

^{19}F NMR (471 MHz, CD_2Cl_2): δ = –63.2 (s, 3F).

^{13}C NMR (151 MHz, CD$_2$Cl$_2$): δ = 136.9 (q, J = 1.5 Hz), 136.4, 135.9 (q, J = 3.8 Hz), 134.5, 130.0 (q, J = 32.8 Hz), 126.9 (q, J = 3.6 Hz), 124.1 (q, J = 271.9 Hz), 49.6, 31.2.

HRMS *m/z* (GC-EI): calcd. For C$_{11}$H$_{12}$S$_1$F$_3$Br$_1$ ([M]$^+$): 311.978983; found: 311.979340.

3-(2-(*tert*-butylthio)-4-(trifluoromethyl)phenyl)thiophene (134)
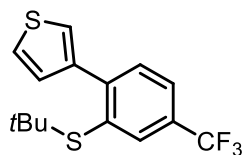
A Schlenk flask was charged with (2-bromo-5-(trifluoromethyl)phenyl)(*tert*-butyl)sulfane (**133**, 5.27 g, 16.8 mmol, 1.00 eq.), 3-thienylboronic acid (4.31 g, 33.7 mmol, 2.00 eq.), LiCl (2.14 g, 50.5 mmol, 3.00 eq.), aqueous Na$_2$CO$_3$ (2 M, 18.5 mL, 37.0 mmol, 2.20 eq.) and 1,4-dioxane (28 mL). Subsequently the suspension was sparged with argon for 30 min, Pd(PPh$_3$)$_4$ (5 mol%, 970 mg) was added under argon, and the mixture was heated to 110 °C for 19 h. After addition of water the aqueous phase was extracted with DCM (3 x 75 mL). The combined organic layers were washed with water, dried over anhydrous Na$_2$SO$_4$ and concentrated under reduced pressure. Purification via flash column chromatography on silica gel (100% hexanes) furnished the title compound as a white solid (5.27 g, 99%).

R_F (100% hexanes) = 0.37.

^{1}H NMR (501 MHz, CD$_2$Cl$_2$): δ = 7.94 (d, J = 2.0 Hz, 1H), 7.64 (dd, J = 8.2, 2.0 Hz, 1H), 7.60 (d, J = 8.1 Hz, 1H), 7.50 (dd, J = 3.0, 1.4 Hz, 1H), 7.36 (dd, J = 5.0, 2.9 Hz, 1H), 7.34 (dd, J = 5.0, 1.4 Hz, 1H), 1.08 (s, 9H).

^{19}F NMR (471 MHz, CD$_2$Cl$_2$): δ = −62.9 (s, 3F).

^{13}C NMR (151 MHz, CD$_2$Cl$_2$): δ = 146.81 (q, J = 1.4 Hz), 141.3, 136.41 (q, J = 3.8 Hz), 133.0, 131.3, 130.3, 129.25 (q, J = 32.5 Hz), 125.91 (q, J = 3.7 Hz), 125.8, 124.8, 124.4 (q, J = 272.1 Hz), 48.6, 31.0.

13C NMR (151 MHz, CD2Cl2) δ 146.81 (q, J = 1.4 Hz), 136.41 (q, J = 3.8 Hz), 129.25 (q, J = 32.5 Hz), 125.91 (q, J = 3.7 Hz).

HRMS *m/z* (GC-EI): calcd. For C$_{15}$H$_{15}$S$_2$F$_3$ ([M]$^+$): 316.056181; found: 316.056670.

2-bromo-6-(trifluoromethyl)benzo[*b*]thieno[3,2-*d*]thiophene (131)
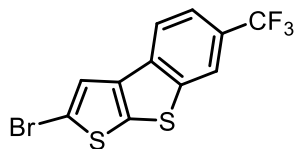
In a flame-dried Schlenk flask under argon 3-(2-(*tert*-butylthio)-4-(trifluoromethyl)phenyl)thiophene (**134**, 5.14 g, 16.3 mmol, 1.00 eq.) was dissolved in dry CHCl$_3$ (40 mL) and AcOH (40 mL). *N*-Bromosuccinimide (6.51 g, 36.6 mmol, 2.25 eq.) was added, and the reaction mixture was stirred at room temperature for 5 h.

The reaction was then quenched with water, and the aqueous phase was extracted with DCM (3 x 75 mL). The combined organic layers were washed with 3% NaOH solution and water, dried over anhydrous Na_2SO_4 and concentrated under reduced pressure. Purification by flash column chromatography on silica gel (100% hexanes) afforded a white solid containing 90% of the desired title compound (4.76 g, 90% purity, 78% yield). The material was suitable for use in the subsequent Suzuki coupling without significantly affecting the reaction outcome. Alternatively, recrystallization from hexanes/DCM provided the pure title compound as a white solid.

R_F (100% hexanes) = 0.57.

^{1}H NMR (501 MHz, CDCl$_3$): δ = 8.06 (s, 1H), 7.85 (d, J = 8.3 Hz, 1H), 7.63 (dd, J = 8.4, 1.6 Hz, 1H), 7.49 (s, 1H).

^{19}F NMR (471 MHz, CDCl$_3$): δ = –61.4 (s, 3F).

^{13}C NMR (126 MHz, CDCl$_3$): δ = 142.6, 140.2, 139.4, 134.4, 126.8 (q, J = 32.7 Hz), 124.42 (q, J = 272.3 Hz), 122.4, 121.8 (q, J = 3.4 Hz), 121.6, 120.6 (q, J = 4.3 Hz), 113.8.

HRMS *m/z* (ESI): calcd. For $C_{11}H_4S_2F_3Br_1$ ([M]$^+$): 335.888456; found: 335.888030.

Synthesis of 2-bromo-4-fluoro-6-(trifluoromethyl)benzo[b]thieno[3,2-d]thiophene (135)
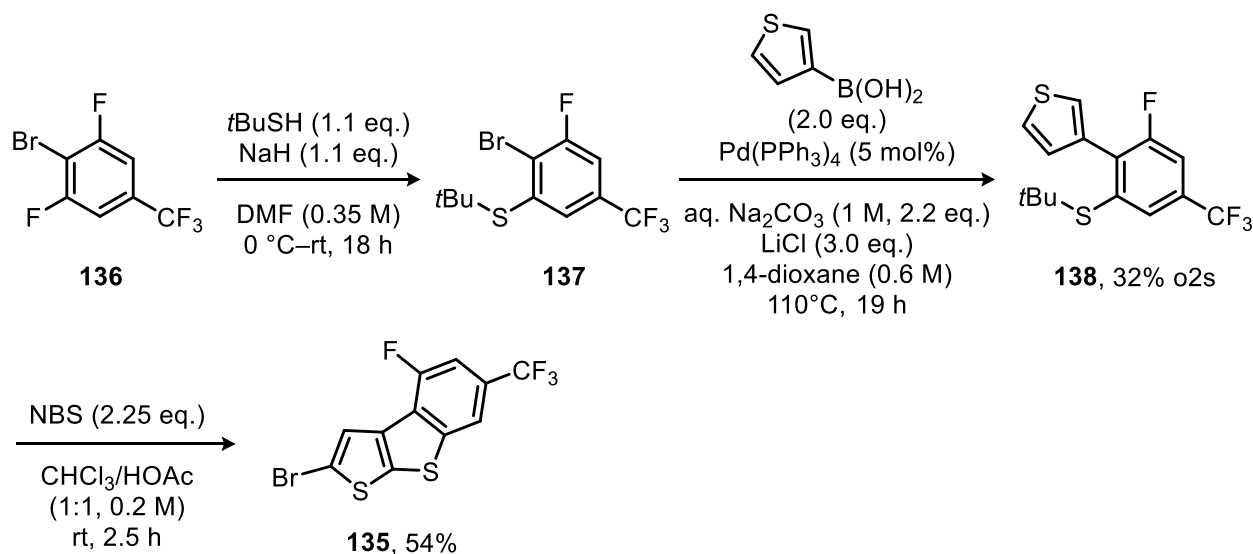
(2-bromo-3-fluoro-5-(trifluoromethyl)phenyl)(*tert*-butyl)sulfane (137)
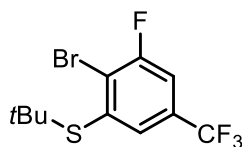
A flame-dried Schlenk flask under argon was charged with NaH (60% in mineral oil, 168 mg, 4.20 mmol, 1.09 eq.) and dry DMF (11 mL), and cooled to 0 °C. After dropwise addition of *tert*-butylthiol (0.46 mL, 4.23 mmol, 1.1 eq.) the reaction mixture was stirred for 1 h. 2-Bromo-1,3-difluoro-5-(trifluoromethyl)benzene (**136**, 1.00 g, 3.85 mmol, 1.00 eq.) was added in one portion at 0 °C. The reaction was allowed to warm to room temperature and stirred for 18 h until TLC indicated full consumption of the starting material. It was then diluted with MTBE and quenched with 10% HCl. The aqueous layer was extracted with MTBE (2 x 40 mL), and the combined organic phases were washed with brine (4 x 50 mL), dried over anhydrous Na_2SO_4 and concentrated under reduced pressure. Purification by flash column chromatography on silica gel (100% hexanes) afforded a mixture containing the desired thioether **137** as a yellow oil (1.04 g). As further purification was not feasible, the crude material was used directly in the subsequent step.

MS *m/z* (GC-EI): calcd. For $C_{11}H_{11}S_1F_4Br_1$ ([M]$^+$): 330; found: 330.

3-(2-(*tert*-butylthio)-6-fluoro-4-(trifluoromethyl)phenyl)thiophene (138)
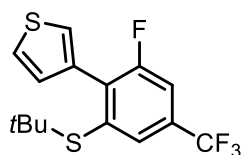
A Schlenk flask was charged with (2-bromo-3-fluoro-5-(trifluoromethyl)phenyl)(*tert*-butyl)sulfane (**137**, 1.00 g, 3.02 mmol, 1.00 eq.), 3-thienylboronic acid (773 mg, 6.04 mmol, 2.00 eq.), LiCl (384 mg, 9.06 mmol, 3.00 eq.), aqueous Na_2CO_3 (2 M, 3.32 mL, 6.64 mmol, 2.20 eq.) and 1,4-dioxane (28 mL). Subsequently the suspension was sparged with argon for 30 min, Pd(PPh$_3$)$_4$ (5 mol%, 174 mg) was added under argon, and the mixture was heated to 110 °C for 19 h. After addition of water the aqueous phase was extracted with DCM (3 x 30 mL). The combined organic layers were washed with water, dried over anhydrous Na_2SO_4 and concentrated under reduced pressure. Purification via flash column chromatography on silica gel (100% hexanes) furnished the title compound as a white solid (414 mg, 32% over two steps).

¹H NMR (501 MHz, CD$_2$Cl$_2$): δ = 7.78 (dt, *J* = 1.9, 0.9 Hz, 1H), 7.45–7.41 (m, 2H), 7.41–7.38 (m, 1H), 7.20 (dt, *J* = 5.0, 1.4 Hz, 1H), 1.11 (s, 9H).

¹⁹F NMR (471 MHz, CD$_2$Cl$_2$): δ = –63.2 (s, 3F), –109.2 (s, 1F).

MS *m/z* (GC-EI): calcd. For $C_{15}H_{14}S_2F_4$ ([M]$^+$): 334; found: 334.

2-bromo-4-fluoro-6-(trifluoromethyl)benzo[*b*]thieno[3,2-*d*]thiophene (135)
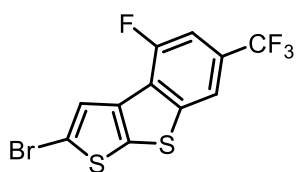
In a flame-dried Schlenk flask under argon 3-(2-(*tert*-butylthio)-6-fluoro-4-(trifluoromethyl)phenyl)thiophene (**134**, 414 mg, 1.24 mmol, 1.00 eq.) was dissolved in dry CHCl$_3$ (3 mL) and AcOH (3 mL). *N*-Bromosuccinimide (496 mg, 2.79 mmol, 2.25 eq.) was added, and the reaction mixture was stirred at room temperature for 2.5 h. The reaction was then quenched with water, and the aqueous phase was extracted with DCM (3 x 25 mL). The combined organic layers were washed with 3% NaOH solution and water, dried over anhydrous Na$_2$SO$_4$ and concentrated under reduced pressure. Purification by flash column chromatography on silica gel (100% hexanes) afforded a yellow solid containing 92% of the desired title compound (257 mg, 92% purity, 54% yield). The material was suitable for use in the subsequent Suzuki coupling without significantly affecting the reaction outcome. Alternatively, recrystallization from hexanes/DCM provided the pure title compound as a yellow solid.

^{1}H NMR (501 MHz, CD$_2$Cl$_2$): δ = 7.80 (t, *J* = 1.1 Hz, 1H), 7.49 (d, *J* = 1.3 Hz, 1H), 7.28 (dd, *J* = 10.0, 1.4 Hz, 1H).

^{19}F NMR (471 MHz, CD$_2$Cl$_2$): δ = –61.77 (s, 3F), –117.08 (s, 1F).

HRMS *m/z* (GC-EI): calcd. For C$_{11}$H$_3$S$_2$F$_4$Br$_1$ ([M]$^+$): 353.879034; found: 353.879350.

Synthesis of substituted (*S*)-BINOLs

139, (*S*)-MOM-BINOL Bpin ester
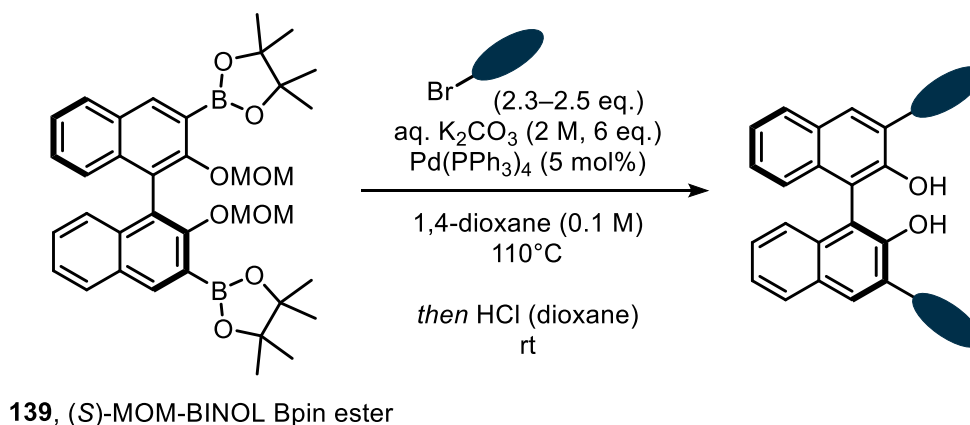
(*S*)-3,3'-bis(benzo[*b*]thiophen-2-yl)-[1,1'-binaphthalene]-2,2'-diol (140)

A Schlenk flask was charged (*S*)-MOM-BINOL Bpin ester **139** (500 mg, 0.798 mmol, 1.00 eq.), 2-bromobenzothiophene (425 mg, 2.00 mmol, 2.50 eq.), aqueous K$_2$CO$_3$ (2 M, 2.4 mL, 4.8 mmol, 6.0 eq.)

and 1,4-dioxane (24 mL). Subsequently the suspension was sparged with argon for 30 min, Pd(PPh$_3$)$_4$ (5 mol%, 46 mg) was added under argon, and the mixture was heated to 110 °C overnight. After addition of saturated NH$_4$Cl solution the aqueous phase was extracted with DCM (3 x 50 mL). The combined organic layers were washed with water, dried over anhydrous Na$_2$SO$_4$ and concentrated under reduced pressure. The crude material was dissolved in HCl (4 M in 1,4-dioxane, 2 mL) and stirred at room temperature overnight. The reaction mixture was diluted with 10% HCl and DCM. The aqueous phase was washed with DCM (3 x 25 mL), the combined organic layers were washed with water, dried over anhydrous Na$_2$SO$_4$ and concentrated under reduced pressure. Purification via flash column chromatography on silica gel (2% ethyl acetate, pentane) furnished the title compound as a white solid (307 mg, 70%).

R_F (50% DCM, hexanes) = 0.52.

^{1}H NMR (600 MHz, CD$_2$Cl$_2$): δ = 8.45 (d, J = 0.8 Hz, 2H), 8.03–7.98 (m, 4H), 7.92–7.88 (m, 2H), 7.87–7.80 (m, 2H), 7.43 (ddd, J = 8.1, 6.8, 1.2 Hz, 2H), 7.41–7.35 (m, 4H), 7.33 (ddd, J = 8.2, 6.8, 1.3 Hz, 2H), 7.19 (ddt, J = 8.5, 1.4, 0.8 Hz, 2H), 5.81 (d, J = 0.6 Hz, 2H).

^{13}C NMR (151 MHz, CD$_2$Cl$_2$): δ = 150.5, 140.9, 140.1, 139.6, 133.4, 131.3, 129.8, 129.1, 128.3, 125.2, 125.1, 124.9, 124.7, 124.4, 124.3, 123.8, 122.3, 112.7.

HRMS m/z (ESI): calcd. For C$_{36}$H$_{21}$S$_2$O$_2$ ([M–H]$^-$): 549.098850; found: 549.099530.

$[\alpha]_D^{25}$ = +127.7 (c = 0.13, CHCl$_3$).

(S)-3,3'-bis(6-(perfluorophenyl)benzofuran-2-yl)-[1,1'-binaphthalene]-2,2'-diol (141)
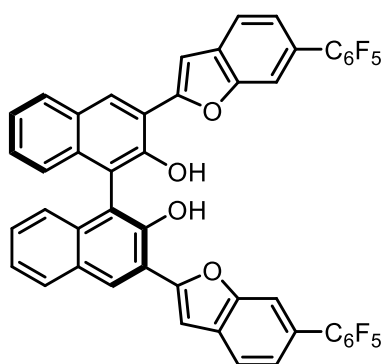
A Schlenk flask was charged (S)-MOM-BINOL Bpin ester **139** (113 mg, 0.180 mmol, 1.00 eq.), iodide **119** (170 mg, 0.415 mmol, 2.30 eq.), aqueous K$_2$CO$_3$ (2 M, 0.54 mL, 1.08 mmol, 6.0 eq.) and 1,4-dioxane (24 mL). Subsequently the suspension was sparged with argon for 30 min, Pd(PPh$_3$)$_4$ (5 mol%, 46 mg) was added under argon, and the mixture was heated to 110 °C overnight. After addition of saturated NH$_4$Cl solution the aqueous phase was extracted with DCM (3 x 30 mL). The combined organic layers were washed with water, dried over anhydrous Na$_2$SO$_4$ and concentrated under reduced pressure. The crude material was dissolved in HCl (4 M in 1,4-dioxane, 2 mL) and stirred at room temperature overnight. The reaction mixture was diluted with

10% HCl and DCM. The aqueous phase was washed with DCM (3 x 25 mL), the combined organic layers were washed with water, dried over anhydrous Na_2SO_4 and concentrated under reduced pressure. Purification via flash column chromatography on silica gel (15–30% DCM, hexanes) furnished the title compound as a white solid (144 mg, 94%).

¹H NMR (501 MHz, $(CD_3)_2CO$): δ = 8.79 (s, 2H), 8.73 (s, 2H), 8.12 (d, J = 8.1 Hz, 2H), 7.89–7.84 (m, 4H), 7.75 (d, J = 1.0 Hz, 2H), 7.46–7.39 (m, 4H), 7.33 (ddd, J = 8.2, 6.8, 1.3 Hz, 2H), 7.10 (dd, J = 8.5, 1.1 Hz, 2H).

¹⁹F NMR (471 MHz, $(CD_3)_2CO$): δ = –144.6 (dd, J = 23.0, 7.7 Hz, 4F), –158.5 (t, J = 20.5 Hz, 2F), –164.8 (td, J = 22.1, 7.6 Hz, 4F).

¹³C NMR (126 MHz, $(CD_3)_2CO$): δ = 155.2, 154.8, 152.5, 146.3, 144.4, 139.8, 137.8, 135.3, 131.8, 129.9, 129.8, 128.8, 128.5, 126.1, 125.1, 125.0, 123.2, 122.5, 120.7, 117.3, 117.1, 114.6, 113.6, 108.3.

HRMS *m/z* (ESI): calcd. For $C_{48}H_{19}O_4F_{10}$ ([M]⁻): 849.112920; found: 849.113310.

(*S*)-3,3'-bis(benzo[*b*]thieno[3,2-*d*]thiophen-2-yl)-[1,1'-binaphthalene]-2,2'-diol (142)
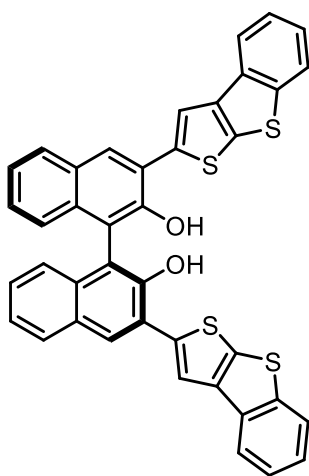
A Schlenk flask was charged (*S*)-MOM-BINOL Bpin ester **139** (216 mg, 0.345 mmol, 1.00 eq.), 2-bromobenzo[*b*]thieno[3,2-*d*]thiophene (214 mg, 0.80 mmol, 2.31 eq.), aqueous K_2CO_3 (2 M, 1.0 mL, 2.1 mmol, 6.0 eq.) and 1,4-dioxane (3.4 mL). Subsequently the suspension was sparged with argon for 30 min, $Pd(PPh_3)_4$ (5 mol%, 20 mg) was added under argon, and the mixture was heated to 110 °C overnight. After addition of saturated NH_4Cl solution the aqueous phase was extracted with DCM (3 x 50 mL). The combined organic layers were washed with water, dried over anhydrous Na_2SO_4 and concentrated under reduced pressure. The crude material was dissolved in HCl (4 M in 1,4-dioxane, 2 mL) and stirred at room temperature overnight. The reaction mixture was diluted with 10% HCl and DCM. The aqueous phase was washed with DCM (3 x 25 mL), the combined organic layers were washed with water, dried over anhydrous Na_2SO_4 and concentrated under reduced pressure. Purification via flash column chromatography on silica gel (30% DCM, pentane) furnished the title compound as a light yellow solid (195 mg, 85%).

R_F (50% DCM, hexanes) = 0.53.

¹H NMR (600 MHz, CD$_2$Cl$_2$): δ = 8.43 (d, J = 0.8 Hz, 2H), 8.23 (s, 2H), 8.01 (tdd, J = 7.9, 1.2, 0.6 Hz, 4H), 7.88 (ddd, J = 8.0, 1.1, 0.7 Hz, 2H), 7.47–7.43 (m, 4H), 7.41–7.33 (m, 4H), 7.19 (dd, J = 8.4, 1.0 Hz, 2H).

¹³C NMR (151 MHz, CD$_2$Cl$_2$): δ = 150.1, 144.0, 142.6, 142.0, 138.7, 133.3, 133.1, 129.9, 129.9, 129.0, 128.2, 125.3, 125.2, 124.9, 124.4, 124.1, 123.6, 122.0, 119.5, 112.7.

HRMS *m/z* (ESI): calcd. For C$_{40}$H$_{21}$S$_4$O$_2$ ([M–H]⁻): 661.04299; found: 661.04392.

$[\alpha]_D^{25}$ = +150.5 (c = 0.16, CHCl$_3$).

(*S*)-3,3'-bis(benzo[*b*]thieno[2,3-*d*]thiophen-2-yl)-[1,1'-binaphthalene]-2,2'-diol (143)
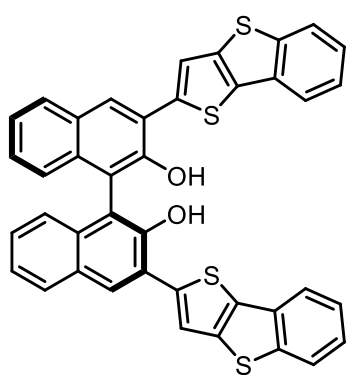
A Schlenk flask was charged (*S*)-MOM-BINOL Bpin ester **139** (155 mg, 0.248 mmol, 1.00 eq.), bromide **125** (150 mg, 0.56 mmol, 2.25 eq.), aqueous K$_2$CO$_3$ (2 M, 0.74 mL, 1.49 mmol, 6.0 eq.) and 1,4-dioxane (2.5 mL). Subsequently the suspension was sparged with argon for 30 min, Pd(PPh$_3$)$_4$ (10 mol%, 29 mg) was added under argon, and the mixture was heated to 110 °C overnight. After addition of saturated NH$_4$Cl solution the aqueous phase was extracted with DCM (3 x 30 mL). The combined organic layers were washed with water, dried over anhydrous Na$_2$SO$_4$ and concentrated under reduced pressure. The crude material was dissolved in HCl (4 M in 1,4-dioxane, 2 mL) and stirred at room temperature overnight. The reaction mixture was diluted with 10% HCl and DCM. The aqueous phase was washed with DCM (3 x 25 mL), the combined organic layers were washed with water, dried over anhydrous Na$_2$SO$_4$ and concentrated under reduced pressure. Purification via flash column chromatography on silica gel (10–40% DCM, hexanes) furnished the title compound as a bright yellow solid (139 mg, 85%).

¹H NMR (501 MHz, CDCl$_3$): δ = 8.37 (s, 2H), 7.97 (s, 2H), 7.95–7.91 (m, 2H), 7.89–7.84 (m, 4H), 7.45–7.39 (m, 4H), 7.39–7.30 (m, 4H), 7.18 (dd, J = 8.4, 1.1 Hz, 2H).

¹³C NMR (126 MHz, CDCl$_3$): δ = 149.8, 142.7, 141.8, 138.6, 135.0, 132.9, 132.7, 129.9, 129.6, 128.8, 128.1, 125.1, 124.9, 124.7, 124.2, 124.0, 123.7, 121.2, 120.6, 112.1.

HRMS *m/z* (ESI): calcd. For C$_{40}$H$_{21}$S$_4$O$_2$ ([M–H]⁻): 661.042995; found: 661.043540.

(S)-3,3'-bis(5-(trifluoromethyl)benzo[b]thieno[3,2-d]thiophen-2-yl)-[1,1'-binaphthalene]-2,2'-diol (144)
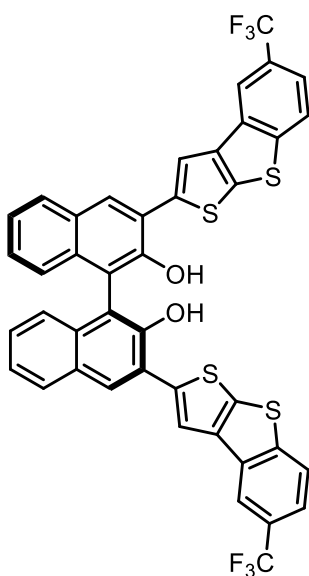
A Schlenk flask was charged (S)-MOM-BINOL Bpin ester **139** (200 mg, 0.32 mmol, 1.00 eq.), bromide **127** (285 mg, 87% purity, 0.73 mmol, 2.30 eq.), aqueous K_2CO_3 (2 M, 0.96 mL, 1.92 mmol, 6.0 eq.) and 1,4-dioxane (3.2 mL). Subsequently the suspension was sparged with argon for 30 min, Pd(PPh$_3$)$_4$ (10 mol%, 37 mg) was added under argon, and the mixture was heated to 110 °C overnight. After addition of saturated NH$_4$Cl solution the aqueous phase was extracted with DCM (3 x 30 mL). The combined organic layers were washed with water, dried over anhydrous Na_2SO_4 and concentrated under reduced pressure. The crude material was dissolved in HCl (4 M in 1,4-dioxane, 2 mL) and stirred at room temperature overnight. The reaction mixture was diluted with 10% HCl and DCM. The aqueous phase was washed with DCM (3 x 25 mL), the combined organic layers were washed with water, dried over anhydrous Na_2SO_4 and concentrated under reduced pressure. Purification via flash column chromatography on silica gel (15–40% DCM, hexanes) furnished the title compound as a beige solid (229 mg, 90%).

^{1}H NMR (501 MHz, (CD$_3$)$_2$CO): δ = 8.80 (br, 2H), 8.63 (s, 2H), 8.58 (s, 2H), 8.54 (d, J = 1.9 Hz, 2H), 8.22 (d, J = 8.5 Hz, 2H), 8.03 (d, J = 8.1 Hz, 2H), 7.70 (dd, J = 8.5, 1.9 Hz, 2H), 7.39 (ddd, J = 8.0, 6.7, 1.2 Hz, 2H), 7.29 (ddd, J = 8.2, 6.7, 1.3 Hz, 2H), 7.11 (d, J = 8.4 Hz, 2H).

^{19}F NMR (471 MHz, (CD$_3$)$_2$CO): δ = –61.8 (s, 6F).

^{13}C NMR (126 MHz, (CD$_3$)$_2$CO): δ = 151.9, 148.1, 144.7, 142.0, 141.1, 134.8, 133.8, 130.1, 129.3, 129.2, 129.1, 128.0, 127.9, 127.7, 127.4, 127.2, 126.9, 125.4, 125.09, 125.08, 124.9, 124.8, 122.6, 121.39, 121.36, 121.33, 121.30, 119.53, 119.50, 119.46, 119.4, 119.0, 114.9.

HRMS *m/z* (ESI): calcd. For $C_{42}H_{19}S_4F_6O_2$ ([M–H]$^-$): 797.017767; found: 797.018210.

(S)-3,3'-bis(6-(trifluoromethyl)benzo[b]thieno[3,2-d]thiophen-2-yl)-[1,1'-binaphthalene]-2,2'-diol (145)

A Schlenk flask was charged (S)-MOM-BINOL Bpin ester (1.50 g, 2.40 mmol, 1.00 eq.), 2-bromo-6-(trifluoromethyl)benzo[b]thieno[3,2-d]thiophene (2.07 g, 5.51 mmol, 2.30 eq.), aqueous K_2CO_3 (2 M, 7.2 mL, 14 mmol, 6.0 eq.) and 1,4-dioxane (24 mL). Subsequently the suspension was sparged with argon
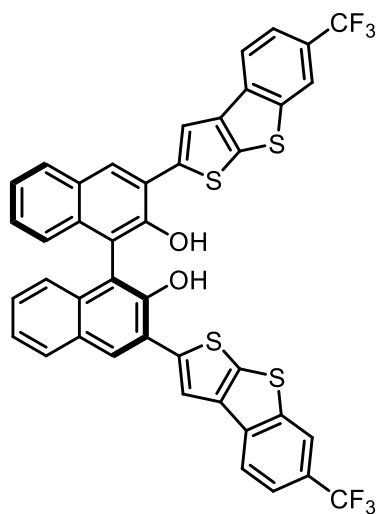
for 30 min, Pd(PPh₃)₄ (5 mol%, 139 mg) was added under argon, and the mixture was heated to 110 °C for 2 d. After addition of saturated NH₄Cl solution the aqueous phase was extracted with DCM (3 x 50 mL). The combined organic layers were washed with water, dried over anhydrous Na₂SO₄ and concentrated under reduced pressure. The crude material was dissolved in HCl (4 M in 1,4-dioxane, 4 mL) and stirred at room temperature for 26 h. The reaction mixture was diluted with 10% HCl and DCM. The aqueous phase was washed with DCM (3 x 25 mL), the combined organic layers were washed with water, dried over anhydrous Na₂SO₄ and concentrated under reduced pressure. Purification via flash column chromatography on silica gel (30% DCM, hexanes) furnished the title compound as a yellow solid (1.68 g, 88%).

R_F (30% DCM, hexanes) = 0.26.

¹H NMR (501 MHz, (CD₃)₂CO): δ = 8.77 (s, 2H), 8.56 (s, 2H), 8.53 (s, 2H), 8.42 (s, 2H), 8.33 (d, J = 8.3 Hz, 2H), 8.03 (d, J = 8.1 Hz, 2H), 7.78 (dd, J = 8.4, 1.7 Hz, 2H), 7.38 (ddd, J = 8.0, 6.8, 1.2 Hz, 2H), 7.29 (ddd, J = 8.2, 6.8, 1.3 Hz, 2H), 7.11 (d, J = 8.1 Hz, 2H).

¹⁹F NMR (471 MHz, (CD₃)₂CO): δ = –61.7 (s, 6F).

¹³C NMR (126 MHz, (CD₃)₂CO): δ = 151.9, 144.8, 144.5, 142.2, 141.8, 136.6, 134.8, 130.1, 129.3, 128.9, 127.9, 127.0, 126.8, 126.7, 126.5, 126.2, 125.3, 125.1, 124.9, 124.6, 123.0, 122.5, 122.4, 122.4, 122.4, 122.3, 121.7, 121.6, 121.6, 121.6, 119.1, 114.9.

HRMS *m/z* (ESI): calcd. For C₄₂H₁₉S₄F₆O₂ ([M–H]⁻): 797.01776; found: 797.01830.

$[\alpha]_D^{25}$ = +142.0 (c = 0.30, CHCl₃).

(*S*)-3,3'-bis(4-fluoro-6-(trifluoromethyl)benzo[*b*]thieno[3,2-*d*]thiophen-2-yl)-[1,1'-binaphthalene]-2,2'-diol (146)

A Schlenk flask was charged (*S*)-MOM-BINOL Bpin ester **139** (188 mg, 0.30 mmol, 1.00 eq.), bromide **135** (257 mg, 92% purity, 0.67 mmol, 2.22 eq.), aqueous K₂CO₃ (2 M, 0.90 mL, 1.80 mmol, 6.0 eq.) and 1,4-dioxane (3.0 mL). Subsequently the suspension was sparged with argon for 30 min, Pd(PPh₃)₄ (5 mol%, 17 mg) was added under argon, and the mixture was heated to 110 °C overnight. After addition of saturated NH₄Cl solution the aqueous phase was extracted with DCM (3 x 30 mL). The combined organic layers were washed with water, dried over anhydrous Na₂SO₄ and concentrated under reduced pressure. The crude
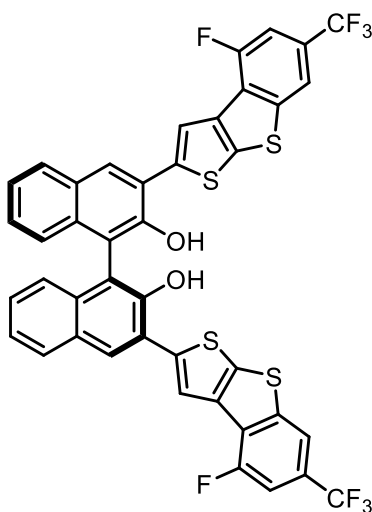
material was dissolved in HCl (4 M in 1,4-dioxane, 2 mL) and stirred at room temperature overnight. The reaction mixture was diluted with 10% HCl and DCM. The aqueous phase was washed with DCM (3 x 25 mL), the combined organic layers were washed with water, dried over anhydrous Na_2SO_4 and concentrated under reduced pressure. Purification via flash column chromatography on silica gel (30% DCM, CyH) furnished the title compound as a white solid (165 mg, 66%).

¹H NMR (501 MHz, $(CD_3)_2CO$): δ = 8.62 (s, 2H), 8.43 (d, J = 1.3 Hz, 2H), 8.29 (s, 2H), 8.07 (d, J = 8.1 Hz, 2H), 7.57 (dd, J = 10.3, 1.4 Hz, 2H), 7.39 (ddd, J = 8.0, 6.6, 1.2 Hz, 2H), 7.30 (ddd, J = 8.2, 6.7, 1.3 Hz, 2H), 7.11 (dd, J = 8.5, 1.0 Hz, 2H).

¹⁹F NMR (471 MHz, $(CD_3)_2CO$): δ = –61.73 (s, 6F), –118.04 (s, 2F).

¹³C NMR (126 MHz, $(CD_3)_2CO$): δ = 158.6, 156.6, 151.9, 147.13, 147.07, 145.6, 142.5, 137.84, 137.82, 134.9, 130.2, 129.4, 128.0, 127.8, 127.7, 127.5, 127.4, 126.0, 125.2, 125.04, 124.99, 124.9, 123.84, 123.82, 120.12, 120.09, 118.0, 117.95, 117.91, 117.88, 114.9, 108.50, 108.47, 108.32, 108.29.

HRMS m/z (ESI): calcd. For $C_{42}H_{17}S_4F_8O_2$ ([M–H]⁻): 832.998923; found: 832.999710.

Synthesis of IDPi catalysts

1) DMAP (1.0 eq.),
   NEt₃ (19 eq.), 1 h
2) HMDS (1.0 eq.), 15 min
   then 120 °C, 5 d

PhMe (0.1 M)

(2.0 eq.)   (2.0 eq.)   (*S,S*)-IDPi
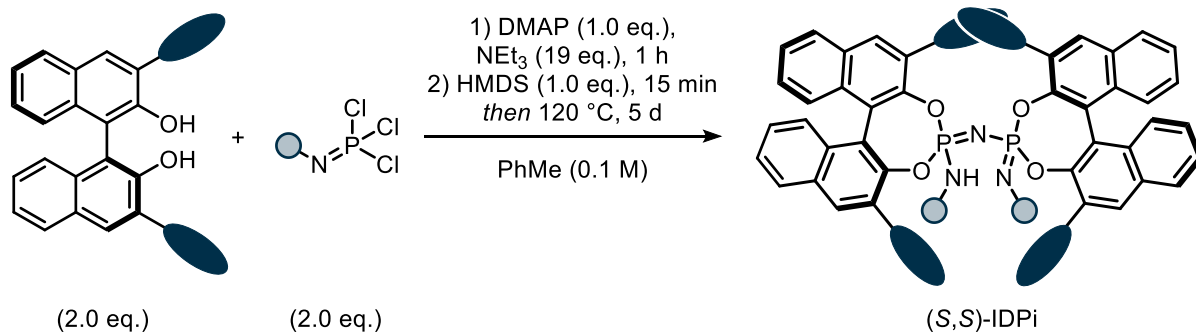
(*S,S*)-(benzothiophen-2-yl)-CF₃-IDPi (82a)
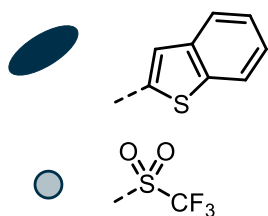
(*S*)-BINOL **140** (180 mg, 0.327 mmol, 2.00 eq.) was added to a flame-dried Schlenk flask under argon and dried at 50 °C under high vacuum overnight. The flask was then placed under argon. $P(NSO_2CF_3)Cl_3$ (52 μL, 0.325 mmol, 2.00 eq.), toluene (3.3 mL) and NEt₃ (0.45 mL, 3.26 mmol, 20.0 eq.) were added and the reaction mixture was stirred at room temperature for 1 h. Subsequently,

HMDS (34.0 µL, 0.163 mmol, 1.00 eq.) was added, the mixture was stirred at room temperature for 15 min, and then heated to 120 °C for 3 d. After cooling to room temperature the mixture was diluted with DCM and quenched by addition of 1 M HCl. The aqueous phase was extracted with DCM (3 x 25 mL), the combined organic layers were washed with 1 M HCl and water, dried over anhydrous Na_2SO_4 and concentrated under reduced pressure. Purification via flash column chromatography on silica gel (1st column: 0–3% EtOAc, DCM, 2nd column: 20–30% EtOAc, hexanes) afforded a white solid. The product was acidified by dissolving it in DCM and vividly stirring it with 6 M HCl for 10 min. The organic layer was concentrated under reduced pressure and dried under high vacuum, furnishing the title compound as an off-white solid (168 mg, 70%).

R_F (50% EtOAc, hexanes) = 0.29.

¹H NMR (501 MHz, CD_2Cl_2): δ = 8.32 (s, 2H), 8.05 (d, J = 8.3 Hz, 2H), 8.01 (d, J = 8.2 Hz, 2H), 7.85 (ddd, J = 8.0, 6.7, 1.1 Hz, 2H), 7.83–7.78 (m, 2H), 7.73 (dd, J = 6.9, 2.1 Hz, 2H), 7.66 (ddd, J = 8.2, 6.8, 1.2 Hz, 2H), 7.61–7.52 (m, 4H), 7.44 (d, J = 7.8 Hz, 2H), 7.42–7.37 (m, 2H), 7.37–7.31 (m, 6H), 7.31–7.25 (m, 4H), 7.03 (s, 2H), 6.90 (td, J = 7.5, 1.2 Hz, 2H), 6.85 (td, J = 7.6, 1.3 Hz, 2H), 6.81 (s, 2H).

¹⁹F NMR (471 MHz, CD_2Cl_2): δ = –78.53 (s, 6F).

³¹P NMR (203 MHz, CD_2Cl_2): δ = –15.79.

¹³C NMR (151 MHz, CD_2Cl_2): δ = 143.74, 143.71, 143.68, 142.8, 142.71, 142.68, 140.9, 140.4, 140.2, 139.9, 137.3, 137.2, 132.4, 132.14, 132.08, 132.0, 131.1, 130.4, 129.6, 129.1, 128.1, 127.9, 127.6, 127.4, 127.3, 127.24, 127.18, 127.15, 126.53, 126.52, 126.51, 126.37, 126.35, 126.3, 125.2, 125.11, 125.06, 124.99, 124.95, 124.72, 124.70, 124.62, 124.59, 124.0, 123.92, 123.91, 123.90, 122.87, 122.61, 122.61, 122.60, 121.97, 121.95, 120.7, 118.6, 116.5.

HRMS *m/z* (ESI): calcd. For $C_{74}H_{40}S_6F_6O_8N_3P_2$ ([M–H]⁻): 1466.05246; found: 1466.05376.

$[\alpha]_D^{25}$ = +377.1 (c = 0.32, CHCl₃).

(*S,S*)-(benzothiophen-2-yl)-C₆F₅-IDPi (82b)
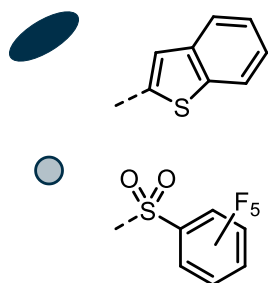
(*S*)-BINOL **140** (210 mg, 0.381 mmol, 2.04 eq.) was added to a flame-dried Schlenk flask under argon and dried at 50 °C under high vacuum overnight. The flask was then placed under argon. P(NSO₂C₆F₅)Cl₃ (144 mg, 0.377 mmol, 2.01 eq.), toluene (3.7 mL) and NEt₃ (0.52 mL, 3.73 mmol, 19.9 eq.) were added and the reaction mixture was stirred at room temperature for 1 h. Subsequently, HMDS (39.0 µL, 0.187 mmol, 1.00 eq.) was added, the mixture was stirred at

room temperature for 15 min, and then heated to 120 °C for 3 d. After cooling to room temperature the mixture was diluted with DCM and quenched by addition of 1 M HCl. The aqueous phase was extracted with DCM (3 x 25 mL), the combined organic layers were washed with 1 M HCl and water, dried over anhydrous Na_2SO_4 and concentrated under reduced pressure. Purification via flash column chromatography on silica gel (1st column: 0–4% EtOAc, DCM, 2nd column: 10–40% EtOAc, hexanes) afforded a white solid. The product was acidified by dissolving it in DCM and vividly stirring it with 6 M HCl for 20 min. The organic layer was concentrated under reduced pressure and dried under high vacuum, furnishing the title compound as an off-white solid (181 mg, 58%).

R_F (50% EtOAc, hexanes) = 0.32.

^{1}H NMR (501 MHz, CD_2Cl_2): δ = 8.26 (s, 2H), 8.01 (dd, J = 17.6, 8.2 Hz, 4H), 7.89–7.84 (m, 2H), 7.82–7.75 (m, 4H), 7.61–7.53 (m, 4H), 7.43 (d, J = 8.6 Hz, 2H), 7.38–7.29 (m, 8H), 7.25 (d, J = 7.7 Hz, 2H), 7.23–7.16 (m, 4H), 7.09 (s, 2H), 6.80–6.69 (m, 6H).

^{19}F NMR (471 MHz, CD_2Cl_2): δ = -136.59 (d, J = 21.4 Hz, 4F), -146.07 (t, J = 21.7 Hz, 2F), -159.60 (t, J = 21.0 Hz, 4F).

^{31}P NMR (203 MHz, CD_2Cl_2): δ = -16.89.

^{13}C NMR (126 MHz, CD_2Cl_2): δ = 145.4, 144.8, 143.43, 143.39, 143.35, 142.8, 142.5, 140.9, 140.4, 139.8, 139.2, 138.6, 137.0, 136.9, 136.6, 132.4, 132.2, 131.9, 131.8, 130.13, 130.09, 129.4, 129.0, 128.1, 127.8, 127.6, 127.5, 127.3, 127.0, 126.5, 125.9, 125.84, 125.82, 125.4, 125.2, 125.0, 124.9, 124.8, 124.5, 123.9, 123.8, 122.6, 121.8, 121.7, 117.7.

HRMS *m/z* (ESI): calcd. For $C_{74}H_{40}S_6F_6O_8N_3P_2$ ([M–H]$^-$): 1662.04607; found: 1662.04538.

$[\alpha]_D^{25}$ = +329.6 (c = 0.26, CHCl$_3$).

(*S,S*)-(6-(perfluorophenyl)benzofuran-2-yl)-C$_6$F$_5$-IDPi (87b)
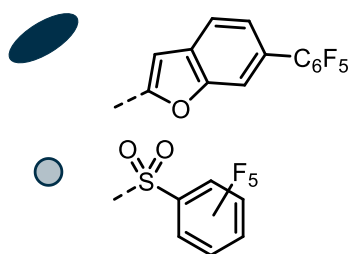
(*S*)-BINOL **141** (142 mg, 0.167 mmol, 2.01 eq.) was added to a flame-dried Schlenk flask under argon and dried at 50 °C under high vacuum overnight. The flask was then placed under argon. P(NSO$_2$C$_6$F$_5$)Cl$_3$ (63.5 mg, 0.166 mmol, 2.0 eq.), toluene (1.7 mL) and NEt$_3$ (0.23 mL, 1.66 mmol, 20.0 eq.) were added and the reaction mixture was stirred at room temperature for 1 h. Subsequently, HMDS (17.3 µL, 0.083 mmol, 1.00 eq.) was added, the mixture was stirred at room temperature for 15 min, and then heated to 120 °C for 3 d. After cooling to room temperature the mixture was diluted with DCM and quenched by addition of

1 M HCl. The aqueous phase was extracted with DCM (3 x 25 mL), the combined organic layers were washed with 1 M HCl and water, dried over anhydrous Na_2SO_4 and concentrated under reduced pressure. Purification via flash column chromatography on silica gel (1st column: 0–3% EtOAc, DCM, 2nd column: 90% EtOAc, hexanes) afforded a white solid. The product was acidified by filtration over a short plug of DOWEX 50WX8 (H-form, eluted with DCM). The product was concentrated under reduced pressure and dried under high vacuum, furnishing the title compound as an off-white solid (54 mg, 29%).

1H NMR (501 MHz, $(CD_3)_2CO$): δ = 8.88 (s, 2H), 8.66 (s, 2H), 8.24 (d, *J* = 8.2 Hz, 2H), 7.99 (s, 2H), 7.92 (d, *J* = 8.0 Hz, 2H), 7.80 (s, 2H), 7.74 (d, *J* = 8.3 Hz, 4H), 7.63 (ddd, *J* = 8.1, 6.7, 1.1 Hz, 2H), 7.57 (ddd, *J* = 8.2, 6.8, 1.1 Hz, 2H), 7.39–7.28 (m, 8H), 7.09 (d, *J* = 7.9 Hz, 2H), 7.04 (t, *J* = 9.2 Hz, 4H), 6.86 (dd, *J* = 8.0, 1.9 Hz, 2H).

19F NMR (471 MHz, $(CD_3)_2CO$): δ = –137.6 (dd, *J* = 21.5, 6.1 Hz, 4F), –144.1 (dd, *J* = 23.4, 7.9 Hz, 4F), –144.5 (dd, *J* = 23.0, 7.5 Hz, 4F), –151.9 (t, *J* = 21.2 Hz, 2F), –158.6 (t, *J* = 20.4 Hz, 2F), –159.2 (t, *J* = 20.3 Hz, 2F), –163.3 (td, *J* = 23.7, 7.5 Hz, 4F), –164.5 (td, *J* = 22.1, 7.8 Hz, 4F), –165.0 (td, *J* = 21.9, 7.5 Hz, 4F).

31P NMR (203 MHz, $(CD_3)_2CO$): δ = –1.36.

13C NMR (126 MHz, $(CD_3)_2CO$): δ = 154.7, 154.5, 152.6, 152.5, 144.4, 143.9, 132.6, 132.5, 132.1, 132.0, 131.9, 131.8, 130.5, 129.8, 128.5, 128.2, 128.1, 127.7, 127.5, 127.3, 127.0, 126.7, 125.8, 125.3, 124.1, 123.6, 123.5, 123.3, 123.1, 122.9, 122.3, 122.1, 113.8, 112.5, 111.6, 109.1.

HRMS *m/z* (ESI): calcd. For $C_{108}H_{36}S_2F_{30}O_{12}N_3P_2$ ([M–H]$^-$): 2262.07421; found: 2262.07463.

(*S*,*S*)-(benzo[*b*]thieno[3,2-*d*]thiophen-2-yl)-C₆F₅-IDPi (88b)
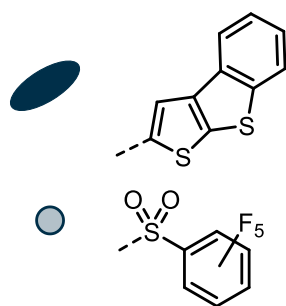
(*S*)-BINOL **142** (158 mg, 0.238 mmol, 2.01 eq.) was added to a flame-dried Schlenk flask under argon and dried at 50 °C under high vacuum overnight. The flask was then placed under argon. $P(NSO_2C_6F_5)Cl_3$ (92 mg, 0.24 mmol, 2.03 eq.), toluene (2.4 mL) and NEt_3 (0.33 mL, 2.37 mmol, 19.9 eq.) were added and the reaction mixture was stirred at room temperature for 1 h. Subsequently, HMDS (24.7 µL, 0.119 mmol, 1.00 eq.) was added, the mixture was stirred at room temperature for 15 min, and then heated to 120 °C for 3 d. After cooling to room temperature the mixture was diluted with DCM and quenched by addition of 1 M HCl. The aqueous phase was extracted with DCM (3 x 25 mL), the combined organic layers were washed with 1 M HCl and water, dried over anhydrous Na_2SO_4 and concentrated under reduced pressure. Purification via flash column chromatography

on silica gel (1st column: 0–3% EtOAc, DCM, 2nd column: 10–20% EtOAc, hexanes) afforded a light yellow solid. The product was acidified by filtration over a short plug of DOWEX 50WX8 (H-form, eluted with DCM). The product was concentrated under reduced pressure and dried under high vacuum, furnishing the title compound as a light yellow solid (95 mg, 42%).

R_F (50% EtOAc, hexanes) = 0.44.

^{1}H NMR (600 MHz, CD$_2$Cl$_2$): δ = 8.18 (s, 2H), 8.06–7.98 (m, 4H), 7.89 (d, J = 8.2 Hz, 2H), 7.78 (d, J = 7.9 Hz, 2H), 7.77–7.66 (m, 3H), 7.58 (ddd, J = 8.1, 6.8, 1.1 Hz, 2H), 7.55–7.43 (m, 6H), 7.43–7.23 (m, 13H), 7.20–7.13 (m, 2H), 6.84 (t, J = 7.4 Hz, 2H), 6.66 (t, J = 7.4 Hz, 2H).

^{19}F NMR (471 MHz, CD$_2$Cl$_2$): δ = –136.2 (s, 4F), –146.7 (s, 2F), –160.1 (s, 4F).

^{31}P NMR (203 MHz, CD$_2$Cl$_2$): δ = –15.95.

^{13}C NMR (151 MHz, CD$_2$Cl$_2$): δ = 145.0, 143.6, 143.4, 143.2, 142.91, 142.87, 142.8, 142.7, 142.3, 134.0, 139.6, 138.7, 138.2, 136.5, 133.1, 132.9, 132.3, 131.84, 131.79, 131.4, 129.6, 129.3, 128.6, 127.9, 127.7, 127.41, 127.37, 127.2, 127.1, 127.0, 126.9, 126.1, 125.1, 124.7, 124.4, 124.1, 123.6, 123.1, 123.0, 122.9, 122.5, 121.7, 120.9, 118.7.

HRMS m/z (ESI): calcd. For C$_{92}$H$_{40}$S$_{10}$F$_{10}$O$_8$N$_3$P$_2$ ([M–H]$^-$): 1885.93435; found: 1885.93518.

$[\alpha]_D^{25}$ = +451.1 (c = 0.12, CHCl$_3$).

(*S*,*S*)-(benzo[*b*]thieno[2,3-*d*]thiophen-2-yl)-C$_6$F$_5$-IDPi (89b)
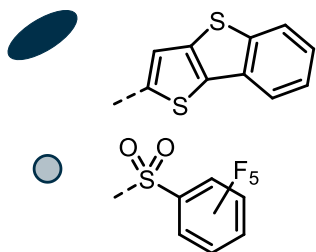
(*S*)-BINOL **143** (101 mg, 0.152 mmol, 2.01 eq.) was added to a flame-dried Schlenk flask under argon and dried at 50 °C under high vacuum overnight. The flask was then placed under argon. P(NSO$_2$C$_6$F$_5$)Cl$_3$ (57.8 mg, 0.151 mmol, 2.00 eq.), toluene (1.5 mL) and NEt$_3$ (84 μL, 0.60 mmol, 8.0 eq.) were added and the reaction mixture was stirred at room temperature for 1 h. Subsequently, HMDS (15.8 μL, 0.076 mmol, 1.00 eq.) was added, the mixture was stirred at room temperature for 15 min, and then heated to 120 °C for 3 d. After cooling to room temperature the mixture was diluted with DCM and quenched by addition of 1 M HCl. The aqueous phase was extracted with DCM (3 x 25 mL), the combined organic layers were washed with 1 M HCl and water, dried over anhydrous Na$_2$SO$_4$ and concentrated under reduced pressure. Purification via flash column chromatography on silica gel (0–4% EtOAc, DCM) afforded a yellow solid. The product was acidified by dissolving it in DCM and vividly stirring it with 6 M HCl for 15 min. The organic layer was concentrated under reduced pressure and dried under high vacuum, furnishing the title compound as a yellow solid (48 mg, 34%).

¹H NMR (501 MHz, CDCl₃): δ = 8.11 (s, 2H), 7.96 (t, J = 7.6 Hz, 4H), 7.85 (dd, J = 8.0, 5.1 Hz, 4H), 7.74 (ddd, J = 8.1, 5.2, 2.6 Hz, 2H), 7.63–7.46 (m, 6H), 7.46–7.38 (m, 2H), 7.38–7.28 (m, 6H), 7.24–7.16 (m, 6H), 7.14 (s, 2H), 6.96–6.86 (m, 2H), 6.65 (t, J = 7.5 Hz, 2H), 6.40 (s, 2H).

¹⁹F NMR (471 MHz, CDCl₃): δ = –135.2 (d, J = 21.5 Hz, 4F), –145.9 (s, 2F), –159.2 (t, J = 20.5 Hz, 4F).

³¹P NMR (203 MHz, CDCl₃): δ = –17.1.

(*S*,*S*)-(5-(trifluoromethyl)benzo[*b*]thieno[3,2-*d*]thiophen-2-yl)-C₆F₅-IDPi (91b)
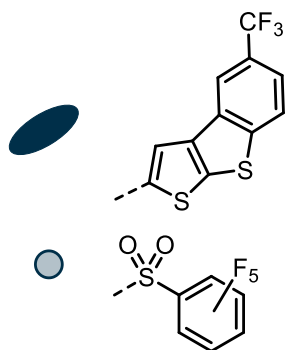
(*S*)-BINOL **144** (101 mg, 0.126 mmol, 2.11 eq.) was added to a flame-dried Schlenk flask under argon and dried at 50 °C under high vacuum overnight. The flask was then placed under argon. P(NSO₂C₆F₅)Cl₃ (47 mg, 0.123 mmol, 2.05 eq.), toluene (1.2 mL) and NEt₃ (0.17 mL, 1.22 mmol, 20.3 eq.) were added and the reaction mixture was stirred at room temperature for 1 h. Subsequently, HMDS (12.5 µL, 0.060 mmol, 1.00 eq.) was added, the mixture was stirred at room temperature for 15 min, and then heated to 120 °C for 3 d. After cooling to room temperature the mixture was diluted with DCM and quenched by addition of 1 M HCl. The aqueous phase was extracted with DCM (3 x 25 mL), the combined organic layers were washed with 1 M HCl and water, dried over anhydrous Na₂SO₄ and concentrated under reduced pressure. Purification via flash column chromatography on silica gel (1st column: 10–20% EtOAc, hexanes, 2nd column: 3% EtOAc, PhMe) afforded a white solid. The product was acidified by filtration over a short plug of DOWEX 50WX8 (H-form, eluted with DCM). The product was concentrated under reduced pressure and dried under high vacuum, furnishing the title compound as a beige solid (24 mg, 19%).

¹H NMR (501 MHz, CD₂Cl₂): δ = 8.31–8.17 (m, 2H), 8.03 (d, J = 8.4 Hz, 1H), 8.00–7.87 (m, 2H), 7.87–7.77 (m, 1H), 7.77–7.48 (m, 6H), 7.44 (d, J = 8.5 Hz, 1H), 7.37 (t, J = 7.7 Hz, 1H), 7.34–7.21 (m, 2H), 7.20–7.12 (m, 2H).

¹⁹F NMR (471 MHz, CD₂Cl₂): δ = –61.8 (s, 6F), –62.0 (s, 6F), –136.1 (s, 4F), –146.7 (s, 2F), –159.8 (s, 4F).

³¹P NMR (203 MHz, CD₂Cl₂): δ = –15.7.

HRMS *m/z* (ESI): calcd. For C₉₆H₃₆S₁₀F₂₂O₈N₃P₂ ([M–H]⁻): 2157.88389; found: 2157.88617.

(*S*,*S*)-(6-(trifluoromethyl)benzo[*b*]thieno[3,2-*d*]thiophen-2-yl)-C₆F₅-IDPi (92b)
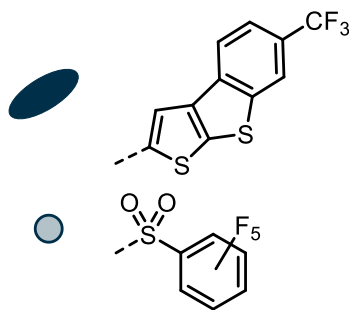
(*S*)-BINOL **145** (1.01 g, 1.23 mmol, 2.01 eq.) was added to a flame-dried Schlenk flask under argon and dried at 50 °C under high vacuum overnight. The flask was then placed under argon. P(NSO₂C₆F₅)Cl₃ (481 mg, 1.26 mmol, 2.00 eq.), DMAP (77 mg, 0.6 mmol, 1.0 eq.), toluene (12.6 mL) and NEt₃ (1.7 mL, 12 mmol, 19 eq.) were added and the reaction mixture was stirred at room temperature for 1 h. Subsequently, HMDS (131 μL, 0.63 mmol, 1.00 eq.) was added, the mixture was stirred at room temperature for 15 min, and then heated to 120 °C for 5 d. After cooling to room temperature the mixture was diluted with DCM and quenched by addition of 1 M HCl. The aqueous phase was extracted with DCM (3 x 25 mL), the combined organic layers were washed with 1 M HCl and water, dried over anhydrous Na₂SO₄ and concentrated under reduced pressure. Purification via flash column chromatography on silica gel (1st column: 30% to 60% EtOAc, hexanes, 2nd column: 80% DCM, hexanes to 100% DCM to 2% EtOAc, DCM) afforded a white solid. The product was acidified by dissolving it in DCM and vividly stirring it with 6 M HCl for 20 min. The organic layer was concentrated under reduced pressure and dried under high vacuum, furnishing the title compound as a beige solid (424 mg, 31%).

R_F (70% EtOAc, hexanes) = 0.26.

¹H NMR (501 MHz, CD₂Cl₂): δ = 8.27 (s, 2H), 8.12–8.01 (m, 6H), 7.85–7.73 (m, 6H), 7.67–7.59 (m, 6H), 7.57–7.47 (m, 6H), 7.41–7.32 (m, 4H), 7.20 (d, *J* = 8.4 Hz, 2H), 7.12 (s, 2H), 6.81 (dd, *J* = 8.0, 1.7 Hz, 2H), 5.66 (s, 2H).

¹⁹F NMR (471 MHz, CD₂Cl₂): δ = –61.7 (s, 6F), –61.8 (s, 6F), –136.0 (d, *J* = 20.3 Hz, 4F), –145.6 (s, 2F), –159.6 (t, *J* = 20.2 Hz, 4F).

³¹P NMR (203 MHz, CD₂Cl₂): δ = –16.6.

¹³C NMR (151 MHz, CD₂Cl₂): δ = 145.1, 145.0, 144.6, 143.30, 143.28, 142.9, 142.68, 142.65, 142.6, 142.3, 142.24, 142.20, 142.0, 141.7, 141.2, 140.61, 140.55, 140.5, 138.4, 138.3, 136.7, 136.6, 136.5, 135.2, 135.0, 132.3, 131.9, 131.8, 131.5, 130.1, 129.8, 128.8, 128.2, 128.04, 128.01, 127.8, 127.7, 127.5, 127.40, 127.36, 127.2, 127.0, 126.8, 126.6, 126.42, 126.39, 126.2, 126.0, 125.9, 125.7, 125.5, 125.4, 125.09, 125.08, 125.07, 124.1, 123.7, 123.6, 123.2, 123.0, 122.3, 122.01, 121.99, 121.97, 121.94, 121.88, 121.8, 121.2, 121.14, 121.12, 121.10, 120.9, 120.62, 120.59, 120.57, 120.5, 119.71, 119.68, 119.66, 119.6, 118.6, 117.2.

HRMS *m/z* (ESI): calcd. For C₉₆H₃₆S₁₀F₂₂O₈N₃P₂ ([M–H]⁻): 2157.883923; found: 2157.883720.

LC (10 mm Chiralpak QN-AX, 4.0 mm i.d., MeOH/AcOH/NH₄OAc = 98:2:0.5 (v/v/w), 1.0 mL/min, 2.1 MPa, RT, 254 nm): t_{R1} = 2.62 min (minor), t_{R2} = 5.39 min (major), er = 99.5:0.5 (99% ee).

$[\alpha]_D^{25}$ = +398.1 (c = 0.31, CHCl₃).

(*S,S*)-(4-fluoro-6-(trifluoromethyl)benzo[*b*]thieno[3,2-*d*]thiophen-2-yl)-C₆F₅-IDPi (94b)
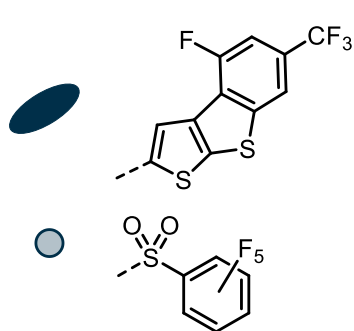
(*S*)-BINOL **146** (118 mg, 0.141 mmol, 2.08 eq.) was added to a flame-dried Schlenk flask under argon and dried at 50 °C under high vacuum overnight. The flask was then placed under argon. P(NSO₂C₆F₅)Cl₃ (52.1 mg, 0.136 mmol, 2.00 eq.), toluene (1.4 mL) and NEt₃ (0.19 mL, 1.36 mmol, 20.0 eq.) were added and the reaction mixture was stirred at room temperature for 1 h. Subsequently, HMDS (14.2 µL, 0.068 mmol, 1.00 eq.) was added, the mixture was stirred at room temperature for 15 min, and then heated to 120 °C for 3 d. After cooling to room temperature the mixture was diluted with DCM and quenched by addition of 1 M HCl. The aqueous phase was extracted with DCM (3 x 25 mL), the combined organic layers were washed with 1 M HCl and water, dried over anhydrous Na₂SO₄ and concentrated under reduced pressure. Purification via flash column chromatography on silica gel (1st column: 10–20% EtOAc, pentane, 2nd column: 80% DCM, pentane to 100% DCM to 1% EtOAc, DCM) afforded a white solid. The product was acidified by dissolving it in DCM and vividly stirring it with 6 M HCl for 20 min. The organic layer was concentrated under reduced pressure and dried under high vacuum, furnishing the title compound as a beige solid (41 mg, 27%).

¹H NMR (501 MHz, CD₂Cl₂): δ = 8.33 (s, 2H), 8.21–8.03 (m, 3H), 7.92 (s, 3H), 7.88–7.74 (m, 4H), 7.72–7.45 (m, 10H), 7.45–7.35 (m, 5H), 7.35–7.22 (m, 5H).

¹⁹F NMR (471 MHz, CD₂Cl₂): δ = –61.8 (s, 6F), –62.1 (s, 6F), –116.1 (s, 4F), –136.0 (s, 4F), –146.9 (s, 2F), –159.9 (s, 4F).

³¹P NMR (203 MHz, CD₂Cl₂): δ = –17.3.

HRMS *m/z* (ESI): calcd. For C₉₆H₃₂S₁₀F₂₆O₈N₃P₂ ([M–H]⁻): 2229.84621; found: 2229.84781.

IDPis from other group members
IDPis **77a**, **78a**, **78b**, **79a**, **79b**, **75a**, **75b**, **80a**, **81a**, and **81b** were provided by the technicians of the List group. IDPi **83b** was provided by Dr. Manuel Scharf. IDPi **84b** was provided by Dr. Benjamin Mitschke.

IDPis **85b** and **86b** were provided by Dr. Sebastian Brunen. IDPis **90b** and **91b** were provided by Michael Merher.

4.3.6 Mechanistic Studies

Convergent Reactivity of Styrene Isomers

Following GP5, the ionic hydrogenations of the respective styrenes **70a** and **68k**/**70k** were performed using EtMe$_2$SiH (10.0 eq.), benzoic acid (1.20 eq.) and IDPi **92b** (2 mol%) under neat reaction conditions at the indicated temperatures and reaction times.

E- or *Z*-**70a**   69a
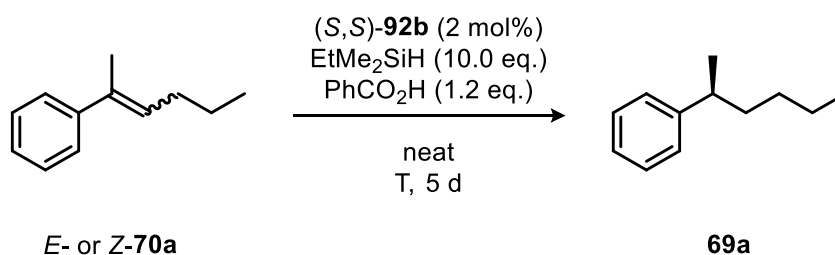
Table 4.99 Ionic hydrogenation of *E*- and *Z*-**68a** at elevated temperatures.

	from *E*-**70a**		from *Z*-**70a**	
temp.	**yield**	**er**	**yield**	**er**
80 °C	95%	79.5:20.5	49%	79.5:20.5
60 °C	64%	81.5:18.5	12%	81:19
40 °C	traces	n.d.	traces	n.d.
20 °C	traces	n.d.	traces	n.d.
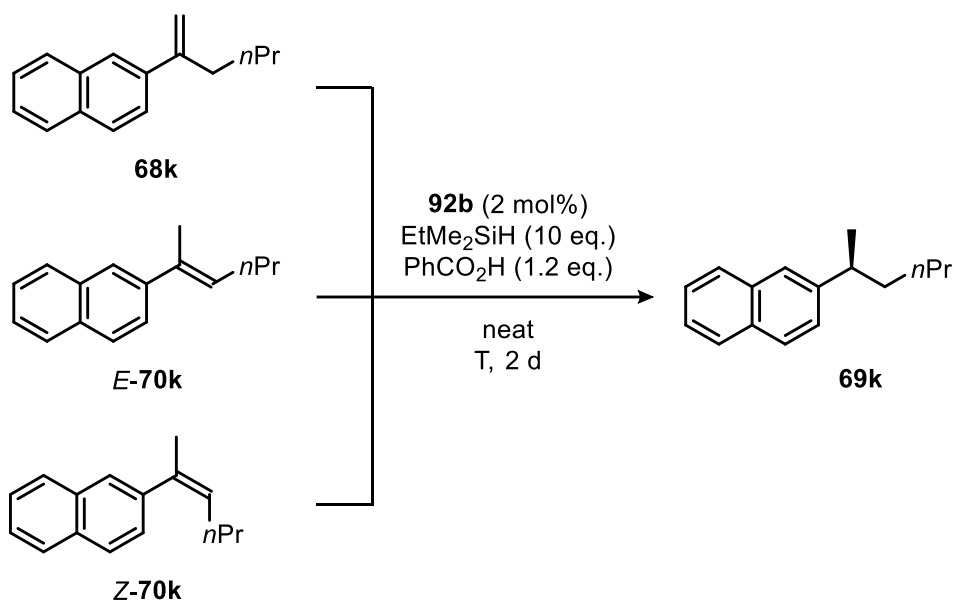
Table 4.100 Ionic hydrogenation of **68k**, *E*- and *Z*-**70k** at elevated temperatures.

	from **68k**		from *E*-**70k**		from *Z*-**70k**	
temp.	**yield**	**er**	**yield**	**er**	**yield**	**er**
80 °C	87%	84:16	>99%	81.5:18.5	>99%	82:18
60 °C	83%	86.5:13.5	>99%	86:14	94%	86:14
40 °C	79%	90.5:9.5	>99%	89:11	43%	89:11
20 °C	78%	94.5:5.5	59%	92.5:7.5	3%	92:8

Reversibility of Styrene Protonation
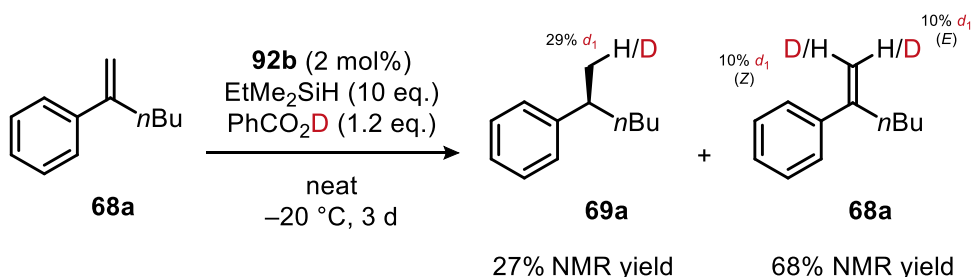
A 2 mL GC vial, equipped with a magnetic stirring bar, was charged with the IDPi **92b** (2 mol%) and benzoic acid-d_1 (0.030 mmol, 1.2 eq.), and then placed under argon. EtMe$_2$SiH (0.25 mmol, 10 eq.) was added, and the vial was cooled to –78 °C. After addition of styrene **68a** (0.025 mmol, 1.0 eq.), the reaction was stirred at –20 °C for 3 d. The reaction was quenched by addition of pyridine (5 μL) followed by addition of mesitylene (3 μL) as internal standard. An aliquot of the mixture was taken and diluted with C$_6$D$_6$ for subsequent ^{1}H, ^{2}H, and ^{13}C NMR analysis.

Product Analysis (**69a**):
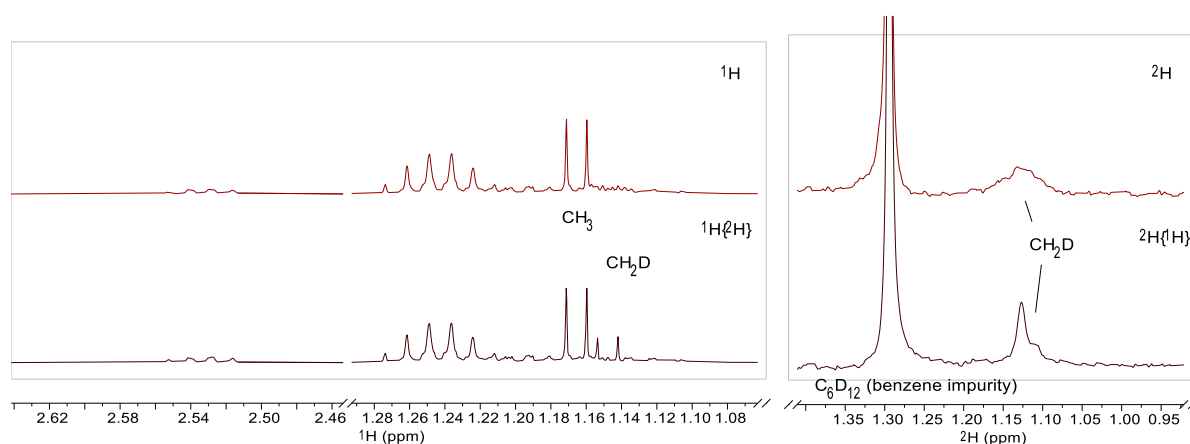
Figure 4.23 Selected region of the ^{1}H and ^{2}H NMR spectra from the crude reaction mixture for the product analysis.

Integration based on ^{1}H NMR was challenging due to signal overlap with other components. Therefore, the ratio was determined using the relative integral of the neighboring ^{13}C signal, which differs between the two species.
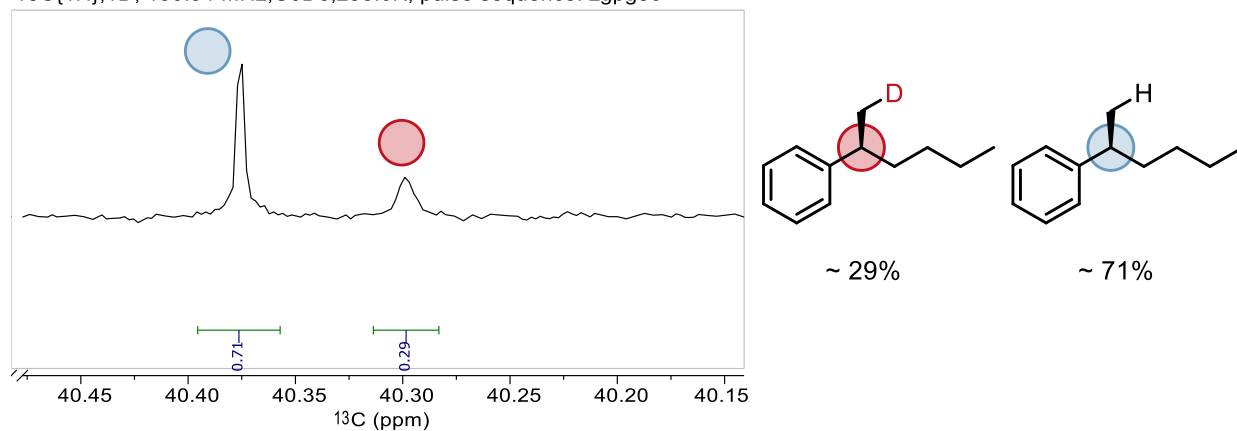
Figure 4.24 Selected region of the ^{13}C NMR spectrum from the crude reaction mixture for the product analysis.

Starting Material Analysis (**68a**):
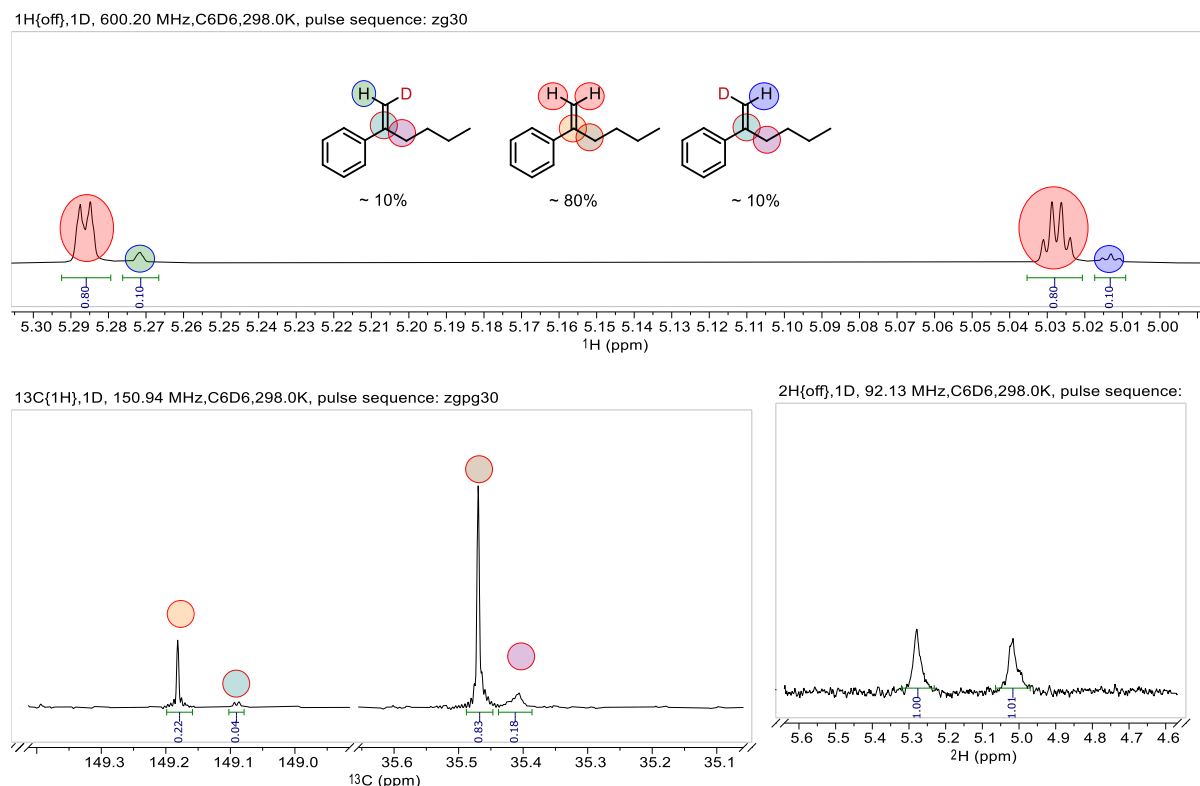
Figure 4.25 Selected region of the ^{1}H, ^{2}H, ^{13}C NMR spectra from the reaction crude for the starting material analysis.

Influence of a Chiral Proton Source on Stereocontrol

For the reduction of styrene **68a**, (*R*)- or (*S*)-α-methoxyphenylacetic acid was employed as the proton source according to GP5, using EtMe₂SiH (5.0 eq.) in CyMe (0.5 M) at room temperature for 1 d. In an additional experiment, (*S*)-(+)-phenylpropionic acid was applied as the enantiopure proton source in combination with either (*R*,*R*)-**92b** or (*S*,*S*)-**92b** as catalyst, under otherwise identical conditions (EtMe₂SiH, 5.0 eq., CyMe, 0.5 M, rt, 1 d).

Formation of Silylation of IDPi Species

The kinetic studies were carried out in collaboration with Dr. Markus Leutzsch.

To detect the silylated IDPi as a catalytic intermediate via NMR spectroscopy, slightly modified reaction conditions were employed. To ensure a homogeneous reaction medium, the experiment was conducted at higher dilution in dry CD₂Cl₂. Additionally, exclusion of proton sources (e.g., benzoic acid or water) was critical to prevent rapid protodesilylation of the intermediate species. To facilitate the detection of low-concentration species, the catalyst loading was increased.

To this end, a dry 3 mm NMR tube under argon was charged with IDPi **75a** (2.2 mg, 1.2 µmol, 22 mol%), dry CD$_2$Cl$_2$ (0.16 mL) and PhMe$_2$SiH (4.2 µL, 27 µmol, 5.0 eq.). Initial ^{1}H and ^{31}P NMR spectra were recorded. Subsequently, styrene **68a** (1.0 µL, 5.5 µmol, 1.0 eq.) was added, and the reaction was monitored at room temperature.

For acquisition of a reference spectrum of the silylated IDPi **75a**, a dry 3 mm NMR tube under argon was charged with IDPi **75a** (2.9 mg, 1.6 µmol, 1.0 eq.), dry CD$_2$Cl$_2$ (0.16 mL) and dimethyl(2-methylallyl)(phenyl)silane (3.5 µL, 16 µmol, 10 eq.). ^{1}H and ^{31}P NMR spectra were recorded immediately.
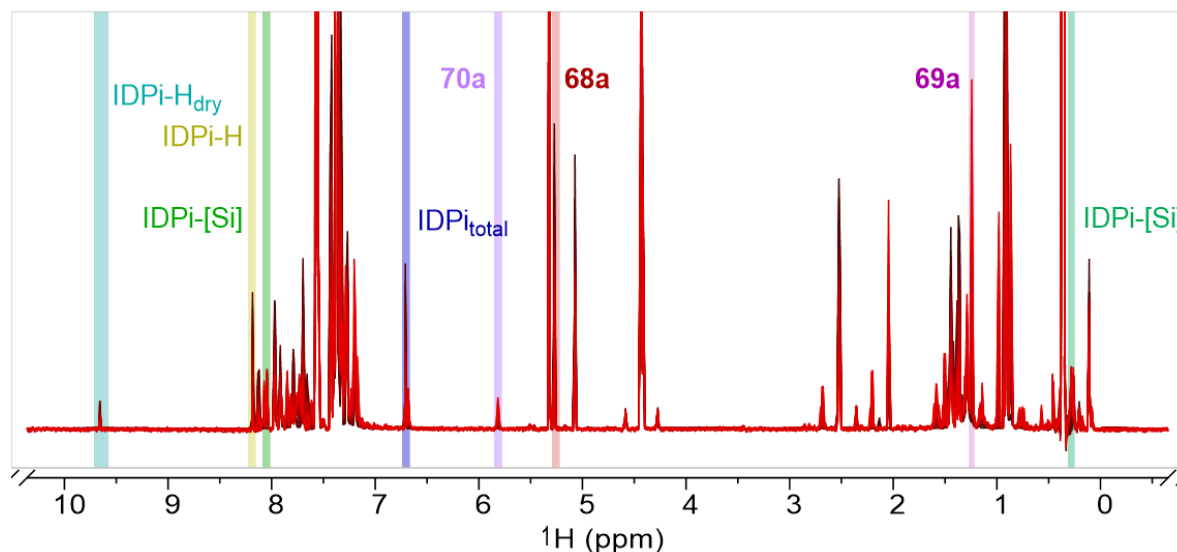
Figure 4.26 Superimposed ^{1}H NMR spectra at selected time points, with highlighted regions used for integration of the respective reaction components. The integrals were used to plot the reaction progress.
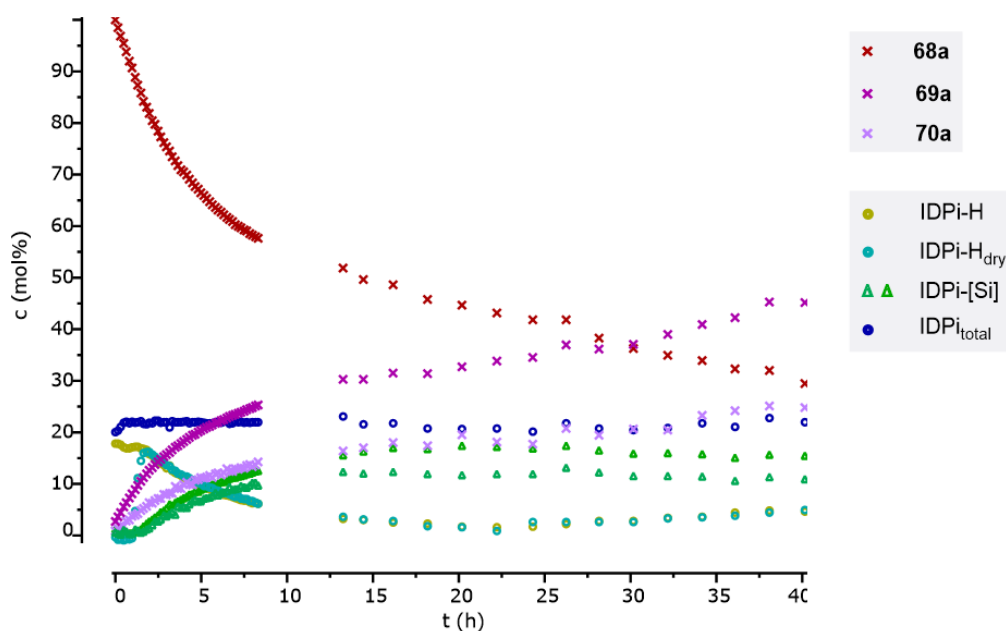
Figure 4.27 Reaction progress plot showing the concentration (mol%) of different reaction components over time (h), derived from 1H NMR spectra.
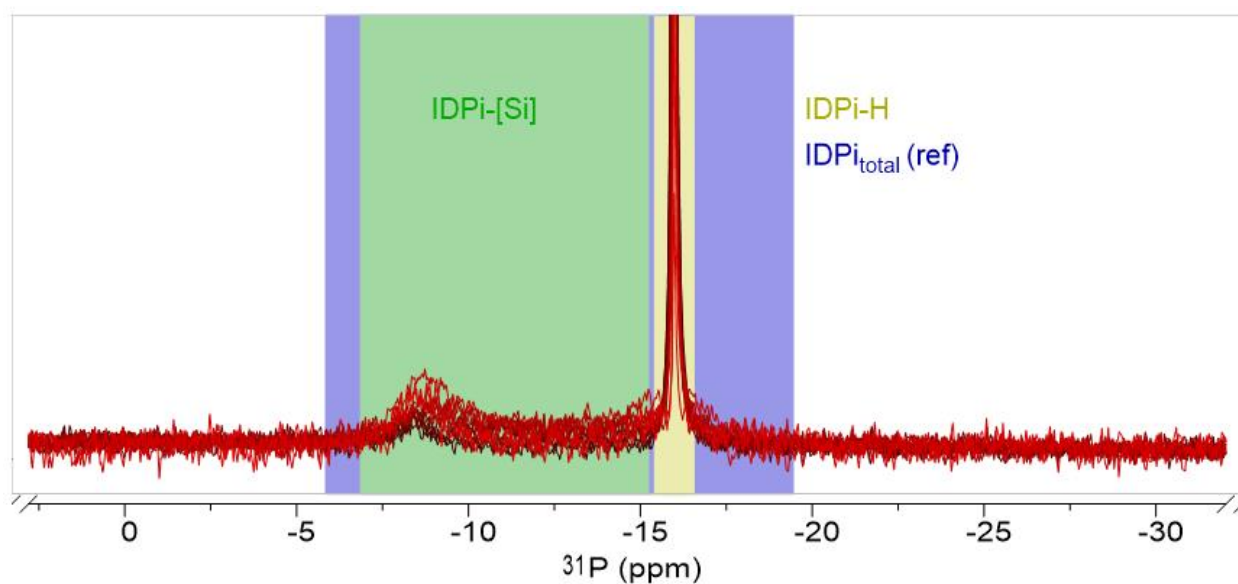
Figure 4.28 Superimposed ^{31}P NMR spectra at selected time points, with highlighted regions used for integration of the respective reaction components. The integrals were used to plot the reaction progress. The ^{31}P NMR spectra were normalized to the integral of the whole region (as the sample was removed from the magnet and retuned at later time points).
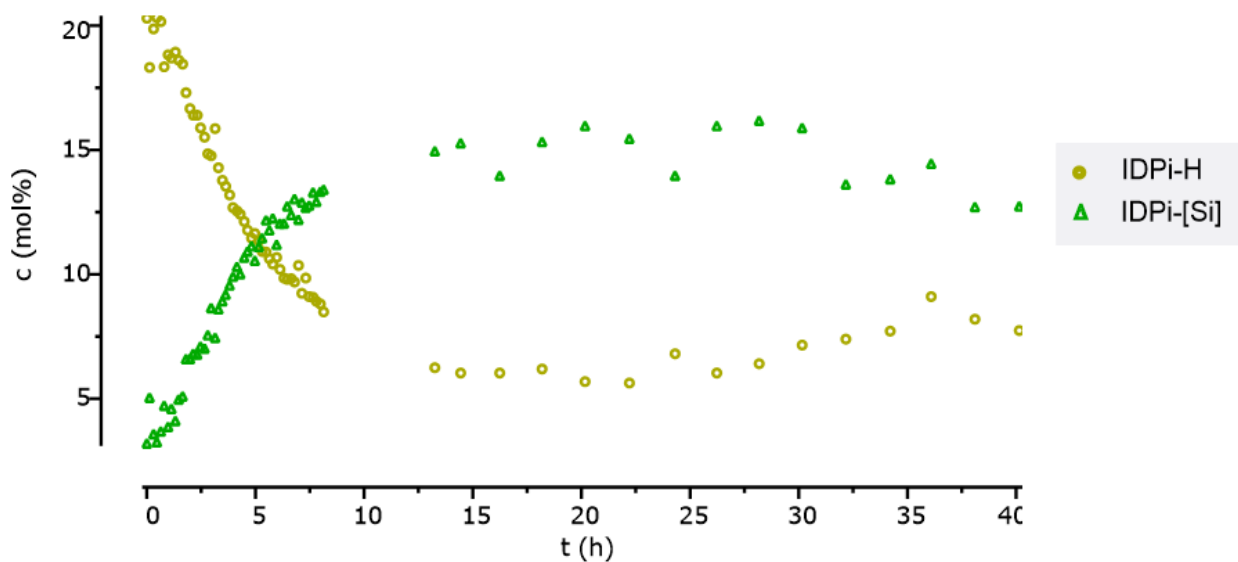
Figure 4.29 Reaction progress plot showing the concentration (mol%) of catalytic species over time (h), derived from 31P NMR spectra.

Catalyst Turnover and Regeneration

The NMR spectroscopic analysis was carried out in collaboration with Dr. Markus Leutzsch.

To simulate the catalyst regeneration step of the catalytic cycle, silylation of IDPi **92b** was performed using dimethyl(2-methylallyl)(phenyl)silane. Upon addition of benzoic acid, the regeneration of the protonated IDPi catalyst was monitored.

In a flame-dried 5 mm NMR tube under argon, IDPi **92b** (15.2 mg) was dissolved in dry CD_2Cl_2 (0.7 mL), and the initial ^{1}H and ^{31}P NMR spectra were recorded. Dimethyl(2-methylallyl)(phenyl)silane (0.8 μL, 0.5 eq. or 1.5 μL, 1.0 eq.) was then added sequentially, with NMR spectra recorded after each addition. Upon addition of an excess of silane (4.0 eq.), the NMR spectrometer was cooled stepwise to 233 K, with spectra recorded after each interval. At room temperature, a stock solution of benzoic acid (0.25 M in CD_2Cl_2, 2.8 μL, 1.0 eq.) was added incrementally, and NMR spectra were recorded after each addition.

Upon initial addition of dimethyl(2-methylallyl)(phenyl)silane to **92b**, drying of the acidic IDPi was observed through scavenging of residual water. This was evident from the appearance of the protic signal corresponding to the acidic proton of the IDPi (δ = 9.87 ppm (t, J = 2.1 Hz, 1H)). In a ^{1}H–^{31}P HMBC spectrum, cross-signals were observed between the phosphorus resonance and both the aromatic BINOL backbone and this acidic proton, supporting the assignment (Figure 4.30).
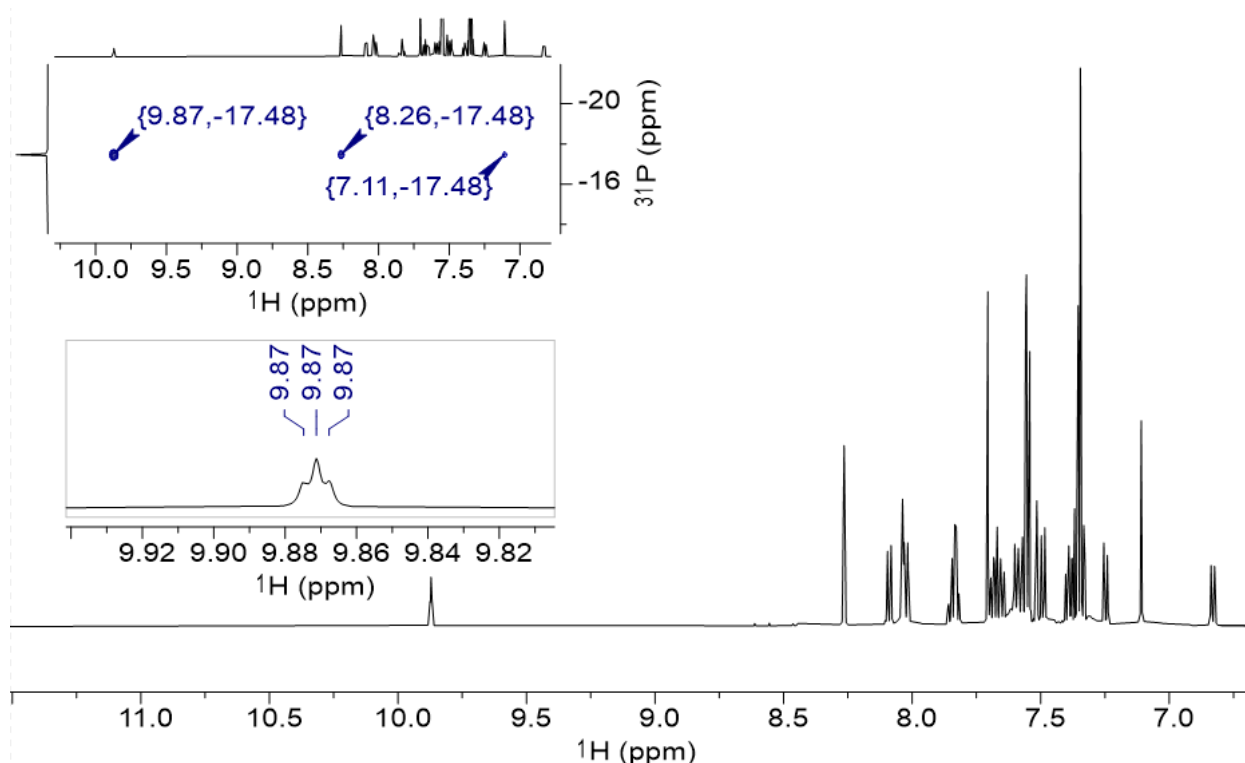
Figure 4.30 ^{1}H NMR spectrum of **92b** after addition of 2 eq. dimethyl(2-methylallyl)(phenyl)silane, showing the acidic proton upon drying, and corresponding ^{1}H–^{31}P HMBC spectrum with cross-peaks between the phosphorus resonance, the acidic proton, and the BINOL backbone.

Upon further addition of silane equivalents, broad signals appeared in the ^{1}H NMR spectrum. The sharp singlet in the ^{31}P spectrum, originally caused by IDPi **92b**, disappeared and was replaced by three broad signals. Cooling the NMR tube to 233 K within the spectrometer did not yield sharp signals; however,

partial resolution was observed at 253 K, resulting in a pattern resembling a doublet of doublets, consistent with the presence of the silylated catalyst (Figure 4.31).
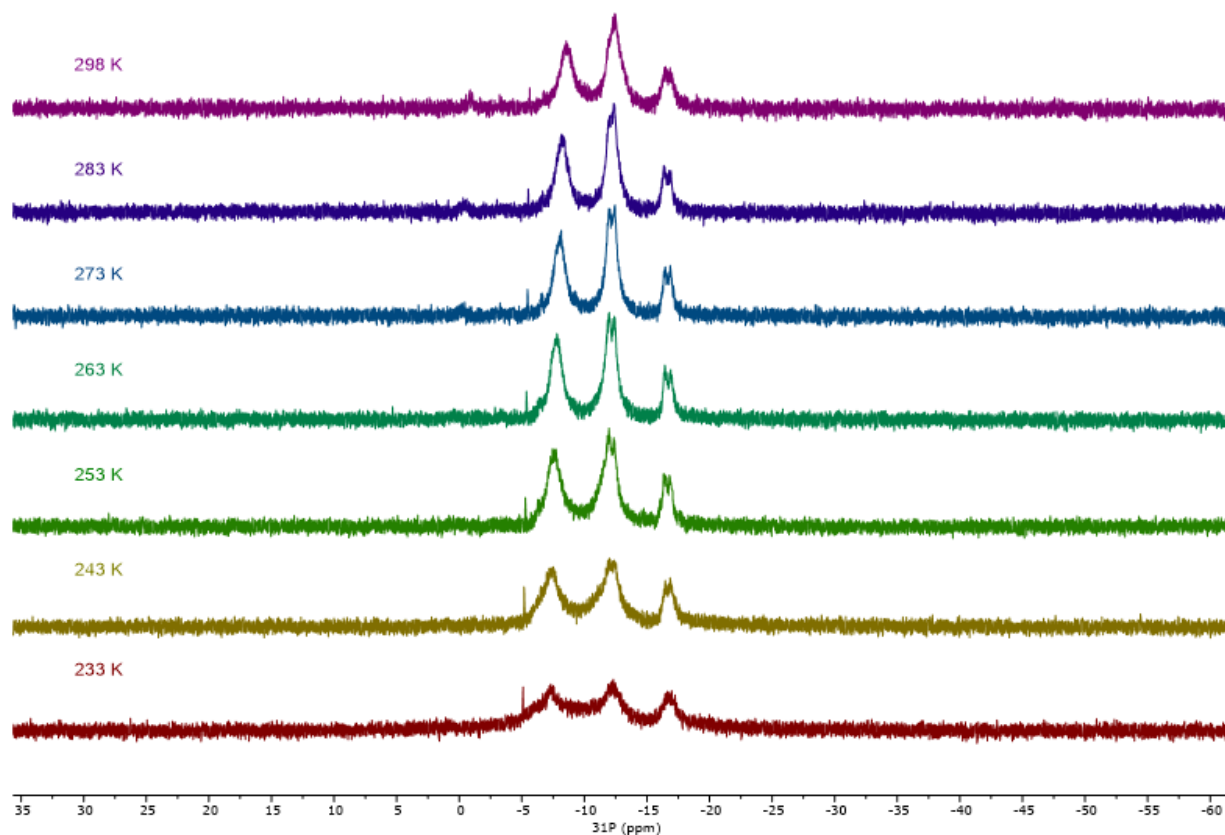
Figure 4.31 Stacked ^{31}P NMR spectra of silylated IDPi species in CD_2Cl_2 recorded at progressively lower temperatures, reaching 233 K.

In an attempt to obtain sharper ^{31}P NMR signals of the silylated IDPi species, the experiment was repeated in PhMe-d_8. A similar pattern of broad signals was observed in the ^{31}P NMR spectrum, and variation of the temperature (cooling and heating) did not lead to complete resolution (Figure 4.32, Figure 4.33).
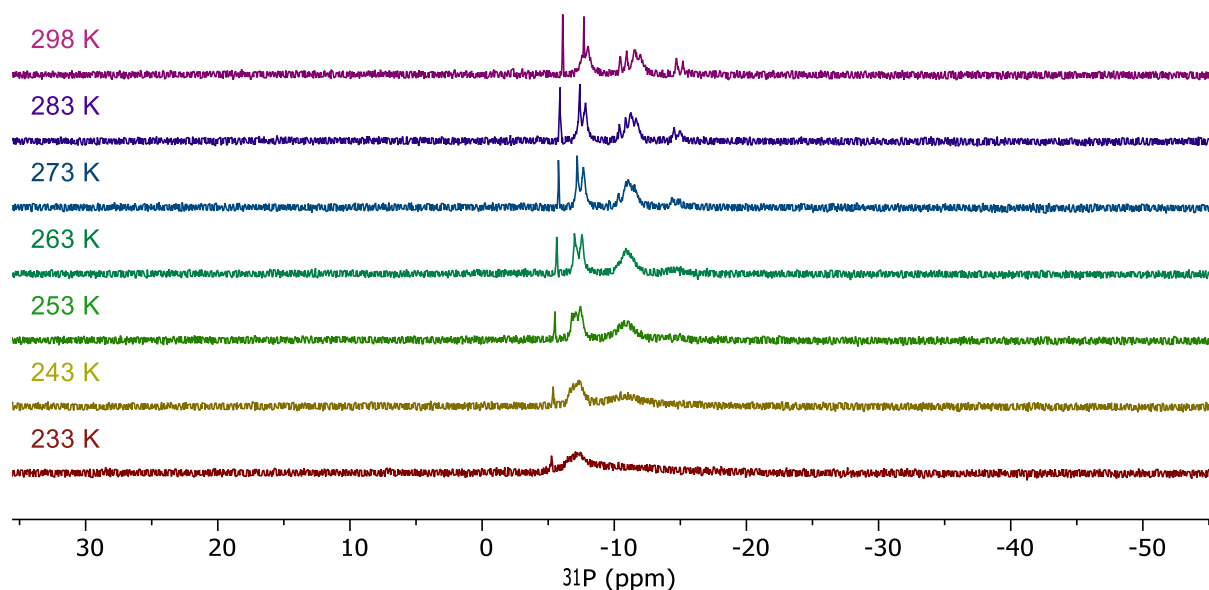
Figure 4.32 Stacked ^{31}P NMR spectra of silylated IDPi species in PhMe-*d₈* recorded at progressively lower temperatures, reaching 233 K.
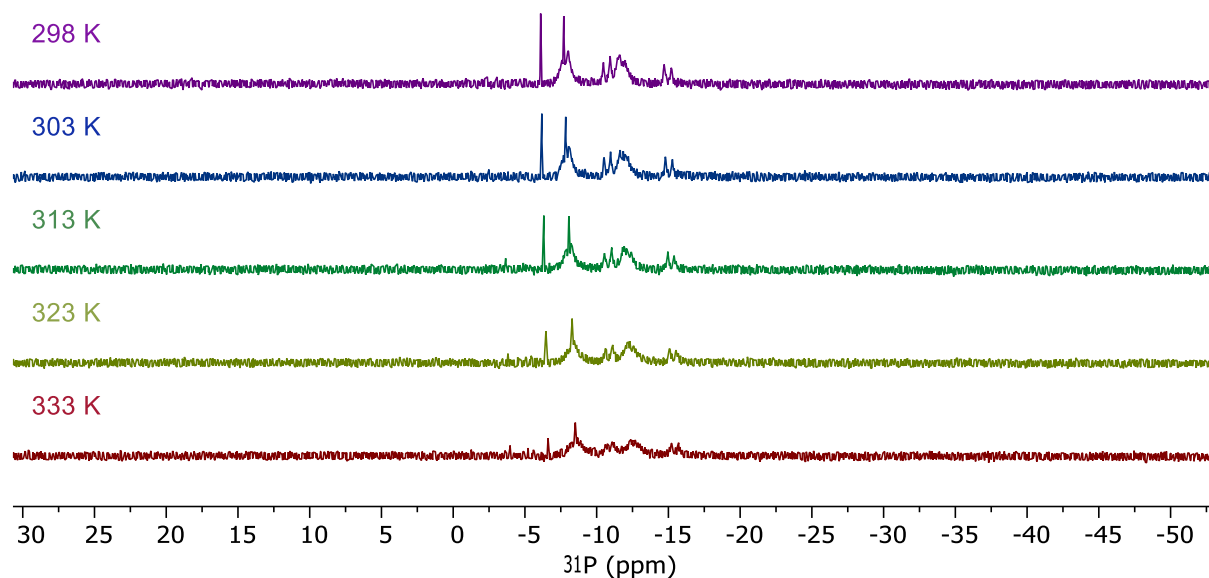
Figure 4.33 Stacked ^{31}P NMR spectra of silylated IDPi species in PhMe-*d₈* recorded at progressively higher temperatures, reaching 333 K.

Computational Details

The computational studies were carried out in collaboration with Prof. Dr. Nobuya Tsuji.

Possible TS conformations were explored by the artificial force induced reaction (AFIR) method[310] implemented in the global route reaction mapping (GRRM) program.[311] An extensive conformational search has been performed on possible catalyst substrate orientations at GFN2-xTB level of theory[279] implemented in Orca 4.2.1[281], using SC-AFIR with constraint. Molecular geometries were optimized at r²SCAN-3c[253] implemented in Orca 5.0.3 program.[312] In the case of transition state optimization, they were combined with GRRM program. Thermal free energy corrections have been performed at the same level of theory using Orca 6.0.1 program[254], and the temperature was set at 253.15 K. Transition state structures were verified by the presence of a single imaginary vibrational frequency and the corresponding intrinsic reaction coordinates (IRC). Solvation effect has been accounted by using SMD (cyclohexane) solvation model as implemented in Orca 6.0.1 program. All single point energy is calculated at SMD(methylcyclohexane)-ωB97X-V/def2-TZVPP level of theory.[252,285] RI approximation was used with AutoAux option implemented in Orca 6.0.1 program. IGMH analysis was performed using Multiwfn[210,211] using the default parameters with isovalue of 0.004 a.u. The wavefunction file was generated at ωB97XD/def2-TZVPP level of theory using Gaussian 16.[313] The visualizations of the molecular geometries were generated using the ChimeraX[314] version 1.9 followed by rendering with Blender version 4.0.[315] Conversion of enantiomeric ratio and ΔΔG was performed based on the Boltzmann distribution as follows: $\Delta\Delta G = RT\ln(\text{pdt}(R)/\text{pdt}(S))$.[316]

Results and Discussion

The DFT calculation is performed using substrate **68a** and catalyst **92b**, and the temperature is set at 253.15 K. Intermediates **I**–**IV** in the free energy diagram (Figure 3.25) correspond to the reactants and products connected by the IRC pathway from each transition state. **TS-5** was calculated in the absence of silane; therefore, the energy of silane is added to **I**, **TS-5**, and **II** in the energy diagram for better comparison. For all **TS-5**, **TS-6**, and **TS-7**, a few negative vibrational modes were initially observed; however, each transition state was confirmed by a single distinct imaginary frequency corresponding to the reaction coordinate, as well as by intrinsic reaction coordinate (IRC) analysis. The additional negative frequencies, all greater than −30 cm⁻¹, are likely numerical artifacts and do not correspond to meaningful reaction coordinates. The calculated energy difference between **TS-6** and **TS-7** agreed well with the experimental one (1.7 kcal/mol (calc) vs. 1.6 kcal/mol (exp)). The anion of catalyst **92b** appears to possess a relatively rigid structure, as indicated by the nearly identical geometries observed in **TS-6** and **TS-7** (Figure 4.34A). This rigidity is presumably due to multiple π–π interactions between the wings or between a wing and the

backbone. Additionally, the anion is further stabilized by noncovalent interactions between aromatic C–H bonds and the oxygen atoms of the sulfonyl groups at the catalytic active site, further rigidifying the structure of the counterion. These interactions in **TS-6** is visualized by IGMH analysis (Figure 4.34B).
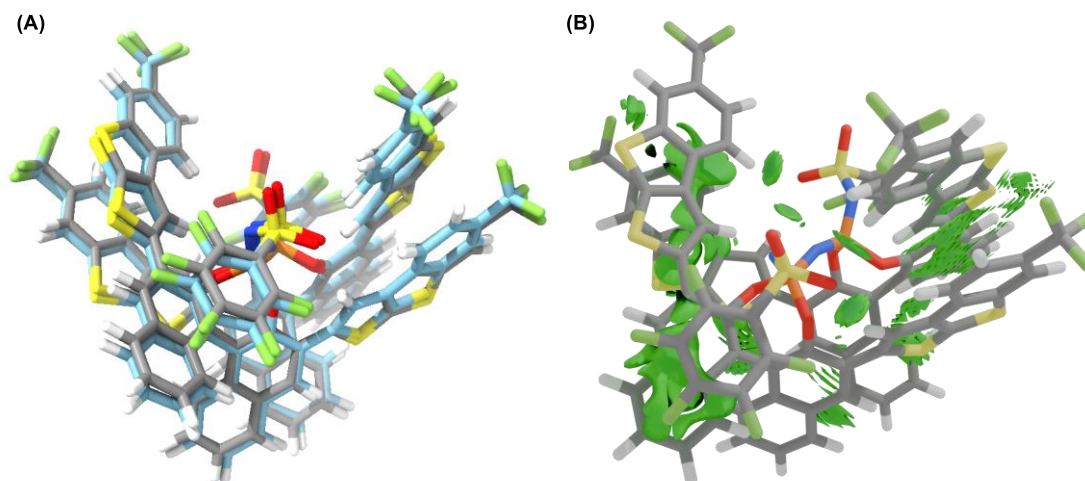
Figure 4.34 (A) Overlaid image of the counteranion structures of **TS-6** and **TS-7**, visualized using ChimeraX. Gray: **TS-6**, light blue: **TS-7**. (B) Visualization of multiple intramolecular noncovalent interactions within the catalyst anion, contributing to the stabilization of **TS-6**.

For a better understanding of the origin of enantioselectivity, distortion-interaction analysis was conducted following the Houk-Bickelhaupt protocol[298] (Table 4.101). Gas phase single point energies of the optimized **TS-6** and **TS-7**, leading to the major enantiomer and minor enantiomer, respectively, were calculated at ωB97X-V/def2-TZVPP level of theory. Then they were decomposed into the catalyst fragment and the substrate fragment. The result suggests that the interactions between the catalyst and the substrates would be the major factor in controlling the enantioselectivity.

Table 4.101 Summary of the distortion-interaction analysis of **TS-6** and **TS-7**.

TS	ωB97X-V/def2-TZVPP (in hartree)	Relative energy $\Delta\Delta E$ (kcal/mol)
TS-6	-12224.30919	4.22
TS-7	-12224.30247	
Substrate fragment		
subst-**TS-6**	-916.451405	1.19
subst-**TS-7**	-916.4495155	

Catalyst fragment		
cat-**TS-6**	-11307.69917	-0.18
cat-**TS-7**	-11307.69945	
Total distortion		1.01
Total interaction		3.21 (major factor)

Table 4.102 Energy table of the optimized structures. Energies are given in Hartree. Computed single point energies (*E*), Gibbs free energy corrections (*G*corr), Gibbs free energies (*G*), and the most negative imaginary frequencies for transition states are provided.

Structures	*E* (solv)	*G*corr	*G* (solv)	Imaginary Frequency
1a	-466.9527635	0.21588128	-466.7368823	-
92b (H-X*)	-11308.24367	1.02415917	-11307.21951	-
I	-11775.21621	1.26204838	-11773.95416	-
TS1	-11775.19437	1.25792388	-11773.93645	-87.16552907
II	-11775.21131	1.26150441	-11773.94981	-
EtMe₂SiH	-449.155673	0.12116426	-449.0345087	-
III	-12224.37949	1.40123965	-12222.97825	-
III'	-12224.37563	1.40053054	-12222.9751	-
TS-6	-12224.37715	1.40256706	-12222.97458	-973.85598462
TS-7	-12224.37255	1.40061657	-12222.97193	-863.08787083
IV	-12224.38988	1.4048345	-12222.98504	-
IV'	-12224.38319	1.40486367	-12222.97833	-
69a'	-468.185491	0.23836337	-467.9471276	-
[Si]-X*	-11756.24477	1.14717926	-11755.09759	-

Nonlinear Effect Study

Heterogeneous conditions:

According to GP5, NLE experiments were set up using styrene **68a**, EtMe₂SiH (10.0 eq.), benzoic acid (1.2 eq.) and scalemic mixtures of IDPi **92b** (2 mol%) at –20 °C for 4–5 d. The enantiomeric excess of the product **69a** was subsequently plotted against the enantiomeric excess of the catalyst.

To probe the potential origin of the (+)-NLE, experiments with scalemic mixtures of **92b** (18%, 36%, 61% ee) were conducted as previously, using EtMe₂SiH (10.0 eq.) under neat reaction conditions on a

0.05 mmol scale. After 3 d, the mixture was centrifuged, and the liquid phase was separated using a Hamilton syringe. The solid phase was dissolved in DCM, and both fractions were purified by preparative thin-layer chromatography (20% EtOAc, hexanes) to isolate **92b**. The enantiomeric excess of the catalyst in both the liquid and solid phases was determined by chiral HPLC analysis.

Homogeneous conditions:

According to GP5, NLE experiments were set up using styrene **68a**, $EtMe_2SiH$ (5.0 eq.), benzoic acid (1.20 eq.) and scalemic mixtures of IDPi **92b** (2 mol%) in $CHCl_3$ (0.25 M) at rt for 3 d. The enantiomeric excess of the product **69a** was subsequently plotted against the enantiomeric excess of the catalyst.

4.3.7 Crystallographic Data
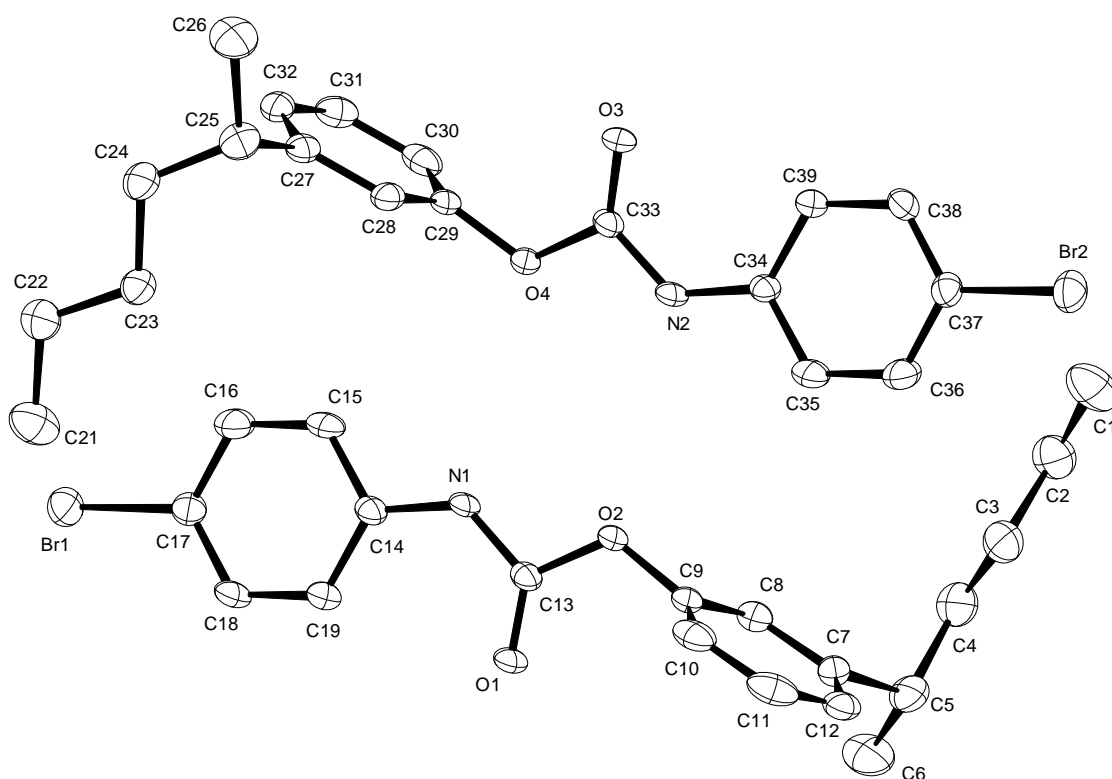
Figure 4.35 X-Ray structure of compound **95** (H atoms omitted).

Table 4.103 Crystal data and structure refinement.

Identification code	16205
Empirical formula	$C_{19} H_{22} Br N O_2$
Color	colorless
Formula weight	376.28 $g \cdot mol^{-1}$
Temperature	100(2) K
Wavelength	0.71073 Å
Crystal system	MONOCLINIC
Space group	**P2$_1$, (no. 4)**
Unit cell dimensions	a = 9.5575(3) Å $\qquad$ α= 90°.
	b = 9.6647(2) Å $\qquad$ β= 99.7280(10)°.
	c = 19.7404(5) Å $\qquad$ γ = 90°.
Volume	1797.21(8) $Å^3$
Z	4
Density (calculated)	1.391 $Mg \cdot m^{-3}$
Absorption coefficient	2.296 mm^{-1}
F(000)	776 e
Crystal size	0.220 x 0.053 x 0.046 mm^3
θ range for data collection	2.093 to 31.548°.
Index ranges	$-14 \leq h \leq 14, -14 \leq k \leq 14, -29 \leq l \leq 29$
Reflections collected	252398
Independent reflections	11968 [R_{int} = 0.0936]
Reflections with I>2σ(I)	9970
Completeness to θ = 25.242°	99.9 %
Absorption correction	Gaussian
Max. and min. transmission	0.94 and 0.76
Refinement method	Full-matrix least-squares on F^2
Data / restraints / parameters	11968 / 1 / 435
Goodness-of-fit on F^2	1.015
Final R indices [I>2σ(I)]	R_1 = 0.0328 $\qquad$ wR^2 = 0.0722
R indices (all data)	R_1 = 0.0475 $\qquad$ wR^2 = 0.0785

Absolute structure parameter   0.006(4)

Largest diff. peak and hole   0.6 and -0.3 e · Å^{-3}

Table 4.104 Bond lengths [Å] and angles [°].

Br(1)-C(17)	1.899(3)	O(1)-C(13)	1.210(4)
O(2)-C(9)	1.404(4)	O(2)-C(13)	1.360(4)
N(1)-H(1)	0.81(4)	N(1)-C(13)	1.349(4)
N(1)-C(14)	1.406(4)	C(1)-C(2)	1.519(6)
C(2)-C(3)	1.518(5)	C(3)-C(4)	1.509(5)
C(4)-C(5)	1.534(5)	C(5)-H(5)	1.02(4)
C(5)-C(6)	1.531(6)	C(5)-C(7)	1.520(4)
C(7)-C(8)	1.392(4)	C(7)-C(12)	1.386(4)
C(8)-C(9)	1.379(4)	C(9)-C(10)	1.373(5)
C(10)-C(11)	1.376(5)	C(11)-C(12)	1.383(5)
C(14)-C(15)	1.388(5)	C(14)-C(19)	1.397(5)
C(15)-C(16)	1.386(5)	C(16)-C(17)	1.387(5)
C(17)-C(18)	1.379(4)	C(18)-C(19)	1.385(5)
Br(2)-C(37)	1.901(3)	O(3)-C(33)	1.207(4)
O(4)-C(29)	1.405(4)	O(4)-C(33)	1.367(4)
N(2)-H(2)	0.77(4)	N(2)-C(33)	1.348(4)
N(2)-C(34)	1.411(4)	C(21)-C(22)	1.523(7)
C(22)-C(23)	1.500(5)	C(23)-C(24)	1.521(5)
C(24)-C(25)	1.523(4)	C(25)-H(25)	0.93(3)
C(25)-C(26)	1.537(5)	C(25)-C(27)	1.518(4)
C(27)-C(28)	1.382(4)	C(27)-C(32)	1.393(4)
C(28)-C(29)	1.380(4)	C(29)-C(30)	1.379(5)
C(30)-C(31)	1.388(5)	C(31)-C(32)	1.384(4)
C(34)-C(35)	1.389(5)	C(34)-C(39)	1.392(5)
C(35)-C(36)	1.386(5)	C(36)-C(37)	1.378(5)
C(37)-C(38)	1.378(4)	C(38)-C(39)	1.391(4)
C(13)-O(2)-C(9)	117.6(3)	C(13)-N(1)-H(1)	113(3)
C(13)-N(1)-C(14)	127.8(3)	C(14)-N(1)-H(1)	119(3)
C(3)-C(2)-C(1)	114.9(3)	C(4)-C(3)-C(2)	113.7(3)
C(3)-C(4)-C(5)	115.3(3)	C(4)-C(5)-H(5)	105(2)

C(6)-C(5)-C(4)	111.5(3)	C(6)-C(5)-H(5)	110(2)
C(7)-C(5)-C(4)	112.2(3)	C(7)-C(5)-H(5)	107(2)
C(7)-C(5)-C(6)	111.1(3)	C(8)-C(7)-C(5)	121.8(3)
C(12)-C(7)-C(5)	120.4(3)	C(12)-C(7)-C(8)	117.8(3)
C(9)-C(8)-C(7)	119.7(3)	C(8)-C(9)-O(2)	117.5(3)
C(10)-C(9)-O(2)	120.0(3)	C(10)-C(9)-C(8)	122.3(3)
C(9)-C(10)-C(11)	118.3(3)	C(10)-C(11)-C(12)	120.1(3)
C(11)-C(12)-C(7)	121.8(3)	O(1)-C(13)-O(2)	124.0(3)
O(1)-C(13)-N(1)	128.0(3)	N(1)-C(13)-O(2)	108.0(3)
C(15)-C(14)-N(1)	116.4(3)	C(15)-C(14)-C(19)	119.9(3)
C(19)-C(14)-N(1)	123.6(3)	C(16)-C(15)-C(14)	120.5(3)
C(15)-C(16)-C(17)	119.0(3)	C(16)-C(17)-Br(1)	118.9(3)
C(18)-C(17)-Br(1)	120.2(2)	C(18)-C(17)-C(16)	120.9(3)
C(17)-C(18)-C(19)	120.2(3)	C(18)-C(19)-C(14)	119.4(3)
C(33)-O(4)-C(29)	118.0(3)	C(33)-N(2)-H(2)	113(3)
C(33)-N(2)-C(34)	127.3(3)	C(34)-N(2)-H(2)	120(3)
C(23)-C(22)-C(21)	114.9(3)	C(22)-C(23)-C(24)	112.6(3)
C(23)-C(24)-C(25)	115.3(3)	C(24)-C(25)-H(25)	107(2)
C(24)-C(25)-C(26)	110.8(3)	C(26)-C(25)-H(25)	107(2)
C(27)-C(25)-C(24)	111.8(3)	C(27)-C(25)-H(25)	110(2)
C(27)-C(25)-C(26)	110.3(3)	C(28)-C(27)-C(25)	120.3(3)
C(28)-C(27)-C(32)	118.1(3)	C(32)-C(27)-C(25)	121.7(3)
C(29)-C(28)-C(27)	120.2(3)	C(28)-C(29)-O(4)	118.4(3)
C(30)-C(29)-O(4)	118.8(3)	C(30)-C(29)-C(28)	122.4(3)
C(29)-C(30)-C(31)	117.6(3)	C(32)-C(31)-C(30)	120.7(3)
C(31)-C(32)-C(27)	121.2(3)	O(3)-C(33)-O(4)	123.5(3)
O(3)-C(33)-N(2)	128.7(3)	N(2)-C(33)-O(4)	107.8(3)
C(35)-C(34)-N(2)	116.6(3)	C(35)-C(34)-C(39)	119.6(3)
C(39)-C(34)-N(2)	123.8(3)	C(36)-C(35)-C(34)	120.2(3)
C(37)-C(36)-C(35)	119.6(3)	C(36)-C(37)-Br(2)	119.3(3)
C(36)-C(37)-C(38)	120.9(3)	C(38)-C(37)-Br(2)	119.8(2)
C(37)-C(38)-C(39)	119.7(3)	C(38)-C(39)-C(34)	119.9(3)

Note: Two additional crystals from the same batch were measured to confirm the correct assignment of the absolute configuration. The analysis is consistent with the data presented.

5 REFERENCES

[1]   H. B. Kagan, *Angew. Chem. Int. Ed.* **2012**, *51*, 7376–7382.

[2]   E. Knoevenagel, B. Bergdolt, *Ber. Dtsch. Chem. Ges.* **1903**, *36*, 2861–2863.

[3]   R. A. Streatfeild, *Electron. Green J.* **2002**, *1*, DOI 10.5070/G311710494.

[4]   T. Kaneko, F. Derbyshire, E. Makino, D. Gray, M. Tamura, K. Li, *Ullmann's Encycl. Ind. Chem.* **2012**, DOI 10.1002/14356007.A07_197.PUB2.

[5]   H. Fischer, F.; Tropsch, *Process for the Synthesis of Alcohols and Other Oxygen-Compounds via Catalytic Reduction of Carbon Monoxide.*, **1922**, German Patent DRP 411216.

[6]   H. Fischer, F.; Tropsch, *Brennst. Chem.* **1923**, *4*, 276–285.

[7]   F. Fischer, H. Tropsch, *Eur. J. Inorg. Chem.* **1923**, *56*, 2428–2443.

[8]   J. J. Berzelius, *Edinburgh New Philos. J.* **1836**, *21*, 223–228.

[9]   G. Rothenberg, *Catalysis: Concepts and Green Applications*, Wiley, **2008**.

[10]   FIREFLY Project, "FIREFLY Factsheet," can be found under ttps://www.firefly-project.eu/wp-content/uploads/2024/02/Factsheet_v3.pdf, **2024**.

[11]   L. Pasteur, *Ann. Chim. Phys.* **1848**, *24*, 442–459.

[12]   J. H. van't Hoff, *Arch. Néerlandaises des Sci. Exactes Nat.* **1874**, *9*, 445–454.

[13]   J.-A. Le Bel, *Bull. la Société Chim. Paris* **1874**, *22*, 337–347.

[14]   J. M. Brown, in *Asymmetric Hydrog. Transf. Hydrog.* (Eds.: V. Ratovelomanana-Vidal, P. Phansavath), Wiley-VCH, **2021**, pp. 1–24.

[15]   W. S. Knowles, *Angew. Chem. Int. Ed.* **2002**, *41*, 1998–2007.

[16]   W. S. Knowles, M. J. Sabacky, *Chem. Commun.* **1968**, 1445–1446.

[17]   W. S. Knowles, M. J. Sabacky, B. D. Vineyard, *L-Dopa Process and Intermediates*, **1975**, US4005127A.

[18]   R. Noyori, T. Ohkuma, *Angew. Chem. Int. Ed.* **2001**, *40*, 40–73.

[19]   C. K. Winkler, J. H. Schrittwieser, W. Kroutil, *ACS Cent. Sci.* **2021**, *7*, 55–71.

[20]   J. Murray, D. R. W. Hodgson, A. M. C. O'Donoghue, *J. Org. Chem.* **2023**, *88*, 7619–7629.

[21]   B. List, *Chem. Rev.* **2007**, *107*, 5413–5415.

[22]   D. W. C. MacMillan, *Nature* **2008**, *455*, 304–308.

[23]   B. List, R. A. Lerner, C. F. Barbas, *J. Am. Chem. Soc.* **2000**, *122*, 2395–2396.

[24]   K. A. Ahrendt, C. J. Borths, D. W. C. MacMillan, *J. Am. Chem. Soc.* **2000**, *122*, 4243–4244.

[25]   S. G. Ouellet, A. M. Walji, D. W. C. Macmillan, *Acc. Chem. Res.* **2007**, *40*, 1327–1339.

[26]   S. J. Connon, *Org. Biomol. Chem.* **2007**, *5*, 3407–3417.

[27]   C. Zheng, S. L. You, *Chem. Soc. Rev.* **2012**, *41*, 2498–2518.

[28] A. M. Faísca Phillips, A. J. L. Pombeiro, *Org. Biomol. Chem.* **2017**, *15*, 2307–2340.

[29] Á. M. Pálvölgyi, F. Scharinger, M. Schnürch, K. Bica-Schröder, *Eur. J. Org. Chem.* **2021**, *2021*, 5367–5381.

[30] P. J. Walsh, M. C. Kozlowski, *Fundamentals of Asymmetric Catalysis*, University Science Books, **2009**.

[31] J. N. Israelachvili, *Intermolecular and Surface Forces*, **2011**.

[32] R. R. Knowles, E. N. Jacobsen, *Proc. Natl. Acad. Sci. U. S. A.* **2010**, *107*, 20678–20685.

[33] "The Nobel Prize in Chemistry 2021 - NobelPrize.org," can be found under https://www.nobelprize.org/prizes/chemistry/2021/summary/, **n.d.**

[34] O. García Mancheño, M. Waser, *Eur. J. Org. Chem.* **2023**, *26*, DOI 10.1002/ejoc.202200950.

[35] J. von Liebig, *Justus Liebigs Ann. Chem.* **1860**, *113*, 246–247.

[36] W. Langenbeck, *Angew. Chem. Int. Ed.* **1928**, *41*, 740–745.

[37] E. Knoevenagel, *Ber. Dtsch. Chem. Ges.* **1896**, *29*, 172–174.

[38] P. S. Fiske, G. Bredig, *Biochem. Z.* **1912**, *46*, 7–23.

[39] H. Pracejus, *Justus Liebigs Ann. Chem.* **1960**, *634*, 9–22.

[40] G. Tanriver, B. Dedeoglu, S. Catak, V. Aviyente, *Acc. Chem. Res.* **2016**, *49*, 1250–1262.

[41] S. S. Jew, H. G. Park, *Chem. Commun.* **2009**, 7090–7103.

[42] U. Eder, G. Sauer, R. Wiechert, *Angew. Chem. Int. Ed.* **1971**, *10*, 496–497.

[43] Z. G. Hajos, D. R. Parrish, *J. Org. Chem.* **1974**, *39*, 1615–1621.

[44] B. List, *Acc. Chem. Res.* **2004**, *37*, 548–557.

[45] G. Lelais, D. W. C. MacMillan, *Aldrichimica Acta* **2006**, *39*, 79–87.

[46] I. Seayad, B. List, *Org. Biomol. Chem.* **2005**, *3*, 719–724.

[47] W. P. Jencks, *Acc. Chem. Res.* **1976**, *9*, 425–432.

[48] T. Akiyama, J. Itoh, K. Fuchibe, *Adv. Synth. Catal.* **2006**, *348*, 999–1010.

[49] A. G. Doyle, E. N. Jacobsen, *Chem. Rev.* **2007**, *107*, 5713–5743.

[50] M. S. Sigman, E. N. Jacobsen, *J. Am. Chem. Soc.* **1998**, *120*, 4901–4902.

[51] J. P. Malerich, K. Hagihara, V. H. Rawal, *J. Am. Chem. Soc.* **2008**, *130*, 14416–14417.

[52] H. Konishi, T. Y. Lam, J. P. Malerich, V. H. Rawal, *Org. Lett.* **2010**, *12*, 2028–2031.

[53] Y. Huang, A. K. Unni, A. N. Thadani, V. H. Rawal, *Nature* **2003**, *424*, 146.

[54] N. T. McDougal, S. E. Schaus, *J. Am. Chem. Soc.* **2003**, *125*, 12094–12095.

[55] T. Akiyama, J. Itoh, K. Yokota, K. Fuchibe, *Angew. Chem. Int. Ed.* **2004**, *43*, 1566–1568.

[56] D. Uraguchi, M. Terada, *J. Am. Chem. Soc.* **2004**, *126*, 5356–5357.

[57] M. Hatano, K. Moriyama, T. Maki, K. Ishihara, *Angew. Chem. Int. Ed.* **2010**, *49*, 3823–3826.

[58] M. Rueping, B. J. Nachtsheim, R. M. Koenigs, W. Ieawsuwan, *Chem. - A Eur. J.* **2010**, *16*, 13116–

13126.

[59] M. Klussmann, L. Ratjen, S. Hoffmann, V. Wakchaure, R. Goddard, B. List, *Synlett* **2010**, 2189–2192.

[60] M. Terada, K. Kanomata, *Synlett* **2011**, 1255–1258.

[61] X. del Corte, E. Martínez de Marigorta, F. Palacios, J. Vicario, A. Maestro, *Org. Chem. Front.* **2022**, *9*, 6331–6399.

[62] S. Hoffmann, A. M. Seayad, B. List, *Angew. Chem. Int. Ed.* **2005**, *44*, 7424–7427.

[63] J. P. Handjaya, N. Patankar, J. P. Reid, *Chem. - A Eur. J.* **2024**, *30*, DOI 10.1002/chem.202400921.

[64] J. Kikuchi, H. Aramaki, H. Okamoto, M. Terada, *Chem. Sci.* **2019**, *10*, 1426–1433.

[65] M. Rueping, E. Sugiono, T. Theissmann, A. Kuenkel, A. Köckritz, A. Pews-Davtyan, N. Nemati, M. Beller, *Org. Lett.* **2007**, *9*, 1065–1068.

[66] X. H. Chen, X. Y. Xu, H. Liu, L. F. Cun, L. Z. Gong, *J. Am. Chem. Soc.* **2006**, *128*, 14802–14803.

[67] M. R. Monaco, S. Prévost, B. List, *J. Am. Chem. Soc.* **2014**, *136*, 16982–16985.

[68] C. Romano, M. Jia, M. Monari, E. Manoni, M. Bandini, *Angew. Chem. Int. Ed.* **2014**, *53*, 13854–13857.

[69] I. Čorić, S. Müller, B. List, *J. Am. Chem. Soc.* **2010**, *132*, 17370–17373.

[70] D. M. Rubush, M. A. Morges, B. J. Rose, D. H. Thamm, T. Rovis, *J. Am. Chem. Soc.* **2012**, *134*, 13554–13557.

[71] Z. Wang, Z. Chen, J. Sun, *Angew. Chem. Int. Ed.* **2013**, *52*, 6685–6688.

[72] G. B. Rowland, H. Zhang, E. B. Rowland, S. Chennamadhavuni, Y. Wang, J. C. Antilla, *J. Am. Chem. Soc.* **2005**, *127*, 15696–15697.

[73] E. B. Rowland, G. B. Rowland, E. Rivera-Otero, J. C. Antilla, *J. Am. Chem. Soc.* **2007**, *129*, 12084–12085.

[74] Y. Liang, E. B. Rowland, G. B. Rowland, J. A. Perman, J. C. Antilla, *Chem. Commun.* **2007**, 4477–4479.

[75] A. A. Desai, W. D. Wulff, *Synthesis (Stuttg).* **2010**, *2010*, 3670–3680.

[76] Z. Ding, W. E. G. Osminski, H. Ren, W. D. Wulff, *Org. Process Res. Dev.* **2011**, *15*, 1089–1107.

[77] T. Akiyama, Y. Saitoh, H. Morita, K. Fuchibe, *Adv. Synth. Catal.* **2005**, *347*, 1523–1526.

[78] D. Nakashima, H. Yamamoto, *J. Am. Chem. Soc.* **2006**, *128*, 9626–9627.

[79] P. S. J. Kaib, B. List, *Synlett* **2016**, *27*, 156–158.

[80] P. Burk, I. A. Koppel, I. Koppel, L. M. Yagupolskii, R. W. Taft, *J. Comput. Chem.* **1996**, *17*, 30–41.

[81] L. M. Yagupolskii, V. N. Petrik, N. V. Kondratenko, L. Soováli, I. Kaljurand, I. Leito, I. A. Koppel, *J. Chem. Soc. Perkin Trans. 2* **2002**, *2*, 1950–1955.

[82] H. C. Cheol, H. Yamamoto, *J. Am. Chem. Soc.* **2008**, *130*, 9246–9247.

[83] F. G. Bordwell, *Acc. Chem. Res.* **1988**, *21*, 456–463.

[84] A. Kütt, T. Rodima, J. Saame, E. Raamat, V. Mäemets, I. Kaljurand, I. A. Koppel, R. Y. Garlyauskayte, Y. L. Yagupolskii, L. M. Yagupolskii, E. Bernhardt, H. Willner, I. Leito, *J. Org. Chem.* **2011**, *76*, 391–395.

[85] B. Peng, J. Ma, J. Guo, Y. Gong, R. Wang, Y. Zhang, J. Zeng, W. W. Chen, K. Ding, B. Zhao, *J. Am. Chem. Soc.* **2022**, *144*, 2853–2860.

[86] T. Gatzenmeier, M. Van Gemmeren, Y. Xie, D. Höfler, M. Leutzsch, B. List, *Science* **2016**, *351*, 949–952.

[87] P. Garcia-Garcia, F. Lay, P. Garcia-Garcia, C. Rabalakos, B. List, *Angew. Chem. Int. Ed.* **2009**, *48*, 4363–4366.

[88] M. Treskow, J. Neudörfl, R. Giernoth, *Eur. J. Org. Chem.* **2009**, 3693–3697.

[89] K. Kaupmees, N. Tolstoluzhsky, S. Raja, M. Rueping, I. Leito, *Angew. Chem. Int. Ed.* **2013**, *52*, 11569–11572.

[90] A. Kütt, S. Selberg, I. Kaljurand, S. Tshepelevitsh, A. Heering, A. Darnell, K. Kaupmees, M. Piirsalu, I. Leito, *Tetrahedron Lett.* **2018**, *59*, 3738–3748.

[91] A. Kütt, S. Tshepelevitsh, J. Saame, M. Lõkov, I. Kaljurand, S. Selberg, I. Leito, *Eur. J. Org. Chem.* **2021**, *2021*, 1407–1419.

[92] L. Schreyer, R. Properzi, B. List, *Angew. Chem. Int. Ed.* **2019**, *58*, 12761–12777.

[93] H. Y. Bae, D. Höfler, P. S. J. Kaib, P. Kasaplar, C. K. De, A. Döhring, S. Lee, K. Kaupmees, I. Leito, B. List, *Nat. Chem.* **2018**, *10*, 888–894.

[94] M. J. Scharf, N. Tsuji, M. M. Lindner, M. Leutzsch, M. Lõkov, E. Parman, I. Leito, B. List, *J. Am. Chem. Soc.* **2024**, *146*, 28339–28349.

[95] A. Berkessel, P. Christ, N. Leconte, J. M. Neudörfl, M. Schäfer, *Eur. J. Org. Chem.* **2010**, 5165–5170.

[96] S. C. Pan, B. List, *Chem. Asian J.* **2008**, *3*, 430–437.

[97] D. Kampen, A. Ladépêche, G. Claßen, B. Lista, *Adv. Synth. Catal.* **2008**, *350*, 962–966.

[98] M. Hatano, T. Maki, K. Moriyama, M. Arinobe, K. Ishihara, *J. Am. Chem. Soc.* **2008**, *130*, 16858–16860.

[99] I. Čorić, B. List, *Nature* **2012**, *483*, 315–319.

[100] L. Liu, P. S. J. Kaib, A. Tap, B. List, *J. Am. Chem. Soc.* **2016**, *138*, 10822–10825.

[101] P. S. J. Kaib, L. Schreyer, S. Lee, R. Properzi, B. List, *Angew. Chem. Int. Ed.* **2016**, *55*, 13200–13203.

[102] J. A. A. Grimm, H. Zhou, R. Properzi, M. Leutzsch, G. Bistoni, J. Nienhaus, B. List, *Nature* **2023**,

615, 634–639.

[103] H. Zhou, Y. Zhou, H. Y. Bae, M. Leutzsch, Y. Li, C. K. De, G. J. Cheng, B. List, *Nature* **2022**, *605*, 84–89.

[104] S. Brunen, B. Mitschke, M. Leutzsch, B. List, *J. Am. Chem. Soc.* **2023**, *145*, 15708–15713.

[105] V. N. Wakchaure, W. DeSnoo, C. J. Laconsay, M. Leutzsch, N. Tsuji, D. J. Tantillo, B. List, *Nature* **2024**, *625*, 287–292.

[106] R. K. Raut, S. Matsutani, F. Shi, S. Kataoka, M. Poje, B. Mitschke, S. Maeda, N. Tsuji, B. List, *Science* **2024**, *386*, 225–230.

[107] B. Mitschke, M. Turberg, B. List, *Chem* **2020**, *6*, 2515–2532.

[108] J. K. Cheng, S. H. Xiang, B. Tan, *Chin. J. Chem.* **2023**, *41*, 685–694.

[109] M. Hatano, Y. Goto, A. Izumiseki, M. Akakura, K. Ishihara, *J. Am. Chem. Soc.* **2015**, *137*, 13472–13475.

[110] Y. L. Pan, H. L. Zheng, J. Wang, C. Yang, X. Li, J. P. Cheng, *ACS Catal.* **2020**, *10*, 8069–8076.

[111] Q. X. Zhang, Y. Li, J. Wang, C. Yang, C. J. Liu, X. Li, J. P. Cheng, *Angew. Chem. Int. Ed.* **2020**, *59*, 4550–4556.

[112] G. P. Wang, M. Q. Chen, S. F. Zhu, Q. L. Zhou, *Chem. Sci.* **2017**, *8*, 7197–7202.

[113] L. Zhang, J. Zhang, J. Ma, D. J. Cheng, B. Tan, *J. Am. Chem. Soc.* **2017**, *139*, 1714–1717.

[114] S. Mayer, B. List, *Angew. Chem. Int. Ed.* **2006**, *45*, 4193–4195.

[115] M. Mahlau, B. List, *Angew. Chem. Int. Ed.* **2013**, *52*, 518–533.

[116] G. L. Hamilton, J. K. Eun, M. Mba, F. D. Toste, *Science* **2007**, *317*, 496–499.

[117] L. M. Entgelmeier, O. G. Mancheño, *Synth.* **2022**, *54*, 3907–3927.

[118] M. S. Taylor, E. N. Jacobsen, *J. Am. Chem. Soc.* **2004**, *126*, 10558–10559.

[119] M. Rueping, J. Dufour, F. R. Schoepke, *Green Chem.* **2011**, *13*, 1084–1105.

[120] A. Hantzsch, *Ber. Dtsch. Chem. Ges.* **1881**, *14*, 1637–1638.

[121] A. Hantzsch, *Justus Liebigs Ann. Chem.* **1882**, *215*, 1–82.

[122] K. Saito, H. Miyashita, T. Akiyama, *Org. Lett.* **2014**, *16*, 5312–5315.

[123] C. Zhu, K. Saito, M. Yamanaka, T. Akiyama, *Acc. Chem. Res.* **2015**, *48*, 388–398.

[124] M. W. Chen, Q. Yang, Z. Deng, Y. Zhou, Q. Ding, Y. Peng, *J. Org. Chem.* **2018**, *83*, 8688–8694.

[125] Q. A. Chen, K. Gao, Y. Duan, Z. S. Ye, L. Shi, Y. Yang, Y. G. Zhou, *J. Am. Chem. Soc.* **2012**, *134*, 2442–2448.

[126] B. Gao, W. Meng, X. Feng, H. Du, *Org. Lett.* **2022**, *24*, 3955–3959.

[127] J. W. Yang, M. T. Hechavarria Fonseca, B. List, *Angew. Chem. Int. Ed.* **2004**, *43*, 6660–6662.

[128] S. Das, V. N. Wakchaure, B. List, in *Asymmetric Hydrog. Transf. Hydrog.* (Eds.: V. Ratovelomanana-Vidal, P. Phansavath), Wiley-VCH, **2021**, pp. 339–374.

[129] S. G. Ouellet, J. B. Tuttle, D. W. C. MacMillan, *J. Am. Chem. Soc.* **2005**, *127*, 32–33.

[130] J. W. Yang, M. T. Hechavarria Fonseca, N. Vignola, B. List, *Angew. Chem. Int. Ed.* **2005**, *44*, 108–110.

[131] J. B. Tuttle, S. G. Ouellet, D. W. C. MacMillan, *J. Am. Chem. Soc.* **2006**, *128*, 12662–12663.

[132] K. Akagawa, H. Akabane, S. Sakamoto, K. Kudo, *Org. Lett.* **2008**, *10*, 2035–2037.

[133] T. M. Bräuer, Q. Zhang, K. Tiefenbacher, *J. Am. Chem. Soc.* **2017**, *139*, 17500–17507.

[134] R. Kumar, V. Maurya, A. Avinash, C. Appayee, *J. Org. Chem.* **2024**, *89*, 8586–8600.

[135] N. J. A. Martin, B. List, *J. Am. Chem. Soc.* **2006**, *128*, 13368–13369.

[136] A. Carioscia, E. Cocco, M. E. Casacchia, G. Gentile, M. Mamone, G. Giorgianni, E. Incerto, M. Prato, F. Pesciaioli, G. Filippini, A. Carlone, *ACS Catal.* **2024**, *14*, 13429–13438.

[137] N. J. A. Martin, L. Ozores, B. List, *J. Am. Chem. Soc.* **2007**, *129*, 8976–8977.

[138] N. J. A. Martin, X. Cheng, B. List, *J. Am. Chem. Soc.* **2008**, *130*, 13862–13863.

[139] J. F. Schneider, M. B. Lauber, V. Muhr, D. Kratzer, J. Paradies, *Org. Biomol. Chem.* **2011**, *9*, 4323–4327.

[140] E. Massolo, M. Benaglia, M. Orlandi, S. Rossi, G. Celentano, *Chem. - A Eur. J.* **2015**, *21*, 3589–3595.

[141] E. Martinelli, A. C. Vicini, M. Mancinelli, A. Mazzanti, P. Zani, L. Bernardi, M. Fochi, *Chem. Commun.* **2015**, *51*, 658–660.

[142] A. Ferraro, L. Bernardi, M. Fochi, *Adv. Synth. Catal.* **2016**, *358*, 1561–1565.

[143] Z. Wang, F. Ai, Z. Wang, W. Zhao, G. Zhu, Z. Lin, J. Sun, *J. Am. Chem. Soc.* **2015**, *137*, 383–389.

[144] K. Autumn, M. Sitti, Y. A. Liang, A. M. Peattie, W. R. Hansen, S. Sponberg, T. W. Kenny, R. Fearing, J. N. Israelachvili, R. J. Full, *Proc. Natl. Acad. Sci. U. S. A.* **2002**, *99*, 12252–12256.

[145] S. Singla, D. Jain, C. M. Zoltowski, S. Voleti, A. Y. Stark, P. H. Niewiarowski, A. Dhinojwala, *Direct Evidence of Acid-Base Interactions in Gecko Adhesion*, **2021**.

[146] P. W. Atkins, P. W. Atkins, J. de Paula, in *Atkins' Phys. Chem.*, **2014**, p. 871.

[147] J. P. Wagner, P. R. Schreiner, *Angew. Chem. Int. Ed.* **2015**, *54*, 12274–12296.

[148] L. Rummel, P. R. Schreiner, *Angew. Chem. Int. Ed.* **2024**, *63*, e202316364.

[149] S. Grimme, *The Chemical Bond*, (Eds. G. Frenking, S. Shaik), Wiley-VCH, Weinheim, **2014**.

[150] K. T. Tang, J. P. Toennies, *Angew. Chem. Int. Ed.* **2010**, *49*, 9574–9579.

[151] F. London, *Zeitschrift für Phys.* **1930**, *63*, 245–279.

[152] S. Grimme, *J. Comput. Chem.* **2004**, *25*, 1463–1473.

[153] J. G. Brandenburg, M. Hochheim, T. Bredow, S. Grimme, *J. Phys. Chem. Lett.* **2014**, *5*, 4275–4284.

[154] W. S. Jen, J. J. M. Wiener, D. W. C. MacMillan, *J. Am. Chem. Soc.* **2000**, *122*, 9874–9875.

[155] D. Seebach, U. Grošelj, W. B. Schweizer, S. Grimme, C. Mück-Lichtenfeld, *Helv. Chim. Acta* **2010**,

93, 1–16.

[156] E. J. Corey, R. K. Bakshi, S. Shibata, C. pin Chen, V. K. Singh, *J. Am. Chem. Soc.* **1987**, *109*, 7925–7926.

[157] E. J. Corey, R. K. Bakshi, S. Shibata, *J. Am. Chem. Soc* **1987**, *109*, 5551–5553.

[158] E. J. Corey, S. Shibata, R. K. Bakshi, *J. Org. Chem.* **1988**, *53*, 2861–2863.

[159] E. J. Corey, J. O. Link, *Tetrahedron Lett.* **1989**, *30*, 6275–6278.

[160] E. J. Corey, R. K. Bakshi, *Tetrahedron Lett.* **1990**, *31*, 611–614.

[161] E. J. Corey, C. J. Helal, *Tetrahedron Lett.* **1995**, *36*, 9153–9156.

[162] E. J. Corey, C. J. Helal, *Angew. Chem. Int. Ed.* **1998**, *37*, 1986–2012.

[163] E. J. Corey, J. O. Link, R. K. Bakshi, *Tetrahedron Lett.* **1992**, *33*, 7107–7110.

[164] C. Eschmann, L. Song, P. R. Schreiner, *Angew. Chem. Int. Ed.* **2021**, *60*, 4823–4832.

[165] S. Grimme, R. Huenerbein, S. Ehrlich, *ChemPhysChem* **2011**, *12*, 1258–1261.

[166] J. M. McBride, *Tetrahedron* **1974**, *30*, 2009–2022.

[167] H. Lankamp, W. T. Nauta, C. MacLean, *Tetrahedron Lett.* **1968**, *9*, 249–254.

[168] B. Kahr, D. Van Engen, K. Mislow, *J. Am. Chem. Soc.* **1986**, *108*, 8305–8307.

[169] S. Grimme, P. R. Schreiner, *Angew. Chem. Int. Ed.* **2011**, *50*, 12639–12642.

[170] G. Mayer, S. Pfriem, U. Schäfer, R. Matusch, *Angew. Chem.* **1978**, *90*, 552–553.

[171] P. R. Schreiner, L. V Chernish, P. A. Gunchenko, E. Y. Tikhonchuk, H. Hausmann, M. Serafin, S. Schlecht, J. E. P. Dahl, R. M. K. Carlson, A. A. Fokin, *Nature* **2011**, *477*, 308–311.

[172] Y. Ishigaki, T. Shimajiri, T. Takeda, R. Katoono, T. Suzuki, *Chem* **2018**, *4*, 795–806.

[173] T. Shimajiri, Y. Kawakami, S. Kawaguchi, Y. Hayashi, K. Hada, T. Suzuki, Y. Ishigaki, *Synlett* **2022**, *34*, 1147–1152.

[174] S. Rösel, H. Quanz, C. Logemann, J. Becker, E. Mossou, L. Cañadillas-Delgado, E. Caldeweyher, S. Grimme, P. R. Schreiner, *J. Am. Chem. Soc.* **2017**, *139*, 7428–7431.

[175] C. Valente, S. Çalimsiz, K. H. Hoi, D. Mallik, M. Sayah, M. G. Organ, *Angew. Chem. Int. Ed.* **2012**, *51*, 3314–3332.

[176] Y. Xi, B. Su, X. Qi, S. Pedram, P. Liu, J. F. Hartwig, *J. Am. Chem. Soc.* **2020**, *142*, 18213–18222.

[177] S. Singha, M. Buchsteiner, G. Bistoni, R. Goddard, A. Fürstner, *J. Am. Chem. Soc.* **2021**, *143*, 5666–5673.

[178] T. Zheng, J. Ma, H. Chen, H. Jiang, S. Lu, Z. Shi, F. Liu, K. N. Houk, Y. Liang, *J. Am. Chem. Soc.* **2024**, *146*, 25058–25066.

[179] G. Lu, R. Y. Liu, Y. Yang, C. Fang, D. S. Lambrecht, S. L. Buchwald, P. Liu, *J. Am. Chem. Soc.* **2017**, *139*, 16548–16555.

[180] A. A. Thomas, K. Speck, I. Kevlishvili, Z. Lu, P. Liu, S. L. Buchwald, *J. Am. Chem. Soc.* **2018**, *140*,

13976–13984.

[181]　M. Marin-Luna, B. Pölloth, F. Zott, H. Zipse, *Chem. Sci.* **2018**, *9*, 6509–6515.

[182]　B. Pölloth, M. P. Sibi, H. Zipse, *Angew. Chem. Int. Ed.* **2021**, *60*, 774–778.

[183]　M. C. Schwarzer, A. Fujioka, T. Ishii, H. Ohmiya, S. Mori, M. Sawamura, *Chem. Sci.* **2018**, *9*, 3484–3493.

[184]　S. M. Maley, R. Steagall, G. R. Lief, R. M. Buck, Q. Yang, O. L. Sydora, S. M. Bischof, D. H. Ess, *Organometallics* **2022**, *41*, 581–593.

[185]　V. R. Yatham, W. Harnying, D. Kootz, J. M. Neudörfl, N. E. Schlörer, A. Berkessel, *J. Am. Chem. Soc.* **2016**, *138*, 2670–2677.

[186]　W. Harnying, P. Sudkaow, A. Biswas, A. Berkessel, *Angew. Chem. Int. Ed.* **2021**, *60*, 19631–19636.

[187]　W. Harnying, J. M. Neudörfl, A. Berkessel, *Org. Lett.* **2020**, *22*, 386–390.

[188]　M. Paul, J. Neudörfl, A. Berkessel, *Angew. Chem. Int. Ed.* **2019**, *58*, 10596–10600.

[189]　M. Paul, P. Sudkaow, A. Wessels, N. E. Schlörer, J. Neudörfl, A. Berkessel, *Angew. Chem. Int. Ed.* **2018**, *57*, 8310–8315.

[190]　M. Paul, M. Breugst, J. M. Neudörfl, R. B. Sunoj, A. Berkessel, *J. Am. Chem. Soc.* **2016**, *138*, 5044–5051.

[191]　A. Seitz, R. C. Wende, P. R. Schreiner, *Chem. - A Eur. J.* **2023**, *29*, 3907–3922.

[192]　A. C. Colgan, R. S. J. Proctor, D. C. Gibson, P. Chuentragool, A. S. K. Lahdenperä, K. Ermanis, R. J. Phipps, *Angew. Chem. Int. Ed.* **2022**, *61*, DOI 10.1002/anie.202200266.

[193]　J. Miró, T. Gensch, M. Ellwart, S. J. Han, H. H. Lin, M. S. Sigman, F. D. Toste, *J. Am. Chem. Soc.* **2020**, *142*, 6390–6399.

[194]　J. Gramüller, M. Franta, R. M. Gschwind, *J. Am. Chem. Soc.* **2022**, *144*, 19861–19871.

[195]　R. C. Wende, A. Seitz, D. Niedek, S. M. M. Schuler, C. Hofmann, J. Becker, P. R. Schreiner, *Angew. Chem. Int. Ed.* **2016**, *55*, 2719–2723.

[196]　K. M. Lippert, K. Hof, D. Gerbig, D. Ley, H. Hausmann, S. Guenther, P. R. Schreiner, *Eur. J. Org. Chem.* **2012**, *2012*, 5919–5927.

[197]　L. Rummel, M. H. J. Domanski, H. Hausmann, J. Becker, P. R. Schreiner, *Angew. Chem. Int. Ed.* **2022**, *61*, DOI 10.1002/anie.202204393.

[198]　I. Sandler, F. A. Larik, N. Mallo, J. E. Beves, J. Ho, *J. Org. Chem.* **2020**, *85*, 8074–8084.

[199]　M. H. J. Domanski, M. Fuhrmann, P. R. Schreiner, *J. Am. Chem. Soc.* **2025**, DOI 10.1021/JACS.5C09212.

[200]　A. Shoja, J. P. Reid, *J. Am. Chem. Soc.* **2021**, *143*, 7209–7215.

[201]　G. Bistoni, *Wiley Interdiscip. Rev. Comput. Mol. Sci.* **2020**, *10*, DOI 10.1002/wcms.1442.

[202]　A. Altun, R. Izsák, G. Bistoni, *Int. J. Quantum Chem.* **2021**, *121*, 26339.

[203] C. Riplinger, P. Pinski, U. Becker, E. F. Valeev, F. Neese, *J. Chem. Phys.* **2016**, *144*, 24109.

[204] C. Riplinger, B. Sandhoefer, A. Hansen, F. Neese, *J. Chem. Phys.* **2013**, *139*, 134101.

[205] C. Riplinger, F. Neese, *J. Chem. Phys.* **2013**, *138*, 34106.

[206] A. Hansen, D. G. Liakos, F. Neese, *J. Chem. Phys.* **2011**, *135*, 214102.

[207] D. G. Liakos, A. Hansen, F. Neese, *J. Chem. Theory Comput.* **2011**, *7*, 76–87.

[208] F. Neese, A. Hansen, D. G. Liakos, *J. Chem. Phys.* **2009**, *131*, 64103.

[209] F. Neese, A. Hansen, F. Wennmohs, S. Grimme, *Acc. Chem. Res.* **2009**, *42*, 641–648.

[210] T. Lu, Q. Chen, *J. Comput. Chem.* **2022**, *43*, 539–555.

[211] T. Lu, F. Chen, *J. Comput. Chem.* **2012**, *33*, 580–592.

[212] T. Lu, *J. Chem. Phys.* **2024**, *161*, 82503.

[213] S. G. Ouellet, J. B. Tuttle, D. W. C. MacMillan, *J. Am. Chem. Soc.* **2005**, *127*, 32–33.

[214] J. Burés, *Angew. Chem. Int. Ed.* **2016**, *55*, 16084–16087.

[215] J. P. Wagner, P. R. Schreiner, *Angew. Chem.* **2015**, *127*, 12446–12471.

[216] B. Wang, D. A. Gandamana, F. Gagosz, S. Chiba, *Org. Lett.* **2019**, *21*, 2298–2301.

[217] B. Wolff, Z. W. Qu, S. Grimme, M. Oestreich, *Angew. Chem. Int. Ed.* **2023**, *62*, e202305295.

[218] J. L. Fry, M. G. Adlington, *J. Am. Chem. Soc.* **1978**, *100*, 7641–7644.

[219] M. Franta, A. Pattanaik, W. Silva, K. Motiram-Corral, J. Rehbein, R. M. Gschwind, *J. Am. Chem. Soc* **2025**, *147*, 2549–2558.

[220] M. Žabka, R. M. Gschwind, *Chem. Sci.* **2021**, *12*, 15263–15272.

[221] T. Marcelli, P. Hammar, F. Himo, *Chem. - A Eur. J.* **2008**, *14*, 8562–8571.

[222] I. Chatterjee, M. Oestreich, *Org. Lett.* **2016**, *18*, 2463–2466.

[223] D. N. Kursanov, Z. N. Parnes, *Russ. Chem. Rev.* **1969**, *38*, 812–821.

[224] D. N. Kursanov, Z. N. Parnes, N. M. Loim, *Synth.* **1974**, 633–651.

[225] Y. Bao, S. Ma, J. Zhu, Z. Dai, Q. Zhou, X. Yang, Q. Zhou, F. Yang, *Green Chem.* **2024**, *26*, 1356–1362.

[226] Y. Arakawa, T. Kohda, K. Minagawa, Y. Imada, *SynOpen* **2017**, *1*, 11–14.

[227] N. Frank, M. Leutzsch, B. List, *J. Am. Chem. Soc.* **2025**, *147*, 7932–7938.

[228] J. F. Teichert, T. Den Hartog, M. Hanstein, C. Smit, B. Ter Horst, V. Hernandez-Olmos, B. L. Feringa, A. J. Minnaard, *ACS Catal.* **2011**, *1*, 309–315.

[229] Y. Imada, H. Iida, T. Naota, *J. Am. Chem. Soc.* **2005**, *127*, 14544–14545.

[230] C. Smit, M. W. Fraaije, A. J. Minnaard, *J. Org. Chem.* **2008**, *73*, 9482–9485.

[231] Y. Imada, H. Iida, T. Kitagawa, T. Naota, *Chem. - A Eur. J.* **2011**, *17*, 5908–5920.

[232] M. Lamani, R. Siddappa Guralamata, K. Ramaiah Prabhu, *Chem. Commun.* **2012**, *48*, 6583–6585.

[233] Y. Imada, T. Kitagawa, T. Ohno, H. Iida, T. Naota, *Org. Lett.* **2010**, *12*, 32–35.

[234] B. Wolff, M. Oestreich, *Isr. J. Chem.* **2023**, *63*, e202300027.

[235] J. L. Fry, *J. Am. Chem. Soc.* **1971**, *93*, 3558–3559.

[236] J. C. L. Walker, M. Oestreich, *Synlett* **2019**, *30*, 2216–2232.

[237] N. Tsuji, J. L. Kennemur, T. Buyck, S. Lee, S. Prévost, P. S. J. Kaib, D. Bykov, C. Farès, B. List, *Science* **2018**, *359*, 1501–1505.

[238] R. Maji, S. Ghosh, O. Grossmann, P. Zhang, M. Leutzsch, N. Tsuji, B. List, *J. Am. Chem. Soc.* **2023**, *145*, 8788–8793.

[239] J. Kikuchi, M. Terada, *Angew. Chem. Int. Ed.* **2019**, *58*, 8458–8462.

[240] R. Properzi, P. S. J. Kaib, M. Leutzsch, G. Pupo, R. Mitra, C. K. De, L. Song, P. R. Schreiner, B. List, *Nat. Chem.* **2020**, *12*, 1174–1179.

[241] P. Zhang, N. Tsuji, J. Ouyang, B. List, *J. Am. Chem. Soc.* **2021**, *143*, 675–680.

[242] L. Ackermann, A. Althammer, *Synlett* **2008**, 995–998.

[243] J. Lin, P. Yu, L. Huang, P. Zhang, B. Tan, X.-Y. Liu, *Angew. Chem. Int. Ed.* **2015**, *54*, 7847–7851.

[244] Z. L. Yu, Y. F. Cheng, N. C. Jiang, J. Wang, L. W. Fan, Y. Yuan, Z. L. Li, Q. S. Gu, Q. S. Gu, X. Y. Liu, *Chem. Sci.* **2020**, *11*, 5987–5993.

[245] R. Takagi, D. T. Duong, T. Ichiki, *Tetrahedron* **2021**, *94*, 132332.

[246] S. Guria, A. N. Volkov, R. Khudaverdyan, R. Van Lommel, R. Pan, C. G. Daniliuc, F. De Proft, U. Hennecke, *J. Am. Chem. Soc.* **2024**, *146*, 17180–17188.

[247] T. L. Cottrell, *The Strengths of Chemical Bonds.*, Butterworths Scientific, **1958**.

[248] L. R. C. Barclay, H. R. Sonawane, M. C. MacDonald, *Can. J. Chem.* **1972**, *50*, 281–290.

[249] C. Margarita, P. G. Andersson, *J. Am. Chem. Soc.* **2017**, *139*, 1346–1356.

[250] S. Das, B. Mitschke, C. K. De, I. Harden, G. Bistoni, B. List, *Nat. Catal.* **2021**, *4*, 1043–1049.

[251] J. T. Han, N. Tsuji, H. Zhou, M. Leutzsch, B. List, *Nat. Commun.* **2024**, *15*, DOI 10.1038/s41467-024-49988-2.

[252] N. Mardirossian, M. Head-Gordon, *Phys. Chem. Chem. Phys.* **2014**, *16*, 9904–9924.

[253] S. Grimme, A. Hansen, S. Ehlert, J. M. Mewes, *J. Chem. Phys.* **2021**, *154*, 64103.

[254] F. Neese, *Wiley Interdiscip. Rev. Comput. Mol. Sci.* **2025**, *15*, e70019.

[255] F. M. Bickelhaupt, K. N. Houk, *Angew. Chem. Int. Ed.* **2017**, *56*, 10070–10086.

[256] T. Satyanarayana, S. Abraham, H. B. Kagan, *Angew. Chem. Int. Ed.* **2009**, *48*, 456–494.

[257] M. Klussmann, H. Iwamura, S. P. Mathew, D. H. Wells, U. Pandya, A. Armstrong, D. G. Blackmond, *Nature* **2006**, *441*, 621–623.

[258] Y. Hayashi, M. Matsuzawa, J. Yamaguchi, S. Yonehara, Y. Matsumoto, M. Shoji, D. Hashizume, H. Koshino, *Angew. Chem.* **2006**, *118*, 4709–4713.

[259] N. Li, X. H. Chen, S. M. Zhou, S. W. Luo, J. Song, L. Ren, L. Z. Gong, *Angew. Chem. Int. Ed.* **2010**,

49, 6378–6381.

[260] J. B. Metternich, R. Gilmour, *J. Am. Chem. Soc.* **2015**, *137*, 11254–11257.

[261] J. M. Obrien, K. S. Lee, A. H. Hoveyda, *J. Am. Chem. Soc.* **2010**, *132*, 10630–10633.

[262] A. G. Bush, J. L. Jiang, P. R. Payne, W. W. Ogilvie, *Tetrahedron* **2009**, *65*, 8502–8506.

[263] M. Shevlin, M. R. Friedfeld, H. Sheng, N. A. Pierson, J. M. Hoyt, L. C. Campeau, P. J. Chirik, *J. Am. Chem. Soc.* **2016**, *138*, 3562–3569.

[264] J. Zheng, C. Margarita, S. Krajangsri, P. G. Andersson, *Org. Lett.* **2018**, *20*, 5676–5679.

[265] S. E. Denmark, L. K. Marble, *Heterocycles* **2014**, *88*, 559–590.

[266] A. C. P. Rivera, R. Still, D. E. Frantz, *Angew. Chem. Int. Ed.* **2016**, *55*, 6689–6693.

[267] D. A. Engel, G. B. Dudley, *Org. Lett.* **2006**, *8*, 4027–4029.

[268] A. Narczyk, S. Stecko, *Org. Biomol. Chem.* **2020**, *18*, 5972–5981.

[269] Y. Xiao, Y. Huang, Z. Zeng, X. Luo, X. Qian, Y. Yang, *J. Org. Chem.* **2022**, *87*, 85–93.

[270] J. H. Sahner, H. Sucipto, S. C. Wenzel, M. Groh, R. W. Hartmann, R. Müller, *ChemBioChem* **2015**, *16*, 946–953.

[271] P. Castelani, J. V. Comasseto, *Tetrahedron* **2005**, *61*, 2319–2326.

[272] T. Brégent, J. P. Bouillon, T. Poisson, *Org. Lett.* **2020**, *22*, 7688–7693.

[273] M. Asikainen, W. Lewis, A. J. Blake, S. Woodward, *Tetrahedron Lett.* **2010**, *51*, 6454–6456.

[274] L. Næsborg, V. Corti, L. A. Leth, P. H. Poulsen, K. A. Jørgensen, *Angew. Chem. Int. Ed.* **2018**, *57*, 1606–1610.

[275] J. Tummatorn, G. B. Dudley, *Org. Lett.* **2011**, *13*, 1572–1575.

[276] A. J. Neel, A. Milo, M. S. Sigman, F. D. Toste, *J. Am. Chem. Soc.* **2016**, *138*, 3863–3875.

[277] B. J. Bench, C. Liu, C. R. Evett, C. M. H. Watanabe, *J. Org. Chem.* **2006**, *71*, 9458–9463.

[278] R. Shintani, T. Kimura, T. Hayashi, *Chem. Commun.* **2005**, 3213–3214.

[279] C. Bannwarth, S. Ehlert, S. Grimme, *J. Chem. Theory Comput.* **2019**, *15*, 1652–1671.

[280] P. Pracht, F. Bohle, S. Grimme, *Phys. Chem. Chem. Phys.* **2020**, *22*, 7169–7192.

[281] F. Neese, *Wiley Interdiscip. Rev. Comput. Mol. Sci.* **2012**, *2*, 73–78.

[282] J. P. Perdew, K. Burke, M. Ernzerhof, *Phys. Rev. Lett.* **1996**, *77*, 3865–3868.

[283] S. Grimme, J. Antony, S. Ehrlich, H. Krieg, *J. Chem. Phys.* **2010**, *132*, 15104.

[284] S. Grimme, S. Ehrlich, L. Goerigk, *J. Comput. Chem.* **2011**, *32*, 1456–1465.

[285] F. Weigend, R. Ahlrichs, *Phys. Chem. Chem. Phys.* **2005**, *7*, 3297–3305.

[286] D. Yepes, F. Neese, B. List, G. Bistoni, *J. Am. Chem. Soc.* **2020**, *142*, 3613–3625.

[287] K. Eichkorn, O. Treutler, H. Öhm, M. Häser, R. Ahlrichs, *Chem. Phys. Lett.* **1995**, *242*, 652–660.

[288] F. Neese, *J. Comput. Chem.* **2003**, *24*, 1740–1747.

[289] F. Weigend, *Phys. Chem. Chem. Phys.* **2006**, *8*, 1057–1065.

[290] V. Barone, M. Cossi, *J. Phys. Chem. A* **1998**, *102*, 1995–2001.

[291] "GitHub - duartegroup/otherm: thermochemical contributions from ORCA calculations," can be found under https://github.com/duartegroup/otherm, **2020**.

[292] A. D. Becke, *J. Chem. Phys.* **1993**, *98*, 5648–5652.

[293] C. Lee, W. Yang, R. G. Parr, *Phys. Rev. B* **1988**, *37*, 785–789.

[294] Y. Zhao, D. G. Truhlar, *Theor. Chem. Acc.* **2008**, *120*, 215–241.

[295] S. Grimme, F. Neese, *J. Chem. Phys.* **2007**, *127*, 154116.

[296] N. Mardirossian, M. Head-Gordon, *J. Chem. Phys.* **2016**, *144*, 214110.

[297] C. Riplinger, P. Pinski, U. Becker, E. F. Valeev, F. Neese, *J. Chem. Phys.* **2016**, *144*, 24109.

[298] F. M. Bickelhaupt, K. N. Houk, *Angew. Chem. Int. Ed.* **2017**, *56*, 10070–10086.

[299] S. H. Smallcombe, S. L. Patt, P. A. Keifer, *J. Magn. Reson. Ser. A* **1995**, *117*, 295–303.

[300] T. Rigotti, T. Bach, *Org. Lett.* **2022**, *24*, 8821–8825.

[301] S. Kolb, D. B. Werz, *Chem. - A Eur. J.* **2023**, *29*, DOI 10.1002/chem.202300849.

[302] T. He, Z. W. Qu, H. F. T. Klare, S. Grimme, M. Oestreich, *Angew. Chem. Int. Ed.* **2022**, *61*, DOI 10.1002/anie.202203347.

[303] S. G. Pyne, *J. Org. Chem.* **1986**, *51*, 81–87.

[304] H. L. Goering, C. C. Tseng, *J. Org. Chem.* **1985**, *50*, 1597–1599.

[305] P. Lu, X. Ren, H. Xu, D. Lu, Y. Sun, Z. Lu, *J. Am. Chem. Soc.* **2021**, *143*, 12433–12438.

[306] M. R. Friedfeld, M. Shevlin, G. W. Margulieux, L. C. Campeau, P. J. Chirik, *J. Am. Chem. Soc.* **2016**, *138*, 3314–3324.

[307] M. Magrez, Y. Le Guen, O. Baslé, C. Crévisy, M. Mauduit, *Chem. - A Eur. J.* **2013**, *19*, 1199–1203.

[308] X. Tang, L. Qian, G. Liu, Z. Huang, *Org. Lett.* **2023**, *25*, 4950–4954.

[309] S. M. Rafiq, R. Sivasakthikumaran, A. K. Mohanakrishnan, *Org. Lett.* **2014**, *16*, 2720–2723.

[310] S. Maeda, Y. Harabuchi, M. Takagi, T. Taketsugu, K. Morokuma, *Chem. Rec.* **2016**, *16*, 2232–2248.

[311] S. Maeda, K. Ohno, K. Morokuma, *Phys. Chem. Chem. Phys.* **2013**, *15*, 3683–3701.

[312] F. Neese, *Wiley Interdiscip. Rev. Comput. Mol. Sci.* **2022**, *12*, e1606.

[313] M. J. Frisch, G. W. Trucks, H. B. Schlegel, G. E. Scuseria, M. A. Robb, J. R. Cheeseman, G. Scalmani, V. Barone, G. A. Petersson, X. Nakatsuji, H.; Li, M. Caricato, A. V Marenich, J. Bloino, B. G. Janesko, R. Gomperts, B. Mennucci, H. P. Hratchian, J. V Ortiz, A. F. Izmaylov, J. L. Sonnenberg, D. Williams-Young, F. Ding, F. Lipparini, F. Egidi, J. Goings, B. Peng, A. Petrone, T. Henderson, D. Ranasinghe, V. G. Zakrzewski, J. Gao, N. Rega, G. Zheng, W. Liang, M. Hada, M. Ehara, K. Toyota, R. Fukuda, J. Hasegawa, M. Ishida, T. Nakajima, Y. Honda, O. Kitao, H. Nakai, T. Vreven, K. Throssell, J. Montgomery, J. A., J. E. Peralta, F. Ogliaro, M. J. Bearpark, J. J. Heyd, E. N. Brothers, K. N. Kudin, V. N. Staroverov, T. A. Keith, R. Kobayashi, J. Normand, K.

Raghavachari, A. P. Rendell, J. C. Burant, S. S. Iyengar, J. Tomasi, M. Cossi, J. M. Millam, M. Klene, C. Adamo, R. Cammi, J. W. Ochterski, R. L. Martin, K. Morokuma, O. Farkas, J. B. Foresman, D. J. Fox, **2016**.

[314] E. C. Meng, T. D. Goddard, E. F. Pettersen, G. S. Couch, Z. J. Pearson, J. H. Morris, T. E. Ferrin, *Protein Sci.* **2023**, *32*, e4792.

[315] "Blender Online Community, 'Blender - a 3D modelling and rendering package' (Stichting Blender Foundation, 2018)," can be found under https://www.blender.org, **n.d.**

[316] Q. Peng, F. Duarte, R. S. Paton, *Chem. Soc. Rev.* **2016**, *45*, 6093–6107.

[317] N. F. Hall, J. B. Conant, *J. Am. Chem. Soc* **1927**, *49*, 3047–3061.

[318] G. A. Olah, *Angew. Chem. Int. Ed.* **1995**, *34*, 1393–1405.

APPENDIX

Cartesian coordinates of optimized structures in Chapter 2
TS-1
54 conformers were generated by CREST, all of which were used for constrained DFT optimizations followed by transition state and frequency calculations.
Electronic energy (a. u.) | DLPNO-CCSD(T)/cc-pVTZ: –4111.23553028788
Thermochemical Corrections (a. u.) | PBE-D3(BJ)/def2-SVP: 1.377326615848
Imaginary Frequencies: one (–587.05 cm^{-1})
Gibbs Free Energy (a. u.): –4116.415342903240

182

```
  C    3.66916939159229    -2.16779132812554     0.46704356259096
  C    5.51422098630449    -1.21005863490217    -1.03211868577402
  C    6.13635157519248    -0.04700797259461    -1.61606009461278
  C    5.51591875492624     1.22651969520515    -1.46950747607233
  C    4.28569774464126     1.37653566500592    -0.84296290083396
  C    3.67391201708912     0.20806989394791    -0.28497381135580
  H    6.02789248153986     2.11341677147031    -1.87200616162969
  C    4.40245995709047    -2.88115955657019     1.48368279575297
  C    2.33312756539934    -2.51805923345353     0.23403386371157
  C    3.78499634013339    -4.01379949032619     2.12944103647421
  C    2.45022331334453    -4.36939284209497     1.78737883768940
  C    1.70153413853831    -3.62675403648145     0.88363962882473
  H    1.99131245093996    -5.24290839856985     2.27561071336398
  O    2.45734895029572     0.35563507587984     0.35001256331843
  O    1.60260255944772    -1.82510643947587    -0.70512878850483
  P    1.09349736235602    -0.25194383720057    -0.41981942394066
  O   -0.03112089343170    -0.17315443415070     0.59157501177372
  O    0.95951578079090     0.35945982521705    -1.81530977838032
  N   -1.73693561008059     2.39763767506177     2.57772883353844
  C   -2.37570308051657     1.48425800132703     1.81555214927576
  C   -0.28982705157165     2.31043100862385     2.79700388726562
  C   -0.03193732864340     2.01314084951569     4.27737399779960
  H    0.17680773894732     3.28348977498643     2.52758936683118
  H    0.12883411020209     1.52008644023830     2.14175010816290
  O   -0.64672400963202     2.98349236007490     5.11527353760768
  H    1.05273369952982     2.03972564708348     4.49392192404463
  H   -0.41576797278255     0.99070997187260     4.51531936106720
  C   -2.04648984085980     3.02310911780157     4.91530233043615
  C   -2.39201740233740     3.35760138865356     3.45761741399446
  H   -3.48506860057064     3.34293723368426     3.29578694897906
  H   -2.02190157004319     4.37384855523291     3.20356673966694
  C   -3.74740566327703     1.30553107745461     1.67884953710384
  H   -1.67465541538254     0.82719229278678     1.27012714459380
  C   -4.32631817437380     0.33455348620613     0.77694536752064
  C   -3.47705661622335    -0.83199898324525     0.31366258785535
  H   -3.89955884011335    -1.29833410248180    -0.59588864152838
  H   -3.43629548410133    -1.61599981704013     1.09425050986369
  H   -2.42729623088201    -0.55723899949941     0.10084274622395
  C   -5.80028748277270     0.06985139881692     0.92091606870706
  C   -6.71290896621549     1.14652522228262     0.99370054478498
```

```
C    -6.31567064127169    -1.24410233666306     0.93659712072522
H    -4.44677980430233     1.94904759833716     2.23254707317600
C    -7.69565772640002    -1.47365472433783     1.04397072717693
C    -8.09095657402840     0.91776982147364     1.09372720224915
C    -8.59036107992030    -0.39558505073217     1.12297054517368
H    -5.63225911779755    -2.10271386630522     0.87300827479650
H    -8.07332959217966    -2.50747676391754     1.06471965338164
H    -9.67304068594082    -0.57653852888479     1.20198192842148
H    -6.33045949000923     2.17653956682858     0.92819675441020
H    -8.78408918804877     1.77187138928458     1.13898682366252
H    -2.51245640889745     2.04111009487886     5.18131914501599
H    -2.45153922506060     3.79873585388862     5.59627546834835
N    -1.49581181408165     1.27142529354855    -2.17364440996369
C    -2.44498640810865     0.51315092476582    -2.81963843249766
C    -3.78576430972647     0.73807030209701    -2.51813957975505
C    -4.12937633393170     1.72326736856341    -1.49433700335351
C    -3.08494088627107     2.63226188852330    -1.04278802745192
H    -4.36890911278864     1.01880607973443    -0.39353486077374
H    -5.14953914041179     2.13533600151422    -1.54144687005327
C    -1.75332179879941     2.31885453457289    -1.33848786176926
H    -0.47483081974002     0.92636075113551    -2.17797344408564
C    -1.93260360553234    -0.54662529662517    -3.77119676761976
C    -0.56274397464319     3.07150438044071    -0.84273581431311
H     0.37465193684911     2.55626715341577    -1.10864003561990
H    -0.62127907512102     3.22326468822521     0.24793652055569
H    -0.55032652317815     4.08869887126249    -1.28083809213398
C    -3.41953140704677     3.79567206185447    -0.20187845275876
O    -2.63868366688041     4.58888997332807     0.31166950000392
O    -4.77763438926652     3.92619179592516    -0.04946327836706
C    -5.19080643963190     5.04415381771702     0.73717502354229
C    -4.88123534438619    -0.11444531914712    -3.05068304845986
O    -6.03068889146736     0.12822158516512    -2.35707978781148
C    -7.14336059157068    -0.70961795239300    -2.67856890888599
O    -4.82316532319750    -0.96145338077656    -3.93154383003256
H    -4.77227491523196     5.98939958660282     0.33754672384420
H    -4.85071148596561     4.93899978985889     1.78871334638116
H    -7.95209926553403    -0.41343541663017    -1.98728209429842
H    -6.88337059570558    -1.77709983021209    -2.52802314692768
C     7.35968187855267    -0.19779902619055    -2.33320686715776
C     6.12826680096771    -2.48096277456097    -1.23961008651041
C     7.31084947818726    -2.59589768708327    -1.95626185791574
C     7.94139707547342    -1.44527863378440    -2.49888757241773
H     5.64382383877287    -3.37835735861655    -0.83074959079475
H     7.76036175301172    -3.58873446306757    -2.10955678952357
H     8.88251389733876    -1.54780108417538    -3.06003878047444
H     7.82781541154834     0.70052636731037    -2.76540284733598
C     4.28812469265563    -1.04901551795350    -0.29263663833919
C     4.51359414508461    -4.73677472126725     3.11966299467987
C     5.70793744993506    -2.49331547374261     1.91131032019441
C     6.38425717809053    -3.20817549432186     2.88954976259163
C     5.79139615946979    -4.34916505990969     3.49150163284710
H     4.03085453551000    -5.60496472589750     3.59531154249884
H     6.34021444623713    -4.91270054006730     4.26112447028842
H     6.17524333268969    -1.60662145523950     1.46183574194908
H     7.38745075710391    -2.88313857571200     3.20469287887240
```

```
C    3.62510118578457      2.70650084676279     -0.66328299923226
C    3.60571204051371      3.29083874620192      0.63273452368379
C    2.92605240139668      4.50532932131746      0.82412012465090
C    2.28751210419530      5.17709271809837     -0.23284823920445
C    2.36243492167106      4.60380847628320     -1.51254103180329
C    3.00420975747201      3.37353743367068     -1.75332764854662
H    1.87612293403975      5.12715122644201     -2.35115171051162
H    2.90702796927510      4.94779557958532      1.83345357915403
C    4.34418760134618      2.65896471080787      1.80985347088685
C    3.39185792946389      2.24974697618864      2.94347537419015
H    2.86728922215794      3.13267074937384      3.36588714881979
H    3.95245807279786      1.76885899155710      3.77160654694162
H    2.63653826162866      1.52987130345391      2.57372981030649
C    5.46306199834172      3.58470835576737      2.31857159853581
H    4.83225801106590      1.73426507095629      1.44279956473160
H    6.16411296623420      3.85395478649977      1.50319272775008
H    6.04423949860271      3.08997250113453      3.12394678321564
H    5.05305279036648      4.52901988005374      2.73381063725958
C    3.04196656119741      2.79513803821200     -3.16577790642933
C    1.71519977758755      2.93772251598820     -3.92566778656343
H    1.77095963471436      2.39827536660724     -4.89292123787343
H    1.47605259248563      3.99668276505293     -4.15679920553425
H    0.87590363741373      2.50569616675567     -3.35212028007592
C    4.18753914326781      3.42531184005497     -3.97998181585578
H    3.24154753300730      1.70924021404366     -3.06314749323812
H    5.16986343473902      3.28729129924533     -3.48820299531191
H    4.02724009157165      4.51730643965711     -4.10108585751951
H    4.24600770048836      2.97512982304421     -4.99258219993832
C    1.56441010919590      6.49763466030960     -0.00218250632206
C    0.27472866278745     -3.95320508765501      0.58117162703385
C   -0.73781091272151     -3.64924867846960      1.52826191214087
C   -0.06096918449358     -4.57166192426121     -0.65308951347919
C   -2.07089376504993     -3.96986779092204      1.21133295276475
C   -1.41241443756842     -4.83907861129331     -0.93541445299652
C   -2.43635971380246     -4.54662088911591     -0.01582035387525
H   -2.86053116348428     -3.76588848608105      1.95346982862956
H   -1.66918095348398     -5.31430887371825     -1.89607410968474
C   -0.41059336686588     -3.03978468373110      2.88920668836908
C   -1.27424797750469     -1.81512785929783      3.22215620701525
H   -0.95859901776090     -1.37876710093288      4.19291458185543
H   -2.35023374991823     -2.07097976029287      3.31829356116568
H   -1.15613420365884     -1.04873055061946      2.43480782069984
C   -0.50183135110081     -4.10554054817308      3.99572116760106
H    0.63917478622929     -2.68643019773191      2.84540136976747
H   -0.22048675295245     -3.67793988683618      4.98041998963352
H    0.16712994975785     -4.96554017959802      3.79219605758721
H   -1.53562588060472     -4.50142463976674      4.08056378699999
C    1.02588449872249     -5.02697594579733     -1.62464439834314
C    1.02054522369601     -6.56008708214440     -1.75890040923433
H    0.07965321899141     -6.92204478490676     -2.22374870284145
H    1.11506517622056     -7.05066281228383     -0.76919848169022
H    1.86203787137928     -6.90213126575078     -2.39616264299583
C    0.94609344002088     -4.33990138159262     -2.99533640365481
H    2.00113334892301     -4.74490420081734     -1.17904978870756
H   -0.00294871643490     -4.57990249389468     -3.51903704616542
```

```
H    1.77773375857647      -4.68032557457710      -3.64616308787494
H    1.01923527509543      -3.24108936488223      -2.88978644358573
C   -3.89019029305108      -4.91158247416602      -0.29365255115089
C    2.55823300605877       7.61465845760809       0.36249738333144
H    3.34801148761903       7.71947603240908      -0.40808716325993
H    3.06113431626270       7.40046483572698       1.32874711710070
H    2.04022740459838       8.59087312069837       0.46348195469813
C    0.44908558173609       6.37949524439905       1.05166880482032
H    1.08720901711265       6.77611116915922      -0.96777553215087
H    0.86069609941629       6.07098714469286       2.03579770851095
H   -0.32764824101802       5.64716925160549       0.75667506152177
H   -0.05304946082675       7.35800819221118       1.19930242873894
C   -4.42518545062386      -4.32549461432008      -1.60928325429390
H   -5.48709794184792      -4.60815406376185      -1.76304412499256
H   -3.85436342806850      -4.69689605246963      -2.48467591113751
H   -4.36448412391800      -3.21951425004347      -1.62314494698091
C   -4.08369249003600      -6.43828781053797      -0.24889944801101
H   -4.49070067225979      -4.47658778129348       0.53717578896714
H   -3.50587535087821      -6.93302535105859      -1.05705300256111
H   -5.15130517587886      -6.71147459642421      -0.38086272054651
H   -3.73402977308328      -6.85778164415601       0.71538389019989
H   -7.45129757334798      -0.57155150396347      -3.73463228116287
H   -6.29477114606098       5.05940513534504       0.69464892676575
C   -0.69327105877810      -0.11367815635937      -4.56911451185941
H   -0.47586677621097      -0.88217600452691      -5.33716624909936
H    0.20515007371111      -0.02181058408353      -3.92781673791395
H   -0.85776073025563       0.84959834544973      -5.09319416740199
C   -1.68981093150785      -1.85870107985935      -2.99917844305751
H   -2.76460061275491      -0.73979453542195      -4.47230440366316
H   -2.60701601322616      -2.20018882893789      -2.48661215514117
H   -0.88576179387039      -1.75707983100763      -2.24485399457714
H   -1.38788869892172      -2.65462758915138      -3.70644258326858
```

TS-2

385 conformers were generated by CREST, all of which were used for constrained optimizations at the GFN2-xTB level of theory. Subsequently, the number of conformers was reduced to 191 by RMSD calculation and cutoff following RMSD $\geq$ 0.20 Å^2. After constrained DFT optimizations, the number of conformers was again reduced from 191 to 143 by RMSD $\geq$ 0.25 Å^2. All 143 conformers were subjected to transition state optimizations and frequency calculations.

Electronic energy (a. u.) | DLPNO-CCSD(T)/cc-pVTZ: –4111.23227588186

Thermochemical Corrections (a. u.) | PBE-D3(BJ)/def2-SVP: 1.378167177460

Imaginary Frequencies: one (–664.24 cm^{-1})

Gibbs Free Energy (a. u.):   –4109.854108704400

182

```
C    3.12757822667729      -2.07516375554245       0.94051806765247
C    5.21838461541356      -1.28807449910797      -0.26623472480098
C    5.93605597141385      -0.23659188552705      -0.94030375504962
C    5.27100862402927       0.98939222884652      -1.20850418628551
C    3.93314256120608       1.19951011368444      -0.89007188517950
C    3.23576426127698       0.15701042053297      -0.19842645912107
```

H	5.82726619120903	1.79357788988848	-1.71411799499328
C	3.65497922160241	-2.62275467540376	2.16335366610159
C	1.90914544533508	-2.56501928040315	0.45505917537864
C	3.01284914440342	-3.77489266998886	2.74570504276077
C	1.83963499522027	-4.29919115361030	2.13524457650179
C	1.24057281455894	-3.69018065228212	1.03635490332787
H	1.36626728052412	-5.19027150124514	2.57638211715566
O	1.92447364059415	0.37017244074491	0.17772687606433
O	1.36491802949214	-1.99310988052965	-0.67286861739785
P	0.66336813554519	-0.47819227645945	-0.57609781287953
O	-0.50176080570269	-0.44834877254492	0.39526763955598
O	0.49506742135663	-0.00851927207667	-2.01651475903366
N	-0.87321708268768	2.19869838469389	3.41018398381380
C	-2.18026753418980	2.10719552402814	3.08326554151266
C	-0.39761134765470	3.15005936219615	4.40827138640279
C	0.56076070101289	2.44898709252533	5.37944753469737
H	-1.26379602195565	3.57368361739773	4.95491011617920
H	0.13494321819847	3.98207050929323	3.89607131191730
O	1.62587858134404	1.82111041050906	4.69373831648808
H	-0.01370999687774	1.69992745818465	5.98091682338602
H	1.00747519955382	3.18828247261969	6.07435631477560
C	1.13449444895459	0.84221946037841	3.78071211936886
C	0.19923300676400	1.45942974476015	2.74482096391053
H	0.77254075833483	2.17314381128497	2.11793993657166
H	-0.19963688880511	0.68116265237906	2.06676445603848
C	-2.75718810558176	1.26130887484463	2.15166854760188
H	-2.81780225268201	2.79216974398807	3.66580214639534
C	-4.17277545763603	1.24971955590346	1.83649087269765
C	-5.11891084131353	2.09227914378591	2.67803409411630
H	-5.35990002730583	1.58680587421043	3.63663220238507
H	-6.06737531625105	2.27879354195496	2.14040182163899
H	-4.68441609625184	3.08277130259300	2.90178845659957
C	-4.74107120137576	0.00341133001619	1.22812082857926
C	-3.94171741433026	-0.84017606730238	0.41866278793229
C	-6.11173356573364	-0.32238152327090	1.36806909152502
H	-2.09927382042559	0.57958912387533	1.59428295030263
C	-6.66462092064178	-1.43454900793812	0.72078070985245
C	-4.49996944958397	-1.94897406082291	-0.23164991115788
C	-5.86241129122640	-2.24735042731652	-0.09643994296270
H	-6.76371759966654	0.30159349843434	1.99391562729453
H	-7.73204262415864	-1.66759319866385	0.85624681856935
H	-6.29579500270737	-3.11149537332059	-0.62221564649298
H	-2.86449372265264	-0.65032543299818	0.29549322373685
H	-3.85056683780376	-2.58755792378385	-0.84452776729710
H	2.01070080440007	0.39468129702967	3.27287509609882
H	0.59986473765585	0.03308380964376	4.33709269675481
N	-1.86359971002173	1.37174881659414	-1.78577725318857
C	-3.13046696749110	0.93890325316921	-2.08154869086378
C	-4.20817981620465	1.61447560734891	-1.49745505199857
C	-3.95688467681062	2.61646102989669	-0.46810730677561
C	-2.58644966542899	3.08099561720987	-0.29128833604838
H	-4.18320458754373	1.96959705368088	0.67789327549892
H	-4.75167275750627	3.36159798139978	-0.30813694815335
C	-1.55583026868411	2.42713607376595	-0.96748926788965
H	-1.02106866346568	0.79548241596996	-2.08643552449577

```
C    -3.25726507994485     -0.19798231859627     -3.07551351819880
C    -0.12051891233276      2.81467063120469     -0.89972228473066
H     0.32887621667729      2.46742344981173      0.04953055981078
H    -0.01203855897932      3.91045084566905     -0.89886552886486
H     0.45844909238774      2.36569347321062     -1.72148954117028
C    -2.29680825050733      4.17778609181850      0.65468830036842
O    -1.19988294598503      4.60120537116032      1.00125349938834
O    -3.45888641019982      4.71115610015849      1.15302167516305
C    -3.27955342673256      5.77409406644083      2.08854436139107
C    -5.61822475352835      1.26600833456462     -1.79941282923088
O    -6.46980098720929      1.93805601973914     -0.96642069455629
C    -7.85454891967743      1.63782592133589     -1.15243989188122
O    -6.03119988038529      0.50219736716552     -2.66079551947964
H    -2.70727806329194      6.61032094768486      1.63856077904218
H    -2.72264902370133      5.42708584086304      2.98419102214722
H    -8.40755790400879      2.30431434157486     -0.46645604489079
H    -8.05460086229856      0.57576273681302     -0.90401172961523
C     7.28444399211661     -0.45556194436081     -1.35059257299094
C     5.87658101222062     -2.54321866409913     -0.09205674314212
C     7.18347142736365     -2.73199305335118     -0.51742413517046
C     7.90319398053894     -1.67716000428835     -1.13883652565938
H     5.33070586359452     -3.37321021090408      0.37564646318321
H     7.66371636933197     -3.71234298085477     -0.37740736203694
H     8.94191637486561     -1.83770877902066     -1.46498162013812
H     7.81844820142129      0.36502089662233     -1.85492827954275
C     3.86447732516810     -1.04320305416306      0.16626418828287
C     3.55190893850484     -4.34371244007123      3.93779661330740
C     4.77905221901987     -2.05981576939826      2.83827520016578
C     5.26635092993996     -2.62453963801799      4.00828806418025
C     4.65897526677404     -3.78490520039576      4.55758477942589
H     3.05783782974493     -5.23006387141441      4.36602576204060
H     5.05954047358324     -4.22938250896324      5.48123288892145
H     5.25401024667453     -1.16027607266810      2.42206715627370
H     6.12854572119954     -2.16680542701738      4.51654855507869
C     3.30083583086468      2.49674280534167     -1.28925242670272
C     3.10235864283727      3.52817652600429     -0.32932953238667
C     2.63281022418444      4.77829939049579     -0.76407415600690
C     2.33982022054443      5.03851973299147     -2.11503385553090
C     2.51965314604781      3.99844726320133     -3.03794452471574
C     2.99123779405566      2.72700949566579     -2.65608499478336
H     2.27525293315509      4.18357066988747     -4.09657705057784
H     2.47162767751052      5.57262241144749     -0.02145610830136
C     3.41233615484166      3.29265148774402      1.14709370892687
C     2.60175888979844      4.18883839921876      2.09658342475936
H     2.66828156555156      3.79453306340743      3.13014778626470
H     1.53114463498272      4.23454449128381      1.80963868396341
H     2.98685095715374      5.22984574871618      2.10519890560291
C     4.91806177063466      3.43793922713442      1.43639267112548
H     3.13058019372247      2.24078111462140      1.36548442295468
H     5.25652624115849      4.47014473694597      1.20840329770432
H     5.52237332053507      2.73794501372443      0.82786270077888
H     5.13192089667658      3.23457427903251      2.50601639773086
C     3.16346614962773      1.64283844448966     -3.71800451731944
C     1.90914107450675      1.46337940859696     -4.58836390392221
H     1.03895333199995      1.19800516266447     -3.95939841547609
```

```
H    2.06451578178989      0.63714894717345     -5.31215647504604
H    1.67430098804573      2.37528505881887     -5.17591221405519
C    4.40320376320090      1.91896899530502     -4.58722507340200
H    3.32346141277879      0.68322883502966     -3.18683709073880
H    5.32544170574381      1.98519679668182     -3.97683104157280
H    4.29635183321207      2.87777586616702     -5.13674589248520
H    4.54714461902094      1.11299334096081     -5.33610221797110
C    1.76893721491826      6.38055048703770     -2.55306061926159
C   -0.07733128520545     -4.15468811596315      0.51219805238064
C   -1.22424221823158     -4.10128336392517      1.35593605870413
C   -0.19938308830419     -4.64701135514634     -0.81675995039777
C   -2.46011303326959     -4.53700091987465      0.84482209836164
C   -1.46058207651432     -5.06471310839798     -1.27696112336064
C   -2.60587279139904     -5.02079450734892     -0.46547670560725
H   -3.35374936728074     -4.48081583667587      1.48771176542452
H   -1.54192099165012     -5.45105341851675     -2.30477227776989
C   -1.17883748747525     -3.55852090755604      2.78355532207678
C   -1.99129141828703     -2.26191634379162      2.91565926209239
H   -1.62146164299941     -1.51695616764286      2.18713434466251
H   -1.89169572271495     -1.83779144625014      3.93727342721390
H   -3.07206708386597     -2.42261584695850      2.72260596231950
C   -1.61005381602169     -4.61699237206770      3.81092306657532
H   -0.12867439192061     -3.29185072429486      3.00831768667712
H   -0.98983106766815     -5.53377297491421      3.73670071351956
H   -2.66796751551777     -4.91979483245483      3.66635396449962
H   -1.51587407006053     -4.22109987243345      4.84334019560263
C    1.00344757935713     -4.81204874024169     -1.74157206439594
C    1.29900587372134     -6.30386314786518     -1.98148482511318
H    2.20905213446656     -6.42785043239541     -2.60421399659873
H    0.45982919749155     -6.80270416467938     -2.50986134755090
H    1.45938261550873     -6.84162196678544     -1.02521225685689
C    0.83300818203335     -4.04864887416841     -3.06490978938244
H    1.88878620643438     -4.38757240571218     -1.22905502253898
H    1.74020244345868     -4.15928399981247     -3.69389881253861
H    0.67511680301070     -2.96932443148224     -2.87929893841775
H   -0.02558830988741     -4.43604355229670     -3.65252233649684
C   -3.95599670010215     -5.53269705184148     -0.95097403319545
C    2.57802127999068      7.57299250986868     -2.02132067060553
H    2.18721066879635      8.52732424629723     -2.43011935877273
H    3.64829054801936      7.49065888163287     -2.29715167614745
H    2.51977086010490      7.64179593726751     -0.91525631029843
C    0.28412897546929      6.49461546640168     -2.15795621621380
H    1.82261832913290      6.40496923763374     -3.66382009637474
H   -0.14475517290247      7.46207385882030     -2.49276454737106
H    0.15795098990800      6.42700927906185     -1.05695461017584
H   -0.31440525190066      5.67919902857980     -2.61138457668662
C   -4.28751339380669     -5.11193913840151     -2.39043217044490
H   -4.20752943162210     -4.01460570659617     -2.52783318353901
H   -5.31888443901986     -5.41717758191560     -2.66125196887858
H   -3.60434120881729     -5.58921910926923     -3.12273109913759
C   -4.03959994374263     -7.06182019607549     -0.78966394297521
H   -4.72319971911573     -5.08469273602130     -0.28127121881928
H   -3.84774158907160     -7.36470291838119      0.25890248845557
H   -3.28151764541058     -7.56353009211935     -1.42659759907573
H   -5.03976904066331     -7.44264938789444     -1.08422159094610
```

```
H    -8.16229346980222        1.81500358876556       -2.20232517774149
H    -4.29344352642524        6.10827571513804        2.37311231692440
C    -3.30348515799250        0.38092301934813       -4.50525414579816
H    -2.36185954607710        0.91433617551887       -4.75096193048540
H    -4.15430299865191        1.07901188099828       -4.62419840175399
H    -3.42946579682154       -0.44164952306180       -5.23749586272004
C    -2.18294418549525       -1.28807948984257       -2.94642306054098
H    -4.24730021395921       -0.64941251658853       -2.88235722071288
H    -2.05415697534800       -1.63639423257855       -1.90324845379459
H    -1.18648371598559       -0.96156319236475       -3.29962849423169
H    -2.48760614435924       -2.16203278929516       -3.55596757103010
```

TS-2b

250 conformers were generated by CREST, all of which were used for constrained optimizations at the GFN2-xTB level of theory. Subsequently, the number of conformers was reduced to 156 by RMSD calculation and cutoff following RMSD ≥ 0.15 Å². After constrained DFT optimizations, the number of conformers was again reduced from 156 to 137 by RMSD ≥ 0.20 Å². All 137 conformers were subjected to transition state optimizations and frequency calculations.

Electronic energy (a. u.) | DLPNO-CCSD(T)/cc-pVTZ: –4111.22933365562
Thermochemical Corrections (a. u.) | PBE-D3(BJ)/def2-SVP: 1.378416051103
Imaginary Frequencies: one (–656.95 cm^{-1})
Gibbs Free Energy (a. u.)   –4109.850917604520


```
182

  C    4.22811595333883       -1.01973738451625       -0.13363963435567
  C    5.39564187097862        0.74130064823584       -1.57722090892940
  C    5.50488192774828        2.12265455709381       -1.97804140203002
  C    4.52436059459083        3.05564769164473       -1.53883547597793
  C    3.42086484167038        2.66568313261964       -0.78913962506269
  C    3.32215609132698        1.28958504732061       -0.40741671708584
  H    4.63479647292184        4.11454863910241       -1.81960310934390
  C    5.31221674739612       -1.57766382956899        0.63620773259306
  C    3.06688497463681       -1.78330861030687       -0.30898731163690
  C    5.22701382710843       -2.94935402675384        1.07313524404965
  C    4.05420813959355       -3.70099205425780        0.78244096550530
  C    2.95901278189711       -3.13691678301560        0.14006365121557
  H    4.00941891572798       -4.75703731269430        1.08958823605869
  O    2.24395514156635        0.91111896100088        0.36123855827225
  O    2.00679910175686       -1.24949486563108       -1.00782749532190
  P    1.04966604195744       -0.07236293522079       -0.29267845023426
  O    0.24505947672097       -0.60066844107244        0.87353870115297
  O    0.36702659603182        0.63104300669194       -1.46804303578910
  N   -2.47084568299990        1.62892740556015        2.77398959306635
  C   -3.27901402294271        0.78314357338724        2.10703301760728
  C   -1.02244701515726        1.41333076539140        2.84712441245047
  C   -0.64897171428143        1.07499224986362        4.29046237351706
  H   -0.50846950591253        2.35187717498425        2.54707186360067
  H   -0.70434592484333        0.61327864790694        2.14397476011621
  O   -1.07395687278439        2.09522913030968        5.18673062996081
  H    0.44936990048315        0.98956783032818        4.39015638709341
  H   -1.10624438571253        0.09284731551695        4.56968960292660
```

```
C   -2.47274378376923      2.28726202737749      5.12207592115068
C   -2.92751148275112      2.65969762332809      3.70231764013149
H   -4.02435641553691      2.77816655848990      3.65149105367838
H   -2.46625113022504      3.62404835347202      3.40256925951790
C   -4.67341656066436      0.78901403436946      2.08371762051708
H   -2.72847119291767      0.02589356011496      1.52383119790481
C   -5.49090305867577     -0.12376850851491      1.33097693566579
C   -6.99619236701005      0.08304176863046      1.45909871365656
H   -7.24864247398410      1.16019898854947      1.43734382276518
H   -7.35555045990354     -0.35106602207166      2.41619551011883
H   -7.54668052196462     -0.41539870244418      0.63925621890690
C   -5.07523850393751     -1.55090687429771      1.11326958992104
C   -4.18497243619797     -2.21788909890670      1.98612481475429
C   -5.65362669910959     -2.29544441017462      0.05718907648479
H   -5.20417007380876      1.61107578715646      2.58730524838345
C   -5.34073608616123     -3.64782751419101     -0.12880225283613
C   -3.88197967513574     -3.57426535939052      1.80447743654832
C   -4.45385414311476     -4.29475568670406      0.74571954713236
H   -6.36077346026210     -1.80484045480074     -0.62650261949701
H   -5.79623340767575     -4.20217880117678     -0.96372785073461
H   -4.21202746907217     -5.35832895894162      0.60594245317572
H   -3.75544118760412     -1.67853486582240      2.84201050104387
H   -3.19610581473443     -4.07216168465748      2.50448458809810
H   -3.01514614518771      1.36193174414951      5.44253359663040
H   -2.72468399627167      3.10253395652800      5.82983267338551
N   -2.29649953565864      0.72169799837735     -1.44996254419240
C   -3.10055368126178     -0.20218817681069     -2.07993414107420
C   -4.48135995165064     -0.00817543552810     -2.03612477860200
C   -5.02951373404545      0.98665825602090     -1.10746978165635
C   -4.11303249625463      2.02134752656741     -0.63111556791302
H   -5.32808143087631      0.36689126850834     -0.00898661083357
H   -6.05532860906449      1.31795433490587     -1.34115506879014
C   -2.73712108484946      1.84463953010277     -0.80928343033140
H   -1.22577016594378      0.59768348148150     -1.48098245076867
C   -2.38301353874374     -1.39661784623734     -2.67189913794626
C   -1.68780516710266      2.81027856014945     -0.36445876636691
H   -1.82559821649718      3.07664215933542      0.69682372493463
H   -1.79296437713011      3.76435335355020     -0.91565891967149
H   -0.67554599055932      2.40909745786386     -0.53956547929500
C   -4.64124905497498      3.18335458561389      0.10660614963661
O   -4.00021882348358      4.08463679786282      0.63520827379785
O   -6.00945164139042      3.15389104681286      0.15791198802985
C   -6.61108239738700      4.23924422612952      0.86512671963099
C   -5.51099632441983     -0.72856169302419     -2.82074220623452
O   -5.04890700375916     -1.39221179107825     -3.90821705397757
C   -6.04339478470557     -2.09675378184997     -4.66358742963109
O   -6.70774855420112     -0.68611452470132     -2.54676461064323
H   -7.70281146537757      4.09201677770992      0.78309828171026
H   -6.31585999523708      5.21327072874943      0.42584949690771
H   -5.50598722496678     -2.57558511774026     -5.50115655184539
H   -6.81484705621778     -1.39810704903743     -5.04436544253627
C    6.58721031164461      2.52247308901769     -2.81644373712574
C    6.35423633410094     -0.18563286531265     -2.08520410131890
C    7.38662464189409      0.23239411731669     -2.91263066367226
C    7.51548019655479      1.59979634277384     -3.27303647742115
```

```
H    6.25915082475957      -1.24756955525805      -1.82015399425880
H    8.10818802034393      -0.50445208282271      -3.29696829270444
H    8.34244210487956       1.92098056140295      -3.92426588988894
H    6.66214160874421       3.58271461279017      -3.10498298749285
C    4.31245156588112       0.34747923084626      -0.71186161683324
C    6.30899063117582      -3.51776994733230       1.80817531334782
C    6.46191258086743      -0.82151921365132       1.01543286696743
C    7.49003734896348      -1.39847113904508       1.74706714998475
C    7.42390266781760      -2.76236913302538       2.13630650658769
H    6.23186798279374      -4.57015801699608       2.12365432482137
H    8.24912452799217      -3.21118345353482       2.70964274859803
H    6.52229394069994       0.23688601748333       0.72788620957203
H    8.36213624821110      -0.79058149916463       2.03217646417317
C    2.38129774203351       3.64775403825660      -0.35861606755544
C    2.25003954418184       3.97300565448303       1.02100081877233
C    1.27206112742782       4.90273720395255       1.41261890821771
C    0.44389414229089       5.55442172563073       0.48098420515348
C    0.60697676187413       5.23133586218010      -0.87490059780635
C    1.54512741698658       4.27875614520704      -1.31876530149508
H   -0.03247835352595       5.73853898090102      -1.61662122370924
H    1.17941883896577       5.15253938069444       2.48200690110449
C    3.19356360695803       3.40440458193146       2.07909198226514
C    2.45322486258021       2.57499039822525       3.13884530424402
H    1.71194805324231       3.18472523641626       3.69789703916267
H    3.16791397118367       2.16194882440249       3.88052507506248
H    1.93057047079659       1.72644396991773       2.65810662616716
C    4.03510184192753       4.52298112851829       2.71837435866856
H    3.89954746725421       2.72119218695376       1.56687618206185
H    4.58804608995914       5.09954604339328       1.94972691997501
H    4.77409842866120       4.09980748088355       3.42972352514884
H    3.40015462020254       5.23850061249265       3.28141108164151
C    1.63203769239432       3.96493497299634      -2.81117234504305
C    0.30449598406238       3.42874717929920      -3.37231846608834
H    0.40249766688751       3.22015886111523      -4.45774353963616
H   -0.52353646378047       4.15808464680359      -3.24776070784505
H    0.03279548693660       2.48441813184419      -2.86476846385617
C    2.13186250666270       5.18366250820406      -3.60568545480040
H    2.37612854654783       3.15417149874217      -2.93703060691872
H    2.25248103973973       4.93024316121680      -4.67915130849192
H    3.10940576699697       5.54537584793923      -3.22656638950405
H    1.41786661648801       6.03117979820115      -3.53929834445997
C   -0.54827432269105       6.62304723931706       0.92048929187494
C    1.72404293826703      -3.94263969112995      -0.11562460267039
C    0.77205561161779      -4.13615982272185       0.92030787395807
C    1.53426903621086      -4.54894713379773      -1.38479332164131
C   -0.32594925203609      -4.98124357617708       0.67357755874535
C    0.41507462822774      -5.37597679465677      -1.58332371029406
C   -0.51981070160164      -5.61888791720009      -0.56274508189824
H   -1.06527572201454      -5.14920437114954       1.47199613016050
H    0.27389005439092      -5.84909519785894      -2.56836876492460
C    0.93786631523252      -3.45852539311221       2.27845859032674
C   -0.38888138871747      -2.95921394469175       2.86730161697883
H   -0.19222763797804      -2.32829845790254       3.75907534596373
H   -1.03597650826356      -3.79752404642756       3.20165549581509
H   -0.93706536486946      -2.34688995283105       2.12745125133517
```

```
C    1.66197616997057     -4.37589338794561      3.27994932199779
H    1.56512225102742     -2.56017463675113      2.10802256161411
H    2.66701870090125     -4.66655166521949      2.91912930207782
H    1.08267619348572     -5.30734977871081      3.45331606312703
H    1.78820170723699     -3.86661535139148      4.25799703369635
C    2.50146862862988     -4.30652283385877     -2.53893469542186
C    3.06637823555106     -5.61714259971544     -3.10920551222544
H    2.27050186504299     -6.24451548736111     -3.56218476234505
H    3.56073857177641     -6.22001968829147     -2.32092584679199
H    3.81320381562706     -5.40774584163404     -3.90238836968769
C    1.84345330260228     -3.44400479744030     -3.63053294162128
H    3.35874111962259     -3.72909267466380     -2.13729958440686
H    0.97644471864749     -3.96775265331407     -4.08667070100451
H    2.56574851467158     -3.21929387480228     -4.44241933350689
H    1.48665141302449     -2.48489766736756     -3.20841728918332
C   -1.70085210308517     -6.55309151174111     -0.78677329048331
C    0.19251255396031      7.88113863476075      1.40897426180181
H   -0.52284345069742      8.69047687092332      1.66376177837925
H    0.88863952652829      8.26385612642837      0.63611765361732
H    0.79087893878806      7.66185387787052      2.31795386498729
C   -1.54405543750790      6.11713758970210      1.97715182226977
H   -1.13469189113903      6.90826894187112      0.01943399569127
H   -2.23240247676229      6.93212331393049      2.28307084899719
H   -1.01878176135704      5.77203803668406      2.89290455831382
H   -2.16535292245563      5.28844657219447      1.58628407634223
C   -2.60262397882025     -6.08687470656119     -1.94197470923824
H   -3.48602770055279     -6.75091747402514     -2.04669931479340
H   -2.05818936721398     -6.10617326814900     -2.90894198967967
H   -2.96223318335417     -5.05193999846707     -1.77970131390517
C   -1.23434438698654     -8.00418704569630     -0.99463580934740
H   -2.30747546425845     -6.52816421338081      0.14561260199035
H   -2.09996249049384     -8.69077078226073     -1.10033296817442
H   -0.61645452715628     -8.35309139126915     -0.14336183632229
H   -0.61865858919376     -8.09554320233000     -1.91353123841608
H   -6.54853577252893     -2.86159620534011     -4.03920571352686
H   -6.30161040988296      4.23913275231183      1.93113948683659
C   -1.31493301819482     -1.01222702381488     -3.71012972696727
H   -0.89949891375458     -1.93384385646508     -4.16326639329117
H   -0.47196771530129     -0.45566185305952     -3.25528341766086
H   -1.75459018132732     -0.39907357440364     -4.52243204546244
C   -1.82476352524583     -2.25622134315558     -1.51662948655538
H   -3.15221143138270     -1.99311633580189     -3.18827273563096
H   -1.28944071164782     -3.13665703192125     -1.92257782116856
H   -2.64562256556483     -2.62161866553739     -0.86795125607797
H   -1.11109255964662     -1.70921017230570     -0.87139724800555
```

TS-3

174 conformers were generated by GOAT. Subsequently, the number of conformers was reduced to 109 by RMSD calculation and cutoff following RMSD $\geq$ 0.10 Å^2. All 109 conformers were subjected to constrained DFT optimizations followed by transition state optimizations and frequency calculations.

Electronic energy (a. u.) | DLPNO-CCSD(T)/cc-pVTZ: –5199.14938975462

Thermochemical Corrections (a. u.) | PBE-D3(BJ)/def2-SVP: 1.918448315521

Imaginary Frequencies: one (–566.00 cm^{-1})

Gibbs Free Energy (a. u.)   –5197.230941439100

```
C    -0.15196725590091    -4.64094817236051     1.07078252128286
C     1.90517217134921    -5.85319940892892     0.18142304135856
C     3.28857927525065    -5.80927604082442    -0.22179157309134
C     3.94443509379975    -4.55118515685713    -0.31581831098644
C     3.28667861831521    -3.35387470101199    -0.06104953096450
C     1.93875708673517    -3.41512239255865     0.41830384234365
H     4.99554403107120    -4.52379511262758    -0.64184783534726
C    -0.57660128257273    -5.47012521435770     2.16976460501546
C    -1.10989006155191    -3.84087419454471     0.43598737298288
C    -1.98351051590689    -5.56212182073789     2.47317108214173
C    -2.91709799159553    -4.80565503883742     1.71001148179152
C    -2.51021588282839    -3.91547606544143     0.72336805459682
H    -3.98986577587851    -4.90948283641055     1.93195577532737
O     1.33525620969435    -2.23622827085901     0.79832153687338
O    -0.70691607285902    -2.98058859046797    -0.56120760943825
P     0.07533805489268    -1.57466022633276    -0.11540140931166
O    -0.72763443915661    -0.73545861818675     0.85735952468231
O     0.62070580609384    -1.00760430413201    -1.42450928443623
N    -0.32763019194516     1.39470641501698     3.77918739302757
C    -0.89903445784079     1.77726752091571     2.61343400248303
C     0.50125874743864     0.19178896431722     3.83930780430294
C     0.22347317055420    -0.63564751624815     5.10617162480615
H     1.57178275824126     0.49722809114976     3.85795341088664
H     0.31903917655495    -0.40089366097630     2.92154644942265
O     0.34921590162129     0.22277686141888     6.25125225397585
C    -0.54281713328711     1.31882764970049     6.21298875026529
C    -0.30774552501165     2.20701085958806     4.98688310637942
H    -1.09426641397392     2.98239089368186     4.92893349946191
H     0.67611604102072     2.72097548092332     5.07833654131445
C    -1.55271823117171     2.97601184663150     2.36417855038907
H    -0.83255864869882     1.00026648895369     1.83069685856833
C    -2.18458075567700     3.30114509596440     1.10320412130841
C    -2.59971914767073     2.18190510445775     0.16707660026110
H    -2.74688994041022     2.56153000479281    -0.86086228528442
H    -3.56013584992103     1.73711325040799     0.49646924152471
H    -1.86767050216057     1.35282638530146     0.13792231289935
C    -3.04823592825295     4.53419757601762     1.10998090370330
C    -4.37656546904851     4.50763768209336     0.63684476664504
C    -2.52372890242720     5.75920600014983     1.58302200068264
H    -1.55360904785600     3.76689269447862     3.12842183752481
C    -3.30929260742470     6.91883529290687     1.58735899047327
C    -5.16645752293762     5.66778674433783     0.65442235175492
C    -4.63621759298459     6.87821265357386     1.12598659936126
H    -1.47595344722099     5.80293133849322     1.92323181176004
H    -2.87942625887925     7.86559321750525     1.94875314151013
H    -5.25337634446656     7.78943457022891     1.13053917579618
H    -4.80759216159413     3.56914468132265     0.26023812617168
H    -6.20451641143823     5.62278320008916     0.29095555386332
N     0.84611434057085     1.60124849686657    -1.17232970415471
C     0.12462773598910     2.35780100874609    -2.06169230550913
C    -0.26806555819523     3.63513660580692    -1.67336828456206
```

```
C   -0.03146093785544      4.04292444105819     -0.29327770445016
C    0.94101488779824      3.29011705000153      0.49005535937936
H   -1.15928739797823      3.78999745984804      0.37344589983683
H   -0.05798661987887      5.12513571951068     -0.08749450478100
C    1.32350644903087      2.02546726121484      0.03478018552778
H    0.90269148198947      0.54328395548829     -1.36585731842170
C   -0.13063262730036      1.68546079831298     -3.37483753262730
H   -0.37799876229760      0.61892516200610     -3.19915066428601
H    0.79603615980095      1.70402130299811     -3.98743385102172
H   -0.91722264511532      2.19899172067766     -3.94910667888473
C    2.24381175292053      1.06264553865771      0.71496831290682
H    1.78565112379997      0.66772552627419      1.63813407191547
H    3.17891107470002      1.56356629881944      1.01726221177509
H    2.48350962855211      0.21220728853423      0.05518120222299
C    1.40265995945068      3.95827388427807      1.72566065777177
O    1.05288386494992      5.08898751252401      2.05079979251737
O    2.27378357727525      3.22234665751639      2.46641060519761
C    2.83051067297494      3.87921325963385      3.62248483135294
C   -0.99728005407955      4.55287315900212     -2.58562742073882
O   -1.43373137953587      5.64446983827163     -1.90616554399105
C   -2.16533619660528      6.63525525004807     -2.66399062005930
O   -1.19844141198883      4.38552106075597     -3.78211385803004
C    3.67261797502889      2.87058855194911      4.37735044478537
H    2.00151672915342      4.28863038154898      4.23840897058302
H    3.42839197979379      4.75091188453484      3.28057163754464
H    4.16430495108759      3.36112430335360      5.24049381566113
H    4.46203310826044      2.44355446370621      3.72751064647282
H    3.05766913033819      2.03390166208529      4.76651098568002
C   -3.63316389198951      6.26772731746497     -2.80021674116307
H   -1.68596298393544      6.74499739344350     -3.65813399211226
H   -2.03443634744192      7.57089713809545     -2.08635841716779
H   -4.08853678420990      6.09680061999131     -1.80543225814886
H   -3.75344970583292      5.35435878040991     -3.41354311306650
H   -4.18092399224580      7.09295892585975     -3.29856889116506
C    3.95832865854652     -7.01930640364857     -0.57005744174501
C    1.23654334893670     -7.11403243467942      0.13775802590315
C    1.91000439264090     -8.27160540172510     -0.22480344824336
C    3.28782166511295     -8.23196769540630     -0.56497175877288
H    0.16827625246738     -7.16152707126623      0.38675154048762
H    1.36713423429372     -9.22848199177213     -0.25516958288720
H    3.81304899133148     -9.15829710691510     -0.84242710460468
H    5.01872118338324     -6.96560255772311     -0.86260061348164
C    1.25093660115652     -4.62864656310020      0.57576980589520
C   -2.40969840451557     -6.38621371576953      3.55658637698084
C    0.34192671386598     -6.17510530011679      3.00277397758243
C   -0.10317424615161     -6.95245031663693      4.06245966994874
C   -1.49135059906412     -7.07091216827072      4.33762531755461
H   -3.48781989252631     -6.45350444584558      3.77096982395959
H   -1.83371698995459     -7.69585482818695      5.17618867272488
H    1.41821159020228     -6.08016271420744      2.80384747286647
H    0.62648070152319     -7.47731403937858      4.69751777948589
C    3.99663793508729     -2.05731891149950     -0.31184547173756
C    4.69600683812678     -1.41020951933475      0.73970752663400
C    5.47203893993767     -0.27353741043022      0.44617448387398
C    5.57811975705211      0.23223646501702     -0.86176555041258
```

```
C    4.83348804926237     -0.39296417686724     -1.87780318723322
C    4.03985677391061     -1.52844901883397     -1.63260768592207
H    4.90706867572499      0.00517469985153     -2.90032082725555
H    6.03906930213070      0.22252134804838      1.24834210691067
C    4.68534021091840     -1.97880670978920      2.15486959867531
C    4.53417263032754     -0.89998380500384      3.23576872584507
H    5.40330678874079     -0.21087296689084      3.26215978455455
H    4.45883519100394     -1.36536592371925      4.23933742095057
H    3.62353640727188     -0.29222442242120      3.07051011336621
C    5.94394901849207     -2.83206987217719      2.39506664545804
H    3.80693487573057     -2.65231435450206      2.23416113553338
H    6.01200607339418     -3.66195019907006      1.66392112097897
H    5.93741141443198     -3.27286263354638      3.41340971879659
H    6.86229197744502     -2.21638531239941      2.29299591860300
C    3.29335526852165     -2.19599422967351     -2.78870110386224
C    2.72780263856832     -1.18858581255257     -3.79676288538617
H    2.05723233780288     -1.70754414115062     -4.51076438554135
H    3.52454975415325     -0.69735447414813     -4.39354395553205
H    2.13385563501741     -0.41096541565146     -3.28458203603001
C    4.20385476652216     -3.21159043337458     -3.51146972022831
H    2.43895988153353     -2.74185063371214     -2.35154449687083
H    5.09309311124282     -2.70681357556857     -3.94448681297677
H    3.65356325400147     -3.70223265050071     -4.34057339430283
H    4.56386484316599     -4.00579157570242     -2.83005669560434
C    6.52761950470813      1.34182051248982     -1.19177404125195
C   -3.47525213385914     -3.05548070064620     -0.02684575706738
C   -4.22290926116406     -2.05326944446286      0.65369732426560
C   -3.64965182192252     -3.24161959190547     -1.42679972520717
C   -5.11432289750678     -1.25374354948320     -0.08494462598797
C   -4.57313171408461     -2.43512642436721     -2.11331495934875
C   -5.31249009477400     -1.43193592156684     -1.46485885885649
H   -5.69939690734401     -0.47579698222178      0.42958934809955
H   -4.74603760573206     -2.60730848388336     -3.18646009158655
C   -4.13157761500041     -1.83534963509699      2.16175838717805
C   -3.85209891604003     -0.37109924810048      2.52435899812769
H   -2.90186561506769     -0.04173414805989      2.06711172881618
H   -3.77457254954070     -0.25026064850218      3.62422769225895
H   -4.66250919013511      0.30699669887638      2.18554905461265
C   -5.40098788839210     -2.35031544352880      2.86402681231230
H   -3.27370081017804     -2.42734967234886      2.53589793842293
H   -5.58912572772379     -3.41972641938388      2.64033734473994
H   -6.29727923503048     -1.78374237669515      2.53497406141144
H   -5.31519997097184     -2.23991952504179      3.96501829154814
C   -2.91765096852804     -4.32995699889109     -2.20646798667451
C   -3.90035913227324     -5.40942694155486     -2.69381132421262
H   -3.35832243430706     -6.22720127075116     -3.21201200513432
H   -4.64133912835361     -4.99313133420001     -3.40782088455825
H   -4.46305690765059     -5.85205020369384     -1.84709261514136
C   -2.08769066894740     -3.74860575781892     -3.36308688324345
H   -2.21327839061314     -4.82870667009752     -1.51257959898836
H   -2.73451387192824     -3.28087669984235     -4.13503419076858
H   -1.50522453399924     -4.55019906835158     -3.86225142797282
H   -1.37629975958038     -2.98541503056084     -2.99297126332912
C   -6.34100354255073     -0.62814411533185     -2.19839211982271
C    6.06513321404084      2.66091437677633     -1.44621693672308
```

```
C    7.91611128286183      1.05028129165641     -1.28218607495817
C   -7.70012641105496     -1.03299670492404     -2.14031183312993
C   -5.97477216262365      0.53035123999925     -2.93779271047558
C    6.99698976917146      3.65801400831889     -1.78397066031786
C    8.80968655146281      2.08664478967724     -1.61066357344243
C    8.37520135330585      3.39600510563929     -1.86908018029310
H    6.63201061152236      4.67856923184983     -1.98259723508181
H    9.88786311277086      1.86693144007180     -1.67858611155713
C    8.45809589981190     -0.35582425945756     -1.03470873507551
C    9.33172975348161     -0.85564029866146     -2.19653850842136
H    9.64144617725128     -1.90719390323201     -2.02592944216891
H   10.25711731442022     -0.25339757861468     -2.30726897607968
H    8.78347489345447     -0.81064156490482     -3.15883585916150
C    9.20902839701727     -0.43388744939573      0.30569401496852
H    7.58784184363801     -1.03849871953233     -0.96289393908945
H    9.56381012499515     -1.46716092824930      0.50157251417454
H    8.55713627828304     -0.13075239951502      1.14958520251514
H   10.09498231566229      0.23520443476752      0.31125924696931
C    4.58559278211361      3.02192553401497     -1.35677798913091
C    3.98692067759731      3.32073256439754     -2.74203823353889
H    4.10787375391200      2.45737906350556     -3.42701056104999
H    4.47968851267884      4.19509007108245     -3.21637404037604
H    2.90284513679773      3.54807257408225     -2.66379037289060
C    4.34037706225823      4.18314381592622     -0.37935552466041
H    4.06032486298445      2.13004225490801     -0.96274497142397
H    3.25902276663406      4.41359123667744     -0.30746265548422
H    4.85236085257827      5.11032010118403     -0.70897078905539
H    4.71109515604466      3.93965122262720      0.63693857575831
C    9.36553263535213      4.49103321101262     -2.24024507946102
C    9.34354437455318      5.64935487907879     -1.22893042439537
H   10.11151271794101      6.40963780172875     -1.48036114493069
H    9.53726116800377      5.28913512926828     -0.19881663461960
H    8.35798996788715      6.15973614184798     -1.22583168936307
C    9.13300623523996      4.99745808468766     -3.67402621371876
H   10.37826592258873      4.03265582745468     -2.20516814899189
H    9.89514404776773      5.75240400719572     -3.95769233250711
H    8.13594955985783      5.47535044695066     -3.77125583227753
H    9.17877950769578      4.16705713008941     -4.40652769444285
C   -8.67021045211413     -0.26351608241846     -2.81067102402329
C   -6.97990148568298      1.25988967003142     -3.59576261081874
C   -8.33466304455195      0.88481284511233     -3.54269856108039
H   -9.72866261741907     -0.56826588334904     -2.76264182466889
H   -6.69706281204843      2.15643835717614     -4.16791239654879
C   -8.12904321450579     -2.27026076813073     -1.35551858657047
C   -8.96873008709146     -3.23734756838260     -2.20492508979486
H   -9.19408021759168     -4.16193760741622     -1.63465386102232
H   -8.43190713362055     -3.52668343348791     -3.13056018765307
H   -9.93947371344494     -2.79034887608836     -2.50411936885244
C   -8.86057162961973     -1.87739339403422     -0.06047975771170
H   -7.20582737028740     -2.80907720243669     -1.06141573338572
H   -9.14044574457087     -2.77736078055122      0.52551948037012
H   -9.79037654632762     -1.31179335966940     -0.27985132739874
H   -8.22233804917926     -1.23699083377779      0.58096302453163
C   -4.51394344297029      0.95795937853327     -3.05761788369591
C   -4.32828949893693      2.48099366030132     -3.09764456994185
```

```
    H    -4.73710780229130         2.92408404016747        -4.02915240859978
    H    -3.25230224603507         2.74379892882181        -3.07924536337083
    H    -4.82265460798560         2.98386802536860        -2.24239863939185
    C    -3.85432924816703         0.30846886452104        -4.28930774442283
    H    -3.98608772525085         0.57435886921534        -2.15795604339715
    H    -3.89545734185337        -0.79600839459937        -4.23820518147015
    H    -2.78811076766680         0.60339682977191        -4.36711434812472
    H    -4.36768172051966         0.62687648431733        -5.22040526226288
    C    -9.40515574257920         1.70098175844324        -4.25378236022649
    C    -9.18962955136323         1.72158949338115        -5.77636239190821
    H    -8.23624817148176         2.22518207598106        -6.03989885565310
    H   -10.00839900343706         2.27045865500607        -6.28596314697084
    H    -9.15079658454483         0.69479035937565        -6.19170172728223
    C    -9.50167004185623         3.12673525777477        -3.68466790063049
    H   -10.37612707363544         1.19475503293373        -4.05866505789697
    H    -9.68647840654756         3.11172837450365        -2.59189381187845
    H   -10.32494194725332         3.69277183455352        -4.16758085392241
    H    -8.56160780632174         3.69092327597463        -3.85814953947993
    H    -1.60436255099385         0.97491113845741         6.21864674962760
    H    -0.37072345921306         1.90732447409310         7.13676935650803
    C     1.23115831928464        -1.78362695800478         5.24261929350609
    C    -1.12276185158734        -1.38545261203438         5.01758211461981
    C     0.70741995983551        -2.89300170522364         4.30929587675714
    H     1.20402390548730        -2.09633568695757         6.30680304565924
    H     2.26703480004544        -1.46005105273532         5.02090561286424
    C    -0.81509866369002        -2.61060997854151         4.13347797676694
    H     0.89973064728020        -3.90031248290189         4.72514949319564
    H     1.21413491161741        -2.85746838344148         3.32413150959393
    H    -1.44234216281105        -3.48035804148321         4.40618919462821
    H    -1.03594861035461        -2.38215247068306         3.07194499962520
    H    -1.94232841783504        -0.76393246622447         4.60953600156919
    H    -1.40152242359004        -1.68590628026377         6.04947906075626
```

TS-4

45 conformers were generated by GOAT, all of which were subjected to constrained DFT optimizations followed by transition state optimizations and frequency calculations.

Electronic energy (a. u.) | DLPNO-CCSD(T)/cc-pVTZ: –5199.14698169226

Thermochemical Corrections (a. u.) | PBE-D3(BJ)/def2-SVP: 1.919610586735

Imaginary Frequencies: one (–630.64 cm^{-1})

Gibbs Free Energy (a. u.)   –5197.227371105520

```
248

    C    -0.33501076724424        -4.62983214313133         0.20645211655079
    C     1.41317533688767        -5.72897945491957        -1.28122741596308
    C     2.70013737957584        -5.66694235985876        -1.92619141241783
    C     3.44683691949347        -4.45891071252743        -1.86541856045362
    C     2.96065633234087        -3.31300053481958        -1.24475349379875
    C     1.69952170663480        -3.39909731041788        -0.57357621831806
    H     4.43367608612619        -4.42215209986493        -2.35181806713090
    C    -0.60389826600341        -5.62539156381462         1.21168901916056
    C    -1.33499705790582        -3.69902618188797        -0.09838797696060
    C    -1.92707507595496        -5.70660348688371         1.77996864940859
    C    -2.93824194124022        -4.81238151949060         1.32667787531658
```

```
C   -2.66891428972234    -3.80296417497298     0.41089299703460
H   -3.95949206015433    -4.91953273575508     1.72315963556890
O    1.23655702173191    -2.29510530147530     0.11007363404026
O   -1.06055198497646    -2.68608856097264    -0.99140379791985
P   -0.08115161665891    -1.41946361801888    -0.49487268213160
O   -0.64994237337345    -0.67293447713305     0.69466266956441
O    0.32216328556857    -0.69715937620489    -1.77840743379217
N    0.66145690893030     0.84706842920614     3.76836448662302
C   -0.12843161585376     1.59607484990034     2.96915814385493
C    1.29986131454726     1.31566857836859     4.99302967031054
C    1.10808104855429     0.26238050269616     6.09114466656753
H    0.84933310980252     2.27321366014213     5.31396824636135
H    2.38019214651647     1.48630142517664     4.79385669957954
O    1.56700396545744    -1.01328996874674     5.69557829667700
H    0.02944085891121     0.23289568538396     6.38207137253328
H    1.69355710819207     0.54996898427741     6.98802676446294
C    0.89454479142789    -1.51145641515051     4.52025542278786
C    1.07624188891992    -0.49964944439043     3.38012411769265
H    2.15717772154841    -0.46677250770096     3.11917167029585
H    0.50461891221528    -0.80813656196829     2.48243311787857
C   -0.38950189794430     2.95331579943794     3.12889641937484
C   -1.19733570148373     3.83052419949677     2.30477366563856
C   -1.31191436065572     5.24789259019967     2.85774587753537
H   -0.32934800072173     5.57966458721931     3.24459607991785
H   -2.03822358360908     5.29372382920031     3.69626081240992
H   -1.62700106593337     5.95760959249565     2.06990868853810
C   -2.36685245654025     3.35297540431937     1.48903956759301
C   -2.27879023570812     2.25101036189194     0.60608911700266
C   -3.59612139068612     4.05423392954116     1.53943954412927
H    0.16970762723450     3.47858459066790     3.91849963909704
C   -4.69255120613867     3.65760356779784     0.76329803307805
C   -3.37399599560458     1.86249296076403    -0.17931875423108
C   -4.58729523715476     2.56227885779065    -0.10853377209848
H   -3.70565668124799     4.91982394561716     2.20611484692958
H   -5.64079249269696     4.21260829852099     0.83519888449089
H   -5.44539355855492     2.25317728922942    -0.72258492869969
H   -1.36315029873162     1.65218399200372     0.52266341615012
H   -3.27463170240086     0.98093690239704    -0.82973302750291
N    0.81111254130748     1.83321395440961    -1.08382676499553
C   -0.05116092361709     2.76714324790484    -1.59640705211760
C   -0.15785135817796     3.99402067876869    -0.94611071193411
C    0.55531899557906     4.20355315478246     0.30906182655145
C    1.53024256385540     3.19765118378312     0.72455110984660
H   -0.36650062549846     4.09411806584510     1.25505681374717
H    0.78117809727284     5.25465626931920     0.55527915109522
C    1.60523426851852     1.99781854179634     0.01597723468113
H    0.72530863234434     0.83510704180854    -1.46854867896308
C   -0.80072514524706     2.31486262479933    -2.81118249490562
H   -0.67205693618049     1.22465967952203    -2.94998035244000
H   -0.44415757644638     2.84867108561842    -3.71454436341923
H   -1.87295824911960     2.55218813048037    -2.71245487468607
C    2.49687178554646     0.84318150285825     0.32336364673375
H    1.95720303873748     0.11345773908857     0.95650967511243
H    3.38929018359587     1.16244618585395     0.88217151953765
H    2.77761494723482     0.31510762958624    -0.60388613962479
```

```
C    2.35817989271662      3.43403883690111      1.92766536934352
O    3.06264289452289      2.62116555702217      2.51727827325330
O    2.26279132776981      4.73537016229950      2.33246616308356
C    3.03319210670755      5.08408965020656      3.49649625493497
C   -1.08030673879154      5.09335170480827     -1.31684497770926
O   -1.66549734881210      4.94308548768864     -2.53107125015419
C   -2.64191486661496      5.94367073501294     -2.90174468576058
O   -1.29370232329459      6.04934667112887     -0.57913285207696
C    2.85976976235736      6.56841909664649      3.74462516115548
H    4.09393352602085      4.80594190191814      3.32192480681341
H    2.68306077080269      4.47065852399820      4.35575725336895
H    3.45187249445118      6.87721195985020      4.62865937435304
H    1.79802949841433      6.82413750376480      3.93431637133405
H    3.20525110400701      7.15825126044185      2.87272104569591
C   -4.01856061898091      5.61467979578061     -2.34748475994418
H   -2.63417284244700      5.93965853692438     -4.00929987577192
H   -2.29223229086954      6.93004213863317     -2.53622273939113
H   -4.75235333049427      6.37376486963993     -2.68688352635379
H   -4.00707420550031      5.61348956155945     -1.24079561202980
H   -4.36531224716232      4.61978713431257     -2.69053641101258
C    3.18348715271399     -6.80348343407707     -2.63958454860128
C    0.63829063147348     -6.91741765925326     -1.44184651696601
C    1.12817929203574     -8.00035916492903     -2.15730884435499
C    2.41800519516136     -7.95341824020230     -2.74971600705058
H   -0.36536552261870     -6.96401379511865     -0.99861528514968
H    0.50733438415392     -8.90188562854418     -2.27174604347465
H    2.79834166660875     -8.82197487155158     -3.30822326692836
H    4.17431729690623     -6.74076873660424     -3.11620636610403
C    0.95074857749973     -4.58428678098123     -0.53776481577154
C   -2.19350324054423     -6.68267427282176      2.78486309035086
C    0.39744120696259     -6.51900305706489      1.69746621133580
C    0.10648066851012     -7.45478747573654      2.68014585474272
C   -1.20046862700682     -7.54313881469019      3.22774475518388
H   -3.20862171077477     -6.73432168155949      3.20883205852380
H   -1.42020038691131     -8.28801541880993      4.00731046643873
H    1.41577040986235     -6.44721165970894      1.29113269878041
H    0.89876074338309     -8.12569375186202      3.04506614261602
C    3.78699913049356     -2.06371656112954     -1.29176377910977
C    4.62623534349617     -1.72810895553033     -0.19530689353700
C    5.52483651051945     -0.65484750319612     -0.33006587168417
C    5.61901640748189      0.08867635771470     -1.52083334448632
C    4.73215318314745     -0.21849343624224     -2.56709395719627
C    3.80818758694183     -1.27696187519734     -2.47624089057389
H    4.78859041099356      0.37278267068952     -3.49300018576800
H    6.19281172612997     -0.39532789762082      0.50400332012184
C    4.60773201964540     -2.55579268517699      1.08614236918334
C    4.86058313421741     -1.72617001931096      2.35250959977299
H    4.19717399706121     -0.83958712920091      2.40436281833591
H    5.90788015884770     -1.36446847738206      2.40882920630436
H    4.68019595643482     -2.34044251874044      3.25746910012111
C    5.61179410550492     -3.72011061396932      0.98705281669671
H    3.59268838428582     -2.99580449370928      1.17608786652093
H    6.44494537294919     -3.33323482353017      0.86088079445062
H    5.38613450554247     -4.37553867103641      0.12318244474196
H    5.58831812448397     -4.34330612795596      1.90490584810490
```

```
C    2.88155329858138    -1.57295110654426    -3.65245726810298
C    2.30006134249549    -0.29950538439872    -4.28550908913080
H    1.81882526908382     0.33984473761222    -3.52319061364146
H    1.52729566901253    -0.56929924977019    -5.03330110921508
H    3.07293443864896     0.29809939326921    -4.81238341697255
C    3.59017035157340    -2.42562674044286    -4.72097612160351
H    2.02543028933689    -2.15127681697356    -3.25042352659588
H    3.93621214520851    -3.39399789168436    -4.31189319181143
H    4.47606800206727    -1.89339815942117    -5.12704954563979
H    2.90490092973172    -2.64079505937061    -5.56652358509658
C    6.68648778357325     1.12214235496583    -1.70648846698855
C   -3.72110120761384    -2.86868701321770    -0.09041408285023
C   -4.25899863534667    -1.85926914873894     0.75210047164421
C   -4.17217611718161    -2.98577417604263    -1.43341390336929
C   -5.18005884945074    -0.94990747441631     0.20859056656056
C   -5.15108534405638    -2.09526308934030    -1.90648852117206
C   -5.64499088526906    -1.04045858203970    -1.11843177666771
H   -5.53893091399361    -0.12245459786232     0.83596163869748
H   -5.53174443020103    -2.22123877332112    -2.92978751150610
C   -3.90016867394527    -1.74820826101845     2.23000159263715
C   -3.44998249689880    -0.33848948346796     2.63299835372142
H   -2.55500212158037    -0.05099665809377     2.05324138876999
H   -3.19968415806630    -0.30801233881501     3.71322284011433
H   -4.23474581053518     0.42583529454975     2.45844430108327
C   -5.07628998691728    -2.23127638237948     3.09828571570091
H   -3.04518502857304    -2.42706911079938     2.41259142875415
C   -3.63417439218503    -4.04802320464258    -2.38711601937733
C   -4.73760062641277    -5.02780747701265    -2.82026194384889
H   -4.31935868078219    -5.82772480684814    -3.46540043994249
H   -5.53342100940584    -4.51526843929836    -3.40028749660037
H   -5.21744314598197    -5.50777746162398    -1.94362400283090
C   -2.93245800667112    -3.40758301251387    -3.59798654601195
H   -2.87303869620988    -4.63996421562063    -1.84068111752242
H   -2.46984107775513    -4.18684008197584    -4.23821243550709
H   -2.13562648162264    -2.71399208274252    -3.26707987228997
H   -3.65071719252015    -2.84174387418289    -4.22770237772791
C   -6.58105475420061     0.00031538886057    -1.64053917202512
C    6.39476564765422     2.50874521162884    -1.63202839823157
C    8.01311902344043     0.69139090107637    -1.99045871860873
C   -7.77871921162521     0.30352903906620    -0.92885876907394
C   -6.24009411929258     0.78305506323916    -2.78749341549184
C    7.43299733462916     3.43458473739349    -1.84930244062486
C    9.01745405223380     1.65543243892572    -2.18126862825627
C    8.75017899943475     3.03425291966416    -2.12033096321428
H    7.21165824414460     4.51329970235569    -1.80026665138632
H   10.04399769760957     1.31614399309889    -2.39343144879544
C    8.36924712232814    -0.79089979645735    -2.08534274370275
C    9.12562743623057    -1.13005572139704    -3.37966693048985
H    8.56055369672298    -0.79843982803328    -4.27373514644461
H    9.28637754750671    -2.22476774024062    -3.46052998846766
H   10.12479487519294    -0.64850267944948    -3.41481427782720
C    9.15118215621007    -1.25168550141151    -0.84274637803421
H    7.41759484575213    -1.35905515281559    -2.10456669584495
H   10.11452740530243    -0.70735438598314    -0.75202566847860
H    9.37725020152838    -2.33705387558448    -0.89586885867533
```

```
H    8.57451551385360      -1.06749502509765       0.08570596883025
C    4.98686713150701       3.01508816048675      -1.33091854146290
C    4.31058882108824       3.58584126627996      -2.59004024884690
H    4.26008265337634       2.83037546726728      -3.39952176461456
H    4.86840374750838       4.46175865324208      -2.98223788346902
H    3.27444025679446       3.91578604170373      -2.36501588728047
C    4.96995752517456       4.03411469817789      -0.18016086842986
H    4.39270382224279       2.13740540638069      -1.00974007866409
H    5.58949905995642       4.92528750332625      -0.40935439526642
H    5.35070139625326       3.58671583575392       0.75942613329965
H    3.93959500574852       4.39732663018390       0.00496440448092
C    9.85173364692375       4.06152950779433      -2.34180799241959
C   10.43652174833239       3.96904689605146      -3.76130342397094
H   10.93208440269051       2.98975838744654      -3.92663639921223
H   11.19569033045334       4.76035949505324      -3.93113113964533
H    9.64565549333670       4.07702006753852      -4.53018596267059
C   10.95397930467337       3.94906187228686      -1.27498445330493
H    9.38159186214386       5.06396257300581      -2.23604107680169
H   11.47064401174287       2.96867556161792      -1.33640975800134
H   10.53589205379473       4.04318614594523      -0.25287790843874
H   11.72127141767363       4.73926988028650      -1.40996904048781
C   -8.55388514240880       1.41257667377195      -1.31628430669560
C   -7.06192529024792       1.86702600149604      -3.13997641398989
C   -8.20382049500631       2.22525122164830      -2.40458366990777
H   -9.46419465470512       1.64419786966010      -0.74262344494070
H   -6.78947257366406       2.48179613076341      -4.01286717589204
C   -8.28872561051672      -0.56006431493559       0.22426600157108
C   -9.65007580476050      -1.19025403292177      -0.11979825373081
H  -10.43723598440573      -0.41943050333840      -0.25483811786213
H   -9.98268624446796      -1.86882248777159       0.69270036527180
H   -9.59274596261088      -1.77845999863031      -1.05732709652455
C   -8.35580161668401       0.21864231588897       1.54868838442494
H   -7.57226684989106      -1.39302824475643       0.36173430284205
H   -8.65145455936024      -0.44991272339443       2.38346052200128
H   -9.10089972043691       1.03991798001662       1.49925979672481
H   -7.37776571606204       0.67374754904694       1.80508361770630
C   -5.00538581107981       0.50665665705294      -3.64363348608237
C   -4.21936014474826       1.77922026375633      -3.99436592241518
H   -3.26765571473918       1.51488991671668      -4.49766104612513
H   -3.97872262598308       2.36543788910015      -3.08586021143940
H   -4.77944954840306       2.44068694179061      -4.68708716116273
C   -5.38729396387599      -0.25101414770552      -4.92879899850919
H   -4.32786690596887      -0.14406338132091      -3.05459204468731
H   -6.04746487768105       0.37167995507569      -5.56820315232774
H   -5.93496358104610      -1.18866435133504      -4.70922602630395
H   -4.48424732880778      -0.51049248602288      -5.51909742225543
C   -8.95909690338478       3.49863610777441      -2.75920663787777
C   -8.28006032249954       4.70761221591567      -2.08444138505260
H   -8.33092338498300       4.61269668393561      -0.97929819901902
H   -8.77544788413604       5.65884399460853      -2.36999247124317
H   -7.20910560415518       4.77690432251452      -2.36294480668386
C  -10.45543723554191       3.45210425767511      -2.42847606202935
H   -8.85897832265214       3.63336474359229      -3.85948852706524
H  -10.94509716079171       2.56350926316587      -2.87472798926299
H  -10.96754189540034       4.35746713419264      -2.81220174682575
```

```
H    -10.63085977377815      3.42130230022986     -1.33309511950347
C      1.54197355278611     -2.87146930808264      4.14227805751259
C     -0.60403767438741     -1.83467577724030      4.77772551011594
C     -0.83659203596669     -3.16831757109372      4.05602982710030
H     -1.28510541912669     -1.02580041035921      4.45026757891124
H     -0.73691435255999     -1.97402977616726      5.87159641914337
C      0.45555254799389     -3.93921197248542      4.35215790992679
H      2.45349979464969     -3.02125954065965      4.75255915373686
H      1.85250719294620     -2.84901262317331      3.07674275244206
H      0.45206655571987     -4.28300212096398      5.40879135519015
H      0.58926417166463     -4.83123634905630      3.71186276158007
H     -0.92699707432395     -2.99897340499746      2.96117871001874
H     -1.75798357536485     -3.69107439994987      4.38121805467513
H     -4.80163136364154     -2.22218142989311      4.17365293157504
H     -5.38441499230860     -3.26164517869790      2.83171520651193
H     -5.96170419587280     -1.57340415486676      2.96924510805628
H     -0.55071398199561      1.01549804151278      2.13381375758376
```

TS-4b

39 conformers were generated by GOAT, all of which were subjected to constrained DFT optimizations followed by transition state optimizations and frequency calculations.

Electronic energy (a. u.) | DLPNO-CCSD(T)/cc-pVTZ: –5199.14595863599

Thermochemical Corrections (a. u.) | PBE-D3(BJ)/def2-SVP: 1.919054203187

Imaginary Frequencies: one (–616.82 cm^{-1})

Gibbs Free Energy (a. u.)   –5197.226904432800

```
248

  C     -0.21085067030366     -4.51808058887981      0.83987959810129
  C      1.43131084555585     -5.67162577705448     -0.72121489329549
  C      2.64203631827935     -5.61809419457663     -1.50069030834452
  C      3.32873070773485     -4.37961654402381     -1.62624149901421
  C      2.85055453429558     -3.20392214781078     -1.05939027878684
  C      1.67473193075738     -3.27855822912664     -0.24584598338140
  H      4.25265211300764     -4.34403714259829     -2.22370310975907
  C     -0.34789158831282     -5.45233287794988      1.92763271629598
  C     -1.28022136982251     -3.66038007227446      0.55911946126987
  C     -1.62291654748271     -5.57311906043996      2.59034899446797
  C     -2.72041417768373     -4.78023896372441      2.14479173444967
  C     -2.57346290778967     -3.81527444894828      1.15789179370554
  H     -3.71041473815015     -4.95180155792420      2.59261785323254
  O      1.25058128852156     -2.13959239801635      0.39758071877348
  O     -1.13048797788025     -2.69074119961507     -0.40971424467944
  P     -0.18609054072695     -1.35208935279519     -0.04721698977710
  O     -0.65439571658652     -0.61716160135748      1.19079666363433
  O      0.02774143573768     -0.63402277718195     -1.37664433567145
  N      0.36724447278642      1.27952020367234      4.54889577556815
  C     -0.08687399984456      2.37945858477934      3.89936904752024
  C      0.99715978647205      1.42748154033861      5.85838573637471
  C      1.98510812258340      0.28874575303335      6.09401515056558
  H      0.21542505100907      1.39556134933699      6.65473352313877
  H      1.50470194351766      2.41182667758290      5.90993884729582
  O      1.35066037335172     -0.96199156853182      5.96971892876849
  H      2.39256846649838      0.34785597475634      7.12351795303521
```

```
H     2.83980220318274      0.39433322225952      5.38101439445614
C     0.79391266014030     -1.19094225418563      4.64952357373430
C    -0.17275477398654     -0.05833673673789      4.27923220094214
H    -0.43023135220658     -0.15955316915542      3.20738833991324
H    -1.10564462678375     -0.17613081716300      4.87908794048995
C    -0.90497584619865      2.39565053182632      2.78238831095481
C    -1.51807847258528      3.58026593583767      2.22753111768444
C    -1.56612552991864      4.85413038011821      3.05492005187318
H    -2.34189102063687      4.78391808466335      3.84614245702474
H    -1.79694943099027      5.72882727591023      2.41757261522164
H    -0.58861687075986      5.05557724313340      3.53058722895939
C    -2.61802358116437      3.34217819606642      1.24202553534919
C    -2.57069163521182      2.22572477317993      0.36993495420811
C    -3.72124737732124      4.21904199621047      1.13128111736212
H    -1.12496634497627      1.43460834263614      2.29817199291263
C    -4.74487739726258      3.97849788101870      0.20336625006994
C    -3.59263472542649      1.99081939761324     -0.55619598344581
C    -4.68858864023079      2.86322678696031     -0.64779674379191
H    -3.79612928973892      5.09216416924815      1.79419526684844
H    -5.60100461663824      4.66864811859490      0.14884198452557
H    -5.49269965529852      2.66512954441912     -1.37200468153803
H    -1.74449903403006      1.50124018200218      0.42724939657949
H    -3.53632329063858      1.09975066805714     -1.19554011121313
N     0.73790899971676      1.88067759082432     -0.83220017221428
C    -0.04952062701223      2.82222345961891     -1.44692307013386
C    -0.17263759148960      4.07470222342402     -0.85280410549345
C     0.39905996115028      4.27520273753927      0.47880581698763
C     1.41580766865871      3.32313633553467      0.92535224095046
H    -0.56640489188414      4.02769020631669      1.28724592786847
H     0.57270396451173      5.31983272973283      0.78633222225886
C     1.51034012336356      2.09254943897320      0.27898824774491
H     0.60661117246313      0.86834771752216     -1.15325972420421
C    -0.69466306374469      2.36631432426566     -2.71606140242242
H    -1.62230837870040      2.92542916029122     -2.91772990246831
H    -0.88530820187581      1.27696700028507     -2.66035953737327
H    -0.01384030718277      2.55074919832586     -3.57408353369843
C     2.39857239052643      0.95676159587744      0.66542517537568
H     3.45814177932237      1.26913227917224      0.63102709613638
H     2.26900239001330      0.09802579903649     -0.01291680474302
H     2.19595515669900      0.63548343562261      1.70260852477981
C     2.17922637471912      3.73619269749647      2.11933263892786
O     1.94383991572987      4.76575343424429      2.74718106296756
O     3.18212498652869      2.88798339310454      2.46639270180451
C     3.96936709194612      3.27829229996634      3.60634209939257
C    -0.96682733073577      5.15290895943059     -1.48207325336765
O    -1.14729898458036      6.19382865898648     -0.61481821694223
C    -1.84964365142231      7.33962140591492     -1.14287699378693
O    -1.40595599156394      5.15917452700644     -2.62435083726815
C     5.03651500219525      2.22437386194241      3.81800220308070
H     3.30190651236006      3.38424925806848      4.48901716189475
H     4.40058176898860      4.28413101243139      3.41765744057943
H     5.67957936913866      2.50102307606981      4.67660499313129
H     5.67935649687641      2.12322487343661      2.92117345614642
H     4.58593957668614      1.23375003069484      4.02805086998053
C    -3.35758354072449      7.18990738360121     -1.02949899687742
```

```
H    -1.55065039941229        7.47765162983330       -2.20171782017377
H    -1.47805436578569        8.19438807908093       -0.54391267188148
H    -3.70980332285162        6.32544434858101       -1.62435129971412
H    -3.85404136719060        8.10385942040755       -1.41417682924757
H    -3.67015102882081        7.04220897879983        0.02269147261244
C     3.10362531917666       -6.79297448212006       -2.16432926229174
C     0.69937990213884       -6.89760420476676       -0.70444513778275
C     1.16430806100908       -8.01915710591575       -1.37591985030846
C     2.38500395747213       -7.97622114974712       -2.09992418295754
H    -0.25198520260399       -6.94486308049086       -0.15816344721829
H     0.57617291805778       -8.94908794873536       -1.35184272273722
H     2.74693030296090       -8.87481129061853       -2.62193138587814
H     4.03728025256075       -6.73376813014537       -2.74546559859922
C     0.99401820793840       -4.48487626833712       -0.02843744830837
C    -1.76166103497431       -6.49968301284327        3.66541341213752
C     0.73688385141239       -6.25408729943622        2.39232672968654
C     0.57056406365874       -7.14176439899567        3.44594391137133
C    -0.68990926891003       -7.27260959374165        4.08635654407904
H    -2.74145631535425       -6.58496878650690        4.16093007614511
H    -0.81128622149491       -7.97987748802042        4.92054916447594
H     1.71897210577632       -6.14827388182165        1.91120607972996
H     1.42540670925129       -7.74120794203430        3.79363444039993
C     3.57519872266609       -1.91945924247999       -1.32405702313234
C     4.57170723280910       -1.46542110123645       -0.42029985593355
C     5.34298543613010       -0.34181210040272       -0.76776571335050
C     5.15092383410148        0.34123657320990       -1.98235570898130
C     4.11690662411093       -0.08864653789204       -2.83233382292917
C     3.32212420184409       -1.20988599184284       -2.53043452928208
H     3.95731153803380        0.45129252386926       -3.77730048275117
H     6.13557438934104        0.00795274849183       -0.09000832855325
C     4.84877275337765       -2.21604312575500        0.87843454143401
C     5.24608445067305       -1.29388005247324        2.03924706843982
H     6.25349154949239       -0.85202002000848        1.89266332846631
H     5.27749332757069       -1.86380005745297        2.98980787268775
H     4.52607697821680       -0.46211931745721        2.16135060621978
C     5.91878737178747       -3.30227946682140        0.66052803676159
H     3.90561695114600       -2.72365706459453        1.16949508671142
H     6.10441910423592       -3.86757469233342        1.59716808808717
H     6.87767976220630       -2.84387038777735        0.33903971911479
H     5.61055757985460       -4.02552808198871       -0.11913223008319
C     2.25619030532404       -1.67290340512229       -3.52034980431626
C     1.53186330093266       -0.50743521793724       -4.20857731389601
H     1.16487513992653        0.22341655635344       -3.46709223777223
H     0.65412219820534       -0.88598904717092       -4.77006483088074
H     2.18467777600712        0.01891272406189       -4.93587104989185
C     2.85450252225890       -2.62037693745065       -4.57703773760367
H     1.49381842321684       -2.22830308234684       -2.93741926472545
H     3.29502138995461       -3.52724174739655       -4.12118541231633
H     3.65205938852071       -2.10694050257612       -5.15417963954047
H     2.07241077321576       -2.94780515396251       -5.29259189995545
C     6.08127627530882        1.43565708688766       -2.40528954568599
C    -3.69110652613564       -3.00153716280799        0.58580419841747
C    -4.11859604867778       -1.79588781155342        1.20614377647425
C    -4.22808777866238       -3.38815656545063       -0.66932679306727
C    -4.97438800014594       -0.94393807771240        0.49031150787865
```

```
C    -5.14326718578101      -2.53502185139828      -1.31117348205889
C    -5.48250289253457      -1.27893485089758      -0.78277305925557
H    -5.23798260744142       0.03350455595098       0.91319301991042
H    -5.57697905975505      -2.84211473534201      -2.27298559374157
C    -3.69338311310588      -1.45031961094128       2.62970182540002
C    -3.71996342730493       0.04865976247005       2.93772056927668
H    -3.13799264081820       0.62276703316040       2.19684142784447
H    -3.29320923735906       0.24621789627420       3.94121883679664
H    -4.75379178013409       0.45264192317939       2.94531325582933
C    -4.58024194141782      -2.19462707897054       3.64754255852303
H    -2.64653604591355      -1.80235811401732       2.74935718601015
C    -3.80621106660891      -4.67700869743099      -1.37058329406620
C    -5.01286700861750      -5.57302334175536      -1.69401277970279
H    -4.67850351426775      -6.52892570103456      -2.14695147381925
H    -5.69912624549158      -5.08725386436302      -2.41847514699755
H    -5.59854821831702      -5.80864594515003      -0.78265387172006
C    -2.97112000158602      -4.37878648856980      -2.62985735535242
H    -3.15859526210834      -5.24286860422173      -0.67053211669274
H    -2.58652104142579      -5.31929846404200      -3.07597918157600
H    -2.10844836291322      -3.72708296689618      -2.39100885854979
H    -3.58313463356339      -3.86611031510542      -3.40143074916244
C    -6.30075929608187      -0.28595774441229      -1.54329229870546
C     5.70689229539447       2.80250620515507      -2.31282759226419
C     7.35496126084526       1.08479214725553      -2.93050896876484
C    -7.48164208084676       0.26479347209837      -0.96691153257944
C    -5.86236484917249       0.18728345412482      -2.81959152184610
C     6.61153727415122       3.78863535781959      -2.74426186977008
C     8.23003161240953       2.10975815568093      -3.33504346970556
C     7.88100254656440       3.46701570021796      -3.25413675982002
H     6.31359812675957       4.84706429275043      -2.67479165158698
H     9.22118899893034       1.84460725030630      -3.73807852713386
C     7.79183342885529      -0.37257337708541      -3.05951057683982
C     8.31254145847742      -0.70653386215574      -4.46637233946458
H     8.52776880515908      -1.79139569342754      -4.55351652730635
H     9.25286267678436      -0.16622316365549      -4.70240091571493
H     7.56794562758030      -0.44081630372357      -5.24331750591249
C     8.82311415672565      -0.74027133550996      -1.97852593324428
H     6.89568535920117      -1.00203274776466      -2.88670618118235
H     8.41878032898461      -0.56421985975457      -0.96167431627055
H     9.74623904114410      -0.13238235088228      -2.08264922500909
H     9.11028176266155      -1.80986434739821      -2.05190773978794
C     4.34627956926890       3.22453932460216      -1.76629770386473
C     3.43179386743539       3.75260319421478      -2.88550215446134
H     3.86504730592197       4.65428146673441      -3.36666029398726
H     2.43438088025596       4.03067047867028      -2.48557999526208
H     3.28473731942253       2.99014454473854      -3.67657462214702
C     4.47733483084253       4.24351959977691      -0.62292956265983
H     3.86604245375748       2.31476226593503      -1.35419105728176
H     3.47778790965184       4.52819297668689      -0.23938974605657
H     4.97901148143506       5.17441838090454      -0.95821123214912
H     5.06482810192972       3.82962097944393       0.22136251703792
C     8.84870183023216       4.55229146733588      -3.70513227136576
C     9.26168447455522       5.46403308870188      -2.53716520429913
H     8.38973638245211       6.02225817152549      -2.13690247476719
H    10.01550476246995       6.21056731932551      -2.86240821606160
```

```
H    9.69385119521626     4.87652579889678    -1.70266307653644
C    8.28245877942675     5.36811741827715    -4.87929913374342
H    9.76436894390727     4.03478552116167    -4.06682025148868
H    9.02235948308950     6.11271062820559    -5.23908114848786
H    7.36968143937749     5.92367328354250    -4.57909230058167
H    8.00986509297378     4.71236802769791    -5.73015851523865
C   -8.16507498810341     1.29127484188344    -1.64465577061094
C   -6.58715222876556     1.21244649758326    -3.45274689692378
C   -7.73158333572157     1.79322120807593    -2.88023330741016
H   -9.07315209044488     1.72217527383190    -1.19124061198239
H   -6.22918510022942     1.58596070452141    -4.42434274310347
C   -8.05816844240778    -0.23572302576939     0.35585723279859
C   -9.48295164365688    -0.78744306464328     0.17603633894745
H  -10.19393449335042     0.00268690126468    -0.14355460384914
H   -9.86143544271856    -1.20925283347262     1.13003492230367
H   -9.50783403147120    -1.58978758781342    -0.58816115324193
C   -8.01343563124315     0.84995020875350     1.44475425149235
H   -7.42609182568706    -1.07839171549676     0.69805309067202
H   -8.35696423345881     0.44559341798487     2.41944848473508
H   -8.66934357952685     1.70825124963126     1.18852594915839
H   -6.98823425517810     1.25019038139387     1.58013439018032
C   -4.62716609023176    -0.36616681492531    -3.53235850101719
C   -3.72616459913937     0.72846346104022    -4.12954450696075
H   -2.76711315115757     0.28823192636923    -4.47099030928632
H   -3.49292257780472     1.51829403638208    -3.39081755093124
H   -4.19088057879826     1.21923886838778    -5.00961293908584
C   -5.03318403380168    -1.36375548740711    -4.63379740450602
H   -4.02266627606408    -0.91822827181952    -2.78387128212103
H   -5.63477512037757    -0.85696458453734    -5.41713501626016
H   -5.64677338059087    -2.19577704931970    -4.23612207738059
H   -4.13673878835255    -1.80046758235734    -5.12053715990917
C   -8.44427391281478     2.96248601332274    -3.54379448241241
C   -8.81048641183103     2.68124655202505    -5.00894077401964
H   -7.90462954124212     2.55240446629225    -5.63681826049848
H   -9.39074972714087     3.52336504228977    -5.43862704457026
H   -9.41786730135261     1.75898592276257    -5.10293595153294
C   -7.60886800785422     4.24958917238029    -3.41189542123015
H   -9.39226313112368     3.12069765321100    -2.98369494592708
H   -7.38856380591897     4.47783507746578    -2.34928086292302
H   -8.14169963212536     5.11979125571179    -3.84836371892513
H   -6.63687988185768     4.14818422103860    -3.93844521071582
C    1.91315179592566    -1.47567628432331     3.62114446384694
C    0.07259465226236    -2.54231699667389     4.73707347803784
C    1.22605186917310    -3.54955378854424     4.78012442053391
H   -0.53230642234264    -2.67754515448204     3.81500260206552
H   -0.60595905590529    -2.58297891428931     5.61243505415044
C    2.23870236792549    -2.98877349511401     3.75429563515724
H    2.79565936319182    -0.82725559501462     3.78319725021842
H    1.53114056233261    -1.25610795086339     2.60716074727901
H    3.28613870486308    -3.17146872734932     4.06658237206271
H    2.10677435841047    -3.48438914538470     2.77130802081125
H    0.90558997184735    -4.58326894857103     4.55147461518715
H    1.66646695080129    -3.54315130274522     5.79692825358853
H   -4.56611255630102    -3.29039325367579     3.50050098483586
H   -5.63458205406972    -1.85868869234722     3.55604227615587
```

```
   H   -4.24427804952648      -1.98584629865438       4.68473512398667
   H    0.23650074426053       3.32869635576850       4.35673057760566
```

TS-3b

251 conformers were generated by CREST, all of which were used for constrained optimizations at the GFN2-xTB level of theory. Subsequently, the number of conformers was reduced to 102 by RMSD calculation and cutoff following RMSD ≥ 0.20 Å^2. All 102 conformers were subjected to constrained DFT optimizations followed by transition state optimizations and frequency calculations.

Electronic energy (a. u.) | DLPNO-CCSD(T)/cc-pVTZ:　　　　–5199.14153903724
Thermochemical Corrections (a. u.) | PBE-D3(BJ)/def2-SVP:　1.916419816326
Imaginary Frequencies:　　　　one (–601.04 cm^{-1})
Gibbs Free Energy (a. u.)　　　–5197.225119220910

```
248

   C    0.09422807874680      -4.60800276859242       0.73958862658690
   C    2.20930147340619      -5.69618050810399      -0.17132035135697
   C    3.58783347690148      -5.57113902538602      -0.57291896453502
   C    4.17556422997305      -4.27812278274923      -0.63465851865661
   C    3.45491297446671      -3.12162323614265      -0.35959878254175
   C    2.10334784522949      -3.26102922790282       0.09331151331645
   H    5.22916331629789      -4.18890647547784      -0.94148579191239
   C   -0.26324665292869      -5.45034144792250       1.85215711929401
   C   -0.91402038736349      -3.87001117754379       0.10867863873195
   C   -1.65816145679465      -5.62444953189714       2.17472295170899
   C   -2.64182618439283      -4.92013795541138       1.42527905259852
   C   -2.30129200481210      -4.01000603588747       0.43060937821620
   H   -3.70356448621659      -5.07703071790734       1.66848492435934
   O    1.41917652599341      -2.12527800396372       0.46804324898848
   O   -0.56617394589572      -3.00207105691019      -0.90570029285617
   P    0.13013692375411      -1.54858635445633      -0.47024242821983
   O   -0.74587776232116      -0.75482362345448       0.47644337914684
   O    0.67309386607486      -0.94513685188905      -1.76300868191393
   N    0.00805142640496       1.04660759653443       3.43366487240609
   C   -0.70905041822397       1.57073343057758       2.41268562297851
   C    0.35941017900336      -0.37603324207920       3.45906815663059
   C   -0.40649388391962      -1.05400674757296       4.59603410218332
   H    1.45230338142302      -0.47142041871767       3.64101909495793
   H    0.11248918826833      -0.83051273312985       2.47930750980473
   O   -0.19177079014951      -0.39795743777117       5.83992939887057
   H   -0.05775057623059      -2.09839682139211       4.72216278258460
   H   -1.49150948249923      -1.08338264360223       4.33918361150810
   C   -0.56368096686918       0.98717873850107       5.83228249508366
   C    0.22865016730216       1.70179022350406       4.71168005399297
   H   -0.04824514968193       2.76986766794488       4.65186656655457
   H    1.31129185836628       1.64186694183922       4.95944458114135
   C   -1.30996534424295       2.82215224926961       2.36428133030230
   H   -0.80529324027502       0.86823097259448       1.56494858627361
   C   -2.07586507339731       3.30085716131972       1.23407876964950
   C   -2.64131829111499       2.29862480437078       0.24418229906547
   H   -3.55594248885114       1.82222236302848       0.65067500493562
   H   -1.93409750401181       1.47881666756090       0.01623264070946
   H   -2.91849132633073       2.79371890261660      -0.70443096588050
```

```
C    -2.88662235762503       4.54379307436520       1.48527037341837
C    -4.24312939617811       4.62920535191711       1.10552584827369
C    -2.29057831036829       5.66251650668685       2.11325660761481
H    -1.19569228678987       3.51851914524112       3.20747539853079
C    -3.04113145509140       6.81347042414026       2.38496846498403
C    -4.99405970895212       5.78185984953110       1.38271813210030
C    -4.39941340010477       6.87616367552750       2.02926768592726
H    -1.21572320763201       5.63647893511110       2.35520070032181
H    -2.55713709844145       7.67588382643390       2.86832379692540
H    -4.98846265163916       7.78076345680393       2.24355804543013
H    -4.72816547012797       3.77940960092643       0.60477193957329
H    -6.05476273729381       5.82178888866782       1.09120578624780
N     0.84275676923703       1.67688874376209      -1.30555881112172
C     0.03427087693525       2.42043557893782      -2.13304489876281
C    -0.39782346983815       3.66588632165172      -1.69105137225259
C    -0.06301199451539       4.08828878852195      -0.33263837092050
C     0.96814780001406       3.34447633530394       0.37809554063613
H    -1.12666920891105       3.83800647952345       0.41896116762326
H    -0.08933112892775       5.17169670570422      -0.12746593572253
C     1.34537702300596       2.08776983548779      -0.10466038677624
H     0.93653887864480       0.63792679278823      -1.55239476512391
C    -0.27536769077581       1.76477234311335      -3.44285881318005
H     0.58550966298277       1.89300194640980      -4.13370005014543
H    -1.15195069421365       2.22288497399585      -3.92741130504465
H    -0.40777820171804       0.67505500037160      -3.28910574251861
C     2.27025881360613       1.12451643156602       0.56394970433610
H     3.27036572921885       1.57292445967652       0.69927079738283
H     2.37771625183003       0.19823798907300      -0.02314582741196
H     1.90881474219071       0.88206831715586       1.57830034557923
C     1.46317126128626       3.98549032125904       1.61411637901436
O     1.07355185358259       5.08166075344171       2.00805537767180
O     2.41540176612812       3.27420418205269       2.27088084760137
C     2.98601020031040       3.90580921764822       3.43282131394957
C    -1.31263074254289       4.51034088927894      -2.49889205715959
O    -1.82828921418207       5.50570551191682      -1.72962385696169
C    -2.80230062387426       6.36701991889022      -2.35484296432833
O    -1.61747222113070       4.35405966642847      -3.67451698473853
C     4.06437618763296       2.98878473143470       3.97153883000482
H     2.18080923572878       4.09228119961735       4.17559030232239
H     3.38314367299686       4.90044745706753       3.13969810399560
H     3.64547146628255       2.00415759042117       4.26030225959932
H     4.53811098409966       3.44058657515291       4.86511329997109
H     4.85184338126071       2.81227423914849       3.21168392234353
C    -2.98549611947689       7.58335609992757      -1.47252721856609
H    -3.74728097155508       5.79217964975533      -2.46968694835987
H    -2.45179420582732       6.62093365669394      -3.37641762956423
H    -3.74864820987531       8.25540343443443      -1.91305431146820
H    -2.03820323411617       8.15076682886142      -1.37829405213598
H    -3.32100933487726       7.29329796585958      -0.45804935483376
C     4.32262492230401      -6.73794075466628      -0.93686138230538
C     1.61179995471081      -6.99188326336704      -0.22253222784552
C     2.34792623762759      -8.10623714250524      -0.59819514752739
C     3.71996696940756      -7.98580117188304      -0.94357397386653
H     0.54887783017119      -7.10127999720590       0.03083910320718
H     1.86017728625141      -9.09214064126061      -0.63496910263831
```

```
H     4.29487747074491      -8.87850847815505      -1.23255725250370
H     5.37819441799013      -6.62279967279011      -1.22922027740014
C     1.48829527940653      -4.51461137767772       0.23217135919038
C    -2.02116081489175      -6.47842708664508       3.25815994036895
C     0.70673670661892      -6.10016546254679       2.67240056366697
C     0.32126020029237      -6.90958900505605       3.73152715320081
C    -1.05394386111017      -7.11399704835503       4.02124088070303
H    -3.09062994237564      -6.61018022623983       3.48574164402937
H    -1.34791450487336      -7.76473850189225       4.85858701183640
H     1.77322912478035      -5.94441573663914       2.45834541763688
H     1.08859738177910      -7.39408827041795       4.35421158128759
C     4.12463400004405      -1.79180038139711      -0.53206025262915
C     4.77496136411793      -1.18193069957018       0.57260035072244
C     5.53823639896880      -0.01885430956985       0.35992911672325
C     5.67499907724331       0.55230051473593      -0.91887952340905
C     4.97336674578215      -0.03620804140295      -1.98605964560166
C     4.19534501022789      -1.19702474052364      -1.82227078560762
H     5.07111909696856       0.41136352446678      -2.98582158206025
H     6.06909576065587       0.44698453053520       1.20417953052725
C     4.71676185701706      -1.81209794688142       1.96074392184174
C     4.48470900689434      -0.78562616284093       3.07880983895080
H     4.33694604813435      -1.29801369527511       4.05133439130019
H     3.58866125380320      -0.16717471960131       2.87564716302929
H     5.34799372721245      -0.09930048661857       3.20025736474041
C     5.98485522664999      -2.64351172925828       2.22607492465482
H     3.85409947911298      -2.50942329327154       1.96910519961209
H     5.94386509070659      -3.12421158450627       3.22539085410570
H     6.89078240351905      -2.00249466146200       2.19008844988216
H     6.10679707807857      -3.44236464249298       1.46787457603064
C     3.49823064005649      -1.81675310677036      -3.03063085350321
C     2.93170742796154      -0.76625786386994      -3.99711690514809
H     2.29393736644318      -1.25794292547945      -4.75868374135613
H     3.73329614611774      -0.22392321354702      -4.54071893096916
H     2.30518559049212      -0.02941855546913      -3.46258666071769
C     4.44135306468843      -2.77499676946004      -3.78121601484613
H     2.63726386962994      -2.39846652024422      -2.64446253739862
H     4.79137368600478      -3.60201527559761      -3.13434355723453
H     5.33580154380146      -2.23274146271863      -4.15377895217332
H     3.92618329711699      -3.22445171389588      -4.65497688656306
C     6.60975866023909       1.69523015738739      -1.16747800808608
C    -3.33072526931852      -3.18041654095284      -0.26381055389681
C    -4.09684005092068      -2.23748389427026       0.47950015606217
C    -3.55274893450715      -3.33176830306767      -1.66044046147286
C    -5.06575891763246      -1.47091910234310      -0.19191482146810
C    -4.54525500635948      -2.55376394202084      -2.28107930600977
C    -5.31422256716191      -1.61948713828586      -1.56693757660252
H    -5.66896247135496      -0.74151397556795       0.37075368517766
H    -4.75114235629934      -2.69454732350948      -3.35315735718121
C    -3.93277671259275      -2.04119577773806       1.98474350326652
C    -3.69500926643498      -0.57164926488418       2.35519886965012
H    -4.56304608688855       0.07042238458496       2.09844405283691
H    -2.80458171070839      -0.18979183352966       1.82471161888693
H    -3.53064235068218      -0.46660579780709       3.44733865957498
C    -5.13738862869784      -2.61881300361864       2.74892264165407
H    -3.02984962242543      -2.60005666561796       2.30096608736140
```

```
H   -4.99600140711685    -2.51791007679981     3.84513774596966
H   -5.29301615747000    -3.69245835446300     2.52093034466990
H   -6.07367862218825    -2.08714712022500     2.47829076402752
C   -2.80156293035497    -4.35859183589043    -2.50274335838598
C   -3.75008094261307    -5.47507689906129    -2.97458593820233
H   -3.19267774758795    -6.25047672334517    -3.53952485108758
H   -4.54313799520953    -5.07815300798816    -3.64217766669236
H   -4.25006482645382    -5.96709123575304    -2.11587297238848
C   -2.06100064002727    -3.70366548578372    -3.67994154257992
H   -2.03861821103339    -4.83482876359919    -1.85672885837821
H   -2.76749167162999    -3.23598410803118    -4.39743207240346
H   -1.47562154644823    -4.46231296347764    -4.23915687920366
H   -1.36003216191638    -2.92543340076267    -3.32141463623445
C   -6.41845287067255    -0.85671025119713    -2.23012419334369
C    6.12754534997537     3.01111816846116    -1.39328412401246
C    8.00908283152456     1.43767466325936    -1.21374295299688
C   -7.74068982419125    -1.37493728228543    -2.18102443921397
C   -6.15962925649189     0.37052500744784    -2.89574781689593
C    7.05230446173359     4.03878180507767    -1.65913143221223
C    8.89164016263829     2.50119168420509    -1.46920752212912
C    8.43631094780945     3.81126867837045    -1.69836819373285
H    6.68301390933222     5.06185672807843    -1.83820043354445
H    9.97370312282425     2.29560651723128    -1.50071780845298
C    8.57362953319676     0.03455785993945    -1.00028369128101
C    9.48537276243106    -0.40558322237372    -2.15700239266504
H    8.95772048705866    -0.34131893401529    -3.12967420988556
H    9.81703128104521    -1.45458896748520    -2.01415697729261
H   10.39791426460127     0.22201221962805    -2.22742776756315
C    9.29254781360883    -0.07551986723821     0.35508280320042
H    7.71680733551187    -0.66807470233265    -0.97531239837017
H    8.61405355797727     0.18560770211839     1.19208764945448
H   10.16392936652985     0.61054630110115     0.40631058436628
H    9.66396420365193    -1.10758700958445     0.52447104130596
C    4.63793304422631     3.33908938314214    -1.35437570895171
C    4.07403216813816     3.59848524571404    -2.76233853984399
H    4.56422119252985     4.47436065383159    -3.23655878789799
H    2.98375138775448     3.80439679954838    -2.71824136785134
H    4.23117538659346     2.72582025908600    -3.42719577436959
C    4.33051865717789     4.51136175927447    -0.40900439321730
H    4.12090041698659     2.44289075015291    -0.95958167546286
H    3.23976408103447     4.70052979508961    -0.36332495229822
H    4.81049299505651     5.45103099770870    -0.75103969569494
H    4.69064508547645     4.30543306667257     0.61895100919362
C    9.40745848079069     4.94446363070367    -1.99856228570161
C   10.10826606451868     4.73560939866089    -3.35206785607041
H   10.73344066288832     3.81853074866019    -3.33939280993323
H   10.77251159656611     5.59126903820438    -3.59292200207654
H    9.37230940345660     4.62684481062848    -4.17350026773692
C   10.42869052061939     5.14353928103092    -0.86641387543930
H    8.80167138828698     5.87423097455138    -2.07340305039346
H    9.92513146929907     5.31454836587210     0.10600610101313
H   11.08528378418392     6.01328801077552    -1.07446769771835
H   11.08211402739168     4.25349680586361    -0.75411672785279
C   -8.78029384133773    -0.65232020516409    -2.79209485913855
C   -7.23315395646154     1.05172819059562    -3.49949468564865
```

```
C    -8.54906140849275     0.56274500868910    -3.45904619691120
H    -9.80481582957793    -1.05487977917902    -2.74588990744417
H    -7.04419486424276     2.00272621167532    -4.02203634938907
C    -8.05267672392977    -2.67895666915002    -1.45154774883861
C    -8.87703888275748    -3.65265227453758    -2.30738694973976
H    -9.00638717069703    -4.61999165464306    -1.77994912125935
H    -8.38062304346718    -3.85442802188264    -3.27779649718364
H    -9.89205049979479    -3.25923167692579    -2.52392235510523
C    -8.73667784631076    -2.39858685450581    -0.10185051950054
H    -7.08437373015745    -3.17275515989028    -1.23222047396244
H    -8.93033431847068    -3.34198125102647     0.44979578587530
H    -9.70874821350137    -1.88192315520650    -0.24605230106891
H    -8.10468068362777    -1.75148779833321     0.53903881305242
C    -4.74020671617592     0.92178562718568    -3.00005516172866
C    -4.67179832208113     2.45196698446311    -2.89115624872613
H    -5.16115265276874     2.95256371639146    -3.75170387674677
H    -3.61861841809742     2.79424942755498    -2.89569119201940
H    -5.16032476643390     2.81850536433553    -1.96540207428026
C    -4.06608978708491     0.44153113152986    -4.29919617884018
H    -4.16322681805876     0.49459509028738    -2.15189499417129
H    -3.02091421089211     0.80724711193910    -4.35937557527834
H    -4.61436706186444     0.81797751535316    -5.18779532215468
H    -4.04181575101702    -0.66370898510372    -4.35769182090914
C    -9.68969499098669     1.33790093815269    -4.10449691108923
C   -10.66729914555962     1.87807280715617    -3.04619331757538
H   -11.15870517235296     1.04748172021920    -2.49780106910378
H   -11.46579325232634     2.48944429250348    -3.51548637722799
H   -10.14290436209979     2.50709790873801    -2.29932837129299
C   -10.42318888913280     0.50576051068488    -5.16868250327299
H    -9.23333333656806     2.21300969310273    -4.61749338160896
H   -10.92320808833943    -0.37582832182949    -4.71613390596952
H    -9.72251227643166     0.13242567716397    -5.94195268694789
H   -11.20646373308675     1.10861513640887    -5.67285543646122
C    -2.09345971634559     1.21033904962861     5.67174125700428
C    -0.21438242017111     1.58582467746196     7.22214967154289
C    -1.52179595043462     2.17776473162238     7.78966623737299
H     0.56869150974818     2.36619304580222     7.11766308237651
H     0.21342079484273     0.78278632693116     7.85221812477716
C    -2.39006018889546     2.43259165051492     6.54735767625218
H    -2.60297359516103     0.31571733881991     6.08860439434736
H    -2.41894484012679     1.32540057430335     4.61943566859225
H    -3.46775249222166     2.55440088403721     6.77508149634128
H    -2.06595812686124     3.36282130566114     6.02985535666242
H    -1.35675740498879     3.08274526693883     8.40739198834788
H    -2.02516022901963     1.43056555627441     8.43853225202190
```

TS-4c

329 conformers were generated by CREST, all of which were used for constrained optimizations at the GFN2-xTB level of theory. Subsequently, the number of conformers was reduced to 62 by RMSD calculation and cutoff following RMSD ≥ 0.50 Å^2. All 62 conformers were subjected to constrained DFT optimizations followed by transition state optimizations and frequency calculations.

Electronic energy (a. u.) | DLPNO-CCSD(T)/cc-pVTZ: –5199.13908137966

Thermochemical Corrections (a. u.) | PBE-D3(BJ)/def2-SVP: 1.917406181065
Imaginary Frequencies: one (–724.80 cm^{-1})
Gibbs Free Energy (a. u.)   –5197.221675198590

248

```
C    -0.51336830912119    -4.53605319174477     0.81413541408959
C     1.28239683705291    -5.92994922385491    -0.32878451608226
C     2.60257896358686    -6.01552271583651    -0.90024488000213
C     3.36887511867203    -4.82773809228438    -1.04885466102643
C     2.87463685033309    -3.57474945870303    -0.70277494151210
C     1.57570752823440    -3.50498968712038    -0.10113494018059
H     4.38233562104901    -4.89920486551549    -1.47336681751594
C    -0.84124409295830    -5.30603610927882     1.98684248351149
C    -1.47941882734575    -3.66816266134783     0.29279564573367
C    -2.19380667785380    -5.27628934848331     2.48635438309464
C    -3.16067571792578    -4.46015301475241     1.83443137293475
C    -2.82603528329657    -3.62423555773255     0.77578949616283
H    -4.19707383416313    -4.47083307195306     2.20335024339064
O     1.11393051037870    -2.28193186584744     0.33153704571214
O    -1.13942818840440    -2.84822797759048    -0.76451665190494
P    -0.20555173660241    -1.50693383219109    -0.40329900324709
O    -0.83351156445358    -0.64023575657088     0.66778817943172
O     0.23109741573877    -0.91950693957589    -1.74183776335832
N     0.48145209590935     0.80247799319961     3.57889485570907
C    -0.22655726300430     1.62599809886260     2.77881345614619
C     0.31316052101891    -0.65233568202457     3.52009154612162
C    -0.31096223246091    -1.13420721974034     4.82817708105224
H     1.31622792407904    -1.11401184049134     3.40183751139571
H    -0.29618538579327    -0.91541152503063     2.63235638905739
O     0.44243418523258    -0.70818064149648     5.95673417348813
H    -0.32575141289820    -2.24225867080122     4.85409275212945
H    -1.36680295735014    -0.77631729782246     4.89172070636827
C     0.60419646707147     0.71386515289652     6.03705551405255
C     1.26462698322454     1.21949649737949     4.73214416850507
H     1.38129912167075     2.31685941587350     4.74924079462285
H     2.28085967725428     0.78099422328374     4.64348245454245
C    -0.27285184294249     3.01589205796615     2.85126305393711
C    -1.01520944552507     3.92380290622851     2.00340695756295
C    -1.04249415604808     5.35735591774675     2.52168559662132
H    -1.34304899682187     6.06706046040646     1.72794330982876
H    -0.03596585078451     5.64793770218371     2.87863551787232
H    -1.74756283336308     5.46281685677824     3.37301250168461
C    -2.21125004771442     3.48864214338608     1.20734713089131
C    -2.17096232197320     2.37396110973470     0.33704646947241
C    -3.41940465897859     4.22224926001301     1.27710169832659
H     0.34995686718262     3.51352607942792     3.61030969568920
C    -4.54046154647427     3.84879695211570     0.52379921390840
C    -3.29097465001268     2.00470716207690    -0.41953776929628
C    -4.48246952431513     2.74042926514734    -0.33535995774293
H    -3.49510298041074     5.09149104429163     1.94498773899861
H    -5.47148083385214     4.43020836511799     0.60899154374512
H    -5.36152992796894     2.44321672972480    -0.92578009836017
H    -1.27523460389859     1.74738331656436     0.25211801262208
H    -3.22744532685128     1.11116924506071    -1.05670971410389
```

```
N     0.94422482686661      1.60679308453888     -1.16026657281009
C     0.19622028611809      2.55748581045899     -1.80635910129396
C     0.14436930975595      3.84063107679961     -1.26862097394886
C     0.79195639750668      4.11183836532551      0.01444731819571
C     1.68785789872737      3.08668171744277      0.54442948858742
H    -0.15885754905566      4.11215536197593      0.92736754710202
H     1.08866706924254      5.15871281824820      0.19034506149363
C     1.69229316439186      1.81792036127963     -0.03623447870719
H     0.80037502518173      0.59489704782978     -1.47639146480470
C    -0.50880069768056      2.07703586194460     -3.03567154162621
H    -0.54200259415281      0.97076312493356     -3.04043697261065
H     0.01722745794423      2.43160193945221     -3.94564785583098
H    -1.52734663769728      2.49834001961687     -3.09211560667210
C     2.45735821406962      0.64408688020800      0.46750910920099
H     3.48785692915989      0.92740740237161      0.73982918465561
H     2.47262404872126     -0.17193571206105     -0.27271037629180
H     1.99584538942224      0.26894638434980      1.40022586846941
C     2.50939394114838      3.37137131428658      1.73880918460694
O     3.19461130015624      2.57936226471410      2.37555395255680
O     2.44229580999050      4.69860453776940      2.07099090475495
C     3.23884127036382      5.09616856580870      3.20081379037159
C    -0.66621706578587      4.89291681700441     -1.91798284218915
O    -0.79937671875999      5.97909965607046     -1.09783192436724
C    -1.59979674404306      7.06291212469430     -1.61779134190531
O    -1.17279075236877      4.83434352054939     -3.02997503752573
C     3.11804836102230      6.59845951884782      3.35441755844078
H     4.28749808615749      4.77166617928198      3.03345626520751
H     2.88229953695464      4.55273794138405      4.10382969411388
H     2.06815773112957      6.90231258120252      3.53959286675171
H     3.47184221133686      7.11880263888155      2.44244253247882
H     3.73176400347645      6.94337551096665      4.20988969883930
C    -3.08231901328232      6.83461950584248     -1.37240880707325
H    -1.39259327934757      7.16651709319168     -2.70214390368669
H    -1.22996231146375      7.96274856295767     -1.08772855825020
H    -3.29817300154450      6.71066425660312     -0.29341862880931
H    -3.43034485198215      5.92630585280364     -1.90108507915396
H    -3.66419551954168      7.70028806370605     -1.74874424381988
C     3.10006220590735     -7.27980070865296     -1.33408330389918
C     0.49567203447979     -7.12044285661338     -0.27753475242377
C     1.00133570759274     -8.33309736863241     -0.72302745975614
C     2.31980506518402     -8.42144257270058     -1.24304653275777
H    -0.52978972804193     -7.06767179024257      0.11198334362004
H     0.37053508055343     -9.23388502051185     -0.67857688006467
H     2.71159271347192     -9.39061096564142     -1.58687066618476
H     4.11525611492223     -7.32570936877584     -1.75856574948832
C     0.80368086947267     -4.65240985069763      0.13570881932673
C    -2.52846179346393     -6.04994589088772      3.63705344565509
C     0.12669657270902     -6.07438335288299      2.70008217488402
C    -0.22691781476885     -6.80121823157720      3.82799590479473
C    -1.56778416152187     -6.80163418312717      4.29593853464957
H    -3.56771866948862     -6.02576702736562      4.00084074212890
H    -1.83819274336492     -7.38814155906435      5.18698106558537
H     1.16760298046881     -6.07535210347933      2.34787289516382
H     0.53973102681160     -7.37881673138900      4.36640904910381
C     3.72369519392697     -2.36437145659852     -0.95201682247251
```

C	4.67578006169839	-1.95300351441108	0.02140624611344
C	5.53566231073589	-0.87950349624152	-0.27886855713505
C	5.49566226750256	-0.22212719587319	-1.52162354494204
C	4.52919981157066	-0.63001620025828	-2.45756480479280
C	3.64372955171236	-1.69366594204332	-2.20464516673191
H	4.50647536823979	-0.12939329438953	-3.43617916346095
H	6.28771927172369	-0.56193343417578	0.45790304571202
C	4.77001784704438	-2.65287301935535	1.37528179431016
C	3.85276893909617	-1.97441760539463	2.41013589196338
H	4.16810197699619	-0.92471849852317	2.58824668756073
H	3.88726698737562	-2.51202780229338	3.38048256529316
H	2.80413936595022	-1.95924451592948	2.05702551503753
C	6.20701886253481	-2.76744627425462	1.90303029740966
H	4.38803471543625	-3.68504974065086	1.23099324712793
H	6.23296786162770	-3.40206635532551	2.81201948930507
H	6.62496316551862	-1.77953633469709	2.18737829883995
H	6.88547259242776	-3.21656278935408	1.14976670413449
C	2.68890598775830	-2.15708741442661	-3.30150882176793
C	2.18993521393342	-1.01353128726162	-4.19598639299108
H	1.80198926066944	-0.17121888121584	-3.59457161947530
H	1.36374281912785	-1.37165558069466	-4.84199954329315
H	2.98842572461782	-0.63119290134579	-4.86559792235191
C	3.34507120310245	-3.25230488893784	-4.16385314395646
H	1.79915134964227	-2.58706240500532	-2.79969602757078
H	3.62991396276588	-4.13685818305529	-3.56306405927575
H	4.26190433858248	-2.86376674936514	-4.65501703619838
H	2.64914760352582	-3.59276949648936	-4.95811138141771
C	6.53683341932642	0.78325431763530	-1.90976170676254
C	-3.81431937141445	-2.69385495323299	0.15383874668612
C	-4.31599344139669	-1.58780207010415	0.89596281391405
C	-4.24331619678952	-2.90112353380768	-1.18480864036651
C	-5.19837633631731	-0.69725000926531	0.26412184777769
C	-5.17427833516674	-2.01264834240068	-1.75013601560849
C	-5.65059389356473	-0.88696370186511	-1.05674983188051
H	-5.54286308953543	0.18908599249995	0.81395056557925
H	-5.54109388769507	-2.20455510003293	-2.76830073558441
C	-3.95820471579416	-1.34928328392514	2.36118012481565
C	-3.57319083524760	0.10622059538298	2.65492801454452
H	-4.43225240673339	0.80139821837976	2.55536082910026
H	-2.78664568065632	0.44192943990443	1.95821800891221
H	-3.19533151124505	0.20505698220421	3.69385487464551
C	-5.11204388293472	-1.79851478000325	3.27760055475311
H	-3.07228758761856	-1.97448834542295	2.59238829248423
C	-3.75172684557597	-4.07003555875520	-2.03240943080729
C	-4.89845391141992	-5.04142767891490	-2.36151041458976
H	-5.68128844856563	-4.55252629431402	-2.97834416233050
H	-5.38495465506994	-5.41833052725493	-1.43926543264074
H	-4.52016280595561	-5.91381896455030	-2.93321985495189
C	-3.03699585054173	-3.58146777008063	-3.30444359275260
H	-3.01022219560456	-4.63721149645983	-1.43489591654960
H	-3.73307479211217	-3.03911380348914	-3.97832082529798
H	-2.62515635329161	-4.44055806585297	-3.87317618678527
H	-2.20007880382093	-2.90357862896407	-3.04863468457669
C	-6.59108556284549	0.10040990586013	-1.66823345070975
C	6.27276775179384	2.17893974321554	-1.89457931752977

```
C    7.80417093048098      0.30894437573787     -2.34657030106269
C   -7.82621782486925      0.39200291925280     -1.01953834475028
C   -6.24104731984276      0.81598292923242     -2.85520756651870
C    7.27570919533882      3.06694192641714     -2.32156942393778
C    8.78077346489131      1.24040546533985     -2.74561696325689
C    8.53910816357532      2.62253621374951     -2.74708615661193
H    7.06189194844341      4.14743882801888     -2.31820664243452
H    9.76688896527713      0.87769623639888     -3.07907863573134
C    8.13167251103268     -1.18208905675259     -2.38658770011231
C    8.68635070395012     -1.62424575858265     -3.75013378333490
H    7.99589812823745     -1.34997200868740     -4.57283377305848
H    8.82860386256213     -2.72425402357129     -3.77321120928197
H    9.67107995986008     -1.16126242025729     -3.96857236603454
C    9.08420316936217     -1.56795795129301     -1.24167204819759
H    7.18376211766212     -1.73376584030497     -2.22659991230695
H   10.05446841186306     -1.03586523628004     -1.33108919052626
H    9.29294845968770     -2.65807415408438     -1.24964109373907
H    8.65103655748538     -1.30996274015285     -0.25475164805831
C    4.92325905804687      2.73315027087068     -1.44647967705481
C    4.06587300487443      3.16465780872280     -2.64920611436332
H    3.88895894234118      2.31878719366322     -3.34304342925491
H    4.56433643621188      3.97306566920689     -3.22383833606895
H    3.07823842276353      3.54453985539861     -2.31278963241497
C    5.07250245075286      3.87830223176006     -0.43225487983837
H    4.38730811338411      1.90581707119597     -0.94110737429122
H    5.63872991441370      4.73303691551659     -0.85587221915631
H    5.59933987866148      3.54105778188598      0.48262154950732
H    4.07989982747766      4.26912655515105     -0.13460534737192
C    9.61414520628058      3.60624847423624     -3.18797742247935
C   10.06204100914039      4.50823160834842     -2.02504995862616
H   10.88240241825552      5.18619756802418     -2.33951579318744
H   10.41948156289587      3.90745894265416     -1.16500852668680
H    9.22368078310882      5.14087423115437     -1.66587485787949
C    9.16544430997928      4.43924777940862     -4.40009505453052
H   10.49300899109481      3.00132096610821     -3.50216804201156
H    8.29626957531798      5.08109845273600     -4.14612889628088
H    8.86566679125245      3.78961125182913     -5.24648222946480
H    9.98153834374651      5.10617627437090     -4.74700474897363
C   -8.64633713583291      1.41558779457328     -1.52935834385178
C   -7.10327840352757      1.82253980572166     -3.32349656292019
C   -8.30142441349243      2.15548198432729     -2.66913466334544
H   -9.59686357380709      1.64615548851115     -1.02028435707464
H   -6.81753228360449      2.38095911321436     -4.22832446191838
C   -8.32390640552643     -0.39548757599907      0.19227902811194
C   -9.66285628770185     -1.09267297599829     -0.10515354731218
H   -9.58334074994529     -1.74956648699460     -0.99427492995315
H  -10.47477898285799     -0.36140601053050     -0.29959535361553
H   -9.97685955136859     -1.71730004690773      0.75654434027111
C   -8.42257431311580      0.48434191104814      1.44976822508392
H   -7.58353521385282     -1.19228710245603      0.39996590368846
H   -7.45314233915927      0.96809227641516      1.68557911750889
H   -8.72699850827398     -0.11870089658149      2.33026663687915
H   -9.17276173401273      1.29240287212772      1.32147105717617
C   -4.96331849890935      0.53362924390278     -3.64437420066581
C   -4.20649904402811      1.80704679120721     -4.05615472257743
```

```
H   -4.77049284149788      2.40312895314413     -4.80284612222010
H   -3.23903040812276      1.53862883317887     -4.52629599302503
H   -3.99665568684604      2.46525736057685     -3.19049611009933
C   -5.27154807336343     -0.31897890245798     -4.89040662098810
H   -4.28893419823685     -0.05810514632250     -2.99263770905732
H   -5.92273459544825      0.23934066401033     -5.59504060774680
H   -5.79911437226278     -1.25809741824602     -4.63135176637378
H   -4.33763477899294     -0.58673790694270     -5.42635749627142
C   -9.18190190027276      3.29298107089904     -3.16506137272681
C   -9.64893911102558      3.07639004080727     -4.61354236031127
H   -8.79091621908154      3.07172790986582     -5.31745522158930
H  -10.33593345753845      3.88677180821048     -4.93327463207099
H  -10.17868901593141      2.10937615064265     -4.72544797610249
C   -8.47310029463202      4.64919469124870     -3.00139979857849
H  -10.08614774673063      3.30544006475889     -2.51747815439333
H   -8.16906951296020      4.81840212687471     -1.94869517001087
H   -9.13411604674057      5.48545149016321     -3.30998255143136
H   -7.55600564145643      4.69668367197178     -3.62484079802030
C   -0.72866457055988      1.46283743444634      6.32073112172415
C    1.50682719040599      1.02378649140604      7.26270046711831
C    0.70064073238512      1.96926778888360      8.17773722043820
H    2.45492783807836      1.49597546436460      6.93042264849053
H    1.77688296763703      0.06712435117966      7.74895878811245
C   -0.32078480181999      2.62397408986180      7.23438770911324
H   -1.38925683690128      0.76317667601325      6.87522847430814
H   -1.26508155291272      1.78068314242267      5.40459564020913
H   -1.17867576907090      3.08833586885692      7.76069529553135
H    0.16369547601347      3.42866752245499      6.63723072098166
H    1.33657642125771      2.69922444200988      8.71689335000642
H    0.15874256367481      1.38106303104762      8.94784208461547
H   -5.38285803081252     -2.86089936007579      3.11683851240373
H   -6.02256262683233     -1.19261017516930      3.08537446962203
H   -4.84018662703263     -1.67208896819003      4.34637235701486
H   -0.78872239918602      1.07518065586514      2.01007961599568
```

TS-4d

948 conformers were generated by CREST, all of which were used for constrained optimizations at the GFN2-xTB level of theory. Subsequently, the number of conformers was reduced to 650 by RMSD calculation and cutoff following RMSD $\geq$ 0.15 Å^2. After constrained DFT optimizations, the number of conformers was again reduced from 650 to 337 by RMSD $\geq$ 0.20 Å^2. All 337 conformers were subjected to transition state optimizations and frequency calculations.

Electronic energy (a. u.) | DLPNO-CCSD(T)/cc-pVTZ: –5199.13885404644
Thermochemical Corrections (a. u.) | PBE-D3(BJ)/def2-SVP: 1.917685659392
Imaginary Frequencies: one (–715.85 cm^{-1})
Gibbs Free Energy (a. u.)   –5197.221168387050

```
248

C   -0.23530307789734     -4.49685417164055      0.75214719740913
C    1.56993853921369     -5.79723108474331     -0.47833910588854
C    2.86378667722121     -5.81961155701404     -1.11249225261786
C    3.56625357431739     -4.59714929465410     -1.29153675125061
C    3.03469669624225     -3.36973090609843     -0.91069688977076
```

```
C    1.76929560565203     -3.36402779390232     -0.23702609832292
H    4.55758127024154     -4.62048711903453     -1.77036205365498
C   -0.48922192037698     -5.30341275166464      1.91853574927957
C   -1.26054067743996     -3.67118914134077      0.27640732157208
C   -1.82874883961238     -5.36194214711248      2.45035754791982
C   -2.85783682023312     -4.59346362902830      1.83604369191465
C   -2.59660846722575     -3.71853939973443      0.78806748456482
H   -3.88260062909933     -4.66956791196205      2.23001678827654
O    1.27788073633353     -2.16856869519721      0.24054504944651
O   -0.99607910843161     -2.80955583394725     -0.76809624648386
P   -0.09919370649107     -1.43841159124012     -0.42734192207308
O   -0.70986537574896     -0.60434298623864      0.68079481883511
O    0.25134420624316     -0.82050680459522     -1.77744517774448
N    0.75779151690378      0.87230392051855      4.10565770803936
C    0.08710728639467      1.97243653812011      3.70432549631364
C    0.74911200070544     -0.41570216529011      3.41612228672176
C    0.14942266400395     -1.48055188759080      4.33258844121113
H    1.80332911367319     -0.68471436947375      3.19460503072105
H    0.19304160004656     -0.37439952429846      2.45886235736019
O    0.81835253325002     -1.52748611850812      5.58748806995130
H    0.26396132655500     -2.48046106415423      3.86849476019926
H   -0.94219951002201     -1.28801757437150      4.46250832758761
C    0.80034811095574     -0.27912142202670      6.29020514587409
C    1.43375558058771      0.81122854274256      5.39043929288669
H    1.37842284553703      1.80050853391133      5.88620941896617
H    2.50538314816651      0.56081471563709      5.22698536096565
C   -0.70544343310727      2.10917848670649      2.57699344096777
C   -1.41379244508188      3.32151729935702      2.22664703057267
C   -1.39791614809143      4.48772765271682      3.20217786907807
H   -2.09903286771650      4.31545858555365      4.04570683448383
H   -1.69000855024573      5.42867491306367      2.69948971737219
H   -0.38481838857066      4.65011799398584      3.61207865912251
C   -2.62379830327356      3.17716231010866      1.35637247146205
C   -2.70318667101778      2.14954380579700      0.38393975857241
C   -3.70909591654042      4.08119239370424      1.45149102613915
H   -0.81024587625218      1.24057674987328      1.91145175075233
C   -4.83078486796693      3.95989427852293      0.62008021471614
C   -3.82160904360978      2.04057058200659     -0.45168587096115
C   -4.89259758755623      2.94039153674390     -0.34408508018914
H   -3.69028036452255      4.88312172703050      2.20201954437035
H   -5.66916331793985      4.66513404824672      0.73053524745586
H   -5.77075449574378      2.83473701878538     -0.99892097712784
H   -1.91224376049495      1.38934191672650      0.29484532582012
H   -3.86370915279965      1.22026857522236     -1.17960412976934
N    0.74060238186064      1.72920928466815     -1.09924110514612
C   -0.17732192174711      2.61543011986490     -1.59686959050129
C   -0.35593689838069      3.82921413940925     -0.93697990331801
C    0.33542576360101      4.06796794370486      0.32777873943278
C    1.38129433705500      3.12166245235356      0.71681946324575
H   -0.58700757621459      3.83871830370935      1.24168512539722
H    0.49850552396677      5.12207091649435      0.60386188705945
C    1.52571265430974      1.93374173223734     -0.00108225052407
H    0.69475740932440      0.73542840276182     -1.49020781198908
C   -0.90616313580196      2.15103026941279     -2.81750785947490
H   -0.76714007725766      1.06083886342801     -2.94734423006868
```

```
H    -0.53911788307790     2.68407876461275    -3.71802358026720
H    -1.97914664756663     2.39573840491461    -2.74107530401527
C     2.47840225212774     0.83454261653641     0.32104254288124
H     2.10627817711003     0.25600005427719     1.18559638664875
H     3.45945066421793     1.23352218905656     0.62560072223204
H     2.58919535613895     0.14364968191793    -0.53058977092693
C     2.21083701865547     3.38320854449942     1.91038892600210
O     3.02686396454952     2.62755694325431     2.42554715543633
O     1.95783442477005     4.63603897070217     2.41140038245324
C     2.74900326072782     5.03319081727430     3.54824572885560
C    -1.36571789108362     4.80104668227310    -1.41289074065145
O    -1.54385539233094     5.79866314760968    -0.49872228227299
C    -2.58562413263273     6.74234900985121    -0.81098553928692
O    -1.99594394672214     4.74654004072403    -2.45946849178298
C     4.09662517461596     5.59443303277059     3.12353324478689
H     2.88205929342677     4.15605370818090     4.21492061444494
H     2.13439796986806     5.79693981173031     4.06550076027628
H     4.65318081114536     5.96246182320456     4.00904427693953
H     3.96901654063612     6.43875948798459     2.41732763855033
H     4.70540750400403     4.81072064683631     2.63308028600517
C    -2.67300501575439     7.73381400602564     0.33060463434181
H    -3.53469543205341     6.18358778598707    -0.95436103888676
H    -2.35058907716648     7.23356933477586    -1.77908285305553
H    -3.45101652853948     8.49305587035277     0.11642280699527
H    -1.70855594003170     8.25907924419508     0.47987851611850
H    -2.94171239157885     7.22466543737154     1.27785809519608
C     3.39645084796248    -7.05744212563850    -1.57967064540085
C     0.83943488211808    -7.02191805081152    -0.40349942949591
C     1.37709779253524    -8.20764808469179    -0.88255704038961
C     2.67313923653415    -8.23361605611754    -1.46229612987967
H    -0.16844567418793    -7.01759725455258     0.03225930426174
H     0.78918591820229    -9.13580668833424    -0.81789152407562
H     3.09153057340937    -9.18198087116596    -1.83184912224710
H     4.39182193770394    -7.05506280317866    -2.05102062683711
C     1.05917379877417    -4.54577663015658     0.02288504566510
C    -2.08823782272255    -6.17273571368689     3.59476680357062
C     0.53954187892778    -6.02568247610891     2.59372377882750
C     0.25758511840949    -6.78963265592586     3.71727509103310
C    -1.06877338624595    -6.87657966571813     4.21717054045243
H    -3.11760473044620    -6.21542573728778     3.98403118774931
H    -1.28177224224920    -7.49158546961768     5.10454901735144
H     1.56932558288670    -5.96012091462346     2.21560518758794
H     1.07011771324812    -7.32892117854174     4.22732578475448
C     3.80908188996074    -2.11927110046288    -1.20428666792881
C     4.79381854967382    -1.66138751974585    -0.28583301930291
C     5.56937067900287    -0.53665491637294    -0.62463461881133
C     5.41719020921803     0.12563292458436    -1.85578175337269
C     4.43137994364003    -0.33905597787992    -2.74371909055766
C     3.62375046564478    -1.45267667304396    -2.44807090060805
H     4.32136780951368     0.16805045768097    -3.71316096105364
H     6.33856332434959    -0.17542520581774     0.07336969023837
C     5.01420281736532    -2.37149204744954     1.04788031171705
C     4.10603924171994    -1.78563535820777     2.14512608113283
H     4.34792805448498    -0.71804329256967     2.33190371602575
H     4.23118594068232    -2.33793294111810     3.09953907876235
```

```
H    3.04203099268020     -1.84560324914980      1.84798577917605
C    6.48254308916364     -2.38623162221046      1.49512314582877
H    4.70330028984766     -3.42697584787975      0.90112226808284
H    7.15016809275820     -2.76778439044971      0.69620590328221
H    6.60524772583819     -3.03459427357544      2.38624574906093
H    6.84144530732575     -1.37529082418107      1.77940283110668
C    2.63847875479800     -1.96895354263615     -3.49381713769547
C    2.01750471215493     -0.85658515151650     -4.35028011024841
H    1.18763500963942     -1.26890540403586     -4.95834395155602
H    2.75238738953957     -0.41457824925823     -5.05546753296602
H    1.59960870791281     -0.04929453875575     -3.72123318706811
C    3.31346978813026     -3.01706485285264     -4.39918476516786
H    1.80843097215570     -2.45898432096449     -2.94698616167151
H    2.59502350756662     -3.40365490436659     -5.15112881514994
H    3.69358777493234     -3.88013595785051     -3.82024729902229
H    4.17088743631547     -2.56821074623423     -4.94348163312510
C    6.34801594338123      1.22357467910107     -2.27161937059303
C   -3.64231865093110     -2.82347955660857      0.21056022543511
C   -4.18405250981583     -1.76584810155611      0.99394949784441
C   -4.07774337384437     -3.00409646641084     -1.12948464271385
C   -5.08837375726101     -0.87630073144376      0.39212423233324
C   -5.04986340776485     -2.13581894902452     -1.65569641395137
C   -5.55072362666891     -1.04079727288094     -0.93011590907311
H   -5.44898493081471     -0.01500077999918      0.97106987333779
H   -5.42954262407754     -2.32148515495298     -2.66941777796845
C   -3.86428183629399     -1.59495552358308      2.47708840440146
C   -3.41718347453313     -0.17592037669982      2.84234648463068
H   -3.16351211333241     -0.11375686410316      3.92163680743628
H   -4.20110460200943      0.58369391894357      2.64490575330316
H   -2.52228843821230      0.09718141984395      2.25851662021037
C   -5.06921620291824     -2.03484447898621      3.32946691573046
H   -3.01730032931983     -2.26850367082487      2.71391725605649
C   -3.55447819226883     -4.12809787602267     -2.01783763527113
C   -4.66615239685130     -5.13787036673245     -2.35156949546620
H   -5.47901271819249     -4.66696385084908     -2.94322709984108
H   -5.12079994365591     -5.55638654776261     -1.43103646655056
H   -4.26300940831297     -5.98001042624973     -2.95104487803373
C   -2.88594663607415     -3.57771734529114     -3.28981874126793
H   -2.77842056165524     -4.67914275179394     -1.44966311254872
H   -3.61796662057037     -3.05071436580014     -3.93698618645671
H   -2.44832634805398     -4.40376361339451     -3.88752513348295
H   -2.07468619612069     -2.87011379390131     -3.03198455737244
C   -6.52901533185826     -0.06703525456910     -1.50478161230870
C    5.95161634612317      2.58518202156753     -2.22697220496275
C    7.64179996714923      0.87898677525950     -2.75459771641228
C   -7.73289926834774      0.22447295811152     -0.79630805668782
C   -6.25475754098831      0.63654789238153     -2.72058528403291
C    6.85387320394223      3.57293870461945     -2.66544661303186
C    8.50992479586804      1.90292491099770     -3.17008591186291
C    8.13719241409625      3.25820335390505     -3.13710771555561
H    6.54943459044303      4.63214717385715     -2.63535072835627
H    9.51135185501269      1.63131529816705     -3.54059665825675
C    8.10886435609834     -0.57316860108033     -2.82291839437752
C    8.65086805950384     -0.94998277515180     -4.21079344510825
H    8.89670639254247     -2.03107641860957     -4.25137098175191
```

```
H     9.57806598259694    -0.39371814963690    -4.46172138871075
H     7.90621189385774    -0.73733613676470    -5.00389531103079
C     9.13651607958451    -0.87436129045871    -1.71807611282571
H     7.22477861070586    -1.21463283526368    -2.63427254688839
H     8.71831889852170    -0.66719697518595    -0.71279125418060
H    10.04706475425178    -0.25051136728625    -1.83798568108241
H     9.44852756897968    -1.93921387190117    -1.74596602808847
C     4.57558898819666     2.99899897917537    -1.71543263443168
C     3.66802072509342     3.49485559019972    -2.85387838520731
H     4.08693912977247     4.40188381839476    -3.33786713771693
H     2.65913149457204     3.75254656436302    -2.46824831327780
H     3.54701609276692     2.72137311842201    -3.63872332924931
C     4.67180200887326     4.03468886009500    -0.58351671760978
H     4.10614191741502     2.08872252752627    -1.29636216219104
H     5.16610699079157     4.96863711236188    -0.92187117620392
H     5.24920506549592     3.63826565502331     0.27559937017690
H     3.66166287417664     4.31139779113352    -0.22070392730211
C     9.08841084836123     4.34910940780269    -3.60942681272075
C     9.35781048113549     4.24276003513975    -5.12044197869647
H     9.86558962109621     3.28759560095404    -5.36926446336568
H    10.01010948160155     5.07038873041399    -5.46835056105375
H     8.41382063559799     4.27885596376272    -5.70001208546604
C    10.39977625212440     4.35330202889613    -2.80671413540937
H     8.57820454162880     5.32056469672947    -3.42719950820003
H    11.05427717412748     5.19303900616668    -3.11926273589331
H    10.96837766582347     3.41301021780336    -2.96252426529568
H    10.20664058595633     4.45092825997077    -1.71969253872713
C    -8.58521190546216     1.23894727171118    -1.26977995864852
C    -7.14925570987487     1.63252077593683    -3.15010522952318
C    -8.30937851406718     1.96946520199528    -2.43341552864226
H    -9.50767976009028     1.46880001125135    -0.71109421146915
H    -6.91878748521165     2.18026802484029    -4.07648163367783
C    -8.17645953883576    -0.55631399724491     0.44090978165875
C    -9.51586952493790    -1.27318223155960     0.19666643758615
H   -10.34259287953092    -0.55444528943824     0.01868381157720
H    -9.79384575202651    -1.88954470438847     1.07659459925126
H    -9.45693446690454    -1.94170888373755    -0.68539823245136
C    -8.24344785691287     0.33593327566910     1.69178173901049
H    -7.42118565890557    -1.34299842791955     0.63108336042013
H    -8.49401527062195    -0.26394128883209     2.59116673262365
H    -9.01993725339389     1.12237016076791     1.58777111585888
H    -7.27878602311753     0.84958796298483     1.87889985626641
C    -5.02807446305906     0.36011674797405    -3.59128306454091
C    -4.35216973080631     1.63799700801510    -4.11843547130107
H    -3.39197130958125     1.38413803306963    -4.61096697140143
H    -4.14241603372636     2.36982960367966    -3.31389012331327
H    -4.97566229755902     2.15089053302156    -4.87900453792897
C    -5.39879245081745    -0.54920864595032    -4.77966472622363
H    -4.28478279398452    -0.18136865062385    -2.96988382143804
H    -4.49874401799518    -0.80917628207046    -5.37414343162731
H    -6.11545895850895    -0.03282735179453    -5.45181518956328
H    -5.87968903086651    -1.49229087576708    -4.45400565102856
C    -9.21557216986358     3.10516364655968    -2.88445775343646
C    -9.71984099715124     2.91548045495310    -4.32383922971305
H    -8.88303118240700     2.94274583952361    -5.05225450963261
```

```
H    -10.42812748685515      3.72208984987899     -4.60390803782300
H    -10.23749809793926      1.94297997384370     -4.44448677870631
C     -8.51430840471274      4.46458818464025     -2.71139865528115
H    -10.10205824829194      3.09608046679825     -2.21258295051686
H     -8.19161195497541      4.61897491289544     -1.66179374824624
H     -9.18751610227375      5.30090552745283     -2.99245640024518
H     -7.60985108672718      4.52880136723508     -3.35154806243649
C     -0.62772176582933      0.12571150065634      6.75974383452538
C      1.61863555968282     -0.45930912996551      7.59758278930915
C      0.63105079128305     -0.25525027218950      8.76130785134692
H      2.43653438277098      0.29084180493729      7.64173931877007
H      2.09399861857776     -1.45848960664910      7.58420475998918
C     -0.42727618520571      0.68886540583470      8.17235258709333
H     -1.23271104943315     -0.80356238826114      6.81329026987150
H     -1.14439306890871      0.81738689886918      6.06452439107974
H     -1.36518033322190      0.73350288776607      8.76153426466609
H     -0.02727568587329      1.72626596576794      8.12167522226386
H      1.11348445515957      0.13358908809401      9.68009950762666
H      0.15244847931345     -1.22163772039343      9.02667847391727
H     -5.38689735345264     -3.07081917419663      3.09362244838832
H     -5.94271794756035     -1.37331669364158      3.14941097906731
H     -4.82647553874481     -1.98708531840401      4.41156674767672
H      0.20769530983909      2.82503110838996      4.39203260658371
```

1d2a4a

18 conformers were generated by GOAT, all of which were used for optimization and frequency calculation at the PBE-D3(BJ)/def2-SVP level of theory.

Electronic energy (a. u.) | ωB97M-V/def2-TZVPP: –4118.27199046396
Thermochemical Corrections (a. u.) | PBE-D3(BJ)/def2-SVP: 1.380282790774
Imaginary Frequencies: none
Gibbs Free Energy (a. u.)   –4116.891707673190

182

```
C      3.62935835700265     -2.13342821955336      0.55761637614849
C      5.50515176420166     -1.26038835149184     -0.95335982745696
C      6.15462334714891     -0.12962368838217     -1.57017874146238
C      5.55138502708277      1.15751759529227     -1.48162554366722
C      4.31122257420977      1.34688977308751     -0.88636829825721
C      3.66772226065498      0.20811714160829     -0.30269209554616
H      6.08778151837535      2.02311351969879     -1.89859185996300
C      4.34272258567275     -2.80413647212495      1.61683198191879
C      2.29517861538057     -2.48715116710318      0.31906585888510
C      3.70807162883490     -3.90282582448432      2.30346494412281
C      2.37878598820819     -4.27011884965594      1.95284907455987
C      1.64855670230923     -3.56804815634630      1.00191465930095
H      1.90716293029907     -5.12022432557925      2.47025215511145
O      2.44281572857159      0.39808661157657      0.30027705080178
O      1.58597697372946     -1.82975592642978     -0.65982894686547
P      1.07699757787119     -0.24595356484925     -0.44482986787233
O     -0.01921871245469     -0.13678416995308      0.60091904977007
O      0.91250714562516      0.31069539237170     -1.85168128161809
```

```
N    -1.74784063421845     2.28247843307421      2.56770919972529
C    -2.31381742160777     1.33578511871914      1.82636886210184
C    -0.28402869187957     2.37567731336117      2.67298123784536
C     0.11063964414819     2.13183614290715      4.13373230377380
H     0.02971353942320     3.39531884805946      2.36496283524939
H     0.17211856429615     1.62613791601058      1.99519786756072
O    -0.54090212645134     3.04326929675136      5.00640479612460
H     1.19881303319130     2.28177018017919      4.25696094480262
H    -0.13347045059961     1.07635849806520      4.40806858074166
C    -1.94330830016779     2.92050408001039      4.91703861228913
C    -2.44322185235464     3.18157291266206      3.48778072993952
H    -3.53493952731057     3.03057765537829      3.42079677944440
H    -2.21937978728929     4.22041047058533      3.17112694770861
C    -3.69361419490252     1.01727801809232      1.78530381655214
H    -1.58112508651497     0.74564060063351      1.23923402992721
C    -4.19573410828904    -0.05767508758844      1.05992207457000
C    -3.32295942387028    -0.91349095894164      0.20461605807359
H    -3.54227017151657    -0.70417602809798     -0.86689833893948
H    -3.52806191837798    -1.98834670435884      0.36405336647491
H    -2.24044220864439    -0.75276527187080      0.34756556325645
C    -5.63683060396123    -0.38962225344695      1.10891881185623
C    -6.49945953208247     0.12393586124717      2.11064717699425
C    -6.20127920172985    -1.26029999165467      0.14127463201932
H    -4.40174881993256     1.64809619103535      2.33953844447478
C    -7.56268328244871    -1.58348405042284      0.16376445509376
C    -7.85923996986763    -0.20107677309372      2.13391661813510
C    -8.40088505839391    -1.05443029415802      1.15762981003458
H    -5.57008659197294    -1.68007226528760     -0.65314333238781
H    -7.97162859294939    -2.25652410173335     -0.60484333830035
H    -9.47037525757680    -1.31254110323976      1.17856679701764
H    -6.09540042575695     0.76824449483464      2.90456328873460
H    -8.50266744642609     0.20613109457241      2.92841479356347
H    -2.27451891297512     1.89994138363531      5.23554502129647
H    -2.38583575192781     3.66325902395714      5.61051988000486
N    -1.58124170922406     1.38056851699483     -2.21434439897033
C    -2.57192226043336     0.65982842121098     -2.85248917969934
C    -3.89587562501607     0.91141454244001     -2.53965741514117
C    -4.27292153895448     1.97093523256996     -1.52620951420613
C    -3.09720001196467     2.72114291334301     -0.94729208240802
H    -4.86137319628900     1.50297623003436     -0.69843108901945
H    -5.00585297130029     2.68079398250766     -1.96742413219466
C    -1.80064993860772     2.39044285284540     -1.30753248579798
H    -0.59505290320997     1.00706388265829     -2.24743089381651
C    -2.08706817202336    -0.39183492374001     -3.83380497073668
C    -0.56263579907417     3.09422452283961     -0.84436041733665
H    -0.44761327846526     4.04652820377753     -1.40095680411414
H     0.33786023345654     2.48621596710811     -1.03469335154705
H    -0.62906470176062     3.37673846225716      0.21585793909246
C    -3.36919263020180     3.79873259163010      0.00482226261868
O    -2.57064334305175     4.51651944088035      0.61090384778452
O    -4.72502848132771     3.93213343594870      0.20118047146921
C    -5.11780107433158     4.97846865852705      1.08283304567914
C    -5.00019510167969     0.13023745001583     -3.12449011290883
O    -6.20933247810535     0.65888609510653     -2.74622195894220
C    -7.35440815529935    -0.04627774451642     -3.21812330773596
```

```
O   -4.94000740298123      -0.88310173176226      -3.81660324132762
H   -4.81927129557804       4.76019633989646       2.13068253984512
H   -6.21914167343330       5.04226480415071       1.01593937954881
H   -7.29109027558218      -1.12423417727458      -2.96525980510409
H   -7.44728683836195       0.03700607223326      -4.32083083390752
C    7.38915729622576      -0.32481715121350      -2.25671052820545
C    6.10583255292582      -2.54632771473063      -1.09874392892087
C    7.30009626781180      -2.70516432381980      -1.78699972223986
C    7.95671788500665      -1.58529599388803      -2.36204057494703
H    5.60140984379885      -3.42049078148063      -0.66430748679339
H    7.73847487427815      -3.70915546963323      -1.89246228641839
H    8.90663501320067      -1.72212607941016      -2.90058703020077
H    7.87800571902496       0.54954194386658      -2.71442344149531
C    4.26798529543467      -1.05490058198035      -0.24363488626558
C    4.41625085997191      -4.58292482046933       3.33790899999710
C    5.64381188500590      -2.40468617922990       2.04689228262011
C    6.30006831814830      -3.07713058673660       3.06809422518717
C    5.69029640625060      -4.18554775087078       3.71249961361070
H    3.92118829312504      -5.42636417170758       3.84451078216562
H    6.22330677423796      -4.71621302470151       4.51588039827432
H    6.12376856302002      -1.54290916910418       1.56357149183482
H    7.30049983740967      -2.74393401182563       3.38352912526995
C    3.67680965004967       2.69451867986692      -0.74097150930184
C    3.71505011393068       3.32870392188237       0.53036136271286
C    3.05106644538623       4.55518235998475       0.70202573065927
C    2.37577542231627       5.19031519103062      -0.35465188033073
C    2.39529281023355       4.56695925182786      -1.61290183838067
C    3.01762809326382       3.32275280212108      -1.83067953024311
H    1.88093981325697       5.06212105880245      -2.45148392851182
H    3.07517828421749       5.03717669405566       1.69306947208000
C    4.48069972982249       2.72422023279345       1.70453950320135
C    3.54065940748082       2.30085514819933       2.84369644241943
H    3.00603674773490       3.18052177646910       3.26128843841781
H    4.11035021570676       1.83159079530922       3.67239680836100
H    2.79360760273296       1.56932433970805       2.47834202406941
C    5.58274203909301       3.67332745828326       2.20479065851504
H    4.98411005694243       1.80726545290272       1.33851681699075
H    6.27248598993353       3.95612612614975       1.38445627736155
H    6.17930785629189       3.19089873200923       3.00631279931807
H    5.15788324821825       4.60954067688725       2.62336404336086
C    2.99988393312083       2.68513410874988      -3.21722105489134
C    1.67622574190969       2.87889533939274      -3.96950297953911
H    1.68675730204623       2.29449462889255      -4.91157983342683
H    1.50386248619315       3.93949911797027      -4.24784363647350
H    0.81597263587732       2.52953773107039      -3.37110413868006
C    4.17131806673127       3.20832182060883      -4.06991199196804
H    3.13342516036168       1.59391419337132      -3.06946634738128
H    4.07869896108817       4.30313370325020      -4.23035130750366
H    4.18335549618039       2.71725684602987      -5.06491443307681
H    5.15057373080370       3.02442930260251      -3.58778443002827
C    1.66648222694294       6.52229887110742      -0.14729080513949
C    0.23160509532609      -3.91707093424031       0.68447025036226
C   -0.79310145561377      -3.69278267703816       1.64199396727554
C   -0.08737404230330      -4.48476432854112      -0.57989121821952
C   -2.11778810010928      -4.02406030252846       1.30072147613480
```

```
C    -1.42961022151432      -4.77692973588632      -0.87853251490705
C    -2.46504025170607      -4.54969573291446       0.04556402703944
H    -2.91802240567029      -3.85718098571637       2.04130965075450
H    -1.66933563690533      -5.21571502701314      -1.86010106400689
C    -0.51064393798609      -3.11483945627332       3.02742442536626
C    -1.24829473755400      -1.78611809230580       3.25777089179885
H    -1.02498507066468      -1.38949906671377       4.27114340052194
H    -2.35001754620951      -1.90220101507992       3.18228343197860
H    -0.91764763738947      -1.04681189837617       2.50400407657776
C    -0.82130339997049      -4.13982004531554       4.13128501900059
H     0.57239069128397      -2.88850039498739       3.07893357447604
H    -0.55896358423750      -3.73448760153699       5.13049314811147
H    -0.25272259732049      -5.08013625724848       3.98242335346750
H    -1.89942191461889      -4.40377393061476       4.14849520179512
C     1.00534866708391      -4.86886562460862      -1.57451545946725
C     1.08423607922652      -6.40012299950745      -1.71343514894406
H     0.15154131040309      -6.81559266659867      -2.14900118770143
H     1.23893316906693      -6.88496519773371      -0.72837476067155
H     1.92419292532011      -6.69179004636637      -2.37726336645444
C     0.85399201140107      -4.18098771523917      -2.93854394543542
H     1.97280963732262      -4.53505182982506      -1.14944494129410
H     1.68231070825560      -4.47929032599697      -3.61365139669807
H     0.88059276535575      -3.08095608097062      -2.82656837286445
H    -0.09747465775097      -4.46134625384175      -3.43678406064168
C    -3.91197625399140      -4.92128955914760      -0.25726002388084
C     2.67149020549686       7.64137826215051       0.17738988729746
H     2.16043264945333       8.62291187248076       0.26059292496206
H     3.45176261916533       7.72224863292872      -0.60564717927325
H     3.18569877853771       7.44882484428766       1.14225719328103
C     0.56372866581342       6.43703501860428       0.92304576855564
H     1.17800804764786       6.78003704149626      -1.11285728475924
H     0.98532576026413       6.14098854794394       1.90697135284859
H    -0.22641160424491       5.70914027593823       0.65299700687779
H     0.07523823885908       7.42399791246738       1.06033151000993
C    -4.39996835581795      -4.42639408089133      -1.62683382617836
H    -5.47129636336383      -4.67416430983533      -1.77290148338058
H    -3.83853333066149      -4.89901820587058      -2.45849608408360
H    -4.28619965264088      -3.33026256368436      -1.74167288062585
C    -4.11507570151622      -6.44115290325240      -0.11581018823909
H    -4.53785877084989      -4.42800952158107       0.52049585031723
H    -3.80848204838657      -6.79484474236116       0.88870030646105
H    -3.50363221366127      -6.98805245152553      -0.86345135258322
H    -5.17732103732316      -6.72125333325277      -0.27418870862790
H    -8.22732158918834       0.41626760738197      -2.72318848364267
H    -4.65305563624843       5.94352084765194       0.79613432242371
C    -0.85271560121408       0.04702386180657      -4.63686447349165
H    -0.65793445822287      -0.69980690541942      -5.43229855132930
H     0.05728493409602       0.10190454141085      -4.00752855441167
H    -1.00700419024530       1.02977960953383      -5.12652951256613
C    -1.84044249110691      -1.72369196456128      -3.10117510993452
H    -2.92784857102435      -0.56673744173212      -4.52949297673008
H    -2.76864835970688      -2.09176097522472      -2.62777554289072
H    -1.05564209743089      -1.62955438066616      -2.32579680864207
H    -1.50754018472772      -2.49401667978155      -3.82375348515256
```

1d2b6e

58 conformers were generated by GOAT, all of which were used for optimization and frequency calculation at the PBE-D3(BJ)/def2-SVP level of theory.

Electronic energy (a. u.) | ωB97M-V/def2-TZVPP: –5208.11047695836

Thermochemical Corrections (a. u.) | PBE-D3(BJ)/def2-SVP: 1.921211795535

Imaginary Frequencies: none

Gibbs Free Energy (a. u.)   –5206.189265162820

```
248

  C    0.29066841687917    -4.97917973257130     0.34454334559928
  C    2.24621991497280    -5.93144703545335    -0.99245329036550
  C    3.58141136982728    -5.76687063763398    -1.51247206372363
  C    4.22865532409499    -4.50663519233551    -1.38481471947124
  C    3.59910945542827    -3.40806626317804    -0.81177066286132
  C    2.29833068464425    -3.60190829143589    -0.24963283712834
  H    5.25050853043394    -4.39152307631644    -1.77727670937504
  C    0.00066758701430    -6.02453821069646     1.29292840769056
  C   -0.73972798641153    -4.09751239985943    -0.00978957606752
  C   -1.36299457517030    -6.22813426107086     1.71817295106490
  C   -2.38414185754670    -5.36786116712318     1.22506541770537
  C   -2.09839114639061    -4.28650655051493     0.39935748699766
  H   -3.42645593869528    -5.55175964619505     1.52902675550255
  O    1.71353520940388    -2.54040919700760     0.40310716350760
  O   -0.47053249259591    -3.04813702940392    -0.85399768381837
  P    0.41916802308127    -1.73709370293898    -0.30740345748692
  O   -0.26591179828610    -1.03746164153741     0.85678323270002
  O    0.84012142646416    -1.00759930110689    -1.57130243172547
  N   -0.11166455984912     1.55472024947426     3.29781898359733
  C   -0.83620069061453     1.53128996864189     2.19105950482351
  C    0.76793246835313     0.43460420557851     3.65702474010961
  C    0.29034740083143    -0.14053672597190     4.99589221495983
  H    1.80041650690681     0.83117206755636     3.73158426539298
  H    0.71077663355938    -0.33226070040124     2.85877839986948
  O    0.18082970972523     0.85386244103967     6.00357965727935
  H    1.02847466505798    -0.88300073543176     5.35767129743231
  H   -0.68069213529794    -0.66663910306156     4.84353884357357
  C   -0.68870638752324     1.93042049066976     5.65903910196732
  C   -0.17679385282506     2.56685628784214     4.34600783459954
  H   -0.79736283929218     3.41837694147687     4.01936412671831
  H    0.85884149431914     2.92831318546093     4.50367331279019
  C   -1.88813244662065     2.43055550706708     1.86376675725672
  H   -0.62150575010579     0.66347866942792     1.53377383099116
  C   -2.74932385879434     2.21016398807391     0.80121299662198
  C   -2.61314576154364     1.07355258321180    -0.15793459887040
  H   -2.63883236550374     1.46655894636398    -1.19308161752825
  H   -3.47620557913996     0.37884462336988    -0.07203511061761
  H   -1.70528647006312     0.46489252916662    -0.01324458857766
  C   -3.89725179151424     3.11911089781906     0.60892697589035
  C   -5.11580606765332     2.62466132420072     0.08280822222143
  C   -3.81585142188443     4.49473491644864     0.93917654092624
  H   -2.10476869812874     3.27215752230604     2.53696329301792
```

```
C    -4.91520007064740     5.33999467503207     0.75241940107846
C    -6.21820838900618     3.46958892155029    -0.08815825331612
C    -6.12228196696647     4.83006466419751     0.24287471119352
H    -2.86117272530309     4.91361243511652     1.28949230697529
H    -4.82593760844676     6.41017366019205     0.99309233661522
H    -6.98592811429025     5.49640313208458     0.09532966273098
H    -5.21228052106461     1.56310131108180    -0.18116425462560
H    -7.15044106678668     3.05449618630779    -0.49599782701813
N     1.00696801296095     1.67538436667570    -1.18297462515930
C     0.01527482554699     2.39570148484478    -1.82861876358476
C    -0.36763536981568     3.62563683589940    -1.33902936631903
C     0.34354316948695     4.23457292226891    -0.14214754148344
C     1.24583119773106     3.25528470471947     0.58582253548219
H    -0.40674108914016     4.64531782478964     0.56528754386822
H     0.92160703723204     5.13687303663413    -0.45476352207965
C     1.57253823622553     2.03649116612675     0.01681398391234
H     1.07629074712782     0.65530795846440    -1.43998612806550
C    -0.51491707225278     1.69258540326504    -3.04357662066615
H    -1.37015139766984     2.23353426028442    -3.47555380682859
H    -0.78508077817896     0.64743820339858    -2.78685765530219
H     0.29501209589588     1.61875950870582    -3.80037745377615
C     2.50994973345995     1.01255676855514     0.58163450803708
H     3.30152821643028     1.47412830027560     1.19242395938152
H     2.94882798119561     0.40200428269352    -0.22820362772352
H     1.95848055334670     0.31100749809540     1.23509185164020
C     1.81815816831200     3.66797603732948     1.86423638191525
O     2.49557540980796     3.00261001885498     2.65386641502554
O     1.47669096177247     4.97296654297840     2.14401300984220
C     2.05453959822162     5.55610726011891     3.32241365693039
C    -1.45779519990226     4.40201585039688    -1.94958927122499
O    -1.58399164278643     5.62006243251528    -1.32323849485517
C    -2.62901384781003     6.47635030863933    -1.81669300566807
O    -2.21003033023042     4.07931268618005    -2.86791680073143
C     3.46055296061538     6.07466109969444     3.06217905361266
H     2.06493978918463     4.80476592940998     4.13987855628094
H     1.36446691606253     6.37874253073305     3.59815901202724
H     3.84789768615035     6.60009720705674     3.95852579964814
H     3.46761261264053     6.78430122071542     2.21110281709910
H     4.14521265141373     5.23686039284118     2.82890648054540
C    -2.19789472152869     7.23966734972775    -3.05966326427878
H    -2.84690177692989     7.16415568600205    -0.97513282900102
H    -3.53043661003303     5.86294532964475    -2.02098475432232
H    -2.99036616606548     7.95376026705432    -3.36308281403175
H    -2.02289851156467     6.53987891954852    -3.89916706968907
H    -1.26815504581994     7.81286520371941    -2.87072765906620
C     4.21327078277498    -6.85747620443751    -2.18003147765428
C     1.58198669831784    -7.17195380803697    -1.23308610263766
C     2.21728935509460    -8.20811936417422    -1.90244460415424
C     3.55040408464200    -8.06001736204144    -2.36775712040743
H     0.54694776542366    -7.29990407512260    -0.88891952782544
H     1.67841195687067    -9.15130679872920    -2.07956062391505
H     4.04619957741266    -8.89156467489459    -2.89095493856206
H     5.23722008116551    -6.71576600551486    -2.55997627759660
C     1.63109132907374    -4.83410917204313    -0.28631704289171
C    -1.65741752062477    -7.27862985320058     2.63716947668975
```

```
C    1.01385002091547      -6.85668633752473       1.85619784454544
C    0.69671425758402      -7.85875326978116       2.76185624953867
C   -0.65125509636352      -8.08375864988331       3.14795637548124
H   -2.70472529652704      -7.42877041374713       2.94322524424143
H   -0.89206686288952      -8.88707420555217       3.86053730403016
H    2.06063449455655      -6.68655486838294       1.56883241017073
H    1.49816631368326      -8.48168919368119       3.18718888501991
C    4.29216854432072      -2.07961217809084      -0.79226200165743
C    4.95551131206891      -1.63221003999774       0.38051663206166
C    5.72877687464626      -0.45774511564108       0.32168870363443
C    5.89049762516639       0.26552482744524      -0.87406667136311
C    5.17352093883212      -0.16279715459963      -2.00570826298721
C    4.35898831702627      -1.30901602811708      -1.98696708936374
H    5.27906059036936       0.40896043129923      -2.93950305569738
H    6.25798309684368      -0.11032868645797       1.22234852356055
C    4.87031372959175      -2.40821599577998       1.69159167700661
C    4.01658456153158      -1.65750870382655       2.72960129397985
H    3.96227234838808      -2.22928559698062       3.67947066648578
H    2.98698876046711      -1.51941702652390       2.34841240821975
H    4.44429180174827      -0.65854132221655       2.95717757233215
C    6.26097020160467      -2.75857094847332       2.24577990102960
H    4.35432615360963      -3.36540439935389       1.47318814119402
H    6.82954837985722      -1.85111332683790       2.53650387386089
H    6.86670276319843      -3.30677583177766       1.49611499942694
H    6.17180846958287      -3.39646933406180       3.14900525283198
C    3.59219903845207      -1.70490689042218      -3.24646612261363
C    2.95723851332443      -0.49359127396454      -3.94869881754139
H    2.25077233839637      -0.83498829712528      -4.73204854386361
H    3.71635567782253       0.14511366970846      -4.44670254993003
H    2.39207364674895       0.13015175382505      -3.23271643407776
C    4.48222004247378      -2.48549880669270      -4.22973606259785
H    2.76098432552475      -2.36312675137213      -2.92267925751832
H    3.91103731183244      -2.76110731727584      -5.14020272280306
H    4.87344479328422      -3.41879519876960      -3.78144526315118
H    5.35120703151694      -1.87060279769906      -4.54547773969940
C    6.86153655337473       1.39954912157250      -0.97761609389564
C   -3.16961579353905      -3.35157874003802      -0.06409819385312
C   -3.83707505320096      -2.50950673269978       0.86700439209416
C   -3.55075919127446      -3.32312236180255      -1.43388827789080
C   -4.84902076781859      -1.64797933399037       0.40513932220663
C   -4.60785390247483      -2.48776854569413      -1.83350489217147
C   -5.27294564724711      -1.62969184526361      -0.93947332114215
H   -5.34613013775155      -0.97639866264612       1.12228429623476
H   -4.93957073296730      -2.52159740189171      -2.87996857935950
C   -3.51138292749503      -2.51788408279333       2.35734385162790
C   -3.02715437497649      -1.14649859046672       2.84685367743470
H   -3.79806884195804      -0.35713910354813       2.72109225227484
H   -2.12072565792244      -0.85603719390526       2.28347607517607
H   -2.77800548859363      -1.19336179805067       3.92755939090060
C   -4.70327051157132      -3.03145072038677       3.18306776200694
H   -2.66963125922224      -3.22101096446026       2.51011843646257
H   -4.44066168780554      -3.08977470798042       4.25965331339415
H   -5.01985067766900      -4.04180672418698       2.85304112055607
H   -5.58294611733615      -2.36121396244978       3.08719978702274
C   -2.87959950720775      -4.19545679678400      -2.48937872472572
```

```
C   -3.87250486404129    -5.19403259349729    -3.10878677724998
H   -4.35151589812913    -5.82336121293073    -2.33171334515482
H   -3.35304822655211    -5.86483378202884    -3.82343862020518
H   -4.67972337323409    -4.67605233231760    -3.66762348765029
C   -2.18741772640349    -3.33877981114475    -3.56504312189535
H   -2.09425594456971    -4.79220739053010    -1.98494331075772
H   -2.92084755416777    -2.71865356213740    -4.12258582342646
H   -1.67054950545211    -3.98753708004128    -4.30185305519197
H   -1.43311897411535    -2.66930178338696    -3.10895492279246
C   -6.40989138706474    -0.75757809498112    -1.37084880805595
C    6.42083367395307     2.73837409368960    -1.17190122578152
C    8.25579193798409     1.11873303258137    -0.92702473376271
C   -7.67591456907555    -0.88206765394055    -0.72458191578047
C   -6.25574503123993     0.20448123417419    -2.41829589944935
C    7.37826246985838     3.75826430118402    -1.31171608205813
C    9.17168931593770     2.17927792492294    -1.05749259813142
C    8.75911946080715     3.50556065221310    -1.25411127161071
H    7.02929289068797     4.79198869229971    -1.46563089121735
H   10.25248066527106     1.96469515456792    -1.01734691792278
C    8.79372805088292    -0.30200560358388    -0.76700464243837
C    9.70743017254967    -0.70154009225241    -1.93769108625353
H   10.62520629830652    -0.07878655089223    -1.97748801488626
H    9.18429835103217    -0.59057041090320    -2.90864798673330
H   10.02830026406827    -1.75922829867393    -1.83912504636251
C    9.50034545275124    -0.48889777549181     0.58618376161049
H    7.92670725836919    -0.99130620326126    -0.78333448465563
H    8.82336198673605    -0.24835353454458     1.43055138078697
H   10.38880018017182     0.17085232085764     0.67345175834295
H    9.84425984978443    -1.53658637553037     0.71165214489897
C    4.94120288464101     3.10855129503416    -1.22347393882300
C    4.50420859412210     3.52010024718277    -2.64038957840069
H    5.03528358587246     4.43504045962257    -2.97674231418748
H    3.41433363803224     3.72824902735257    -2.66721298574317
H    4.71603847349598     2.72056130718438    -3.37818549753065
C    4.59349237935387     4.20120610733883    -0.19946180891200
H    4.36125225397478     2.20398719341788    -0.95755919286034
H    3.51079581086179     4.43472238183344    -0.23185974015882
H    5.14408289876047     5.14332224777384    -0.40073212729170
H    4.84123515868343     3.87827534549824     0.83136275672120
C    9.77444832312237     4.62951385614930    -1.40595053856022
C    9.62909089687478     5.68221928944366    -0.29410903039535
H    8.64380572402201     6.19015918886934    -0.35027076323686
H   10.41248436486460     6.46330658848752    -0.38133317576140
H    9.71043191891704     5.22049300469926     0.71016285342399
C    9.69781383945603     5.27494598205154    -2.79999057191505
H   10.78140309842410     4.16837861769861    -1.30340681053782
H    9.83519809166236     4.52084133391207    -3.60046278140853
H   10.47755908074220     6.05524164787958    -2.92107661084151
H    8.71219250543159     5.75887901213274    -2.96229264259000
C   -8.73117865900704    -0.03310179006322    -1.10799500046193
C   -7.34677568154852     1.02377213496711    -2.75916157160866
C   -8.59440186316306     0.92802278228112    -2.11954700031652
H   -9.70984892480285    -0.13807362402561    -0.61140540789723
H   -7.21452535087944     1.76364776949239    -3.56366466426798
C   -7.96651036638419    -1.94931919320998     0.33074566528984
```

```
C    -9.10714746492184    -2.88285718619545    -0.11062295626526
H    -9.24986293963487    -3.69842247635287     0.62805218400617
H    -8.88824748812478    -3.34480149045810    -1.09395271827126
H   -10.07291493798059    -2.34355718015041    -0.20005755733837
C    -8.25795952136558    -1.32765747216215     1.70690689779160
H    -7.06089676069973    -2.57722557816222     0.43436346722251
H    -9.17501601565695    -0.70265083120542     1.68329060877811
H    -7.42577861936440    -0.67723926947331     2.04496918153426
H    -8.40894758860309    -2.11614369136841     2.47292557834850
C    -4.96390574030181     0.35628667433393    -3.22166737973284
C    -4.53482735301989     1.81580572415660    -3.43326928980961
H    -5.25649288487465     2.37455572617897    -4.06395576039829
H    -3.55957218619980     1.85716640240382    -3.95470289914455
H    -4.42122850703719     2.37520820291187    -2.48593362648801
C    -5.09440553989177    -0.34316172658535    -4.58980947999976
H    -4.15451827108609    -0.15127863888449    -2.65721635750149
H    -4.13124908136611    -0.31030295414509    -5.13934513091077
H    -5.86006264178381     0.16341127644130    -5.21362869318391
H    -5.40013674063916    -1.40368518013493    -4.49529835280910
C    -9.76229210161027     1.82138241738114    -2.51591900304667
C   -10.10122694492940     1.69236132177899    -4.01003040905723
H    -9.27138167393940     2.06401653355299    -4.64615666511524
H   -11.00419051345191     2.28493465179444    -4.26365013481500
H   -10.29076544750261     0.63685876109596    -4.28931960092742
C    -9.51408457711896     3.28891801875139    -2.12623753140913
H   -10.64498615096873     1.46728196911308    -1.93938323165350
H    -8.61859584963616     3.69347467886394    -2.64266237842053
H    -9.35193289263140     3.39299776876109    -1.03417267159102
H   -10.37900629173141     3.92644152820471    -2.40303987174499
C    -2.18384462543234     1.54559826398694     5.56557550803429
C    -0.68045819825484     2.95925188445390     6.79774423650726
C    -1.96515128557879     3.78666984448176     6.60019001443501
H     0.24841306439707     3.56358951125569     6.81518494516013
H    -0.71081397309883     2.37758801307775     7.74169199040049
C    -2.94389624301644     2.86601571390228     5.80802669353763
H    -2.37864320015073     0.81441216788334     6.37731062007442
H    -2.46063737351894     1.05772476274773     4.61089381477696
H    -3.89148856638765     2.69030563065314     6.35335794411057
H    -3.23232941773809     3.33652555237909     4.84525093735226
H    -1.75226078614126     4.71339640992410     6.02862848073910
H    -2.38837888262851     4.11603804046336     7.56890041385430
```

Cartesian coordinates of the optimized structures in Chapter 3

68a

```
C    -1.184631   -1.194955   -0.941685      H    -1.258776    1.350001    1.964122
C    -0.213718   -1.249602    0.050952      H    -2.977124    1.444154    0.206229
C    -0.224518   -0.344780    1.120668      H    -2.942138   -0.183079   -1.668654
C    -1.227436    0.633496    1.148497      C     0.804311   -0.420529    2.185522
C    -2.201092    0.685422    0.158253      C     1.225924   -1.601109    2.652666
C    -2.185090   -0.228701   -0.891287      H     0.796638   -2.536869    2.307152
H    -1.152616   -1.902987   -1.765053      H     1.997821   -1.657703    3.414551
H     0.582340   -1.986635   -0.007307      C     1.367867    0.880406    2.705533
```

H	2.108694	0.656010	3.482382	C	3.031963	5.067694	2.598945
H	0.572327	1.458769	3.195458	C	3.821954	5.383882	3.677962
C	2.011210	1.744406	1.609685	H	6.426370	2.628959	0.697620
H	1.249595	2.023955	0.869164	H	6.701405	3.812433	2.777128
H	2.365163	2.680854	2.062117	C	5.395079	2.963099	0.610867
C	3.171341	1.049315	0.900958	C	2.763817	3.951969	0.380932
H	2.810823	0.117861	0.445177	H	2.003314	5.409070	2.561018
H	3.924734	0.752571	1.644469	H	3.411096	5.975860	4.490334
C	3.812806	1.930313	-0.168258	C	7.825754	0.071230	3.004832
H	4.642293	1.418322	-0.666413	C	6.934448	-0.648329	2.245318
H	3.080768	2.205995	-0.935772	C	5.539241	-0.471967	2.402053
H	4.203946	2.858068	0.265037	C	5.077258	0.519361	3.321882
				C	6.021188	1.219153	4.113512
				C	7.366776	0.996383	3.965111
92b				H	8.892497	-0.078791	2.867578
				H	7.299568	-1.361017	1.514633
O	2.500882	2.670018	-1.606054	C	4.569737	-1.219317	1.663036
O	0.491420	2.356010	-0.087538	C	3.701650	0.803589	3.418308
O	2.312999	-1.609496	1.045387	H	5.656437	1.951439	4.828445
O	3.758733	-1.243170	-0.985016	H	3.388215	1.571602	4.121638
S	-0.045904	-2.415116	-1.833877	C	7.325360	-5.612838	2.020148
S	0.159124	2.672258	-3.841201	C	7.021094	-5.454851	0.692251
O	-1.053751	-3.003880	-0.943177	C	6.215204	-4.372704	0.256992
O	-0.414043	-1.097019	-2.422888	C	5.750928	-3.420506	1.215176
O	0.552706	3.951283	-3.271258	C	6.056588	-3.630219	2.580503
O	0.689029	2.183382	-5.110140	C	6.824073	-4.700641	2.972005
N	1.419193	-2.415294	-1.203938	H	6.216981	-4.992741	-1.786769
N	0.518839	1.474822	-2.670455	H	7.377771	-6.168495	-0.045850
P	2.206932	-1.230057	-0.523644	H	5.669401	-2.941191	3.323221
N	1.748982	0.268755	-0.657464	H	7.039922	-4.850154	4.025638
P	1.343491	1.628726	-1.237880	C	5.841521	-4.245329	-1.092923
H	0.211911	0.506989	-2.870921	C	4.967954	-2.319968	0.752019
C	0.315813	3.740512	-0.054772	H	0.675379	9.815175	-0.055022
C	3.306678	3.075356	-0.529419	H	5.782710	5.227634	4.584460
C	3.239179	-0.879636	1.790950	H	8.081377	1.540084	4.576449
C	4.569577	-2.298785	-0.570545	H	7.935595	-6.450395	2.344360
C	-1.015069	4.232583	-0.167208	C	-2.177987	3.369960	-0.351367
C	4.986203	-3.252123	-1.543711	C	-2.298413	2.039147	-0.682623
C	4.631829	2.562988	-0.472562	S	-3.789575	4.129831	-0.240234
C	2.755221	0.152435	2.644183	C	-3.637169	1.627044	-0.901040
C	2.135194	8.218750	0.050839	H	-1.465027	1.362392	-0.786131
C	2.347954	6.862359	0.107493	C	-4.545957	2.652171	-0.697987
C	1.259391	5.958651	0.098710	C	-4.280127	0.421677	-1.343282
C	-0.062200	6.485762	-0.015332	C	-5.677957	0.593124	-1.452585
C	-0.248038	7.890503	-0.055583	S	-6.202321	2.225426	-1.003488
C	0.826879	8.740741	-0.015877	C	-3.720381	-0.820976	-1.662257
H	2.984561	8.895222	0.048121	H	-2.650316	-0.975386	-1.582955
H	3.360856	6.477293	0.144540	C	-4.543254	-1.852115	-2.070239
C	1.421941	4.539678	0.150091	H	-4.112860	-2.818636	-2.313885
C	-1.156233	5.610346	-0.122050	C	-6.514782	-0.437733	-1.861495
H	-1.259725	8.279633	-0.134646	H	-7.587803	-0.301067	-1.933121
H	-2.141225	6.056821	-0.225183	C	-5.930511	-1.659243	-2.168280
C	5.162874	4.951343	3.736368	C	-6.775382	-2.818519	-2.609123
C	5.677939	4.172909	2.730914	F	-6.376901	-3.294708	-3.814430
C	4.880587	3.800501	1.620620	F	-8.083130	-2.498156	-2.717102
C	3.541638	4.291606	1.532284				

```
F    -6.688448   -3.856163   -1.738367        C     5.908249   -1.355782   -7.241553
C     4.520720   -3.226434   -2.924955        H     4.298360   -0.131008   -7.986089
C     3.675405   -2.365904   -3.583381        C     6.107673   -2.042294   -8.561270
S     5.001528   -4.568593   -3.999742        F     4.938008   -2.237193   -9.215131
C     3.369214   -2.770997   -4.903665        F     6.703179   -3.249455   -8.427756
H     3.277293   -1.466102   -3.144847        F     6.894807   -1.307534   -9.389991
C     4.024000   -3.934816   -5.269001        C     0.144938   -3.548954   -3.241602
C     2.476685   -2.310551   -5.924762        C     1.029794   -4.630615   -3.233496
S     3.637745   -4.506985   -6.864760        C    -0.666949   -3.381787   -4.367670
C     2.513042   -3.152365   -7.059113        C     1.148392   -5.469153   -4.335502
C     1.611004   -1.209896   -5.923008        C    -0.548782   -4.209458   -5.475836
C     1.719651   -2.914138   -8.174630        C     0.366065   -5.252803   -5.461809
H     1.569152   -0.547167   -5.063389        F     1.780741   -4.920847   -2.174051
C     0.812474   -0.967141   -7.023419        F     2.000236   -6.494941   -4.308574
H     1.753346   -3.564065   -9.041805        F     0.472658   -6.056880   -6.515014
C     0.868979   -1.816628   -8.140384        F    -1.317165   -4.012838   -6.545868
H     0.139233   -0.115710   -7.024184        F    -1.599485   -2.432446   -4.423986
C    -0.027863   -1.511434   -9.304275        C    -1.638100    2.588178   -3.956423
F     0.236137   -0.286909   -9.828409        C    -2.466598    3.680461   -3.685633
F    -1.332761   -1.496887   -8.936654        C    -2.224128    1.403387   -4.406765
F     0.097212   -2.408844  -10.305014        C    -3.842420    3.577995   -3.863266
C     1.347926    0.533947    2.683154        F    -1.988252    4.848696   -3.273215
C     0.207470   -0.154446    2.342076        C    -3.594932    1.287089   -4.569192
S     0.957954    2.180348    3.232453        F    -1.464015    0.345798   -4.687960
C    -0.978088    0.606482    2.512896        C    -4.404674    2.386771   -4.305756
H     0.216347   -1.180247    1.999426        F    -4.625978    4.626418   -3.620008
C    -0.719636    1.883401    2.989790        F    -4.132885    0.147106   -4.985141
C    -2.387272    0.375513    2.344450        F    -5.715253    2.298366   -4.484097
S    -2.132517    2.857880    3.263702
C    -3.145073    1.507701    2.730275
C    -3.063437   -0.759547    1.880616   I
C    -4.531921    1.512005    2.697070
H    -2.505508   -1.628336    1.542248        O     1.772302    2.599708   -2.197170
C    -4.446719   -0.764869    1.844443        O    -0.090575    2.012365   -0.588345
H    -5.102274    2.380769    3.007606        O     1.489000   -1.596097    0.141259
C    -5.174534    0.358618    2.261174        O     2.897144   -1.253357   -1.933446
H    -4.975280   -1.641635    1.483100        S    -0.304744   -3.647321   -1.230655
C    -6.671462    0.273824    2.320051        S     0.006250    2.969501   -4.599054
F    -7.192864   -0.367271    1.246880        O    -1.061729   -3.007557   -0.137405
F    -7.257125    1.491323    2.387146        O    -1.050299   -4.476628   -2.178973
F    -7.081908   -0.418182    3.415298        O     1.367343    2.709331   -5.054368
C     5.155103    1.679038   -1.506372        O    -1.118204    2.807443   -5.514510
C     4.788156    1.536875   -2.824277        N     0.586384   -2.593006   -2.079900
S     6.501627    0.596188   -1.097415        N    -0.400192    1.973712   -3.268178
C     5.559370    0.571482   -3.517624        P     1.357501   -1.361529   -1.453711
H     4.008626    2.125726   -3.288361        N     0.777098    0.040095   -1.904101
C     6.515824   -0.021202   -2.706036        P     0.577055    1.555535   -1.975475
C     5.571910    0.028023   -4.847093        H    -1.055587    1.224720   -3.572661
S     7.466730   -1.249038   -3.488190        C    -0.399112    3.360235   -0.416707
C     6.553281   -0.983299   -4.981346        C     2.583638    2.948771   -1.105033
C     4.765291    0.335370   -5.947667        C     2.516538   -1.033746    0.884805
C     6.730603   -1.680363   -6.167378        C     3.675848   -2.369966   -1.641644
H     3.995574    1.097752   -5.865901        C    -1.776995    3.715105   -0.396642
C     4.935678   -0.352691   -7.135908        C     3.998492   -3.249830   -2.712810
H     7.477308   -2.462030   -6.257805        C     3.924777    2.479567   -1.117899
                                              C     2.144585   -0.087507    1.880999
```

C	1.000207	7.965538	-0.027752	C	-4.110383	0.811985	-0.967754
C	1.341056	6.638065	-0.132601	H	-1.950831	0.761642	-0.575704
C	0.344169	5.634061	-0.133766	C	-5.103303	1.776769	-1.033209
C	-1.029061	6.027251	-0.073223	C	-4.628898	-0.507167	-1.204470
C	-1.343616	7.403929	0.060492	C	-6.024106	-0.479940	-1.412599
C	-0.351750	8.351027	0.089578	S	-6.695621	1.157465	-1.330341
H	1.777217	8.723694	-0.042531	C	-3.961618	-1.736018	-1.254330
H	2.383453	6.350630	-0.224589	H	-2.891117	-1.791143	-1.087947
C	0.645523	4.242067	-0.229729	C	-4.676604	-2.893181	-1.493847
C	-2.045321	5.059334	-0.178684	H	-4.154545	-3.844399	-1.540674
H	-2.388670	7.696619	0.117047	C	-6.757879	-1.636703	-1.642441
H	-3.074148	5.402750	-0.112767	H	-7.832230	-1.606732	-1.784346
C	4.518371	4.587411	3.228512	C	-6.067169	-2.840875	-1.680648
C	5.018819	3.888378	2.159946	C	-6.806814	-4.129358	-1.895186
C	4.198855	3.578214	1.046900	F	-6.246449	-4.872081	-2.877243
C	2.846687	4.041920	1.025137	F	-8.102787	-3.933517	-2.227275
C	2.355569	4.736938	2.155612	F	-6.797291	-4.898180	-0.774829
C	3.169753	4.998743	3.231034	C	3.539754	-3.016689	-4.077304
H	5.744435	2.505803	0.006512	C	2.795711	-1.997507	-4.628821
H	6.049279	3.544687	2.153905	S	3.961378	-4.218825	-5.325164
C	4.704680	2.822118	-0.027634	C	2.547010	-2.160106	-6.010418
C	2.039062	3.743149	-0.119100	H	2.445625	-1.137455	-4.082028
H	1.319617	5.055241	2.176206	C	3.128557	-3.305540	-6.524455
H	2.769380	5.527256	4.090931	C	1.868700	-1.400157	-7.017908
C	7.207308	-0.502632	1.936612	S	2.912017	-3.514154	-8.235685
C	6.231023	-1.120447	1.192636	C	2.000776	-1.997277	-8.290275
C	4.860674	-0.846507	1.417466	C	1.166679	-0.198033	-6.901994
C	4.517420	0.121870	2.412179	C	1.475071	-1.410670	-9.432393
C	5.547099	0.720943	3.179228	H	1.051936	0.269917	-5.929904
C	6.864687	0.415416	2.950516	C	0.636674	0.396942	-8.030132
H	8.252116	-0.725678	1.742176	H	1.591319	-1.868087	-10.408653
H	6.509999	-1.823111	0.415577	C	0.798133	-0.205171	-9.287267
C	3.809713	-1.466228	0.667839	H	0.091842	1.332210	-7.942801
C	3.168442	0.464642	2.628507	C	0.156323	0.442625	-10.475605
H	5.268433	1.438874	3.945734	F	0.609027	-0.052965	-11.648080
H	2.935964	1.175192	3.418552	F	0.365232	1.781913	-10.496833
C	6.212325	-6.082758	0.578125	F	-1.194582	0.267210	-10.470311
C	5.895226	-5.786951	-0.722865	C	0.747341	0.267052	2.103889
C	5.168468	-4.612524	-1.045183	C	-0.394837	-0.479004	1.943545
C	4.804605	-3.714632	0.006931	S	0.376088	1.897278	2.703318
C	5.119762	-4.064947	1.340888	C	-1.572622	0.232891	2.288808
C	5.804941	-5.223171	1.619607	H	-0.394215	-1.501255	1.586970
H	5.081680	-5.055742	-3.135964	C	-1.306552	1.533161	2.692338
H	6.174829	-6.463120	-1.526291	C	-2.982757	-0.046148	2.284424
H	4.803149	-3.413411	2.148874	S	-2.716024	2.485336	3.051618
H	6.023513	-5.484746	2.650479	C	-3.736083	1.093649	2.655166
C	4.779107	-4.344497	-2.371878	C	-3.659580	-1.226741	1.962774
C	4.096019	-2.524287	-0.336465	C	-5.122303	1.083642	2.674717
H	-0.606019	9.402906	0.177313	H	-3.100115	-2.108558	1.663874
H	5.154788	4.816755	4.078179	C	-5.043326	-1.250882	1.992107
H	7.645706	0.881232	3.544476	H	-5.691799	1.968230	2.939225
H	6.753233	-6.994402	0.812781	C	-5.767194	-0.100715	2.331830
C	-2.843210	2.745800	-0.615355	H	-5.572984	-2.158017	1.718924
C	-2.832753	1.369959	-0.714203	C	-7.265694	-0.162399	2.387693
S	-4.497487	3.372435	-0.820643	F	-7.778026	-0.984767	1.442928

F	−7.834597	1.054243	2.215095
F	−7.704177	−0.629506	3.585903
C	4.449486	1.679896	−2.217209
C	4.149566	1.710281	−3.557224
S	5.702203	0.477431	−1.860232
C	4.905500	0.779453	−4.314145
H	3.420225	2.383465	−3.987112
C	5.767454	0.034376	−3.521137
C	4.986439	0.393524	−5.696281
S	6.676228	−1.175559	−4.373036
C	5.898162	−0.673287	−5.880814
C	4.314750	0.904704	−6.811157
C	6.126066	−1.238848	−7.126085
H	3.601983	1.715297	−6.692218
C	4.542724	0.354879	−8.060429
H	6.815016	−2.066798	−7.254416
C	5.435218	−0.714274	−8.213110
H	4.007867	0.735939	−8.924595
C	5.704615	−1.256103	−9.586469
F	4.597401	−1.246762	−10.365883
F	6.166680	−2.527141	−9.556649
F	6.640670	−0.517238	−10.238997
C	0.926379	−4.750763	−0.456590
C	1.145702	−4.822169	0.918901
C	1.644989	−5.621630	−1.278584
C	2.014481	−5.765372	1.457615
C	2.507460	−6.570645	−0.750186
C	2.678556	−6.654973	0.625704
F	0.541685	−4.005151	1.783156
F	2.209053	−5.822728	2.777292
F	3.485332	−7.576914	1.144700
F	3.176699	−7.398259	−1.555857
F	1.525770	−5.567012	−2.604324
C	−0.052407	4.628875	−3.908718
C	1.075193	5.454014	−3.839255
C	−1.300775	5.180372	−3.601917
C	0.944511	6.803269	−3.532891
F	2.303889	5.001214	−4.063193
C	−1.434436	6.524710	−3.293233
F	−2.396594	4.427427	−3.604248
C	−0.310888	7.343438	−3.285695
F	2.021895	7.583250	−3.483764
F	−2.630746	7.032948	−3.007576
F	−0.434812	8.638921	−3.033839
C	−0.669704	−3.844946	−6.058320
C	−0.782034	−3.809160	−7.445833
C	−1.427607	−2.735467	−8.049580
C	−1.951513	−1.705961	−7.276966
C	−1.852065	−1.728765	−5.877354
C	−1.205240	−2.825467	−5.285394
H	−0.178483	−4.678903	−5.564709
H	−0.373872	−4.614315	−8.050175
H	−1.519736	−2.689670	−9.131078
H	−2.432739	−0.875302	−7.782197
H	−1.137870	−2.914897	−4.207945

C	−2.450307	−0.654227	−5.048233
C	−2.177822	−0.538650	−3.735313
H	−1.489349	−1.206442	−3.228200
H	−2.736307	0.157244	−3.118689
C	−3.405555	0.297171	−5.727863
H	−4.142473	−0.295277	−6.288789
H	−2.842835	0.861031	−6.487309
C	−4.140348	1.292904	−4.835308
H	−4.768033	0.754647	−4.109620
H	−3.423103	1.887605	−4.252676
C	−5.005742	2.255142	−5.648613
H	−5.716213	1.681790	−6.259877
H	−4.363016	2.802508	−6.351862
C	−5.766169	3.244621	−4.769254
H	−6.364530	3.937669	−5.369514
H	−6.443709	2.718948	−4.086647
H	−5.074896	3.837334	−4.159114

II

O	1.836714	2.715115	−2.040433
O	−0.031234	2.119303	−0.441101
O	1.505710	−1.503835	0.163396
O	2.936493	−1.095206	−1.880850
S	−0.253479	−3.503061	−1.314003
S	−0.083529	2.989023	−4.390182
O	−1.051288	−2.924012	−0.216214
O	−0.977132	−4.292646	−2.321653
O	1.252596	2.657447	−4.922379
O	−1.210855	2.882653	−5.332336
N	0.656743	−2.431393	−2.097245
N	−0.479436	2.185859	−3.055761
P	1.381698	−1.175466	−1.422667
N	0.788412	0.203794	−1.839680
P	0.544415	1.741230	−1.907720
H	−1.367552	0.284264	−3.868600
C	−0.329297	3.460561	−0.245149
C	2.636393	3.015960	−0.948506
C	2.519425	−0.963392	0.939694
C	3.693490	−2.224553	−1.608139
C	−1.700326	3.843426	−0.252723
C	4.002675	−3.096914	−2.690449
C	3.981561	2.550417	−0.980957
C	2.137401	−0.050278	1.963316
C	1.137324	8.040399	0.198726
C	1.458203	6.707888	0.095384
C	0.445944	5.719689	0.072536
C	−0.921651	6.136705	0.108860
C	−1.215466	7.517543	0.242444
C	−0.209409	8.448524	0.292637
H	1.927033	8.785588	0.198102
H	2.496844	6.403666	0.017238
C	0.726005	4.323888	−0.034420
C	−1.953398	5.187680	−0.027748

```
H    -2.256577    7.827254    0.276573        C    -6.602905   -1.438144   -1.984491
H    -2.977528    5.550118    0.009665        H    -7.665717   -1.404433   -2.196579
C     4.623889    4.552741    3.406795        C    -5.904120   -2.638498   -2.040947
C     5.111761    3.874662    2.318501        C    -6.613005   -3.912595   -2.393443
C     4.281696    3.590989    1.206346        F    -5.999499   -4.558319   -3.417182
C     2.930727    4.059749    1.206160        F    -7.896802   -3.707964   -2.763361
C     2.453032    4.733372    2.355487        F    -6.632554   -4.779138   -1.349489
C     3.277162    4.969462    3.429644        C     3.482429   -2.871087   -4.034125
H     5.815952    2.543820    0.123486        C     2.764573   -1.824878   -4.564537
H     6.141302    3.528411    2.296037        S     3.701334   -4.158150   -5.250942
C     4.775555    2.860700    0.107558        C     2.360969   -2.039411   -5.902167
C     2.111517    3.795646    0.063121        H     2.539705   -0.915042   -4.031590
H     1.419242    5.058624    2.387511        C     2.811673   -3.247453   -6.409999
H     2.886790    5.483421    4.303007        C     1.590637   -1.305545   -6.859969
C     7.201840   -0.444653    2.042062        S     2.372779   -3.535434   -8.065696
C     6.233518   -1.041118    1.270436        C     1.508700   -1.990720   -8.092106
C     4.860512   -0.783466    1.497611        C     0.964415   -0.062019   -6.727094
C     4.505623    0.148460    2.522178        C     0.817458   -1.466604   -9.174984
C     5.526944    0.725027    3.316696        H     1.046075    0.498260   -5.800698
C     6.847567    0.433916    3.086391        C     0.278978    0.473919   -7.801257
H     8.249222   -0.653480    1.845340        H     0.759851   -1.995205  -10.120158
H     6.521182   -1.712617    0.469332        C     0.199638   -0.230548   -9.012776
C     3.817371   -1.383322    0.722842        H    -0.188092    1.450470   -7.705036
C     3.153551    0.479502    2.737333        C    -0.623043    0.351257  -10.121502
H     5.239873    1.417304    4.103232        F    -0.458526   -0.299746  -11.292717
H     2.913310    1.167418    3.544925        F    -0.342236    1.654713  -10.336826
C     6.235346   -5.988361    0.529511        F    -1.957260    0.291266   -9.825558
C     5.921212   -5.663301   -0.765292        C     0.738238    0.298346    2.181022
C     5.189678   -4.485314   -1.061466        C    -0.401649   -0.438016    1.969930
C     4.820177   -3.611263    0.008686        S     0.358674    1.907799    2.828056
C     5.131626   -3.992689    1.335098        C    -1.584770    0.266660    2.309794
C     5.819622   -5.155040    1.588780        H    -0.395265   -1.446764    1.577628
H     5.092106   -4.887532   -3.161495        C    -1.323935    1.550846    2.765505
H     6.206033   -6.319258   -1.583609        C    -2.994847    0.000434    2.243311
H     4.811316   -3.360635    2.156827        S    -2.739591    2.500834    3.107250
H     6.035332   -5.439690    2.614159        C    -3.753698    1.133879    2.623700
C     4.791189   -4.193523   -2.380587        C    -3.667658   -1.160630    1.850045
C     4.113327   -2.412050   -0.307471        C    -5.139499    1.138062    2.579150
H    -0.447964    9.504431    0.376070        H    -3.102743   -2.037900    1.547817
H     5.269277    4.762380    4.254927        C    -5.051288   -1.170198    1.813491
H     7.622189    0.884147    3.700443        H    -5.711858    2.019483    2.848169
H     6.779965   -6.902541    0.744915        C    -5.779427   -0.024665    2.160368
C    -2.769823    2.889387   -0.523501        H    -5.577086   -2.061354    1.485529
C    -2.754342    1.522413   -0.681567        C    -7.278467   -0.072193    2.139298
S    -4.414906    3.528207   -0.777877        F    -7.749571   -0.855972    1.139818
C    -4.015868    0.979379   -1.026317        F    -7.829006    1.154633    1.982124
H    -1.877164    0.910882   -0.537322        F    -7.782522   -0.578419    3.295604
C    -5.006643    1.945127   -1.099717        C     4.487125    1.786576   -2.116080
C    -4.515237   -0.325544   -1.349143        C     4.129469    1.829503   -3.440912
C    -5.896453   -0.291357   -1.645274        S     5.768085    0.590196   -1.829733
S    -6.579790    1.335168   -1.512862        C     4.855857    0.908542   -4.238788
C    -3.843163   -1.553768   -1.397241        H     3.364923    2.487746   -3.832380
H    -2.793428   -1.620144   -1.127773        C     5.759207    0.161974   -3.496521
C    -4.532157   -2.700024   -1.748306        C     4.845159    0.514540   -5.619853
H    -4.004909   -3.649076   -1.789129        S     6.611439   -1.054033   -4.402611
```

C	5.732755	-0.563208	-5.857454
C	4.095328	1.019335	-6.687259
C	5.850483	-1.155140	-7.105781
H	3.405337	1.841924	-6.521869
C	4.215625	0.443382	-7.939916
H	6.516269	-1.995096	-7.273337
C	5.074788	-0.644915	-8.142639
H	3.623270	0.820514	-8.767648
C	5.211099	-1.226836	-9.517869
F	4.041405	-1.198774	-10.202939
F	5.629605	-2.514366	-9.492246
F	6.111679	-0.540749	-10.269073
C	0.944156	-4.650718	-0.550026
C	1.147344	-4.754381	0.826065
C	1.671946	-5.503972	-1.381027
C	2.011937	-5.708628	1.353095
C	2.529733	-6.463625	-0.865951
C	2.687944	-6.577645	0.509249
F	0.530199	-3.961298	1.701670
F	2.189719	-5.797181	2.672995
F	3.491588	-7.509272	1.015701
F	3.209927	-7.271138	-1.684208
F	1.569087	-5.421307	-2.709629
C	-0.030266	4.734357	-3.865637
C	1.140719	5.491101	-3.819249
C	-1.225937	5.358537	-3.504945
C	1.108798	6.837522	-3.470838
F	2.336898	4.977105	-4.105432
C	-1.268595	6.701037	-3.161451
F	-2.372076	4.677126	-3.477490
C	-0.097655	7.448380	-3.161363
F	2.236775	7.550440	-3.442655
F	-2.426396	7.277203	-2.829866
F	-0.130651	8.744228	-2.862702
C	-0.616884	-4.331488	-6.105708
C	-0.981313	-4.505154	-7.440377
C	-1.720949	-3.522727	-8.105118
C	-2.095472	-2.372218	-7.444423
C	-1.732342	-2.166843	-6.086119
C	-0.975133	-3.180183	-5.435439
H	-0.048642	-5.094240	-5.582718
H	-0.695861	-5.412379	-7.965257
H	-1.999603	-3.662013	-9.145078
H	-2.655763	-1.618821	-7.983878
H	-0.682441	-3.086695	-4.397395
C	-2.104443	-0.981104	-5.386186
C	-1.709263	-0.753135	-4.000322
H	-0.975053	-1.439001	-3.588600
H	-2.626226	-0.802789	-3.385839
C	-2.891671	0.106904	-6.009638
H	-3.436448	-0.224415	-6.896816
H	-2.120893	0.817795	-6.365691
C	-3.818545	0.911344	-5.082020
H	-4.553295	0.237719	-4.615961
H	-3.238294	1.373971	-4.276712

C	-4.530349	2.015021	-5.861237
H	-5.131418	1.572675	-6.668061
H	-3.772023	2.649285	-6.338015
C	-5.417471	2.867077	-4.958736
H	-5.902752	3.669080	-5.523620
H	-6.200256	2.262389	-4.487659
H	-4.824943	3.327357	-4.159983

EtMe$_2$SiH

Si	1.112291	-2.612087	-0.193748
H	0.771049	-1.787443	-1.390494
C	-0.480126	-3.096946	0.684814
H	-1.020678	-2.215125	1.045675
H	-1.148644	-3.645432	0.012402
H	-0.276861	-3.741920	1.546984
C	2.025922	-4.156003	-0.763317
H	1.420182	-4.732606	-1.470714
H	2.966811	-3.899238	-1.262202
H	2.262874	-4.812683	0.081160
C	2.206679	-1.579353	0.947346
H	3.097164	-1.265246	0.385637
H	1.670582	-0.653759	1.198424
C	2.627078	-2.306742	2.232970
H	3.257588	-1.674155	2.867412
H	1.756153	-2.601663	2.828617
H	3.196063	-3.216337	2.010841

III

O	1.768152	2.424278	-2.363061
O	-0.151187	1.896314	-0.804228
O	1.488029	-1.616994	0.054884
O	2.939996	-1.253242	-1.990056
S	-0.142342	-3.784714	-1.337421
S	-0.052428	2.649727	-4.750389
O	-0.974770	-3.181797	-0.278812
O	-0.826654	-4.651519	-2.309964
O	1.314989	2.362778	-5.222136
O	-1.126828	2.530680	-5.752528
N	0.737557	-2.723038	-2.165492
N	-0.492804	1.802748	-3.455525
P	1.384125	-1.397332	-1.551589
N	0.709638	-0.086606	-2.068045
P	0.477024	1.449842	-2.231197
H	-1.101312	-0.976451	-3.465000
C	-0.478031	3.238298	-0.680761
C	2.521576	2.823524	-1.270739
C	2.480642	-1.016272	0.813423
C	3.745548	-2.336291	-1.666087
C	-1.857067	3.586911	-0.719080
C	4.129913	-3.218044	-2.715442
C	3.885029	2.413610	-1.242973
C	2.062809	-0.068087	1.788633

C	0.873253	7.869776	-0.448609	C	-4.135959	0.611144	-1.076855
C	1.226512	6.541868	-0.478919	H	-1.967657	0.635667	-0.720584
C	0.237768	5.529819	-0.470927	C	-5.149026	1.546425	-1.213510
C	-1.139014	5.915394	-0.481683	C	-4.640082	-0.732124	-1.111813
C	-1.467341	7.293594	-0.424656	C	-6.047323	-0.751969	-1.241867
C	-0.484065	8.249686	-0.401468	S	-6.742347	0.870528	-1.365876
H	1.645565	8.632597	-0.471949	C	-3.953686	-1.946709	-0.996272
H	2.273253	6.259310	-0.521819	H	-2.874489	-1.964537	-0.878734
C	0.552423	4.136967	-0.495594	C	-4.661628	-3.133406	-0.984487
C	-2.145616	4.935296	-0.577620	H	-4.128652	-4.073894	-0.876353
H	-2.515695	7.579989	-0.425287	C	-6.769949	-1.937176	-1.219883
H	-3.178378	5.273864	-0.565799	H	-7.851880	-1.940688	-1.290591
C	4.338154	4.693057	3.030803	C	-6.061996	-3.125092	-1.084350
C	4.876493	3.963642	2.001157	C	-6.788814	-4.434567	-1.013670
C	4.088058	3.588100	0.885891	F	-6.291606	-5.333426	-1.902099
C	2.725219	4.014730	0.817761	F	-8.109522	-4.312294	-1.268705
C	2.196241	4.745460	1.908274	F	-6.669740	-5.004435	0.213190
C	2.980861	5.071985	2.988198	C	3.678307	-3.031719	-4.090155
H	5.687911	2.538663	-0.096383	C	2.920025	-2.042962	-4.672958
H	5.915071	3.645941	2.028833	S	4.107852	-4.277305	-5.293504
C	4.636999	2.813064	-0.154429	C	2.656266	-2.267692	-6.044955
C	1.945979	3.651753	-0.327826	H	2.570461	-1.165531	-4.152688
H	1.153460	5.041557	1.892467	C	3.249621	-3.425051	-6.518489
H	2.550228	5.627511	3.815984	C	1.907078	-1.591177	-7.062184
C	7.132219	-0.310404	1.948713	S	2.976365	-3.733440	-8.207106
C	6.191799	-0.970427	1.194681	C	1.994026	-2.263218	-8.301616
C	4.808669	-0.742795	1.392440	C	1.158402	-0.413302	-6.978458
C	4.415055	0.225918	2.367242	C	1.359366	-1.785642	-9.439063
C	5.408357	0.869190	3.145698	H	1.112650	0.140907	-6.045909
C	6.739674	0.606062	2.945578	C	0.512135	0.068571	-8.101892
H	8.187576	-0.497702	1.774215	H	1.440770	-2.299925	-10.390679
H	6.510353	-1.668832	0.429366	C	0.612398	-0.618064	-9.322435
C	3.793143	-1.407621	0.632710	H	-0.058812	0.990681	-8.037126
C	3.051575	0.527736	2.548851	C	-0.172860	-0.121214	-10.497498
H	5.091701	1.589239	3.895211	F	-1.484810	-0.498509	-10.405936
H	2.777788	1.244592	3.319527	F	0.283586	-0.607220	-11.672338
C	6.374618	-5.926493	0.655156	F	-0.170084	1.225831	-10.584750
C	6.079841	-5.656189	-0.656664	C	0.652426	0.252566	1.981705
C	5.312923	-4.516654	-1.009010	C	-0.462918	-0.541912	1.880421
C	4.883090	-3.625053	0.022734	S	0.232136	1.906681	2.463687
C	5.177567	-3.949523	1.368080	C	-1.662847	0.151942	2.192139
C	5.903517	-5.074936	1.676292	H	-0.423674	-1.584174	1.588023
H	5.299268	-4.978880	-3.097772	C	-1.435381	1.488322	2.491420
H	6.408590	-6.326988	-1.445912	C	-3.061797	-0.173480	2.257305
H	4.813807	-3.302836	2.159912	S	-2.869718	2.422699	2.792320
H	6.106574	-5.316677	2.715199	C	-3.846492	0.969939	2.544156
C	4.946589	-4.275901	-2.347490	C	-3.706078	-1.404823	2.096026
C	4.139481	-2.465519	-0.350398	C	-5.230311	0.913766	2.617191
H	-0.748478	9.302391	-0.375743	H	-3.123402	-2.295564	1.880287
H	4.951676	4.973362	3.882128	C	-5.084937	-1.476805	2.189856
H	7.493010	1.106873	3.546797	H	-5.822598	1.800955	2.813724
H	6.948035	-6.811450	0.913581	C	-5.841057	-0.321531	2.429483
C	-2.904701	2.587232	-0.894108	H	-5.588023	-2.428217	2.047634
C	-2.865340	1.210787	-0.890553	C	-7.332143	-0.432947	2.548517
S	-4.572080	3.165257	-1.138107	F	-7.849783	-1.313444	1.657056

F	-7.953374	0.752175	2.346795
F	-7.709221	-0.867280	3.779160
C	4.455791	1.627766	-2.330310
C	4.149762	1.627415	-3.668116
S	5.768671	0.490579	-1.964097
C	4.945300	0.722010	-4.414991
H	3.376742	2.247257	-4.103494
C	5.845939	0.027954	-3.620274
C	5.019395	0.312347	-5.789094
S	6.791468	-1.161375	-4.466107
C	5.967560	-0.723709	-5.969549
C	4.304147	0.774346	-6.898707
C	6.184450	-1.312500	-7.206126
H	3.566114	1.562299	-6.778076
C	4.522671	0.201378	-8.139237
H	6.899603	-2.118547	-7.331433
C	5.446034	-0.842497	-8.287787
H	3.959561	0.546192	-9.000774
C	5.690165	-1.417304	-9.651152
F	4.558181	-1.462463	-10.396566
F	6.186034	-2.675934	-9.598115
F	6.583947	-0.677300	-10.358127
C	1.088578	-4.849184	-0.509939
C	1.270270	-4.891691	0.872083
C	1.866055	-5.701960	-1.295700
C	2.161429	-5.789856	1.450440
C	2.749897	-6.607316	-0.728929
C	2.885350	-6.663617	0.652396
F	0.603695	-4.091562	1.704734
F	2.318155	-5.821094	2.775680
F	3.712355	-7.545471	1.208009
F	3.472832	-7.420668	-1.503107
F	1.784503	-5.673478	-2.627633
C	-0.080332	4.400966	-4.238330
C	1.058362	5.204588	-4.179908
C	-1.315175	4.999339	-3.982119
C	0.958600	6.569882	-3.932726
F	2.286122	4.718715	-4.362955
C	-1.425227	6.359486	-3.737567
F	-2.436827	4.276611	-3.970051
C	-0.284604	7.152120	-3.734047
F	2.057274	7.326628	-3.893113
F	-2.619075	6.909637	-3.503384
F	-0.381630	8.463687	-3.533268
C	-1.167702	-3.592800	-8.134204
C	-0.368119	-4.544034	-7.493876
C	-0.120069	-4.448118	-6.126287
C	-0.692665	-3.428298	-5.389432
C	-1.516581	-2.460669	-6.015645
C	-1.727328	-2.559152	-7.412912
H	-1.355671	-3.666285	-9.200847
H	0.060396	-5.361648	-8.066023
H	0.515901	-5.171917	-5.626054
H	-0.480284	-3.378032	-4.328309
H	-2.359648	-1.847038	-7.929071
C	-2.119315	-1.420857	-5.231981
C	-2.045662	-1.469027	-3.765018
H	-2.026461	-2.482763	-3.363572
H	-2.845455	-0.889949	-3.304421
C	-2.675651	-0.204383	-5.846617
H	-3.040272	-0.396976	-6.860309
H	-1.786812	0.447338	-5.996397
C	-3.693069	0.609896	-5.039274
H	-4.437017	-0.066861	-4.592918
H	-3.183161	1.130124	-4.218886
C	-4.408816	1.634316	-5.916219
H	-4.931256	1.112530	-6.731423
H	-3.664257	2.292181	-6.380833
C	-5.406744	2.464220	-5.113662
H	-5.927231	3.185859	-5.750989
H	-6.161660	1.824549	-4.640212
H	-4.897131	3.021508	-4.320345
Si	-5.022407	-3.554038	-5.441934
H	-4.262115	-2.267351	-5.302377
C	-5.069747	-3.994113	-7.270738
H	-5.719361	-4.862659	-7.432235
H	-5.456767	-3.171704	-7.881709
H	-4.072686	-4.252740	-7.641917
C	-6.751526	-3.197925	-4.791177
H	-6.671278	-3.010533	-3.713667
H	-7.369017	-4.100934	-4.895735
C	-7.425373	-2.001842	-5.478080
H	-8.411923	-1.793978	-5.049480
H	-6.822458	-1.092083	-5.369339
H	-7.565180	-2.176751	-6.550461
C	-4.117114	-4.868570	-4.461143
H	-4.680822	-5.808294	-4.449707
H	-3.129631	-5.075502	-4.889368
H	-3.967354	-4.561112	-3.421256

III'

O	1.627391	2.799077	-2.320630
O	-0.128250	2.325900	-0.541302
O	1.678201	-1.506550	0.525616
O	2.957459	-1.408807	-1.653893
S	-0.489341	-3.195235	-0.947536
S	-0.294525	1.965399	-4.520151
O	-0.915530	-2.882830	0.426039
O	-1.553408	-3.602490	-1.886838
O	1.050537	1.707994	-5.071526
O	-1.439546	1.504273	-5.319753
N	0.358427	-2.037235	-1.664698
N	-0.482652	1.428187	-3.010686
P	1.482523	-1.097998	-1.030342
N	1.362515	0.445124	-1.217752
P	0.584854	1.648048	-1.841852
H	-1.111455	-1.296249	-3.510262
C	-0.503774	3.658185	-0.592816

C	2.460463	3.303085	-1.326626	H	-0.969156	9.702339	-1.162863
C	2.741278	-0.883094	1.172582	H	4.997803	5.803344	3.604779
C	3.662355	-2.525158	-1.242378	H	8.082662	1.361697	3.019721
C	-1.895351	3.972917	-0.564505	H	6.629660	-6.997087	1.640161
C	3.882704	-3.562803	-2.195797	C	-2.934336	2.951974	-0.492718
C	3.801890	2.837007	-1.269423	C	-2.870413	1.579248	-0.499335
C	2.454333	0.224081	2.016838	S	-4.632178	3.497873	-0.394901
C	0.693014	8.316004	-1.112025	C	-4.142084	0.957364	-0.450248
C	1.089264	7.008573	-0.960195	H	-1.948038	1.022568	-0.536379
C	0.135493	5.986645	-0.743074	C	-5.181889	1.868771	-0.387883
C	-1.249979	6.332964	-0.721203	C	-4.618032	-0.391524	-0.484889
C	-1.622324	7.693906	-0.856441	C	-6.029661	-0.448489	-0.444014
C	-0.671698	8.665052	-1.042482	S	-6.766512	1.156378	-0.358662
H	1.436598	9.085694	-1.295407	C	-3.890237	-1.581997	-0.554260
H	2.140767	6.746920	-1.020433	H	-2.806510	-1.559208	-0.546474
C	0.495397	4.615222	-0.593532	C	-4.558628	-2.790917	-0.602836
C	-2.219138	5.320739	-0.601547	H	-3.986721	-3.712878	-0.657044
H	-2.678144	7.951056	-0.834474	C	-6.714194	-1.656629	-0.489210
H	-3.260442	5.630570	-0.582016	H	-7.797469	-1.694345	-0.461127
C	4.371033	5.477953	2.779657	C	-5.962833	-2.823042	-0.580474
C	4.877750	4.645911	1.813196	C	-6.633405	-4.159177	-0.669635
C	4.070470	4.210080	0.733196	F	-7.979185	-4.071205	-0.696917
C	2.720263	4.672439	0.641384	F	-6.303241	-4.963718	0.369977
C	2.224718	5.515651	1.663566	F	-6.256225	-4.826945	-1.799155
C	3.029646	5.906934	2.706640	C	3.371655	-3.501207	-3.563375
H	5.618977	3.009360	-0.150617	C	2.695064	-2.524223	-4.259111
H	5.906410	4.297785	1.862607	S	3.655688	-4.923719	-4.602437
C	4.581018	3.322624	-0.235269	C	2.388582	-2.892830	-5.596707
C	1.915118	4.207540	-0.444189	H	2.445506	-1.559463	-3.843627
H	1.191840	5.844696	1.625997	C	2.850808	-4.160695	-5.912791
H	2.627311	6.549049	3.484519	C	1.748849	-2.268332	-6.722673
C	7.502776	-0.308037	1.768055	S	2.568299	-4.653551	-7.554928
C	6.463505	-1.032379	1.234925	C	1.784315	-3.098433	-7.866958
C	5.119896	-0.681049	1.503444	C	1.159182	-1.004026	-6.828669
C	4.864951	0.464126	2.321623	C	1.297477	-2.678915	-9.097398
C	5.959578	1.179903	2.867045	H	1.127362	-0.336606	-5.973907
C	7.251694	0.803482	2.598513	C	0.660571	-0.578469	-8.045937
H	8.526592	-0.590971	1.542297	H	1.364654	-3.311187	-9.976023
H	6.671033	-1.876940	0.586482	C	0.743056	-1.406903	-9.175941
C	4.005183	-1.370619	0.932692	H	0.221312	0.411490	-8.124168
C	3.539615	0.871789	2.576385	C	0.299578	-0.870886	-10.504728
H	5.751646	2.040648	3.497767	F	1.225002	-0.029246	-11.033051
H	3.379570	1.723046	3.234162	F	-0.852199	-0.162158	-10.408996
C	6.128938	-6.090664	1.313723	F	0.092972	-1.849242	-11.415430
C	5.745660	-5.949342	0.004123	C	1.082378	0.650589	2.256169
C	5.075693	-4.778702	-0.431480	C	-0.077689	-0.084418	2.260326
C	4.833758	-3.726007	0.502810	S	0.772392	2.358201	2.622886
C	5.221016	-3.913625	1.850468	C	-1.221932	0.696209	2.563064
C	5.851083	-5.069281	2.245104	H	-0.109341	-1.147180	2.055743
H	4.846325	-5.468147	-2.438110	C	-0.912145	2.033923	2.764432
H	5.932552	-6.742636	-0.715170	C	-2.626070	0.443151	2.723101
H	5.002208	-3.137878	2.576469	S	-2.280821	3.048695	3.112933
H	6.128402	-5.201319	3.286569	C	-3.336833	1.632145	3.017064
C	4.618728	-4.652481	-1.756194	C	-3.331877	-0.761524	2.639323
C	4.173814	-2.546999	0.043651	C	-4.710783	1.638294	3.206537

```
H    -2.806742   -1.681605    2.399019      C    -2.180368   -4.068487   -4.836581
C    -4.700986   -0.767762    2.839655      C    -3.113918   -5.014465   -4.360069
H    -5.248443    2.556052    3.419635      H    -3.666122   -7.079739   -4.270513
C    -5.385005    0.424650    3.113072      H    -1.819275   -7.817838   -5.752190
H    -5.255058   -1.698132    2.764380      H    -0.203900   -6.161163   -6.655756
C    -6.858969    0.376723    3.384298      H    -0.413732   -3.788985   -6.062993
F    -7.491703   -0.543134    2.614709      H    -3.912910   -4.701947   -3.695851
F    -7.463053    1.568024    3.166430      C    -2.308547   -2.681040   -4.494408
F    -7.121471    0.039424    4.674865      C    -1.157063   -1.789637   -4.493759
C     4.311766    1.859673   -2.223807      H    -1.320243   -0.951389   -5.188966
C     3.986367    1.638407   -3.538771      H    -0.205651   -2.283568   -4.671805
S     5.545547    0.719371   -1.656993      C    -3.614243   -2.129759   -4.085046
C     4.719550    0.566261   -4.113610      H    -3.717670   -2.423303   -3.018761
H     3.241693    2.215257   -4.071576      H    -4.421632   -2.655178   -4.609198
C     5.582068   -0.029420   -3.203514      C    -3.782558   -0.612542   -4.190438
C     4.792048   -0.064560   -5.403115      H    -3.148314   -0.102432   -3.453878
S     6.472336   -1.388127   -3.825063      H    -3.432198   -0.270176   -5.172097
C     5.694366   -1.157423   -5.396305      C    -5.236227   -0.188991   -4.001135
C     4.132536    0.252136   -6.595243      H    -5.614399   -0.576597   -3.046823
C     5.917368   -1.934638   -6.522198      H    -5.853643   -0.648278   -4.786355
H     3.427938    1.078309   -6.618813      C    -5.388970    1.329110   -4.044806
C     4.362819   -0.506231   -7.730597      H    -6.432807    1.628430   -3.908160
H     6.599455   -2.778128   -6.500437      H    -4.794901    1.801003   -3.255282
C     5.239452   -1.598145   -7.690416      H    -5.038747    1.732526   -5.001667
H     3.840134   -0.270754   -8.652367      Si   -3.616504   -1.843015   -8.039376
C     5.516778   -2.372768   -8.943745      H    -2.866408   -2.134589   -6.780021
F     4.437327   -2.431169   -9.760616      C    -5.401635   -2.377003   -7.771583
F     5.894353   -3.647899   -8.685449      H    -5.468826   -3.439703   -7.512643
F     6.518807   -1.812298   -9.670840      H    -5.870198   -1.801241   -6.965963
C     0.639419   -4.626654   -0.825418      H    -5.999783   -2.216918   -8.675886
C     1.292698   -4.963921    0.362802      C    -2.811209   -2.874239   -9.395656
C     0.857874   -5.438398   -1.940296      H    -2.942463   -3.934097   -9.133228
C     2.106234   -6.089331    0.441249      H    -1.728519   -2.694846   -9.370532
C     1.650632   -6.574018   -1.866481      C    -3.357817   -2.606354  -10.804820
C     2.279380   -6.897926   -0.671963      H    -2.865261   -3.237943  -11.551903
F     1.176049   -4.236690    1.470070      H    -4.433904   -2.805684  -10.863727
F     2.727343   -6.389165    1.581082      H    -3.195218   -1.565404  -11.101812
F     3.068252   -7.968856   -0.606179      C    -3.522100    0.003042   -8.358301
F     1.827205   -7.351324   -2.938816      H    -4.053846    0.559801   -7.578655
F     0.318291   -5.150876   -3.126086      H    -2.485881    0.353539   -8.363332
C    -0.464770    3.780738   -4.396630      H    -3.971548    0.265039   -9.322675
C     0.582670    4.671776   -4.633844
C    -1.704996    4.313500   -4.040700      IV
C     0.389301    6.046120   -4.541700
F     1.810086    4.266857   -4.958501      O     1.709928    2.414544   -2.354586
C    -1.909671    5.682514   -3.953122      O    -0.206572    1.901904   -0.783983
F    -2.737347    3.517728   -3.760846      O     1.465082   -1.657736    0.057076
C    -0.860024    6.553187   -4.215706      O     2.895602   -1.283668   -2.006208
F     1.402074    6.883863   -4.774663      S    -0.200171   -3.789051   -1.347493
F    -3.106769    6.167650   -3.613917      S    -0.123445    2.571271   -4.750831
F    -1.051402    7.868127   -4.157647      O    -1.043943   -3.184785   -0.296508
C    -2.968220   -6.352068   -4.672459      O    -0.887579   -4.658587   -2.318985
C    -1.923113   -6.766037   -5.501077      O     1.238187    2.247339   -5.216659
C    -1.011122   -5.840533   -6.004823      O    -1.205983    2.442691   -5.737781
C    -1.120606   -4.506119   -5.658484      N     0.693164   -2.739805   -2.165606
```

N	-0.563702	1.784463	-3.418735	H	5.245200	-5.015340	-3.121373
P	1.344125	-1.417384	-1.547551	H	6.355913	-6.366594	-1.475083
N	0.674484	-0.090866	-2.014074	H	4.794379	-3.330463	2.134844
P	0.421266	1.435448	-2.208604	H	6.082827	-5.347991	2.686249
H	-0.984040	-1.009433	-3.989497	C	4.899160	-4.309037	-2.371348
C	-0.528529	3.245511	-0.679771	C	4.106151	-2.496762	-0.373477
C	2.467051	2.815577	-1.267005	H	-0.764869	9.316989	-0.459121
C	2.459892	-1.048522	0.804486	H	4.902230	4.980377	3.878094
C	3.702924	-2.367349	-1.687444	H	7.492793	1.074053	3.501105
C	-1.905505	3.603341	-0.724272	H	6.906758	-6.849940	0.882064
C	4.086337	-3.247482	-2.739515	C	-2.961416	2.607194	-0.872813
C	3.828426	2.398975	-1.235598	C	-2.924007	1.231861	-0.895296
C	2.050478	-0.093292	1.776215	S	-4.638989	3.190506	-1.033617
C	0.848345	7.873557	-0.503842	C	-4.202640	0.637064	-1.036010
C	1.193903	6.543450	-0.515079	H	-2.021660	0.651297	-0.779420
C	0.198950	5.537357	-0.498426	C	-5.220207	1.573773	-1.109956
C	-1.175055	5.931291	-0.520522	C	-4.707737	-0.704478	-1.053742
C	-1.495634	7.312006	-0.484465	C	-6.121386	-0.724509	-1.104803
C	-0.506873	8.262422	-0.469153	S	-6.820723	0.897918	-1.182511
H	1.625376	8.631391	-0.533385	C	-4.013731	-1.918494	-0.974932
H	2.239045	6.254049	-0.549022	H	-2.929624	-1.934214	-0.912002
C	0.505326	4.142736	-0.503687	C	-4.720391	-3.104898	-0.919694
C	-2.186467	4.955397	-0.606398	H	-4.182514	-4.043924	-0.821972
H	-2.542235	7.604495	-0.494757	C	-6.840716	-1.911248	-1.048550
H	-3.216770	5.301629	-0.607602	H	-7.924834	-1.915176	-1.060441
C	4.288559	4.699715	3.026965	C	-6.125096	-3.098145	-0.949877
C	4.823892	3.960455	2.002679	C	-6.841383	-4.411186	-0.894429
C	4.035426	3.584146	0.887543	F	-6.534963	-5.188844	-1.979610
C	2.675686	4.019679	0.814472	F	-8.183511	-4.278002	-0.882975
C	2.149851	4.761645	1.898939	F	-6.495227	-5.135849	0.193863
C	2.934358	5.089203	2.978681	C	3.654012	-3.052934	-4.119478
H	5.630700	2.521517	-0.087461	C	2.860834	-2.091244	-4.702431
H	5.860406	3.636266	2.034104	S	4.186828	-4.240928	-5.340832
C	4.581167	2.800563	-0.148053	C	2.653946	-2.291375	-6.088278
C	1.896311	3.652995	-0.329456	H	2.448615	-1.247331	-4.172575
H	1.109203	5.065389	1.878691	C	3.323000	-3.402255	-6.570839
H	2.506232	5.653326	3.801977	C	1.924190	-1.613456	-7.119238
C	7.119812	-0.349091	1.910931	S	3.146357	-3.662986	-8.280018
C	6.173906	-1.008380	1.163276	C	2.104553	-2.235469	-8.374454
C	4.792382	-0.775165	1.365917	C	1.129465	-0.466449	-7.037205
C	4.406516	0.197229	2.340194	C	1.515620	-1.739650	-9.528553
C	5.405439	0.840822	3.111266	H	1.005884	0.048368	-6.089780
C	6.734969	0.572942	2.905770	C	0.535452	0.037459	-8.179023
H	8.173742	-0.540760	1.732532	H	1.666496	-2.217443	-10.490425
H	6.486462	-1.710568	0.398934	C	0.726876	-0.599872	-9.414949
C	3.770851	-1.438583	0.613206	H	-0.069798	0.937397	-8.114351
C	3.044926	0.503583	2.528025	C	-0.003092	-0.076215	-10.612593
H	5.094331	1.564677	3.859527	F	-1.325209	-0.423899	-10.576124
H	2.777789	1.224913	3.296870	F	0.487018	-0.557803	-11.776412
C	6.335359	-5.963058	0.625607	F	0.031031	1.273017	-10.685741
C	6.033829	-5.693696	-0.684842	C	0.642671	0.235167	1.974393
C	5.269930	-4.551255	-1.034846	C	-0.477724	-0.552239	1.878118
C	4.849388	-3.656859	-0.002345	S	0.235076	1.893335	2.453959
C	5.150764	-3.979994	1.341967	C	-1.671574	0.150106	2.194231
C	5.874081	-5.107654	1.648124	H	-0.446067	-1.594920	1.586562

C	-1.434366	1.485738	2.489491
C	-3.070098	-0.169243	2.280517
S	-2.860695	2.426326	2.809626
C	-3.846213	0.977305	2.579652
C	-3.720817	-1.399704	2.137113
C	-5.228165	0.924079	2.684512
H	-3.144358	-2.292405	1.912571
C	-5.096822	-1.468891	2.266372
H	-5.813704	1.813202	2.892403
C	-5.845506	-0.311166	2.519325
H	-5.604663	-2.420425	2.143651
C	-7.331875	-0.420665	2.682470
F	-7.876263	-1.306615	1.810006
F	-7.959487	0.762690	2.491987
F	-7.674748	-0.849393	3.924821
C	4.397311	1.608496	-2.319708
C	4.089874	1.603165	-3.657278
S	5.720060	0.483202	-1.952927
C	4.896344	0.708170	-4.403958
H	3.310899	2.214532	-4.093447
C	5.804253	0.023845	-3.609322
C	4.991620	0.317118	-5.782061
S	6.779981	-1.137242	-4.459336
C	5.966829	-0.692339	-5.966864
C	4.280853	0.781666	-6.893361
C	6.222695	-1.246460	-7.211977
H	3.517676	1.544528	-6.768435
C	4.537382	0.243080	-8.142011
H	6.962013	-2.029649	-7.341758
C	5.494245	-0.769193	-8.296994
H	3.979034	0.590801	-9.005437
C	5.787843	-1.296800	-9.669429
F	4.676289	-1.357159	-10.443489
F	6.325452	-2.538952	-9.641155
F	6.672816	-0.506838	-10.333760
C	1.016955	-4.862034	-0.509927
C	1.195047	-4.899537	0.872436
C	1.800115	-5.713893	-1.291337
C	2.090217	-5.790296	1.455879
C	2.686289	-6.613862	-0.719043
C	2.820166	-6.663416	0.662647
F	0.520378	-4.101407	1.701181
F	2.243583	-5.816657	2.781966
F	3.648990	-7.540415	1.223677
F	3.410839	-7.430170	-1.488512
F	1.720463	-5.691079	-2.622712
C	-0.109925	4.338862	-4.280690
C	1.045152	5.119409	-4.239640
C	-1.328294	4.968360	-4.022081
C	0.977526	6.488782	-4.002907
F	2.261708	4.607985	-4.430633
C	-1.407896	6.333116	-3.790947
F	-2.466466	4.271638	-3.993219
C	-0.250594	7.100671	-3.800864
F	2.093007	7.222067	-3.977386

F	-2.589285	6.911598	-3.557716
F	-0.317001	8.416284	-3.610100
C	-1.064269	-3.632544	-8.389590
C	-0.258959	-4.590089	-7.777671
C	-0.101705	-4.572497	-6.396416
C	-0.772197	-3.630077	-5.624764
C	-1.612752	-2.682783	-6.226287
C	-1.730207	-2.686140	-7.623832
H	-1.168176	-3.613319	-9.470551
H	0.260227	-5.331389	-8.377606
H	0.549936	-5.289926	-5.905984
H	-0.623667	-3.649576	-4.550862
H	-2.339685	-1.946313	-8.130854
C	-2.414581	-1.728539	-5.385170
C	-1.940741	-1.544474	-3.962953
H	-1.781505	-2.487497	-3.441254
H	-2.639129	-0.936395	-3.386556
C	-2.868532	-0.434659	-6.052224
H	-3.413629	-0.657957	-6.977541
H	-1.952255	0.094630	-6.352131
C	-3.715545	0.483602	-5.170724
H	-4.462295	-0.109591	-4.617875
H	-3.078640	0.967009	-4.421381
C	-4.434976	1.565611	-5.971840
H	-5.038452	1.101937	-6.766906
H	-3.685853	2.193164	-6.469110
C	-5.327878	2.425841	-5.081627
H	-5.825905	3.214574	-5.654179
H	-6.102678	1.818191	-4.596559
H	-4.739852	2.903746	-4.291301
Si	-4.649131	-3.518553	-5.144972
H	-3.512121	-2.287888	-5.225405
C	-4.816702	-3.945293	-6.942822
H	-5.673191	-4.623981	-7.057750
H	-5.013031	-3.062188	-7.558809
H	-3.923386	-4.448918	-7.321863
C	-6.068772	-2.560048	-4.414970
H	-5.685507	-1.974455	-3.569535
H	-6.738089	-3.306984	-3.960194
C	-6.835344	-1.674657	-5.405280
H	-7.628694	-1.123992	-4.890518
H	-6.182426	-0.935248	-5.879940
H	-7.301600	-2.267711	-6.198160
C	-3.790988	-4.765929	-4.090783
H	-4.511455	-5.554408	-3.834931
H	-2.945737	-5.220188	-4.616003
H	-3.420497	-4.341807	-3.153734

IV'

O	1.568145	2.765143	-2.358214
O	-0.153144	2.319340	-0.534959
O	1.615032	-1.506807	0.513823
O	2.850617	-1.451455	-1.691129

S	-0.590838	-3.217736	-0.854384	H	3.387099	1.729957	3.166922
S	-0.450172	2.001168	-4.504351	C	6.026747	-6.123355	1.282034
O	-0.973934	-2.857719	0.520102	C	5.630782	-5.990891	-0.024751
O	-1.674182	-3.655031	-1.751533	C	4.968682	-4.817644	-0.465109
O	0.861159	1.712600	-5.118687	C	4.747572	-3.753326	0.461302
O	-1.641588	1.581597	-5.263203	C	5.148556	-3.931250	1.806321
N	0.246802	-2.082148	-1.629848	C	5.770607	-5.089512	2.205825
N	-0.596415	1.461182	-2.998526	H	4.720652	-5.519359	-2.465656
P	1.383376	-1.131391	-1.046945	H	5.801022	-6.793589	-0.737678
N	1.274643	0.408485	-1.272351	H	4.945619	-3.145879	2.526553
P	0.509909	1.634823	-1.858691	H	6.057566	-5.214134	3.245608
H	-1.101307	-2.005498	-3.553813	C	4.503759	-4.697264	-1.787851
C	-0.509781	3.657337	-0.576923	C	4.091175	-2.573500	-0.000362
C	2.429502	3.254273	-1.381815	H	-0.889022	9.709481	-1.130641
C	2.692288	-0.883344	1.131889	H	5.129610	5.729775	3.477414
C	3.561795	-2.561259	-1.279599	H	8.081898	1.315779	2.893667
C	-1.895137	3.994456	-0.518177	H	6.520620	-7.032142	1.612307
C	3.775444	-3.603538	-2.229640	C	-2.949869	2.991972	-0.427154
C	3.765390	2.770831	-1.356123	C	-2.915518	1.619428	-0.484088
C	2.428438	0.233140	1.972282	S	-4.630322	3.567071	-0.241271
C	0.751265	8.296321	-1.119969	C	-4.196431	1.021019	-0.406399
C	1.129325	6.982305	-0.978310	H	-2.009500	1.044537	-0.583385
C	0.164371	5.975716	-0.739551	C	-5.213348	1.949488	-0.269414
C	-1.214274	6.344292	-0.685256	C	-4.699739	-0.318156	-0.464637
C	-1.567244	7.711407	-0.810796	C	-6.108591	-0.349189	-0.358148
C	-0.605654	8.667332	-1.018254	S	-6.809098	1.266812	-0.190358
H	1.502913	9.053976	-1.319942	C	-3.999658	-1.519969	-0.601842
H	2.174777	6.703617	-1.063133	H	-2.917041	-1.517616	-0.660964
C	0.504384	4.598090	-0.600187	C	-4.693076	-2.713874	-0.640169
C	-2.196975	5.347794	-0.546950	H	-4.142980	-3.644473	-0.744315
H	-2.617983	7.985536	-0.763906	C	-6.818133	-1.542751	-0.392471
H	-3.232751	5.673766	-0.508476	H	-7.898891	-1.561292	-0.307599
C	4.476463	5.409556	2.670915	C	-6.094310	-2.720660	-0.543023
C	4.946497	4.569212	1.693300	C	-6.795625	-4.042729	-0.605321
C	4.104612	4.140089	0.637362	F	-8.141066	-3.923318	-0.604689
C	2.758452	4.618888	0.579940	F	-6.464965	-4.842125	0.439260
C	2.300938	5.469585	1.613855	F	-6.459010	-4.731956	-1.731630
C	3.138482	5.853552	2.633625	C	3.281999	-3.529360	-3.603530
H	5.613164	2.917395	-0.286136	C	2.627030	-2.539774	-4.300967
H	5.971623	4.208291	1.715802	S	3.600813	-4.932301	-4.660120
C	4.577567	3.244394	-0.342309	C	2.376790	-2.877867	-5.658132
C	1.919696	4.166261	-0.485363	H	2.357578	-1.585240	-3.874663
H	1.271355	5.810561	1.603619	C	2.852845	-4.137363	-5.984752
H	2.764628	6.501437	3.420886	C	1.811499	-2.215107	-6.800279
C	7.467927	-0.353403	1.657467	S	2.666224	-4.579329	-7.655627
C	6.413809	-1.069536	1.142354	C	1.915744	-3.009676	-7.967065
C	5.077591	-0.702792	1.426746	C	1.237196	-0.942574	-6.903517
C	4.845692	0.449930	2.241311	C	1.514880	-2.545912	-9.212712
C	5.955137	1.156110	2.769011	H	1.147863	-0.302980	-6.031078
C	7.239626	0.764653	2.485657	C	0.826426	-0.473150	-8.137793
H	8.485572	-0.648657	1.419808	H	1.638200	-3.150129	-10.104887
H	6.603896	-1.920137	0.496438	C	0.976667	-1.265892	-9.287131
C	3.947544	-1.385776	0.878151	H	0.408142	0.526177	-8.213919
C	3.528440	0.873321	2.511801	C	0.622563	-0.688993	-10.622901
H	5.764649	2.022167	3.397897	F	1.578934	0.156729	-11.077736

F	-0.531710	0.033031	-10.575530	C	-1.790036	4.383210	-3.985403
F	0.452316	-1.638865	-11.570868	C	0.333222	6.064160	-4.541794
C	1.063880	0.669876	2.232097	F	1.699099	4.249652	-4.990778
C	-0.102419	-0.055404	2.240491	C	-1.958767	5.757305	-3.897341
S	0.771767	2.374806	2.628549	F	-2.834827	3.614421	-3.678181
C	-1.236100	0.729947	2.566339	C	-0.895406	6.602064	-4.188167
H	-0.147412	-1.115280	2.024850	F	1.360148	6.875903	-4.804446
C	-0.913756	2.061352	2.786179	F	-3.135490	6.272399	-3.531727
C	-2.639452	0.482903	2.740509	F	-1.054120	7.921597	-4.131178
S	-2.269890	3.078015	3.175823	C	-2.706598	-6.479698	-4.465855
C	-3.336626	1.669322	3.073322	C	-1.607823	-6.930985	-5.188161
C	-3.354253	-0.714883	2.636832	C	-0.800937	-6.015711	-5.859887
C	-4.705845	1.678333	3.293572	C	-1.089488	-4.660782	-5.797192
H	-2.839686	-1.630597	2.359465	C	-2.197746	-4.193913	-5.077387
C	-4.718983	-0.718055	2.865733	C	-3.008790	-5.123194	-4.418205
H	-5.233301	2.593485	3.540705	H	-3.331962	-7.184222	-3.925751
C	-5.388747	0.470473	3.187793	H	-1.373592	-7.991011	-5.220487
H	-5.280450	-1.642783	2.777129	H	0.066465	-6.353621	-6.419276
C	-6.854469	0.424079	3.499877	H	-0.440135	-3.959990	-6.315526
F	-7.514484	-0.480170	2.735264	H	-3.855175	-4.793865	-3.825931
F	-7.459483	1.621653	3.319671	C	-2.465904	-2.720482	-4.986242
F	-7.081265	0.067568	4.792588	C	-1.267719	-1.877888	-4.629159
C	4.244888	1.794069	-2.327722	H	-1.437984	-0.817618	-4.825782
C	3.923842	1.613921	-3.649759	H	-0.362798	-2.208342	-5.138569
S	5.445109	0.611172	-1.779381	C	-3.747220	-2.296434	-4.296451
C	4.641512	0.542611	-4.247571	H	-3.648049	-2.614936	-3.248879
H	3.194629	2.222322	-4.169846	H	-4.597933	-2.852798	-4.711501
C	5.477095	-0.099691	-3.343263	C	-4.025869	-0.794642	-4.337374
C	4.740063	-0.036541	-5.559507	H	-3.340981	-0.263361	-3.664651
S	6.352310	-1.454494	-3.993343	H	-3.808768	-0.390776	-5.338013
C	5.620432	-1.147275	-5.572426	C	-5.466898	-0.454890	-3.967882
C	4.139793	0.354242	-6.761588	H	-5.708300	-0.910518	-2.999914
C	5.869897	-1.876072	-6.725362	H	-6.152985	-0.911474	-4.697110
H	3.459705	1.200951	-6.774006	C	-5.698002	1.052535	-3.906973
C	4.404150	-0.349194	-7.924059	H	-6.731436	1.288979	-3.635837
H	6.533466	-2.734342	-6.718071	H	-5.039781	1.514222	-3.162952
C	5.250985	-1.465491	-7.902033	H	-5.479467	1.524973	-4.871873
H	3.934463	-0.050197	-8.856012	Si	-3.189257	-1.984213	-7.706788
C	5.562942	-2.177868	-9.183429	H	-2.669092	-2.390630	-6.170283
F	4.492520	-2.227481	-10.015880	C	-4.978090	-2.470564	-7.588794
F	5.969074	-3.452888	-8.979088	H	-5.090227	-3.510151	-7.263671
F	6.555638	-1.559571	-9.875022	H	-5.528699	-1.819984	-6.903033
C	0.547207	-4.641132	-0.731522	H	-5.439397	-2.377770	-8.580877
C	1.197735	-4.990663	0.453235	C	-2.120460	-3.152263	-8.682833
C	0.769831	-5.435421	-1.858463	H	-2.268759	-4.175930	-8.318503
C	2.008580	-6.119247	0.520253	H	-1.066771	-2.901861	-8.510329
C	1.561817	-6.572045	-1.796259	C	-2.447725	-3.055914	-10.188028
C	2.181643	-6.914812	-0.602146	H	-1.778518	-3.706550	-10.759262
F	1.082466	-4.272170	1.567026	H	-3.474879	-3.370352	-10.400819
F	2.629508	-6.433552	1.657355	H	-2.314176	-2.039696	-10.572477
F	2.969423	-7.988378	-0.547840	C	-2.823792	-0.176321	-7.872551
F	1.754508	-7.328586	-2.881672	H	-3.723959	0.426015	-7.716372
F	0.243938	-5.121257	-3.041057	H	-2.076231	0.159942	-7.144746
C	-0.571867	3.820233	-4.371121	H	-2.425006	0.023894	-8.873908
C	0.490506	4.685316	-4.634688				

69a

```
C    -1.121043   -3.204043   -7.916284
C    -1.807323   -4.378768   -7.618057
C    -2.407910   -4.521093   -6.372229
C    -2.322021   -3.495466   -5.434042
C    -1.637698   -2.313415   -5.719179
C    -1.037564   -2.183799   -6.975747
H    -0.648193   -3.082583   -8.887001
H    -1.872665   -5.176042   -8.352713
H    -2.946860   -5.432417   -6.128295
H    -2.797932   -3.611915   -4.462781
H    -0.498977   -1.272978   -7.226045
C    -1.551223   -1.199244   -4.696235
C    -2.228208    0.089484   -5.193731
H    -1.691628    0.459676   -6.079522
H    -2.112406    0.862682   -4.420520
C    -3.708106   -0.080812   -5.526915
H    -3.821803   -0.849936   -6.303272
H    -4.239290   -0.459916   -4.640911
C    -4.367492    1.215417   -5.995827
H    -3.834407    1.590384   -6.880443
H    -4.251812    1.984929   -5.219762
C    -5.847960    1.036898   -6.325321
H    -6.302471    1.974902   -6.660183
H    -5.985855    0.294856   -7.119779
H    -6.405582    0.689162   -5.448242
H    -2.098863   -1.534964   -3.803213
C    -0.097514   -0.930602   -4.285599
H     0.385289   -1.844924   -3.926671
H     0.486313   -0.554163   -5.132911
H    -0.053483   -0.179325   -3.489454
```

[Si]-X*

```
O     2.398726    2.899675   -1.792718
O     0.377318    2.338156   -0.335101
O     1.965256   -1.499493    0.628647
O     3.627547   -1.253137   -1.281579
S     0.452579   -2.137416   -3.062246
S     0.777237    2.612219   -4.227123
O    -1.005958   -2.320199   -2.994995
O     0.955803   -0.998010   -3.863451
O     2.062497    2.258763   -4.821019
O    -0.371291    2.477028   -5.265087
N     1.082390   -2.205605   -1.585578
N     0.304126    1.915265   -2.916261
P     2.036100   -1.113362   -0.944372
N     1.802118    0.426282   -1.146657
P     1.238354    1.781662   -1.589284
C     0.063115    3.692250   -0.286516
C     3.103307    3.263167   -0.641537
C     2.876140   -0.861259    1.469540
```

```
C     4.359489   -2.329690   -0.800152
C    -1.307010    4.074234   -0.397147
C     4.907808   -3.254528   -1.737720
C     4.420847    2.760744   -0.461020
C     2.397111    0.164526    2.333711
C     1.506686    8.306943   -0.116316
C     1.827077    6.971175   -0.068748
C     0.812691    5.984613   -0.094585
C    -0.547988    6.401070   -0.210168
C    -0.845185    7.787645   -0.232214
C     0.159182    8.720135   -0.180710
H     2.297682    9.050662   -0.109704
H     2.866131    6.661754   -0.020773
C     1.092041    4.586581   -0.052705
C    -1.564287    5.436759   -0.327624
H    -1.883969    8.097332   -0.310754
H    -2.585943    5.798890   -0.400988
C     4.521326    5.059366    3.832029
C     5.135328    4.305034    2.864512
C     4.453024    3.957910    1.672188
C     3.123655    4.439954    1.465432
C     2.511516    5.195971    2.492907
C     3.192489    5.494510    3.648641
H     6.087302    2.811491    0.882935
H     6.152016    3.946994    3.001301
C     5.068016    3.143887    0.701503
C     2.460538    4.096758    0.245880
H     1.488483    5.533135    2.367160
H     2.701904    6.069917    4.427981
C     7.418489   -0.199275    3.012713
C     6.534807   -0.882752    2.212829
C     5.147377   -0.606024    2.259635
C     4.692769    0.431009    3.129583
C     5.625787    1.099503    3.960597
C     6.961213    0.790631    3.907251
H     8.479317   -0.424075    2.954634
H     6.902943   -1.637381    1.527128
C     4.186868   -1.285804    1.444832
C     3.328660    0.774939    3.154951
H     5.260139    1.871273    4.632513
H     3.007235    1.542197    3.855152
C     6.586797   -5.844717    2.034251
C     6.468599   -5.644009    0.682597
C     5.792565   -4.505817    0.175887
C     5.257657   -3.548869    1.089809
C     5.376299   -3.796997    2.477670
C     6.023517   -4.918804    2.937130
H     6.076430   -5.048860   -1.868289
H     6.878704   -6.363091   -0.021773
H     4.938922   -3.096847    3.181490
H     6.095040   -5.098401    4.005682
C     5.632606   -4.309711   -1.206756
C     4.596687   -2.400404    0.559434
H    -0.078561    9.779081   -0.212147
H     5.052611    5.316729    4.743697
```

Atom	X	Y	Z	Atom	X	Y	Z
H	7.669189	1.309694	4.546966	H	-5.460791	2.321858	2.939018
H	7.099419	-6.723988	2.412636	C	-5.535510	0.241693	2.374997
C	-2.393970	3.117647	-0.565481	H	-5.339576	-1.828586	1.805702
C	-2.400118	1.750064	-0.715431	C	-7.032714	0.171395	2.443213
S	-4.061151	3.757472	-0.616981	F	-7.456476	-0.330847	3.632490
C	-3.696020	1.205664	-0.898071	F	-7.549693	-0.631669	1.482385
H	-1.508921	1.142014	-0.702991	F	-7.611874	1.386675	2.307055
C	-4.687030	2.171382	-0.857708	C	5.062005	1.885985	-1.434310
C	-4.230281	-0.099599	-1.163286	C	4.918302	1.803303	-2.798207
C	-5.638001	-0.066815	-1.275788	S	6.281397	0.741351	-0.841590
S	-6.299157	1.566766	-1.090123	C	5.786465	0.847442	-3.388689
C	-3.564582	-1.318557	-1.328293	H	4.226468	2.416860	-3.360195
H	-2.481132	-1.367780	-1.292705	C	6.565282	0.190729	-2.445696
C	-4.295520	-2.465768	-1.571003	C	6.076004	0.395119	-4.722228
H	-3.780276	-3.409581	-1.718292	S	7.640898	-1.009806	-3.095729
C	-6.384718	-1.215305	-1.501127	C	7.059485	-0.623900	-4.721395
H	-7.466584	-1.184260	-1.564190	C	5.548494	0.817149	-5.947058
C	-5.696525	-2.414104	-1.643407	C	7.496610	-1.225552	-5.892041
C	-6.450392	-3.694998	-1.847856	H	4.785669	1.589908	-5.970618
F	-5.912942	-4.443082	-2.840469	C	5.986081	0.231802	-7.121950
F	-7.749645	-3.488202	-2.157825	H	8.242460	-2.012973	-5.878810
F	-6.429919	-4.467941	-0.729325	C	6.947726	-0.786861	-7.092332
C	4.720225	-3.126221	-3.176622	H	5.565456	0.545346	-8.072417
C	4.044234	-2.194708	-3.927518	C	7.447603	-1.356176	-8.387316
S	5.418302	-4.392071	-4.228592	F	6.455333	-1.509352	-9.296473
C	4.032350	-2.488509	-5.313652	F	8.036431	-2.563189	-8.226768
H	3.555385	-1.325327	-3.517902	F	8.372798	-0.543303	-8.963186
C	4.731199	-3.643126	-5.620047	C	1.074647	-3.641167	-3.894489
C	3.453998	-1.885712	-6.478470	C	1.793296	-4.674082	-3.294000
S	4.731174	-4.061598	-7.307678	C	0.805542	-3.751857	-5.260507
C	3.754667	-2.622943	-7.645566	C	2.246188	-5.759007	-4.038354
C	2.716581	-0.701746	-6.590969	C	1.260902	-4.821850	-6.015176
C	3.343819	-2.204882	-8.904931	C	1.990088	-5.830203	-5.399202
H	2.477340	-0.128273	-5.702350	F	2.089770	-4.687007	-1.995240
C	2.319557	-0.269117	-7.839954	F	2.936783	-6.734165	-3.442837
H	3.585491	-2.771551	-9.797019	F	2.439415	-6.861793	-6.109945
C	2.627001	-1.018302	-8.986763	F	1.001127	-4.887777	-7.321844
H	1.765038	0.658693	-7.938428	F	0.089915	-2.819622	-5.892840
C	2.195112	-0.482876	-10.318118	C	0.726609	4.401582	-3.967709
F	2.351815	-1.376557	-11.316926	C	1.880197	5.187847	-3.957133
F	2.901671	0.627158	-10.662951	C	-0.500213	5.021274	-3.714235
F	0.888259	-0.111922	-10.310793	C	1.801495	6.558957	-3.739608
C	0.993322	0.552864	2.381726	F	3.090513	4.673059	-4.151509
C	-0.146671	-0.175030	2.143860	C	-0.587578	6.390383	-3.516932
S	0.606673	2.205010	2.904389	F	-1.629751	4.313985	-3.664911
C	-1.336615	0.561599	2.386793	C	0.567677	7.163138	-3.539258
H	-0.124275	-1.210214	1.828489	F	2.908301	7.298680	-3.733376
C	-1.075548	1.865925	2.781802	F	-1.770722	6.965560	-3.310248
C	-2.747939	0.294345	2.340517	F	0.493033	8.476507	-3.370545
S	-2.487974	2.836935	3.071102	Si	-1.729991	1.411625	-5.625852
C	-3.504259	1.443267	2.677535	C	-1.048397	0.067414	-6.702531
C	-3.427675	-0.889560	2.035475	H	-1.806144	-0.710254	-6.853687
C	-4.890937	1.432648	2.691603	H	-0.741234	0.436651	-7.686266
H	-2.871709	-1.782972	1.767859	H	-0.191349	-0.410883	-6.219418
C	-4.810701	-0.914721	2.057333	C	-2.489874	0.796559	-4.058669

```
H     -1.839597    0.080991    -3.547794        C     -4.059286    1.899086    -7.161828
H     -2.724646    1.618730    -3.377229        H     -4.685561    1.444442    -6.386655
H     -3.425555    0.275162    -4.296421        H     -4.686596    2.604808    -7.715518
C     -2.832071    2.602298    -6.556964        H     -3.764993    1.106333    -7.858045
H     -2.242980    3.081344    -7.350534
H     -3.150484    3.404218    -5.877840
```

TS-5

O	1.755447654061	2.580668615224	-2.213786520090
O	-0.117809920925	2.014908291765	-0.606201777887
O	1.505186498409	-1.641771581281	0.153916373881
O	2.912471542398	-1.275690314595	-1.918751321997
S	-0.311519337708	-3.642575874017	-1.264712058686
S	-0.072954968330	2.815506935377	-4.576157185130
O	-1.084056357308	-3.016926558256	-0.173826940665
O	-1.050767943688	-4.452069443515	-2.238607571681
O	1.280358990054	2.561681964554	-5.079389843882
O	-1.198135421637	2.678861332048	-5.505395953500
N	0.597363833035	-2.588777872665	-2.086260746031
N	-0.458931119848	1.862386405693	-3.275718764865
P	1.369160779020	-1.361171876643	-1.436964178865
N	0.797582880265	0.040534383447	-1.843292180879
P	0.535670115546	1.547694415817	-2.007261409880
H	-1.284621081454	0.825868498191	-3.605743507227
C	-0.419187524380	3.360097707677	-0.435382546385
C	2.559686871306	2.928267858019	-1.123829329414
C	2.522916991692	-1.061790517724	0.897961886345
C	3.691987771486	-2.387937499647	-1.623083697570
C	-1.793914511580	3.727506956955	-0.397025210554
C	4.029437849876	-3.266810015131	-2.691024963376
C	3.902846928772	2.461892442993	-1.130308795246
C	2.145457854312	-0.105180607215	1.881741733071
C	1.009749982411	7.961512268355	-0.091472493280
C	1.341132636484	6.630833458696	-0.184098028123
C	0.337613887332	5.633523389092	-0.169315367073
C	-1.031902878358	6.037301311824	-0.102491223922
C	-1.336735665685	7.417080791446	0.018051774014
C	-0.338568438220	8.357865140529	0.029990129190
H	1.791776209184	8.714120930745	-0.120688308126
H	2.380741002893	6.335362056704	-0.281691791623
C	0.629802940595	4.239041109709	-0.256509364988
C	-2.054366491620	5.073587588452	-0.187203850447
H	-2.379549622248	7.717251982538	0.076886575818
H	-3.080770619930	5.422955451925	-0.113219220947
C	4.498928549569	4.597262316331	3.201681560860
C	4.998236253515	3.888745402047	2.138699000821
C	4.178293674241	3.571588425854	1.027730139632
C	2.827290195321	4.037597818382	1.000455481138
C	2.337424927373	4.742856487690	2.125376669119
C	3.151247690498	5.011587098489	3.199485324688
H	5.723969917668	2.495106122670	-0.007884606516
H	6.028193385479	3.543288040563	2.135417879309
C	4.683416552444	2.808978205650	-0.042533344906
C	2.020160992059	3.732834242828	-0.142636196462
H	1.302453477784	5.064717768668	2.142163987452
H	2.751326881854	5.548335062886	4.054543041380
C	7.211220483607	-0.488331143015	1.944224950895
C	6.239251301348	-1.118424056492	1.204819158265
C	4.867195546783	-0.852239793517	1.428325183119
C	4.517137386698	0.121628519490	2.414957439412
C	5.542537475248	0.733551350532	3.177501370669

```
C        6.862159961449        0.434877953056        2.951242288709
H        8.257628453894       -0.705106828093        1.751195153165
H        6.523036370857       -1.824406966525        0.432456025955
C        3.819739906859       -1.483854485475        0.684733898685
C        3.165986286095        0.459209138998        2.625132924333
H        5.259306410453        1.456565501237        3.937518863064
H        2.929176173903        1.178009414837        3.406326385925
C        6.239076045240       -6.089702997649        0.609714835736
C        5.928015937701       -5.795913144186       -0.693227784478
C        5.197804054423       -4.624981017230       -1.019625253011
C        4.824387039185       -3.727888511094        0.029296573553
C        5.134844099106       -4.075266242105        1.365175301911
C        5.822645182809       -5.230875938275        1.648237113301
H        5.129017019511       -5.063133522656       -3.112176847536
H        6.215114203043       -6.471077904019       -1.494882234291
H        4.812277000621       -3.423294912363        2.170452593186
H        6.037533748933       -5.490435043580        2.680403466129
C        4.814971210433       -4.356830176711       -2.348094697086
C        4.111807683118       -2.541183044241       -0.317374349112
H       -0.585081502843        9.412502155393        0.106038675170
H        5.135510258069        4.832492398580        4.049670298414
H        7.640004645657        0.911154766687        3.541079296100
H        6.782600528521       -6.998849412383        0.848018332172
C       -2.867580319919        2.760272310390       -0.589426232748
C       -2.858658344090        1.385649407242       -0.675227215803
S       -4.523703576414        3.387674249882       -0.784310741736
C       -4.138792203978        0.827214059827       -0.918380910172
H       -1.973156360892        0.781178623886       -0.543739904806
C       -5.131867211378        1.790997962944       -0.985190974922
C       -4.652808656239       -0.490568203189       -1.168476762243
C       -6.047268099092       -0.465504741913       -1.385895213470
S       -6.722588031895        1.169022203717       -1.293446023676
C       -3.979339871630       -1.716181466787       -1.232406558347
H       -2.910082257892       -1.769998397043       -1.054198346858
C       -4.687461412246       -2.872407755208       -1.496207916163
H       -4.161324833421       -3.821028917580       -1.551401680653
C       -6.773884820476       -1.622606241709       -1.636581920271
H       -7.847508958888       -1.595275611239       -1.784816937573
C       -6.077444856229       -2.822998052451       -1.691400453515
C       -6.808542865353       -4.110432804234       -1.937181969948
F       -6.236207438934       -4.828425190061       -2.932394893843
F       -8.102813323897       -3.914975236799       -2.275471824834
F       -6.802241242062       -4.903628514380       -0.835005562288
C        3.578804256823       -3.036776392844       -4.058820053904
C        2.862085215802       -2.004635626179       -4.620009461408
S        3.977723107466       -4.259501908821       -5.294668003760
C        2.618117590057       -2.172672346703       -6.002644114304
H        2.531570220887       -1.132969892256       -4.078576202035
C        3.171966309120       -3.336622912306       -6.504830195850
C        1.952815803796       -1.410714502642       -7.016352126404
S        2.948123691519       -3.558355667252       -8.215287001524
C        2.062410913750       -2.026073504190       -8.282505158762
C        1.276475139793       -0.193859913782       -6.906897436321
C        1.534094231491       -1.443846024615       -9.426063042870
H        1.194430980329        0.298230903678       -5.943744359249
```

C	0.742604588396	0.395892109374	-8.036350715353
H	1.635855269863	-1.911931095023	-10.399009175933
C	0.876897009031	-0.226028771433	-9.287382150467
H	0.223542345059	1.346232495290	-7.952740657047
C	0.227179642444	0.413127126215	-10.476020983462
F	0.671031606322	-0.090637198410	-11.647916008780
F	0.429199800163	1.751239502374	-10.508245800165
F	-1.125529514925	0.231134278120	-10.458939166805
C	0.747792087371	0.250779789726	2.098590844896
C	-0.394773643832	-0.495882824096	1.944441490966
S	0.379111092470	1.884620631524	2.688672811345
C	-1.571199825713	0.217705413438	2.292471888005
H	-0.394425647972	-1.519599893446	1.591928087583
C	-1.302535696621	1.519686374818	2.689452175476
C	-2.981344688263	-0.060470370094	2.299392450463
S	-2.708979659306	2.473100604102	3.056655430621
C	-3.731706693834	1.080963702213	2.672435241227
C	-3.661773466745	-1.241460943206	1.986327211103
C	-5.117824374028	1.072211917910	2.700552297681
H	-3.104935895863	-2.125031273962	1.687607446316
C	-5.045302663773	-1.264128559616	2.024162814228
H	-5.684428831898	1.958576670353	2.965369575303
C	-5.766273713447	-0.111997808657	2.364084760421
H	-5.577805395425	-2.171708326825	1.758068255392
C	-7.264272171077	-0.171766246242	2.424687807314
F	-7.780477455233	-0.989985978868	1.477330035306
F	-7.832567537714	1.045928988277	2.258201987803
F	-7.701109970802	-0.643707479873	3.621586895188
C	4.433827420877	1.667138663052	-2.230626940001
C	4.140361132509	1.702204482243	-3.571609356984
S	5.695761915118	0.473769361231	-1.872154924431
C	4.913079527420	0.784313802719	-4.328947471178
H	3.399435876938	2.364065139676	-4.000972959418
C	5.774980650257	0.040599286103	-3.534834124032
C	5.008805607263	0.409185376349	-5.712816340258
S	6.695171973389	-1.161081990416	-4.387573551902
C	5.924753018646	-0.654460310654	-5.897249476593
C	4.348575093055	0.929641136459	-6.830524208222
C	6.159982900705	-1.214470464234	-7.143797235661
H	3.637228247363	1.741520032032	-6.711156355564
C	4.586036782390	0.387029105711	-8.081086005956
H	6.849598197013	-2.041959167391	-7.271506813506
C	5.475513370413	-0.685119919375	-8.232627211729
H	4.059484917194	0.774652005092	-8.947493795256
C	5.744004843514	-1.226554424117	-9.605732937560
F	4.630659334117	-1.232153042460	-10.378365169445
F	6.218920920360	-2.493050391945	-9.576072614509
F	6.666619436104	-0.479982789883	-10.267757058690
C	0.899405000026	-4.766234217809	-0.488635621381
C	1.099557537283	-4.858736017106	0.888442705624
C	1.641026817907	-5.613474444226	-1.314469719883
C	1.977272866220	-5.796297012420	1.423043278953
C	2.511335686794	-6.557564804172	-0.790782236747
C	2.667549625355	-6.660436301089	0.585677193770
F	0.467419479310	-4.069470644305	1.757651861614

F	2.154023278315	-5.873834497282	2.744083035779
F	3.482204111057	-7.577947037864	1.100123294067
F	3.202653020582	-7.362605765312	-1.601151392748
F	1.537961557266	-5.539496491764	-2.641615231162
C	-0.102762152657	4.517412747405	-3.950868218808
C	1.033454574607	5.330224122092	-3.907977840910
C	-1.334754994110	5.094460516314	-3.633577524936
C	0.927455416989	6.685770811384	-3.616788320058
F	2.256124757144	4.863525687877	-4.146537500704
C	-1.447895194584	6.444677001157	-3.341660876091
F	-2.446359078149	4.360082221297	-3.609776385251
C	-0.314631874571	7.248449070908	-3.357741521061
F	2.017932945207	7.451443113371	-3.593990305710
F	-2.635841114272	6.973006075495	-3.047773147882
F	-0.416397990193	8.549962325630	-3.116340828143
C	-0.639076645457	-3.632539658554	-5.898938302275
C	-0.759853032746	-3.625541177842	-7.285629343687
C	-1.409998601941	-2.568839501380	-7.922056333312
C	-1.935689756201	-1.525491914472	-7.179819178157
C	-1.829239434825	-1.517152007494	-5.774054075131
C	-1.170907865856	-2.594969738156	-5.151070384016
H	-0.145114603915	-4.452796536494	-5.386695808093
H	-0.349539310287	-4.442748019781	-7.872095874633
H	-1.494355971719	-2.551478641509	-9.004283993096
H	-2.412948936862	-0.703759596057	-7.702417691775
H	-1.100235735585	-2.658899106715	-4.073135167333
C	-2.441144346833	-0.460257625669	-4.975779544121
C	-2.108734901192	-0.256757480908	-3.644877013831
H	-1.490580963371	-0.993376006611	-3.135525553376
H	-2.862041981915	0.229214754395	-3.028802723505
C	-3.432127939473	0.449841407965	-5.635468632015
H	-4.148377661249	-0.169632536305	-6.193434486350
H	-2.879719589651	1.017599832615	-6.400819836762
C	-4.178953172195	1.438407017511	-4.744898123102
H	-4.828066867937	0.895018049759	-4.042127235683
H	-3.467575086433	2.018207601211	-4.144915708618
C	-5.018758396928	2.411442657213	-5.571963676707
H	-5.709610287563	1.848675211697	-6.215280975943
H	-4.350988359346	2.968992217567	-6.243007462482
C	-5.805276116726	3.387920511447	-4.701458337272
H	-6.386168021697	4.087062881239	-5.311338834385
H	-6.502138698770	2.853776439266	-4.045396663179
H	-5.131955593722	3.973696865904	-4.065973255186

TS-6

O	1.749022678943	2.416589345230	-2.373414763778
O	-0.173108065393	1.899303481112	-0.813927732462
O	1.466408028964	-1.632753707188	0.046828698853
O	2.918850918277	-1.267191537716	-2.000061134039
S	-0.169768082759	-3.790779627991	-1.354931369579

S	-0.075038201660	2.626978025122	-4.764496071284
O	-1.005704030057	-3.190204190392	-0.297457064637
O	-0.853018256699	-4.656063417157	-2.330230888074
O	1.291190835137	2.331378001052	-5.234699773231
O	-1.151353552141	2.505956593670	-5.763133708706
N	0.714020313787	-2.729496012505	-2.177343628461
N	-0.515504286544	1.793290851213	-3.461215336898
P	1.362866195137	-1.406549182075	-1.559151602069
N	0.692482440632	-0.090431234228	-2.063301179548
P	0.456278047480	1.443266535580	-2.238398517829
H	-1.060411750052	-1.061156688651	-3.572534423411
C	-0.495240436856	3.242779049787	-0.696831484248
C	2.502506298128	2.814966920452	-1.280946104415
C	2.458662515127	-1.030991335460	0.804792030571
C	3.723955859761	-2.350651108727	-1.675946850669
C	-1.872603344700	3.598146802740	-0.736637282355
C	4.113712326404	-3.230107973202	-2.725602743930
C	3.864208716671	2.399783891876	-1.248557939431
C	2.042152987216	-0.080575528321	1.778188135579
C	0.876075034427	7.869630319943	-0.480083573110
C	1.223333738831	6.540019171526	-0.504600721798
C	0.229871689439	5.532621841214	-0.494669174202
C	-1.144945386817	5.924572076892	-0.509319285111
C	-1.467171022727	7.304406921367	-0.458420648600
C	-0.479545641649	8.256030509758	-0.437111482490
H	1.651933886789	8.628796547442	-0.504875564255
H	2.268821348259	6.252374833929	-0.544196006436
C	0.538138326767	4.138325307090	-0.513351500935
C	-2.155517207138	4.948353436831	-0.602059103628
H	-2.514210498833	7.595528838924	-0.462217455044
H	-3.186830000030	5.291396951898	-0.592808521393
C	4.314083898952	4.681684023980	3.024520390398
C	4.852525063667	3.948590547718	1.997508841650
C	4.066189844837	3.575661123850	0.879874624146
C	2.705770105373	4.008815159119	0.806625242842
C	2.176457298568	4.743473933771	1.894348117002
C	2.958806274858	5.067261817287	2.976748503607
H	5.664306889419	2.518790216328	-0.096918904017
H	5.889595977089	3.626335140817	2.028918346343
C	4.614624627238	2.797153225700	-0.158056183178
C	1.928825970692	3.647635877608	-0.340916498145
H	1.135154959634	5.044618684298	1.874482169079
H	2.528010977878	5.625754362923	3.802457696292
C	7.110682515312	-0.333593374740	1.943789140841
C	6.169715928536	-0.991464622215	1.188591861978
C	4.786862230646	-0.760388304738	1.384385466626
C	4.394342710540	0.209572537448	2.358398588881
C	5.388128982340	0.850737324311	3.137957302302
C	6.719064208459	0.584185422672	2.939825541843
H	8.165811134357	-0.523586220795	1.770830391211
H	6.487549413300	-1.691026873464	0.424037157508
C	3.770642277267	-1.423444486089	0.624107687951
C	3.031317876883	0.514546047806	2.538323820616
H	5.072149730664	1.571647859010	3.886940676096
H	2.758104903590	1.232731236206	3.307956870188

C	6.344105029915	-5.945223416983	0.650095541477
C	6.053275817243	-5.673629958682	-0.662337534338
C	5.289045415169	-4.532667208044	-1.015993622808
C	4.857162026611	-3.641616275193	0.015101469663
C	5.147731602075	-3.967165765385	1.361069624229
C	5.871333873904	-5.093743204903	1.670562034135
H	5.282514658122	-4.991981559586	-3.104806505388
H	6.383724108570	-6.344008618407	-1.451241759733
H	4.782531794237	-3.320555985570	2.152321497204
H	6.071459047107	-5.336313345765	2.709846695230
C	4.927822908841	-4.289341192448	-2.355232827785
C	4.115542256418	-2.481389042406	-0.359386300605
H	-0.739099015021	9.310044991362	-0.415975550752
H	4.925902380334	4.959706061699	3.877828919149
H	7.472824233488	1.083362538700	3.541876076872
H	6.915433771229	-6.831260080552	0.909481280139
C	-2.924834607591	2.601972623438	-0.901184677645
C	-2.888555546248	1.225898311182	-0.891442901078
S	-4.593770810481	3.183446462227	-1.128330652910
C	-4.162822430403	0.629117500602	-1.058204343266
H	-1.990916345454	0.649352602983	-0.726888307091
C	-5.175786274667	1.565595668726	-1.185080490752
C	-4.669765980010	-0.712739862909	-1.069311652124
C	-6.079916819997	-0.731089636844	-1.166496673935
S	-6.773734144813	0.891363968257	-1.295935737965
C	-3.981911740855	-1.926776648241	-0.957981122475
H	-2.900153133014	-1.945388636675	-0.865378986087
C	-4.691839971505	-3.111757129811	-0.918135033673
H	-4.157961052581	-4.051644366112	-0.808720876039
C	-6.803529288410	-1.915039244755	-1.118904767782
H	-7.886486797655	-1.918150868988	-1.169851072652
C	-6.093951157209	-3.102596996189	-0.990445760547
C	-6.819812513566	-4.410991925403	-0.907731944157
F	-6.335581724715	-5.309201257100	-1.805965959480
F	-8.143989496544	-4.288982314123	-1.144100836280
F	-6.682873070649	-4.983716070263	0.315370752328
C	3.676364717331	-3.038774491223	-4.104343498170
C	2.911596148320	-2.056562400208	-4.690042683290
S	4.147573056521	-4.263648069795	-5.313804463301
C	2.677572764484	-2.269411632802	-6.069501909197
H	2.536858222487	-1.191625744821	-4.166244377396
C	3.297601795766	-3.411696596419	-6.544593440505
C	1.937962329309	-1.592689208271	-7.093586940182
S	3.062547330065	-3.704507112002	-8.241846684123
C	2.058494633678	-2.249426382939	-8.338340236828
C	1.172564424359	-0.425650201368	-7.011957351366
C	1.438774537014	-1.768284559645	-9.482578303497
H	1.101930518770	0.118617007147	-6.075211032193
C	0.542129706489	0.060217474437	-8.142513874520
H	1.545609159701	-2.271065328615	-10.437767280465
C	0.674444953373	-0.611864839487	-9.368050648981
H	-0.042304867463	0.973921609498	-8.078724162127
C	-0.094494571909	-0.111020736667	-10.551854712578
F	-1.407487495929	-0.488646091100	-10.480492945153
F	0.378413054177	-0.591641173312	-11.722587174809

```
F    -0.091173329964     1.236815708035    -10.633825580128
C     0.632144441438     0.241981105553      1.971579969748
C    -0.482996954718    -0.553814344093      1.880681258927
S     0.213402420318     1.899397400003      2.442833163515
C    -1.681886987069     0.141421609969      2.194059598712
H    -0.443836819113    -1.598069611257      1.595262283996
C    -1.453629909734     1.480442128432      2.481318932019
C    -3.079427096589    -0.185737872770      2.277069259310
S    -2.886517913152     2.415181482515      2.788106135248
C    -3.863051561506     0.958683061947      2.563091793228
C    -3.723210441826    -1.420167293994      2.137329345938
C    -5.245664220713     0.900043606061      2.655978234020
H    -3.141312810534    -2.311818188762      1.923246991741
C    -5.100204149235    -1.494728079900      2.252971649656
H    -5.837262920914     1.787837233100      2.851870594090
C    -5.855866413903    -0.338637189860      2.490827640648
H    -5.602919530292    -2.448855204559      2.129210033876
C    -7.344531119843    -0.452866032148      2.633489836127
F    -7.873286160177    -1.341431392463      1.756135637967
F    -7.972176783968     0.728888780437      2.431987416856
F    -7.702083637915    -0.879147279694      3.872629495839
C     4.436230755302     1.613228066297     -2.334337493239
C     4.135550405436     1.616021701471     -3.673372261289
S     5.749680756835     0.477702351534     -1.965664510854
C     4.937492459382     0.715891128484     -4.419581183039
H     3.363393631308     2.235906965806     -4.110258769450
C     5.835858055804     0.021164212080     -3.622941336170
C     5.024497746375     0.316447286023     -5.795877228988
S     6.793482071049    -1.157761213035     -4.469324890756
C     5.980744577521    -0.712013790479     -5.976483792015
C     4.316640272274     0.783645948869     -6.908040551589
C     6.214561171656    -1.287063178709     -7.216473433906
H     3.571511129637     1.564874558124     -6.787337674773
C     4.551546894175     0.224114107244     -8.151680718619
H     6.936648861773    -2.086810701544     -7.342240775105
C     5.484468248404    -0.811141367635     -8.301065534517
H     3.994569112359     0.573320675848     -9.015435357288
C     5.747366649813    -1.369410426583     -9.667762510672
F     4.622416892338    -1.421198392403    -10.423441050114
F     6.258764834456    -2.622040005288     -9.623214742269
F     6.637607148709    -0.610997621439    -10.359845829399
C     1.057353737328    -4.859307737824     -0.526811190286
C     1.235197858180    -4.906416465910      0.855460672078
C     1.837325630734    -5.709143793927     -1.313362502179
C     2.125285173354    -5.805945692286      1.433315243415
C     2.719804068966    -6.616197389358     -0.747089705776
C     2.851726278466    -6.676792082292      0.634393855004
F     0.565910660015    -4.109172027743      1.688914531541
F     2.278257423732    -5.841601516513      2.758969483443
F     3.676855683570    -7.560800291875      1.189483102788
F     3.444986215883    -7.426955014730     -1.521889734875
F     1.759163622793    -5.676468985455     -2.645295042787
C    -0.093816416747     4.382269669602     -4.262702423276
C     1.048320958654     5.181237063530     -4.209913915308
C    -1.325172662552     4.987473072271     -4.006114479771
```

C	0.955447753031	6.547887312707	-3.967238311842
F	2.273734008279	4.689538360889	-4.393940140319
C	-1.428643101450	6.349060165929	-3.766574397366
F	-2.450416679536	4.270210322200	-3.987942219885
C	-0.284583998199	7.136651646937	-3.768378076766
F	2.057622429673	7.300037668325	-3.933654860453
F	-2.619791090776	6.905611761690	-3.532661178766
F	-0.375147708152	8.449366972503	-3.571012822596
C	-1.092536706502	-3.602686925740	-8.197438143421
C	-0.287454257874	-4.547553736365	-7.556347907921
C	-0.072052805706	-4.466252406971	-6.183328532807
C	-0.683626466597	-3.469240600449	-5.442491935596
C	-1.515215141273	-2.515569422632	-6.070374630391
C	-1.693179557444	-2.594848968021	-7.469866245285
H	-1.252031642303	-3.658096787911	-9.269871188148
H	0.174083389648	-5.344322500293	-8.132036365808
H	0.570801581796	-5.182052087957	-5.680084327823
H	-0.496539856113	-3.432440936374	-4.375921246041
H	-2.327431549473	-1.885528689412	-7.988395689707
C	-2.180949881507	-1.503741247553	-5.278321279099
C	-2.037669999818	-1.517864075283	-3.808283906196
H	-2.034902908502	-2.522791477293	-3.383831539498
H	-2.795370420509	-0.904605438997	-3.322229030594
C	-2.699376623381	-0.260257449267	-5.894225231343
H	-3.071904802309	-0.442603275220	-6.906893202866
H	-1.794531249315	0.366160123420	-6.034258024250
C	-3.703771594809	0.561806154489	-5.081264511372
H	-4.442990413594	-0.110424968353	-4.617955516465
H	-3.183499147678	1.083967935044	-4.268925909981
C	-4.430216560384	1.587422147889	-5.947487712791
H	-4.962587474294	1.068894227873	-6.758793277017
H	-3.690375535342	2.245265814626	-6.419603191171
C	-5.416916847816	2.416426673230	-5.130219475115
H	-5.942988617800	3.142666787362	-5.757631888111
H	-6.168092074352	1.776661908678	-4.650388823759
H	-4.896588689626	2.968351592276	-4.340063822619
Si	-4.844589535390	-3.468255086449	-5.322398549048
H	-3.911948415859	-2.266429349104	-5.274368734311
C	-4.955537545247	-3.964561700849	-7.128960448264
H	-5.709289887563	-4.751793831846	-7.254059620347
H	-5.243351222629	-3.124651503597	-7.769822244167
H	-3.999591013516	-4.357527252114	-7.489562186402
C	-6.481208485418	-2.830332541136	-4.657109434540
H	-6.291403253657	-2.412325735312	-3.660826796710
H	-7.158109019755	-3.682529764834	-4.500150570453
C	-7.140824329478	-1.775208629635	-5.555896553537
H	-8.055279496854	-1.379512906411	-5.101273913379
H	-6.470773533730	-0.925264269519	-5.732685478912
H	-7.411015433757	-2.189911043431	-6.532671944765
C	-4.035393370690	-4.794544516339	-4.287276082970
H	-4.648061024541	-5.703453256749	-4.274295468417
H	-3.049596207364	-5.057829073811	-4.686824299179
H	-3.897726847867	-4.473080221617	-3.251015673333

TS-7

O	1.597418918773	2.785303119706	-2.344903596052
O	-0.146677815265	2.325704906981	-0.549978609328
O	1.625099192050	-1.505117914556	0.511438860832
O	2.881726415244	-1.436319213042	-1.680891348474
S	-0.550708282806	-3.218481804050	-0.891085584088
S	-0.365514320981	2.007260951659	-4.530951799274
O	-0.944748348572	-2.889650841674	0.487266926825
O	-1.629168520744	-3.642618010640	-1.803534898265
O	0.968143144422	1.733433363210	-5.102102792713
O	-1.528442917500	1.572693658181	-5.320135997365
N	0.272872771107	-2.058719004619	-1.644536459485
N	-0.544148180258	1.460859573432	-3.025021150182
P	1.413730639003	-1.112990633442	-1.046416139991
N	1.300878782010	0.425198131765	-1.264135038256
P	0.538345821727	1.648553281642	-1.866061618643
H	-0.887595237160	-1.762667795428	-3.518332757555
C	-0.510998540906	3.661693991982	-0.591218112952
C	2.441753758332	3.277978928410	-1.355425304983
C	2.697805567322	-0.886137708605	1.145532987660
C	3.592416062254	-2.547673273759	-1.269022002588
C	-1.899044671209	3.989218847973	-0.545077341073
C	3.815476095499	-3.583355597758	-2.223940169709
C	3.779443361265	2.800530372017	-1.310997996936
C	2.424480137562	0.224919811873	1.989464207371
C	0.724012434630	8.310229891981	-1.105259507091
C	1.109516654836	6.998440759974	-0.963560962262
C	0.148706977281	5.984552181474	-0.739743202285
C	-1.233104396944	6.343612427413	-0.700633281538
C	-1.594001267732	7.708627906811	-0.825820928740
C	-0.636503869253	8.671673845995	-1.018516963398
H	1.472682448057	9.073700743670	-1.293893103287
H	2.157756489798	6.727148558466	-1.037040675122
C	0.497099824256	4.609082033064	-0.599875213536
C	-2.210444717452	5.340184067709	-0.573802245740
H	-2.647029560821	7.975550081686	-0.790618302759
H	-3.248615084692	5.659306875510	-0.541563836474
C	4.414433270190	5.432259539243	2.733673617746
C	4.903812014006	4.597170475933	1.761015895445
C	4.081037910752	4.168218139001	0.690013533828
C	2.733831728478	4.641493230952	0.612653401800
C	2.256177454868	5.487170096574	1.641480841180
C	3.075481973157	5.871093444577	2.676015526893
H	5.609784767781	2.955173611803	-0.212086849784
H	5.930161157137	4.240919483589	1.798590600027
C	4.573590931148	3.277146622148	-0.284266839751
C	1.913729959950	4.186399439862	-0.466091002910
H	1.225517099146	5.824072075860	1.615909731254
H	2.686438674418	6.515156202718	3.459033250786
C	7.467167554768	-0.346388887115	1.711825408171
C	6.419294140630	-1.063463168697	1.185674961882
C	5.079827209148	-0.702048177333	1.461591266659
C	4.838591807625	0.446595781007	2.279053738664
C	5.941752924336	1.154258220823	2.817851722822

384

C	7.229426527587	0.767650386451	2.542738006162
H	8.487413284330	-0.637306656769	1.480131933699
H	6.617203236142	-1.910125085103	0.537051091576
C	3.956086706228	-1.384908022226	0.899513805366
C	3.518153002377	0.865392464328	2.540892738979
H	5.743840643102	2.017292429958	3.448606384633
H	3.368790759713	1.718612432717	3.198629924753
C	6.074973604947	-6.107036452703	1.279614204242
C	5.685422723377	-5.967798678323	-0.028374452996
C	5.012476099843	-4.798355110536	-0.462508462009
C	4.774061119223	-3.744429750886	0.471401281437
C	5.167452393763	-3.930165017835	1.817559348662
C	5.800337110290	-5.084722805286	2.210882819500
H	4.783449821755	-5.485895938612	-2.470385420726
H	5.869831826610	-6.761821622917	-0.747504849141
H	4.951055570018	-3.153712693879	2.543521948993
H	6.082107761210	-5.215254567760	3.251337357781
C	4.553247200440	-4.672518601285	-1.786592920799
C	4.111840858223	-2.565752638348	0.014037827133
H	-0.925585822839	9.712218456186	-1.130991510393
H	5.052931891566	5.752315761779	3.551867286426
H	8.067000044272	1.319692597902	2.958990955734
H	6.577990400183	-7.012592575555	1.604917062905
C	-2.946025990786	2.977660253372	-0.463901656278
C	-2.893610429812	1.604648339143	-0.481138750648
S	-4.637516239821	3.536486827122	-0.336330170013
C	-4.168969419968	0.992764978858	-0.417240458704
H	-1.976902437101	1.040548132167	-0.536914925449
C	-5.200300912949	1.911581704224	-0.331592900847
C	-4.654972192501	-0.352379643265	-0.456655647833
C	-6.065973682912	-0.399289047422	-0.392960700521
S	-6.789641098678	1.210768799541	-0.283942700577
C	-3.936623665014	-1.547066141818	-0.548623113787
H	-2.852636179361	-1.529717242428	-0.567114903248
C	-4.614018134978	-2.750564793552	-0.590984447570
H	-4.050149847128	-3.676312492057	-0.660220154488
C	-6.759618679216	-1.602218241160	-0.432833904086
H	-7.842424596537	-1.632907072705	-0.385533426458
C	-6.017593481895	-2.773124356927	-0.542821652242
C	-6.698971923515	-4.104741547141	-0.618059673086
F	-8.044616843745	-4.005742483398	-0.641353321806
F	-6.372881349740	-4.901554524412	0.429521750012
F	-6.331414179486	-4.786972787832	-1.740879546898
C	3.314505553457	-3.512674800928	-3.594846380148
C	2.664354305312	-2.521268299974	-4.295099487035
S	3.598553196268	-4.931405465398	-4.639146638410
C	2.386603277315	-2.872489417807	-5.643508820695
H	2.417338528532	-1.556932130346	-3.876711655405
C	2.838164638585	-4.143351566519	-5.961520364659
C	1.793976954148	-2.222664417754	-6.780539087049
S	2.600791290229	-4.610050332665	-7.618758687395
C	1.853990615186	-3.037989195149	-7.934655250128
C	1.225287059588	-0.948217399457	-6.887075916173
C	1.410318200989	-2.595706203537	-9.173627538645
H	1.170077824734	-0.292198836841	-6.024224804044

```
C        0.770017278097       -0.500986679885       -8.113188553016
H        1.492084322574       -3.218714535338      -10.057532248951
C        0.873834433604       -1.316179945347       -9.251128630189
H        0.348418621672        0.496643698426       -8.192291738066
C        0.450259352664       -0.764840715003      -10.579309506651
F        1.367161598702        0.104573761895      -11.074831333017
F       -0.718862685635       -0.080752734607      -10.492934207723
F        0.278883224089       -1.730202430628      -11.510618147522
C        1.056947332787        0.658589353502        2.240240710691
C       -0.106133645067       -0.071612556210        2.254073145368
S        0.757540286984        2.366341894743        2.615502257077
C       -1.243956136383        0.712677061639        2.569841953629
H       -0.144464819307       -1.133941474620        2.048845629296
C       -0.926966535634        2.048325923207        2.772915295229
C       -2.647452394758        0.464128436453        2.741672699113
S       -2.288219430450        3.066677244232        3.139250018004
C       -3.350532083993        1.654239999428        3.048584245399
C       -3.358514136443       -0.737342642045        2.656754105722
C       -4.722399132585        1.664388334545        3.252399194561
H       -2.839354705933       -1.657758193277        2.404954798153
C       -4.725623009640       -0.739472294851        2.870285094695
H       -5.254488713337        2.582880499119        3.476011014998
C       -5.402005470683        0.453788258976        3.158782334597
H       -5.284081667531       -1.667113932815        2.793857893644
C       -6.873128463751        0.409838305149        3.445641876634
F       -7.517988487692       -0.502733722807        2.677635557190
F       -7.474978229277        1.604819022684        3.241874123279
F       -7.122852994197        0.065723183608        4.737087686959
C        4.275118547570        1.823562678648       -2.273840688890
C        3.958757340509        1.626827631694       -3.594787000864
S        5.485008972901        0.656632274908       -1.711505541462
C        4.684535700128        0.554050390865       -4.179291162062
H        3.226413377420        2.222959465849       -4.124194510621
C        5.525866668087       -0.070163483433       -3.268048492206
C        4.775875409707       -0.048694504571       -5.481214759250
S        6.407784304693       -1.428768803756       -3.901095213047
C        5.662343883555       -1.154514058396       -5.480521008619
C        4.155065534250        0.310093081273       -6.682478690277
C        5.900590996034       -1.907976386550       -6.619572615436
H        3.467474567870        1.150520099591       -6.704163709979
C        4.404588134795       -0.421223013522       -7.831197582927
H        6.568740626463       -2.762563184348       -6.601908186537
C        5.259625861645       -1.530466418898       -7.795753088498
H        3.914412176176       -0.150590154278       -8.761227690038
C        5.554641581742       -2.276214296814       -9.062453826942
F        4.481593155024       -2.326749196114       -9.889268598844
F        5.940851691024       -3.553007336323       -8.828913276579
F        6.556350608490       -1.690751183004       -9.769677112469
C        0.591035854494       -4.639456045195       -0.785050468301
C        1.252192416462       -4.985347943272        0.395751175963
C        0.800846421742       -5.441648418718       -1.908698153136
C        2.061675191072       -6.114691157286        0.460715170989
C        1.591386288553       -6.579394376658       -1.848631389862
C        2.224536624778       -6.915499287455       -0.659651673610
F        1.147960792069       -4.262478624713        1.507137472647
```

```
F        2.689877263247      -6.425063192513       1.593916161068
F        3.010272846415      -7.989609169571      -0.606840949197
F        1.763134705376      -7.346582764164      -2.929286697529
F        0.257080508916      -5.139760354649      -3.088227791608
C       -0.508038994096       3.824095027081      -4.391601777330
C        0.548702138955       4.701941932979      -4.635403625564
C       -1.737632399281       4.371748481716      -4.021027148003
C        0.374659710187       6.078451667353      -4.537198604356
F        1.767271392455       4.281515227693      -4.974405923314
C       -1.922924292801       5.743185411529      -3.927061421043
F       -2.777973623210       3.589215686109      -3.733565791448
C       -0.864667237814       6.600903841179      -4.197824805411
F        1.396208469565       6.903290769760      -4.778606739722
F       -3.109940278598       6.243139393711      -3.574053765883
F       -1.038284388249       7.918218612365      -4.134769162274
C       -2.854725733722      -6.391039297956      -4.514716333465
C       -1.815849117238      -6.842160345262      -5.327503793653
C       -0.957670873673      -5.930354566690      -5.939680488614
C       -1.121368422419      -4.574250244445      -5.721311897690
C       -2.169367774605      -4.101566442744      -4.907308745559
C       -3.045771894604      -5.034153686516      -4.319390178272
H       -3.514282995285      -7.102032752878      -4.027032015932
H       -1.673987415333      -7.907841515085      -5.482738304496
H       -0.152650932071      -6.276462108759      -6.580489671748
H       -0.456547821124      -3.874813337987      -6.218448682827
H       -3.838602489976      -4.698427461069      -3.659783079625
C       -2.325762570001      -2.682764096375      -4.649963649989
C       -1.148857627466      -1.816590012113      -4.594757231970
H       -1.354843951643      -0.790902997078      -4.909411500872
H       -0.275706176169      -2.226935024859      -5.096155207103
C       -3.601433119032      -2.160533760079      -4.100604105501
H       -3.583899835502      -2.466850562133      -3.036409761154
H       -4.449007013807      -2.694894431839      -4.546195158941
C       -3.800176319934      -0.646312462039      -4.173354706969
H       -3.161120253635      -0.143266428434      -3.435795915447
H       -3.469587478461      -0.273242958563      -5.151598271512
C       -5.255893539591      -0.243596936177      -3.956965014576
H       -5.618588961041      -0.653551544336      -3.006258745990
H       -5.877363765309      -0.696277087499      -4.743386831520
C       -5.425015577441       1.273551321676      -3.971784330526
H       -6.468597407637       1.561472851873      -3.811224980996
H       -4.820109720556       1.738029104971      -3.185849302657
H       -5.094584901496       1.695681469598      -4.927726338774
Si      -3.380931944751      -1.985048186893      -7.788162484664
H       -2.779773737949      -2.161329094035      -6.406772380589
C       -5.176324901830      -2.513932258494      -7.643798671325
H       -5.265299501960      -3.546628908210      -7.288569982356
H       -5.727992862680      -1.865195108601      -6.955093124598
H       -5.674363426617      -2.454202437686      -8.618778981955
C       -2.403040428282      -3.146736796981      -8.896937995710
H       -2.546540221038      -4.172185341148      -8.527961707766
H       -1.333733835799      -2.928071908807      -8.775920460384
C       -2.794148799591      -3.053377969900     -10.380823977251
H       -2.207701852529      -3.750007649417     -10.989153441353
H       -3.852212902225      -3.293019016797     -10.534439188389
```

```
H        -2.616448103624        -2.048463015993       -10.776274412350
C        -3.219908476593        -0.176598193595        -8.239129831095
H        -3.857241400283         0.443039239723        -7.599549188873
H        -2.190735535795         0.172666716721        -8.117323533503
H        -3.515248899017        -0.006238748542        -9.280822272488
```